MITOCHONDRIAL OXPHOS SYSTEM: EMERGING CONCEPTS AND TECHNOLOGIES AND ROLE IN DISEASE

EDITED BY: David Pacheu-Grau, Erika Fernandez-Vizarra, Gloria Garrabou and Sylvie Callegari

PUBLISHED IN: Frontiers in Cell and Developmental Biology and Frontiers in Molecular Biosciences

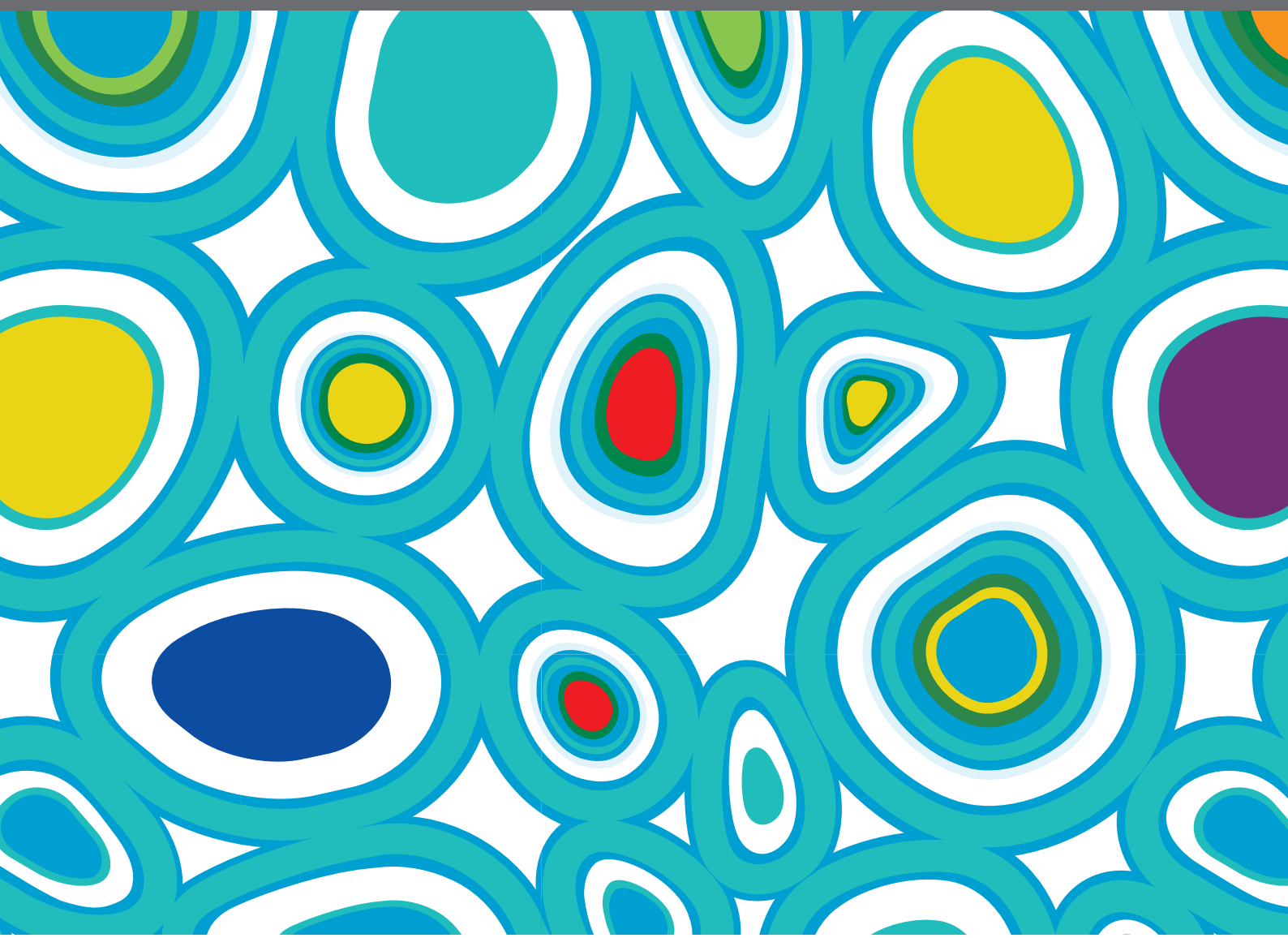

frontiers Research Topics

ISSN 1664-8714
ISBN 978-2-88976-330-6
DOI 10.3389/978-2-88976-330-6

About Frontiers

Frontiers is more than just an open-access publisher of scholarly articles: it is a pioneering approach to the world of academia, radically improving the way scholarly research is managed. The grand vision of Frontiers is a world where all people have an equal opportunity to seek, share and generate knowledge. Frontiers provides immediate and permanent online open access to all its publications, but this alone is not enough to realize our grand goals.

Frontiers Journal Series

The Frontiers Journal Series is a multi-tier and interdisciplinary set of open-access, online journals, promising a paradigm shift from the current review, selection and dissemination processes in academic publishing. All Frontiers journals are driven by researchers for researchers; therefore, they constitute a service to the scholarly community. At the same time, the Frontiers Journal Series operates on a revolutionary invention, the tiered publishing system, initially addressing specific communities of scholars, and gradually climbing up to broader public understanding, thus serving the interests of the lay society, too.

Dedication to Quality

Each Frontiers article is a landmark of the highest quality, thanks to genuinely collaborative interactions between authors and review editors, who include some of the world's best academicians. Research must be certified by peers before entering a stream of knowledge that may eventually reach the public - and shape society; therefore, Frontiers only applies the most rigorous and unbiased reviews.
Frontiers revolutionizes research publishing by freely delivering the most outstanding research, evaluated with no bias from both the academic and social point of view. By applying the most advanced information technologies, Frontiers is catapulting scholarly publishing into a new generation.

What are Frontiers Research Topics?

Frontiers Research Topics are very popular trademarks of the Frontiers Journals Series: they are collections of at least ten articles, all centered on a particular subject. With their unique mix of varied contributions from Original Research to Review Articles, Frontiers Research Topics unify the most influential researchers, the latest key findings and historical advances in a hot research area! Find out more on how to host your own Frontiers Research Topic or contribute to one as an author by contacting the Frontiers Editorial Office: frontiersin.org/about/contact

MITOCHONDRIAL OXPHOS SYSTEM: EMERGING CONCEPTS AND TECHNOLOGIES AND ROLE IN DISEASE

Topic Editors:
David Pacheu-Grau, University of Zaragoza, Spain
Erika Fernandez-Vizarra, Veneto Institute of Molecular Medicine (VIMM), Italy
Gloria Garrabou, Institut de Recerca Biomèdica August Pi i Sunyer (IDIBAPS), Spain
Sylvie Callegari, The University of Melbourne, Australia

Citation: Pacheu-Grau, D., Fernandez-Vizarra, E., Garrabou, G., Callegari, S., eds. (2022). Mitochondrial OXPHOS System: Emerging Concepts and Technologies and Role in Disease. Lausanne: Frontiers Media SA.
doi: 10.3389/978-2-88976-330-6

Table of Contents

frontiers | Frontiers in Cell and Developmental Biology

EDITORIAL
published: 19 May 2022
doi: 10.3389/fcell.2022.924272

Editorial: Mitochondrial OXPHOS System: Emerging Concepts and Technologies and Role in Disease

Erika Fernández-Vizarra[1,2]*, *Sylvie Callegari*[3,4]*, *Glòria Garrabou*[5,6]* and *David Pacheu-Grau*[6,7,8]*

[1]Istituto Veneto di Medicina Molecolare (VIMM), Padova, Italy, [2]Dipartimento di Scienze Biomediche, Università di Padova, Padova, Italy, [3]Walter and Eliza Hall Institute of Medical Research, Parkville, VIC, Australia, [4]Department of Medical Biology, University of Melbourne, Melbourne, VIC, Australia, [5]Muscle Research and Mitochondrial Function Laboratory, Internal Medicine Department-Hospital Clínic of Barcelona, Cellex-IDIBAPS, Faculty of Medicine and Health Sciences, University of Barcelona, Barcelona, Spain, [6]Centro de Investigaciones Biomédicas en Red de Enfermedades Raras (CIBERER), Madrid, Spain, [7]Departamento de Bioquímica, Biología Molecular y Celular, Universidad de Zaragoza, Zaragoza, Spain, [8]Instituto de Investigación Sanitaria (IIS) de Aragón, Zaragoza, Spain

Keywords: mitochondria, OXPHOS, mtDNA, mitochondrial proteome, mitochondrial dysfunction, mitochondrial quality control

OPEN ACCESS

Edited and reviewed by:
Cecilia Giulivi,
University of California, Davis, United States

***Correspondence:**
Erika Fernández-Vizarra
erika.fernandezvizarra@unipd.it
Sylvie Callegari
callegari.s@wehi.edu.au
Glòria Garrabou
GARRABOU@clinic.cat
David Pacheu-Grau
dpacheu@unizar.es

Specialty section:
This article was submitted to Cellular Biochemistry, a section of the journal Frontiers in Cell and Developmental Biology

Received: *20 April 2022*
Accepted: *28 April 2022*
Published: *19 May 2022*

Citation:
Fernández-Vizarra E, Callegari S, Garrabou G and Pacheu-Grau D (2022) Editorial: Mitochondrial OXPHOS System: Emerging Concepts and Technologies and Role in Disease. Front. Cell Dev. Biol. 10:924272. doi: 10.3389/fcell.2022.924272

Editorial on the Research Topic

Mitochondrial OXPHOS System: Emerging Concepts and Technologies and Role in Disease

Mitochondria are eukaryotic organelles responsible for generating the main bulk of ATP, the cellular energy currency, via the process of oxidative phosphorylation (OXPHOS). The OXPHOS system is unique because it comprises subunits of dual genetic origin, encoded in the mitochondrial and the nuclear genomes. Therefore, to form the multimeric membrane-bound complexes responsible for this energy production process, proteins translated inside the organelle must be assembled in coordination with those expressed in the cytosol and imported into mitochondria by using a sophisticated import and translocation machinery. The idea that the OXPHOS system plays a role not only in ATP production but also in regulating many physiological and pathological processes has been emerging for more than 10 years. Recent evidence points to the existence of intricate quality control systems that guarantee the functionality of mitochondria, as well as the interactions of intramitochondrial and extramitochondrial factors that ultimately influence mitochondrial bioenergetics. For these reasons this Research Topic is a timely release, covering emerging concepts relating to the structure, function, and regulation of the OXPHOS system. In addition, the Research Topic also presents novel technological approaches to unravel the yet unknown intricacies involving this group of protein complexes as well as new mechanisms or pathways linking OXPHOS dysfunction and pathological states.

This Research Topic comprises thirteen contributions, including nine reviews, one perspective and three original research articles that highlight relevant new aspects influencing mitochondrial OXPHOS fitness. Guitart-Mampel et al. analyze the role of inorganic polyphosphate (polyP) in bioenergetics by using wild-type and MitoPPX SH-SY5Y (cells enzymatically deprived of mitochondrial polyP) via a thorough analysis of the changes in cell physiology, proteome and metabolome. Two key metabolic mitochondrial pathways (OXPHOS and TCA cycle) were affected by deficiency in polyP. This observation could be linked to a regulatory role of polyP in processes altered in neurodegenerative disorders, such as reactive oxygen species (ROS) production, apoptosis, inflammation, or energy metabolism. Illescas et al. explore mitochondrial function within a broader cellular context, depicting how cytoskeleton dynamics is related not only to mitochondrial trafficking, dynamics, and apoptosis but also to biogenesis and metabolism. Interestingly, they

report novel findings of actin filaments located outside and inside mitochondria and the relevance of gelsolin (one of the most abundant actin-binding proteins) to mitochondrial function. Other articles in the Research Topic offer an updated view of key molecular pathways inside mitochondria. Padavannil et al. explore the intriguing question of why accessory subunits of Complex I (CI) have been added during evolution to the fourteen conserved core subunits. To explain the evolutionary and functional reasons for these additions, they used a combination of available structural information from CI assembly, subunit knockout, knockdown, and mutagenesis, and clinical studies. As a result of this analysis, they propose more sophisticated molecular functions for each of the accessory subunits, including, for example, assembly coordination, scaffold for protein localization to the cristae, response to ROS generation and sensors for energy supply/output. Eaglesfield and Tokatlidis provide an updated overview concerning the structure and mechanisms of protein insertion into mitochondria, highlighting the most exciting features of the various molecular machineries conducting protein translocation and insertion (including the TOM, MIM, SAM, TIM22 and TIM23 complexes, and OXA1). Den Brave et al. summarized the most recent and compelling insights on protein quality control mechanisms at the mitochondrial surface. They describe the current molecular pathways by which cells can survey and cleanup the mislocalization of mitochondrial proteins and protein blockages of the mitochondrial import channel in order to ensure optimal mitochondrial function.

An important focus of this Research Topic has been to highlight new experimental approaches that can be implemented to uncover different aspects of mitochondrial biology. Mitochondrial disorders affect various tissues and organs, and developing physiologically relevant cellular models is critical to understanding the basis of their pathology. Pavez-Giani and Cyganek present the latest advances in the use of human induced pluripotent stem cells to study mitochondrial cardiomyopathies. They analyzed different reported iPSC-CM models used to study a range of mitochondrial genetic mutations and their characteristics. They additionally describe the general limitations of this approach and different strategies to overcome them. Cabrera-Orefice et al. summarize the most relevant aspects of Complexome Profiling. This resolutive approach combines the separation of membrane complexes by native electrophoresis, size exclusion chromatography, or density gradient centrifugation with proteomic mass spectrometry analysis. This technique has proven its usefulness in evaluating the inventory, abundance, and arrangement of OXPHOS Complexes and related factors in health and disease. The authors give examples of different uses for this technical approach and discuss the limitations, improvements, and the use of Complexome Profiling to complement, for example, structural methods. Finally, Robinson et al. present an elegant original research article illustrating the application of carbonate extraction of mitochondrial membrane proteins, coupled to mass spectrometry, to investigate OXPHOS structural defects. In this way, they generated membrane association profiles for >800 mitochondrial proteins and clustered them into 6 different groups based on resistance to carbonate extraction at different pH Using Complex III (CIII) knockout cell lines as an example, they used this technique to assess the destabilization of protein associations within the mitochondrial membranes induced by CIII assembly defects.

The last group of articles uncovers new concepts related to mitochondrial dysfunction and disease. Zhang et al. link mitochondrial dysfunction and severe liver disease. Their review discusses how liver dysfunction impacts mitochondrial fitness and consequently which mitochondrial parameters could be used as a hallmark of liver disease. They further define novel methodologies for assessing mitochondrial function in this context and propose strategies to reverse the metabolic reprogramming observed in advanced liver disease. In their perspective article, Fløtnes and Tzoulis evaluate the role and influence of OXPHOS in idiopathic Parkinson's disease (PD) neurodegeneration. They consider different aspects of OXPHOS dysfunction in PD patients to enlighten the nature of this defect in the brain. More specifically, they explore the discrepancies found in the OXPHOS phenotypes of PD patients, possible molecular causes for the defects, links to other known hallmarks of PD, such as alpha-synuclein, and the potential downstream impact of OXPHOS dysfunction in PD pathology. Chowdhury et al. summarize the most recent insights into the role of released mitochondrial nucleic acids and immune system activation. They provide a comprehensive review of the main pathways involved in nucleic acid release from mitochondria, sensing mechanisms, and the consequences of these molecular processes on human health. They point out how mitochondrial RNA and DNA release may play an essential role in critical diseases such as autoimmune disorders and neuroinflammatory diseases. Interestingly, mitochondrial gene expression requires approximately 25% of the mitochondrial proteome, highlighting the complexity and relevance of this process for mitochondrial physiology. Wang et al. present a thorough review analyzing the connection between mitochondrial translation and disease. They review the different molecular steps in the process and the known mutations that affect these steps. Furthermore, they discuss the possibility of different regulatory mechanisms mediated by microRNAs, as well as the coordination between cytosolic and mitochondrial translation. Finally, Jennings et al. contributed an original research article describing the molecular consequences of DNAJC3 mutations associated with a multisystemic neurological disorder and diabetes. Disruption of this Endoplasmic Reticulum (ER) BiP co-chaperone leads to alteration of lipid and cholesterol metabolism, resulting in ER stress, activation of the unfolded protein response (UPR), β-amyloid accumulation, and ultimately an alteration of the OXPHOS system. Interestingly, the abundance of OXPHOS subunits and, concomitantly, mitochondrial respiration rates were increased in these mutants, indicating a possible pro-survival mechanism triggered by ER-stress.

In conclusion, this Research Topic of articles summarizes and describes novel molecular aspects of mitochondrial fitness, state-of-the-art technologies to study mitochondrial organization, and novel associations of mitochondrial dysfunction to diseases. It provides an update on the most relevant insights into

mitochondrial pathophysiology, setting the path to bringing discoveries into current experimental and clinical practices.

AUTHOR CONTRIBUTIONS

DP-G wrote the first draft of the manuscript. EF-V, SC, and GG revised and edited the manuscript. All authors approved the final version.

Conflict of Interest: The authors declare that the research was conducted in the absence of any commercial or financial relationships that could be construed as a potential conflict of interest.

Publisher's Note: All claims expressed in this article are solely those of the authors and do not necessarily represent those of their affiliated organizations, or those of the publisher, the editors and the reviewers. Any product that may be evaluated in this article, or claim that may be made by its manufacturer, is not guaranteed or endorsed by the publisher.

frontiers in Cell and Developmental Biology

REVIEW
published: 01 July 2021
doi: 10.3389/fcell.2021.675465

Mitochondrial Protein Translation: Emerging Roles and Clinical Significance in Disease

*Fei Wang[1], Deyu Zhang[1], Dejiu Zhang[1], Peifeng Li[1] and Yanyan Gao[1,2]**

[1] *Institute for Translational Medicine, The Affiliated Hospital of Qingdao University, College of Medicine, Qingdao University, Qingdao, China,* [2] *Key Laboratory of Nuclear Medicine, Ministry of Health, Jiangsu Key Laboratory of Molecular Nuclear Medicine, Jiangsu Institute of Nuclear Medicine, Wuxi, China*

Mitochondria are one of the most important organelles in cells. Mitochondria are semi-autonomous organelles with their own genetic system, and can independently replicate, transcribe, and translate mitochondrial DNA. Translation initiation, elongation, termination, and recycling of the ribosome are four stages in the process of mitochondrial protein translation. In this process, mitochondrial protein translation factors and translation activators, mitochondrial RNA, and other regulatory factors regulate mitochondrial protein translation. Mitochondrial protein translation abnormalities are associated with a variety of diseases, including cancer, cardiovascular diseases, and nervous system diseases. Mutation or deletion of various mitochondrial protein translation factors and translation activators leads to abnormal mitochondrial protein translation. Mitochondrial tRNAs and mitochondrial ribosomal proteins are essential players during translation and mutations in genes encoding them represent a large fraction of mitochondrial diseases. Moreover, there is crosstalk between mitochondrial protein translation and cytoplasmic translation, and the imbalance between mitochondrial protein translation and cytoplasmic translation can affect some physiological and pathological processes. This review summarizes the regulation of mitochondrial protein translation factors, mitochondrial ribosomal proteins, mitochondrial tRNAs, and mitochondrial aminoacyl-tRNA synthetases (mt-aaRSs) in the mitochondrial protein translation process and its relationship with diseases. The regulation of mitochondrial protein translation and cytoplasmic translation in multiple diseases is also summarized.

Keywords: mitochondria, protein translation, translation factors, mitochondrial ribosome, mitoribosome assembly factors, mitochondrial aminoacyl-tRNA synthetase, translation activators, cytoplasmic translation

OPEN ACCESS

Edited by:
Erika Fernandez-Vizarra, University of Glasgow, United Kingdom

Reviewed by:
Joanna Rorbach, Karolinska Institutet (KI), Sweden
Juliane Mueller, University of Cambridge, United Kingdom

***Correspondence:**
Yanyan Gao
gaoyanyan@qdu.edu.cn

Specialty section:
This article was submitted to Cellular Biochemistry, a section of the journal Frontiers in Cell and Developmental Biology

Received: *03 March 2021*
Accepted: *09 June 2021*
Published: *01 July 2021*

Citation:
Wang F, Zhang D, Zhang D, Li P and Gao Y (2021) Mitochondrial Protein Translation: Emerging Roles and Clinical Significance in Disease. Front. Cell Dev. Biol. 9:675465. doi: 10.3389/fcell.2021.675465

INTRODUCTION

Mitochondria are important, semi-autonomous organelles in eukaryotic cells. Their independent genetic system includes mitochondrial DNA (mtDNA), messenger RNA (mRNA), transfer RNA (tRNA), ribosomal RNA (rRNA), and ribosomes. Mitochondrial DNA replication, mRNA transcription, and protein translation occur independently, including the synthesis of polypeptides encoded by mtDNA. Human mtDNA comprises 16,569 base pairs and exists in multiple copies

(Surovtseva et al., 2011). The mitochondrial genome lacks introns and contains only one major non-coding region, as well as a displacement loop (D-loop), which contains the promoter for transcription initiation. Mitochondrial DNA has heavy (H) and light (L) strands. The L-chain is rich in adenine and thymine, encoding one protein (ND6) and eight tRNAs. The H-strand is rich in guanine and encodes the remaining 12 proteins and 14 tRNAs (Shokolenko and Alexeyev, 2015). Despite the presence of this system, most mitochondrial proteins are encoded by nuclear DNA (nDNA). Only 13 of the proteins involved in the respiratory chain of mitochondria are encoded by mtDNA. These 13 are the core components of the mitochondrial respiratory chain complex. ND1–ND6 and ND4L are subunits of complex I. Cytochrome b (CYTB) is a subunit of complex III. COX1–COX3 are subunits of complex IV. Finally, ATP6 and ATP8 are subunits of ATPase (complex V). All complex II subunits are encoded by nDNA and are translocated through the mitochondrial membrane (Schulz et al., 2015).

Mitochondrial translation includes initiation, elongation, termination, and ribosome-recycling stages (**Figure 1**). The mtDNA encodes two rRNAs, 22 tRNAs, and 13 proteins, which are important for mitochondrial function and biogenesis (Yokokawa et al., 2018). Mammalian mitochondrial ribosomes (mitoribosomes) synthesize proteins essential for ATP production via oxidative phosphorylation (OXPHOS). Mitochondrial translation mechanisms differ from those of cytoplasmic ribosomes, and are more similar to prokaryotic translation (Koripella et al., 2019a). At each stage, mitochondrial protein synthesis requires a series of mitochondrial factors (Mai et al., 2017). These include two initiation factors (MTIF2 and MTIF3), three elongation factors (EFTU, EF-TS, and mtEF-G1), a release factor (MTRF1L), and two ribosome recycling factors (MRRF and EF-G2mt). All are necessary for mitochondrial translation. Deficiency or mutation of these factors leads to abnormal mitochondrial translation and a series of metabolic disorders.

Translation in mitochondria is carried out by specialized mitoribosomes. Mammalian mitochondrial ribosomes consist of a large subunit (39S) and a small subunit (28S). The large subunit contains a 16S rRNA and 48 proteins, while the small subunit contains a 12S rRNA and 30 proteins. To visualize the process of translation in human mitochondria, Aibara et al. (2020) determined eight cryogenic electron microscopy (cryo-EM) structures of human mitoribosomes in complex with mitochondrial mRNA (mt-mRNA), mitochondrial tRNAs (mt-tRNAs) and additional factors in different states. Most mutations in nuclear genes encoding mitoribosomal proteins, as well as mitochondrial DNA encoding tRNAs and 12S rRNA, lead to clinically and genetically heterogeneous infant multisystem diseases, such as Leigh's syndrome, sensorineural hearing loss, encephalomyopathy, and hypertrophic cardiomyopathy (Jacobs and Turnbull, 2005; Perez-Martinez et al., 2008; Rotig, 2011).

Mitochondria are involved in many physiological and pathological processes, including electron transport, OXPHOS, fatty acid metabolism, and the tricarboxylic acid cycle. Changes in mitochondrial protein structure and function are involved in many human diseases, including nervous diseases, cardiovascular diseases, and cancers (De Silva et al., 2015; Mai et al., 2017; Ferrari et al., 2020; Kummer and Ban, 2021). Most mitochondrial diseases are characterized by oxygen- and phosphorus-related damage, affecting the OXPHOS system (Torraco et al., 2015). Many mitochondrial diseases are caused by defective mitochondrial protein synthesis. Mutations or deficiencies in mitochondrial protein translation factors (**Table 1**), mitochondrial tRNAs, mitochondrial aminoacyl-tRNA synthetases (mt-aaRSs), mitochondrial ribosomal proteins (MRPs), or mRNA, rRNA, and tRNA modification enzymes can lead to translation disorders and a wide range of phenotypes and diseases.

ABNORMAL MITOCHONDRIAL TRANSLATION INITIATION AND DISEASE

The translation initiation process is a highly regulated and rate-limiting step in mitochondrial protein synthesis, which begins with the formation of an initiation complex. In bacteria, the first step of translation initiation is the dissociation of the ribosome into its small subunit (SSU) and large subunit (LSU). Then in the presence of mRNA, formylated methionine (fMet)-tRNA^{Met} (fMet-tRNA^{Met}), and three initiation factors (IF1, IF2, and IF3), the initiation complex can be formed to initiate protein synthesis. In mammalian mitochondria, the separation of the 28S and 39S mitochondrial ribosomal subunits leads to the formation of an initiation complex consisting of the 28S subunit,

Abbreviations: AD, Alzheimer's disease; aa-tRNA, aminoacyl-tRNA; CTD, C-terminal domain; COXPD7, OXPHOS deficiency type 7; CPEO, chronic progressive external ophthalmoplegia; CRC, colorectal carcinoma; CTEs, mito-specific C-terminal extensions; MT-CYB, mitochondrial cytochrome b; EMT, epithelial-to-mesenchymal transition; ETS, electron transport system; fMet, formyl-methionine; GDP, guanosine diphosphate; GGQ, Gly-Gly-Gln; GTP, guanosine triphosphate; GTPBP6, GTP binding protein 6; GUF1, GTPase of unknown function 1; HUPRA syndrome, hyperuricemia, pulmonary hypertension, renal failure in infancy, and alkalosis; ISCU, iron-sulfur cluster assembly enzyme; ISR, integrated stress response; LBSL, leukoencephalopathy with brainstem and spinal cord involvement and lactate elevation; LRPPRC, leucine rich pentatricopeptide repeat containing; ISR, integrated stress response; LSU, large subunit; LTBL, leukoencephalopathy with thalamus and brainstem involvement and high lactate; MELAS, mitochondrial encephalomyopathy, lactic acidosis, and stroke-like episodes; MERRF, myoclonic epilepsy with ragged-red fiber; MIDD, maternally inherited diabetes and deafness; miRNA, microRNA; mitomiRs, mitochondrial miRNAs; MITRAC, mitochondrial translation regulation assembly intermediate of cytochrome c oxidase; MLASA, syndrome, myopathy, lactic acidosis, and sideroblastic anemia; mt-tRNA, mitochondrial transfer RNA; MT-TI, mt-tRNA^{Ile}; MT-TL1, mt-tRNA^{Leu}; MT-TK, mt-tRNA^{Lys}; mt-aaRSs, mitochondrial aminoacyl-tRNA synthetases; mitoribosomes, mitochondrial ribosomes; mRNA, messenger RNA; mtDNA, mitochondrial DNA; mtPIC, mitochondrial preinitiation step; mTOR, mammalian target of rapamycin; MTRF, mitochondrial release factor; nDNA, nuclear DNA; NGS, next-generation sequencing; NTD, N-terminal domain; NTEs, mito-specific N-terminal extensions; OXPHOS, oxidative phosphorylation; PD, Parkinson's disease; PoTC, post-termination complex; PTC, peptidyltransferase center; RCC, respiratory chain complexes; ROS, reactive oxygen species; RRF, mitochondrial ribosome recycling factor; rRNA, ribosomal RNA; SNP, single nucleotide polymorphism; SRL, sarcin/ricin loop; SSU, small subunit; TACO1, translational activator of cytochrome oxidase I; TFAM, mitochondrial transcription factor A; tRNA, transfer RNA; UPRmt, mitochondrial unfolded protein response; USP5, ubiquitin-specific peptidase 5; UTR, untranslated region; WES, whole-exome sequencing.

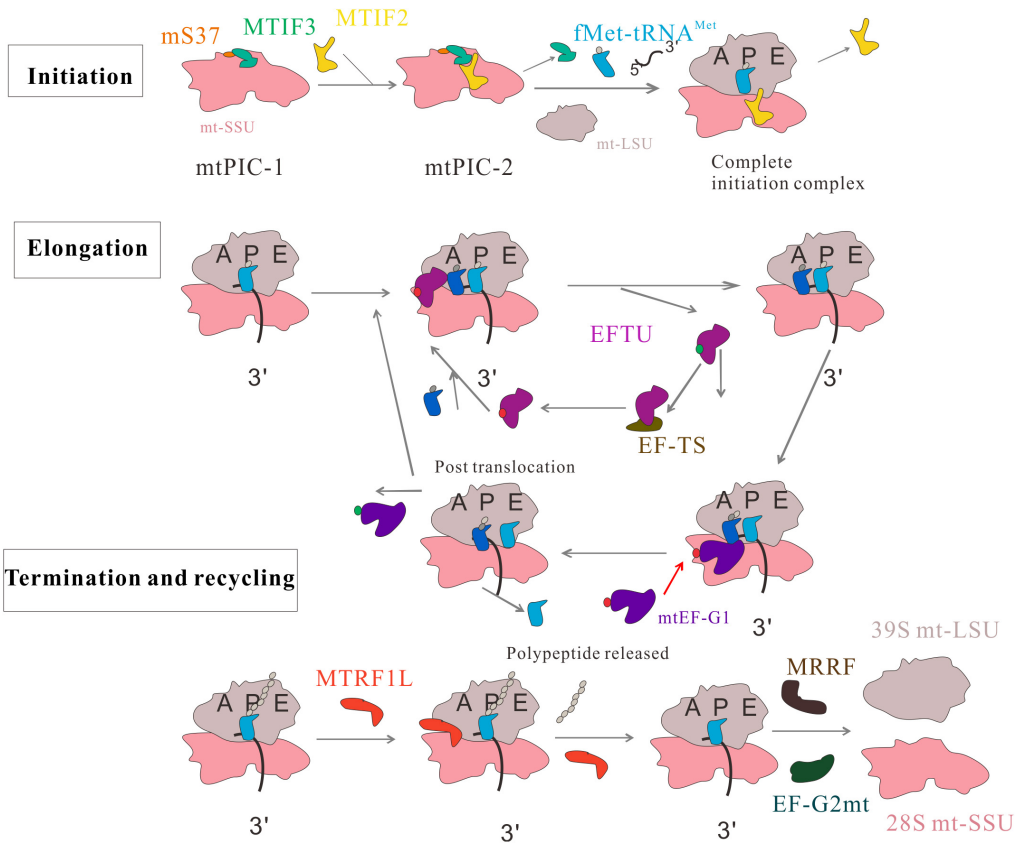

FIGURE 1 | Human mitochondrial translation. The process includes four phases: initiation, elongation, termination, and recycling. In the initiation phase, two distinct pre-initiation assembly steps, termed mitochondrial preinitiation steps 1 and 2 (mtPIC-1, mtPIC-2) are established. In the elongation phase, the aminoacyl-tRNA is transferred to the A site of mitochondrial ribosome by GTP · EFTU, and GTP · EFTU is transformed into GDP · EFTU. EF-TS converts GDP · EFTU to GTP · EFTU. The peptide-tRNA in the P site is transferred from the P site to the A site. mtEF-G1 binds to the ribosome at the A site and promotes translocation of the ribosome along the mRNA by inducing movement of A-tRNAs and P-tRNAs to the P site and E site. The tRNA at the E site leaves the monomer and this cycle continues until the polypeptide is completed and the stop codon appears at the A site. MRRF and EF-G2mt promote the separation of ribosomal subunits; MTIF3 combines with the small mitochondrial ribosomal subunits to prevent the premature reassociation of the large and small subunits.

mRNA, fMet-tRNA^{Met}, and initiation factors (Kuzmenko et al., 2014). These initiation factors (MTIFs) are encoded by nuclear genes that regulate the initiation of mitochondrial translation. One of these, MTIF2, closes the decoding center and stabilizes the binding of fMet-tRNA^{Met} to leaderless mRNAs (Rudler et al., 2019). Therefore, MTIF2 promotes the binding of fMet-tRNA^{Met} with the SSU of mitoribosomes (Gaur et al., 2008). Another important initiation factor is MTIF3, whose function has been widely studied. It enables the initiation codon (AUG) to correctly localize to the peptide (P) site of the mitoribosome and helps the mRNA bind to the mitochondrial SSU. In the absence of mRNA, fMet-tRNA^{Met} and MTIF2 bind weakly to mitochondrial SSU; MTIF3 acts to prevent or correct the premature binding of these components (Christian and Spremulli, 2009). Furthermore, a recent paper mentioned two distinct pre-initiation assembly steps, termed mitochondrial preinitiation steps 1 and 2 (mtPIC-1, mtPIC-2). The study applied cryo-EM and fluorescence analysis to reveal that the interaction between mitochondrial-specific protein mS37 and MTIF3 keeps the mitochondrial SSU in a conformation favorable for the accommodation of MTIF2 in the second step. Then, MTIF2 produces an intermediate state mtPIC-2, which binds to the mitochondrial LSU, replaces MTIF3 with the initial tRNA, and accommodates mitochondrial leaderless mRNA, resulting in the formation of a complete elongation-competent initiation complex (Khawaja et al., 2020) (**Figure 1**). Some diseases are associated with abnormal mitochondrial translation initiation and mutations in the genes encoding translation initiation factors.

MTIF2

Despite its role in mitochondrial translation, MTIF2 is encoded by a nuclear gene. It participates in the activation of mitochondrial protein translation and is the main regulatory factor for initiation. It is considered to be the functional equivalent of bacterial IF1 and IF2 (Liao and Spremulli, 1990). A 37-residue sequence was inserted into the V and VI domains of MTIF2, making it substitute for the function of IF1. A cryo-EM study showed that this 37 amino acid insertion into MTIF2 produced a similar function to that

of IF1, which could stereoscopically block the ribosomal A site, thus promoting the binding of the initial tRNA to the ribosomal P site during translation initiation (Yassin et al., 2011). This insert interacts with the decoding center of the small ribosomal subunit A-site and the 3′-CCA end of the sarcin/ricin loop (SRL) and fMet-tRNA^{Met} near the large ribosome subunit peptidyltransferase center (PTC), under the action of guanosine triphosphate (GTP) and the mRNA template

TABLE 1 | Mitochondrial translation factor mutations and related diseases.

Gene	Protein	Related disease/clinical presentation	References
(1) Mitochondrial translation initiation process			
MTIF2	**MTIF2**	Pathological myocardial hypertrophy	Lee et al., 2019
MTIF3	**MTIF3**	Parkinson's disease	Behrouz et al., 2010
		Obesity	Abadi et al., 2016
		Cardiomyopathy	Rudler et al., 2019
(2) Mitochondrial translation elongation process			
TUFM	**EFTU**	Lactic acidosis and fatal encephalopathy	Cao and Qin, 2016
		Lung cancer, colorectal carcinoma	Shi et al., 2012; He et al., 2016; Xu et al., 2019
		Hyperlactatemia	Di Nottia et al., 2017
		Metabolic cardiomyopathy	Hershkovitz et al., 2019
		MELAS	Sasarman et al., 2008
		Myocardial ischemia and reperfusion	He et al., 2001
		Polycystic encephalopathy, micropolygyria	Valente et al., 2009
TSFM	**EF-TS**	Early onset encephalocardiomyopathy	Emperador et al., 2016
		Mitochondrial cardiomyopathy	Perli et al., 2019
		Hypertrophic or dilated cardiomyopathy	Seo et al., 2019
		Encephalomyopathy and hypertrophic cardiomyopathy	Smeitink et al., 2006
		Infant liver failure	Vedrenne et al., 2012
GFM1	**mtEF-G1**	Early onset Leigh syndrome	Valente et al., 2007
		MELAS	Ahola et al., 2014; Emperador et al., 2016
GUF1	**mtEF4**	Cancer	Zhu et al., 2018
		Western syndrome	Alfaiz et al., 2016
		Male infertility	Gao et al., 2016
		Peripheral neuropathy, spastic paraparesis	Temperley et al., 2003
		Axonal neuropathy and optic atrophy	Tucci et al., 2014
		Distal motor neuropathy, optic atrophy	Fang et al., 2017b
		Leigh syndrome	Imagawa et al., 2016
		Leigh syndrome, optic atrophy, ophthalmoplegia	Antonicka et al., 2010
		Classical Behr's syndrome phenotype	Pyle et al., 2014
		Optic atrophy and mild developmental delays	Heidary et al., 2014
		Spastic paraplegia and strabismus	Buchert et al., 2013
(3) Mitochondrial termination and ribosome recycling			
MRRF	***RRF***	Parkinson's disease	Wu et al., 2020
GFM2	**EF-G2mt**	Leigh syndrome with arthrogryposis multiplex congenital	Fukumura et al., 2015
MTRFR	**C12orf65**	Early onset optic atrophy, progressive encephalomyopathy	Fang et al., 2017a
(4) Mitochondrial translational activators and disease			
LRPPRC	**LRPPRC**	French-Canadian Leigh syndrome	Kohler et al., 2015
(5) Mitochondrial miRNA			
miR-181c		Heart failure	Das et al., 2012, 2014
miR-1		Myogenesis	Das et al., 2014
miR-92a		Diabetic cardiomyopathy	Li et al., 2019
miR-21		Myocardial hypertrophy	Li et al., 2016

to generate a pre-start complex (Gaur et al., 2008). Mutation of this insertion domain seriously affects the ability of MTIF2 to bind to mitochondrial SSU and the formation of initiation complexes (Spencer and Spremulli, 2005). Similar to other protein synthesis systems, mitochondrial translation is initiated by methionine residues. However, for mitochondria, only one type of $tRNA^{Met}$ is used, which is in the form of fMet-$tRNA^{Met}$ at initiation and Met-$tRNA^{Met}$ during elongation. Formylation of Met-$tRNA^{Met}$ markedly enhances its affinity for MTIF2 (Spencer and Spremulli, 2004; Kummer et al., 2018). MTIF2 contains domains III to VI which are homologous to *Escherichia coli* IF2. Of these, subunit IV is the domain that mainly binds to fMet-$tRNA^{Met}$ (Spencer and Spremulli, 2004). Subsequently, Kummer et al. (2018) analyzed the cryo-EM structure of the complete translation initiation complex of mammalian mitochondria. They showed that the function of the additional domain insertion of MTIF2, which stabilizes the binding of leaderless mRNAs by closing the decoding center, induces the conformational changes of rRNA nucleotides involved in decoding. H678 of MTIF2 domain IV interacts with formyl of fMet-$tRNA^{Met}$, while F632 interacts with methionine. The results showed that MTIF2 has a unique function in the identification of fMet-$tRNA^{Met}$ and the regulation of GTPase activity (Kummer et al., 2018). Thus, MTIF2 has dual functions in mammalian mitochondria (Gaur et al., 2008). Therefore, mtIF2 guides the association of fMet-$tRNA^{Met}$ with mRNA and the assembly of mitochondrial 55S ribosomes (D'Souza and Minczuk, 2018).

Previous studies have found a relationship between MTIF2 and cardiomyocyte death (Lee et al., 2019), but no mutation of the *MTIF2* gene leading to mitochondrial diseases has been found. Specifically, in cell and animal models, MTIF2 has been linked to the oxidative capacity and redox state of cardiomyocytes (Lee et al., 2019). Its expression is reduced in the hearts of aged and obese mice, which decreases the oxidative capacity of cardiomyocytes. After *in vitro* hypoxic exposure, insufficient expression of MTIF2 can reduce oxygen consumption and increase cardiomyocyte death. Therefore, MTIF2 is necessary to maintain the oxidative properties of the myocardium, which plays a role in pathological myocardial hypertrophy during aging and obesity (Lee et al., 2019). The lack of MTIF2 in *Saccharomyces cerevisiae* reportedly results in disordered mitochondrial protein synthesis, which affects respiration. This defect was restored by either the *S. cerevisiae MTIF2* gene (*IFM1*) or cDNA encoding bovine MTIF2 (Tibbetts et al., 2003). A recent study showed that the upregulation of MTIF2 is associated with poor prognosis of lung cell malignancy induced by inorganic arsenic (Zhang et al., 2019).

MTIF3

Mammalian MTIF3 is encoded by nuclear genes. It catalyzes the formation of initiation complexes in the presence of mitoribosomes, mRNA, mitochondrial initiator tRNA, and MTIF2 *in vitro*, and regulates mitochondrial protein translation. It contains N-terminal and C-terminal domains (NTD and CTD, respectively) that are separated by unstructured, flexible connection zones (Koc and Spremulli, 2002). Unlike its bacterial homolog, MTIF3 possesses unique terminal extensions on its N- and C-termini (Next and Cext, respectively). These extensions may have evolved as adaptations to the mitochondrial environment (Chicherin et al., 2019). The CTD participates in translation regulation *in vitro* (Haque and Spremulli, 2008). It may also play a role in the kinetics of translation initiation complex formation (Haque and Spremulli, 2008). One finding also showed that the NTD increases the fidelity function of MTIF3 in terms of the selection of the initiation codon and initiator tRNA (through its anticodon stem) (Ayyub et al., 2017). Koripella et al. (2019a) analyzed the cryo-EM structure of the mammalian mitochondrial 28S-MTIF3 complex. Unique contacts between the N-terminal domain (NTD) of MTIF3 and the 28S subunit were observed in the cryo-EM structure, which also explained the high affinity of MTIF3 for the 28S subunit. The location of mito-specific N-terminal extensions (NTE) of MTIF3 indicated the role of NTE in binding of the initial tRNA to the 28S subunit. The location of the CTD imparts anti-association activity, and the orientation of mito-specific C-terminal extensions (CTEs) explains why it can destabilize initiator tRNA in the absence of mRNA. The authors also speculate that CTD can recruit leaderless mRNAs and initiate translation. The study investigated the role of the NTD and CTD of MTIF3 in stabilization of the pre-initiator complex with mitochondrial SSU, also demonstrating the mutual binding site of MTIF3 and tRNA on the ribosome (Koripella et al., 2019a).

Mammalian MTIF3 has an affinity for small mitoribosome subunits. It locates the AUG or AUA promoter of mRNA at the P-site of 28S SSU, prevents the premature binding of 39S large subunits with the 28S SSU, and promotes the dissociation of mitoribosomes (55S) into small (28S) and large (39S) ribosomal subunits (Koc and Spremulli, 2002). It changes the equilibrium between the 55S mitoribosome and the separated 39S and 28S subunits by binding with free 28S, preventing further subunit rebinding. In addition, MTIF3 binds to the 55S mitoribosome and promotes its dissociation. This may be due to the formation of a transient intermediate that is rapidly distributed to the 28S subunit combined with MTIF3 and the free 39S subunit (Christian and Spremulli, 2009). Moreover, mammalian MTIF3 promotes the separation of the initiator tRNA from mitoribosomes with a lack of mRNA (Bhargava and Spremulli, 2005).

Another key role of MTIF3 is in mitochondrial translation initiation by regulating mitochondrial function. One study indicated that MTIF3 is essential for mitochondrial translation initiation and the coordinated assembly of respiratory complexes. Heart-specific and skeletal muscle-specific loss of MTIF3 in mice caused abnormal mitochondrial protein synthesis and induced cardiomyopathy (Rudler et al., 2019). Changes in the function or expression of MTIF3 protein may affect mitochondrial function, ATP production, or the formation of reactive oxygen species (ROS), affecting susceptibility to Parkinson's disease (PD) and promoting its occurrence (Behrouz et al., 2010). The latter investigators also described an association of the rs7669 variant of *MTIF3* with PD risk. Whether rs7669 is a functional variant

remains to be confirmed. Thus, *MTIF3* mutations are associated with multiple pathological processes such as PD, obesity, and diabetes. A synonymous polymorphism (Asp266Asp, caused by c.798C>T) is associated with sporadic PD, indicating that MTIF3 may be involved in the pathogenesis of PD (Anvret et al., 2010), and this single-nucleotide polymorphism (SNP, c.798C>T) in *MTIF3* was shown to be strongly related to the PD allele by another group (Abahuni et al., 2007). MTIF3 is also involved in obesity (Abadi et al., 2016). It was reported that an *MTIF3* SNP (rs4771122) is associated with increased body mass index (BMI) in Mexican children (Abadi et al., 2016). In addition, MTIF3 autoantibodies were found in patients with type I diabetes, indicating that MTIF3 is related to diabetes (Bian et al., 2017).

MITOCHONDRIAL TRANSLATION ELONGATION AND DISEASE

Elongation is the core of protein synthesis and is the most conserved (Ott et al., 2016). In the process of protein synthesis, ribosomes move along the mRNA, which is decoded continuously through the interaction between mRNA codons and the anticodons of cognate tRNAs on the SSU. The aminoacyl (A) site, the peptidyl (P) site, and the exit (E) site are three binding sites for tRNAs in the ribosome. EFTU, EF-TS, mtEF-G1, and GUF1 are involved in the regulation of mitochondrial translation elongation. EFTU brings aminoacyl-tRNA (aa-tRNA) to the ribosomal A-site and coordinates specific codon: anticodon pairing between the mRNA and tRNA. Then, EFTU mediates hydrolysis of GTP and release of newly formed EFTU · guanosine diphosphate (GDP). EF-TS promotes GDP release from EFTU. GDP, regenerating EFTU · GTP. Next, under the catalysis of the large ribosomal subunit, peptide bonds are formed between the peptide-tRNA at the P site and aa-tRNA at the A site. mtEF-G1 (also called GFM1) then binds to the ribosomal A site and promotes ribosomal translocation along the mRNA by inducing A- and P-tRNAs to move to the P and E sites, respectively (Christian and Spremulli, 2012; Hallberg and Larsson, 2014; Ott et al., 2016) (**Figure 1**). The clinical expression levels of EFTU, EF-TS, and mtEF-G1 can reflect the function and translational speed of mitochondria; they can be used to evaluate the functional state of cells. Mutations in genes encoding these factors lead to mitochondrial disease (Wang X. Q. et al., 2017). Clinical manifestations include diverse diseases and phenotypes. These are usually disabling, progressive, and/or fatal, affecting the brain, liver, skeletal muscle, heart, and other organs (Boczonadi and Horvath, 2014; Diodato et al., 2014).

EFTU

A highly conserved GTPase, EFTU is encoded by the *TUFM* gene. EFTU is highly conserved and has 55–60% homology with bacterial EFTU (Woriax et al., 1995). In its active form (EFTU · GTP), aa-tRNA is transferred to the A-site of the mitoribosome to coordinate codon:anticodon pairing between the mRNA and tRNA through the formation of a ternary complex. Because this process requires energy, EFTU · GTP is converted to the EFTU · GDP inactive complex by EFTU-mediated GTP hydrolysis. The latter is released from ribosomes as the substrate of EF-TS, which promotes the exchange of GDP and GTP, reactivating GTP (Di Nottia et al., 2017). After correct codon:anticodon pairing, EFTU · GDP leaves the mitoribosome and aa-tRNA enters the P-site. At the P-site, the formation of peptide bonds is catalyzed by the large ribosomal subunit and the growing peptide chain is elongated (Boczonadi and Horvath, 2014). Binding at the A-site, GFM1 promotes the translocation of the ribosome along the mRNA by inducing movement of A-tRNAs and P-tRNAs to the P site and E site, respectively (Cao and Qin, 2016). The overall structure of EFTU · GTP is similar to that observed in *E. coli*, but the nucleotide binding domain (domain I) is in a different orientation compared with that observed in prokaryotic EFTU. In addition, domain III is followed by a short extension of 11 amino acids, forming one helical turn (Polekhina et al., 1996). It is an important step for EFTU to select the correct aa-tRNA for the ribosome A site to ensure the fidelity of translation. Using structure-based and explicit solvent molecular dynamics simulations based on recent cryo-EM reconstructions, Girodat et al. (2020) investigated the structural mechanism of how EFTU is involved in proofreading. They found that switch I of EFTU is a gate that facilitates aa-tRNA selection. Switch I of EFTU converts from an α-helix to a β-hairpin to control the movement of aa-tRNA in the accommodation corridor through steric interactions between Arg58 and the correct acceptor stem of aa-tRNA. Recent studies have also shown that EFTU plays a non-canonical role in the regulation of mitophagy mediated by PINK1. EFTU has mitochondrial-cytosolic dual localization. Ser222 of EFTU is phosphorylated by PINK1, which localizes it mainly in the cytosol and plays a role in inhibiting mitophagy (Lin et al., 2020).

Mutations in *TUFM* are associated with OXPHOS deficiency, which leads to lactic acidosis and fatal encephalopathy (Cao and Qin, 2016). A study described a patient with a homozygous mutation in *TUFM*. The patient was affected by neonatal lactic acidosis, rapidly progressive encephalopathy due to mitochondrial translation disorder, and mtDNA-related mitochondrial respiratory chain (MRC) complex deficiency (Valente et al., 2007). Another study described the case of a female infant with polycystic encephalopathy, micropolygyria, and leukodystrophy changes. An Arg336Gln substitution in EFTU was identified and associated with the failure to form active EFTU; the GTP·aa-tRNA ternary complex affected mitochondrial translation (Valente et al., 2009). In mitochondrial encephalomyopathy, lactic acidosis, and stroke-like episodes (MELAS) myoblasts, an almost complete lack of respiratory chain complexes I, IV, and V has been attributed to a heteroplasmic m.3243A>G substitution in the mitochondrial $tRNA^{Leu}$(UUR) (Emperador et al., 2016). The authors reported that the overexpression of EFTU or EF-G2mt (also called GFM2), but not EF-TS or GFM1, partially suppressed the phenotype. The finding of EFTU phosphorylation during myocardial ischemia and reperfusion prompted the hypothesis that the phosphorylation of mitochondrial translation factors inhibits mitochondrial protein synthesis,

indicating that mitochondrial protein synthesis is a decisive factor in myocardial ischemia-reperfusion injury (He et al., 2001). Therefore, *TUFM* may affect the function of the mitochondrial respiratory chain by regulating mitochondrial translation and may play an important role in encephalopathy and other diseases.

A novel c.964G>A mutation in *TUFM* changed the evolutionarily conserved EFTU-Gly322 residue to Arg, resulting in an approximately 80% decrease in expression. Patients harboring this pathological variant of *TUFM* displayed metabolic acidosis and hyperlactatemia. Neurological examination revealed severe encephalopathy and leukodystrophy with microlymph nodes (Di Nottia et al., 2017). The cases presented in these studies have expanded the phenotypic characteristics of *TUFM*-related diseases, which are characterized by lactic acidosis and dilated cardiomyopathy, without progressive encephalopathy. These findings have implicated *TUFM* as a candidate gene for early cardiomyopathy and in the differential diagnosis of metabolic cardiomyopathy (Hershkovitz et al., 2019).

Moreover, some studies have shown that EFTU is involved in the process of epithelial-to-mesenchymal transition (EMT); thus, it is expected to become a new prognostic indicator. In human cancer tissues, EFTU has been reported to be downregulated; moreover, EFTU knockdown induced EMT by activating the AMPK-GSK3β/β-catenin pathway (He et al., 2016). Overexpression of EFTU in colorectal carcinoma (CRC) has been described. This may be a promising new prognostic indicator for CRC (Shi et al., 2012). Another study showed that EFTU was deubiquitinated by ubiquitin-specific peptidase 5 (USP5), and its level increased in CRC (Xu et al., 2019). Moreover, EFTU knockout decreased mitochondrial respiratory chain activity, increased glycolysis, and produced ROS, inducing EMT (Samec et al., 2018). However, it has also been reported that high expression of EFTU in gastrointestinal stromal tumors (GISTs) is related to the occurrence, development, and prognosis of the tumors (Weng et al., 2020).

Some studies have shown that EFTU also participates in the process of disease by regulating oxidative stress. Silencing *TUFM* in *Paracoccidioides brasiliensis* reportedly alters translation elongation, causes respiratory defects, and increases the sensitivity of yeast cells to reactive oxygen stress, indicating the involvement of *TUFM* in the pathogenicity of this fungus (Marcos et al., 2019). Moreover, EFTU can physically interact with Xeroderma pigmentosum group D (XPD) protein, which is involved in mitochondrial oxidative DNA damage repair (Liu et al., 2015). Recently published articles have reported that EFTU is associated with Alzheimer's disease (AD)-like pathologies. The expression of EFTU is decreased in the brains of AD patients. Further studies showed that EFTU participates in the pathological process of AD through ROS in Beta-secretase 1 (BACE1) translation, apoptosis, and tau phosphorylation (Zhong et al., 2021).

EF-TS

EF-TS is a guanine nucleotide exchange factor encoded by *TSFM*. This factor combines with the EFTU · GDP complex to promote GDP release and form a stable EFTU · EF-TS heterodimer. GTP then promotes the separation of EF-TS from this complex and regenerates EFTU · GTP, which then binds to another aa-tRNA. This ternary complex combines with the ribosome A site. When the correct codon:anticodon recognition is established, GTP is hydrolyzed, EFTU · GDP is released, and the cycle repeats (Cai et al., 2000; Mai et al., 2017). The three-dimensional crystal structure of the bovine EFTU · EF-TS complex has been determined (Jeppesen et al., 2005).

Studies have described that decreased EF-TS in fibroblasts induced the upregulation of EFTU and mitochondrial biogenesis-related genes, along with increased expression of respiratory chain subunits and an increase in normal oxygen consumption rate (Perli et al., 2019). Forced overexpression of EFTU in cells obtained from carriers of pathogenic *TUFM* mutations can rescue EFTU deficiency. The predicted instability of EF-TS and EFTU in a bioinformatics analysis was consistent with a significant decrease in the steady-state levels of both proteins in clinically affected myocardium (Perli et al., 2019). These findings indicate that the lack of respiratory chain enzymes leads to OXPHOS dysfunction and eventually to multiple mitochondrial diseases.

Symptoms of mitochondrial cardiomyopathy caused by mitochondrial translation disorder have been described for a patient with a new complex heterozygote variant in *TSFM* (Perli et al., 2019). Two novel compound heterozygous mutations, c.944G>A, p.Cys315Tyr and c.856C>T, p.Gln286Xaa, in the *TSFM* gene of patients with juvenile-onset Leigh disease, ataxia, neuropathy, and optic atrophy, were reported to lead to EFTU protein degradation and marginally increased mitochondrial protein translation activity (Ahola et al., 2014). Recently, the first case of a patient with a childhood-onset chorea caused by complex heterozygous mutation of *TSFM* (MIM*604723) without basal ganglis lesions was reported (van Riesen et al., 2021).

A homozygous mutation of EF-TS (p.Cys997Thr) was found in both patients with encephalomyopathy and hypertrophic cardiomyopathy. The mutation resulted in mitochondrial translation defects and reduced amounts of assembled complexes I, IV, and V in fibroblasts (Smeitink et al., 2006). SNP genotyping has been used to detect homozygous *TSFM* mutations. The p.Arg312Trp substitution changed arginine to tryptophan, suggesting that mitochondrial translation deficiency is an increasingly serious cause of infant liver failure (Vedrenne et al., 2012). Another homozygous missense mutation was found in the mitochondrial translation elongation factor *TSFM* gene in a patient with slow progressive childhood ataxia and hypertrophic cardiomyopathy (Ahola et al., 2014; Emperador et al., 2016). Whole-exome sequencing (WES) was used to identify mutations in the *TSFM* gene leading to p.Gln111ThrfsTer5 and RNA mis-splicing in a patient with rare mitochondrial disorders (Seo et al., 2019). There is evidence that children with hypertrophic or dilated cardiomyopathy who progress slowly due to *TSFM* mutations develop neurological symptoms that include optic-nerve and/or peripheral neuropathy, ataxia, Leigh disease, and others, which are the main manifestations of the disease (Emperador et al., 2016).

A next-generation sequencing (NGS)-based multigene panel for mitochondrial dysfunction was used to identify a *TSFM* homozygous variant, c.547G>A, p.Gly183Ser, associated with early onset encephalomyopathy with sensorineural hearing loss and peculiar neuroimaging features. This result showed that EF-TS-mediated mitochondrial protein translation is valuable for studies of mitochondrial diseases in children with neurological and cardiac involvement (Scala et al., 2019). A patient with a novel *TSFM* mutation has been reported to have an adult-onset complex generalized hyperactivity disorder (Traschutz et al., 2019). The collective findings indicate that *TSFM* mutations are the cause of autosomal recessive mitochondrial cardiomyopathy, encephalopathy with optic and/or peripheral neuropathy, ataxia, and Leigh syndrome.

mtEF-G1

The human genes *GFM1* and *GFM2* encode mtEF-G1 and EF-G2mt, respectively. Both are highly conserved homologs of bacterial translation elongation factor G (EF-G). The mtEF-G1 elongation factor displays mitoribosome translocation activity. The EF-G2mt factor disassembles the mitoribosome at the end of translation to allow a subsequent protein-synthesis cycle (Glasgow et al., 2017).

The sequence homology between the functional human mtEF-G1 and its bacterial counterpart is ∼45%. The main difference is that there is a mito-specific extension of 11 amino acids at the former's C-terminus (Bhargava et al., 2004). It was shown that the CTE in mtEF-G1 is directly involved in the translocation of the mt-tRNA receptor arm at the A site. The complex of human 55S mitochondrial ribosome and human mtEF-G1 has three different conformational states including an intermediate state and post-translocation state (Koripella et al., 2020). mtEF-G1 is a five-domain GTPase that catalyzes the transfer of peptide-tRNA from the A site of the ribosome receptor to the P site after the formation of peptide bonds, while removing the deacylated tRNA, promoting mRNA translocation, and exposing the next codon (Brito et al., 2015). mtEF-G1, as a translational GTPase, uses the energy of GTP hydrolysis to facilitate the rearrangement of the pre-translocation ribosomes and tRNA movement, so as to accelerate the process of translocation (Chen et al., 2013). Cryo-EM structures provide insights into the structures of elongation complexes from mammalian mitochondria at two different steps of the tRNA translocation reaction using *in vitro* reconstitution systems. Results have shown that mtEF-G1 not only controls the conformational changes in SSU to promote the movement of tRNA, but also causes the large rearrangement of the GTPase-associated center of mitochondrial LSU. mtEF-G1 binding leads to GAC closure, which stabilizes mtEF-G1 from a weakly to a tightly bound state with translocation ability (Kummer and Ban, 2020).

A study described two new mutations in *GFM1*, which resulted in decreased levels of mtEF-G1, abrogated assembly of mitochondrial complexes III and V, and decreased activity of mitochondrial complexes I and IV. These changes manifested as OXPHOS defects with complex clinical manifestations (Brito et al., 2015). However, the residual steady-state level of mtEF-G1 protein found in the heart and skeletal muscle was higher than that in the liver and fibroblasts, which reduced the sensitivity of these tissues and accentuated the nerve and liver involvement. The difference in residual protein levels among cells may be due to differing regulatory and compensatory responses of the mitochondrial translation system in different tissues (Brito et al., 2015). A tissue-specific effect of novel *GFM1* mutations has been described in three patients by other investigators. In these patients, the respiratory chain enzyme activity of muscle and fibroblasts decreased slightly, while the liver function was seriously deficient (Ravn et al., 2015). A *GFM1* mutation was found in two siblings with serious defects in mitochondrial translation. This mutation is located in a conserved residue in the GTP binding domain of mtEF-G1 (Coenen et al., 2004). A case report showed a *GFM1* mutation in a patient affected by severe, rapidly progressive mitochondrial encephalopathy. This mutation results in a p.Arg250Trp substitution in the mtEF-G1 G′ subdomain and may block ribosome-dependent GTP hydrolysis (Smits et al., 2011a). Another study showed that patients with *GFM1* mutations were affected by severe lactic acidosis, rapidly progressive and fatal encephalopathy, and early onset Leigh syndrome (Valente et al., 2007). A novel intronic *GFM1* mutation was described. The prognosis of patients with this mutation was poor, with death almost always occurring in infancy, although one child was still alive at 6 years of age (Simon et al., 2017). A comprehensive genomic analysis revealed that *GFM1* is one gene mutation known to cause OXPHOS disease in patients with childhood-onset mitochondrial respiratory chain complex deficiencies (Kohda et al., 2016). Recently, a study reported a family that carries a novel *GFM1* variant, which is associated with a rare fatal mitochondrial disease. A p.Cys1576Thr mutation in exon 13 of *GFM1* resulted in a premature stop codon at amino acid position 526 (Coenen et al., 2004; Su and Wang, 2020). WES revealed a novel composition of two heterozygous mutations of *GFM1* in a Chinese child with epilepsy and mental retardation (You et al., 2020). In recent years, nine unrelated children were found to carry *GFM1* mutation. All of these patients presented with nervous system involvement during the neonatal period, and five of them were diagnosed with West syndrome. mtEF-G1 expression was decreased, mitochondrial translation was impaired, and OXPHOS protein levels were decreased in these patients (Barcia et al., 2020). In conclusion, *GFM1* is one of the known gene mutations causing OXPHOS disease, and its mutations and abnormal expression are closely related to a series of mitochondrial diseases.

GUF1

Bacterial and organellar translation employ a specific regulatory mechanism that differs from that of eukaryotes, involving the highly conserved EF4 translation elongation factor. In this phase of bacterial protein synthesis, EF4 catalyzes the back-translocation of P- and E-tRNAs to A- and P-tRNAs (Zhang et al., 2016). EF4 was originally termed lepA, because the gene encoding the protein is the first cistron of the bicistronic lep operon leader peptidase (lepB or lep) (March and Inouye, 1985). EF4 is highly conserved among all bacteria and almost

all eukaryotes. In bacteria, EF4 catalyzes the translocation of peptidyl-tRNA and deacylated-tRNA in the opposite direction of EF-G catalysis. Therefore, EF4 is a back-translocase that maintains translation fidelity by back-translocating the ribosome under stress conditions (Qin et al., 2006). The *E. coli* lepA translation elongation factor has a mitochondrial homolog, mtEF4. Initial studies on budding yeast identified mtEF4 as an evolutionarily conserved GTPase with unknown function. Accordingly, it was also named GTPase of unknown function 1 (GUF1) (Bauerschmitt et al., 2008). In eukaryotes, the N-termini of GUF1 homologs have a mitochondria-targeting signal localized to the mitochondrial outer membrane and are considered to be mtEF4. Under suboptimal conditions, such as low temperatures and high Mg^{2+} concentrations, GUF1 mutant yeast displayed enhanced mitochondrial protein synthesis. At higher temperatures, the assembly of cytochrome c oxidase was shown to be defective in GUF1-deficient mutants (Bauerschmitt et al., 2008). The observations that mtEF4 ablation can reduce the mitochondrial translation rate and disrupt the assembly of complex IV-containing supercomplexes support the important roles of mtEF4 in mitochondrial translation and adaptation to stressful conditions, suggesting that mtEF4 is a key protein that maintains the fidelity of mitochondrial protein synthesis (Bauerschmitt et al., 2008; Yang et al., 2014). It has been shown that mtEF4 is essential for the quality control of respiratory chain biogenesis. Dysregulation of mitochondrial translation caused by its overexpression may be crucial in the development of human cancers. Different mtEF4 levels induce distinct bioenergetic pathways in cancer cells due to different types of speed-quality imbalances. Specific downregulation of mtEF4 expression in tumor tissue could be a promising new therapy for cancer treatment (Zhu et al., 2018). Other authors used exome sequencing to detect mutations in relatives of patients with isolated West syndrome. A homozygous variant (c.1825G>T, p.Ala609Ser) was identified in *GUF1* in three affected siblings (Alfaiz et al., 2016).

In *Caenorhabditis elegans*, a *GUF1* deletion resulted in delayed growth, and MRC complex assembly defects resulted in mitochondrial dysfunction (Yang et al., 2014). We demonstrated testis-specific dysfunction in OXPHOS by genetic ablation of mtEF4 in mice, leading to male infertility (Gao et al., 2016). Our observations demonstrated crosstalk between the mtEF4-dependent quality control in mitochondria and cytoplasmic mammalian target of rapamycin (mTOR) signaling. We showed that with mtEF4 ablation, the main feedback signal from the somatic cytoplasm was mTOR-upregulated and was accompanied by increased cytoplasmic translation, indicating that mTOR is a critical downstream effector compensating for mitochondrial translation deficiency (Gao et al., 2016). We concluded that cytoplasmic translation regulated by mTOR and mitochondrial translation involving mtEF4 have a bidirectional causal relationship. The essential function of mtEF4 provides a plausible explanation for its high degree of evolutionary conservation throughout eukaryotes. Our findings suggest a disease mechanism involving developmental decoupling of crosstalk, such as during spermatogenesis in the testis or pathological conditions in other tissues. Thus, mtEF4 could be a biomarker for human diseases and a drug target for male contraception (Gao et al., 2016).

MITOCHONDRIAL TRANSLATION TERMINATION/RIBOSOME RECYCLING

Mitochondrial Translation Termination

Once the translation complex reaches the stop codon, the finished protein must be separated from the final tRNA, ribosome, and its homologous mRNA. In human mitochondria, UGA is not a stop codon, but a tryptophan codon. It is striking that AGA and AGG are not arginine codons, but terminating codons, only at the very end of open reading frames (ORFs) of the mitochondrial transcripts *MT-CO1* (also named *COX1*) and *MTND6* (also named *ND6*), respectively. This results in the possibility of a −1 frameshifting mechanism at the termination stage (Richter et al., 2010a). The remaining 11 mitochondrial ORFs are terminated by either the standard stop codon UAA or UAG. Several release factors are required during this termination. The proteins responsible for these functions are termed release factors (RFs). They recognize mRNA stop codons on the ribosome and control termination of protein synthesis (Soleimanpour-Lichaei et al., 2007). When a termination codon appears at the A site, RFs bind to the ribosome and promote ribosomal PTC-dependent hydrolysis of the ester bond of the peptide-based tRNA binding to the P site (Kisselev et al., 2003). Human mitochondria harbor four different members of the class 1 RF family: MTRF1L, MTRF1, MTRFR (previously called C12orf65), and MRPL58 (previously called ICT1) (Akabane et al., 2014). Mammalian MTRF1L is similar to the bacterial RF sequence. The absence of MTRF1L in human cells leads to growth deficiency (Soleimanpour-Lichaei et al., 2007). Changes in MTRF1L levels related to the mitochondrial inner membrane affect assembly of the respiratory complex and ROS production. MTRF1L is responsible for decoding the UAA/UAG termination codon (Kaji et al., 2001), which enables a single MTRF1L to terminate the translation of all 13 mtDNA-encoded peptides. This is sufficient to release all new human mitochondrial gene products from mitoribosomes (Rao and Varshney, 2001). Further analysis of other mitochondrial factors related to mitochondrial translation termination, such as RRFs, will help us to understand the process of mitochondrial translation termination in mammals and the role of MTRF1L (Nozaki et al., 2008). Desai et al. (2020) described the structure of MTRFR and mitochondrial LSU in rescuing the mitoribosome stalled state by analysis of cryo-EM structures of elongating mitoribosomes and revealed that MTRFR ejects the nascent chain (Desai et al., 2020).

The MRPL58 protein is a component of the human mitoribosome. It has codon-independent peptidyl-tRNA hydrolysis activity through its conserved Gly-Gly-Gln (GGQ) motif. Its function is crucial for hydrolysis of peptidyl-tRNAs that have been prematurely terminated in mitoribosomes and for cell viability (Richter et al., 2010b). *MRPL58* gene knockout results in apoptosis, decreased mitochondrial membrane potential and mass, and decreased cytochrome c oxidase activity (Handa et al., 2010). The MTRFR protein is similar to MRPL58

and plays a similar role in rescuing stalled mitoribosomes. Its knockdown can increase ROS production and apoptosis, thus inhibiting cell proliferation. Compared with control cells, the mitochondrial membrane potential and mass of MTRFR knockout cells change considerably. These results indicate that the function of MTRFR is crucial for cell viability and mitochondrial function (Kogure et al., 2012). Some human diseases are caused by a disorder of translation termination in mitochondria (Temperley et al., 2003). MTRFR participates in the process of mitochondrial translation and is related to multiple phenotypes, including early onset optic atrophy, progressive encephalomyopathy, peripheral neuropathy, and spastic paraparesis (Fang et al., 2017a). Loss of *MTRFR* gene function causes mitochondrial translation defects, leading to encephalomyopathy (Temperley et al., 2003). Another study identified a 2-base deletion in *MTRFR* in a Japanese woman with mitochondrial dysfunction in choroid plexus cell bodies (Nishihara et al., 2017). Other groups identified a novel protein-truncating mutation in the *MTRFR* gene in a family with neuropathy and optic atrophy. Cells from these individuals exhibited mitochondrial defects, including reduced mitochondrial respiration complex activity and stability, decreased mitochondrial respiration rate, and decreased mitochondrial membrane potential (Tucci et al., 2014). Another group reported that a compound heterozygous mutation of *MTRFR* caused distal motor neuropathy and optic atrophy in a Chinese patient (Fang et al., 2017b). Siblings diagnosed with combined OXPHOS deficiency type 7 (COXPD7) had *MTRFR* compound heterozygous mutations. They displayed optic atrophy, mild developmental delays, and bilateral brainstem symmetry (Heidary et al., 2014). Homozygosity mapping was used to identify mutations in *MTRFR* in two patients who developed Leigh syndrome, optic atrophy, and ophthalmoplegia. Analysis of mitochondrial translation in fibroblasts from these patients revealed decreased mitochondrial translation, with considerable decreases in complexes I, IV, and V, and with a slight decrease in complex III (Antonicka et al., 2010). Finally, the analyses of two affected siblings with mild intellectual disability, spastic paraplegia, and strabismus revealed a homozygous premature stop mutation at codon 139 of *MTRFR* using homozygosity mapping and exome sequence analysis (Buchert et al., 2013). A homozygous nonsense mutation of *MTRFR* (NM_001143905:c.346delG, p.Val116*) was described in a pair of female twins diagnosed with Leigh syndrome (Imagawa et al., 2016). Other groups described four patients with the classical Behr syndrome phenotype who had homozygous nonsense mutations in the *MTRFR* gene (Pyle et al., 2014). A novel *MTRFR* mutation was identified in seven affected individuals from two closely related families by whole-genome homozygosity mapping and exome sequencing. Disruption of the GGQ domain in the first coding exon led to a more severe phenotype (Spiegel et al., 2014). In one case, a new pathologic variant of the *MTRFR* gene was identified. The mutant protein lacked the GGQ domain (Perrone et al., 2020). The homozygous pathologic variant of *MTRFR* displayed a damaged mitochondrial OXPHOS system. The findings indicated that loss-of-function variants are more likely to lead to disease, while variations affecting the GGQ domain are associated with more severe phenotypes (Perrone et al., 2020). The results of these two cases are consistent, indicating that the GGQ domain of MTRFR is crucial for its phenotype, and its deletion causes a more severe phenotype.

Mitochondrial Translation Recycling

After the termination of protein synthesis, the mRNA and deacylated-tRNA in the peptide/exit (P/E) state remain associated with the ribosome to form the post-termination complex (PoTC) (Kaji et al., 2001). To start a new round of protein synthesis, the ligands binding to ribosomes must be removed from the PoTC and the ribosomes must separate into their two subunits. In this process, the RRF and EF-G2mt cooperate to disassemble the PoTC (Rao and Varshney, 2001), with the EF-G2mt transferred to the A site together with RRF to catalyze the release of mRNAs, deacylated-tRNA, and ribosome subunits, which are necessary for ribosome recycling (Hansen et al., 2000). The binding of EF-G2mt·GTP to the RRF-PoTC results in the disassembly of the 55S ribosome into two subunits during GTP hydrolysis (Peske et al., 2005). The cryo-EM structure of the human 55S mitoribosome-RRF complex revealed that the mito-specific NTE of RRF has α-helix and loop structures. These structures produce a functional key region that interacts with mitochondrial ribosomes. The structure revealed the presence of a tRNA at the P/E position and the rotation of small mitochondrial ribosomal subunits upon RRF binding. The research also revealed the interaction between P/E tRNA and mL64. These findings help to understand the unique features of the mitochondrial ribosome cycle (Koripella et al., 2019b). Furthermore, a recent paper mentioned the role of GTP binding protein 6 (GTPBP6), a homolog of the bacterial ribosome recycling factor HflX, in the division of ribosomal subunits, especially under stress conditions. This study showed that GTPBP6 plays a dual role in the ribosome cycle and biogenesis. On the one hand, it is conducive to the dissociation of ribosomes; on the other hand, it promotes the assembly of mitochondrial ribosomes. These findings contribute to our understanding of the assembly of large ribosomal subunits and the mitochondrial ribosomal recycling pathway (Lavdovskaia et al., 2020).

The EF-G2mt [also designated RRF2mt and GFM2 (Takeuchi et al., 2010)] protein mediates ribosomal recycling together with human RRF, but lacks translocation activity. The functional specificity of EF-G2mt involves domains III and IV. Therefore, EF-G2mt represents a class of guanosine triphosphate hydrolases (GTPases) involved in ribosome recycling. It cooperates with RRF and mediates ribosome dissociation during ribosome recycling, which is essential for the recycling stage.

The MRRF protein (also called RRF) was previously named mtRRF-1 (Takeuchi et al., 2010). It is a GTP-binding protein. Its binding can stabilize the rotational conformational state of mitoribosomes and has multiple weakened specific subunit bridges, preparing the complex for the dissociation of the EF-G2mt-binding subunits (Zhang and Spremulli, 1998). Deletion of MRRF in yeast does not decrease mitochondrial protein synthesis or stability of mtDNA. Thus, MRRF is involved in the coordination between yeast mitochondrial translation and

OXPHOS assembly (Ostojic et al., 2016). Only the combination of EF-G2mt and MRRF can rescue the temperature-sensitive characteristics of *E. coli* RRF (Qin et al., 2006).

The MRRF protein is essential for the survival of human cell lines. Depletion of MRRF in human cell lines is fatal, which initially leads to severe mitochondrial abnormalities, mitoribosome aggregation, increased mitochondrial superoxide production, and eventual loss of the OXPHOS complex. Hence, MRRF loss results in decreased growth rate and cell death, leading to a variety of mitochondrial dysfunctions and diseases (Rorbach et al., 2008). Two biomarkers, RRF and ribosomal protein S18 (RPS18), distinguish early PD from normal control samples and are thus considered high-confidence biomarkers of distinct protein autoantibodies for early PD (Wu et al., 2020). These findings could help establish a timely and accurate method for the diagnosis of early PD (Wu et al., 2020). Mutations in *GFM2* have been found in patients with Leigh syndrome. *GFM2* mutations (c.206 + 4A>G and c.2029-1G>A) were found in both siblings, resulting in abnormal splicing of the premature stop codon (p.Gly50Glufs*4 and p.Ala677Leufs*2, respectively). Thus, the *GFM2* mutation may be the cause of Leigh syndrome with multiple congenital arthritis phenotypes (Fukumura et al., 2015). WES was used to identify compound heterozygous (c.569G>A, p.Arg190Gln; c.636delA, p.Glu213Argfs*3) and homozygous (c.275A>C, p.Tyr92Ser) recessive variants of *GFM2* in patients presenting in early childhood with global developmental delay, elevated cerebrospinal fluid levels of lactate, and abnormalities on cranial magnetic resonance imaging (Zhang et al., 2016). Further research also identified these recessive *GFM2* variants in two unrelated patients with early-onset neurological presentations of mitochondrial disease (Glasgow et al., 2017).

MITORIBOSOMES AND RELATED DISEASE

Mammalian Mitoribosomes and Mitochondrial Ribosome Assembly

Unlike 70S ribosomes in prokaryotes and 80S ribosomes in the cytoplasm of eukaryotes, human (mammalian) mitochondria contain 55S ribosomes (O'Brien, 2003). The mitochondrial genome encodes both 12S rRNA and 16S rRNA, but all MRPs are encoded by the nuclear genome. The rRNAs have catalytic function, while ribosomal proteins have not only structural but also biological function in the process of translation. The MRPs are imported into mitochondria and assembled with the rRNAs transcribed by the mitochondria to form ribosomes responsible for translating mRNAs of 13 essential proteins in the OXPHOS system (O'Brien, 2003). The bovine 55S mitochondrial ribosome with a molecular weight of 2.71 MDa consists of two subunits of different sizes: a small subunit (28S) and large subunit (39S) (O'Brien, 1971). Compared with bacterial 30S consisting of 16S rRNA (1,542 nucleotides) and 21 proteins (S1–S21), the 28S SSU contains a 12S rRNA (950 nucleotides) and 29 proteins (Suzuki et al., 2001). Compared with bacterial 50S composed of two rRNA molecules (5S, 120 nucleotides; 23S, 2904 nucleotides) and 33 proteins (L1–L36), the 39S LSU of mitoribosomes contains a 16S rRNA (1560 nucleotides) and 48 proteins (Koc et al., 2001). Therefore, compared with bacterial ribosomes (33% protein and 67% RNA), the ratio of MRP to RNA is completely reversed, with 69% protein and 31% RNA. Of the 77 mitoribosomal component proteins, almost half are mitoribosome-specific and the remainder are bacterial protein homologs. Sharma et al. (2003) first analyzed the 3-dimensional cryo-EM map of the bovine mitochondrial 55S ribosome with a resolution of 13.5 Å. It was found that many proteins occupied a new position in ribosomes. Mitochondrial ribosomes have intersubunit bridges composed of proteins and have a gate-like structure at the mRNA entrance, which may be involved in the recruitment of unique mitochondrial mRNAs (Sharma et al., 2003). Subsequently, in 2009, the mitochondrial ribosomes of *Leishmania tarentolae* were reconstructed with a resolution of 14.1 Å. Greber et al. (2015) published the complete structure of the porcine 28S mitoribosome SSU and the reconstruction model of the 55S mitoribosome complexes with mRNA and tRNA. This structure revealed that the interaction between subunits in mitochondria is not as extensive as that in bacteria, and many bridges are formed by mitochondria-specific RNA and protein components. Reduced peripheral contacts may result in increased conformational flexibility of mitoribosomal subunits, including relative tilt between subunits (Greber et al., 2015). Subsequent studies confirmed the previous structure discovery that the large reduction in ribosomal RNA led to topological changes in some function-related regions in mammalian mitoribosomal structures, including the tRNA binding sites and nascent polypeptide-exit tunnels (Kaushal et al., 2015).

Despite the high-resolution mitoribosomal structures, the problem of how these macromolecular structures are assembled remains. Ribosome assembly involves the coordinated processing and modification of the time-related relationship between rRNAs and ribosomal proteins (De Silva et al., 2015). Many ribosome assembly factors act as macromolecular machines to improve efficiency and provide higher levels of control over mitochondrial translation. Mitochondrial assembly factors include GTPases, helicases, pseudouridine synthases, methyltransferases, endonucleases, and factors without known enzyme activity (Lopez Sanchez et al., 2021). To date, many mitochondrial assembly factors are RNA-binding proteins related to 12S and 16S rRNA, which have molecular chaperone activity and help them fold correctly (Lopez Sanchez et al., 2021). Studies have shown that mitoribosome assembly factors play a very important role in the process of mitochondrial translation, and are involved in diseases caused by mitochondrial translation disorders. Next-generation WES helps to identify pathogenic mutations in nuclear genes of different components of the mitochondrial protein translation machinery, including mitoribosome biogenesis and assembly. Pathogenic mutations have been identified in the RNA components of the mitoribosome (12S, 16S, and CP-tRNA^{Val}), MRPs, and mitoribosome

assembly factors. These mutations are associated with a wide range of clinical features, can be present at all stages of life, and are associated with variable tissue specificity (Lopez Sanchez et al., 2021).

MRPs Mutations

In 2004, it was reported for the first time that the nonsense mutation of mitochondrial SSU protein S16 (*MRPS16*) gene significantly reduced the transcription level of 12S rRNA, resulting in mitochondrial protein translation defects. This report found a case of neonatal lactic acidosis with agenesis of corpus callosum, dysmorphism, and lethality. The activities of complexes I and IV in the patient's muscle and liver were significantly decreased, accompanied by extensive mitochondrial translation defects. Analysis of the patient showed a homozygous C-to-T substitution at nucleotide 331 of the *MRPS16* cDNA (Miller et al., 2004). Similar results showed that in *Drosophila*, a missense mutation in mitochondrial ribosomal protein S12 prevented ribosomal proteins from assembling into active ribosomes, resulting in a significant reduction in 12S rRNA transcripts (Toivonen et al., 2001). Another mitochondrial ribosomal SSU protein mutation occurs in *MRPS22*. That report identified *MRPS22* gene mutations in patients with antenatal skin edema, hypotonia, cardiomyopathy, and tubulopathy born to the same set of consanguineous parents. Transfection with wild-type *MRPS22* cDNA could increase 12S rRNA content and normalize enzyme activity (Saada et al., 2007). Another study also reported that a patient with Cornelia de Lange-like dysmorphic features, brain abnormalities, and hypertrophic cardiomyopathy had a mutation in *MRPS22*. This study found that a mutation at a conserved site in the *MRPS22* gene resulted in a p.Leu215Pro substitution, which seriously damaged the mitochondrial protein translation in fibroblasts and caused defects in OXPHOS complexes I, III, and IV. The amount and activity of OXPHOS complex IV and the transcription level of 12S rRNA could be restored to normal levels by transfection to increase the expression of MRPS22 in fibroblasts (Smits et al., 2011b). Researchers investigated phenotypes of mice carrying a homozygous mutation in mitochondrial ribosomal protein of small subunit 34 (*MRPS34*) and found that the mutant mice developed cardiac hypertrophy and liver steatosis with age. MRPS34 is one of 15 mammalian mitochondria-specific MRPs, which has not been found in the ancestors of bacterial ribosomes (Greber et al., 2015). Further studies have shown that MRPS34 is required for mitochondrial translation, stability of small ribosomal subunits, and its association with the large subunit. The *MRPS34* mutation caused an obvious decrease in this protein, resulting in reduced levels of mitochondrial proteins and complexes, which led to decreased oxygen consumption and respiratory complex activity (Richman et al., 2015). The research group then identified the *MRPS34* autosomal-recessive mutations in six individuals in four families with OXPHOS deficiency and Leigh syndrome or Leigh-like disease. Further investigation showed that these mutations caused reduced mitochondrial translation and combined OXPHOS deficiency by destabilizing the small mitochondrial ribosome subunit (Lake et al., 2018).

Galmiche et al. (2011) first identified mutations of *MRPL3*, the first large ribosomal subunit protein, through WES of individuals with multiple respiratory chain defects. The compound heterozygotes with a missense *MRPL3* mutation (p.Pro317Arg) and a large-scale deletion were shown to have altered ribosome assembly and mitochondrial translation defects in skin fibroblasts, resulting in abnormal assembly of several respiratory chain complexes (RCC). The investigators also showed that these *MRPL3* mutations were the cause of severe hypertrophic cardiomyopathy in four siblings born to non-consanguineous parents (Galmiche et al., 2011). NGS exome sequencing of two siblings with recessive hypertrophic cardiomyopathy uncovered a homozygous mutation (p.Leu156Arg) in the *MRPL44* gene. MRPL44 is one of 20 mitochondrial ribosomal LSU proteins without a bacterial homolog and is reported to be located near the tunnel exit of the mitochondrial ribosome in yeast. Missense mutations in the *MRPL44* gene affect protein stability, resulting in a severe decline in MRPL44 levels in the heart, skeletal muscle, and fibroblasts of patients. In patient fibroblasts, the reduction in MRPL44 has no effect on *de novo* mitochondrial translation, but seriously affects the assembly of large ribosomal subunits and the stability of 16S rRNA, resulting in the lack of complex IV. These results indicate that MRPL44 directly affects the assembly and stability of nascent mitochondrial polypeptides such as COX1 and likely interacts with chaperones or assembly factors. These studies suggest that some mitochondrial ribosomal subunit defects can produce tissue-specific phenotypes such as cardiomyopathy (Carroll et al., 2013). This conclusion was further confirmed by another study, which found that the heart muscle is particularly vulnerable to metabolic defects. This study expands the clinical spectrum of mitochondrial diseases associated with MRPL44 and indicates that the defect also leads to slowly progressive multisystem diseases, including those of skeletal muscle, liver, kidney, and the central nervous system. Therefore, *MRPL44* mutations are more likely to occur in patients with slowly progressing mitochondrial multisystem diseases, especially in patients with cardiomyopathy (Distelmaier et al., 2015). In addition, one research group sequenced the mitochondrial ribosomal protein L12 (*MRPL12*) gene in a patient who was born to consanguineous parents and presented with growth retardation and neurological deterioration; they identified a c.542C>T missense mutation in exon 5, which converted a highly conserved alanine to valine (p.Ala181Val). This mutation led to decreased MRPL12 protein levels, which affected the assembly of large ribosomal subunits, caused overall mitochondrial translation defects, and significantly reduced the synthesis of COX1, COX2, and COX3 subunits. Studies in eubacteria have shown that eubacterial L7/L12, which are MRPL12 homologs, play an important role in protein synthesis by interacting with translation factors and regulating the speed and accuracy of protein synthesis (Pettersson and Kurland, 1980; Dey et al., 1995; Helgstrand et al., 2007). Modeling of MRPL12 showed that the p.Ala181Val change may alter the binding with elongation factor, thus

reducing the affinity of mutant MRPL12 for the ribosome (Serre et al., 2013).

mt-tRNA (MT-T) MUTATIONS AND DISEASE

mt-tRNA (MT-T) Overview

Among the 37 genes encoded by mtDNA, 13 encode electron transfer chain components, 2 encode mt-rRNAs, and the remaining 22 encode mt-tRNA (MT-T) genes. The *MT-T* gene has a unique secondary structure and forms endonuclease sites (Ojala et al., 1981; Taanman, 1999). After transcription, 14 cytosine-rich "light" mt-tRNAs and 8 guanine-rich "heavy" mt-tRNAs are released into the matrix (Anderson et al., 1981; Larsson and Clayton, 1995; Taanman, 1999). The secondary structure of tRNAs typically consists of a cloverleaf-shaped base-pairing pattern containing four domains: the acceptor stem, D-stem/loop, TψC-stem/loop, and anticodon stem/loop. Compared with cytoplasmic or bacterial tRNAs, the intrinsic thermodynamic stability of mt-tRNAs is decreased, mainly due to decreased GC content and increased non-Watson–Crick base pair frequency in the stem region. Thermodynamic instability may lead to inactivation of mt-tRNAs due to pathologic mutations; a single base substitution is more likely to destroy these weaker structures than structures with stronger contact sets (Wittenhagen and Kelley, 2003). There are more than 300 pathological mutations in the region of mtDNA encoding the *MT-T* gene. Although these mutations are widely distributed in the *MT-T* gene, three tRNAs, namely mt-tRNA^{Ile} (MT-TI), mt-tRNA^{Leu} (UUR) (MT-TL1) and mt-tRNA^{Lys} (MT-TK), contain almost 50% of the known pathologic mutations (Wittenhagen and Kelley, 2003).

mt-tRNA (MT-T) Mutations

MT-T gene mutations are associated with many clinical characteristics, many of which also occur in mitochondrial diseases (Taylor and Turnbull, 2005). In general, there is little correlation between *MT-T* gene mutations and clinical manifestations. Mutations at different sites of the same *MT-T* gene may lead to completely different clinical symptoms, and the same point mutation may also lead to several different clinical phenotypes. The MITOMAP and Mamit-tRNA databases show the clinical variability of *MT-T* mutations, and mutations in different *MT-T* genes can lead to the same clinical presentation. For example, MELAS, chronic progressive external ophthalmoplegia (CPEO), and maternally inherited diabetes and deafness (MIDD) are reported clinical syndromes of m.3243A>G mutation within *MT-TL1*, which are also closely related to other *MT-T* gene mutations. Studies have identified many different possible effects of mutations, including interference of 3′ terminal maturation, prevention of aminoacylation, disruption of transcription factor binding, and codon recognition (Florentz et al., 2003). However, the basic molecular mechanism of mutation leading to disease is not well understood (Zifa et al., 2007). The only common feature of *MT-T* mutation is the loss of stability of MT-T. Among all the mutants, m.8344A>G and m.3243A>G are the two most common heteroplasmic *MT-T* genetic variants. Because pathologic changes usually occur in Watson–Crick pairs, which are structurally important in stems, it is unexpected that both mutations occur within loop structures (Yarham et al., 2010).

m.8344A>G, located in the T loop of mt-tRNA^{Lys}, was the first pathologic heteroplasmic mutation of the *MT-T* gene to be identified (Shoffner et al., 1990). m.8344A>G is the sole cause of mitochondrial protein synthesis defects (Chomyn et al., 1991). Mutant transmitochondrial cybrids showed 10-fold reduced oxygen consumption, decreased cytochrome c oxidase activity, and respiratory defects caused by impaired protein synthesis (Chomyn et al., 1991; Masucci et al., 1995). Heteroplasmic mutation of the *MT-T* gene is closely related to the myoclonic epilepsy with ragged-red fiber (MERRF) phenotype. However, the mechanism of m.8344A>G mutation causing this phenotype has not been determined. One report suggested that this mutation causes a decrease in mt-tRNA^{Lys} steady-state levels (Masucci et al., 1995). It was also reported that m.8344A>G causes a decrease in aminoacylation, which may be the primary cause of protein synthesis defects (Enriquez et al., 1995). Some studies have shown that m.8344A>G causes the post-transcriptional taurine modification defect of wobble position uridine in mt-tRNA^{Lys}, which is also a reason for mitochondrial protein synthesis defects (Enriquez et al., 1995; Yasukawa et al., 2000a). Therefore, we suggest that the m.8344A>G mutation leads to the MERRF phenotype mainly by preventing the post-transcriptional taurine modification of wobble position uridine. m.8344A>G weakened the codon-anticodon interaction in mt-tRNA^{Lys}, stalled translation, and reduced protein synthesis. Furthermore, ribosomal shifting may then occur, leading to premature translation termination and resulting in abnormal translation products. Although m.8344A>G is the most common mutation associated with MERRF (∼80% of cases) (Ozawa et al., 1997), other mutations such as m.8356T>C have also been reported (Masucci et al., 1995).

Mitochondrial disease MELAS syndrome is usually associated with many *MT-T* gene point mutations. Approximately 80% of MELAS syndrome patients had m.3243A>G mutations in the *MT-TL1* gene (Morgan-Hughes et al., 1995). The m.3243A>G mutation occurs in the mtDNA binding site of MTERF1, which leads to a decrease in MTERF1 affinity, resulting in mitochondrial protein synthesis defects and respiratory disorders (Chomyn et al., 1992; King et al., 1992). As was previously observed with m.8344A>G, m.3243A>G mutation caused mt-tRNA^{Leu}(UUR) molecules to lack wobble position uridine modification (Yasukawa et al., 2000b, 2002). Because wobble uridine is considered to play an important role in stability, this mutation leads to protein synthesis defects, resulting in the MELAS phenotype (Yasukawa et al., 2002; Sasarman et al., 2008). Interestingly, the m.3243A>G. mutation enhanced the dimerization of mt-tRNA^{Leu} (UUR), resulting in a 10-fold reduction of aminoacylation in dimers (Wittenhagen and Kelley, 2002). Hence, decreased aminoacylation and post-transcriptional

modification defects are crucial to causing respiratory deficiency and MELAS syndrome (Yasukawa et al., 2000b).

MITOCHONDRIAL AMINOACYL-tRNA SYNTHETASES (mt-aaRSs)

Aminoacyl tRNA synthetases (aaRSs) are a group of nuclear-encoded enzymes that conjugate each of the 20 amino acids to their cognate tRNA molecules to ensure correct translation of the genetic code (Sissler et al., 2017; Ognjenovic and Simonovic, 2018). mt-aaRSs are imported into the mitochondrial matrix and supply mt-tRNA conjugates for protein translation. In principle, each amino acid is recognized by its specific aaRS, resulting in 20 aaRS protein synthesis systems per cell. However, in human mitochondria, only 19 aaRSs are present, because Gln-tRNA^{Gln} is synthesized indirectly via misacylated Glu-tRNA^{Gln} through transamidation (Nagao et al., 2009). Recently, mutations in the genes encoding mt-aaRSs have been identified as a new cause of human diseases. They are believed to impair mitochondrial protein synthesis, thereby affecting the OXPHOS system and leading to surprising tissue-specific phenotypes. At present, nine gene mutations encoding mitochondria-specific aaRSs have been reported. Among these mutations, encephalopathy is the most common phenotype, while cardiomyopathy, tubulopathy, myopathy, or sensorineural neuropathy is the next most common phenotype (Konovalova and Tyynismaa, 2013). *DARS2*, *EARS*, and *AARS2* are three typical genes whose mutations lead to rare and well-defined leukodystrophy (LD) syndrome. The mutations occur in mitochondrial aspartyl-tRNA synthetase, mitochondrial glutamate tRNA synthetase, and mitochondrial alanyl-tRNA synthetase, respectively (Fine et al., 2019). Mt-aaRSs as key players in the mitochondrial translation machinery play an important role in cell energy production. In AARS2 ovarian LD, leukoencephalopathy with thalamus and brainstem involvement and high lactate (LTBL), and leukoencephalopathy with brainstem and spinal cord involvement and lactate elevation (LBSL), protein and enzyme activities are reduced to varying degrees, but are not completely lacking. For AARS2 ovario-LD and LTBL, RCC dysfunction occurred, which was not detected in LBSL patient cells (Scheper et al., 2007; Mikhailova et al., 2009; Synofzik et al., 2011; Taskin et al., 2016). In addition, in LTBL, the oxygen consumption rate decreased significantly (Fine et al., 2019). Moreover, *AARS2* was found to be the disease gene for early-onset fatal hypertrophic cardiomyopathy with lactic acidosis (Gotz et al., 2011). The patients died during the perinatal period or within 10 months after birth. Cardiomyopathy was a prominent clinical manifestation, but in addition to the heart, OXPHOS deficiency in the brain and muscle was observed at autopsy. The patients, however, did not show OXPHOS deficiency in fibroblasts or myoblasts. *AARS2* mutations have been identified as homozygous or heterozygous, but to date, all the patients described have a mutation leading to p.Arg592Trp in mitochondrial alanyl-tRNA synthetase (Gotz et al., 2011; Calvo et al., 2012). Mt-aaRSs not only promote the translation of proteins forming the mitochondrial respiratory chain complex, but they also affect cell signaling, transcription, and RNA biological genesis in neurons (Sissler et al., 2017). At present, many studies have reported the non-canonical effects of mt-aaRSs, such as the angiogenic function of rat mitochondrial tryptophanyl-tRNA synthetase (WARS2) and the possible role of mt-aaRS mutations in the integrated stress response (ISR) (Agnew et al., 2018). Complete inhibition of mitochondrial translation in DARS2 knockout mice leads to the accumulation of unassembled nuclear-encoded respiratory chain subunits, resulting in severe protein homeostasis stress and mitochondrial unfolded protein response (UPRmt)-dependent ISR activation. The ISR does not reach steady state, which leads to severe heart disease and decreased survival (Dogan et al., 2014). In addition to mt-aaRS mutations that affect the pathology of the central nervous system, mt-AlaRS, mt-GlyRS, and mt-LysRS mutations are known to cause cardiomyopathies (Hei et al., 2019; Sommerville et al., 2019); mt-TyrRS mutations caused myopathy, lactic acidosis, and sideroblastic anemia (MLASA syndrome) (Shahni et al., 2013); and mt-SerRS mutations caused hyperuricemia, pulmonary hypertension, renal failure in infancy, and alkalosis (HUPRA syndrome) (Rivera et al., 2013). Generally speaking, the characteristics of mt-aaRSs are relatively poorly understood, and future research will provide important knowledge regarding the function of these synthetases. The detection of identified *AARS2* mutations provides some clues for understanding the molecular mechanism of these rare diseases.

MITOCHONDRIAL TRANSLATIONAL ACTIVATORS

Mitochondrial translational activators are nuclear-encoded proteins. A yeast translational activator was proposed in the late 1980s. These activators generally interact with the 5′-untranslated region (UTR) of mitochondrial mRNA. They may also bind to nascent proteins or interact with mitoribosomes. Translation activators are often bound to the membrane, which may limit translation to the region close to the inner membrane (Fox, 2012). It is not clear whether all translational activators exhibit all of these activities. Unfortunately, due to the lack of an *in vitro* translation system, analyzing their activities in the process of translation initiation and elongation is not yet possible. Some protein factors, such as translational activator of cytochrome oxidase I (TACO1), mitochondrial translation regulation assembly intermediate of cytochrome c oxidase (MITRAC), and COX14 (previously called C12orf62), are recruited to bind directly to mitochondrial transcripts and regulate the translation of MT-CO1 (Szklarczyk et al., 2012; Weraarpachai et al., 2012; Richter-Dennerlein et al., 2016). In yeast, the translational activator of COX2 (MT-CO2) is PET111 (Sanchirico et al., 1998), which is necessary for COX2 mRNA translation (Fiori et al., 2005). PET54, PET122, and PET494 are translational activators of COX3 (MT-CO3). They interact with the 5′-UTR of *COX3* mRNA, the small ribosomal subunit protein, and the inner membrane to promote the synthesis of COX3 (Naithani et al., 2003). The mitochondrial translation activators CBS1 and CBS2 interact specifically with the cytochrome b

gene (*MT-CYB* or *COB*) mRNA via its 5′-UTR (Mittelmeier and Dieckmann, 1995). Both activators participate in translation initiation and promote the synthesis of MT-CYB by binding to mRNA-ribosome complexes (Rodel, 1986). CBP1 is another protein that binds to the 5′-UTR of *MT-CYB* mRNA, which is necessary for *MT-CYB* mRNA translation (Dieckmann et al., 1984; Islas-Osuna et al., 2002). In addition, CBP3 and CBP6 participate in the translation of MT-CYB (Gruschke et al., 2011).

Most yeast genes involved in the translation of mitochondria-encoded proteins lack mammalian homologs due to the lack of 5′-UTRs in mammalian mitochondrial mRNAs (Fontanesi et al., 2006). To date, TACO1 is the only specific mitochondrial mammalian translation activator. Expression of TACO1 in fibroblasts rescued the COX1 (MT-CO1) synthesis and assembly defects (Weraarpachai et al., 2009). TACO1 is necessary for the efficient translation of COX1. Investigations on TACO1$^{mut/mut}$ mice showed that TACO1 is required for COX1 translation through its specific binding of *MT-CO1* mRNA and association with mitochondrial ribosomes. These mutant mice developed a late-onset syndrome similar to human patients with visual impairment, motor dysfunction, and cardiac hypertrophy (Richman et al., 2016). MITRAC is a complex IV assembly intermediate that regulates mitochondrial translation. MITRAC was found to interact with multiple assembly factors and efficiently translate *COX1* mRNA (Mick et al., 2012). Lrpl30 and leucine rich pentatricopeptide repeat containing (LRPPRC) are translation activators of the human cytochrome c oxidase subunits (Debray et al., 2011). Both have multiple targets, including COX1 and COX3. Mutations result in a deficiency of cytochrome c oxidase, leading to French–Canadian Leigh syndrome (Kohler et al., 2015).

REGULATION OF MITOCHONDRIAL microRNAs (mitomiRs) IN MITOCHONDRIAL TRANSLATION AND THEIR ROLE IN DISEASE

MicroRNAs (miRNAs) are single-stranded non-coding RNAs that are 18–23 nucleotides in length. They can translocate into the mitochondria and regulate mitochondrial translation (Bandiera et al., 2013). MitomiRs regulate mitochondrial gene expression and function under physiological and pathological conditions (Paramasivam and Vijayashree Priyadharsini, 2020). Several mitomiRs may be derived from mitochondrial genomic mRNA. MitomiRs post-translationally regulate gene expression in the mitochondria (Das et al., 2012; Fan et al., 2019). Most importantly, differentially expressed mitomiRs were observed in heart failure (Pinti et al., 2017; Wang X. et al., 2017). However, the translocation mechanism of nuclear-encoded miRNAs into mitochondria is not clear. MitomiR transport is one of the most controversial fields in mitochondrial research. Researchers have questioned the transport of RNA into mitochondria. In recent years, many miRNA processing proteins, including Ago, Dicer and RISC, have been found in mitochondria (Chen et al., 2010; Wang et al., 2015). Knowledge of the mechanism of miRNA transport to the mitochondrial matrix may provide important insights into the pathophysiology of disease and may become a new target for therapeutic intervention.

MicroRNAs miR-1, miR-210, and miR-338 can enhance mitochondrial translation and regulate mitochondrial proteomics and mitochondrial bioenergetics in myocytes (Aschrafi et al., 2008; Colleoni et al., 2013; Zhang et al., 2014; Srinivasan and Das, 2015). In mitochondria, miR-1 unexpectedly stimulates, rather than inhibits, translation of mitochondrial genome-encoded transcripts. The observed positive role of mitomiRs in mitochondrial translation suggests that miR-1 regulates the myogenic program by mediating mitochondrial translational activation and inhibiting cytoplasmic translation. Thus, mitomiRs play an important role in the crosstalk between mitochondrial and cytoplasmic translation. However, another study showed that hypoxia induced the expression of miR-210 in fibroblasts, while the expression of its downstream targets, iron-sulfur cluster assembly enzyme (ISCU) and the COX10 cytochrome c oxidase assembly protein, decreased. Moreover, miR-210 inhibited protein synthesis, thus reducing the level of the electron transport system (ETS) complex protein (Colleoni et al., 2013). MicroRNA-181c (miR-181c) inhibits the translation of COX1, resulting in the remodeling of complex IV and enhancement of mitochondrial function in ventricular myocytes. It regulates the mitochondrial genome and bioenergy and may potentially regulate heart failure *in vivo* (Das et al., 2012, 2014). The microRNA miR-762 translocates into mitochondria and is upregulated during hypoxia/reoxygenation in cardiomyocytes. Therefore, miR-762 can directly reduce MT-ND2 translation, mitochondrial complex I enzyme activity, and ATP levels, and increase ROS levels and cardiomyocyte apoptosis (Yan et al., 2019). It can also be translocated to the mitochondria to inhibit the downregulation of MT-CYB. Overexpression of miR-92a enhances mitochondrial translation and reduces ROS production and lipid deposition, thus improving diabetic cardiomyopathy (Li et al., 2019). Another study reported significant upregulation of miR-21 in spontaneously hypertensive rats. Computational prediction and biochemical analyses revealed that miR-21 directly targets MT-CYB and positively regulates its mitochondrial translation. miR-21 also reduces blood pressure and myocardial hypertrophy in spontaneously hypertensive rats by upregulating the mitochondrial translation level of MT-CYB (Li et al., 2016). Therefore, some mitomiRs promote mitochondrial translation, while others inhibit it. The mechanism of mitomiRs regulating mitochondrial translation needs further study.

CROSSTALK BETWEEN MITOCHONDRIAL AND CYTOPLASMIC PROTEIN SYNTHESIS

OXPHOS subunits are encoded by both the nuclear and mitochondrial genomes. However, the co-regulation of OXPHOS subunit genes remains poorly understood. This cooperative translation program provides one-way control

through complex and dynamic cytoplasmic translation control. Therefore, the nuclear genome precisely guides the coordination of mitochondrial and cytoplasmic translation to coordinate the synchronous synthesis of the OXPHOS complex (Tang et al., 2020). Recently, Guo et al. (2020) identified the molecular pathway of the mitochondrial stress signal relayed to the cytoplasm. In mammalian cells, mitochondrial dysfunction caused by mitochondrial translation disorders leads to an ISR. This ISR is mediated through eIF2α phosphorylation. Phosphorylation of eIF2α decreases overall protein synthesis, but increases the translation of only ATF4, the master transcriptional regulator of ISR. Mitochondrial stress stimulates a mitochondrial stress-activated protease (OMA1)-dependent cleavage of DAP3 binding cell death enhancer 1 (DELE1), a protein found to be associated with the inner mitochondrial membrane. Hence, DELE1 accumulates in the cytosol and interacts with eukaryotic translation initiation factor 2 alpha kinase 1 (HRI or EIF2AK1), an eIF2α kinase necessary for activating eIF2α kinase (Guo et al., 2020). Another investigation further uncovered the OMA1-DELE1-HRI signaling axis that constitutes a link between mitochondrial perturbation and the cytosolic ISR. Moreover, this research combined genome engineering and haploid genetics to identify a suite of additional regulators in ISR. Therefore, this pathway is a potential therapeutic target, which can fine-tune ISR and obtain beneficial results in treating diseases involving mitochondrial dysfunction (Fessler et al., 2020). The serine/threonine kinase mTOR integrates extracellular and intracellular signals to drive growth and proliferation. mTORC1 is an important upstream regulator of integrated mitochondrial stress response (ISRmt). Khan et al. (2017) reported that mTORC1 is activated by mitochondrial DNA replication defects, which drive ISRmt through ATF4 activation. mTORC1 activation induces the mitochondrial one-carbon cycle, fibroblast growth factor 21 (FGF21), and the UPRmt. Downregulation of this response by rapamycin reverts progression of mitochondrial myopathy in mice (Khan et al., 2017). In mammals, mTOR coordinates the energy consumption of mRNA translation mechanisms with mitochondrial energy production by stimulating the synthesis of nuclear-encoded mitochondrial-related proteins, including mitochondrial transcription factor A (TFAM), mitochondrial ribosomal protein, and components of complexes I and V (Chapman et al., 2018). We have shown that mTOR, which is the upstream regulator of mitochondria, can sense mitochondrial translation defects and subsequently activate cytoplasmic translation to compensate for them (Gao et al., 2016). We recently found that mTOR adapts cytoplasmic translation to mitochondrial translation defects caused by mtEF4 ablation in *C. elegans* and mice (Gao et al., 2016) (**Figure 2**). Another example of mTOR regulation by mitochondrial stress is the ubiquitination of mTOR by Parkin, an E3 ubiquitin ligase located in mitochondria. Parkin is required to maintain mTORC1 activity during mitochondrial stress (Park et al., 2014). Thus,

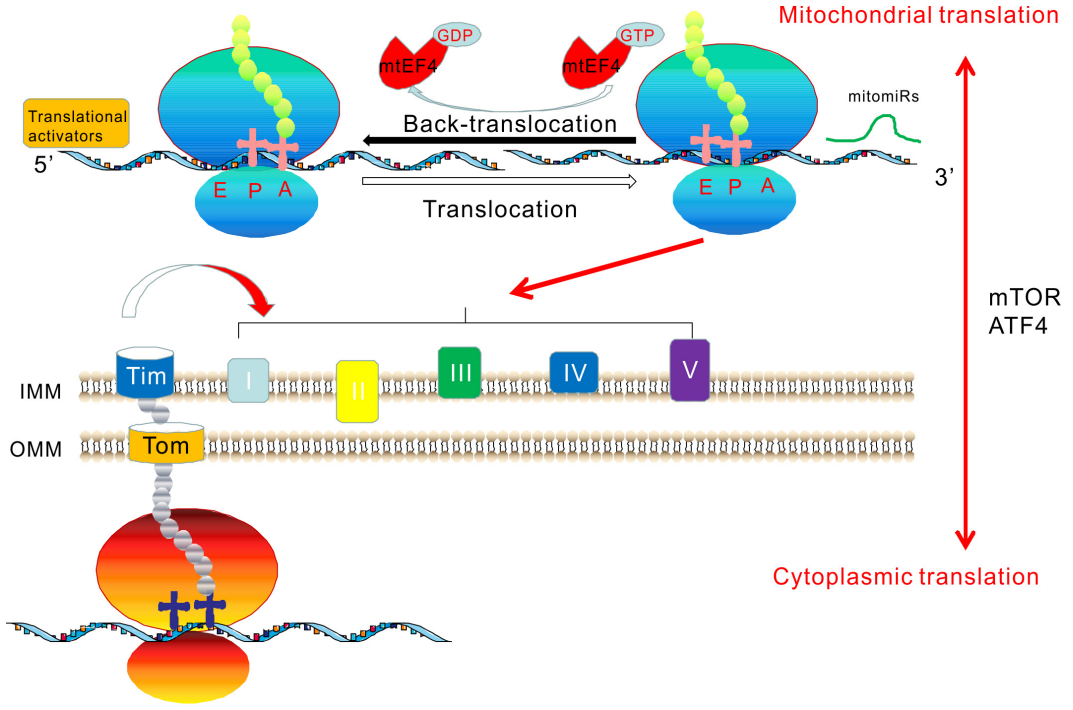

FIGURE 2 | Crosstalk between mitochondrial and cytoplasmic translation. mtEF4, translation activators, and mitomiRs are important regulators that directly affect mitochondrial translation. The components of mitochondrial complexes I, II, III, IV, and V are produced by both mitochondrial and cytoplasmic translation, requiring coordination between the two translation systems. mtEF4 has a back-translocation effect and catalyzes the back-translocation of the P- and E-tRNAs to A- and P-tRNAs. Mitochondrial translation activator promotes mRNA-specific translation initiation. MitomiRs function at the 3′ end of mRNA. mTOR and ATF4 play an important role in the crosstalk between mitochondrial and cytoplasmic translation.

mTOR may be important in sensing mitochondrial translation defects and subsequently activating cytoplasmic translation. It is conceivable that cytoplasmic translation regulated by mTOR and mitochondrial translation controlled by mitochondrial translation factors, such as mtEF4, have a bidirectional causal relationship (Gao et al., 2016).

RNA interference to reduce expression of mitochondrial ribosomal protein MRPS5 leads to an imbalance of OXPHOS subunits (mitonuclear protein imbalance) encoded by nDNA and mtDNA. Expression of the mtDNA-encoded MT-CO1 homolog MTCE.26 and nDNA-encoded ATP5PF homolog H28O16.1 can be unbalanced (Houtkooper et al., 2013). In mammalian cells, MRP knockout results in mitochondrial protein imbalance, decreased mitochondrial respiration, and activation of the UPRmt. Specific antibiotics or ethidium bromide, targeting mitochondrial translation, can extend lifespan by inducing mitonuclear protein imbalance (Houtkooper et al., 2013). Silencing miRNA-382-5p significantly increases the expression of genes related to mitochondrial dynamics and biogenesis. Conventional microarray analysis revealed the downregulation of MRPs and respiratory chain proteins in C2C12 myotubes upon silencing of miRNA-382-5p. This effect was accompanied by an imbalance between mitochondrial proteins encoded by nDNA and mtDNA and induction of heat shock protein 60 (HSP60), indicating that UPRmt was activated and that silencing of miR-382-5p resulted in mitonuclear protein imbalance and activated UPRmt in skeletal muscle (Dahlmans et al., 2019). Chloramphenicol and other antibiotics inhibit mitochondrial protein translation, effectively decreasing the synthesis of mitochondrial proteins in INS-1E cells and reducing the expression of mtDNA encoding the COX1 subunit of the respiratory chain, rather than the ATP synthase subunit ATP5PF. Although expression of the important respiratory chain subunit COX1 was significantly reduced, the INS-1E cells maintained a normal respiratory rate, indicating that inhibition of mitochondrial protein translation caused mitonuclear protein imbalance. However, in insulin-secreting cells, a compensatory mechanism effectively maintained a normal respiratory rate and even increased ATP synthase-dependent respiration and calcium signaling pathways (Santo-Domingo et al., 2017).

CONCLUSION

Mitochondria participate in important life activities of cells and are important in the study of evolution. Mitochondrial protein translation is an important and unique mitochondrial function, essential for the biogenesis of mitochondrial OXPHOS, cellular energy supply, and other mitochondrial functions. Mitochondrial protein translation is directly regulated by mitochondrial translation initiation, elongation, termination factors, translation activators, and mitomiRs. Mitochondrial translation and cytoplasmic translation are regulated by mTOR and other signaling pathways. Mitochondrial translation defects are the main causes of devastating human diseases. In this group of diseases, most mutations in mtDNA-encoding tRNAs, as well as mutations in nuclear genes encoding mitoribosomal proteins, translation initiation factors, and elongation factors, are the causes of clinical and genetic heterogeneity of infant multisystem diseases, such as Leigh syndrome, sensorineural hearing loss, encephalomyopathy, and hypertrophic cardiomyopathy (Perez-Martinez et al., 2008; Rotig, 2011). Many patients with mitochondrial diseases have multiple OXPHOS defects of unknown genetic causes, which indicates that many genes related to the biogenesis and function of mitochondrial translation mechanisms still need to be identified. Comprehensive clinical diagnosis and treatment based on mitochondrial translation defects remain challenging. With the advent of a boom in mitochondrial research and the progress in modern sequencing technology, the study of protein function will be more in-depth, and research on mitochondrial protein translation regulation will increase in importance. Research on mitochondrial protein translation will enhance our understanding of the pathogenesis and early diagnosis of human diseases.

AUTHOR CONTRIBUTIONS

YG conceived of the manuscript. YG, FW, DYZ, DJZ, and PL drafted the manuscript, constructed the figures, and revised the manuscript. All authors read and approved the final manuscript.

FUNDING

This study was funded by grants from the National Natural Science Foundation of China (Nos. 81602353 and 31870816), Major Research Program of the National Natural Science Foundation of China (No. 91849209), the Natural Science Foundation of Jiangsu Province (BK20171145), the China Postdoctoral Science Foundation (2019M652314 and 2020T130333), the Qingdao Applied Basic Research Project (19-6-2-39-cg), and the Qingdao Science and Technology Plan Fund (18-6-1-63-nsh).

ACKNOWLEDGMENTS

We would like to thank Editage (www.editage.cn) for English language editing.

REFERENCES

Abadi, A., Peralta-Romero, J., Suarez, F., Gomez-Zamudio, J., Burguete-Garcia, A. I., Cruz, M., et al. (2016). Assessing the effects of 35 European-derived BMI-associated SNPs in Mexican children. *Obesity (Silver Spring)* 24, 1989–1995. doi: 10.1002/oby.21590

Abahuni, N., Gispert, S., Bauer, P., Riess, O., Kruger, R., Becker, T., et al. (2007). Mitochondrial translation initiation factor 3 gene polymorphism associated with Parkinson's disease. *Neurosci. Lett.* 414, 126–129. doi: 10.1016/j.neulet.2006.12.053

Agnew, T., Goldsworthy, M., Aguilar, C., Morgan, A., Simon, M., Hilton, H., et al. (2018). A Wars2 mutant mouse model displays OXPHOS deficiencies

and activation of tissue-specific stress response pathways. *Cell Rep.* 25, 3315–3328.e6. doi: 10.1016/j.celrep.2018.11.080

Ahola, S., Isohanni, P., Euro, L., Brilhante, V., Palotie, A., Pihko, H., et al. (2014). Mitochondrial EFTs defects in juvenile-onset Leigh disease, ataxia, neuropathy, and optic atrophy. *Neurology* 83, 743–751. doi: 10.1212/WNL.0000000000000716

Aibara, S., Singh, V., Modelska, A., and Amunts, A. (2020). Structural basis of mitochondrial translation. *Elife* 9:e58362. doi: 10.7554/eLife.58362

Akabane, S., Ueda, T., Nierhaus, K. H., and Takeuchi, N. (2014). Ribosome rescue and translation termination at non-standard stop codons by ICT1 in mammalian mitochondria. *PLoS Genet.* 10:e1004616. doi: 10.1371/journal.pgen.1004616

Alfaiz, A. A., Muller, V., Boutry-Kryza, N., Ville, D., Guex, N., De Bellescize, J., et al. (2016). West syndrome caused by homozygous variant in the evolutionary conserved gene encoding the mitochondrial elongation factor GUF1. *Eur. J. Hum. Genet.* 24, 1001–1008. doi: 10.1038/ejhg.2015.227

Anderson, S., Bankier, A. T., Barrell, B. G., De Bruijn, M. H., Coulson, A. R., Drouin, J., et al. (1981). Sequence and organization of the human mitochondrial genome. *Nature* 290, 457–465. doi: 10.1038/290457a0

Antonicka, H., Ostergaard, E., Sasarman, F., Weraarpachai, W., Wibrand, F., Pedersen, A. M., et al. (2010). Mutations in C12orf65 in patients with encephalomyopathy and a mitochondrial translation defect. *Am. J. Hum. Genet.* 87, 115–122. doi: 10.1016/j.ajhg.2010.06.004

Anvret, A., Ran, C., Westerlund, M., Thelander, A. C., Sydow, O., Lind, C., et al. (2010). Possible involvement of a mitochondrial translation initiation factor 3 variant causing decreased mRNA levels in Parkinson's disease. *Parkinsons Dis.* 2010:491751. doi: 10.4061/2010/491751

Aschrafi, A., Schwechter, A. D., Mameza, M. G., Natera-Naranjo, O., Gioio, A. E., and Kaplan, B. B. (2008). MicroRNA-338 regulates local cytochrome c oxidase IV mRNA levels and oxidative phosphorylation in the axons of sympathetic neurons. *J. Neurosci.* 28, 12581–12590. doi: 10.1523/JNEUROSCI.3338-08.2008

Ayyub, S. A., Dobriyal, D., and Varshney, U. (2017). Contributions of the N- and C-terminal domains of initiation factor 3 to its functions in the fidelity of initiation and antiassociation of the ribosomal subunits. *J. Bacteriol.* 199, e51–e17. doi: 10.1128/JB.00051-17

Bandiera, S., Mategot, R., Girard, M., Demongeot, J., and Henrion-Caude, A. (2013). MitomiRs delineating the intracellular localization of microRNAs at mitochondria. *Free Radic. Biol. Med.* 64, 12–19. doi: 10.1016/j.freeradbiomed.2013.06.013

Barcia, G., Rio, M., Assouline, Z., Zangarelli, C., Gueguen, N., Dumas, V. D., et al. (2020). Clinical neuroimaging and biochemical findings in patients and patient fibroblasts expressing ten novel GFM1 mutations. *Hum. Mutat.* 41, 397–402. doi: 10.1002/humu.23937

Bauerschmitt, H., Funes, S., and Herrmann, J. M. (2008). The membrane-bound GTPase Guf1 promotes mitochondrial protein synthesis under suboptimal conditions. *J. Biol. Chem.* 283, 17139–17146. doi: 10.1074/jbc.M710037200

Behrouz, B., Vilarino-Guell, C., Heckman, M. G., Soto-Ortolaza, A. I., Aasly, J. O., Sando, S., et al. (2010). Mitochondrial translation initiation factor 3 polymorphism and Parkinson's disease. *Neurosci. Lett.* 486, 228–230. doi: 10.1016/j.neulet.2010.09.059

Bhargava, K., and Spremulli, L. L. (2005). Role of the N- and C-terminal extensions on the activity of mammalian mitochondrial translational initiation factor 3. *Nucleic Acids Res.* 33, 7011–7018. doi: 10.1093/nar/gki1007

Bhargava, K., Templeton, P., and Spremulli, L. L. (2004). Expression and characterization of isoform 1 of human mitochondrial elongation factor G. *Protein Expr. Purif.* 37, 368–376. doi: 10.1016/j.pep.2004.06.030

Bian, X., Wasserfall, C., Wallstrom, G., Wang, J., Wang, H., Barker, K., et al. (2017). Tracking the antibody immunome in type 1 diabetes using protein arrays. *J. Proteome Res.* 16, 195–203. doi: 10.1021/acs.jproteome.6b00354

Boczonadi, V., and Horvath, R. (2014). Mitochondria: impaired mitochondrial translation in human disease. *Int. J. Biochem. Cell Biol.* 48, 77–84. doi: 10.1016/j.biocel.2013.12.011

Brito, S., Thompson, K., Campistol, J., Colomer, J., Hardy, S. A., He, L., et al. (2015). Long-term survival in a child with severe encephalopathy, multiple respiratory chain deficiency and GFM1 mutations. *Front. Genet.* 6:102. doi: 10.3389/fgene.2015.00102

Buchert, R., Uebe, S., Radwan, F., Tawamie, H., Issa, S., Shimazaki, H., et al. (2013). Mutations in the mitochondrial gene C12ORF65 lead to syndromic autosomal recessive intellectual disability and show genotype phenotype correlation. *Eur. J. Med. Genet.* 56, 599–602. doi: 10.1016/j.ejmg.2013.09.010

Cai, Y. C., Bullard, J. M., Thompson, N. L., and Spremulli, L. L. (2000). Interaction of mitochondrial elongation factor Tu with aminoacyl-tRNA and elongation factor Ts. *J. Biol. Chem.* 275, 20308–20314. doi: 10.1074/jbc.M001899200

Calvo, S. E., Compton, A. G., Hershman, S. G., Lim, S. C., Lieber, D. S., Tucker, E. J., et al. (2012). Molecular diagnosis of infantile mitochondrial disease with targeted next-generation sequencing. *Sci. Transl. Med.* 4:118ra10.

Cao, X., and Qin, Y. (2016). Mitochondrial translation factors reflect coordination between organelles and cytoplasmic translation via mTOR signaling: implication in disease. *Free Radic. Biol. Med.* 100, 231–237. doi: 10.1016/j.freeradbiomed.2016.04.010

Carroll, C. J., Isohanni, P., Poyhonen, R., Euro, L., Richter, U., Brilhante, V., et al. (2013). Whole-exome sequencing identifies a mutation in the mitochondrial ribosome protein MRPL44 to underlie mitochondrial infantile cardiomyopathy. *J. Med. Genet.* 50, 151–159. doi: 10.1136/jmedgenet-2012-101375

Chapman, N. M., Zeng, H., Nguyen, T. M., Wang, Y., Vogel, P., Dhungana, Y., et al. (2018). mTOR coordinates transcriptional programs and mitochondrial metabolism of activated Treg subsets to protect tissue homeostasis. *Nat. Commun.* 9:2095. doi: 10.1038/s41467-018-04392-5

Chen, Y., Feng, S., Kumar, V., Ero, R., and Gao, Y. G. (2013). Structure of EF-G-ribosome complex in a pretranslocation state. *Nat. Struct. Mol. Biol.* 20, 1077–1084. doi: 10.1038/nsmb.2645

Chen, Z., Li, Y., Zhang, H., Huang, P., and Luthra, R. (2010). Hypoxia-regulated microRNA-210 modulates mitochondrial function and decreases ISCU and COX10 expression. *Oncogene* 29, 4362–4368. doi: 10.1038/onc.2010.193

Chicherin, I. V., Baleva, M. V., Levitskii, S. A., Dashinimaev, E. B., and Krasheninnikov, I. A. (2019). Mitochondrial translation initiation factor 3: structure, functions, interactions, and implication in human health and disease. *Biochemistry (Mosc)* 84, 1143–1150. doi: 10.1134/S0006297919100031

Chomyn, A., Martinuzzi, A., Yoneda, M., Daga, A., Hurko, O., Johns, D., et al. (1992). MELAS mutation in mtDNA binding site for transcription termination factor causes defects in protein synthesis and in respiration but no change in levels of upstream and downstream mature transcripts. *Proc. Natl. Acad. Sci. U.S.A.* 89, 4221–4225. doi: 10.1073/pnas.89.10.4221

Chomyn, A., Meola, G., Bresolin, N., Lai, S. T., Scarlato, G., and Attardi, G. (1991). In vitro genetic transfer of protein synthesis and respiration defects to mitochondrial DNA-less cells with myopathy-patient mitochondria. *Mol. Cell Biol.* 11, 2236–2244. doi: 10.1128/mcb.11.4.2236

Christian, B. E., and Spremulli, L. L. (2009). Evidence for an active role of IF3mt in the initiation of translation in mammalian mitochondria. *Biochemistry* 48, 3269–3278. doi: 10.1021/bi8023493

Christian, B. E., and Spremulli, L. L. (2012). Mechanism of protein biosynthesis in mammalian mitochondria. *Biochim. Biophys. Acta* 1819, 1035–1054. doi: 10.1016/j.bbagrm.2011.11.009

Coenen, M. J., Antonicka, H., Ugalde, C., Sasarman, F., Rossi, R., Heister, J. G., et al. (2004). Mutant mitochondrial elongation factor G1 and combined oxidative phosphorylation deficiency. *N. Engl. J. Med.* 351, 2080–2086. doi: 10.1056/NEJMoa041878

Colleoni, F., Padmanabhan, N., Yung, H. W., Watson, E. D., Cetin, I., Tissot Van Patot, M. C., et al. (2013). Suppression of mitochondrial electron transport chain function in the hypoxic human placenta: a role for miRNA-210 and protein synthesis inhibition. *PLoS One* 8:e55194. doi: 10.1371/journal.pone.0055194

Dahlmans, D., Houzelle, A., Andreux, P., Wang, X., Jorgensen, J. A., Moullan, N., et al. (2019). MicroRNA-382 silencing induces a mitonuclear protein imbalance and activates the mitochondrial unfolded protein response in muscle cells. *J. Cell Physiol.* 234, 6601–6610. doi: 10.1002/jcp.27401

Das, S., Bedja, D., Campbell, N., Dunkerly, B., Chenna, V., Maitra, A., et al. (2014). miR-181c regulates the mitochondrial genome, bioenergetics, and propensity for heart failure *in vivo*. *PLoS One* 9:e96820. doi: 10.1371/journal.pone.0096820

Das, S., Ferlito, M., Kent, O. A., Fox-Talbot, K., Wang, R., Liu, D., et al. (2012). Nuclear miRNA regulates the mitochondrial genome in the heart. *Circ. Res.* 110, 1596–1603. doi: 10.1161/CIRCRESAHA.112.267732

De Silva, D., Tu, Y. T., Amunts, A., Fontanesi, F., and Barrientos, A. (2015). Mitochondrial ribosome assembly in health and disease. *Cell Cycle* 14, 2226–2250. doi: 10.1080/15384101.2015.1053672

Debray, F. G., Morin, C., Janvier, A., Villeneuve, J., Maranda, B., Laframboise, R., et al. (2011). LRPPRC mutations cause a phenotypically distinct form of Leigh

syndrome with cytochrome c oxidase deficiency. *J. Med. Genet.* 48, 183–189. doi: 10.1136/jmg.2010.081976

Desai, N., Yang, H., Chandrasekaran, V., Kazi, R., Minczuk, M., and Ramakrishnan, V. (2020). Elongational stalling activates mitoribosome-associated quality control. *Science* 370, 1105–1110. doi: 10.1126/science.abc7782

Dey, D., Oleinikov, A. V., and Traut, R. R. (1995). The hinge region of *Escherichia coli* ribosomal protein L7/L12 is required for factor binding and GTP hydrolysis. *Biochimie* 77, 925–930. doi: 10.1016/0300-9084(95)80003-4

Di Nottia, M., Montanari, A., Verrigni, D., Oliva, R., Torraco, A., Fernandez-Vizarra, E., et al. (2017). Novel mutation in mitochondrial Elongation Factor EF-Tu associated to dysplastic leukoencephalopathy and defective mitochondrial DNA translation. *Biochim. Biophys. Acta Mol. Basis Dis.* 1863, 961–967. doi: 10.1016/j.bbadis.2017.01.022

Dieckmann, C. L., Koerner, T. J., and Tzagoloff, A. (1984). Assembly of the mitochondrial membrane system. CBP1, a yeast nuclear gene involved in 5′ end processing of cytochrome b pre-mRNA. *J. Biol. Chem.* 259, 4722–4731. doi: 10.1016/S0021-9258(17)42907-3

Diodato, D., Ghezzi, D., and Tiranti, V. (2014). The mitochondrial aminoacyl tRNA synthetases: genes and syndromes. *Int. J. Cell Biol.* 2014:787956. doi: 10.1155/2014/787956

Distelmaier, F., Haack, T. B., Catarino, C. B., Gallenmuller, C., Rodenburg, R. J., Strom, T. M., et al. (2015). MRPL44 mutations cause a slowly progressive multisystem disease with childhood-onset hypertrophic cardiomyopathy. *Neurogenetics* 16, 319–323. doi: 10.1007/s10048-015-0444-2

Dogan, S. A., Pujol, C., Maiti, P., Kukat, A., Wang, S., Hermans, S., et al. (2014). Tissue-specific loss of DARS2 activates stress responses independently of respiratory chain deficiency in the heart. *Cell Metab.* 19, 458–469. doi: 10.1016/j.cmet.2014.02.004

D'Souza, A. R., and Minczuk, M. (2018). Mitochondrial transcription and translation: overview. *Essays Biochem.* 62, 309–320. doi: 10.1042/EBC20170102

Emperador, S., Bayona-Bafaluy, M. P., Fernandez-Marmiesse, A., Pineda, M., Felgueroso, B., Lopez-Gallardo, E., et al. (2016). Molecular-genetic characterization and rescue of a TSFM mutation causing childhood-onset ataxia and nonobstructive cardiomyopathy. *Eur. J. Hum. Genet.* 25, 153–156. doi: 10.1038/ejhg.2016.124

Enriquez, J. A., Chomyn, A., and Attardi, G. (1995). MtDNA mutation in MERRF syndrome causes defective aminoacylation of tRNA(Lys) and premature translation termination. *Nat. Genet.* 10, 47–55. doi: 10.1038/ng0595-47

Fan, S., Tian, T., Chen, W., Lv, X., Lei, X., Zhang, H., et al. (2019). Mitochondrial miRNA determines chemoresistance by reprogramming metabolism and regulating mitochondrial transcription. *Cancer Res.* 79, 1069–1084. doi: 10.1158/0008-5472.CAN-18-2505

Fang, F., Liu, Z., Fang, H., Wu, J., Shen, D., Sun, S., et al. (2017a). The clinical and genetic characteristics in children with mitochondrial disease in China. *Sci. China Life Sci.* 60, 746–757. doi: 10.1007/s11427-017-9080-y

Fang, X. J., Zhang, W., Lyu, H., Wang, Z. X., Wang, W. W., and Yuan, Y. (2017b). Compound heterozygote mutation of C12orf65 causes distal motor neuropathy and optic atrophy. *Chin. Med. J. (Engl)* 130, 242–244. doi: 10.4103/0366-6999.198019

Ferrari, A., Del'olio, S., and Barrientos, A. (2020). The diseased mitoribosome. *FEBS Lett.* 595, 1025–1061. doi: 10.1002/1873-3468.14024

Fessler, E., Eckl, E. M., Schmitt, S., Mancilla, I. A., Meyer-Bender, M. F., and Hanf, M. (2020). A pathway coordinated by DELE1 relays mitochondrial stress to the cytosol. *Nature* 579, 433–437. doi: 10.1038/s41586-020-2076-4

Fine, A. S., Nemeth, C. L., Kaufman, M. L., and Fatemi, A. (2019). Mitochondrial aminoacyl-tRNA synthetase disorders: an emerging group of developmental disorders of myelination. *J. Neurodev. Disord.* 11:29. doi: 10.1186/s11689-019-9292-y

Fiori, A., Perez-Martinez, X., and Fox, T. D. (2005). Overexpression of the COX2 translational activator, Pet111p, prevents translation of COX1 mRNA and cytochrome c oxidase assembly in mitochondria of Saccharomyces cerevisiae. *Mol. Microbiol.* 56, 1689–1704. doi: 10.1111/j.1365-2958.2005.04658.x

Florentz, C., Sohm, B., Tryoen-Toth, P., Putz, J., and Sissler, M. (2003). Human mitochondrial tRNAs in health and disease. *Cell Mol. Life Sci.* 60, 1356–1375. doi: 10.1007/s00018-003-2343-1

Fontanesi, F., Soto, I. C., Horn, D., and Barrientos, A. (2006). Assembly of mitochondrial cytochrome c-oxidase, a complicated and highly regulated cellular process. *Am. J. Physiol. Cell Physiol.* 291, C1129–C1147. doi: 10.1152/ajpcell.00233.2006

Fox, T. D. (2012). Mitochondrial protein synthesis, import, and assembly. *Genetics* 192, 1203–1234. doi: 10.1534/genetics.112.141267

Fukumura, S., Ohba, C., Watanabe, T., Minagawa, K., Shimura, M., Murayama, K., et al. (2015). Compound heterozygous GFM2 mutations with Leigh syndrome complicated by arthrogryposis multiplex congenita. *J. Hum. Genet.* 60, 509–513. doi: 10.1038/jhg.2015.57

Galmiche, L., Serre, V., Beinat, M., Assouline, Z., Lebre, A. S., Chretien, D., et al. (2011). Exome sequencing identifies MRPL3 mutation in mitochondrial cardiomyopathy. *Hum. Mutat.* 32, 1225–1231. doi: 10.1002/humu.21562

Gao, Y., Bai, X., Zhang, D., Han, C., Yuan, J., Liu, W., et al. (2016). Mammalian elongation factor 4 regulates mitochondrial translation essential for spermatogenesis. *Nat. Struct. Mol. Biol.* 23, 441–449. doi: 10.1038/nsmb.3206

Gaur, R., Grasso, D., Datta, P. P., Krishna, P. D., Das, G., Spencer, A., et al. (2008). A single mammalian mitochondrial translation initiation factor functionally replaces two bacterial factors. *Mol. Cell* 29, 180–190. doi: 10.1016/j.molcel.2007.11.021

Girodat, D., Blanchard, S. C., Wieden, H. J., and Sanbonmatsu, K. Y. (2020). Elongation Factor Tu Switch I Element is a gate for aminoacyl-tRNA selection. *J. Mol. Biol.* 432, 3064–3077. doi: 10.1016/j.jmb.2020.01.038

Glasgow, R. I. C., Thompson, K., Barbosa, I. A., He, L., Alston, C. L., Deshpande, C., et al. (2017). Novel GFM2 variants associated with early-onset neurological presentations of mitochondrial disease and impaired expression of OXPHOS subunits. *Neurogenetics* 18, 227–235. doi: 10.1007/s10048-017-0526-4

Gotz, A., Tyynismaa, H., Euro, L., Ellonen, P., Hyotylainen, T., Ojala, T., et al. (2011). Exome sequencing identifies mitochondrial alanyl-tRNA synthetase mutations in infantile mitochondrial cardiomyopathy. *Am. J. Hum. Genet.* 88, 635–642. doi: 10.1016/j.ajhg.2011.04.006

Greber, B. J., Bieri, P., Leibundgut, M., Leitner, A., Aebersold, R., Boehringer, D., et al. (2015). Ribosome. The complete structure of the 55S mammalian mitochondrial ribosome. *Science* 348, 303–308. doi: 10.1126/science.aaa3872

Gruschke, S., Kehrein, K., Rompler, K., Grone, K., Israel, L., Imhof, A., et al. (2011). Cbp3-Cbp6 interacts with the yeast mitochondrial ribosomal tunnel exit and promotes cytochrome b synthesis and assembly. *J. Cell Biol.* 193, 1101–1114. doi: 10.1083/jcb.201103132

Guo, X., Aviles, G., Liu, Y., Tian, R., Unger, B. A., Lin, Y. T., et al. (2020). Mitochondrial stress is relayed to the cytosol by an OMA1-DELE1-HRI pathway. *Nature* 579, 427–432. doi: 10.1038/s41586-020-2078-2

Hallberg, B. M., and Larsson, N. G. (2014). Making proteins in the powerhouse. *Cell Metab.* 20, 226–240. doi: 10.1016/j.cmet.2014.07.001

Handa, Y., Hikawa, Y., Tochio, N., Kogure, H., Inoue, M., Koshiba, S., et al. (2010). Solution structure of the catalytic domain of the mitochondrial protein ICT1 that is essential for cell vitality. *J. Mol. Biol.* 404, 260–273. doi: 10.1016/j.jmb.2010.09.033

Hansen, L. L., Jorgensen, R., and Justesen, J. (2000). Assignment of the human mitochondrial translational release factor 1 (MTRF1) to chromosome 13q14.1–>q14.3 and of the human mitochondrial ribosome recycling factor (MRRF) to chromosome 9q32–>q34.1 with radiation hybrid mapping. *Cytogenet. Cell Genet.* 88, 91–92. doi: 10.1159/000015494

Haque, M. E., and Spremulli, L. L. (2008). Roles of the N- and C-terminal domains of mammalian mitochondrial initiation factor 3 in protein biosynthesis. *J. Mol. Biol.* 384, 929–940. doi: 10.1016/j.jmb.2008.09.077

He, H., Chen, M., Scheffler, N. K., Gibson, B. W., Spremulli, L. L., and Gottlieb, R. A. (2001). Phosphorylation of mitochondrial elongation factor Tu in ischemic myocardium: basis for chloramphenicol-mediated cardioprotection. *Circ. Res.* 89, 461–467. doi: 10.1161/hh1701.096038

He, K., Guo, X., Liu, Y., Li, J., Hu, Y., Wang, D., et al. (2016). TUFM downregulation induces epithelial-mesenchymal transition and invasion in lung cancer cells via a mechanism involving AMPK-GSK3beta signaling. *Cell Mol. Life Sci.* 73, 2105–2121. doi: 10.1007/s00018-015-2122-9

Hei, Z., Wu, S., Liu, Z., Wang, J., and Fang, P. (2019). Retractile lysyl-tRNA synthetase-AIMP2 assembly in the human multi-aminoacyl-tRNA synthetase complex. *J. Biol. Chem.* 294, 4775–4783. doi: 10.1074/jbc.RA118.006356

Heidary, G., Calderwood, L., Cox, G. F., Robson, C. D., Teot, L. A., Mullon, J., et al. (2014). Optic atrophy and a Leigh-like syndrome due to mutations in the c12orf65 gene: report of a novel mutation

and review of the literature. *J. Neuroophthalmol.* 34, 39–43. doi: 10.1097/WNO.0000000000000076

Helgstrand, M., Mandava, C. S., Mulder, F. A., Liljas, A., Sanyal, S., and Akke, M. (2007). The ribosomal stalk binds to translation factors IF2, EF-Tu, EF-G and RF3 via a conserved region of the L12 C-terminal domain. *J. Mol. Biol.* 365, 468–479. doi: 10.1016/j.jmb.2006.10.025

Hershkovitz, T., Kurolap, A., Gonzaga-Jauregui, C., Paperna, T., Mory, A., Wolf, S. E., et al. (2019). A novel TUFM homozygous variant in a child with mitochondrial cardiomyopathy expands the phenotype of combined oxidative phosphorylation deficiency 4. *J. Hum. Genet.* 64, 589–595. doi: 10.1038/s10038-019-0592-6

Houtkooper, R. H., Mouchiroud, L., Ryu, D., Moullan, N., Katsyuba, E., Knott, G., et al. (2013). Mitonuclear protein imbalance as a conserved longevity mechanism. *Nature* 497, 451–457. doi: 10.1038/nature12188

Imagawa, E., Fattal-Valevski, A., Eyal, O., Miyatake, S., Saada, A., Nakashima, M., et al. (2016). Homozygous p.V116* mutation in C12orf65 results in Leigh syndrome. *J. Neurol. Neurosurg. Psychiatry* 87, 212–216. doi: 10.1136/jnnp-2014-310084

Islas-Osuna, M. A., Ellis, T. P., Marnell, L. L., Mittelmeier, T. M., and Dieckmann, C. L. (2002). Cbp1 is required for translation of the mitochondrial cytochrome b mRNA of Saccharomyces cerevisiae. *J. Biol. Chem.* 277, 37987–37990. doi: 10.1074/jbc.M206132200

Jacobs, H. T., and Turnbull, D. M. (2005). Nuclear genes and mitochondrial translation: a new class of genetic disease. *Trends Genet.* 21, 312–314. doi: 10.1016/j.tig.2005.04.003

Jeppesen, M. G., Navratil, T., Spremulli, L. L., and Nyborg, J. (2005). Crystal structure of the bovine mitochondrial elongation factor Tu.Ts complex. *J. Biol. Chem.* 280, 5071–5081. doi: 10.1074/jbc.M411782200

Kaji, A., Kiel, M. C., Hirokawa, G., Muto, A. R., Inokuchi, Y., and Kaji, H. (2001). The fourth step of protein synthesis: disassembly of the posttermination complex is catalyzed by elongation factor G and ribosome recycling factor, a near-perfect mimic of tRNA. *Cold Spring Harb. Symp. Quant. Biol.* 66, 515–529. doi: 10.1101/sqb.2001.66.515

Kaushal, P. S., Sharma, M. R., and Agrawal, R. K. (2015). The 55S mammalian mitochondrial ribosome and its tRNA-exit region. *Biochimie* 114, 119–126. doi: 10.1016/j.biochi.2015.03.013

Khan, N. A., Nikkanen, J., Yatsuga, S., Jackson, C., Wang, L., Pradhan, S., et al. (2017). mTORC1 regulates mitochondrial integrated stress response and mitochondrial myopathy progression. *Cell Metab.* 26, 419–428.e5. doi: 10.1016/j.cmet.2017.07.007

Khawaja, A., Itoh, Y., Remes, C., Spahr, H., Yukhnovets, O., Hofig, H., et al. (2020). Distinct pre-initiation steps in human mitochondrial translation. *Nat. Commun.* 11:2932. doi: 10.1038/s41467-020-16503-2

King, M. P., Koga, Y., Davidson, M., and Schon, E. A. (1992). Defects in mitochondrial protein synthesis and respiratory chain activity segregate with the tRNA(Leu(UUR)) mutation associated with mitochondrial myopathy, encephalopathy, lactic acidosis, and strokelike episodes. *Mol. Cell Biol.* 12, 480–490. doi: 10.1128/mcb.12.2.480

Kisselev, L., Ehrenberg, M., and Frolova, L. (2003). Termination of translation: interplay of mRNA, rRNAs and release factors? *EMBO J.* 22, 175–182. doi: 10.1093/emboj/cdg017

Koc, E. C., Burkhart, W., Blackburn, K., Moyer, M. B., Schlatzer, D. M., Moseley, A., et al. (2001). The large subunit of the mammalian mitochondrial ribosome. Analysis of the complement of ribosomal proteins present. *J. Biol. Chem.* 276, 43958–43969. doi: 10.1074/jbc.M106510200

Koc, E. C., and Spremulli, L. L. (2002). Identification of mammalian mitochondrial translational initiation factor 3 and examination of its role in initiation complex formation with natural mRNAs. *J. Biol. Chem.* 277, 35541–35549. doi: 10.1074/jbc.M202498200

Kogure, H., Hikawa, Y., Hagihara, M., Tochio, N., Koshiba, S., Inoue, Y., et al. (2012). Solution structure and siRNA-mediated knockdown analysis of the mitochondrial disease-related protein C12orf65. *Proteins* 80, 2629–2642. doi: 10.1002/prot.24152

Kohda, M., Tokuzawa, Y., Kishita, Y., Nyuzuki, H., Moriyama, Y., Mizuno, Y., et al. (2016). A comprehensive genomic analysis reveals the genetic landscape of mitochondrial respiratory chain complex deficiencies. *PLoS Genet.* 12:e1005679. doi: 10.1371/journal.pgen.1005679

Kohler, F., Muller-Rischart, A. K., Conradt, B., and Rolland, S. G. (2015). The loss of LRPPRC function induces the mitochondrial unfolded protein response. *Aging (Albany NY)* 7, 701–717. doi: 10.18632/aging.100812

Konovalova, S., and Tyynismaa, H. (2013). Mitochondrial aminoacyl-tRNA synthetases in human disease. *Mol. Genet. Metab.* 108, 206–211. doi: 10.1016/j.ymgme.2013.01.010

Koripella, R. K., Sharma, M. R., Bhargava, K., Datta, P. P., Kaushal, P. S., Keshavan, P., et al. (2020). Structures of the human mitochondrial ribosome bound to EF-G1 reveal distinct features of mitochondrial translation elongation. *Nat. Commun.* 11:3830. doi: 10.1038/s41467-020-17715-2

Koripella, R. K., Sharma, M. R., Haque, M. E., Risteff, P., Spremulli, L. L., and Agrawal, R. K. (2019a). Structure of human mitochondrial translation initiation factor 3 bound to the small ribosomal subunit. *iScience* 12, 76–86. doi: 10.1016/j.isci.2018.12.030

Koripella, R. K., Sharma, M. R., Risteff, P., Keshavan, P., and Agrawal, R. K. (2019b). Structural insights into unique features of the human mitochondrial ribosome recycling. *Proc. Natl. Acad. Sci. U.S.A.* 116, 8283–8288. doi: 10.1073/pnas.1815675116

Kummer, E., and Ban, N. (2020). Structural insights into mammalian mitochondrial translation elongation catalyzed by mtEFG1. *EMBO J.* 39:e104820. doi: 10.15252/embj.2020104820

Kummer, E., and Ban, N. (2021). Mechanisms and regulation of protein synthesis in mitochondria. *Nat. Rev. Mol. Cell Biol.* 22, 307–325. doi: 10.1038/s41580-021-00332-2

Kummer, E., Leibundgut, M., Rackham, O., Lee, R. G., Boehringer, D., Filipovska, A., et al. (2018). Unique features of mammalian mitochondrial translation initiation revealed by cryo-EM. *Nature* 560, 263–267. doi: 10.1038/s41586-018-0373-y

Kuzmenko, A., Atkinson, G. C., Levitskii, S., Zenkin, N., Tenson, T., Hauryliuk, V., et al. (2014). Mitochondrial translation initiation machinery: conservation and diversification. *Biochimie* 100, 132–140. doi: 10.1016/j.biochi.2013.07.024

Lake, N. J., Webb, B. D., Stroud, D. A., Richman, T. R., Ruzzenente, B., Compton, A. G., et al. (2018). Biallelic mutations in MRPS34 lead to instability of the small mitoribosomal subunit and Leigh syndrome. *Am. J. Hum. Genet.* 102:713. doi: 10.1016/j.ajhg.2018.03.015

Larsson, N. G., and Clayton, D. A. (1995). Molecular genetic aspects of human mitochondrial disorders. *Annu. Rev. Genet.* 29, 151–178. doi: 10.1146/annurev.ge.29.120195.001055

Lavdovskaia, E., Denks, K., Nadler, F., Steube, E., Linden, A., Urlaub, H., et al. (2020). Dual function of GTPBP6 in biogenesis and recycling of human mitochondrial ribosomes. *Nucleic Acids Res.* 48, 12929–12942. doi: 10.1093/nar/gkaa1132

Lee, D. E., Perry, R. A. Jr., Brown, J. L., Rosa-Caldwell, M. E., Brown, L. A., Haynie, W. S., et al. (2019). Mitochondrial mRNA translation initiation contributes to oxidative metabolism in the myocardia of aged, obese mice. *Exp. Gerontol.* 121, 62–70. doi: 10.1016/j.exger.2019.03.009

Li, H., Dai, B., Fan, J., Chen, C., Nie, X., Yin, Z., et al. (2019). The different roles of miRNA-92a-2-5p and let-7b-5p in mitochondrial translation in db/db mice. *Mol. Ther. Nucleic Acids* 17, 424–435. doi: 10.1016/j.omtn.2019.06.013

Li, H., Zhang, X., Wang, F., Zhou, L., Yin, Z., Fan, J., et al. (2016). MicroRNA-21 Lowers blood pressure in spontaneous hypertensive rats by upregulating mitochondrial translation. *Circulation* 134, 734–751. doi: 10.1161/CIRCULATIONAHA.116.023926

Liao, H. X., and Spremulli, L. L. (1990). Identification and initial characterization of translational initiation factor 2 from bovine mitochondria. *J. Biol. Chem.* 265, 13618–13622. doi: 10.1016/s0021-9258(18)77393-6

Lin, J., Chen, K., Chen, W., Yao, Y., Ni, S., Ye, M., et al. (2020). Paradoxical mitophagy regulation by PINK1 and TUFm. *Mol. Cell* 80:e612. doi: 10.1016/j.molcel.2020.10.007

Liu, J., Fang, H., Chi, Z., Wu, Z., Wei, D., Mo, D., et al. (2015). XPD localizes in mitochondria and protects the mitochondrial genome from oxidative DNA damage. *Nucleic Acids Res.* 43, 5476–5488. doi: 10.1093/nar/gkv472

Lopez Sanchez, M. I. G., Kruger, A., Shiriaev, D. I., Liu, Y., and Rorbach, J. (2021). Human mitoribosome biogenesis and its emerging links to disease. *Int. J. Mol. Sci.* 22:3827. doi: 10.3390/ijms22083827

Mai, N., Chrzanowska-Lightowlers, Z. M., and Lightowlers, R. N. (2017). The process of mammalian mitochondrial protein synthesis. *Cell Tissue Res.* 367, 5–20. doi: 10.1007/s00441-016-2456-0

March, P. E., and Inouye, M. (1985). Characterization of the lep operon of *Escherichia coli*. Identification of the promoter and the gene upstream of the signal peptidase I gene. *J. Biol. Chem.* 260, 7206–7213. doi: 10.1016/s0021-9258(17)39594-7

Marcos, C. M., Tamer, G., De Oliveira, H. C., Assato, P. A., Scorzoni, L., Santos, C. T., et al. (2019). Down-regulation of TUFM impairs host cell interaction and virulence by Paracoccidioides brasiliensis. *Sci. Rep.* 9:17206. doi: 10.1038/s41598-019-51540-y

Masucci, J. P., Davidson, M., Koga, Y., Schon, E. A., and King, M. P. (1995). In vitro analysis of mutations causing myoclonus epilepsy with ragged-red fibers in the mitochondrial tRNA(Lys)gene: two genotypes produce similar phenotypes. *Mol. Cell Biol.* 15, 2872–2881. doi: 10.1128/mcb.15.5.2872

Mick, D. U., Dennerlein, S., Wiese, H., Reinhold, R., Pacheu-Grau, D., Lorenzi, I., et al. (2012). MITRAC links mitochondrial protein translocation to respiratory-chain assembly and translational regulation. *Cell* 151, 1528–1541. doi: 10.1016/j.cell.2012.11.053

Mikhailova, S. V., Zakharova, E., Banin, A. V., Demushkina, A. A., and Petrukhin, A. S. (2009). Clinical and molecular genetic diagnosis of leukoencephalopathy with brainstem and spinal cord involvement and lactate elevation in children. *Zh Nevrol. Psikhiatr. Im. S S Korsakova* 109, 16–22.

Miller, C., Saada, A., Shaul, N., Shabtai, N., Ben-Shalom, E., Shaag, A., et al. (2004). Defective mitochondrial translation caused by a ribosomal protein (MRPS16) mutation. *Ann. Neurol.* 56, 734–738. doi: 10.1002/ana.20282

Mittelmeier, T. M., and Dieckmann, C. L. (1995). *In vivo* analysis of sequences required for translation of cytochrome b transcripts in yeast mitochondria. *Mol. Cell Biol.* 15, 780–789. doi: 10.1128/mcb.15.2.780

Morgan-Hughes, J. A., Sweeney, M. G., Cooper, J. M., Hammans, S. R., Brockington, M., Schapira, A. H., et al. (1995). Mitochondrial DNA (mtDNA) diseases: correlation of genotype to phenotype. *Biochim. Biophys. Acta* 1271, 135–140. doi: 10.1016/0925-4439(95)00020-5

Nagao, A., Suzuki, T., Katoh, T., Sakaguchi, Y., and Suzuki, T. (2009). Biogenesis of glutaminyl-mt tRNAGln in human mitochondria. *Proc. Natl. Acad. Sci. U.S.A.* 106, 16209–16214. doi: 10.1073/pnas.0907602106

Naithani, S., Saracco, S. A., Butler, C. A., and Fox, T. D. (2003). Interactions among COX1, COX2, and COX3 mRNA-specific translational activator proteins on the inner surface of the mitochondrial inner membrane of Saccharomyces cerevisiae. *Mol. Biol. Cell* 14, 324–333. doi: 10.1091/mbc.e02-08-0490

Nishihara, H., Omoto, M., Takao, M., Higuchi, Y., Koga, M., Kawai, M., et al. (2017). Autopsy case of the C12orf65 mutation in a patient with signs of mitochondrial dysfunction. *Neurol. Genet.* 3:e171. doi: 10.1212/NXG.0000000000000171

Nozaki, Y., Matsunaga, N., Ishizawa, T., Ueda, T., and Takeuchi, N. (2008). HMRF1L is a human mitochondrial translation release factor involved in the decoding of the termination codons UAA and UAG. *Genes Cells* 13, 429–438. doi: 10.1111/j.1365-2443.2008.01181.x

O'Brien, T. W. (1971). The general occurrence of 55 S ribosomes in mammalian liver mitochondria. *J. Biol. Chem.* 246, 3409–3417. doi: 10.1016/s0021-9258(18)62239-2

O'Brien, T. W. (2003). Properties of human mitochondrial ribosomes. *IUBMB Life* 55, 505–513. doi: 10.1080/15216540310001626610

Ognjenovic, J., and Simonovic, M. (2018). Human aminoacyl-tRNA synthetases in diseases of the nervous system. *RNA Biol.* 15, 623–634. doi: 10.1080/15476286.2017.1330245

Ojala, D., Montoya, J., and Attardi, G. (1981). tRNA punctuation model of RNA processing in human mitochondria. *Nature* 290, 470–474. doi: 10.1038/290470a0

Ostojic, J., Panozzo, C., Bourand-Plantefol, A., Herbert, C. J., Dujardin, G., and Bonnefoy, N. (2016). Ribosome recycling defects modify the balance between the synthesis and assembly of specific subunits of the oxidative phosphorylation complexes in yeast mitochondria. *Nucleic Acids Res.* 44, 5785–5797. doi: 10.1093/nar/gkw490

Ott, M., Amunts, A., and Brown, A. (2016). Organization and regulation of mitochondrial protein synthesis. *Annu. Rev. Biochem.* 85, 77–101. doi: 10.1146/annurev-biochem-060815-014334

Ozawa, M., Nishino, I., Horai, S., Nonaka, I., and Goto, Y. I. (1997). Myoclonus epilepsy associated with ragged-red fibers: a G-to-A mutation at nucleotide pair 8363 in mitochondrial tRNA(Lys) in two families. *Muscle Nerve* 20, 271–278. doi: 10.1002/(sici)1097-4598(199703)20:3<271::aid-mus2>3.0.co;2-8

Paramasivam, A., and Vijayashree Priyadharsini, J. (2020). MitomiRs: new emerging microRNAs in mitochondrial dysfunction and cardiovascular disease. *Hypertens Res.* 43, 851–853. doi: 10.1038/s41440-020-0423-3

Park, D., Lee, M. N., Jeong, H., Koh, A., Yang, Y. R., Suh, P. G., et al. (2014). Parkin ubiquitinates mTOR to regulate mTORC1 activity under mitochondrial stress. *Cell Signal.* 26, 2122–2130. doi: 10.1016/j.cellsig.2014.06.010

Perez-Martinez, X., Funes, S., Camacho-Villasana, Y., Marjavaara, S., Tavares-Carreon, F., and Shingu-Vazquez, M. (2008). Protein synthesis and assembly in mitochondrial disorders. *Curr. Top Med. Chem.* 8, 1335–1350. doi: 10.2174/156802608786141124

Perli, E., Pisano, A., Glasgow, R. I. C., Carbo, M., Hardy, S. A., Falkous, G., et al. (2019). Novel compound mutations in the mitochondrial translation elongation factor (TSFM) gene cause severe cardiomyopathy with myocardial fibro-adipose replacement. *Sci. Rep.* 9:5108. doi: 10.1038/s41598-019-41483-9

Perrone, E., Cavole, T. R., Oliveira, M. G., Virmond, L. D. A., Silva, M. F. B., Soares, M. F. F., et al. (2020). Leigh syndrome in a patient with a novel C12orf65 pathogenic variant: case report and literature review. *Genet. Mol. Biol.* 43:e20180271. doi: 10.1590/1678-4685-GMB-2018-0271

Peske, F., Rodnina, M. V., and Wintermeyer, W. (2005). Sequence of steps in ribosome recycling as defined by kinetic analysis. *Mol. Cell* 18, 403–412. doi: 10.1016/j.molcel.2005.04.009

Pettersson, I., and Kurland, C. G. (1980). Ribosomal protein L7/L12 is required for optimal translation. *Proc. Natl. Acad. Sci. U.S.A.* 77, 4007–4010. doi: 10.1073/pnas.77.7.4007

Pinti, M. V., Hathaway, Q. A., and Hollander, J. M. (2017). Role of microRNA in metabolic shift during heart failure. *Am. J. Physiol. Heart Circ. Physiol.* 312, H33–H45. doi: 10.1152/ajpheart.00341.2016

Polekhina, G., Thirup, S., Kjeldgaard, M., Nissen, P., Lippmann, C., and Nyborg, J. (1996). Helix unwinding in the effector region of elongation factor EF-Tu-GDP. *Structure* 4, 1141–1151. doi: 10.1016/s0969-2126(96)00122-0

Pyle, A., Ramesh, V., Bartsakoulia, M., Boczonadi, V., Gomez-Duran, A., Herczegfalvi, A., et al. (2014). Behr's syndrome is typically associated with disturbed mitochondrial translation and mutations in the C12orf65 gene. *J. Neuromuscul. Dis.* 1, 55–63. doi: 10.3233/JND-140003

Qin, Y., Polacek, N., Vesper, O., Staub, E., Einfeldt, E., Wilson, D. N., et al. (2006). The highly conserved LepA is a ribosomal elongation factor that back-translocates the ribosome. *Cell* 127, 721–733. doi: 10.1016/j.cell.2006.09.037

Rao, A. R., and Varshney, U. (2001). Specific interaction between the ribosome recycling factor and the elongation factor G from Mycobacterium tuberculosis mediates peptidyl-tRNA release and ribosome recycling in *Escherichia coli*. *EMBO J.* 20, 2977–2986. doi: 10.1093/emboj/20.11.2977

Ravn, K., Schonewolf-Greulich, B., Hansen, R. M., Bohr, A. H., Duno, M., Wibrand, F., et al. (2015). Neonatal mitochondrial hepatoencephalopathy caused by novel GFM1 mutations. *Mol. Genet. Metab. Rep.* 3, 5–10. doi: 10.1016/j.ymgmr.2015.01.004

Richman, T. R., Ermer, J. A., Davies, S. M., Perks, K. L., Viola, H. M., Shearwood, A. M., et al. (2015). Mutation in MRPS34 compromises protein synthesis and causes mitochondrial dysfunction. *PLoS Genet.* 11:e1005089. doi: 10.1371/journal.pgen.1005089

Richman, T. R., Spahr, H., Ermer, J. A., Davies, S. M., Viola, H. M., Bates, K. A., et al. (2016). Loss of the RNA-binding protein TACO1 causes late-onset mitochondrial dysfunction in mice. *Nat. Commun.* 7:11884. doi: 10.1038/ncomms11884

Richter, R., Pajak, A., Dennerlein, S., Rozanska, A., Lightowlers, R. N., and Chrzanowska-Lightowlers, Z. M. (2010a). Translation termination in human mitochondrial ribosomes. *Biochem. Soc. Trans.* 38, 1523–1526. doi: 10.1042/BST0381523

Richter, R., Rorbach, J., Pajak, A., Smith, P. M., Wessels, H. J., Huynen, M. A., et al. (2010b). A functional peptidyl-tRNA hydrolase, ICT1, has been recruited into the human mitochondrial ribosome. *EMBO J.* 29, 1116–1125. doi: 10.1038/emboj.2010.14

Richter-Dennerlein, R., Oeljeklaus, S., Lorenzi, I., Ronsor, C., Bareth, B., Schendzielorz, A. B., et al. (2016). Mitochondrial protein synthesis adapts to influx of nuclear-encoded protein. *Cell* 167, 471–483.e10. doi: 10.1016/j.cell.2016.09.003

Rivera, H., Martin-Hernandez, E., Delmiro, A., Garcia-Silva, M. T., Quijada-Fraile, P., Muley, R., et al. (2013). A new mutation in the gene encoding mitochondrial

seryl-tRNA synthetase as a cause of HUPRA syndrome. *BMC Nephrol.* 14:195. doi: 10.1186/1471-2369-14-195

Rodel, G. (1986). Two yeast nuclear genes, CBS1 and CBS2, are required for translation of mitochondrial transcripts bearing the 5′-untranslated COB leader. *Curr. Genet.* 11, 41–45. doi: 10.1007/BF00389424

Rorbach, J., Richter, R., Wessels, H. J., Wydro, M., Pekalski, M., Farhoud, M., et al. (2008). The human mitochondrial ribosome recycling factor is essential for cell viability. *Nucleic Acids Res.* 36, 5787–5799. doi: 10.1093/nar/gkn576

Rotig, A. (2011). Human diseases with impaired mitochondrial protein synthesis. *Biochim. Biophys. Acta* 1807, 1198–1205. doi: 10.1016/j.bbabio.2011.06.010

Rudler, D. L., Hughes, L. A., Perks, K. L., Richman, T. R., Kuznetsova, I., Ermer, J. A., et al. (2019). Fidelity of translation initiation is required for coordinated respiratory complex assembly. *Sci. Adv.* 5:eaay2118. doi: 10.1126/sciadv.aay2118

Saada, A., Shaag, A., Arnon, S., Dolfin, T., Miller, C., Fuchs-Telem, D., et al. (2007). Antenatal mitochondrial disease caused by mitochondrial ribosomal protein (MRPS22) mutation. *J. Med. Genet.* 44, 784–786. doi: 10.1136/jmg.2007.053116

Samec, N., Jovcevska, I., Stojan, J., Zottel, A., Liovic, M., Myers, M. P., et al. (2018). Glioblastoma-specific anti-TUFM nanobody for in-vitro immunoimaging and cancer stem cell targeting. *Oncotarget* 9, 17282–17299. doi: 10.18632/oncotarget.24629

Sanchirico, M. E., Fox, T. D., and Mason, T. L. (1998). Accumulation of mitochondrially synthesized Saccharomyces cerevisiae Cox2p and Cox3p depends on targeting information in untranslated portions of their mRNAs. *EMBO J.* 17, 5796–5804. doi: 10.1093/emboj/17.19.5796

Santo-Domingo, J., Chareyron, I., Broenimann, C., Lassueur, S., and Wiederkehr, A. (2017). Antibiotics induce mitonuclear protein imbalance but fail to inhibit respiration and nutrient activation in pancreatic beta-cells. *Exp. Cell Res.* 357, 170–180. doi: 10.1016/j.yexcr.2017.05.013

Sasarman, F., Antonicka, H., and Shoubridge, E. A. (2008). The A3243G tRNALeu(UUR) MELAS mutation causes amino acid misincorporation and a combined respiratory chain assembly defect partially suppressed by overexpression of EFTu and EFG2. *Hum. Mol. Genet.* 17, 3697–3707. doi: 10.1093/hmg/ddn265

Scala, M., Brigati, G., Fiorillo, C., Nesti, C., Rubegni, A., Pedemonte, M., et al. (2019). Novel homozygous TSFM pathogenic variant associated with encephalocardiomyopathy with sensorineural hearing loss and peculiar neuroradiologic findings. *Neurogenetics* 20, 165–172. doi: 10.1007/s10048-019-00582-5

Scheper, G. C., Van Der Klok, T., Van Andel, R. J., Van Berkel, C. G., Sissler, M., Smet, J., et al. (2007). Mitochondrial aspartyl-tRNA synthetase deficiency causes leukoencephalopathy with brain stem and spinal cord involvement and lactate elevation. *Nat. Genet.* 39, 534–539. doi: 10.1038/ng2013

Schulz, C., Schendzielorz, A., and Rehling, P. (2015). Unlocking the presequence import pathway. *Trends Cell Biol.* 25, 265–275. doi: 10.1016/j.tcb.2014.12.001

Seo, G. H., Oh, A., Kim, E. N., Lee, Y., Park, J., Kim, T., et al. (2019). Identification of extremely rare mitochondrial disorders by whole exome sequencing. *J. Hum. Genet.* 64, 1117–1125. doi: 10.1038/s10038-019-0660-y

Serre, V., Rozanska, A., Beinat, M., Chretien, D., Boddaert, N., Munnich, A., et al. (2013). Mutations in mitochondrial ribosomal protein MRPL12 leads to growth retardation, neurological deterioration and mitochondrial translation deficiency. *Biochim. Biophys. Acta* 1832, 1304–1312. doi: 10.1016/j.bbadis.2013.04.014

Shahni, R., Wedatilake, Y., Cleary, M. A., Lindley, K. J., Sibson, K. R., and Rahman, S. (2013). A distinct mitochondrial myopathy, lactic acidosis and sideroblastic anemia (MLASA) phenotype associates with YARS2 mutations. *Am. J. Med. Genet. A* 161A, 2334–2338. doi: 10.1002/ajmg.a.36065

Sharma, M. R., Koc, E. C., Datta, P. P., Booth, T. M., Spremulli, L. L., and Agrawal, R. K. (2003). Structure of the mammalian mitochondrial ribosome reveals an expanded functional role for its component proteins. *Cell* 115, 97–108. doi: 10.1016/s0092-8674(03)00762-1

Shi, H., Hayes, M., Kirana, C., Miller, R., Keating, J., Macartney-Coxson, D., et al. (2012). TUFM is a potential new prognostic indicator for colorectal carcinoma. *Pathology* 44, 506–512. doi: 10.1097/PAT.0b013e3283559cbe

Shoffner, J. M., Lott, M. T., Lezza, A. M., Seibel, P., Ballinger, S. W., and Wallace, D. C. (1990). Myoclonic epilepsy and ragged-red fiber disease (MERRF) is associated with a mitochondrial DNA tRNA(Lys) mutation. *Cell* 61, 931–937. doi: 10.1016/0092-8674(90)90059-n

Shokolenko, I. N., and Alexeyev, M. F. (2015). Mitochondrial DNA: a disposable genome? *Biochim. Biophys. Acta* 1852, 1805–1809. doi: 10.1016/j.bbadis.2015.05.016

Simon, M. T., Ng, B. G., Friederich, M. W., Wang, R. Y., Boyer, M., Kircher, M., et al. (2017). Activation of a cryptic splice site in the mitochondrial elongation factor GFM1 causes combined OXPHOS deficiency. *Mitochondrion* 34, 84–90. doi: 10.1016/j.mito.2017.02.004

Sissler, M., Gonzalez-Serrano, L. E., and Westhof, E. (2017). Recent advances in mitochondrial aminoacyl-tRNA synthetases and disease. *Trends Mol. Med.* 23, 693–708. doi: 10.1016/j.molmed.2017.06.002

Smeitink, J. A., Elpeleg, O., Antonicka, H., Diepstra, H., Saada, A., Smits, P., et al. (2006). Distinct clinical phenotypes associated with a mutation in the mitochondrial translation elongation factor EFTs. *Am. J. Hum. Genet.* 79, 869–877. doi: 10.1086/508434

Smits, P., Antonicka, H., Van Hasselt, P. M., Weraarpachai, W., Haller, W., Schreurs, M., et al. (2011a). Mutation in subdomain G' of mitochondrial elongation factor G1 is associated with combined OXPHOS deficiency in fibroblasts but not in muscle. *Eur. J. Hum. Genet.* 19, 275–279. doi: 10.1038/ejhg.2010.208

Smits, P., Saada, A., Wortmann, S. B., Heister, A. J., Brink, M., Pfundt, R., et al. (2011b). Mutation in mitochondrial ribosomal protein MRPS22 leads to Cornelia de Lange-like phenotype, brain abnormalities and hypertrophic cardiomyopathy. *Eur. J. Hum. Genet.* 19, 394–399. doi: 10.1038/ejhg.2010.214

Soleimanpour-Lichaei, H. R., Kuhl, I., Gaisne, M., Passos, J. F., Wydro, M., Rorbach, J., et al. (2007). mtRF1a is a human mitochondrial translation release factor decoding the major termination codons UAA and UAG. *Mol. Cell* 27, 745–757. doi: 10.1016/j.molcel.2007.06.031

Sommerville, E. W., Zhou, X. L., Olahova, M., Jenkins, J., Euro, L., Konovalova, S., et al. (2019). Instability of the mitochondrial alanyl-tRNA synthetase underlies fatal infantile-onset cardiomyopathy. *Hum. Mol. Genet.* 28, 258–268. doi: 10.1093/hmg/ddy294

Spencer, A. C., and Spremulli, L. L. (2004). Interaction of mitochondrial initiation factor 2 with mitochondrial fMet-tRNA. *Nucleic Acids Res.* 32, 5464–5470. doi: 10.1093/nar/gkh886

Spencer, A. C., and Spremulli, L. L. (2005). The interaction of mitochondrial translational initiation factor 2 with the small ribosomal subunit. *Biochim. Biophys. Acta* 1750, 69–81. doi: 10.1016/j.bbapap.2005.03.009

Spiegel, R., Mandel, H., Saada, A., Lerer, I., Burger, A., Shaag, A., et al. (2014). Delineation of C12orf65-related phenotypes: a genotype-phenotype relationship. *Eur. J. Hum. Genet.* 22, 1019–1025. doi: 10.1038/ejhg.2013.284

Srinivasan, H., and Das, S. (2015). Mitochondrial miRNA (MitomiR): a new player in cardiovascular health. *Can. J. Physiol. Pharmacol.* 93, 855–861. doi: 10.1139/cjpp-2014-0500

Su, C., and Wang, F. (2020). Clinical and molecular findings in a family expressing a novel heterozygous variant of the G elongation factor mitochondrial 1 gene. *Exp. Ther. Med.* 20:173. doi: 10.3892/etm.2020.9303

Surovtseva, Y. V., Shutt, T. E., Cotney, J., Cimen, H., Chen, S. Y., Koc, E. C., et al. (2011). Mitochondrial ribosomal protein L12 selectively associates with human mitochondrial RNA polymerase to activate transcription. *Proc Natl Acad Sci U S A* 108, 17921–17926. doi: 10.1073/pnas.1108852108

Suzuki, T., Terasaki, M., Takemoto-Hori, C., Hanada, T., Ueda, T., Wada, A., et al. (2001). Proteomic analysis of the mammalian mitochondrial ribosome. Identification of protein components in the 28 S small subunit. *J. Biol. Chem.* 276, 33181–33195. doi: 10.1074/jbc.M103236200

Synofzik, M., Schicks, J., Lindig, T., Biskup, S., Schmidt, T., Hansel, J., et al. (2011). Acetazolamide-responsive exercise-induced episodic ataxia associated with a novel homozygous DARS2 mutation. *J. Med. Genet.* 48, 713–715. doi: 10.1136/jmg.2011.090282

Szklarczyk, R., Wanschers, B. F., Cuypers, T. D., Esseling, J. J., Riemersma, M., Van Den Brand, M. A., et al. (2012). Iterative orthology prediction uncovers new mitochondrial proteins and identifies C12orf62 as the human ortholog of COX14, a protein involved in the assembly of cytochrome c oxidase. *Genome Biol.* 13:R12. doi: 10.1186/gb-2012-13-2-r12

Taanman, J. W. (1999). The mitochondrial genome: structure, transcription, translation and replication. *Biochim. Biophys. Acta* 1410, 103–123. doi: 10.1016/s0005-2728(98)00161-3

Takeuchi, N., Tomita, N., and Ueda, T. (2010). EF-G2mt is an exclusive recycling factor in mammalian mitochondrial protein synthesis. *Seikagaku* 82, 825–831.

Tang, J. X., Thompson, K., Taylor, R. W., and Olahova, M. (2020). Mitochondrial OXPHOS biogenesis: Co-regulation of protein synthesis, import, and assembly pathways. *Int. J. Mol. Sci.* 21:3820. doi: 10.3390/ijms21113820

Taskin, B. D., Karalok, Z. S., Gurkas, E., Aydin, K., Aydogmus, U., Ceylaner, S., et al. (2016). Early-onset mild type leukoencephalopathy caused by a homozygous EARS2 mutation. *J. Child Neurol.* 31, 938–941. doi: 10.1177/0883073816630087

Taylor, R. W., and Turnbull, D. M. (2005). Mitochondrial DNA mutations in human disease. *Nat. Rev. Genet.* 6, 389–402. doi: 10.1038/nrg1606

Temperley, R. J., Seneca, S. H., Tonska, K., Bartnik, E., Bindoff, L. A., Lightowlers, R. N., et al. (2003). Investigation of a pathogenic mtDNA microdeletion reveals a translation-dependent deadenylation decay pathway in human mitochondria. *Hum. Mol. Genet.* 12, 2341–2348. doi: 10.1093/hmg/ddg238

Tibbetts, A. S., Oesterlin, L., Chan, S. Y., Kramer, G., Hardesty, B., and Appling, D. R. (2003). Mammalian mitochondrial initiation factor 2 supports yeast mitochondrial translation without formylated initiator tRNA. *J. Biol. Chem.* 278, 31774–31780. doi: 10.1074/jbc.M304962200

Toivonen, J. M., O'dell, K. M., Petit, N., Irvine, S. C., Knight, G. K., Lehtonen, M., et al. (2001). Technical knockout, a *Drosophila* model of mitochondrial deafness. *Genetics* 159, 241–254. doi: 10.1093/genetics/159.1.241

Torraco, A., Peralta, S., Iommarini, L., and Diaz, F. (2015). Mitochondrial diseases Part I: mouse models of OXPHOS deficiencies caused by defects in respiratory complex subunits or assembly factors. *Mitochondrion* 21, 76–91. doi: 10.1016/j.mito.2015.01.009

Traschutz, A., Hayer, S. N., Bender, B., Schols, L., Biskup, S., and Synofzik, M. (2019). TSFM mutations cause a complex hyperkinetic movement disorder with strong relief by cannabinoids. *Parkinsonism Relat. Disord.* 60, 176–178. doi: 10.1016/j.parkreldis.2018.09.031

Tucci, A., Liu, Y. T., Preza, E., Pitceathly, R. D., Chalasani, A., Plagnol, V., et al. (2014). Novel C12orf65 mutations in patients with axonal neuropathy and optic atrophy. *J. Neurol. Neurosurg. Psychiatry* 85, 486–492. doi: 10.1136/jnnp-2013-306387

Valente, L., Shigi, N., Suzuki, T., and Zeviani, M. (2009). The R336Q mutation in human mitochondrial EFTu prevents the formation of an active mt-EFTu.GTP.aa-tRNA ternary complex. *Biochim. Biophys. Acta* 1792, 791–795. doi: 10.1016/j.bbadis.2009.06.002

Valente, L., Tiranti, V., Marsano, R. M., Malfatti, E., Fernandez-Vizarra, E., Donnini, C., et al. (2007). Infantile encephalopathy and defective mitochondrial DNA translation in patients with mutations of mitochondrial elongation factors EFG1 and EFTu. *Am. J. Hum. Genet.* 80, 44–58. doi: 10.1086/510559

van Riesen, A. K., Biskup, S., Kuhn, A. A., Kaindl, A. M., and van Riesen, C. (2021). Novel mutation in the TSFM gene causes an early-onset complex chorea without basal ganglia lesions. *Mov. Disord. Clin. Pract.* 8, 453–455. doi: 10.1002/mdc3.13144

Vedrenne, V., Galmiche, L., Chretien, D., De Lonlay, P., Munnich, A., and Rotig, A. (2012). Mutation in the mitochondrial translation elongation factor EFTs results in severe infantile liver failure. *J. Hepatol.* 56, 294–297. doi: 10.1016/j.jhep.2011.06.014

Wang, W. X., Visavadiya, N. P., Pandya, J. D., Nelson, P. T., Sullivan, P. G., and Springer, J. E. (2015). Mitochondria-associated microRNAs in rat hippocampus following traumatic brain injury. *Exp. Neurol.* 265, 84–93. doi: 10.1016/j.expneurol.2014.12.018

Wang, X., Song, C., Zhou, X., Han, X., Li, J., Wang, Z., et al. (2017). Mitochondria associated microRNA expression profiling of heart failure. *Biomed. Res. Int.* 2017:4042509. doi: 10.1155/2017/4042509

Wang, X. Q., Zhang, X. D., Han, Y. M., Shi, X. F., Lan, Z. B., Men, X. X., et al. (2017). Clinical efficacy of gamma knife and surgery treatment of mesial temporal lobe epilepsy and their effects on EF-Tumt and EF-Tsmt expression. *Eur. Rev. Med. Pharmacol. Sci.* 21, 1774–1779.

Weng, X., Zheng, S., Shui, H., Lin, G., and Zhou, Y. (2020). TUFM-knockdown inhibits the migration and proliferation of gastrointestinal stromal tumor cells. *Oncol. Lett.* 20:250. doi: 10.3892/ol.2020.12113

Weraarpachai, W., Antonicka, H., Sasarman, F., Seeger, J., Schrank, B., Kolesar, J. E., et al. (2009). Mutation in TACO1, encoding a translational activator of COX I, results in cytochrome c oxidase deficiency and late-onset Leigh syndrome. *Nat. Genet.* 41, 833–837. doi: 10.1038/ng.390

Weraarpachai, W., Sasarman, F., Nishimura, T., Antonicka, H., Aure, K., Rotig, A., et al. (2012). Mutations in C12orf62, a factor that couples COX I synthesis with cytochrome c oxidase assembly, cause fatal neonatal lactic acidosis. *Am. J. Hum. Genet.* 90, 142–151. doi: 10.1016/j.ajhg.2011.11.027

Wittenhagen, L. M., and Kelley, S. O. (2002). Dimerization of a pathogenic human mitochondrial tRNA. *Nat. Struct. Biol.* 9, 586–590. doi: 10.1038/nsb820

Wittenhagen, L. M., and Kelley, S. O. (2003). Impact of disease-related mitochondrial mutations on tRNA structure and function. *Trends Biochem. Sci.* 28, 605–611. doi: 10.1016/j.tibs.2003.09.006

Woriax, V. L., Burkhart, W., and Spremulli, L. L. (1995). Cloning, sequence analysis and expression of mammalian mitochondrial protein synthesis elongation factor Tu. *Biochim. Biophys. Acta* 1264, 347–356. doi: 10.1016/0167-4781(95)00176-x

Wu, Y., Yao, Q., Jiang, G. X., Wang, G., and Cheng, Q. (2020). Identification of distinct blood-based biomarkers in early stage of Parkinson's disease. *Neurol. Sci.* 41, 893–901. doi: 10.1007/s10072-019-04165-y

Xu, X., Huang, A., Cui, X., Han, K., Hou, X., Wang, Q., et al. (2019). Ubiquitin specific peptidase 5 regulates colorectal cancer cell growth by stabilizing Tu translation elongation factor. *Theranostics* 9, 4208–4220. doi: 10.7150/thno.33803

Yan, K., An, T., Zhai, M., Huang, Y., Wang, Q., Wang, Y., et al. (2019). Mitochondrial miR-762 regulates apoptosis and myocardial infarction by impairing ND2. *Cell Death Dis.* 10:500. doi: 10.1038/s41419-019-1734-7

Yang, F., Gao, Y., Li, Z., Chen, L., Xia, Z., Xu, T., et al. (2014). Mitochondrial EF4 links respiratory dysfunction and cytoplasmic translation in Caenorhabditis elegans. *Biochim. Biophys. Acta* 1837, 1674–1683. doi: 10.1016/j.bbabio.2014.05.353

Yarham, J. W., Elson, J. L., Blakely, E. L., Mcfarland, R., and Taylor, R. W. (2010). Mitochondrial tRNA mutations and disease. *Wiley Interdiscip. Rev. RNA* 1, 304–324. doi: 10.1002/wrna.27

Yassin, A. S., Haque, M. E., Datta, P. P., Elmore, K., Banavali, N. K., Spremulli, L. L., et al. (2011). Insertion domain within mammalian mitochondrial translation initiation factor 2 serves the role of eubacterial initiation factor 1. *Proc. Natl. Acad. Sci. U.S.A.* 108, 3918–3923. doi: 10.1073/pnas.1017425108

Yasukawa, T., Suzuki, T., Ishii, N., Ueda, T., Ohta, S., and Watanabe, K. (2000a). Defect in modification at the anticodon wobble nucleotide of mitochondrial tRNA(Lys) with the MERRF encephalomyopathy pathogenic mutation. *FEBS Lett.* 467, 175–178. doi: 10.1016/s0014-5793(00)01145-5

Yasukawa, T., Suzuki, T., Ueda, T., Ohta, S., and Watanabe, K. (2000b). Modification defect at anticodon wobble nucleotide of mitochondrial tRNAs(Leu)(UUR) with pathogenic mutations of mitochondrial myopathy, encephalopathy, lactic acidosis, and stroke-like episodes. *J. Biol. Chem.* 275, 4251–4257. doi: 10.1074/jbc.275.6.4251

Yasukawa, T., Suzuki, T., Watanabe, K., Yasukawa, T., and Ohta, S. (2002). Wobble modification defect suppresses translational activity of tRNAs with MERRF and MELAS mutations. *Nihon. Rinsho.* 60 Suppl 4, 197–201.

Yokokawa, T., Kido, K., Suga, T., Isaka, T., Hayashi, T., and Fujita, S. (2018). Exercise-induced mitochondrial biogenesis coincides with the expression of mitochondrial translation factors in murine skeletal muscle. *Physiol. Rep.* 6:e13893. doi: 10.14814/phy2.13893

You, C., Xu, N., Qiu, S., Li, Y., Xu, L., Li, X., et al. (2020). A novel composition of two heterozygous GFM1 mutations in a Chinese child with epilepsy and mental retardation. *Brain Behav.* 10:e01791. doi: 10.1002/brb3.1791

Zhang, D., Yan, K., Liu, G., Song, G., Luo, J., Shi, Y., et al. (2016). EF4 disengages the peptidyl-tRNA CCA end and facilitates back-translocation on the 70S ribosome. *Nat. Struct. Mol. Biol.* 23, 125–131. doi: 10.1038/nsmb.3160

Zhang, L., Huang, Y., Ling, J., Xiang, Y., and Zhuo, W. (2019). Screening of key genes and prediction of therapeutic agents in Arsenic-induced lung carcinoma. *Cancer Biomark* 25, 351–360. doi: 10.3233/CBM-182333

Zhang, X., Zuo, X., Yang, B., Li, Z., Xue, Y., Zhou, Y., et al. (2014). MicroRNA directly enhances mitochondrial translation during muscle differentiation. *Cell* 158, 607–619. doi: 10.1016/j.cell.2014.05.047

Zhang, Y., and Spremulli, L. L. (1998). Identification and cloning of human mitochondrial translational release factor 1 and the ribosome recycling factor. *Biochim. Biophys. Acta* 1443, 245–250. doi: 10.1016/s0167-4781(98)00223-1

Zhong, B. R., Zhou, G. F., Song, L., Wen, Q. X., Deng, X. J., Ma, Y. L., et al. (2021). TUFM is involved in Alzheimer's disease-like pathologies that are associated with ROS. *FASEB J.* 35:e21445. doi: 10.1096/fj.202002461R

Zhu, P., Liu, Y., Zhang, F., Bai, X., Chen, Z., Shangguan, F., et al. (2018). Human elongation factor 4 regulates cancer bioenergetics by acting as a mitochondrial translation switch. *Cancer Res.* 78, 2813–2824. doi: 10.1158/0008-5472.CAN-17-2059

Zifa, E., Giannouli, S., Theotokis, P., Stamatis, C., Mamuris, Z., and Stathopoulos, C. (2007). Mitochondrial tRNA mutations: clinical and functional perturbations. *RNA Biol.* 4, 38–66.

Conflict of Interest: The authors declare that the research was conducted in the absence of any commercial or financial relationships that could be construed as a potential conflict of interest.

frontiers in Cell and Developmental Biology

ORIGINAL RESEARCH
published: 06 October 2021
doi: 10.3389/fcell.2021.710247

Intracellular Lipid Accumulation and Mitochondrial Dysfunction Accompanies Endoplasmic Reticulum Stress Caused by Loss of the Co-chaperone *DNAJC3*

Matthew J. Jennings[1†], Denisa Hathazi[1,2†], Chi D. L. Nguyen[2], Benjamin Munro[1], Ute Münchberg[2], Robert Ahrends[2], Annette Schenck[3], Ilse Eidhof[3], Erik Freier[2], Matthis Synofzik[4,5], Rita Horvath[1‡] and Andreas Roos[2,6*‡]*

[1] Department of Clinical Neuroscience, University of Cambridge, Cambridge, United Kingdom, [2] Leibniz-Institut für Analytische Wissenschaften – ISAS – e.V., Dortmund, Germany, [3] Department of Human Genetics, Donders Institute for Brain, Cognition and Behavior, Radboud University Medical Center, Nijmegen, Netherlands, [4] Department of Neurodegenerative Diseases, Hertie Institute for Clinical Brain Research, University of Tübingen, Tübingen, Germany, [5] German Centre for Neurodegenerative Diseases (DZNE), Tübingen, Germany, [6] Department of Pediatric Neurology, Developmental Neurology and Social Pediatrics, Children's Hospital University of Essen, Essen, Germany

Recessive mutations in *DNAJC3*, an endoplasmic reticulum (ER)-resident BiP co-chaperone, have been identified in patients with multisystemic neurodegeneration and diabetes mellitus. To further unravel these pathomechanisms, we employed a non-biased proteomic approach and identified dysregulation of several key cellular pathways, suggesting a pathophysiological interplay of perturbed lipid metabolism, mitochondrial bioenergetics, ER-Golgi function, and amyloid-beta processing. Further functional investigations in fibroblasts of patients with *DNAJC3* mutations detected cellular accumulation of lipids and an increased sensitivity to cholesterol stress, which led to activation of the unfolded protein response (UPR), alterations of the ER-Golgi machinery, and a defect of amyloid precursor protein. In line with the results of previous studies, we describe here alterations in mitochondrial morphology and function, as a major contributor to the *DNAJC3* pathophysiology. Hence, we propose that the loss of *DNAJC3* affects lipid/cholesterol homeostasis, leading to UPR activation, β-amyloid accumulation, and impairment of mitochondrial oxidative phosphorylation.

Keywords: proteomics, cholesterol-stress, mitochondria, *DNAJC3*, unfolded protein response (UPR)

OPEN ACCESS

Edited by:
Erika Fernandez-Vizarra, University of Glasgow, United Kingdom

Reviewed by:
Gloria Brea-Calvo, Universidad Pablo de Olavide, Spain
Massimo Zeviani, University of Padua, Italy
Estela Area-Gomez, Columbia University, United States

***Correspondence:**
Denisa Hathazi
gdh29@cam.ac.uk
Andreas Roos
Andreas.Roos@uk-essen.de

†These authors have contributed equally to this work and share first authorship

‡These authors have contributed equally to this work and share last authorship

Specialty section:
This article was submitted to Cellular Biochemistry, a section of the journal Frontiers in Cell and Developmental Biology

Received: *15 May 2021*
Accepted: *02 September 2021*
Published: *06 October 2021*

Citation:
Jennings MJ, Hathazi D, Nguyen CDL, Munro B, Münchberg U, Ahrends R, Schenck A, Eidhof I, Freier E, Synofzik M, Horvath R and Roos A (2021) Intracellular Lipid Accumulation and Mitochondrial Dysfunction Accompanies Endoplasmic Reticulum Stress Caused by Loss of the Co-chaperone DNAJC3. Front. Cell Dev. Biol. 9:710247. doi: 10.3389/fcell.2021.710247

INTRODUCTION

DnaJ Heat Shock Protein Family (Hsp40) Member C3 (DNAJC3, p58^{IPK}) is an endoplasmic reticulum (ER)-resident co-chaperone of BiP (GRP78, HSPA5), which transiently binds to a broad range of newly synthesized proteins present in the ER to impede the misfolding of susceptible domains. In its "rested" state, DNAJC3 is localized to the ER lumen. The N-terminus of the protein

Abbreviations: ER, endoplasmic reticulum; DNAJC3, DnaJ heat shock protein family (Hsp40) member C3; UPR, unfolded protein response; PERK, protein kinase R (PKR)-like endoplasmic reticulum kinase; eIF2-α, eukaryotic initiation factor 2A; Aβ, β-amyloid; mtDNA, mitochondrial DNA; MSS, Marinesco–Sjörgen syndrome; ATP/ADP, adenosine tri/di-phosphate.

is able to directly bind to hydrophobic regions of misfolded proteins present in the ER (Rutkowski et al., 2007). Once the misfolded protein is bound to the N-terminus of DNACJ3, further ATP-dependent interaction *via* the J-domain with BiP supports the refolding of the misfolded protein (Oyadomari et al., 2006). Additionally, activated DNAJC3 is thought to downregulate the signaling of the unfolded protein response (UPR) effector PERK [protein kinase R (PKR)-like endoplasmic reticulum kinase], presumably by interaction with its cytoplasmic domain (Yan et al., 2002). Dimerization of PERK *via* the phosphorylation of eukaryotic initiation factor 2 alpha (eIF2-α) reduces protein synthesis. Therefore, inhibition of PERK dimerization by DNAJC3 increases protein synthesis and, during periods of sustained UPR signaling, assists in returning the ER to normal homeostasis. Dysregulation of this process may therefore have toxic effects on cellular protein homeostasis. DNAJC3 affects ER maintenance and apoptosis, particularly under conditions of cellular stress, and it has been highlighted as a protective factor in retinal neurons (Boriushkin et al., 2015).

Mutations in components of the UPR frequently cause neurodegenerative diseases. Expression of mutant BiP lacking the carboxyl terminal in a mouse model results in neurodegeneration and severe muscle weakness, associated with aggregation of proteins in the spinal cord alongside upregulation of UPR-related proteins such as GRP94, calnexin and DDIT3 (Jin et al., 2014). Similarly, transgenic mice expressing just 50% of the wild-type BiP exhibit disruption of neural development, defects of cortical neurons, and cerebellar abnormalities, while homozygous loss-of-function mutations result in intrauterine death in mice (Luo et al., 2006). Biallelic mutations in the BiP co-chaperone *SIL1* cause Marinesco–Sjögren syndrome (MSS) in humans, a condition characterized by cataracts, early-onset cerebellar ataxia, cognitive deficits, short stature, and progressive vacuolar myopathy (Anttonen et al., 2005; Senderek et al., 2005; Krieger et al., 2013). The MSS-mouse-model (*woozy* mouse) lacks a functional *Sil1* gene and replicates the human phenotype (Buchkremer et al., 2016). Pathological examination of the *woozy* mouse reveals the loss of Purkinje cells associated with the accumulation of protein aggregates (Zhao et al., 2010), a process found to be accelerated by additional suppression of GRP170, another BiP interacting protein. This process is partially ameliorated by loss of Dnajc3 (Zhao et al., 2010). Furthermore, mutations in the BiP co-chaperone DNAJB2 have been found to be causative for distal hereditary motor neuropathy, accompanied by an increased rate of SOD1 inclusion formation in a neural cell model (Blumen et al., 2012). These studies suggest a causal relationship between dysfunction of protein processing and ER stress and the manifestation of neurological diseases.

Autosomal recessive mutations in *DNAJC3* have been first reported to cause a neurological disorder in two Turkish families, in which individuals presented with ataxia, upper-motor neuron signs, demyelinating neuropathy, neuronal hearing loss, and cerebral atrophy, complicated with early-onset type 2 diabetes mellitus (MODY, OMIM #616192) (Synofzik et al., 2014) and hypothyroidism in a distant relative of the originally reported family (Bublitz et al., 2017). Moreover, isolated type 2 diabetes mellitus has been reported in association with the heterozygous c.712C > A (p.His238Asn) *DNAJC3* mutation (Kulanuwat et al., 2018); however, the same mutation was also observed in two non-diabetic individuals in the study and has been seen at a low frequency in the ExAC database, questioning the role of *DNAJC3* as a dominant type 2 diabetes-associated gene. The p.His238Asn mutation caused minor decrease in DNAJC3 expression, in contrast to the apparent absence seen in the other reported cases. Moreover, two *DNAJC3* patients presenting with juvenile-onset diabetes, short stature, hypothyroidism, neurodegeneration, facial dysmorphism, hypoacusis, microcephaly, and skeletal bone deformities were described (Lytrivi et al., 2021). Symptoms resulting from mutations in *DNAJC3* are partially overlapping with phenotypes caused by mutations in *DNAJB2* and *SIL1*, but with the addition of diabetes (Bublitz et al., 2017).

The mechanisms underlying the pathophysiology of mutations in other BiP co-chaperones such as SIL1 have been extensively explored (Roos et al., 2014, 2016; Ichhaporia et al., 2015; Kollipara et al., 2017; Phan et al., 2019), while in contrast, there is little known about the precise cellular mechanisms underlying the pathogenicity of *DNAJC3* mutations. Studies of primary patient-derived fibroblasts revealed loss of the DNAJC3 protein and a structurally normal ER, and upon ER stress induction, only minor changes were observed in protein secretion and Ca^{2+} leakage (Synofzik et al., 2014). Studies on DNAJC3-silenced rat and human β cells did not affect insulin content and secretion but sensitized cells to ER stress, triggering mitochondrial apoptosis (Lytrivi et al., 2021). To further unravel this pathophysiological route here, we focused on elucidating the pathomechanism of DNAJC3-related pathology by performing proteomics in patient-derived primary fibroblasts, a suitable model to study the etiology of rare neurological diseases (Hentschel et al., 2021), and further investigation of the suggested cellular phenotype.

RESULTS

Loss of Functional *DNAJC3* Alters Proteomic Signature of Human Fibroblasts

Three human primary fibroblast lines carrying previously reported pathogenic homozygous *DNAJC3* mutations (two with c.580C > T; p.Arg194* and one with a large deletion of 72 kb, spanning the *UGGT2* gene NM_006260.5) alongside three fibroblast lines of age-matched healthy controls were used for our proteomics analysis. While the large deletion is spanning the *UGGT2* gene, which can raise concerns of possible overlapping phenotypes, all DNAJC3 patients present with very similar phenotypes. No disease has been so far associated with mutations in the *UGGT2* gene.

We detected 2,531 proteins in total with a minimum of two unique peptides, of which 165 presented with a p-ANOVA < 0.05, and from these, 24 were considered as altered in abundance (12 are upregulated and 12 are downregulated). The most significantly downregulated protein was DNAJC3, which was

expressed at $\log_2 -2.66$ in DNAJC3^{mut} fibroblasts compared to controls, thus confirming that the mutations lead to reduced protein level and demonstrating the robustness of our untargeted proteomic profiling approach. Thresholds were set to 2 standard deviations from the median in either increase or decrease to identify the most significantly altered proteins, which are highlighted in **Figure 1A**.

Pathways associated with dysregulated proteins (KEGG, Reactome, and DAVID libraries; **Figure 1B**) include lipid homeostasis, specifically cholesterol metabolism, which was perturbed in the DNAJC3^{mut} cells (**Figure 1B**). Furthermore, a dysregulation of ADP-ribosylation factor-binding protein GGA1, involved in the processing of APP as an amyloid precursor (von Arnim et al., 2006), was also observed. Apolipoprotein O (APOOL) was increased, which has important roles in mitochondrial lipids and prevention of mitochondrial lipotoxicity (Montero et al., 2010; Turkieh et al., 2014), as well as the Succinate dehydrogenase subunit B (SDHB), a major subunit of mitochondrial respiratory complex II. We therefore identified loss of DNAJC3 to be associated with a proteomic signature of dysregulation of the ER, lipid and cholesterol metabolism, dysregulation of mitochondrial cholesterol processing, and induction of respiratory complex expression.

Loss of Functional *DNAJC3* Results in Cellular Lipid Increase

Prompted by the proteomic findings and the fact that altered lipid homeostasis impacts a variety of cellular processes, such as energy homeostasis, signaling, and on a general note organelle homeostasis (Greenberg et al., 2011), we investigated perturbed lipid homeostasis in our control and DNAJC3^{mut} fibroblasts. Levels of triglycerides and cholesterol esters were investigated using the fluorescent neutral lipid dye 4,4-difluoro-1,3,5,7,8-pentamethyl-4-bora-3a,4a-diaza-s-indacene (BODIPY) and subsequent fluorescence microscopy. Results of these studies showed an increased diffuse staining with perinuclear accumulation and additional nuclear lipid-enrichment in DNAJC3^{mut} fibroblasts compared to the controls (**Figures 2A,B**), supporting the concept of altered lipid homeostasis in cells lacking functional DNAJC3.

As our proteomic data indicated a specific dysregulation of cholesterol metabolism, we studied free cholesterol levels using the filipin fluorescent staining technique (**Figures 2C,D**). While we did not observe an increase in free cholesterol under basal conditions, induction of ER stress with tunicamycin resulted in a significantly greater accumulation of cholesterol in DNAJC3^{mut} fibroblasts compared to controls, demonstrating that DNAJC3^{mut} fibroblasts have functional dysregulation of ER–cholesterol interactions. Treating cells with cholesterol and an inhibitor of Acyl-CoA-: cholesterol acyltransferase (ACAT-I) resulted in a significant increase of cholesterol in both controls and DNAJC3^{mut} fibroblasts (**Figures 2C,D**). This treatment saturated cholesterol clearance capacity and put both DNAJC3^{mut} and control fibroblasts under hypercholesterolemic stress, with only a non-significant slight increase observed in DNAJC3 patient cells compared to controls.

The Endoplasmic Reticulum Is More Vulnerable Against Stress in DNAJC3^{mut} Fibroblasts

It was previously shown that in the presence of tunicamycin or thapsigargin, which perturbs ER function and thus affects

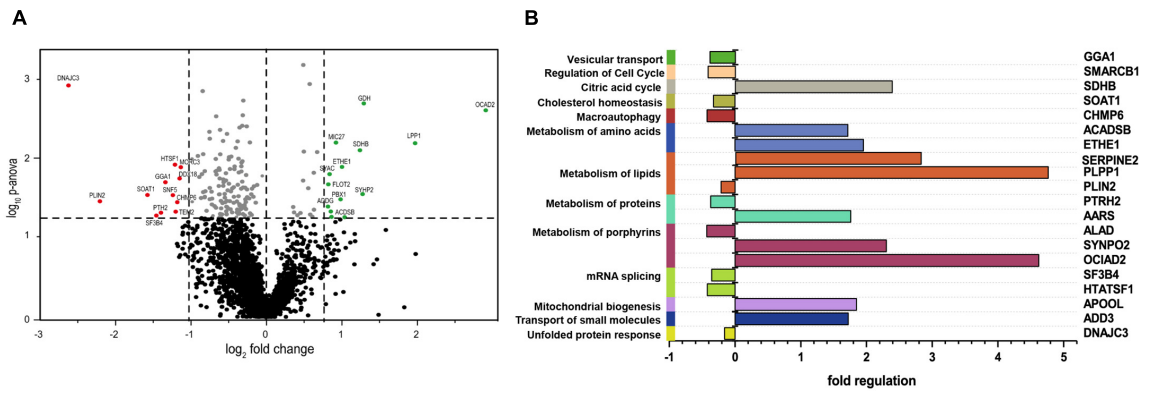

FIGURE 1 | Comparative proteomic profiling results of *DNAJC3*-patient-derived fibroblasts versus control ones. **(A)** The volcano plot depicts all proteins identified in fibroblasts, making a clear delimitation between the statistically significant and non-significant quantified proteins (p-ANOVA < 0.05; horizontal line). Proteins with decreased abundances are represented in red, while the upregulated ones are highlighted in green color. **(B)** *In silico* analyses of proteomic findings included pathway analysis of the regulated proteins. All proteins with altered abundances were searched using KEGG, DAVID, and Reactome databases for protein pathway annotation. Vulnerable pathways (left *Y*-axis) were color-coded and referred to affected proteins (right *Y*-axis). Fold of regulation of the individual proteins is indicated on the *X*-axis. GGA1, ADP-ribosylation factor-binding protein GGA1; SMARCB1, SWI/SNF-related matrix-associated actin-dependent regulator of chromatin subfamily B member 1; SDHB, succinate dehydrogenase; SOAT1, Sterol *O*-acyltransferase 1; CHMP6, charged multivesicular body protein 6; ACADSB, short/branched chain specific acyl-CoA dehydrogenase; ETHE1, persulfide dioxygenase ETHE1; SERPINE2, Glia-derived nexin; PLPP1, phospholipid phosphatase 1; PLIN2, perilipin-2; PTRH2, peptidyl-tRNA hydrolase 2; AARS, alanine–tRNA ligase, cytoplasmic; ALAD, delta-aminolevulinic acid dehydratase; SYNPO2, synaptopodin-2; OCIAD2, OCIA domain-containing protein 2; SF3B4, splicing factor 3B subunit 4; HTATSF1, HIV tat-specific factor 1; APOOL, MICOS complex subunit MIC27; ADD3, gamma-adducin; DNAJC3, DnaJ homolog subfamily C member 3.

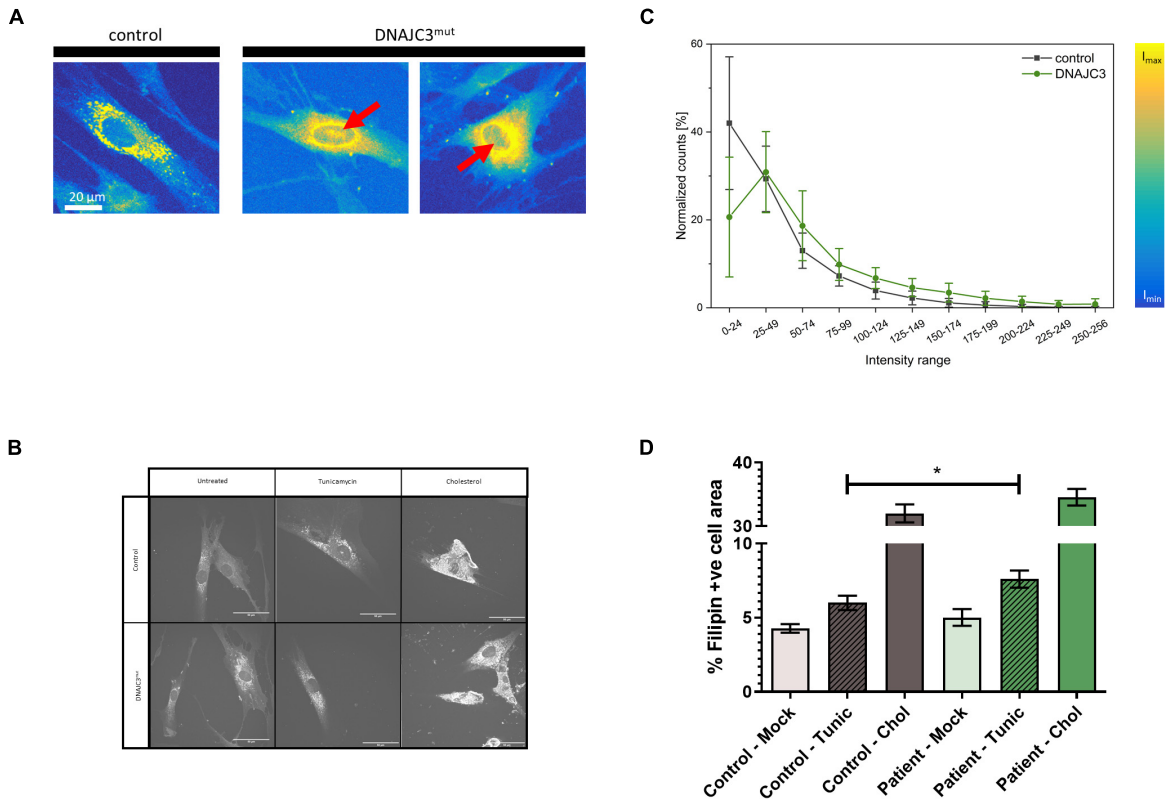

FIGURE 2 | Lipid-level in DNAJC3-pathophysiology. **(A)** Results of BODIPY staining are shown for one representative fibroblast derived from controls (*left panel*) and two from DNAJC3 patients (*right panel*). Notably, in DNAJC3^{mut} cells, nuclear accumulated BODIPY staining can be observed (red arrows), which is absent in controls. **(B)** Single-cell histogram analysis: comparison of intensity histograms for DNAJC3^{mut} cells (green circles) with control cells (gray squares). Two samples per group were analyzed and at least 10 individual cells were used per sample for statistical analyses. For each cell, a histogram analysis was performed giving the frequency of intensity values in the specified ranges. Counts per intensity range were normalized to percentage values for individual cells before calculating the mean and standard deviation for each group. DNAJC3^{mut} fibroblasts tend to have more points with high fluorescence intensity than control cells, indicating an increased level of BODIPY stained lipids and thus an agglomeration/accumulation of lipids in these cells. **(C)** Confocal microscope images of Filipin III staining are shown for one representative fibroblast derived from controls and one DNAJC3 patient in the presence or absence of cholesterol or Tunicamycin. **(D)** Quantification of mean Filipin III positive area relative to cell area (%) for DNAJC3^{mut} and control fibroblasts. Both tunicamycin (Tunic) and cholesterol stress (Chol) treatments increase % Filipin positive area relative to control ($p < 0.01$, Student's *t*-test with Welch's correction) in both DNAJC3^{mut} and control, with * indicating statistical significance between DNAJC3^{mut} and control groups of the same treatment type.

the secretory machinery, DNAJC3 mutant fibroblasts exhibit ER dysfunction (Synofzik et al., 2014). An increased sensitivity against additional ER stress burden was identified in DNAJC3-silenced rat and human β cells (Lytrivi et al., 2021). Notably, several publications demonstrated that cellular cholesterol accumulation leads to UPR activation (Feng et al., 2003; Cunha et al., 2008; Fu et al., 2011). DNAJC3^{mut} fibroblasts present a higher tendency of cholesterol aggregation compared to control cells (**Figures 2C,D**). Taking these findings into consideration, and the fact that neurons (as the vulnerable cellular population of the DNAJC3-phenotype) present with a more pronounced sensitivity against both ER stress and lipid accumulation (Jazvinscak Jembrek et al., 2015), DNAJC3^{mut} and control fibroblasts were further stressed by cholesterol overload to exacerbate ER stress. Parallel reaction monitoring (PRM) was employed to evaluate the respective activation of the UPR (**Figure 3A**). Statistically significant increases ($p < 0.05$) following cholesterol overload were observed for targets in both patient and control fibroblasts. Remarkably, ATF3, DDIT3, ERN1, PR15A, and XBP1 were significantly increased in DNAJC3^{mut} fibroblasts compared to controls (**Figure 3A**). To further elucidate an increased sensitivity of DNAJC3^{mut} fibroblasts against additional ER stress burden, additional immunoblot studies were carried out: BiP, major chaperone of the ER and a key modulator of UPR (Dudek et al., 2009), along with its co-chaperone GRP170 and SIGMAR1, SEC63, and HSP90. We observed an increase in BIP, SEC63, and SIGMAR1 proteins in DNAJC3^{mut} fibroblasts compared to controls. Furthermore, cholesterol treatment leads to a more significant increase of these proteins in DNAJC3^{mut} fibroblasts than controls, suggestive of an increased vulnerability toward ER stress upon cholesterol loading (**Figures 3B,C**). We observed a considerable increase in eIF2α phosphorylation, a master regulator of protein translation upon stress (Boye and Grallert, 2020), while PERK shows a mild increase in DNAJC3^{mut} fibroblasts after cholesterol-treatment (**Figures 3B,C**), which constitutes a hallmark of ER stress and

UPR activation. ATF4 shows a decrease in cholesterol-stressed control fibroblasts in contrast with the increase observed in DNAJC3^{mut} cells after treatment (**Figures 3B,C**). Moreover, ATF6, one of the main UPR branches, seems unaffected by the loss of function of DNAJC3. Our combined proteomic and immunoblot findings suggest that loss of DNAJC3 leads to a very mild UPR activation with a slight increase of some UPR-modulated proteins under basal conditions, while further stress caused by cholesterol accumulation leads to an increase in UPR-associated proteins, which is more severe in DNAJC3^{mut} cells (**Figure 3**).

Cholesterol Accumulation Affects Mitochondrial Homeostasis

The upregulation of several proteins involved in mitochondrial biogenesis observed in the DNAJC3^{mut} proteome (**Figure 1**) prompted us to examine the mitochondrial function in DNAJC3^{mut} fibroblasts. We evaluated mitochondrial function and the structure of mitochondrial networks in control and DNAJC3^{mut} fibroblasts using a redox staining (Mitotracker), with and without cholesterol treatment. Cholesterol treatment induced a clear fragmentation of the mitochondrial network in DNAJC3^{mut} and control cells (**Figure 4A**), indicating that cholesterol treatment induced combined ER/mitochondrial stress. As network imaging by redox staining is dependent on the membrane potential, differences in dye incorporation as a result of cholesterol treatment may be caused by changes in mitochondrial membrane potential. However, further studies would be needed to clarify this.

Next, we investigated mitochondrial copy number in control and DNAJC3^{mut} fibroblasts under basal conditions and after cholesterol treatment. Neither loss of DNAJC3 or cholesterol treatment affected mtDNA copy number, despite the associated changes in mitochondrial morphology (**Figure 4B**).

To further elucidate the effects upon loss of functional DNAJC3 on mitochondria, immunoblot studies focusing on expression of all five mitochondrial complexes were performed. DNAJC3^{mut} fibroblasts display a statistically significant increase in complex I (NDUFB8), complex II (SDHB), complex III (UQCRC2), and complex V (ATP5A) compared to controls, suggestive of a oxidative phosphorylation (OXPHOS) defect. Cholesterol treatment induces an increase in in mitochondrial complexes in both control and patient fibroblasts (**Figure 4C**) with a statistically significant increase of complexes I and III in DNAJC3 cells compared to controls (**Figure 4C**). These biochemical findings suggest that cholesterol accumulation leads to secondary upregulation of the respiratory complexes in DNAJC3^{mut} and, less prominently, in control cells (**Figure 4C**).

To determine whether the upregulation observed in the OXPHOS system has a functional effect on bioenergetic capacity, we performed oxygen consumption studies by Seahorse assay. DNAJC3^{mut} cells have increased basal respiration compared to controls, in accordance with the increased levels of mitochondrial complexes. In contrast, cholesterol-treated DNAJC3^{mut} and control cells show a decrease in basal respiration, ATP-linked respiration, and non-mitochondrial respiration compared to mock-treated cells. The decrease in maximal respiratory capacity after cholesterol treatment was greater in DNAJC3^{mut} cells compared to controls, suggesting that cholesterol treatment is compromising the compensatory capacity of DNAJC3^{mut} cells (**Figure 4D**). Additionally, we can observe an increase in non-mitochondrial respiration (**Figure 4D**) in DNAJC3^{mut} cells compared to controls, suggestive of the hindered bioenergetic health of the cells. This type of respiration has been suggested to increase in the presence of different stressors such as oxygen reactive species (Dranka et al., 2010; Hill et al., 2012).

DNAJC3 Mutant Fibroblasts Have Disrupted Regulation of Intracellular Amyloid Precursor Protein

ER stress may lead to an accumulation of β-amyloid (Aβ) and amyloid precursor protein (APP), and indeed stimulation of expression of other DnaJ family BiP co-chaperones has been shown to ameliorate the accumulation of Aβ in cellular Alzheimer's disease models (Evans et al., 2006; Mansson et al., 2014). Moreover, impaired cholesterol homeostasis has been previously linked to Aβ accumulation (Ledesma and Dotti, 2006). These previously reported findings prompted us to study APP and Aβ in DNAJC3^{mut} fibroblasts compared to controls. Our findings show that cellular loss of functional DNAJC3 results in a significant increase of monomeric APP (**Figure 5B**). Moreover, DNAJC3^{mut} fibroblasts present two extra bands at higher molecular weight corresponding to the immature and mature dimeric form of APP (**Figure 5B**). Similar to DNAJC3^{mut} cells, cholesterol treatment in control cells leads to an increased level of APP compared to the mock-treated controls but without dimerization of APP (**Figures 5A,B**), suggesting that DNAJC3 loss impacts APP dimerization. The increase in the mature and immature APP dimers after cholesterol treatment in DNAJC3^{mut} cells suggests that the additional ER stress triggered by cholesterol treatment and cholesterol accumulation exacerbates this process. It is also worth noting that cholesterol treatment of DNAJC3^{mut} fibroblasts has no impact on the monomeric APP (**Figures 5A,B**).

Next, we assessed the apoptosis in our cell models. Both DNAJC3^{mut} and control cells show similar levels of procaspase (uncleaved caspase-3), while the cleavage product that indicate caspase-3 (CASP3) activation increases in DNAJC3^{mut} cells (**Figures 5A,B**). Cholesterol treatment led to increased CASP3 activation in both patient and control cells, suggesting that the increased stress burden of lipid accumulation induces apoptosis.

DNAJC3^{mut} cells display increased immunoreactivity to anti-Aβ antibody compared to control cells (**Figure 5C**). Cholesterol treatment leads to a significant increase in controls, while patient cells present a non-significant, smaller increase when compared to mock-treated DNAJC3 cells. Interestingly, despite cholesterol accumulation not significantly modifying the amount of Aβ deposition in DNAJC3 cells, we can observe that it induces a major change in the pattern of Aβ, which forms bigger clusters, found mostly around the perinuclear and nuclear region (**Figure 5C**). Cholesterol treatment of control cells does not seem to induce a change in Aβ cluster size and pattern as seen in treated mutant cells. Given that anti-Aβ staining does not

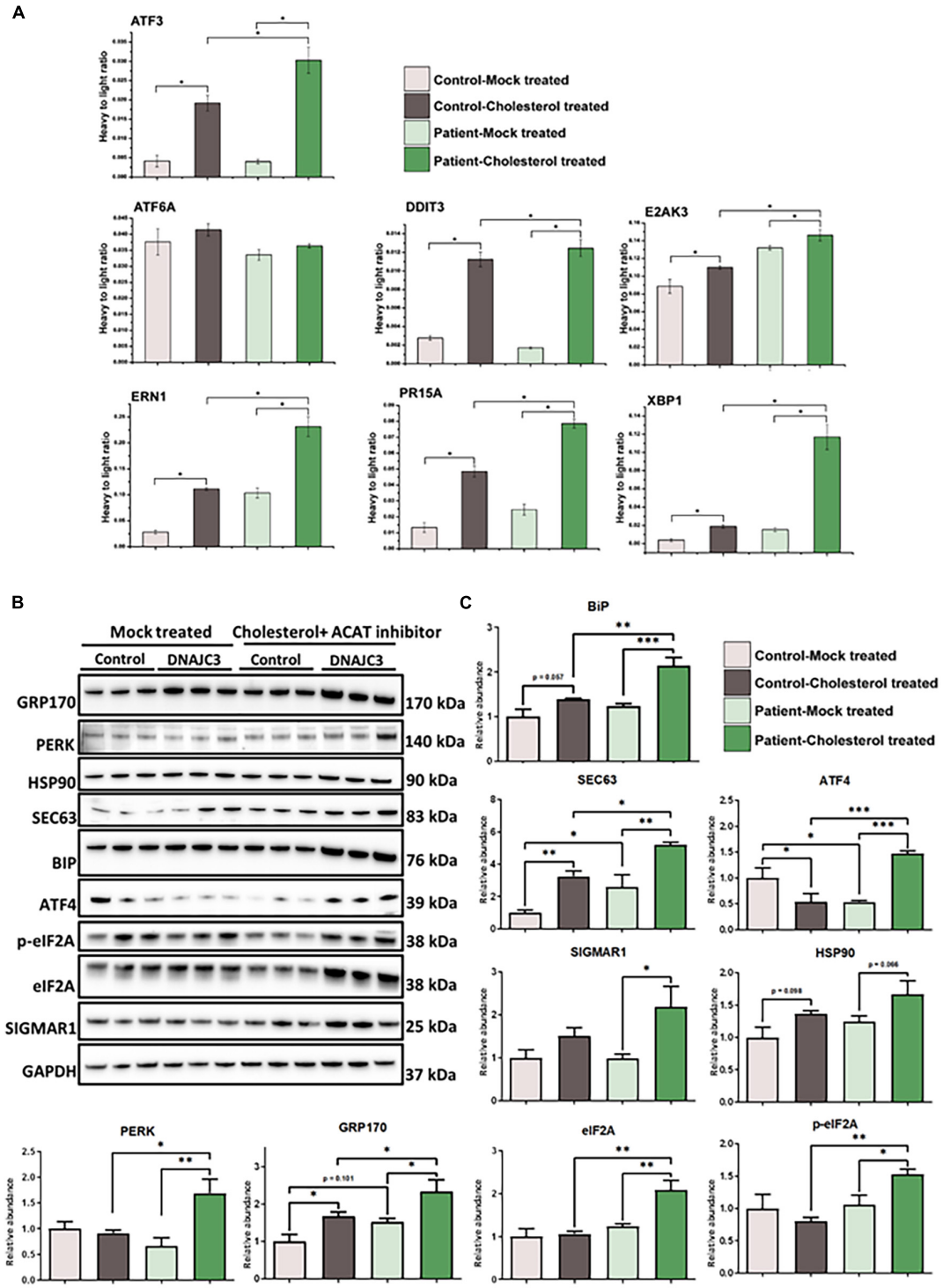

FIGURE 3 | Endoplasmic reticulum (ER) stress in DNAJC3^{mut} fibroblasts. **(A)** Mean values (two technical and two biological replicates for each sample type, respectively) of PRM-based quantification of known ER stress-related proteins following treatment with either DMSO (mock) or soluble cholesterol + ACAT inhibitor in patient and control fibroblasts, respectively. Cholesterol treatment and concomitant inhibition of cholesterol acyltransferase (ACAT; esterifies cholesterol) resulted in pronounced ER stress in both DNAJC3^{mut} and control fibroblasts. Notably, significantly greater increases in ER stress protein expression was seen following soluble cholesterol treatment for ATF3 ($p = 0.026$), DDIT3 ($p = 0.031$), ERN1 ($p = 0.049$), PR15A ($p = 0.028$), and XBP1 ($p = 0.003$) in treated DNAJC3^{mut} cells. Student's *t*-tests compared either mock-treated or cholesterol-treated control versus the correspondingly treated DNAJC3^{mut} fibroblasts. Student's *t*-test ($n = 2$) of changes between mock-treated and cholesterol-treated expression levels is statistically significant between mock-treated DNAJC3^{mut} versus control fibroblasts for ATF3

(Continued)

FIGURE 3 | (Continued)
($p = 0.027$), DDIT3 ($p = 0.031$), ERN1 ($p = 0.049$), PR15A ($p = 0.029$), and XBP1 ($p = 0.0033$). Targeted peptides were ATF3: NFLIQQIK; ATF6: EAQDTSDGIIQK; DDIT3: VAQLAEENER; E2AK3: FLDNPHYNK; ERN1: FPNNLP; PR15A: GAALVEAGLEGEAR and XBP1: LLLENQLLR. **(B)** Results of immunoblot analysis of UPR markers in two DNAJC3-patient-derived and three control cells (treated under the same conditions as for the PRM ER stress investigations) showing changes in UPR markers in DNAJC3 cholesterol-treated cells, thus underlining the vulnerability of these cells to lipid accumulation. GAPDH was used to show equal loading. **(C)** Densitometry analysis of the immunoblotting from panel **(B)**. Graphs show mean±SD of triplicate samples (control fibroblasts and DNAJC3^{mut} fibroblasts under mock-treated and cholesterol-treated). For statistical analysis, Fisher's LSD test was employed where $^{*}p \leq 0.05$, $^{**}p \leq 0.01$, $^{***}p \leq 0.001$ was considered as statistically significant.

detect Aβ in controls cultured under basal conditions, cholesterol treatment seems to trigger accumulation of Aβ even in controls. This finding in turn supports the concept that lipid buildup leads to an increase of Aβ peptide production (Shobab et al., 2005).

Intracellular trafficking of APP through Golgi is crucial for the generation of Aβ (Choy et al., 2012). Thus, we investigated Golgi integrity in fibroblasts using immunofluorescence (**Figure 5C**). Our data show a tightly compacted Golgi in perinuclear localization in control cells while some DNAJC3^{mut} cells present with a more sparce Golgi. Cholesterol treatment does not have any structural effects in controls, while DNAJC3^{mut} display a scattered Golgi, suggesting a vulnerability of this compartment upon lipid loading in patient cells.

DISCUSSION

Bi-allelic loss-of-function mutations in *DNAJC3*, encoding a co-chaperone of BiP, one of the major chaperones of the ER, have been shown to cause neurodegeneration with early-onset ataxia, upper-motor-neuron signs, demyelinating neuropathy, and cerebral atrophy associated with diabetes mellitus (Synofzik et al., 2014). Mutations in genes encoding BiP co-chaperones, localized in the ER or proteins involved in the UPR-modulation have been associated with central and peripheral nervous system abnormalities and non-autoimmune type insulin-dependent diabetes. For example, SIL1 is one of the main co-chaperones of BiP involved in the ATP-ADP cycle, and recessive *SIL1* mutations have been associated with MSS characterized by congenital cataracts, cerebellar ataxia, progressive muscle weakness, and delayed psychomotor development as well as axonal degeneration and disintegration of the neuromuscular junctions (Phan et al., 2019). Clinically overlapping features have been found in patients with recessive *DNAJC3* mutations (Synofzik et al., 2014). Remarkably, a modulating function of DNAJC3 expression in cerebellar degeneration has been demonstrated in the molecular etiology of MSS (Zhao et al., 2010), demonstrating a crucial role of this co-chaperone in neuronal maintenance. Other examples are Wolfram syndrome, caused by mutations in *WFS1* presenting with early-onset ataxia, cognitive deficits, and hearing loss, thus also including clinical hallmarks of the phenotype associated with *DNAJC3* mutations (Khanim et al., 2001) and Wollcot-Rallison syndrome, an autosomal recessive disorder caused by mutations in eukaryotic translation initiation factor 2-alpha kinase 3 (*E2AK3*), characterized by insulin-dependent diabetes, growth retardation, and intellectual disability (Delepine et al., 2000). In addition, a mutation in the *Sec61a1* gene (p.Tyr344His) results in excessive ER stress and apoptosis of pancreatic β cells in C57BL/6 mice, resulting in diabetes and hepatosteatosis (Linxweiler et al., 2017).

To obtain insights into the mechanism underlying the pathophysiology of mutations in *DNAJC3,* unbiased proteomic studies utilizing patient-derived fibroblasts were carried out (**Figure 1**). While fibroblasts are not the primary site of clinical manifestation, these cell models have been previously shown to be suitable to study the etiology of rare neurological diseases (Hentschel et al., 2021) and show very similar levels of DNAJC3 expression to peripheral nerve (**Supplementary Figure 1**). Results of this profiling suggest that lipid metabolism is affected by DNAJC3^{mut} mutations (**Figure 1**) as Sterol-*O*-acyltransferase 1 (SOAT1), an enzyme responsible for the esterification of fatty acids, especially cholesterol (Das et al., 2008), was found to be decreased. Lower levels of SOAT1 were previously linked to a hindered cholesterol clearance suggesting that DNAJC3-deficient cells present an accumulation of cholesterol (Tabas, 2002; Luo et al., 2010). We detected decreased abundance of Periplin 2 (PLIN2), an enzyme involved in lipid droplet formation, which has been linked to acute cholesterol accumulation (Makino et al., 2016), further suggesting a lipid dysregulation in fibroblasts lacking functional DNAJC3. Our functional data on cholesterol and lipid accumulation using immunofluorescence bring further evidence of lipid accumulation in DNAJC3^{mut} cells (**Figure 2**). Cholesterol homeostasis is essential for neuronal functioning and brain development, while perturbed cholesterol metabolism is a major pathophysiological mechanism in neurological diseases such as Alzheimer's disease and Niemann-Pick type C disease, an autosomal recessive storage disorder, characterized by abnormal sequestration of unesterified cholesterol in cells (Fernandez et al., 2009; Marquer et al., 2014).

Label-free proteomics revealed that DNAJC3 is the most decreased protein in the mutant fibroblasts in alignment with previously published results (Synofzik et al., 2014), emphasizing the sensitivity of our proteomic profiling approach. Although DNAJC3 has been widely acknowledged in the attenuation of proteins involved in the initial ER response (Schorr et al., 2015), changes in ER morphology or increased ER calcium leakage were not described previously in the context of the underlying pathophysiology (Synofzik et al., 2014). However, an increased sensitivity against additional ER stress burden was identified in *DNAJC3*-silenced rat and human β cells (Lytrivi et al., 2021). In accordance with these previous observations, our findings suggest only a minor UPR-activation mirrored by the altered abundance of ER-stress-related proteins (**Figure 3**). DNAJC3 has been shown to bind the kinase domain of PERK (also called EIF2AK3), in order to terminate the first phase of ER

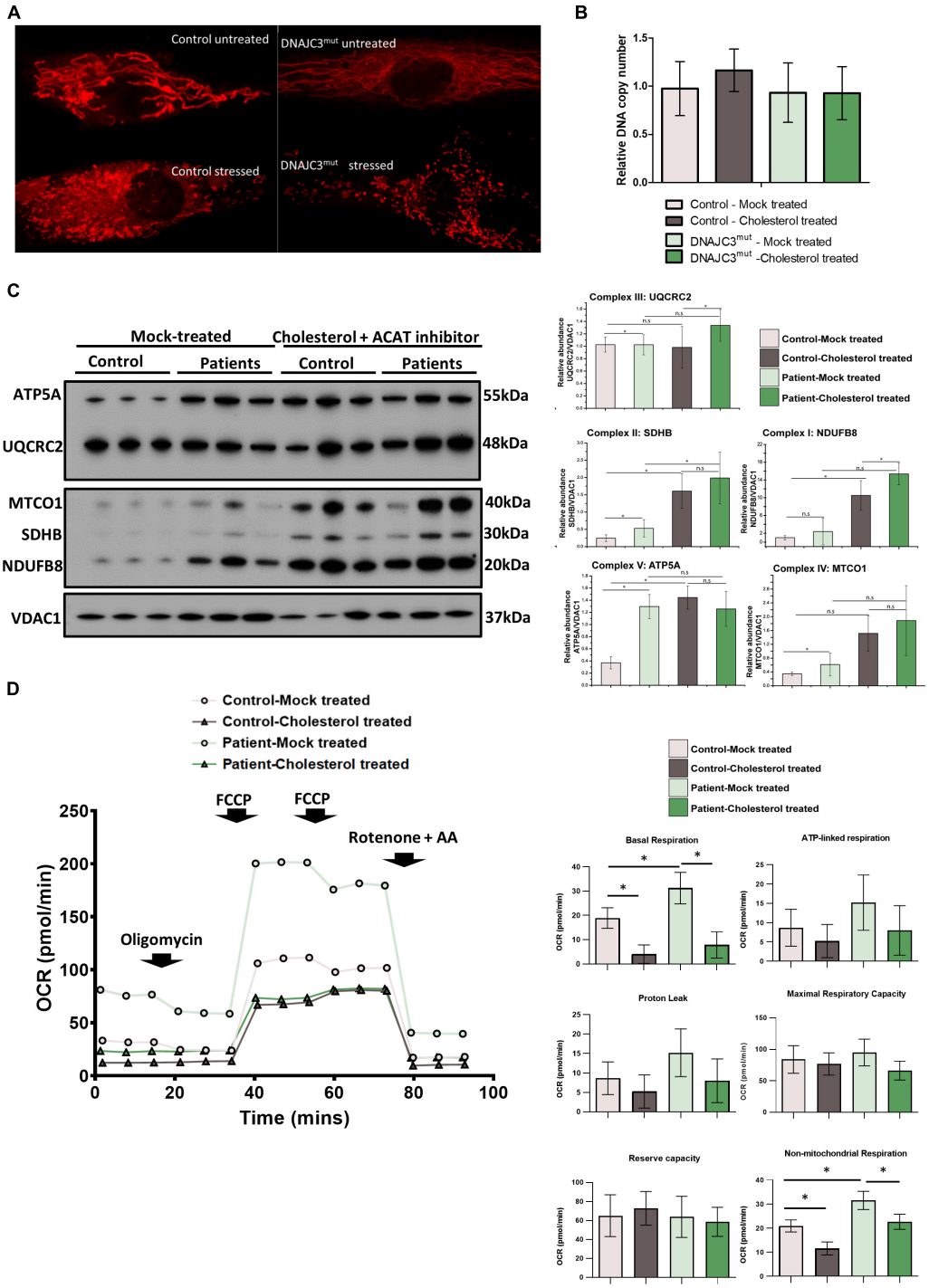

FIGURE 4 | Study of mitochondrial integrity in DNAJC3 pathophysiology. **(A)** Mitotracker staining in DNAJC3^{mut} and control fibroblasts revealed a more fragmented mitochondria in patient cells with reduced staining in DNAJC3^{mut} cells compared to controls. One representative cell is presented per condition, whereby 30 cells have been studied for each of the analyzed conditions. **(B)** Mean mitochondrial DNA copy number quantitative real-time PCR relative abundances (two technical and two biological replicates for each sample type, respectively) show that cholesterol overload results in a mild increase of mtDNA copy in control but not in DNAJC3^{mut} fibroblasts. **(C)** Immunoblot studies of the mitochondrial respiratory chain complexes I–V (*left panel*) revealed a significant increase of complex I and II as well as IV and V in DNAJC3^{mut} cells, which was more pronounced in DNAJC3^{mut} cells after cholesterol-treatment; *t-test < 0.05. Level of the proteins representing the different complexes have been normalized to VDAC1. Densitometry analysis of the Western blotting results is represented in the right panel. **(D)** Mean oxygen consumption rate (OCR) of two biological replicates for each condition (each consisting of ≥12 technical replicates). Statistical significance indicated between treated versus non-treated DNAJC^{mut} or control cells, and between DNAJC^{mut} versus control cells under either treated or non-treated conditions. Student's t-test, *$p < 0.05$.

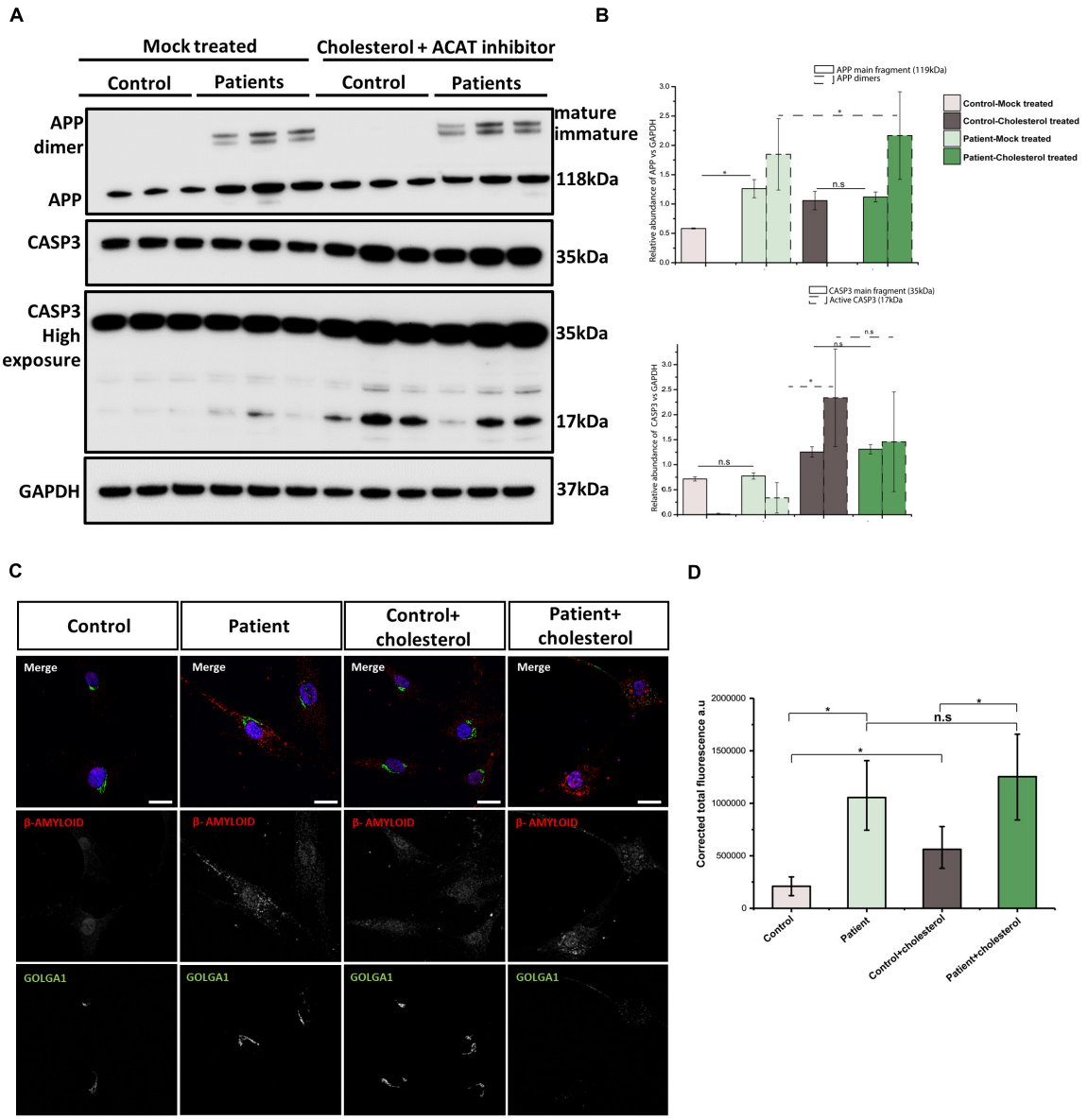

FIGURE 5 | Analysis of amyloid accumulation in DNAJC3^{mut} cells. **(A)** Immunoblotting of APP reveals increased levels of this protein monomer in DNAJC3^{mut} cells, while cholesterol treatment leads to a further increase only in control cells. **(B)** Densitometry analysis of immunoblotting from panel **(A)**. Graphs show ±SD of triplicate samples, and all data were normalized to GAPDH. The mature and immature APP dimers on immunoblotting are present only in the DNAJC3^{mut} cells and cholesterol treatment increases the amount of these proteins, which are further cleaved to form the β-amyloid (Aβ) fragment. Cholesterol treatment induced an activation of caspase-3 protein (corresponding to the 17-kDa fragment), indicating an increase in apoptosis Student's *t*-test, $^{*}p < 0.05$. **(C)** Representative Aβ and GOLOGA1 staining in control and DNAJC3^{mut} cells in the presence and absence of cholesterol. Bar plots represent the corrected total florescence measured for the Aβ in three DNAJC3^{mut} and three controls in mock and cholesterol-treated cells. Immunofluorescence analysis shows that DNAJC3^{mut} fibroblasts present an increase in Aβ while the cholesterol treatment exacerbates the accumulation of the toxic fragment in patient cells. The cholesterol treatment leads to a slight increase in the Aβ in control cells as well; $^{*}t$-test < 0.05.

stress (Yan et al., 2002). Given that DNAJC3^{mut} fibroblasts show slightly increased PERK expression (**Figures 3B,C**), its activation is presumably not terminated by DNAJC3 loss of function.

The ER has been described to tightly regulate the lipid metabolism as it is involved in the synthesis of phospholipids, re-esterification of sterols, and lipid-membrane biosynthesis (Volmer and Ron, 2015). Cholesterol accumulation disturbs the free cholesterol:phospholipid ratio on the normally fluid ER membrane, thus leading to the activation of ER stress (Feng et al., 2003). The impaired lipid/cholesterol metabolism in DNAJC3^{mut} cells was demonstrated by our Filipin-III and BODIPY staining affects ER maintenance and results in irregular lipid accumulation, supporting the concept of perturbed ER membrane structure. Additionally, induction of ER stress with

tunicamycin leads to an increase in cholesterol accumulation in both control and patient cells, but with a more pronounced effect in DNAJC3 cells. We detected increased vulnerability of the ER in DNAJC3^{mut} cells after cholesterol treatment (**Figure 3**) similar to a previous study on *DNAJC3*-silenced rat and human β cells (Lytrivi et al., 2021). These findings provide evidence that lipid accumulation leads to ER stress activation, which is exacerbated in DNAJC3^{mut} patient cells.

There are numerous contact sites between ER and mitochondria [Mitochondria Associated ER Membranes (MAM)], which may enable cholesterol influx from the ER to the mitochondria (Arenas et al., 2017). The interaction of ER and mitochondrial membranes links mitochondrial dysfunction to ER stress. Our proteomic profiling data indicated that DNAJC3^{mut} fibroblasts present with mitochondrial alterations. We found that proteins involved in the maintenance of mitochondrial architecture and biogenesis (APOOL), fatty acid metabolism (ACDSB), or mitochondrial respiratory chain complexes (such as complex II, SDHB) are dysregulated as a results of DNAJC3 loss, suggestive of mitochondrial dysfunction. Further investigation in DNAJC3^{mut} fibroblasts revealed significantly increased level of mitochondrial respiratory chain subunits (except for complex IV) (**Figure 4C**) in line with the significant increase in basal respiration, which can be attributed to a possible increase in cellular energy demands. Mitochondrial respiration has been shown previously to increase due to ER stress (Balsa et al., 2019) and can constitute a pro-survival mechanism from ER stress (Knupp et al., 2019).

Mitochondria are organelles sparse in cholesterol; however, the transport of this lipid to the inner mitochondrial membrane *via* MAM proteins is tightly regulated and of physiological importance (Rone et al., 2009; Marriott et al., 2012). Cholesterol treatment of control and DNAJC3^{mut} fibroblast cells induced clear mitochondrial fragmentation altering the dynamics of the mitochondrial membranes (**Figure 4**) and leads to an increase in OXPHOS complexes in control cells, and an even greater increase in Complex I and III in DNAJC3^{mut} cells when compared to controls (**Figure 4C**). These changes have been previously associated with depletion of glutathione (GSH) (Fernandez et al., 2009). An increase of complex III has been associated with lower GSH levels and with an increase in mitochondrial depolarization, which leads to the release of Cytochrome *c* and activation of caspase-3 (Fernandez et al., 2009). Lipid overload increases caspase-3 levels in both control and patient cells, showing that cholesterol accumulation is a pro-apoptotic factor (**Figures 5A,C**). This may suggest that cholesterol overload exacerbates the DNAJC3^{mut} phenotype to further deplete GSH levels, finally leading to apoptosis. Further experiments focusing on apoptosis key factors would be needed to determine exactly the role of DNJC3 and lipid accumulation in cell death promotion. These findings accord with previous studies in DNAJC3-silenced rat and human β cells (Lytrivi et al., 2021), and in turn could also explain why non-mitochondrial respiration increases dramatically in DNAJC3^{mut} fibroblasts and in cells exposed to cholesterol (**Figure 4D**).

Endoplasmic reticulum stress, mitochondrial dysfunction, and cholesterol metabolism are thought to cause type 2 diabetes mellitus *via* activation of inflammatory pathways thereby inhibiting insulin secretion. Cholesterol treatment of pancreatic β cells triggers apoptosis and ER stress, while inhibition of cholesterol prevents β-cell apoptosis. However, *DNAJC3*-silencing rat and human β cells did not result in perturbed insulin production (Lytrivi et al., 2021).

β-Amyloid regulates the cholesterol flux to the mitochondria and interacts with components of the OXPHOS and thus participates in the molecular etiology of neurodegenerative diseases (Fernandez et al., 2009; Barbero-Camps et al., 2014). Disturbed cholesterol homeostasis has also been shown to affect Aβ accumulation, as cholesterol enhanced the aggregation of Aβ by inhibiting the degradation of this peptide (Yip et al., 2001; Ehehalt et al., 2003). Additionally, the C terminal APP fragment has been shown to regulate lipid homeostasis by acting as a cholesterol sensor in the membrane, contributing to the early pathology in Alzheimer's disease (DelBove et al., 2019; Montesinos et al., 2020). Here, we detected the altered level of GGA1 (**Figure 1**), a Golgi protein that controls APP processing (von Arnim et al., 2006) and Golgi alterations (**Figure 5C**), suggesting that Aβ accumulation (a known hallmark in different neurodegenerative diseases) might be involved in cellular perturbations in DNAJC3^{mut} cells. Indeed, DNAJC3^{mut} cells present with an increase in APP, which is not further affected by cholesterol treatment (**Figure 5**). We also detected two additional bands in the immunoblot corresponding to the mature and immature APP dimer (*N*- and *O*-glycosylated forms of APP dimers) (Isbert et al., 2012), supporting the concept of Aβ accumulation in DNAJC3^{mut} cells, which may further contribute to the neurodegenerative phenotype.

In summary, we show that *DNAJC3* mutations affect cellular lipid metabolism leading to (i) altered ER sensitivity toward stress burden, (ii) mitochondrial vulnerability, and (iii) Aβ accumulation. Neurons are particularly vulnerable to dysfunction of these pathways, which may explain the specifically neurological manifestation of DNAJC3 deficiency. Hence, our study provides molecular and mechanistic insights into the underlying pathophysiology of this rare disease and informs of the physiological function of DNAJC3.

MATERIALS AND METHODS

Cell Culture

We studied two fibroblast lines carrying a homozygous c.580C > T (NM_006260.4, p.Arg194*) premature stop mutation in *DNAJC3*, one line having a large homozygous deletion of 72 kb spanning *DNAJC3* (and the adjacent *UGGT2* gene), and control fibroblasts from three healthy donors, age and sex matched (Synofzik et al., 2014). Both mutations result in a 50% truncation of *DNAJC3* mRNA (Synofzik et al., 2014). Patient fibroblasts were cultured in Dulbecco's Modified Eagle Media (DMEM) containing 4.5 g/L glucose, L-glutamine (Gibco) and phenol red supplemented with 10% fetal bovine serum (FBS) (Gibco) and 1% (v/v) penicillin/streptomycin solution at 37°C in a 5% CO_2 atmosphere. Fibroblasts were grown to 80% confluence prior to harvesting or applying treatment.

Cholesterol Stress Treatment

Fibroblasts (patient and controls) were stressed by supplementing the growth media with 10 μg/ml Sandoz 58-035 (Sigma-Aldrich) (solubilized in DMSO), an inhibitor of Acyl-CoA-: cholesterol acyltransferase (ACAT-I), for 6 h followed by further supplementation with 30 μg/ml of water-soluble cholesterol (Sigma-Aldrich). After 18 h of exposure to the Sandoz 58-035 and cholesterol, the stress treatment is considered complete; this is referred to now only as "Cholesterol-treated." Patient and control fibroblasts were separately mock-treated with 0.1% DMSO and used as controls, referred to as "mock-treated."

Tunicamycin Treatment of Fibroblasts

Fibroblasts were treated for 18 h with 4 μg/ml Tunicamycin (Sigma-Aldrich). The stock solution of Tunicamycin was prepared using DMSO; thus, control and patient cells were treated with the same amount of DMSO as the Tunicamycin-treated cells and are referred to as "mock treated."

Label Free LC-MS/MS Analysis

Reagents

Ammonium hydrogen carbonate (NH_4HCO_3), anhydrous magnesium chloride ($MgCl_2$), guanidine hydrochloride (GuHCl), iodoacetamide (IAA), and urea were purchased from Sigma-Aldrich, Steinheim, Germany. Tris base was obtained from Applichem Biochemica, Darmstadt, Germany and sodium dodecyl sulfate (SDS) was purchased from Carl Roth, Karlsruhe, Germany. Dithiothreitol (DTT) and EDTA-free protease inhibitor (Complete Mini) tablets were obtained from Roche Diagnostics, Mannheim, Germany. Sodium chloride (NaCl) and calcium chloride ($CaCl_2$) were from Merck, Darmstadt. Sequencing grade modified trypsin was from Promega, Madison, WI USA. Benzonase® Nuclease was purchased from Novagen. Bicinchoninic acid assay (BCA) kit was acquired from Thermo Fisher Scientific, Dreieich, Germany. All chemicals for ultra-pure HPLC solvents such as formic acid (FA), trifluoroacetic acid (TFA), and acetonitrile (ACN) were obtained from Biosolve, Valkenswaard, Netherlands.

Cell Lysis, Sample Clean-Up, and Proteolysis

Fibroblasts of patients with *DNAJC3* mutations (see above) and controls were processed independently. Cells were lysed in 100 μl of 50 mM Tris–HCl (pH 7.8) buffer containing 150 mM NaCl, 1% SDS, and EDTA-free protease inhibitor (Complete Mini) on ice for 15 min. Then samples were centrifuged for 5 min at 4°C and 6,000 × *g* and the protein concentration was determined by BCA assay (according to the manufacturer's protocol). Cysteines were reduced by the addition of 10 mM DTT and samples were incubated at 56°C for 30 min, followed by alkylation of free thiol groups with 30 mM IAA at room temperature (RT) in the dark for 30 min.

Sample preparation was performed using filter-aided sample preparation (FASP) with some minor changes: 100 μg of protein lysate was diluted 10-fold with freshly prepared 8 M urea/100 mM Tris-HCl buffer (pH 8.5) (Burkhart et al., 2012; Kollipara and Zahedi, 2013), placed on PALL microsep centrifugal device (30 kDa cutoff), and centrifuged at 13,500 × *g* at RT for 20 min. Three washing steps were carried out with 100 μl of 8 M urea/100 mM Tris–HCl (pH 8.5) and then the buffer was exchanged by washing the device thrice with 100 μl of 50 mM NH_4HCO_3 (pH 7.8). One hundred microliters of digestion buffer [trypsin (Promega) (1:25 w/w, protease to substrate), 0.2 M GuHCl, and 2 mM $CaCl_2$ in 50 mM NH_4HCO_3 (pH 7.8)] was added to the concentrated proteins, and the samples were incubated at 37°C for 14 h. Resulting tryptic peptides were recovered by centrifugation with 50 μl of 50 mM NH_4HCO_3 followed by 50 μl of ultra-pure water, and the resulting peptides were acidified [pH < 3 by addition of 10% TFA (v/v)]. All digests were quality controlled as described previously (Burkhart et al., 2012).

LC-MS/MS Measurement and Data Analysis

One microgram of each sample was measured using an Ultimate 3000 nano RSLC system coupled to an Orbitrap Fusion Lumos mass spectrometer (both Thermo Scientific) and analyzed in a randomized order to minimize systematic errors. Peptides were preconcentrated on a 100 μm × 2 cm C18 trapping column for 10 min using 0.1% TFA (v/v) at a flow rate of 20 μl/min followed by separation on a 75 μm × 50 cm C18 main column (both Pepmap, Thermo Scientific) with a 120-min LC gradient ranging from 3 to 35% of 84% ACN, 0.1% FA (v/v) at a flow rate of 250 nl/min. MS survey scans were acquired in the Orbitrap from 300 to 1,500 *m/z* at a resolution of 120,000 using the polysiloxane ion at *m/z* 445.12002 as lock mass (Olsen et al., 2005), an automatic gain control target value of 2.0×10^5 and maximum injection times of 50 ms. Top 15 most intense signals were selected for fragmentation by HCD with a collision energy of 30% and MS/MS spectra were acquired in the Iontrap using an automatic gain control target value of 2.0×10^5, a maximum injection time of 300 ms, a dynamic exclusion of 15 s.

Data analysis was performed using the Progenesis LC-MS software from Non-linear Dynamics (Newcastle upon Tyne, United Kingdom). Raw MS data were aligned by Progenesis, which automatically selected one of the LC-MS files as reference. After automatic peak picking, only features within retention time and *m/z* windows from 0 to 120 min and 300–1,500 *m/z*, with charge states +2, +3, and +4 were considered for peptide statistics and analysis of variance (ANOVA) and MS/MS spectra were exported as peak lists. Peak lists were searched against a concatenated target/decoy version of the human UniProt database (downloaded on July 22, 2015 containing 20,273 target sequences) using Mascot 2.4 (Matrix Science, Boston, MA, United States), MS-GF+, X!Tandem, and MyriMatch with the help of searchGUI 3.2.5 (Vaudel et al., 2011). Trypsin was selected as enzyme with a maximum of two missed cleavages, carbamidomethylation of Cys was set as fixed, and oxidation of Met was selected as variable modification. MS and MS/MS tolerances were set to 10 ppm and 0.5 Da, respectively.

To obtain peptide-spectrum match and to maximize the number of identified peptides and proteins at a given quality, we used PeptideShaker software 1.4.0 (Vaudel et al., 2015). Combined search results were filtered at a false discovery rate (FDR) of 1% on the peptide and protein level and exported

using the PeptideShaker features that allow direct re-import of the quality-controlled data into Progenesis. Only proteins that were quantified with unique peptides were exported. For each protein, the average of the normalized abundances (obtained from Progenesis) from the analyses was calculated in order to determine the ratios between the patient and control fibroblast lysates. Only proteins that were (i) commonly quantified in all the replicates with (ii) one unique peptide, (iii) an ANOVA p-value of $\leq$0.05 (Progenesis), and (iv) an average $\log_2$ ratio ≤ -1.17 or $\geq$1.7 were considered as dysregulated.

Pathway analysis on the label-free proteomics data was performed using GO term analysis (biological function) enrichment utilizing UniProt (available on www.uniprot.com).

Parallel Reaction Monitoring of Unfolded Protein Response

The synthetic isotopic labeled (SIL) peptides were synthesized in-house and absolute quantified using amino acid analysis (AAA), which was performed as previously described (Nguyen et al., 2019). Tryptic peptides from cholesterol-treated and mock-treated DNAJC3^{mut} and control cells were obtained *via* FASP as described in the previous section. For the measurements, between 212.9 and 1,907.5 amol of the SIL peptides was spiked in each sample containing ∼1 μg of total tryptic peptides. The amounts and sequence of the spiked-in peptide are listed in **Supplementary Table 1**. For this experiment, we have employed two DNAJC3^{mut} patient cell lines from which one has a homozygous c.580C > T (NM_006260.4, p.Arg194*) premature stop mutation in *DNAJC3* and one has a large homozygous deletion of 72 kb spanning *DNAJC3* and two age- and sex-matched controls.

Liquid Chromatography and Mass Spectrometry

For the separation and detection of peptides, an Ultimate 3000 Rapid Separation Liquid Chromatography (RSLC) nano system equipped with ProFlow flow control device was coupled to an Orbitrap Fusion Lumos Tribrid Mass Spectrometer equipped with a nano-electrospray ion source (all from Thermo Scientific, Bremen, Germany). The peptide separation was performed as described previously (Nguyen et al., 2019). The nano-electrospray ion source was run using positive ion mode at a spray voltage of 1,800 V. The mass detection and quantification were performed with the normalized collision energy at 32%, automated gain control (AGC) target value at 2×10^5, resolution at 240,000, isolation width at a mass-to-charge value of 0.4, and injection time at 600 ms.

Data Analysis

Skyline 64-bit version 3.7.0.11317 (MacLean et al., 2010) was used to generate methods and analyze the raw data after measurement. All generated data were reviewed and integrated manually. The choice of peptide as well as the monitored fragments were adapted from Nguyen et al. (2019). The light-to-heavy ratio was built from the total area of all monitored fragments of endogenous peptides (light) and SIL peptides (heavy). All the measurements were performed with two technical replicates.

Mitochondrial Network Analysis

Mitotracker-redTM (MTR) (ThermoFisher), a membrane potential-sensitive dye, was used to label the mitochondria in fibroblasts. Cells were seeded to glass-bottomed dishes 24 h prior to cholesterol stress treatment. Fibroblast growth media was aspirated, and cells were incubated in staining media constituted of minimal essential medium (Gibco), without phenol-red, 10% FBS, and 75 nM MTR for 30 min at 37°C prior to imaging.

Imaging of the mitochondrial network was performed using a Nikon A1R confocal microscope to capture three-dimensional stacks of images, which were then processed to make two-dimensional maximum intensity projections of the mitochondrial network.

Mitochondrial Oxygen Consumption Assay

For this experiment, we use two DNAJC3^{mut} patient cell lines, one with homozygous c.580C > T (NM_006260.4, p.Arg194*) premature stop mutation in *DNAJC3* and the other a large homozygous deletion of 72 kb spanning *DNAJC3*, with two age- and sex-matched healthy controls. The oxygen consumption rate (OCR) of fibroblasts was measured using an XF96 Extracellular Flux Analyzer (Seahorse Bioscience, Agilent Technologies). Fibroblasts were seeded into wells of the 96-well cell culture microplate (Seahorse Bioscience) in 80 μl for 24 h prior to cholesterol stress treatment in the microplate. After this, cell media was replaced with 180 μl of bicarbonate-free DMEM and incubated for 30 min. Supplementation of the media with oligomycin, carbonyl cyanide-*p*-trifluoromethoxy-phenylhydrazone (FCCP), rotenone, and antimycin allows the determination of oxygen consumption rates attributable to basal respiration, proton leakage, maximal respiratory capacity, and non-mitochondrial respiration. ATP-linked respiration and reserve capacity were also calculated. Inhibition of ATP synthase by supplementation of media with oligomycin allows the calculation of ATP-synthesis-linked oxygen consumption. Subsequent supplementation with the uncoupling agent maximizes the respiratory rate. OCR levels were normalized to cellular mass, estimated by total well protein measured by Bradford assay.

Quantification of Mitochondrial DNA Copy Number

The relative mtDNA copy number per cell was quantified by a multiplex Taqman (Bio-rad 4369510) qPCR assay by amplifying *MT-ND1* (mitochondrial encoded gene) and *B2M* (nuclear encoded gene) with a CFX96^{TM} Real-Time PCR Detection System (Bio-Rad) following the protocol described previously (Bartsakoulia et al., 2016). The primers used for template generation of standard curves and the qPCR reaction are as follows B2M: Fw-CACTGAAAAAGATGAGTATGCC, Rv-AA CATTCCCTGACAATCCC; MTND1: Fw-AACA TTCCCTGA CAATCCC, Rv-AACATTCCCTGACAATCCC. Copies per microliter of each template were standardized to 1×10^{10} and a 10-fold dilution series was amplified, with a DNA negative

control on each plate. This was performed in 20 μl reactions in a 96-well plate (Bio-Rad 5496), sealed using microplate "B" plate sealers (VWR 391-1293). The reaction mixture was composed of: 5 μl × 5 × Taqman (Bio-rad 4369510), 0.4 μM of reverse and forward primers, 25–50 ng of DNA template, 0.2 μl of MyTaq HS DNA polymerase (Bioline BIO-21112), and PCR-grade autoclaved sterile deionized water (to make up 20 μl of reaction mixture). The cycling conditions were as follows: (1) initial denaturation at 95°C for 3 min, (2) 40 cycles of denaturation at 95°C for 10 s, and (3) annealing and extension at 62.5°C for 1 min. The relative mtDNA copy number was calculated using the ΔCt data following the equation: CopyNumber $= 2\ (2^{-\Delta Ct})$ where Delta Ct (ΔCt) equals the sample Ct of the mitochondrial gene (MTND1) subtracted from the sample Ct of the nuclear reference gene (B2M).

Immunoblot Analyses

Whole protein extracts of cholesterol- and mock-treated fibroblasts were prepared by lysing cells with RIPA buffer (Sigma Aldrich) containing a protease inhibitor cocktail (Roche). Proteins were separated by utilizing Bis-Tris Gels (Invitrogen) and transferred to PVDF membranes (Invitrogen). Membranes were blocked for 2 h at room temperature with 5% milk in PBS-T and incubated with primary antibodies at 4°C overnight. The primary antibodies and dilutions used are as follows: mouse anti-APP A4 1:1,000 (Merck-Millipore), mouse anti-GRP78 1:2,000 (BD Biosciences), rabbit anti-CASP3 1:1,000 (AB clonal), mouse anti-GAPDH 1:2,000 (Abcam), mouse anti-VDAC1 1:1,000 (Abcam), and mouse anti-total OXPHOS antibody cocktail 1:1,000 (Abcam). Protein signals were detected with a Super SignalTM West Pico PLUS (Thermo Scientific) kit according to the manufacturer's protocol.

Immunofluorescence Studies

For imaging amyloid protein distribution and the Golgi network, cells were grown on coverslips and then fixed with 4% formaldehyde for 15 min at room temperature. Excessive formaldehyde was removed, and samples washed thrice with PBS before permeabilization with 0.5% Triton X in PBS for 10 min at room temperature and then blocked with 1% BSA for 1 h at room temperature. Next, cells were washed thrice with 1 ml of PBS and then incubated at 4°C overnight with an anti-Golgin-97 (rabbit polyclonal, GeneTex) and anti-beta-amyloid (mouse monoclonal, DE2B4, Abcam) primary antibodies. Excessive primary antibody was removed by washing three times with 1 ml of PBS. Fluorescently labeled antibodies rabbit Alexa Fluor 488 and mouse Alexa Fluor 594 (both Thermo Fisher Scientific) diluted in 1% BSA in PBS were added to the samples and incubated at room temperature for 1 h. Samples were washed finally three times with PBS and once very briefly with water and mounted onto microscope slides using ProLong Gold Antifade Mountant with DAPI (Thermo Fisher Scientific). Imaging was performed using a Nikon A1R confocal microscope and acquired images were further analyzed using the open source image-processing package in Fiji.

Cellular Cholesterol and Lipid Quantification Using Florescence Microscopy

To visualize lipid loading in our cells, we have employed Filipin and BODIPY staining. Filipin III was employed to specifically visualize cholesterol deposits in our cell models.

Cell culture medium was removed, and cells were gently washed thrice with 1 × PBS (room temperature). Next, 100 μl of 4% formaldehyde was added to each coverslip and incubated for 15 min at room-temperature. After the formaldehyde has been removed, cells were again washed thrice with 1 × PBS (room-temperature). Cells were next incubated with 1 ml of 1.5 mg/ml glycine at room temperature for 10 min. Filipin III from *Streptomyces filipinensis* (Sigma-Aldrich F4767) was added on cells (125 μg/ml) for 2 h at room temperature. Cells were next rinsed three times with PBS and slides were mounted using ProLong Gold Antifade Mountant (Thermo Fisher Scientific). Imaging was performed using a Leica confocal microscope (excitation approximately 360 nm and emission approximately 480 nm).

Data analysis was performed using Fiji. Two thresholds were set; the higher one to include only filipin-positive areas, and the lower one to also include areas of cellular autofluorescence as a measure of total cellular area. From this percentage, filipin positivity relative to cellular area was calculated for each image, and the mean was determined for all images of the fibroblast/treatment combination to give the percentage filipin positivity per combination. A minimum of 55 cells per combination were employed for quantification.

BODIPY (493/503; green solution; Life technologies, catalog # D-3922) was added followed by an incubation overnight at 4°C in the dark. The next day, BODIPY was removed, and cells were washed three times with 200 μl of PBS and stored at 4°C until microscopic inspection was carried out. Fluorescence measurements were performed on a modified Leica TCS SP8 CARS laser scanning microscope using a 25× water immersion objective [Fluotar VISIR 25x/0.95 WATER, for full description of the system see (Ebersbach et al., 2018)]. BODIPY fluorescence was excited at 488 nm and detected at 495–600 nm with a hybrid detector. Specifications of the hybrid detectors are given by the manufacturer. DAPI imaging was performed using 405 nm for excitation and detection of the fluorescence at 415–475 nm with a PMT. Both fluorescence measurements were carried out sequentially for each sample position. Multiple cell images were acquired as 3D stacks with a resolution of 2,048 × 2,048 pixels and a step size of 227 nm in x and y direction and five to nine layers in the z direction with a step size of 570 nm. 3D images of single cells were acquired with the same objective and a resolution of 512 × 512 pixels using a step size of 303 nm in the x and y direction and 570 nm in the z direction.

All data processing was performed using Matlab R2015a. For comparability of the different samples, all data were preprocessed as follows: For each 3D measurement, the mean intensity was calculated in the z direction. For the resulting 2D image, background noise was reduced by setting all data points with less than 1% of intensity to this lower threshold. To account for

cosmic spikes, an upper intensity threshold was set so that less than 0.1% of the data points showed fluorescence intensity above this value. Intensities exceeding this upper limit were set to this value. Images were then rescaled to full range (8-bit) between these two threshold values.

For statistical analyses, single-cell images were cut from the mean images using an irregular octagon. For each of these cells, an intensity histogram analysis was performed. To account for the different sizes of the single-cell images, the histogram values were normalized to percentage values. From the analyzed cells per sample, the mean and standard deviation were calculated on the normalized histogram data.

Plotting and Statistical Analysis

Data were plotted using GraphPad Prism v.7.0 software (GraphPad Software, United States) or Origin 6.0 (Origin Lab) and Adobe Illustrator Artwork 23.0 (Adobe Systems). The statistical test and method are indicated in the legend of the figures. *p*-values of less than 0.05 were considered statistically significant for all experiments.

DATA AVAILABILITY STATEMENT

The datasets presented in this study can be found in online repositories. The names of the repository/repositories and accession number(s) can be found below: ProteomeXchange with identifier PXD028168 and PXD027372.

ETHICS STATEMENT

The studies involving human participants were reviewed and approved by Ethics Committee of University of Medicine Essen, Germany (19-9011-BO).

AUTHOR CONTRIBUTIONS

DH and AR completed the label free proteomics studies while CN and RA performed the targeted UPR measurements. DH and MJJ performed western blotting of UPR components, filipin staining, and mitochondrial analysis. UM and EF performed the BODIPY staining and analysis. BM studied mtDNA copy numbers. AS, IE, and MS contributed the constructive comments and aided in data interpretation. MS contributed also with the fibroblasts utilized for this study. MJJ, DH, RH, and AR were involved in the design of the experiments, data analysis, and wrote the manuscript. All authors contributed to the article and approved the submitted version.

FUNDING

This work was supported by a grant from the French Muscular Dystrophy Association (AFM-Téléthon; #21644; grant to AR). Financial support by the Ministerium für Innovation, Wissenschaft und Forschung des Landes Nordrhein-Westfalen, the Senatsverwaltung für Wirtschaft, Technologie und Forschung des Landes Berlin and the Bundesministerium für Bildung und Forschung is gratefully acknowledged. RH is a Wellcome Trust Investigator (109915/Z/15/Z), who receives support from the Medical Research Council (United Kingdom) (MR/N025431/1), the European Research Council (309548), the Wellcome Trust Pathfinder Scheme (201064/Z/16/Z), and the Newton Fund (UK/Turkey, MR/N027302/1). This project was supported, in part, by the BMBF under the frame of the E-Rare-3 network PREPARE. (01GM1607 to MS and, as associated partner, RH) via the European Union's Horizon 2020 Research and Innovation Program. MJJ was supported by the Medical Research Council (MRC) (UK) DiMeN and Cambridge DTPs.

SUPPLEMENTARY MATERIAL

The Supplementary Material for this article can be found online at: https://www.frontiersin.org/articles/10.3389/fcell.2021.710247/full#supplementary-material

Supplementary Figure 1 | DNAJC3 expression in different tissues (brain, skin, and muscle) as depicted on GTEx Portal (https://www.gtexportal.org/home/).

REFERENCES

Anttonen, A. K., Mahjneh, I., Hamalainen, R. H., Lagier-Tourenne, C., Kopra, O., Waris, L., et al. (2005). The gene disrupted in Marinesco-Sjogren syndrome encodes SIL1, an HSPA5 cochaperone. *Nat. Genet.* 37, 1309–1311. doi: 10.1038/ng1677

Arenas, F., Garcia-Ruiz, C., and Fernandez-Checa, J. C. (2017). Intracellular cholesterol trafficking and impact in neurodegeneration. *Front. Mol. Neurosci.* 10:382. doi: 10.3389/fnmol.2017.00382

Balsa, E., Soustek, M. S., Thomas, A., Cogliati, S., Garcia-Poyatos, C., Martin-Garcia, E., et al. (2019). ER and nutrient stress promote assembly of respiratory chain supercomplexes through the PERK-eIF2alpha axis. *Mol. Cell* 74, 877–890.e6. doi: 10.1016/j.molcel.2019.03.031

Barbero-Camps, E., Fernandez, A., Baulies, A., Martinez, L., Fernandez-Checa, J. C., and Colell, A. (2014). Endoplasmic reticulum stress mediates amyloid beta neurotoxicity via mitochondrial cholesterol trafficking. *Am. J. Pathol.* 184, 2066–2081. doi: 10.1016/j.ajpath.2014.03.014

Bartsakoulia, M., Mupsilonller, J. S., Gomez-Duran, A., Yu-Wai-Man, P., Boczonadi, V., and Horvath, R. (2016). Cysteine supplementation may be beneficial in a subgroup of mitochondrial translation deficiencies. *J. Neuromuscul. Dis.* 3, 363–379. doi: 10.3233/JND-160178

Blumen, S. C., Astord, S., Robin, V., Vignaud, L., Toumi, N., Cieslik, A., et al. (2012). A rare recessive distal hereditary motor neuropathy with HSJ1 chaperone mutation. *Ann. Neurol.* 71, 509–519. doi: 10.1002/ana.22684

Boriushkin, E., Wang, J. J., Li, J., Jing, G., Seigel, G. M., and Zhang, S. X. (2015). Identification of p58IPK as a novel neuroprotective factor for retinal neurons. *Invest. Ophthalmol. Vis. Sci.* 56, 1374–1386. doi: 10.1167/iovs.14-15196

Boye, E., and Grallert, B. (2020). eIF2alpha phosphorylation and the regulation of translation. *Curr. Genet.* 66, 293–297. doi: 10.1007/s00294-019-01026-1

Bublitz, S. K., Alhaddad, B., Synofzik, M., Kuhl, V., Lindner, A., Freiberg, C., et al. (2017). Expanding the phenotype of DNAJC3 mutations: a case with hypothyroidism additionally to diabetes mellitus and multisystemic neurodegeneration. *Clin. Genet.* 92, 561–562. doi: 10.1111/cge.13069

Buchkremer, S., Gonzalez Coraspe, J. A., Weis, J., and Roos, A. (2016). Sil1-mutant mice elucidate chaperone function in neurological disorders. *J. Neuromuscul. Dis.* 3, 169–181. doi: 10.3233/JND-160152

Burkhart, J. M., Schumbrutzki, C., Wortelkamp, S., Sickmann, A., and Zahedi, R. P. (2012). Systematic and quantitative comparison of digest efficiency and specificity reveals the impact of trypsin quality on MS-based proteomics. *J. Proteomics* 75, 1454–1462. doi: 10.1016/j.jprot.2011.11.016

Choy, R. W., Cheng, Z., and Schekman, R. (2012). Amyloid precursor protein (APP) traffics from the cell surface via endosomes for amyloid beta (Abeta) production in the trans-Golgi network. *Proc. Natl. Acad. Sci. U.S.A.* 109, E2077–E2082. doi: 10.1073/pnas.1208635109

Cunha, D. A., Hekerman, P., Ladriere, L., Bazarra-Castro, A., Ortis, F., Wakeham, M. C., et al. (2008). Initiation and execution of lipotoxic ER stress in pancreatic beta-cells. *J. Cell Sci.* 121, 2308–2318. doi: 10.1242/jcs.026062

Das, A., Davis, M. A., and Rudel, L. L. (2008). Identification of putative active site residues of ACAT enzymes. *J. Lipid Res.* 49, 1770–1781. doi: 10.1194/jlr.M800131-JLR200

DelBove, C. E., Strothman, C. E., Lazarenko, R. M., Huang, H., Sanders, C. R., and Zhang, Q. (2019). Reciprocal modulation between amyloid precursor protein and synaptic membrane cholesterol revealed by live cell imaging. *Neurobiol. Dis.* 127, 449–461. doi: 10.1016/j.nbd.2019.03.009

Delepine, M., Nicolino, M., Barrett, T., Golamaully, M., Lathrop, G. M., and Julier, C. (2000). EIF2AK3, encoding translation initiation factor 2-alpha kinase 3, is mutated in patients with Wolcott-Rallison syndrome. *Nat. Genet.* 25, 406–409. doi: 10.1038/78085

Dranka, B. P., Hill, B. G., and Darley-Usmar, V. M. (2010). Mitochondrial reserve capacity in endothelial cells: the impact of nitric oxide and reactive oxygen species. *Free Radic. Biol. Med.* 48, 905–914. doi: 10.1016/j.freeradbiomed.2010.01.015

Dudek, J., Benedix, J., Cappel, S., Greiner, M., Jalal, C., Muller, L., et al. (2009). Functions and pathologies of BiP and its interaction partners. *Cell. Mol. Life Sci.* 66, 1556–1569. doi: 10.1007/s00018-009-8745-y

Ebersbach, P., Stehle, F., Kayser, O., and Freier, E. (2018). Chemical fingerprinting of single glandular trichomes of *Cannabis sativa* by Coherent anti-Stokes Raman scattering (CARS) microscopy. *BMC Plant Biol.* 18:275. doi: 10.1186/s12870-018-1481-4

Ehehalt, R., Keller, P., Haass, C., Thiele, C., and Simons, K. (2003). Amyloidogenic processing of the Alzheimer beta-amyloid precursor protein depends on lipid rafts. *J. Cell Biol.* 160, 113–123. doi: 10.1083/jcb.200207113

Evans, C. G., Wisen, S., and Gestwicki, J. E. (2006). Heat shock proteins 70 and 90 inhibit early stages of amyloid beta-(1-42) aggregation *in vitro*. *J. Biol. Chem.* 281, 33182–33191. doi: 10.1074/jbc.M606192200

Feng, B., Yao, P. M., Li, Y., Devlin, C. M., Zhang, D., Harding, H. P., et al. (2003). The endoplasmic reticulum is the site of cholesterol-induced cytotoxicity in macrophages. *Nat. Cell Biol.* 5, 781–792. doi: 10.1038/ncb1035

Fernandez, A., Llacuna, L., Fernandez-Checa, J. C., and Colell, A. (2009). Mitochondrial cholesterol loading exacerbates amyloid beta peptide-induced inflammation and neurotoxicity. *J. Neurosci.* 29, 6394–6405. doi: 10.1523/JNEUROSCI.4909-08.2009

Fu, S., Yang, L., Li, P., Hofmann, O., Dicker, L., Hide, W., et al. (2011). Aberrant lipid metabolism disrupts calcium homeostasis causing liver endoplasmic reticulum stress in obesity. *Nature* 473, 528–531. doi: 10.1038/nature09968

Greenberg, A. S., Coleman, R. A., Kraemer, F. B., McManaman, J. L., Obin, M. S., Puri, V., et al. (2011). The role of lipid droplets in metabolic disease in rodents and humans. *J. Clin. Invest.* 121, 2102–2110. doi: 10.1172/JCI46069

Hentschel, A., Czech, A., Munchberg, U., Freier, E., Schara-Schmidt, U., Sickmann, A., et al. (2021). Protein signature of human skin fibroblasts allows the study of the molecular etiology of rare neurological diseases. *Orphanet. J. Rare Dis.* 16:73. doi: 10.1186/s13023-020-01669-1

Hill, B. G., Benavides, G. A., Lancaster, J. R. Jr., Ballinger, S., Dell'Italia, L., Jianhua, Z., et al. (2012). Integration of cellular bioenergetics with mitochondrial quality control and autophagy. *Biol. Chem.* 393, 1485–1512. doi: 10.1515/hsz-2012-0198

Ichhaporia, V. P., Sanford, T., Howes, J., Marion, T. N., and Hendershot, L. M. (2015). Sil1, a nucleotide exchange factor for BiP, is not required for antibody assembly or secretion. *Mol. Biol. Cell* 26, 420–429. doi: 10.1091/mbc.E14-09-1392

Isbert, S., Wagner, K., Eggert, S., Schweitzer, A., Multhaup, G., Weggen, S., et al. (2012). formation is initiated in the endoplasmic reticulum and differs between APP isoforms. *Cell. Mol. Life Sci.* 69, 1353–1375. doi: 10.1007/s00018-011-0882-4

Jazvinscak Jembrek, M., Hof, P. R., and Simic, G. (2015). Ceramides in Alzheimer's disease: key mediators of neuronal apoptosis induced by oxidative stress and abeta accumulation. *Oxid. Med. Cell. Longev.* 2015:346783. doi: 10.1155/2015/346783

Jin, H., Mimura, N., Kashio, M., Koseki, H., and Aoe, T. (2014). Late-onset of spinal neurodegeneration in knock-in mice expressing a mutant BiP. *PLoS One* 9:e112837. doi: 10.1371/journal.pone.0112837

Khanim, F., Kirk, J., Latif, F., and Barrett, T. G. (2001). WFS1/Wolframin mutations, Wolfram syndrome, and associated diseases. *Hum. Mutat.* 17, 357–367. doi: 10.1002/humu.1110

Knupp, J., Arvan, P., and Chang, A. (2019). Increased mitochondrial respiration promotes survival from endoplasmic reticulum stress. *Cell Death Differ.* 26, 487–501. doi: 10.1038/s41418-018-0133-4

Kollipara, L., and Zahedi, R. P. (2013). Protein carbamylation: *in vivo* modification or *in vitro* artefact? *Proteomics* 13, 941–944. doi: 10.1002/pmic.201200452

Kollipara, L., Buchkremer, S., Coraspe, J. A. G., Hathazi, D., Senderek, J., Weis, J., et al. (2017). In-depth phenotyping of lymphoblastoid cells suggests selective cellular vulnerability in Marinesco-Sjogren syndrome. *Oncotarget* 8, 68493–68516. doi: 10.18632/oncotarget.19663

Krieger, M., Roos, A., Stendel, C., Claeys, K. G., Sonmez, F. M., Baudis, M., et al. (2013). SIL1 mutations and clinical spectrum in patients with Marinesco-Sjogren syndrome. *Brain* 136, 3634–3644. doi: 10.1093/brain/awt283

Kulanuwat, S., Tangjittipokin, W., Jungtrakoon, P., Chanprasert, C., Sujjitjoon, J., Binnima, N., et al. (2018). DNAJC3 mutation in Thai familial type 2 diabetes mellitus. *Int. J. Mol. Med.* 42, 1064–1073. doi: 10.3892/ijmm.2018.3678

Ledesma, M. D., and Dotti, C. G. (2006). Amyloid excess in Alzheimer's disease: what is cholesterol to be blamed for? *FEBS Lett.* 580, 5525–5532. doi: 10.1016/j.febslet.2006.06.038

Linxweiler, M., Schick, B., and Zimmermann, R. (2017). Let's talk about Secs: Sec61, Sec62 and Sec63 in signal transduction, oncology and personalized medicine. *Signal Transduct. Target. Ther.* 2:17002. doi: 10.1038/sigtrans.2017.2

Luo, D. X., Cao, D. L., Xiong, Y., Peng, X. H., and Liao, D. F. (2010). A novel model of cholesterol efflux from lipid-loaded cells. *Acta Pharmacol. Sin.* 31, 1243–1257. doi: 10.1038/aps.2010.93

Luo, S., Mao, C., Lee, B., and Lee, A. S. (2006). GRP78/BiP is required for cell proliferation and protecting the inner cell mass from apoptosis during early mouse embryonic development. *Mol. Cell. Biol.* 26, 5688–5697.

Lytrivi, M., Senee, V., Salpea, P., Fantuzzi, F., Philippi, A., Abdulkarim, B., et al. (2021). DNAJC3 deficiency induces beta-cell mitochondrial apoptosis and causes syndromic young-onset diabetes. *Eur. J. Endocrinol.* 184, 459–472.

MacLean, B., Tomazela, D. M., Shulman, N., Chambers, M., Finney, G. L., Frewen, B., et al. (2010). Skyline: an open source document editor for creating and analyzing targeted proteomics experiments. *Bioinformatics* 26, 966–968.

Makino, A., Hullin-Matsuda, F., Murate, M., Abe, M., Tomishige, N., Fukuda, M., et al. (2016). Acute accumulation of free cholesterol induces the degradation of perilipin 2 and Rab18-dependent fusion of ER and lipid droplets in cultured human hepatocytes. *Mol. Biol. Cell* 27, 3293–3304.

Mansson, C., Arosio, P., Hussein, R., Kampinga, H. H., Hashem, R. M., Boelens, W. C., et al. (2014). Interaction of the molecular chaperone DNAJB6 with growing amyloid-beta 42 (Abeta42) aggregates leads to sub-stoichiometric inhibition of amyloid formation. *J. Biol. Chem.* 289, 31066–31076.

Marquer, C., Laine, J., Dauphinot, L., Hanbouch, L., Lemercier-Neuillet, C., Pierrot, N., et al. (2014). Increasing membrane cholesterol of neurons in culture recapitulates Alzheimer;s disease early phenotypes. *Mol. Neurodegener.* 9:60.

Marriott, K. S. C., Prasad, M., Thapliyal, V., and Bose, H. S. (2012). sigma-1 receptor at the mitochondrial-associated endoplasmic reticulum membrane is responsible for mitochondrial metabolic regulation. *J. Pharmacol. Exp. Ther.* 343, 578–586.

Montero, J., Mari, M., Colell, A., Morales, A., Basañez, G., Garcia-Ruiz, C., et al. (2010). Cholesterol and peroxidized cardiolipin in mitochondrial membrane properties, permeabilization and cell death. *Biochim. Biophys. Acta* 1797, 1217–1224.

Montesinos, J., Pera, M., Larrea, D., Guardia-Laguarta, C., Agrawal, R. R., Velasco, K. R., et al. (2020). The Alzheimer's disease-associated C99 fragment of APP regulates cellular cholesterol trafficking. *EMBO J.* 39:e103791.

Nguyen, C. D. L., Malchow, S., Reich, S., Steltgens, S., Shuvaev, K. V., Loroch, S., et al. (2019). A sensitive and simple targeted proteomics approach to quantify transcription factor and membrane proteins of the unfolded protein response pathway in glioblastoma cells. *Sci. Rep.* 9:8836.

Olsen, J. V., de Godoy, L. M., Li, G., Macek, B., Mortensen, P., Pesch, R., et al. (2005). Parts per million mass accuracy on an Orbitrap mass spectrometer via lock mass injection into a C-trap. *Mol. Cell Proteomics* 4, 2010–2021.

Oyadomari, S., Yun, C., Fisher, E. A., Kreglinger, N., Kreibich, G., Oyadomari, M., et al. (2006). Cotranslocational degradation protects the stressed endoplasmic reticulum from protein overload. *Cell* 126, 727–739.

Phan, V., Cox, D., Cipriani, S., Spendiff, S., Buchkremer, S., O'Connor, E., et al. (2019). SIL1 deficiency causes degenerative changes of peripheral nerves and neuromuscular junctions in fish, mice and human. *Neurobiol. Dis.* 124, 218–229.

Rone, M. B., Fan, J. J., and Papadopoulos, V. (2009). Cholesterol transport in steroid biosynthesis: role of protein-protein interactions and implications in disease states. *BBA Mol. Cell Biol.* 1791, 646–658. doi: 10.1016/j.bbalip.2009.03.001

Roos, A., Buchkremer, S., Kollipara, L., Labisch, T., Gatz, C., Zitzelsberger, M., et al. (2014). Myopathy in Marinesco-Sjogren syndrome links endoplasmic reticulum chaperone dysfunction to nuclear envelope pathology. *Acta Neuropathol.* 127, 761–777. doi: 10.1007/s00401-013-1224-4

Roos, A., Kollipara, L., Buchkremer, S., Labisch, T., Brauers, E., Gatz, C., et al. (2016). Cellular signature of SIL1 depletion: disease pathogenesis due to alterations in protein composition beyond the ER machinery. *Mol. Neurobiol.* 53, 5527–5541. doi: 10.1007/s12035-015-9456-z

Rutkowski, D. T., Kang, S. W., Goodman, A. G., Garrison, J. L., Taunton, J., Katze, M. G., et al. (2007). The role of p58IPK in protecting the stressed endoplasmic reticulum. *Mol. Biol. Cell* 18, 3681–3691. doi: 10.1091/mbc.e07-03-0272

Schorr, S., Klein, M. C., Gamayun, I., Melnyk, A., Jung, M., Schauble, N., et al. (2015). Co-chaperone specificity in gating of the polypeptide conducting channel in the membrane of the human endoplasmic reticulum. *J. Biol. Chem.* 290, 18621–18635. doi: 10.1074/jbc.M115.636639

Senderek, J., Krieger, M., Stendel, C., Bergmann, C., Moser, M., Breitbach-Faller, N., et al. (2005). Mutations in SIL1 cause Marinesco-Sjogren syndrome, a cerebellar ataxia with cataract and myopathy. *Nat. Genet.* 37, 1312–1314.

Shobab, L. A., Hsiung, G. Y. R., and Feldman, H. H. (2005). Cholesterol in Alzheimer's disease. *Lancet Neurol.* 4, 841–852.

Synofzik, M., Haack, T. B., Kopajtich, R., Gorza, M., Rapaport, D., Greiner, M., et al. (2014). Absence of BiP co-chaperone DNAJC3 causes diabetes mellitus and multisystemic neurodegeneration. *Am. J. Hum. Genet.* 95, 689–697.

Tabas, I. (2002). Consequences of cellular cholesterol accumulation: basic concepts and physiological implications. *J. Clin. Invest.* 110, 905–911. doi: 10.1172/JCI0216452

Turkieh, A., Caubère, C., Barutaut, M., Desmoulin, F., Harmancey, R., Galinier, M., et al. (2014). Apolipoprotein O is mitochondrial and promotes lipotoxicity in heart. *J. Clin. Invest.* 124, 2277–2286. doi: 10.1172/JCI74668

Vaudel, M., Barsnes, H., Berven, F. S., Sickmann, A., and Martens, L. (2011). SearchGUI: an open-source graphical user interface for simultaneous OMSSA and X!Tandem searches. *Proteomics* 11, 996–999. doi: 10.1002/pmic.201000595

Vaudel, M., Burkhart, J. M., Zahedi, R. P., Oveland, E., Berven, F. S., Sickmann, A., et al. (2015). PeptideShaker enables reanalysis of MS-derived proteomics data sets. *Nat. Biotechnol.* 33, 22–24. doi: 10.1038/nbt.3109

Volmer, R., and Ron, D. (2015). Lipid-dependent regulation of the unfolded protein response. *Curr. Opin. Cell Biol.* 33, 67–73. doi: 10.1016/j.ceb.2014.12.002

von Arnim, C. A. F., Spoelgen, R., Peltan, I. D., Deng, M., Courchesne, S., Koker, M., et al. (2006). GGA1 acts as a spatial switch altering amyloid precursor protein trafficking and processing. *J. Neurosci.* 26, 9913–9922. doi: 10.1523/JNEUROSCI.2290-06.2006

Yan, W., Frank, C. L., Korth, M. J., Sopher, B. L., Novoa, I., Ron, D., et al. (2002). Control of PERK eIF2alpha kinase activity by the endoplasmic reticulum stress-induced molecular chaperone P58IPK. *Proc. Natl. Acad. Sci. U.S.A.* 99, 15920–15925. doi: 10.1073/pnas.252341799

Yip, C. M., Elton, E. A., Darabie, A. A., Morrison, M. R., and McLaurin, J. (2001). Cholesterol, a modulator of membrane-associated A beta-fibrillogenesis and neurotoxicity. *J. Mol. Biol.* 311, 723–734. doi: 10.1006/jmbi.2001.4881

Zhao, L., Rosales, C., Seburn, K., Ron, D., and Ackerman, S. L. (2010). Alteration of the unfolded protein response modifies neurodegeneration in a mouse model of Marinesco-Sjogren syndrome. *Hum. Mol. Genet.* 19, 25–35. doi: 10.1093/hmg/ddp464

Conflict of Interest: The authors declare that the research was conducted in the absence of any commercial or financial relationships that could be construed as a potential conflict of interest.

Publisher's Note: All claims expressed in this article are solely those of the authors and do not necessarily represent those of their affiliated organizations, or those of the publisher, the editors and the reviewers. Any product that may be evaluated in this article, or claim that may be made by its manufacturer, is not guaranteed or endorsed by the publisher.

frontiers in Molecular Biosciences

REVIEW
published: 23 November 2021
doi: 10.3389/fmolb.2021.772174

Mitochondrial Dysfunction in Advanced Liver Disease: Emerging Concepts

Ingrid W. Zhang[1,2]*, *Cristina López-Vicario*[1,2,3], *Marta Duran-Güell*[1,2] and *Joan Clària*[1,2,3,4]

[1]Biochemistry and Molecular Genetics Service, Hospital Clínic–IDIBAPS, Barcelona, Spain, [2]European Foundation for the Study of Chronic Liver Failure (EF Clif) and Grifols Chair, Barcelona, Spain, [3]CIBERehd, Barcelona, Spain, [4]Department of Biomedical Sciences, University of Barcelona, Barcelona, Spain

Mitochondria are entrusted with the challenging task of providing energy through the generation of ATP, the universal cellular currency, thereby being highly flexible to different acute and chronic nutrient demands of the cell. The fact that mitochondrial diseases (genetic disorders caused by mutations in the nuclear or mitochondrial genome) manifest through a remarkable clinical variation of symptoms in affected individuals underlines the far-reaching implications of mitochondrial dysfunction. The study of mitochondrial function in genetic or non-genetic diseases therefore requires a multi-angled approach. Taking into account that the liver is among the organs richest in mitochondria, it stands to reason that in the process of unravelling the pathogenesis of liver-related diseases, researchers give special focus to characterizing mitochondrial function. However, mitochondrial dysfunction is not a uniformly defined term. It can refer to a decline in energy production, increase in reactive oxygen species and so forth. Therefore, any study on mitochondrial dysfunction first needs to define the dysfunction to be investigated. Here, we review the alterations of mitochondrial function in liver cirrhosis with emphasis on acutely decompensated liver cirrhosis and acute-on-chronic liver failure (ACLF), the latter being a form of acute decompensation characterized by a generalized state of systemic hyperinflammation/immunosuppression and high mortality rate. The studies that we discuss were either carried out in liver tissue itself of these patients, or in circulating leukocytes, whose mitochondrial alterations might reflect tissue and organ mitochondrial dysfunction. In addition, we present different methodological approaches that can be of utility to address the diverse aspects of hepatocyte and leukocyte mitochondrial function in liver disease. They include assays to measure metabolic fluxes using the comparatively novel Biolog's MitoPlates in a 96-well format as well as assessment of mitochondrial respiration by high-resolution respirometry using Oroboros' O2k-technology and Agilent Seahorse XF technology.

Keywords: mitochondrial dysfunction, systemic inflammation, organ failure, cirrhosis, acute decompensation, immunometabolism

OPEN ACCESS

Edited by:
David Pacheu-Grau,
University of Zaragoza, Spain

Reviewed by:
Francesca Di Sole,
Des Moines University, United States
Wagner Ferreira Dos Santos,
University of São Paulo Ribeirão Preto, Brazil

***Correspondence:**
Ingrid W. Zhang
iwzhang@clinic.cat

Specialty section:
This article was submitted to Cellular Biochemistry, a section of the journal Frontiers in Molecular Biosciences

Received: *07 September 2021*
Accepted: *04 November 2021*
Published: *23 November 2021*

Citation:
Zhang IW, López-Vicario C, Duran-Güell M and Clària J (2021) Mitochondrial Dysfunction in Advanced Liver Disease: Emerging Concepts. Front. Mol. Biosci. 8:772174. doi: 10.3389/fmolb.2021.772174

1 INTRODUCTION

Although mitochondrial damage has beneficial effects in response to acute injuries or infections through promotion of pro-inflammatory responses, it might be deleterious in diseases associated with chronic inflammation such as advanced liver cirrhosis (Mansouri et al., 2018). Therapeutic interventions aimed at restoring the deranged intermediate metabolism in immune cells might sever the links between excessive mitochondrial damage and deranged immune response and have beneficial effects in patients with acute decompensation (AD) of cirrhosis and acute-on-chronic liver failure (ACLF), a syndrome developing in patients with AD characterized by the presence of organ failure(s).

AD cirrhosis is defined by acute development of ascites, hepatic encephalopathy, gastrointestinal haemorrhage or bacterial infection, or any combination of these, and ACLF is a syndrome with a prevalence of 30% in patients hospitalized for AD cirrhosis (Moreau et al., 2013). An evidence-based definition of ACLF was introduced for the first time in 2013, as a result of the prospective and European-wide CANONIC study (Moreau et al., 2013). The short-term mortality rate of patients with ACLF is 15 times higher than that of patients with mere AD, and the main cause of death is multiple organ failure. The current European and American definitions are based on the presence of organ failures, and the severity of the disease (grade I-III) is determined according to the number of organ failures (Moreau et al., 2013). On the pathophysiological level, ACLF is characterized by the co-existence of systemic inflammation and immunoparesis, thereby rendering these patients more susceptible to bacterial infections (Bernsmeier et al., 2015; Clària et al., 2016; Fernández et al., 2017). ACLF shares pathophysiological similarities with sepsis, during which immune cells undergo metabolic reprogramming to fuel the hyper-inflammatory state. Therefore, it can be assumed that mitochondria, which were recently dubbed as the powerhouses of immunity (Mills et al., 2017), play a crucial role in both conditions. Whereas the evidence is overwhelming and convincing in sepsis, the role of mitochondria in ACLF development due to its relatively recent definition is less well described.

The intricate link between mitochondrial dysfunction and subsequent disturbances in metabolic pathways, leading to shortage in adenosine triphosphate (ATP), excessive storage of fat and leakage of reactive oxygen species (ROS) is well acknowledged (Ott et al., 2007; Aon et al., 2014). In recent years, however, the crosstalk between mitochondria and the immune system has attracted increased attention, to the point that one entire research field termed immunometabolism is dedicated to disentangle this extremely complex network. Recent studies helped to increase the recognition that the metabolic-immunoregulatory crosstalk is bidirectional. On the one hand, immune cells have to transition from a metabolic quiescent to an active state during immune response, and on the other hand, altered metabolism controls immune cell differentiation, function and fate (Angajala et al., 2018). More specifically, mitochondrial intermediate metabolism affects cytokine production, i.e. M1 macrophage polarization is supported by a discontinuous tricarboxylic acid (TCA) cycle, whereas mitochondrial β-oxidation is required for M2 macrophage polarization (Tannahill et al., 2013; Huang et al., 2014; Jha et al., 2015). Additionally, mitochondria are able to activate different intracellular signaling pathways necessary to defend the host against pathogens such as the mitochondrial anti-viral signaling (MAVS) and activation of the nucleotide-binding oligomerization domain (NOD)-, leucine-rich repeat (LRR)- and pyrin domain-containing protein 3 (NLRP3) inflammasome by mitochondrial DNA (mtDNA) (Zhong et al., 2018). Apart from mtDNA, mitochondria also release proteins, lipids, metabolites and ROS. Mitochondria are the major contributor to ROS production in most mammalian cells, and ROS is implicated in redox signaling from mitochondria to other organelles of the cell. The molecules released by mitochondria serve as damage-associated molecular patterns (DAMPs). DAMPs interact with pattern-recognition receptors (PRRs) expressed mainly by cells of the innate immune system in an autocrine, paracrine or endocrine manner (Vénéreau et al., 2015; Miliotis et al., 2019). Since mitochondria are the organelles where metabolic pathways converge, they are also able to reshape the innate and adaptive immune responses by modulating the microenvironment. For instance, a lipid-rich tumor microenvironment favours expansion of the pro-tumoral, interleukin (IL)-17 secreting γδ T cell subset over the anti-tumoral interferon (IFN)γ producing γδ T cells (Lopes et al., 2021), and since glycolysis controls the translation of IFNγ-mRNA, the lack of glucose impairs T cell cytokine production (Chang et al., 2013). Another example is that oligomycin can block the expression of early activation markers after T-cell receptor ligation and blunt subsequent T cell proliferation (Chang et al., 2013).

Mitochondria do not merely release immunostimulatory molecules, but also represent intracellular sites of inflammatory signaling. For example, among the 22 nucleotide-binding leucine-rich repeat receptors or NOD-like receptors (NLRs), NOD5 (or NLRX1) has a predicted mitochondrial import signal (Tattoli et al., 2008). In addition, NLRP3, after being stimulated with monosodium urate, alum or nigericin, relocates from cytoplasmic structures and the ER to mitochondria-associated ER membranes (MAM) (Zhou et al., 2011). Interestingly, NLRP3 has the potential to drive fibrogenesis independent from inflammasome-regulated cytokines IL-1β/IL18 and processing of caspase 1. Instead, NLRP3 operates at mitochondria in fibroblasts and modulates their ROS production to augment profibrogenic pathways (Bracey et al., 2014).

In analogy to mitochondria being the metabolic hub of the cell, the liver can be seen as the metabolic hub of the body. Often, similar to the underestimation of the role of mitochondria in immune responses, the perception of the liver is reduced to its metabolic functions. This notion should be revised, since the liver is a site of complex immunological activity, involved in the production of acute phase proteins, coagulation and complement factors, cytokines and albumin, and contains a large population of resident immune cells. Innate lymphocytes in the liver comprise

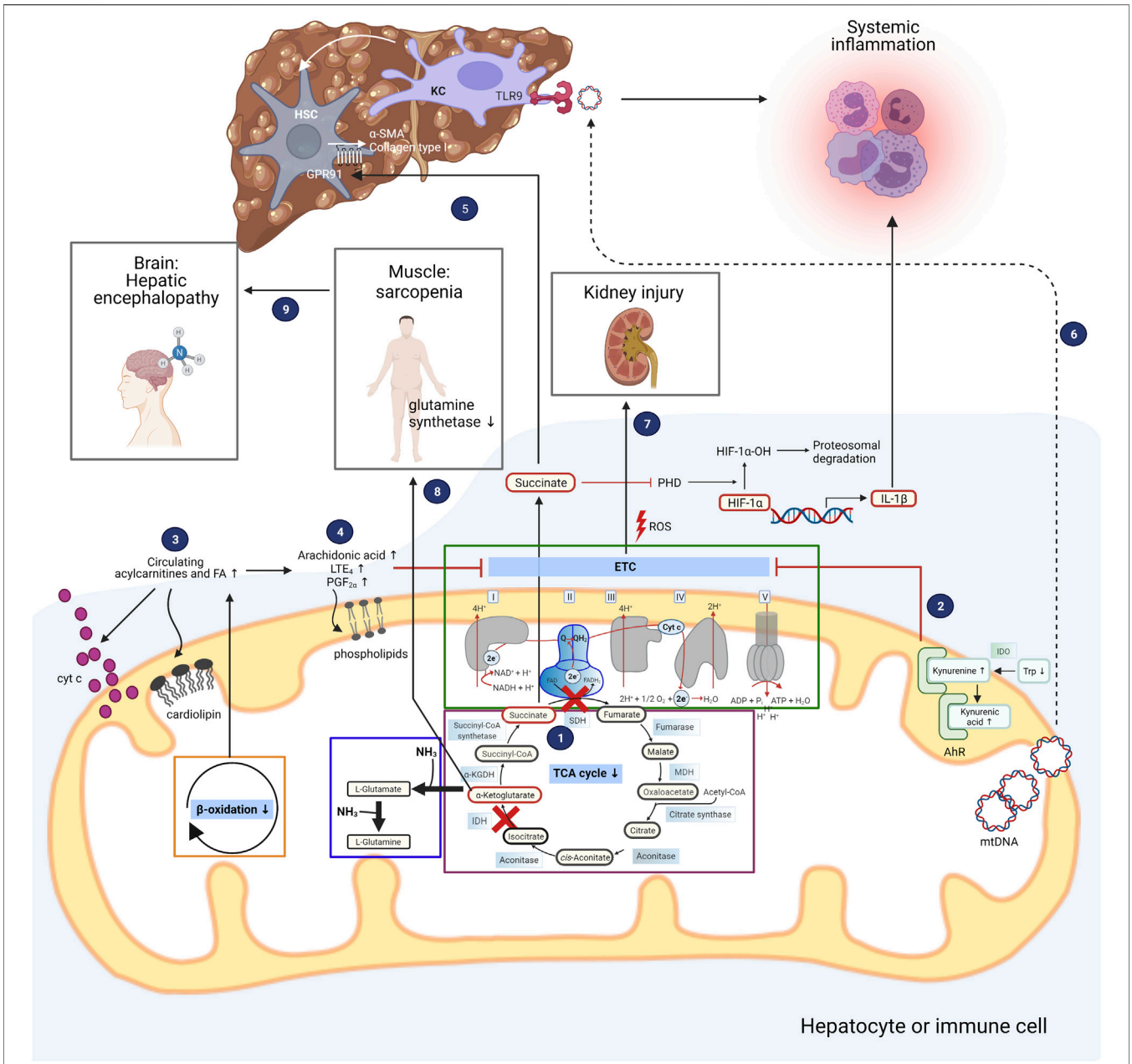

FIGURE 1 | Deranged mitochondrial intermediate metabolism contributes to development of organ dysfunction in patients with acute decompensated liver cirrhosis. The different metabolic intermediate pathways located in mitochondria are depicted, and how their derangements contribute to the clinical symptoms of patients with acutely decompensated liver cirrhosis. The boxes inside the mitochondrion highlight the electron transport chain (ETC), the tricarboxylic acid (TCA) cycle, and glutamine synthesis as one possible pathway for ammonia detoxification. Peripheral mononuclear cells of patients with ACLF exhibit a discontinuous TCA cycle at the isocitrate and succinate dehydrogenase (IDH and SDH) level **(1)**. Succinate is transported into the cytosol where it inhibits prolyl hydroxylase (PHD), resulting in stabilization of hypoxia-inducible factor-1α (HIF-1α) and enhanced production of interleukin-1β (IL-1β). Untargeted metabolomics in serum of patients with AD cirrhosis and ACLF revealed increased degradation of tryptophan (Trp) through the kynurenine pathway with elevated kynurenine and kynurenic acid levels, which bind to aryl hydrocarbon receptor (AhR) localized in the intermembrane space of mitochondria **(2)**. Activation of AhR is implicated in attenuation of mitochondrial maximal respiration. Patients with AD cirrhosis and ACLF also exhibit elevated levels of fatty acids and acylcarnitines, pointing towards impaired β-oxidation **(3)**. Saturated fatty acids (FA) change the composition of cardiolipins which are enriched in the inner mitochondrial membrane, facilitating the release of cytochrome c. Targeted study of bioactive lipid mediators in patients with AD cirrhosis and ACLF revealed elevated levels of arachidonic acid and its products LTE_4 and $PGF_{2\alpha}$ **(4)**. Arachidonic acid is able to modify the phospholipid composition of mitochondrial membranes, resulting in impaired function of the ETC. In addition to being involved in pro-inflammatory responses, succinate promotes fibrogenesis through its receptor GPR91 which is expressed on hepatic stellate cells (HSC), leading to upregulation of alpha-smooth muscle actin (α-SMA) and collagen type I **(5)**. Mitochondrial DNA (mtDNA) released from hepatocytes promote inflammation through binding to toll-like receptor 9 (TLR9) of liver resident Kupffer cells (KC) **(6)**, further contributing to fibrogenesis. Reactive oxygen species (ROS) generated by the electron transport chain and released by mitochondria promote cell death of kidney cells, eventually leading to kidney dysfunction and failure **(7)**. Hyperammonemia in patients with advanced liver cirrhosis leads to depletion of α-ketoglutarate in skeletal muscle and consequently lower TCA flux and ATP synthesis, translating into sarcopenia **(8)**. Along with muscle loss, significant amounts of glutamine synthetase activity is lost, promoting hepatic encephalopathy **(9)**. IDO, indoleamine-2,3-dioxygenase; MDH, malate dehydrogenase. Figure was created with BioRender.com.

natural killer (NK) cells, NK T cells (NKT), mucosal associated invariant T cells and γδ T cells (Doherty et al., 1999; Kenna et al., 2003; Kenna et al., 2004; Dusseaux et al., 2011). Regarding cells of the adaptive immune system, the liver is particularly enriched in $CD8^+$ T cells, activated T cells and memory T cells (Norris et al., 1998). Of note, hepatocytes express variable levels of class II MHC molecules and are capable of presenting antigens to classical T cells (Thomson and Knolle, 2010). The healthy adult liver maintains a basal cytokine level including expression of pro-inflammatory IL-2, IL-7, IL-12, IL-15 and IFNγ, and anti-inflammatory IL-10, IL-13 and transforming growth factor β (TGFβ) (Golden-Mason et al., 2004; Kelly et al., 2006). Worthy of note, the immunological microenvironment in the liver is subjected to direct influence by macronutrients transported to the liver through the portal vein.

Given that recurring commonalities of hepatic diseases include increased ROS and reactive nitrogen species, diminished β-oxidation, defective oxidative phosphorylation and enhanced lipogenesis, we propose that immunometabolic derangement and bioenergetics failure is the phenotype underlying advanced liver cirrhosis including ACLF, similar to sepsis (Cheng et al., 2016).

In the following, we highlight the characteristics of immunometabolism that goes astray in advanced stages of liver cirrhosis, the role of dysfunctional mitochondria in development of organ failures in patients with ACLF, and propose therapeutic strategies aimed at rewiring mitochondrial intermediate metabolism.

2 IMMUNOMETABOLISM IN THE SETTING OF ADVANCED LIVER DISEASE: ROLE OF THE TRICARBOXYLIC ACID CYCLE

Upon polarization of macrophages to the M1 phenotype, a discontinuity in the metabolic flux of the TCA cycle occurs at the isocitrate dehydrogenase (IDH) and succinate dehydrogenase (SDH) levels. As a consequence, succinate, a paradigmatic pro-inflammatory metabolite, is released into the cytosol, where it stabilizes the transcription factor hypoxia-inducible factor-1α (HIF-1α) through inhibition of prolyl hydroxylase (PHD) activity and promotes the production of ROS and IL-1β (Tannahill et al., 2013). In contrast, α-ketoglutarate (α-KG), another TCA cycle intermediate which functions as a branch point between glutamine metabolism and the TCA cycle, attenuates pro-inflammatory responses in M1 macrophages by suppressing nuclear factor-κB (NF-κB) pathway through PHD-dependent proline hydroxylation of IkappaB kinase (IKK) β (Liu et al., 2017). Therefore, M1 macrophage activation is strengthened by a low α-ketoglutarate/succinate ratio (Liu et al., 2017). Recently, we could demonstrate that the break point at SDH also exists in peripheral mononuclear cells of patients with ACLF (**1** in **Figure 1**), probably as a consequence of systemic inflammation in these patients (Zhang et al., 2021). This finding also generates the hypothesis that the break point serves to perpetuate the inflammatory responses through production of cytokines, which is promoted by the pro-inflammatory actions of succinate.

Mitochondria are regarded as the major cellular source of ROS production, but they can also be the target of excessive ROS generation. Mitochondrial ROS can damage metabolic enzymes such as α-ketoglutarate dehydrogenase (α-KGDH) and pyruvate dehydrogenase (Tretter and Adam-Vizi, 2005). α-KGDH, together with citrate synthase and IDH determine the overall rate of the TCA cycle (Cooney et al., 1981; Moreno-Sánchez et al., 1990), and α-KGDH is thought to be the key enzyme which limits the generation of NADH under exposure to oxidative stress (Tretter and Adam-Vizi, 2005). Patients with ACLF exhibit markedly elevated oxidative stress levels as represented by increased human nonmercaptalbumin 1 (HNA1), an oxidized form of albumin (Alcaraz-Quiles et al., 2018). Therefore, it is conceivable that in these patients, when α-KGDH is inhibited under high degree of oxidative stress, the supply of NADH to complex I of the electron transport chain (ETC) becomes limited, thus decreasing mitochondrial respiration and ATP production.

3 AMINO ACID METABOLISM IN ADVANCED LIVER CIRRHOSIS

Systemic inflammation initiated by DAMPs and pathogen-associated molecular patterns most probably is the initiator of metabolic derangements and subsequent organ failures and high mortality in patients with ACLF (Clària et al., 2016; Bajaj et al., 2020; Moreau et al., 2020). Activation of the innate immune system requires the integrated coordination of the metabolism of glucose, nonessential amino acids (AAs) and one-carbon (1C) metabolism, the latter being compartmentalized in the cytosol, mitochondria and nucleus. In decompensated cirrhosis, metabolic alterations comprise intense proteolysis and lipolysis, probably through stimulation of the hypothalamic-pituitary-adrenal axis by glucocorticoids (Ganeshan et al., 2019; Kelly and Pearce, 2020), leading to severe skeletal muscle catabolism (Moreau et al., 2020; Zaccherini et al., 2021). This is clinically most relevant, as sarcopenia is associated with the development of ACLF (Praktiknjo et al., 2019). In physiological conditions, AA catabolism is essential for the conservation of nitrogen and for maintaining physiologic concentrations of AAs, which cannot be stored up in case of dietary excess. Their catabolism occurs in the liver except for branched-chain amino acids, which are mainly metabolized by skeletal muscle and adipose tissue (Brosnan and Brosnan, 2006; Grohmann and Bronte, 2010). AA catabolism is used for controlling pathogen invasion and at the same time for regulating own immune responses (Bronte and Zanovello, 2005; Mellor and Munn, 2008). The metabolomics database of the landmark CANONIC study comprises 137 metabolites of which 43% are related to AAs. Reanalysis using weighted gene co-expression network analysis (WGCNA) identified 9 modules of co-regulated metabolites (Zaccherini et al., 2021). Worthy of note was the parallel increase of metabolite modules with markers of inflammation such as C-reactive protein (CRP), soluble CD163 (sCD163), sCD206, IL-6, tumor necrosis factor α (TNFα) and IL-

10, indicating that inflammatory responses in patients with ACLF is accompanied by changes in AA metabolism (Zaccherini et al., 2021). The same study also suggested that in these patients, production of glutathione via the transsulfuration pathway and methionine renewal through the methionine salvage pathway are prioritized, probably to counteract systemic oxidative stress and to fuel the purine salvage pathway. In addition, N-formyl-L-methionine was reported to be increased in ACLF, suggesting enhanced conversion of serine to glycine and formate production in the folate cycle which forms part of the mitochondrial 1C metabolism.

In addition to reflecting disturbed AA metabolism, certain AAs and their derivatives exert biological functions, with the potential to impair organ functions (Clària et al., 2019). Patients with AD and ACLF present with reduced trytophan (Trp) levels, consistent with increased Trp degradation through the kynurenine pathway, giving rise to kynurenine, kynurenic and quinolinic acids (**2** in **Figure 1**). The first and rate-limiting step of the kynurenine pathway is catalyzed by the enzymes indoleamine-2,3-dioxygenase-1 (IDO-1) and tryptophan-2,3-dioxygenase (TDO) (Clària et al., 2019). *TDO2*, the gene encoding TDO, is mainly expressed in the liver, and IDO is known to be an important regulator of the immune system (Curti et al., 2009). In patients with ACLF, mRNA expression of *IDO1* and *IDO2* in peripheral blood mononuclear cells was increased, which could be related to the elevated plasma IFNγ levels in these patients (Clària et al., 2016; Clària et al., 2019). Increased expression of IDO depletes Trp in T cells, increasing uncharged tRNA levels, upon which the ribosomal stress-response kinase general control non-derepressible 2 (GCN2) is activated, leading to T cell anergy and proliferative arrest (Munn et al., 2005). Kynurenine and kynurenic acid exert immunomodulatory actions by binding to aryl hydrocarbon receptor (AhR) and G protein-coupled receptor 35 (GPR35) on immune cells (Wang et al., 2006; DiNatale et al., 2010). A portion of the AhR pool is localized in the intermembrane space of mitochondria, and ligand-induced activation of AhR attenuated mitochondrial maximal respiration (**2** in **Figure 1**) (Hwang et al., 2016). Increased kynurenine favours immune tolerance by inhibiting proliferation of T and NK cells and increasing proliferation of regulatory T cells and myeloid-derived suppressor cells (MDSCs), which might explain the positive association between higher baseline kynurenine pathway activity and the development of nosocomial infections and mortality in patients with AD cirrhosis (Clària et al., 2019). This finding further exemplifies the intricate link between metabolism and the immune system.

Pleiotropic effects on metabolic and immune processes were also described for glutamine and arginine, which are both inducers of mTORC1 (Chantranupong et al., 2016; Meng et al., 2020). Arginine functions as a precursor for metabolites with immunomodulatory properties such as polyamines and nitric oxide (NO) (Grohmann and Bronte, 2010) and is among the metabolites increased in patients with ACLF (Zaccherini et al., 2021). Increase in extracellular arginine increases oxygen consumption and mitochondrial spare respiratory capacity of T cells, indicating that arginine skews metabolism of activated T cells from glycolysis towards mitochondrial oxidative phosphorylation (OXPHOS), possibly through upregulation of serine biosynthesis which fuels the TCA cycle (Possemato et al., 2011; Geiger et al., 2016). Increase of intracellular arginine levels either through supplementation in medium or by inhibiting arginase (which metabolizes L-arginine to L-ornithine) resulted in less IFN-γ secretion and increased survival of antigen-activated T cells *in vitro* and *in vivo* (Geiger et al., 2016). Interestingly, patients with cirrhosis who developed poor outcome had higher levels of the arginine metabolites asymmetric dimethylarginine (ADMA) and symmetric dimethylarginine (SDMA) which adversely impact vascular reactivity and brain function (Bajaj et al., 2013; Bajaj et al., 2020).

4 CHANGES IN PLASMA AND MITOCHONDRIAL MEMBRANE LIPID COMPOSITION IN PATIENTS WITH CIRRHOSIS—INTERPLAY BETWEEN LIPID MEDIATORS AND MITOCHONDRIAL DYSFUNCTION

Inflammation is often associated with disturbances in cholesterol, fatty acid and phospholipid metabolism. This is also the case for patients with ACLF, who typically present with very low levels of high density lipoprotein (HDL) particles, probably attributed to the downregulation of reverse cholesterol transport mediated by acute phase responses (Feingold and Grunfeld, 2010; Trieb et al., 2020). It was proposed that the innate immune system differentially modifies macrophage cholesterol homeostasis in order to amplify the inflammatory response by activating the inflammasome and then to turn it off (Tall and Yvan-Charvet, 2015).

Untargeted blood lipidomics of cirrhotic patients with AD identified a specific lipid signature characterized by a generalized suppression of lipid species including the total polyunsaturated fatty acid (PUFA) pool and phospholipid families (i.e., lysophosphatidylcholine (LPC) and sphingomyelins), probably reflecting decreased hepatic biosynthetic capacity (López-Vicario et al., 2020; Clària et al., 2021). More specifically, LPC containing omega-3 PUFAs ranked among the lipids with greatest reduction in patients with AD and ACLF from the CANONIC cohort. Importantly, the decrease in LPC paralleled disease severity in patients with cirrhosis (Clària et al., 2021). Metabolomic analysis in a multicentre North American cohort complemented these findings, further demonstrating that patients who developed ACLF had lower serum phospholipids including phosphotidylethanolamine (PE), which is enriched in mitochondrial membranes, and higher estrone-3-sulfate level (Bajaj et al., 2020). An exception are fatty acids, which are notably increased due to enhanced lipolysis as indicated by blood accumulation of 2-hydroxyhexadecanoate, a by-product of lipolysis (Moreau et al., 2020; Zaccherini et al., 2021). At the same time, accumulation of acylcarnitines in the blood of patients indicates impaired translocation of fatty acids into mitochondrial matrix, the site of β-oxidation (**3** in **Figure 1**) (Moreau et al., 2020).

The alterations of blood lipid composition found in patients with decompensated cirrhosis are important, since it was shown that dietary fatty acids can remodel the lipid composition of

mitochondrial membranes (Sullivan et al., 2018). Mitochondrial membranes are enriched with phospholipid species such as phosphatidylcholine (PC), PE, phosphatidylinositol (PI), phosphatidylserine (PS) and cardiolipin (Horvath and Daum, 2013; Sullivan et al., 2018). The latter is a unique structural lipid with four fatty acyl chains that favors mitochondrial membrane fusion and fission, cristae formation and respiratory function (Schlame and Ren, 2009; Paradies et al., 2014; Ren et al., 2014). The PUFA species incorporated into mitochondrial phospholipids are critical for optimal lipid molecular organization, lipid microenvironment and mitochondrial function including the respiratory enzymes involved in OXPHOS (Schlame and Ren, 2009; Genova and Lenaz, 2014; Paradies, 2014; Ruiz-Ramírez et al., 2015; Sullivan et al., 2018; Maekawa et al., 2019). Interestingly, studies using hepatic steatosis high calorie-fed animal models observed that increased hepatic availability of saturated FAs induced changes in the composition of mitochondrial membrane cardiolipins, leading to exacerbated cytochrome c released from the mitochondria to the cytosol and increased mitochondrial ROS generation (**3** in **Figure 1**) (Crescenzo et al., 2015; Ruiz-Ramírez et al., 2015). Furthermore, circulating saturated fatty acids are able to elicit a pro-inflammatory response, since they sensitize hepatocytes to TLR agonists (Csak et al., 2011).

The omega-6 PUFA linoleic acid (LA) is the major fatty acid in mitochondrial membranes and constitutes almost 90% of the cardiolipin fatty acyl chains, which bind with high affinity to respiratory chain enzymes and stabilize them (Planas-Iglesias et al., 2015; Sullivan et al., 2018). Moreover, the high amount of LA in cardiolipin has been positively correlated with cytochrome c oxidase activity (Fajardo et al., 2015). In an animal model of heart failure, LA has been shown to improve mitochondrial OXPHOS capacity in cultured rat cardiomyocytes (Maekawa et al., 2019). Albeit being important for mitochondrial membrane integrity, high amounts of LA directly reduced the mitochondrial marker enzyme citrate synthase, as well as routine and maximal mitochondrial respiration in a concentration-dependent manner (Shrestha et al., 2019). Furthermore, an excessive LA dietary intake leads to exacerbated arachidonic acid-derived lipid mediators, such as prostaglandin E_2 (PGE_2) and leukotriene B_4 (LTB_4) (Shrestha et al., 2019). In fact, this is clinically most relevant as patients with AD cirrhosis present with elevated levels of PGE_2 which suppresses macrophage pro-inflammatory cytokine secretion and bacterial killing, mediated *via* the prostanoid type E receptor-2 (EP2) (O'Brien et al., 2014).

Since mitochondria play a critical role in the regulation of inflammation, bioactive lipid mediators generated under inflammatory conditions could play a paramount feature in mitochondrial function. Lipid mediators play a major role in the regulation of immune responses through generation of omega-6 PUFA-derived pro-inflammatory (i.e., PGs and LTs) and anti-inflammatory lipid mediators (specialized pro-resolving lipid mediators; SPM) derived from omega-3 PUFA (i.e., resolvins (Rv), maresins (MaR) and lipoxins (LX)), which are involved in the initiation and resolution of inflammation (Serhan, 2014; Dennis and Norris, 2015; López-Vicario et al., 2016). The main omega-3 PUFAs which serve as anti-inflammatory and pro-resolving lipid mediators or SPM precursors are docosahexaenoic acid (DHA) and eicosapentaenoic acid (EPA) (Serhan, 2014; López-Vicario et al., 2016). A targeted study of bioactive lipid mediators in patients with AD cirrhosis and ACLF further revealed higher circulating levels of arachidonic acid-derived LTE_4 and $PGF_{2\alpha}$ accompanied by reduced pro-resolving EPA-derived LXA_5 (**4** in **Figure 1**) (López-Vicario et al., 2020). The omega-6 arachidonic acid, biosynthesized from the conversion of LA through desaturation and elongation reactions, is also incorporated into phospholipids of mitochondrial membranes. Arachidonic acid is the major pro-inflammatory lipid mediator precursor and is able to replace the mitochondrial membrane LA leading to changes in membrane permeability, impaired function of respiratory chain complexes, higher cytochrome c release, ROS generation and mitochondrial depolarization through an uncoupling effect (Cocco et al., 1999; Scorrano et al., 2001; Haworth et al., 2010).

SPMs, firstly identified and termed by Serhan (2014), with well recognized potent inflammation-resolving effect on polymorphonuclear neutrophils and macrophages, are described to attenuate mitochondrial dysfunction in a mouse model of liver ischaemia/reperfusion injury and to reduce ROS levels in blood of patients with sepsis by increasing superoxide dismutase activity (Gu et al., 2018; Hecker et al., 2018; Kang et al., 2018). In the model of liver ischaemia/reperfusion injury, RvD1 which is biosynthesized from DHA *via* lipoxygenase (LOX) pathway (Serhan and Petasis, 2011), prevented ROS-mediated mitochondrial dysfunction and reduced mitochondrial swelling, lipid peroxidation and impaired activities of mitochondrial complexes I and III by regulating thioredoxin 2-mediated mitochondrial homeostasis (Kang et al., 2018). Moreover, RvD1 conserves ultrastructural morphology of mitochondria by activating mitophagy (Ren et al., 2020). In the sepsis model of bone marrow derived-macrophages (BMDM) with lipopolysaccharide (LPS), the DHA-derived 12-LOX product MaR1 (Serhan et al., 2009) was able to inhibit ROS production, increase mitochondrial membrane potential and improve ATP content (Gu et al., 2018).

Other lipid mediators worth mentioning are the EPA-derived SPM intermediate 18R-HEPE and RvE1, which also exerted a potent restorative effect in human peripheral mononuclear cells with TNFα-induced mitochondrial dysfunction (Hecker et al., 2018). After exposure to TNFα, cells treated with RvE1 and 18R-HEPE improved routine respiration and the mitochondrial membrane potential compared to those treated with the PUFAs arachidonic acid, DHA and EPA (Hecker et al., 2018). Interestingly, the impaired respiratory capacity and the impaired imbalance of mitochondrial fission and fusion were completely rescued by RvE1 (Mayer et al., 2019).

5 MITOCHONDRIAL DYSFUNCTION AT THE EARLY STAGES OF CHRONIC LIVER INJURY

There is accumulating evidence that mitochondrial dysfunction contributes to the development and progression of fibrosis. Fibrosis development can be regarded as non-homeostatic innate immune response to tissue damage, and the role of hepatic stellate cells

TABLE 1 | Overview of key findings related to mitochondrial dysfunction in patients with cirrhosis and ACLF.

Key findings	Mitochondrial function/process
Cirrhosis	
Increased numbers of mitochondria and swelling in circulating leukocytes of patients with AD cirrhosis (Zhang et al., 2021)	Mitochondrial structure
Systemic oxidative stress in patients with compensated and decompensated cirrhosis (Alcaraz-Quiles et al., 2018)	Oxidative stress
Decreased hepatic expression of COX1 and COX2 in cirrhotic patients (CHILD-Pugh A-C) (Nishikawa et al., 2014)	OXPHOS
Elevated serum mtDNA levels in patients with NASH-associated cirrhosis (An et al., 2020)	Mitochondrial DAMPs
ACLF	
Systemic oxidative stress in patients with ACLF, i.e. elevated levels of oxidized form of albumin (Oettl et al., 2008; Alcaraz-Quiles et al., 2018)	Oxidative stress
Increased extra-mitochondrial utilization of glucose in circulating leukocytes of patients with ACLF (Zhang et al., 2021)	Glucose metabolism
Elevated serum levels of hexanoyl- and tetradecenoylcarnitine (Moreau et al., 2020)	Mitochondrial β-oxidation
Downregulation of *PDP2* in circulating leukocytes of patients with ACLF (Zhang et al., 2021)	Glucose metabolism/TCA cycle
Decreased succinate utilization in leukocytes of patients with ACLF (Zhang et al., 2021)	TCA cycle

Bax, BCL2 associated X; BDL, bile duct ligation; CCl4, carbon tetrachloride; COX, cytochrome c oxidase; DDC, 3,5-diethoxycarbonyl-1,4-dihydrocollidine; DEN, diethylnitrosamine; D-gal: D-galactosamine; eNOS, endothelial nitric oxide synthase; i.p., intraperitoneal; i.v., intravenous; LPS, lipopolysaccharide; ND6, NADH dehydrogenase 6; p.o., per os; OCR, oxygen consumption rate; Ppargc-1α, peroxisome proliferator-activated receptor gamma coactivator 1-alpha; PDP2, pyruvate dehydrogenase phosphatase catalytic subunit 2; TAA, thioacetamide; Tfam, mitochondrial transcription factor A.

(HSCs) as innate immune cells is often under-recognized. Ongoing injury leads to activation of HSCs and their transdifferentiation into myofibroblasts, leading to progressive matrix deposition. This transformation is induced by inflammation-dependent and -independent mechanisms, including secretion of cytokines (i.e., TGFβ and IL-13), signaling through the succinate-GPR91-TGFβ pathway, mitochondrial ROS and apoptotic bodies arising from dying hepatocytes (Chiaramonte et al., 1999; Jiang et al., 2009; Pellicoro et al., 2014; Li et al., 2015a). Similar to immune cells, HSCs undergo metabolic rewiring during their activation. Hedgehog pathway is one of the main player in driving glycolysis and glutaminolysis in activated HSCs, which is essential for their transdifferentiation (Chen et al., 2012; Du et al., 2018). HSCs exert their immunomodulatory effects through production of ROS and pro-inflammatory cytokines and chemokines such as CC-chemokine receptor 2 (CCR2) ligand CCL2, CCL5 (RANTES), CCL3 and CCL4. Activated HSCs and macrophages secrete TGFβ, thereby further promoting myofibroblast activation and deposition of extracellular matrix (ECM). The canonical signaling of TGFβ is mediated by the Smad pathway, which results in repression of epithelial marker gene expression and activation of mesenchymal gene expression (Xu et al., 2009). However, it is less known that Smad2/3 are present and phosphorylated in mitochondria of $CD4^+$ T cells, or that TGFβ impairs mitochondrial function by reducing the basal and ATP-coupled oxygen consumption rate (OCR) of human $CD4^+$ T cells and inhibiting mitochondrial complex V (ATPase activity) (Dimeloe et al., 2019). Inhibition of complex V by TGFβ or oligomycin alone is sufficient to impair IFNγ production by $CD4^+$ T cells. Therefore, through impairing mitochondrial respiration, TGFβ is able to induce T cell paralysis.

Interestingly, succinate also emerges as a key metabolite in the context of fibrosis development. Li et al. (2016) proposed that succinate functions as a paracrine signal between hepatocytes and HSCs, thereby inducing the succinate receptor GPR91 and upregulating the fibrogenic markers alpha-smooth muscle actin (α-SMA), TGFβ and collagen type I (**5** in **Figure 1**). As a proof of concept, inhibition of succinate-GPR91 signaling by Ly2405319, an analog of fibroblast growth factor (FGF)21, attenuated HSC activation.

Mitochondria do not only function as a platform for profibrogenic signaling, but also actively participate in fibrogenesis. Mitochondria-derived DAMPs (mtDAMPs) are particularly immunogenic due to their structural similarities to bacteria. mtDNA from hepatocytes released into circulation promote inflammation through binding to endosomal TLR9 of liver resident Kupffer cells (**6** in **Figure 1**) (Garcia-Martinez et al., 2016). Apart from their pro-inflammatory effect, a recent elegantly conducted study demonstrated that mtDNA is also able to directly activate HSCs and trigger pro-fibrogenic responses in mice (An et al., 2020). More importantly, patients with non-alcoholic steatohepatitis with advanced fibrosis stage have higher circulating levels of mtDNA, supporting the finding that mtDNA are able to drive hepatic fibrogenesis (An et al., 2020).

Non-alcoholic fatty liver disease is a vivid example of how systemic immune responses are regulated by metabolism, and that harmful local fibrosis of the liver can develop if these systemic metabolic disturbances remain unresolved. Therefore, metabolic alterations should not only be regarded as a consequence of immune responses, but they should be at least considered as a root for immune cell impairment.

6 ORGAN DYSFUNCTION AND FAILURE IN ACUTE DECOMPENSATION CIRRHOSIS AND ACUTE-ON-CHRONIC LIVER FAILURE: ROLE OF MITOCHONDRIAL DYSFUNCTION

Systemic inflammation in patients with AD cirrhosis and ACLF require energetically expensive immune responses in order to produce inflammatory mediators, respiratory burst, and positive and negative acute-phase proteins (such as albumin) (Clària et al., 2016; Moreau et al., 2020). As a consequence, a competition for

TABLE 2 | Overview of different animal models of chronic liver injury, cirrhosis and ACLF and findings related to mitochondrial functionality.

Experimental model	Admin. route and induction time	Species	Key findings	Mitochondrial function/process
Animal models of chronic liver injury				
DDC	p.o. 8–10 weeks	Mouse	Reduced respiratory control ratio and complex II activity in hepatocytes (Nikam et al., 2013)	OXPHOS
			Reduction of hepatic ATP content (Nikam et al., 2013)	OXPHOS
DEN	i.p. 8 weeks	Mouse	Inhibition of complex I and complex IV in liver mitochondria (Santos et al., 2012)	OXPHOS
Animal models of cirrhosis				
CCl_4	p.o. 12–14 weeks for compensated cirrhosis and 26–28 weeks for decompensated cirrhosis	Rat	Increased hepatocyte mitochondrial mass (citrate synthase activity) (Nishikawa et al., 2014) and mitochondrial swelling (spectrophotometry) (Natarajan et al., 2006)	Mitochondrial structure
			Increased mitochondrial superoxide levels in hepatocytes and HSC (Vilaseca et al., 2017)	Oxidative stress
			Reduced basal OCR and maximal mitochondrial respiration in hepatocytes from failing cirrhotic livers (Nishikawa et al., 2014)	OXPHOS
			Decreased expression of *COX1*, *COX2*, *ND6* (Nishikawa et al., 2014)	OXPHOS
			Increased dependency on glycolysis as energy source (Nishikawa et al., 2014)	Glucose metabolism/ TCA cycle
			Downregulation of hepatic *PDP2* (Nishikawa et al., 2014)	
TAA	i.p. up to 5 months	Rat	Mitochondrial swelling (Natarajan et al., 2006)	Mitochondrial structure
			Increased malondialdehyde in liver mitochondria (Natarajan et al., 2006)	Oxidative stress
			Decreased respiratory control ratio (Natarajan et al., 2006)	OXPHOS
BDL	4 weeks	Rat	Decrease in mitochondrial membrane potential (Arduini et al., 2011)	Mitochondrial membrane potential
			Reduced hepatic expression of transcription factors regulating mitochondrial biogenesis (*Ppargc-1α*, *Tfam*) (Arduini et al., 2011)	Mitochondrial biogenesis
			Reduced hepatocyte activities of complex I, II and III (Krähenbühl et al., 1994)	OXPHOS
			Reduced fatty acid oxidation and impaired ketogenesis (Krähenbühl et al., 1994)	Mitochondrial β-oxidation
Animal models of ACLF				
Combination CCl_4 + LPS and BDL + LPS	CCl4: inhalation 15–16 weeks BDL: 28 days LPS: i.p. or i.v. (acute injection)	Rat	Increased hepatic superoxide levels, decrease in hepatic eNOS activation (Tripathi et al., 2018)	Oxidative stress
Porcine serum + LPS + D-gal	Porcine serum i.p. 11 weeks LPS: i.v. + D-gal: i.p. (acute injections)	Rat	Increased hepatic expression of Bax and decreased expression of Bcl-2 (Li et al., 2017)	Apoptosis

BDL, bile duct ligation; CCl_4, carbon tetrachloride; COX, cytochrome c oxidase; DDC, 3,5-diethoxycarbonyl-1, 4-dihydrocollidine; DEN, diethylnitrosamine; eNOS, endothelial nitric oxide synthase; i.p., intraperitoneal; i.v., intravenous; ND6, NADH, dehydrogenase 6; p.o., per os; OCR, oxygen consumption rate; Ppargc-1α, peroxisome proliferator-activated receptor gamma coactivator 1-alpha; PDP2, pyruvate dehydrogenase phosphatase catalytic subunit 2; TAA, thioacetamide; Tfam, mitochondrial transcription factor A.

energy with other maintenance programs, including organ function homeostasis, takes place (Ganeshan et al., 2019). In patients with AD and ACLF, glucose is preferentially used in extra-mitochondrial pathways in detriment of ATP production (Moreau et al., 2020), which directly triggers life-threatening organ failure(s), a recurrent feature present in diseases characterized by systemic inflammation (Carré and Singer, 2008; Van Wyngene et al., 2018). The impaired ATP production is especially devastating for the liver whose ATP synthesis rate, estimated at 30 mM/min in healthy volunteers using *in vivo* ^{31}P magnetization transfer experiment, is extraordinarily high compared to human skeletal muscle for example (Schmid et al., 2008).

Hence, mitochondrial dysfunction is typically found as an important hallmark in chronic liver diseases including cirrhosis (Mansouri et al., 2018). An overview of the findings related to mitochondrial dysfunction in patients with cirrhosis and ACLF and in different animal models of chronic liver injury is provided in **Tables 1**, **2**, respectively. In an attempt to compensate for decreased OXPHOS and maintain ATP production, hepatocytes of rats induced to cirrhosis with carbon tetrachloride (CCl_4) undergo a metabolic shift from OXPHOS to glycolysis (Nishikawa et al., 2014). In addition, inflammatory cells release a large amount of oxidants and cytokines (Piano and Angeli, 2021), such as TNFα which imitates the effect of uncouplers in mitochondria, contributing to the decrease in ATP production (Kastl et al., 2014; Song et al., 2019).

In hepatocytes of cirrhotic rats, the OCR as a proxy for the functionality of ETC is similar to that of control hepatocytes at early stages of cirrhosis, but was significantly reduced at the

terminal stage (Nishikawa et al., 2014). The decreased OCR could be a consequence of prolonged exposure of hepatocytes to inflammatory cytokines (Stadler et al., 1992). However, another study in murine hepatocytes detected an increment of OCR after one hour of TNFα-induced damage (Kastl et al., 2014). These findings suggest that the time of exposure to inflammatory cytokines determines if mitochondrial respiration is increased as a first effort of mitochondria to supply enough energy from OXPHOS, or if it is decreased as a secondary damage of prolonged inflammation.

Another aspect of mitochondrial dysfunction of the OXPHOS system in liver cirrhosis is the enhanced production of ROS (Chan, 2006; Natarajan et al., 2006). Oxidative stress produced by mitochondria induces apoptosis in hepatocytes and might consequently lead to deposition of scar tissue, i.e., fibrosis and cirrhosis, and eventually decompensation of liver function (Paradies, 2014; Luangmonkong et al., 2018).

In addition to failure of liver function, kidney, brain, coagulatory and circulatory failure and the combinations thereof are also part of the ACLF syndrome (Moreau et al., 2013). The kidney is one of the most energy-demanding organs in the human body (Wang et al., 2010). During the course of cirrhosis there is a marked decrease of the production of energy by mitochondria from tubular epithelial cells that can be explained by decreased number of mitochondria, swelling of individual organelles and disrupted cristae (Gomez et al., 2014; Tran et al., 2011; Brooks et al., 2009). Additionally, ROS released by damaged mitochondria contributes to oxidative stress, thereby amplifying inflammation and eventually inducing cell death of kidney cells (**7** in **Figure 1**) (Emma et al., 2016).

Another aspect in patients with decompensated cirrhosis is hyperammonemia, which correlates with organ failures and mortality (Shalimar et al., 2019) and impairs neutrophil function (Shawcross et al., 2008), further establishing the intimate connection between disturbed mitochondrial intermediate metabolism and inflammation. Ammonium (NH_3) is detoxified in mitochondria via glutamate or glutamine synthesis from α-KG, resulting in cataplerosis, i.e., depletion of the critical TCA cycle intermediate α-KG (Davuluri et al., 2016). Notably, in skeletal muscle this translates into sarcopenia due to lower flux of the TCA cycle and subsequent decreased ATP synthesis (**8** in **Figure 1**) (Jacobsen et al., 2001). Sarcopenia in turn results in reduced NH_3 clearance from the circulation, as skeletal muscle contain significant amounts of glutamine synthetase, thereby favouring the development of hepatic encephalopathy (**9** in **Figure 1**) (Merli et al., 2013).

In the brain, the cells most vulnerable to ammonia toxicity are astrocytes (Norenberg, 1981). NH_3 inhibits cerebral glutaminase activity (Bradford and Ward, 1976) and state III respiration in mitochondria isolated from acute NH_3-intoxicated rats (Kosenko et al., 1997). It collapses the mitochondrial membrane potential and increases the mitochondrial permeability in cultured astrocytes, possibly through alkalinization and dissipation of the mitochondrial proton gradient. In sparse-fur mice, which are deficient in hepatic ornithine transcarbamylase and therefore congenitally hyperammonemic, a progressive inhibition of electron transport complexes, particularly complex IV (cytochrome c oxidase), was observed (Rama Rao et al., 1997). In addition, the production of glutamine, derived from NH_3 detoxification, might similarly contribute to the induction of the mitochondrial permeability transition (MPT), since inhibition of glutamine synthetase with methionine sulfoximine (MSO) blocks the NH_3-induced collapse of the mitochondrial membrane potential (Bai et al., 2001).

7 THERAPEUTIC STRATEGIES

In this part, we will majorly focus on therapeutic approaches targeted at reversal of the metabolic reprogramming that takes place in advanced liver cirrhosis and ACLF. For strategies based on reduction of oxidative stress levels in cirrhosis, we refer to the excellent review by Li et al. (2015b).

7.1 Targeting the Tricarboxylic Acid Cycle in Macrophages

Supporting anaplerotic reactions, for example by feeding glutamine into the TCA cycle, restores the phagocytic capacity of monocytes which were conditioned with plasma of ACLF patients (Korf et al., 2019). This can be achieved through inhibition of the glutamine synthetase by MSO, a sulfoximine derivative of methionine, or by directly feeding the TCA intermediate α-KG, which promotes M2 activation *via* Jumonji domain-containing protein D3-dependent epigenetic reprogramming (Liu et al., 2017). Another possibility to increase intracellular α-KG availability can be achieved by employing the cell-permeable analogue dimethyl-α-KG. Dimethyl-α-KG suppressed nuclear translocation of NF-κB in glutamine-deprived BMDMs. Furthermore, supplementation of α-KG can relieve nitro-oxidative stress via their antioxidant properties. α-KG treatment in HepG2 increased levels of L-carnitine and restored mitochondrial β-oxidation (Lemire et al., 2011). This is relevant in patients with AD, as they exhibit relative L-carnitine deficiency due to increased circulating acylcarnitines (Zhang et al., 2021). α-KG and succinate, both intermediates of the TCA cycle, act as antagonistic players, thus targeting the α-KG/succinate ratio might be a good manipulation point to tailor macrophage immune responses in patients with ACLF (Liu et al., 2017).

7.2 Inhibition of Succinate-GPR91 Signaling

Since the discovery of succinate as a specific activator of GPR91 in 2004 (He et al., 2004), the involvement of the succinate-GPR91 axis in a multitude of diseases is being gradually unravelled. Activation of GPR91, a plasma membrane receptor, leads to intracellular release of arachidonic acid and production of PGE_2, development of tubulo-interstitial fibrosis in diabetic nephropathy and enhanced activation of HSCs in the liver (Correa et al., 2007; Robben et al., 2009; Peti-Peterdi, 2010). Small molecule antagonists of human GPR91 were firstly identified in 2011, among them two orally bioavailable compounds termed 5g and 7e, identified through a systematic structure-function high-throughput screening analysis (Bhuniya

et al., 2011). Another high-affinity and highly selective human antagonist denoted NF-56-EJ40 was identified later in 2019 (Haffke et al., 2019). These compounds could serve as a promising starting point for preclinical studies investigating their effects in advanced liver cirrhosis.

7.3 Induction of PGC-1α

Activation of peroxisome proliferator-activated receptor γ coactivator 1α (PGC-1α), the master regulator of mitochondrial biogenesis, is a target worth considering. Interestingly, it has been discovered that PGC-1α, apart from its nuclear localization, is also found in mitochondria, where it forms a multiprotein complex with mitochondrial transcription factor A (TFAM) (Aquilano et al., 2010). To our knowledge, only two direct activators of PGC-1α, ZLN005 (2-[4-(1,1-dimethylethyl)phenyl]-1H-benzimidazole) and Mogroside VI B, a cucurbitane glucoside, are available. These compounds have been only investigated in preclinical models of ischaemia-induced neuronal injury and diabetic db/db mice, where they show beneficial effects (Zhang et al., 2013; Xu et al., 2018). All the other pharmacological compounds (metformin, bezafibrate, activators of AMP-activated protein kinase and sirtuins) are indirectly aimed at PGC-1α activation.

7.4 Restoring Lipid Homeostasis

RVX-208 (2-[4-(2-hydroxyethoxy)-3,5-dimethylphenyl]-5,7-dimethoxy-4/3H)-quinazo-linone) is a small molecule which displaces bromodomain and extraterminal (BET) domains from chromatin and increases transcription of APOA1 gene, thereby increasing APO1 and HDL levels in humans (McLure et al., 2013; Picaud et al., 2013). Several phase I and II clinical trials investigating BET inhibitors for its anti-proliferative effect in solid and hematologic malignancies are registered, and one phase III study is currently recruiting patients with myelofibrosis for the treatment with a BET inhibitor in combination with ruxolitinib, a janus kinase (JAK) inhibitor. Given the fact that inhibition of bromodomain-containing protein 4, another member of BET proteins, abrogated activation of HSCs and even reversed liver fibrosis in mice treated with CCl_4 (Ding et al., 2015), BET inhibitors should be evaluated for the treatment of liver fibrosis. One other effect of BET inhibitors, which should be kept in mind, is that they have the potential to reactivate HIV from latency (Banerjee et al., 2012).

Another more general strategy aimed at restoring lipid homeostasis in patients with AD could be the activation of the liver X receptor (LXR). LXR promotes cholesterol efflux through ATP-binding cassette transporters ABCA1 and ABCG1 and induces the expression of genes involved in elongation and unsaturation of fatty acids. Activation of LXRα in the liver also induces lysophosphosphatidylcholine acyltransfase 3 (LPCAT3) which mediates the synthesis of phospholipid-containing PUFAs, thereby decreasing inflammatory responses (Li et al., 2013; Rong et al., 2013). The increase in PUFAs decreases transcriptional responses of NF-κB target genes through altered histone acetylation in their promoter regions (Li et al., 2013), and LPCs ameliorate cytokine secretion and enhance bacterial clearance (Elsbach and Levy, 1968; Yan et al., 2004). Therefore, activation of LXR could be beneficial in patients with AD and ACLF whose plasma is characterised by a decrease in the total PUFA pool (López-Vicario et al., 2020). However, activation of LXRs could be a double-edged sword, as LXRs are highly expressed in haematopoietic stem cells and myeloid progenitor cells, in which they decrease the proliferative responses to IL-3 and GM-CSF (Murphy et al., 2011). LXR also increase expression of MER proto-oncogene tyrosine kinase (MERTK), which suppresses TLR-4 mediated inflammatory responses through enhancement of efferocytosis. ACLF is on the one hand characterized by an exaggerated hyperinflammatory state, and on the other hand by immune paralysis as evidenced by an expansion of immunosuppressive acting monocytes and macrophages which express MERTK. In line with this, MERTK inhibitors restore cytokine production by immune cells from patients with ACLF (Bernsmeier et al., 2015). Therefore, because of the delicate balance between too much inflammation and not enough in patients with ACLF, a generalized therapy concept might be harmful for some patient subsets with ACLF. Therapy in patients with ACLF requires individualized concepts, and diagnostics should also intend to evaluate the extent of inflammation/immune dysfunction in each patient individually. In this case, an elegant solution as to how LXR activation can be targeted to specific cell subsets which exhibit a pro-inflammatory phenotype, but not to those which show exhaustion, would be welcome.

Last but not least, treatment of patients with cirrhosis should take dietary habits and physical activity, which are able to modulate mitochondrial function via direct or indirect mechanisms, into account. The analysis of the mitochondrial membrane phospholipidome in healthy subjects demonstrated that EPA and DHA supplementation is able to increase omega-3 PUFA levels in mitochondrial membranes from skeletal muscle biopsies by replacing omega-6 PUFA in mitochondrial phospholipids (Herbst et al., 2014). This study demonstrated the role for omega-3 PUFAs in the mitochondrial membrane reorganization while ameliorating mitochondrial function and ADP sensitivity (Herbst et al., 2014). Importantly, dietary omega-3 PUFA enrichment favored ATP-linked OCR in both peripheral mononuclear cells and macrophages (Lau et al., 2020).

8 CONCLUSION

The critical mass of research supports the importance of systemic inflammation in development of AD cirrhosis and ACLF. In this review, we focused on the emerging evidence that mitochondrial dysfunction is another hallmark of advanced liver cirrhosis. Mitochondria are not only the executers of the immune system, but they also act as powerful effectors endowed with the ability to shape the immune responses towards a hyperinflammatory or immunosuppressive state. Therefore, we suggest that future strategies to treat patients with AD cirrhosis and ACLF should be focused on restoring metabolic homeostasis in immune cells. In the **Supplementary Material** of this review, we summarize the methodological background of the current methods dedicated to the assessment of mitochondrial function.

AUTHOR CONTRIBUTIONS

Conceptualization and design (IWZ, JC); writing and editing (IWZ, CL-V, MD-G and JC).

FUNDING

Our laboratory is a Consolidated Research Group recognized by the Generalitat de Catalunya (2017SGR1449) and is supported by the Spanish Ministerio de Ciencia e Innovacion (PID2019-105240RB-I00) and EF Clif, a non-profit private organization that receives unrestricted donations from Cellex Foundation, Grifols and European Union's Horizon 2020 research and innovation programme (825694 and 847949). IWZ is supported by the Sheila Sherlock Post Graduate Programme of the European Association for the Study of the Liver (EASL).

SUPPLEMENTARY MATERIAL

The Supplementary Material for this article can be found online at: https://www.frontiersin.org/articles/10.3389/fmolb.2021.772174/full#supplementary-material

REFERENCES

Alcaraz-Quiles, J., Casulleras, M., Oettl, K., Titos, E., Flores-Costa, R., Duran-Güell, M., et al. (2018). Oxidized Albumin Triggers a Cytokine Storm in Leukocytes through P38 Mitogen-Activated Protein Kinase: Role in Systemic Inflammation in Decompensated Cirrhosis. *Hepatology* 68, 1937–1952. doi:10.1002/hep.30135

An, P., Wei, L. L., Zhao, S., Sverdlov, D. Y., Vaid, K. A., Miyamoto, M., et al. (2020). Hepatocyte Mitochondria-Derived Danger Signals Directly Activate Hepatic Stellate Cells and Drive Progression of Liver Fibrosis. *Nat. Commun.* 11, 2362. doi:10.1038/s41467-020-16092-0

Angajala, A., Lim, S., Phillips, J. B., Kim, J. H., Yates, C., You, Z., et al. (2018). Diverse Roles of Mitochondria in Immune Responses: Novel Insights into Immuno-Metabolism. *Front. Immunol.* 9, 1605. doi:10.3389/fimmu.2018.01605

Aon, M. A., Bhatt, N., and Cortassa, S. C. (2014). Mitochondrial and Cellular Mechanisms for Managing Lipid Excess. *Front. Physiol.* 5 (JUL), 282–313. doi:10.3389/fphys.2014.00282

Aquilano, K., Vigilanza, P., Baldelli, S., Pagliei, B., Rotilio, G., and Ciriolo, M. R. (2010). Peroxisome Proliferator-Activated Receptor γ Co-activator 1α (PGC-1α) and Sirtuin 1 (SIRT1) Reside in Mitochondria. *J. Biol. Chem.* 285, 21590–21599. doi:10.1074/jbc.m109.070169

Arduini, A., Serviddio, G., Escobar, J., Tormos, A. M., Bellanti, F., Viña, J., et al. (2011). Mitochondrial Biogenesis Fails in Secondary Biliary Cirrhosis in Rats Leading to Mitochondrial DNA Depletion and Deletions. *Am. J. Physiology-Gastrointestinal Liver Physiol.* 301, G119–G127. doi:10.1152/ajpgi.00253.2010

Bai, G., Rama Rao, K. V., Murthy, C. R. K., Panickar, K. S., Jayakumar, A. R., and Norenberg, M. D. (2001). Ammonia Induces the Mitochondrial Permeability Transition in Primary Cultures of Rat Astrocytes. *J. Neurosci. Res.* 66, 981–991. doi:10.1002/jnr.10056

Bajaj, J. S., Ahluwalia, V., Wade, J. B., Sanyal, A. J., White, M. B., Noble, N. A., et al. (2013). Asymmetric Dimethylarginine Is Strongly Associated with Cognitive Dysfunction and Brain MR Spectroscopic Abnormalities in Cirrhosis. *J. Hepatol.* 58, 38–44. doi:10.1016/j.jhep.2012.08.005

Bajaj, J. S., Reddy, K. R., O'Leary, J. G., Vargas, H. E., Lai, J. C., Kamath, P. S., et al. (2020). Serum Levels of Metabolites Produced by Intestinal Microbes and Lipid Moieties Independently Associated with Acute-On-Chronic Liver Failure and Death in Patients with Cirrhosis. *Gastroenterology* 159, 1715–1730. doi:10.1053/j.gastro.2020.07.019

Banerjee, C., Archin, N., Michaels, D., Belkina, A. C., Denis, G. V., Bradner, J., et al. (2012). BET Bromodomain Inhibition as a Novel Strategy for Reactivation of HIV-1. *J. Leukoc. Biol.* 92, 1147–1154. doi:10.1189/jlb.0312165

Bernsmeier, C., Pop, O. T., Singanayagam, A., Triantafyllou, E., Patel, V. C., Weston, C. J., et al. (2015). Patients with Acute-On-Chronic Liver Failure Have Increased Numbers of Regulatory Immune Cells Expressing the Receptor Tyrosine Kinase MERTK. *Gastroenterology* 148, 603–615. doi:10.1053/j.gastro.2014.11.045

Bhuniya, D., Umrani, D., Dave, B., Salunke, D., Kukreja, G., Gundu, J., et al. (2011). Discovery of a Potent and Selective Small Molecule hGPR91 Antagonist. *Bioorg. Med. Chem. Lett.* 21, 3596–3602. doi:10.1016/j.bmcl.2011.04.091

Bracey, N. A., Gershkovich, B., Chun, J., Vilaysane, A., Meijndert, H. C., Wright, J. R., et al. (2014). Mitochondrial NLRP3 Protein Induces Reactive Oxygen Species to Promote Smad Protein Signaling and Fibrosis Independent from the Inflammasome. *J. Biol. Chem.* 289, 19571–19584. doi:10.1074/jbc.m114.550624

Bradford, H. F., and Ward, H. K. (1976). On Glutaminase Activity in Mammalian Synaptosomes. *Brain Res.* 110, 115–125. doi:10.1016/0006-8993(76)90212-2

Bronte, V., and Zanovello, P. (2005). Regulation of Immune Responses by L-Arginine Metabolism. *Nat. Rev. Immunol.* 5, 641–654. doi:10.1038/nri1668

Brooks, C., Wei, Q., Cho, S.-G., and Dong, Z. (2009). Regulation of Mitochondrial Dynamics in Acute Kidney Injury in Cell Culture and Rodent Models. *J. Clin. Invest.* 119, 1275–1285. doi:10.1172/jci37829

Brosnan, J. T., and Brosnan, M. E. (2006). Branched-Chain Amino Acids: Enzyme and Substrate Regulation. *J. Nutr.* 136, 207S–211S. doi:10.1093/jn/136.1.207s

Carré, J. E., and Singer, M. (2008). Cellular Energetic Metabolism in Sepsis: The Need for a Systems Approach. *Biochim. Biophys. Acta (Bba) - Bioenerg.* 1777, 763–771. doi:10.1016/j.bbabio.2008.04.024

Chan, D. C. (2006). Mitochondria: Dynamic Organelles in Disease, Aging, and Development. *Cell* 125, 1241–1252. doi:10.1016/j.cell.2006.06.010

Chang, C.-H., Curtis, J. D., Maggi, L. B., Faubert, B., Villarino, A. V., O'Sullivan, D., et al. (2013). Posttranscriptional Control of T Cell Effector Function by Aerobic Glycolysis. *Cell* 153, 1239–1251. doi:10.1016/j.cell.2013.05.016

Chantranupong, L., Scaria, S. M., Saxton, R. A., Gygi, M. P., Shen, K., Wyant, G. A., et al. (2016). The CASTOR Proteins Are Arginine Sensors for the mTORC1 Pathway. *Cell* 165, 153–164. doi:10.1016/j.cell.2016.02.035

Chen, Y., Choi, S. S., Michelotti, G. A., Chan, I. S., Swiderska-Syn, M., Karaca, G. F., et al. (2012). Hedgehog Controls Hepatic Stellate Cell Fate by Regulating Metabolism. *Gastroenterology* 143, 1319–1329. doi:10.1053/j.gastro.2012.07.115

Cheng, S.-C., Scicluna, B. P., Arts, R. J. W., Gresnigt, M. S., Lachmandas, E., Giamarellos-Bourboulis, E. J., et al. (2016). Broad Defects in the Energy Metabolism of Leukocytes Underlie Immunoparalysis in Sepsis. *Nat. Immunol.* 17, 406–413. doi:10.1038/ni.3398

Chiaramonte, M. G., Donaldson, D. D., Cheever, A. W., and Wynn, T. A. (1999). An IL-13 Inhibitor Blocks the Development of Hepatic Fibrosis during a T-Helper Type 2-dominated Inflammatory Response. *J. Clin. Invest.* 104, 777–785. doi:10.1172/jci7325

Clària, J., Curto, A., Moreau, R., Colsch, B., López-Vicario, C., Lozano, J. J., et al. (2021). Untargeted Lipidomics Uncovers Lipid Signatures that Distinguish Severe from Moderate Forms of Acutely Decompensated Cirrhosis. *J. Hepatol.* 75, 1116–1127. doi:10.1016/j.jhep.2021.06.043

Clària, J., Moreau, R., Fenaille, F., Amorós, A., Junot, C., Gronbaek, H., et al. (2019). Orchestration of Tryptophan-Kynurenine Pathway, Acute Decompensation, and Acute-on-Chronic Liver Failure in Cirrhosis. *Hepatology* 69, 1686–1701. doi:10.1002/hep.30363

Clària, J., Stauber, R. E., Coenraad, M. J., Moreau, R., Jalan, R., Pavesi, M., et al. (2016). Systemic Inflammation in Decompensated Cirrhosis: Characterization and Role in Acute-On-Chronic Liver Failure. *Hepatology* 64, 1249–1264. doi:10.1002/hep.28740

Cocco, T., Di, M., Papa, P., and Lorusso, M. (1999). Arachidonic Acid Interaction with the Mitochondrial Electron Transport Chain Promotes

Reactive Oxygen Species Generation. *Free Radic. Biol. Med.* 27, 51–59. doi:10.1016/s0891-5849(99)00034-9

Cooney, G. J., Taegtmeyer, H., and Newsholme, E. A. (1981). Tricarboxylic Acid Cycle Flux and Enzyme Activities in the Isolated Working Rat Heart. *Biochem. J.* 200, 701–703. doi:10.1042/bj2000701

Correa, P. R. A. V., Kruglov, E. A., Thompson, M., Leite, M. F., Dranoff, J. A., and Nathanson, M. H. (2007). Succinate Is a Paracrine Signal for Liver Damage. *J. Hepatol.* 47, 262–269. doi:10.1016/j.jhep.2007.03.016

Crescenzo, R., Bianco, F., Mazzoli, A., Giacco, A., Cancelliere, R., di Fabio, G., et al. (2015). Fat Quality Influences the Obesogenic Effect of High Fat Diets. *Nutrients* 7, 9475–9491. doi:10.3390/nu7115480

Csak, T., Ganz, M., Pespisa, J., Kodys, K., Dolganiuc, A., and Szabo, G. (2011). Fatty Acid and Endotoxin Activate Inflammasomes in Mouse Hepatocytes that Release Danger Signals to Stimulate Immune Cells. *Hepatology* 54, 133–144. doi:10.1002/hep.24341

Curti, A., Trabanelli, S., Salvestrini, V., Baccarani, M., and Lemoli, R. M. (2009). The Role of Indoleamine 2,3-dioxygenase in the Induction of Immune Tolerance: Focus on Hematology. *Blood* 113, 2394–2401. doi:10.1182/blood-2008-07-144485

Davuluri, G., Allawy, A., Thapaliya, S., Rennison, J. H., Singh, D., Kumar, A., et al. (2016). Hyperammonaemia-induced Skeletal Muscle Mitochondrial Dysfunction Results in Cataplerosis and Oxidative Stress. *J. Physiol.* 594, 7341–7360. doi:10.1113/jp272796

Dennis, E. A., and Norris, P. C. (2015). Eicosanoid Storm in Infection and Inflammation. *Nat. Rev. Immunol.* 15, 511–523. doi:10.1038/nri3859

Dimeloe, S., Gubser, P., Loeliger, J., Frick, C., Develioglu, L., Fischer, M., et al. (2019). Tumor-derived TGF-β Inhibits Mitochondrial Respiration to Suppress IFN-γ Production by Human CD4+ T Cells. *Sci. Signal.* 12, eaav3334. doi:10.1126/scisignal.aav3334

DiNatale, B. C., Murray, I. A., Schroeder, J. C., Flaveny, C. A., Lahoti, T. S., Laurenzana, E. M., et al. (2010). Kynurenic Acid Is a Potent Endogenous Aryl Hydrocarbon Receptor Ligand that Synergistically Induces Interleukin-6 in the Presence of Inflammatory Signaling. *Toxicol. Sci.* 115, 89–97. doi:10.1093/toxsci/kfq024

Ding, N., Hah, N., Yu, R. T., Sherman, M. H., Benner, C., Leblanc, M., et al. (2015). BRD4 Is a Novel Therapeutic Target for Liver Fibrosis. *Proc. Natl. Acad. Sci. USA* 112, 15713–15718. doi:10.1073/pnas.1522163112

Doherty, D. G., Norris, S., Madrigal-Estebas, L., McEntee, G., Traynor, O., Hegarty, J. E., et al. (1999). The Human Liver Contains Multiple Populations of NK Cells, T Cells, and CD3+CD56+ Natural T Cells with Distinct Cytotoxic Activities and Th1, Th2, and Th0 Cytokine Secretion Patterns. *J. Immunol.* 163, 2314–2321.

Du, K., Hyun, J., Premont, R. T., Choi, S. S., Michelotti, G. A., Swiderska-Syn, M., et al. (2018). Hedgehog-YAP Signaling Pathway Regulates Glutaminolysis to Control Activation of Hepatic Stellate Cells. *Gastroenterology* 154, 1465–1479. doi:10.1053/j.gastro.2017.12.022

Dusseaux, M., Martin, E., Serriari, N., Péguillet, I., Premel, V., Louis, D., et al. (2011). Human MAIT Cells Are Xenobiotic-Resistant, Tissue-Targeted, CD161hi IL-17-secreting T Cells. *Blood* 117, 1250–1259. doi:10.1182/blood-2010-08-303339

Elsbach, P., and Levy, S. (1968). Increased Synthesis of Phospholipid during Phagocytosis. *J. Clin. Invest.* 47, 2217–2229. doi:10.1172/jci105907

Emma, F., Montini, G., Parikh, S. M., and Salviati, L. (2016). Mitochondrial Dysfunction in Inherited Renal Disease and Acute Kidney Injury. *Nat. Rev. Nephrol.* 12, 267–280. doi:10.1038/nrneph.2015.214

Fajardo, V. A., McMeekin, L., Saint, C., and Leblanc, P. J. (2015). Cardiolipin Linoleic Acid Content and Mitochondrial Cytochrome C Oxidase Activity Are Associated in Rat Skeletal Muscle. *Chem. Phys. Lipids* 187, 50–55. doi:10.1016/j.chemphyslip.2015.02.004

Feingold, K. R., and Grunfeld, C. (2010). The Acute Phase Response Inhibits Reverse Cholesterol Transport. *J. Lipid Res.* 51, 682–684. doi:10.1194/jlr.e005454

Fernández, J., Acevedo, J., Wiest, R., Gustot, T., Amoros, A., Deulofeu, C., et al. (2017). Bacterial and Fungal Infections in Acute-On-Chronic Liver Failure: Prevalence, Characteristics and Impact on Prognosis. *Gut* 67, 1870–1880. doi:10.1136/gutjnl-2017-314240

Ganeshan, K., Nikkanen, J., Man, K., Leong, Y. A., Sogawa, Y., Maschek, J. A., et al. (2019). Energetic Trade-Offs and Hypometabolic States Promote Disease Tolerance. *Cell* 177, 399–413. doi:10.1016/j.cell.2019.01.050

Garcia-Martinez, I., Santoro, N., Chen, Y., Hoque, R., Ouyang, X., Caprio, S., et al. (2016). Hepatocyte Mitochondrial DNA Drives Nonalcoholic Steatohepatitis by Activation of TLR9. *J. Clin. Invest.* 126, 859–864. doi:10.1172/jci83885

Geiger, R., Rieckmann, J. C., Wolf, T., Basso, C., Feng, Y., Fuhrer, T., et al. (2016). L-arginine Modulates T Cell Metabolism and Enhances Survival and Anti-tumor Activity. *Cell* 167, 829–842. doi:10.1016/j.cell.2016.09.031

Genova, M. L., and Lenaz, G. (2014). Functional Role of Mitochondrial Respiratory Supercomplexes. *Biochim. Biophys. Acta (Bba) - Bioenerg.* 1837, 427–443. doi:10.1016/j.bbabio.2013.11.002

Golden-Mason, L., Kelly, A. M., Doherty, D. G., Traynor, O., McEntee, G., Kelly, J., et al. (2004). Hepatic Interleuklin 15 (IL-15) Expression: Implications for Local NK/NKT Cell Homeostasis and Development. *Clin. Exp. Immunol.* 138, 94–101. doi:10.1111/j.1365-2249.2004.02586.x

Gomez, H., Ince, C., De Backer, D., Pickkers, P., Payen, D., Hotchkiss, J., et al. (2014). A Unified Theory of Sepsis-Induced Acute Kidney Injury. *Shock* 41, 3–11. doi:10.1097/shk.0000000000000052

Grohmann, U., and Bronte, V. (2010). Control of Immune Response by Amino Acid Metabolism. *Immunol. Rev.* 236, 243–264. doi:10.1111/j.1600-065x.2010.00915.x

Gu, J., Luo, L., Wang, Q., Yan, S., Lin, J., Li, D., et al. (2018). Maresin 1 Attenuates Mitochondrial Dysfunction through the ALX/cAMP/ROS Pathway in the Cecal Ligation and Puncture Mouse Model and Sepsis Patients. *Lab. Invest.* 98, 715–733. doi:10.1038/s41374-018-0031-x

Haffke, M., Fehlmann, D., Rummel, G., Boivineau, J., Duckely, M., Gommermann, N., et al. (2019). Structural Basis of Species-Selective Antagonist Binding to the Succinate Receptor. *Nature* 574, 581–585. doi:10.1038/s41586-019-1663-8

Haworth, R. A., Potter, K. T., and Russell, D. C. (2010). Role of Arachidonic Acid, Lipoxygenase, and Mitochondrial Depolarization in Reperfusion Arrhythmias. *Am. J. Physiol. Heart Circ. Physiol.* 299, H165–H174. doi:10.1152/ajpheart.00906.2009

He, W., Miao, F. J.-P., Lin, D. C.-H., Schwandner, R. T., Wang, Z., Gao, J., et al. (2004). Citric Acid Cycle Intermediates as Ligands for Orphan G-Protein-Coupled Receptors. *Nature* 429, 188–193. doi:10.1038/nature02488

Hecker, M., Sommer, N., Foch, S., Hecker, A., Hackstein, H., Witzenrath, M., et al. (2018). Resolvin E1 and its Precursor 18R-HEPE Restore Mitochondrial Function in Inflammation. *Biochim. Biophys. Acta (Bba) - Mol. Cel Biol. Lipids* 1863, 1016–1028. doi:10.1016/j.bbalip.2018.06.011

Herbst, E. A. F., Paglialunga, S., Gerling, C., Whitfield, J., Mukai, K., Chabowski, A., et al. (2014). Omega-3 Supplementation Alters Mitochondrial Membrane Composition and Respiration Kinetics in Human Skeletal Muscle. *J. Physiol.* 592, 1341–1352. doi:10.1113/jphysiol.2013.267336

Horvath, S. E., and Daum, G. (2013). Lipids of Mitochondria. *Prog. Lipid Res.* 52, 590–614. doi:10.1016/j.plipres.2013.07.002

Huang, S. C.-C., Everts, B., Ivanova, Y., O'Sullivan, D., Nascimento, M., Smith, A. M., et al. (2014). Cell-intrinsic Lysosomal Lipolysis Is Essential for Alternative Activation of Macrophages. *Nat. Immunol.* 15, 846–855. doi:10.1038/ni.2956

Hwang, H. J., Dornbos, P., Steidemann, M., Dunivin, T. K., Rizzo, M., and LaPres, J. J. (2016). Mitochondrial-targeted Aryl Hydrocarbon Receptor and the Impact of 2,3,7,8-Tetrachlorodibenzo-P-Dioxin on Cellular Respiration and the Mitochondrial Proteome. *Toxicol. Appl. Pharmacol.* 304, 121–132. doi:10.1016/j.taap.2016.04.005

Jacobsen, E., Hamberg, O., Quistorff, B., and Ott, P. (2001). Reduced Mitochondrial Adenosine Triphosphate Synthesis in Skeletal Muscle in Patients with Child-Pugh Class B and C Cirrhosis. *Hepatology* 34, 7–12. doi:10.1053/jhep.2001.25451

Jha, A. K., Huang, S. C.-C., Sergushichev, A., Lampropoulou, V., Ivanova, Y., Loginicheva, E., et al. (2015). Network Integration of Parallel Metabolic and Transcriptional Data Reveals Metabolic Modules that Regulate Macrophage Polarization. *Immunity* 42, 419–430. doi:10.1016/j.immuni.2015.02.005

Jiang, J. X., Mikami, K., Venugopal, S., Li, Y., and Török, N. J. (2009). Apoptotic Body Engulfment by Hepatic Stellate Cells Promotes Their Survival by the JAK/STAT and Akt/NF-κb-dependent Pathways. *J. Hepatol.* 51, 139–148. doi:10.1016/j.jhep.2009.03.024

Kang, J.-W., Choi, H.-S., and Lee, S.-M. (2018). Resolvin D1 Attenuates Liver Ischaemia/reperfusion Injury through Modulating Thioredoxin 2-mediated Mitochondrial Quality Control. *Br. J. Pharmacol.* 175, 2441–2453. doi:10.1111/bph.14212

Kastl, L., Sauer, S. W., Ruppert, T., Beissbarth, T., Becker, M. S., Süss, D., et al. (2014). TNF-α Mediates Mitochondrial Uncoupling and Enhances ROS-

dependent Cell migrationviaNF-Kb Activation in Liver Cells. *FEBS Lett.* 588, 175–183. doi:10.1016/j.febslet.2013.11.033

Kelly, A., Goldenmason, L., Traynor, O., Geoghegan, J., McEntee, G., Hegarty, J., et al. (2006). Changes in Hepatic Immunoregulatory Cytokines in Patients with Metastatic Colorectal Carcinoma: Implications for Hepatic Anti-tumour Immunity. *Cytokine* 35, 171–179. doi:10.1016/j.cyto.2006.07.019

Kelly, B., and Pearce, E. L. (2020). Amino Assets: How Amino Acids Support Immunity. *Cel Metab.* 32, 154–175. doi:10.1016/j.cmet.2020.06.010

Kenna, T., Golden-Mason, L., Norris, S., Hegarty, J. E., O'Farrelly, C., and Doherty, D. G. (2004). Distinct Subpopulations of ?? T Cells Are Present in normal and Tumor-Bearing Human Liver. *Clin. Immunol.* 113, 56–63. doi:10.1016/j.clim.2004.05.003

Kenna, T., Mason, L. G., Porcelli, S. A., Koezuka, Y., Hegarty, J. E., O'Farrelly, C., et al. (2003). NKT Cells from Normal and Tumor-Bearing Human Livers Are Phenotypically and Functionally Distinct from Murine NKT Cells. *J. Immunol.* 171, 1775–1779. doi:10.4049/jimmunol.171.4.1775

Korf, H., Du Plessis, J., Van Pelt, J., De Groote, S., Cassiman, D., Verbeke, L., et al. (2019). Inhibition of Glutamine Synthetase in Monocytes from Patients with Acute-On-Chronic Liver Failure Resuscitates Their Antibacterial and Inflammatory Capacity. *Gut.* 68, 1872–1883. doi:10.1136/gutjnl-2018-316888

Kosenko, E., Felipo, V., Montoliu, C., Grisolía, S., and Kaminsky, Y. (1997). Effects of Acute Hyperammonemiain Vivo on Oxidative Metabolism in Nonsynaptic Rat Brain Mitochondria. *Metab. Brain Dis.* 12, 69–82. doi:10.1007/bf02676355

Krähenbühl, S., Talos, C., and Reichen, J. (1994). Mechanisms of Impaired Hepatic Fatty Acid Metabolism in Rats with Long-Term Bile Duct Ligation. *Hepatology* 19, 1272–1281. doi:10.1002/hep.1840190528

Lau, Y. C. C., Ding, J. A., Simental, A., Mirzoyan, H., Lee, W., Diamante, G., et al. (2020). Omega-3 Fatty Acids Increase OXPHOS Energy for Immune Therapy of Alzheimer Disease Patients. *FASEB j.* 34, 9982–9994. doi:10.1096/fj.202000669rr

Lemire, J., Mailloux, R., Darwich, R., Auger, C., and Appanna, V. D. (2011). The Disruption of L-Carnitine Metabolism by Aluminum Toxicity and Oxidative Stress Promotes Dyslipidemia in Human Astrocytic and Hepatic Cells. *Toxicol. Lett.* 203, 219–226. doi:10.1016/j.toxlet.2011.03.019

Li, F., Miao, L., Sun, H., Zhang, Y., Bao, X., and Zhang, D. (2017). Establishment of a New Acute-On-Chronic Liver Failure Model. *Acta Pharmaceutica Sinica B* 7, 326–333. doi:10.1016/j.apsb.2016.09.003

Li, P., Spann, N. J., Kaikkonen, M. U., Lu, M., Oh, D. Y., Fox, J. N., et al. (2013). NCoR Repression of LXRs Restricts Macrophage Biosynthesis of Insulin-Sensitizing omega 3 Fatty Acids. *Cell* 155, 200–214. doi:10.1016/j.cell.2013.08.054

Li, S., Tan, H.-Y., Wang, N., Zhang, Z.-J., Lao, L., Wong, C.-W., et al. (2015). The Role of Oxidative Stress and Antioxidants in Liver Diseases. *Ijms* 16, 26087–26124. doi:10.3390/ijms161125942

Li, Y. H., Choi, D. H., Lee, E. H., Seo, S. R., Lee, S., and Cho, E.-H. (2016). Sirtuin 3 (SIRT3) Regulates α-Smooth Muscle Actin (α-SMA) Production through the Succinate Dehydrogenase-G Protein-Coupled Receptor 91 (GPR91) Pathway in Hepatic Stellate Cells. *J. Biol. Chem.* 291, 10277–10292. doi:10.1074/jbc.m115.692244

Li, Y. H., Woo, S. H., Choi, D. H., and Cho, E.-H. (2015). Succinate Causes α-SMA Production through GPR91 Activation in Hepatic Stellate Cells. *Biochem. Biophysical Res. Commun.* 463, 853–858. doi:10.1016/j.bbrc.2015.06.023

Liu, P. S., Wang, H., Li, X., Chao, T., Teav, T., Christen, S., et al. (2017). α-Ketoglutarate Orchestrates Macrophage Activation through Metabolic and Epigenetic Reprogramming. *Nat Immunol.* 18, 985-994. doi:10.1038/ni.3796

Lopes, N., McIntyre, C., Martin, S., Raverdeau, M., Sumaria, N., Kohlgruber, A. C., et al. (2021). Distinct Metabolic Programs Established in the Thymus Control Effector Functions of γδ T Cell Subsets in Tumor Microenvironments. *Nat. Immunol.* 22, 179–192. doi:10.1038/s41590-020-00848-3

López-Vicario, C., Checa, A., Urdangarin, A., Aguilar, F., Alcaraz-Quiles, J., Caraceni, P., et al. (2020). Targeted Lipidomics Reveals Extensive Changes in Circulating Lipid Mediators in Patients with Acutely Decompensated Cirrhosis. *J. Hepatol.* 73, 817–828. doi:10.1016/j.jhep.2020.03.046

López-Vicario, C., Rius, B., Alcaraz-Quiles, J., García-Alonso, V., Lopategi, A., Titos, E., et al. (2016). Pro-resolving Mediators Produced from EPA and DHA: Overview of the Pathways Involved and Their Mechanisms in Metabolic Syndrome and Related Liver Diseases. *Eur. J. Pharmacol.* 785, 133–143. doi:10.1016/j.ejphar.2015.03.092

Luangmonkong, T., Suriguga, S., Mutsaers, H. A. M., Groothuis, G. M. M., Olinga, P., and Boersema, M. (2018). Targeting Oxidative Stress for the Treatment of Liver Fibrosis. *Rev Physiol Biochem Pharmacol.* 175, 71–102. doi:10.1007/112_2018_10

Maekawa, S., Takada, S., Nambu, H., Furihata, T., Kakutani, N., Setoyama, D., et al. (2019). Linoleic Acid Improves Assembly of the CII Subunit and CIII2/CIV Complex of the Mitochondrial Oxidative Phosphorylation System in Heart Failure. *Cell Commun Signal* 17, 128–211. doi:10.1186/s12964-019-0445-0

Mansouri, A., Gattolliat, C.-H., and Asselah, T. (2018). Mitochondrial Dysfunction and Signaling in Chronic Liver Diseases. *Gastroenterology* 155, 629–647. doi:10.1053/j.gastro.2018.06.083

Mayer, K., Sommer, N., Hache, K., Hecker, A., Reiche, S., Schneck, E., et al. (2019). Resolvin E1 Improves Mitochondrial Function in Human Alveolar Epithelial Cells during Severe Inflammation. *Lipids* 54, 53–65. doi:10.1002/lipd.12119

McLure, K. G., Gesner, E. M., Tsujikawa, L., Kharenko, O. A., Attwell, S., Campeau, E., et al. (2013). RVX-208, an Inducer of ApoA-I in Humans, Is a BET Bromodomain Antagonist. *PLoS One* 8, e83190. doi:10.1371/journal.pone.0083190

Mellor, A. L., and Munn, D. H. (2008). Creating Immune Privilege: Active Local Suppression that Benefits Friends, but Protects Foes. *Nat. Rev. Immunol.* 8, 74–80. doi:10.1038/nri2233

Meng, D., Yang, Q., Wang, H., Melick, C. H., Navlani, R., Frank, A. R., et al. (2020). Glutamine and Asparagine Activate mTORC1 Independently of Rag GTPases. *J. Biol. Chem.* 295, 2890–2899. doi:10.1074/jbc.ac119.011578

Merli, M., Giusto, M., Lucidi, C., Giannelli, V., Pentassuglio, I., Di Gregorio, V., et al. (2013). Muscle Depletion Increases the Risk of Overt and Minimal Hepatic Encephalopathy: Results of a Prospective Study. *Metab. Brain Dis.* 28, 281–284. doi:10.1007/s11011-012-9365-z

Miliotis, S., Nicolalde, B., Ortega, M., Yepez, J., and Caicedo, A. (2019). Forms of Extracellular Mitochondria and Their Impact in Health. *Mitochondrion* 48, 16–30. doi:10.1016/j.mito.2019.02.002

Mills, E. L., Kelly, B., and O'Neill, L. A. J. (2017). Mitochondria Are the Powerhouses of Immunity. *Nat. Immunol.* 18, 488–498. doi:10.1038/ni.3704

Moreau, R., Jalan, R., Gines, P., Pavesi, M., Angeli, P., Cordoba, J., et al. (2013). Acute-on-chronic Liver Failure Is a Distinct Syndrome that Develops in Patients with Acute Decompensation of Cirrhosis. *Gastroenterology* 144 (1426–37), 1426–1429. doi:10.1053/j.gastro.2013.02.042

Moreau, R., Clària, J., Aguilar, F., Fenaille, F., Lozano, J. J., Junot, C., et al. (2020). Blood Metabolomics Uncovers Inflammation-Associated Mitochondrial Dysfunction as a Potential Mechanism Underlying ACLF. *J. Hepatol.* 72, 688–701. doi:10.1016/j.jhep.2019.11.009

Moreno-Sánchez, R., Hogue, B. A., and Hansford, R. G. (1990). Influence of NAD-Linked Dehydrogenase Activity on Flux through Oxidative Phosphorylation. *Biochem. J.* 268, 421–428. doi:10.1042/bj2680421

Munn, D. H., Sharma, M. D., Baban, B., Harding, H. P., Zhang, Y., Ron, D., et al. (2005). GCN2 Kinase in T Cells Mediates Proliferative Arrest and Anergy Induction in Response to Indoleamine 2,3-dioxygenase. *Immunity* 22, 633–642. doi:10.1016/j.immuni.2005.03.013

Murphy, A. J., Akhtari, M., Tolani, S., Pagler, T., Bijl, N., Kuo, C.-L., et al. (2011). ApoE Regulates Hematopoietic Stem Cell Proliferation, Monocytosis, and Monocyte Accumulation in Atherosclerotic Lesions in Mice. *J. Clin. Invest.* 121, 4138–4149. doi:10.1172/jci57559

Natarajan, S. K., Thomas, S., Ramamoorthy, P., Basivireddy, J., Pulimood, A. B., Ramachandran, A., et al. (2006). Oxidative Stress in the Development of Liver Cirrhosis: A Comparison of Two Different Experimental Models. *J. Gastroenterol. Hepatol.* 21, 947–957. doi:10.1111/j.1440-1746.2006.04231.x

Nikam, A., Patankar, J. V., Lackner, C., Schöck, E., Kratky, D., Zatloukal, K., et al. (2013). Transition between Acute and Chronic Hepatotoxicity in Mice Is Associated with Impaired Energy Metabolism and Induction of Mitochondrial Heme Oxygenase-1. *PLoS One* 8, e66094–11. doi:10.1371/journal.pone.0066094

Nishikawa, T., Bellance, N., Damm, A., Bing, H., Zhu, Z., Handa, K., et al. (2014). A Switch in the Source of ATP Production and a Loss in Capacity to Perform Glycolysis Are Hallmarks of Hepatocyte Failure in advance Liver Disease. *J. Hepatol.* 60, 1203–1211. doi:10.1016/j.jhep.2014.02.014

Norenberg, M. D. (1981). The Astrocyte in Liver Disease. *Adv. Cel Neurobiol* 2, 303–352. doi:10.1016/b978-0-12-008302-2.50013-4

Norris, S., Collins, C., Doherty, D. G., Smith, F., McEntee, G., Traynor, O., et al. (1998). Resident Human Hepatitis Lymphocytes Are Phenotypically Different from Circulating Lymphocytes. *J. Hepatol.* 28, 84–90. doi:10.1016/s0168-8278(98)80206-7

O'Brien, A. J., Fullerton, J. N., Massey, K. A., Auld, G., Sewell, G., James, S., et al. (2014). Immunosuppression in Acutely Decompensated Cirrhosis Is Mediated by Prostaglandin E2. *Nat. Med.* 20, 518–523. doi:10.1038/nm.3516

Oettl, K., Stadlbauer, V., Petter, F., Greilberger, J., Putz-Bankuti, C., Hallström, S., et al. (2008). Oxidative Damage of Albumin in Advanced Liver Disease. *Biochim. Biophys. Acta (Bba) - Mol. Basis Dis.* 1782, 469–473. doi:10.1016/j.bbadis.2008.04.002

Ott, M., Gogvadze, V., Orrenius, S., and Zhivotovsky, B. (2007). Mitochondria, Oxidative Stress and Cell Death. *Apoptosis* 12, 913–922. doi:10.1007/s10495-007-0756-2

Paradies, G. (2014). Oxidative Stress, Cardiolipin and Mitochondrial Dysfunction in Nonalcoholic Fatty Liver Disease. *Wjg* 20, 14205. doi:10.3748/wjg.v20.i39.14205

Paradies, G., Paradies, V., Ruggiero, F. M., and Petrosillo, G. (2014). Cardiolipin and Mitochondrial Function in Health and Disease. *Antioxid. Redox Signaling* 20, 1925–1953. doi:10.1089/ars.2013.5280

Pellicoro, A., Ramachandran, P., Iredale, J. P., and Fallowfield, J. A. (2014). Liver Fibrosis and Repair: Immune Regulation of Wound Healing in a Solid Organ. *Nat. Rev. Immunol.* 14, 181–194. doi:10.1038/nri3623

Peti-Peterdi, J. (2010). High Glucose and Renin Release: The Role of Succinate and GPR91. *Kidney Int.* 78, 1214–1217. doi:10.1038/ki.2010.333

Piano, S., and Angeli, P. (2021). Bacterial Infections in Cirrhosis as a Cause or Consequence of Decompensation. *Clin. Liver Dis.* 25, 357–372. doi:10.1016/j.cld.2021.01.006

Picaud, S., Wells, C., Felletar, I., Brotherton, D., Martin, S., Savitsky, P., et al. (2013). RVX-208, an Inhibitor of BET Transcriptional Regulators with Selectivity for the Second Bromodomain. *Proc. Natl. Acad. Sci.* 110, 19754–19759. doi:10.1073/pnas.1310658110

Planas-Iglesias, J., Dwarakanath, H., Mohammadyani, D., Yanamala, N., Kagan, V. E., and Klein-Seetharaman, J. (2015). Cardiolipin Interactions with Proteins. *Biophysical J.* 109, 1282–1294. doi:10.1016/j.bpj.2015.07.034

Possemato, R., Marks, K. M., Shaul, Y. D., Pacold, M. E., Kim, D., Birsoy, K., et al. (2011). Functional Genomics Reveal that the Serine Synthesis Pathway Is Essential in Breast Cancer. *Nature* 476, 346–350. doi:10.1038/nature10350

Praktiknjo, M., Clees, C., Pigliacelli, A., Fischer, S., Jansen, C., Lehmann, J., et al. (2019). Sarcopenia Is Associated with Development of Acute-On-Chronic Liver Failure in Decompensated Liver Cirrhosis Receiving Transjugular Intrahepatic Portosystemic Shunt. *Clin. Transl Gastroenterol.* 10, e00025–8. doi:10.14309/ctg.0000000000000025

Rama Rao, K. V., Mawal, Y. R., and Qureshi, I. A. (1997). Progressive Decrease of Cerebral Cytochrome C Oxidase Activity in Sparse-Fur Mice: Role of Acetyl-L-Carnitine in Restoring the Ammonia-Induced Cerebral Energy Depletion. *Neurosci. Lett.* 224, 83–86. doi:10.1016/s0304-3940(97)13476-0

Ren, M., Phoon, C. K. L., and Schlame, M. (2014). Metabolism and Function of Mitochondrial Cardiolipin. *Prog. Lipid Res.* 55, 1–16. doi:10.1016/j.plipres.2014.04.001

Ren, Y.-Z., Zhang, B.-Z., Zhao, X.-J., and Zhang, Z.-Y. (2020). Resolvin D1 Ameliorates Cognitive Impairment Following Traumatic Brain Injury via Protecting Astrocytic Mitochondria. *J. Neurochem.* 154, 530–546. doi:10.1111/jnc.14962

Robben, J. H., Fenton, R. A., Vargas, S. L., Schweer, H., Peti-Peterdi, J., Deen, P. M. T., et al. (2009). Localization of the Succinate Receptor in the Distal Nephron and its Signaling in Polarized MDCK Cells. *Kidney Int.* 76, 1258–1267. doi:10.1038/ki.2009.360

Rong, X., Albert, C. J., Hong, C., Duerr, M. A., Chamberlain, B. T., Tarling, E. J., et al. (2013). LXRs Regulate ER Stress and Inflammation through Dynamic Modulation of Membrane Phospholipid Composition. *Cel Metab.* 18, 685–697. doi:10.1016/j.cmet.2013.10.002

Ruiz-Ramírez, A., Barrios-Maya, M.-A., López-Acosta, O., Molina-Ortiz, D., and El-Hafidi, M. (2015). Cytochrome C Release from Rat Liver Mitochondria Is Compromised by Increased Saturated Cardiolipin Species Induced by Sucrose Feeding. *Am. J. Physiology-Endocrinology Metab.* 309, E777–E786. doi:10.1152/ajpendo.00617.2014

Santos, N. P., Pereira, I. C., Pires, M. J., Lopes, C., Andrade, R., Oliveira, M. M., et al. (2012). Histology, Bioenergetics and Oxidative Stress in Mouse Liver Exposed to N-Diethylnitrosamine. *In Vivo* 26, 921–929.

Schlame, M., and Ren, M. (2009). The Role of Cardiolipin in the Structural Organization of Mitochondrial Membranes. *Biochim. Biophys. Acta (Bba) - Biomembranes* 1788, 2080–2083. doi:10.1016/j.bbamem.2009.04.019

Schmid, A. I., Chmelík, M., Szendroedi, J., Krššák, M., Brehm, A., Moser, E., et al. (2008). Quantitative ATP Synthesis in Human Liver Measured by localized31P Spectroscopy Using the Magnetization Transfer experiment. *NMR Biomed.* 21, 437–443. doi:10.1002/nbm.1207

Scorrano, L., Penzo, D., Petronilli, V., Pagano, F., and Bernardi, P. (2001). Arachidonic Acid Causes Cell Death through the Mitochondrial Permeability Transition. *J. Biol. Chem.* 276, 12035–12040. doi:10.1074/jbc.m010603200

Serhan, C. N. (2014). Pro-resolving Lipid Mediators Are Leads for Resolution Physiology. *Nature* 510, 92–101. doi:10.1038/nature13479

Serhan, C. N., and Petasis, N. A. (2011). Resolvins and Protectins in Inflammation Resolution. *Chem. Rev.* 111, 5922–5943. doi:10.1021/cr100396c

Serhan, C. N., Yang, R., Martinod, K., Kasuga, K., Pillai, P. S., Porter, T. F., et al. (2009). Maresins: Novel Macrophage Mediators with Potent Antiinflammatory and Proresolving Actions. *J. Exp. Med.* 206, 15–23. doi:10.1084/jem.20081880

ShalimarSheikh, M. F., Mookerjee, R. P., Agarwal, B., Acharya, S. K., and Jalan, R. (2019). Prognostic Role of Ammonia in Patients with Cirrhosis. *Hepatology* 70, 982–994. doi:10.1002/hep.30534

Shawcross, D. L., Wright, G. A. K., Stadlbauer, V., Hodges, S. J., Davies, N. A., Wheeler-Jones, C., et al. (2008). Ammonia Impairs Neutrophil Phagocytic Function in Liver Disease. *Hepatology* 48, 1202–1212. doi:10.1002/hep.22474

Shrestha, N., Cuffe, J. S. M., Holland, O. J., Perkins, A. V., McAinch, A. J., and Hryciw, D. H. (2019). Linoleic Acid Increases Prostaglandin E2 Release and Reduces Mitochondrial Respiration and Cell Viability in Human Trophoblast-like Cells. *Cell Physiol Biochem* 52, 94–108. doi:10.33594/000000007

Song, J., Lu, C., Zhao, W., and Shao, X. (2019). Melatonin Attenuates TNF-α-mediated Hepatocytes Damage via Inhibiting Mitochondrial Stress and Activating the Akt-Sirt3 Signaling Pathway. *J. Cel Physiol* 234, 20969–20979. doi:10.1002/jcp.28701

Stadler, J., Bentz, B. G., Harbrecht, B. G., Silvio, M. D., Curran, R. D., Billiar, T. R., et al. (1992). Tumor Necrosis Factor Alpha Inhibits Hepatocyte Mitochondrial Respiration. *Ann. Surg.* 216, 539–546. doi:10.1097/00000658-199211000-00003

Sullivan, E. M., Pennington, E. R., Green, W. D., Beck, M. A., Brown, D. A., and Shaikh, S. R. (2018). Mechanisms by Which Dietary Fatty Acids Regulate Mitochondrial Structure-Function in Health and Disease. *Adv. Nutr.* 9, 247–262. doi:10.1093/advances/nmy007

Tall, A. R., and Yvan-Charvet, L. (2015). Cholesterol, Inflammation and Innate Immunity. *Nat. Rev. Immunol.* 15, 104–116. doi:10.1038/nri3793

Tannahill, G. M., Curtis, A. M., Adamik, J., Palsson-Mcdermott, E. M., McGettrick, A. F., Goel, G., et al. (2013). Succinate Is an Inflammatory Signal that Induces IL-1β through HIF-1α. *Nature* 496, 238–242. doi:10.1038/nature11986

Tattoli, I., Carneiro, L. A., Jéhanno, M., Magalhaes, J. G., Shu, Y., Philpott, D. J., et al. (2008). NLRX1 Is a Mitochondrial NOD-like Receptor that Amplifies NF-κB and JNK Pathways by Inducing Reactive Oxygen Species Production. *EMBO Rep.* 9, 293–300. doi:10.1038/sj.embor.7401161

Thomson, A. W., and Knolle, P. A. (2010). Antigen-presenting Cell Function in the Tolerogenic Liver Environment. *Nat. Rev. Immunol.* 10, 753–766. doi:10.1038/nri2858

Tran, M., Tam, D., Bardia, A., Bhasin, M., Rowe, G. C., Kher, A., et al. (2011). PGC-1α Promotes Recovery after Acute Kidney Injury during Systemic Inflammation in Mice. *J. Clin. Invest.* 121, 4003–4014. doi:10.1172/jci58662

Tretter, L., and Adam-Vizi, V. (2005). Alpha-ketoglutarate Dehydrogenase: a Target and Generator of Oxidative Stress. *Phil. Trans. R. Soc. B* 360, 2335–2345. doi:10.1098/rstb.2005.1764

Trieb, M., Rainer, F., Stadlbauer, V., Douschan, P., Horvath, A., Binder, L., et al. (2020). HDL-related Biomarkers Are Robust Predictors of Survival in Patients with Chronic Liver Failure. *J. Hepatol.* 73, 113–120. doi:10.1016/j.jhep.2020.01.026

Tripathi, D. M., Vilaseca, M., Lafoz, E., Garcia-Calderó, H., Viegas Haute, G., Fernández-Iglesias, A., et al. (2018). Simvastatin Prevents Progression of Acute

on Chronic Liver Failure in Rats with Cirrhosis and Portal Hypertension. *Gastroenterology* 155, 1564–1577. doi:10.1053/j.gastro.2018.07.022

Van Wyngene, L., Vandewalle, J., and Libert, C. (2018). Reprogramming of Basic Metabolic Pathways in Microbial Sepsis: Therapeutic Targets at Last. *EMBO Mol. Med.* 10, 1–18. doi:10.15252/emmm.201708712

Vénéreau, E., Ceriotti, C., and Bianchi, M. E. (2015). DAMPs from Cell Death to New Life. *Front. Immunol.* 6, 422–511. doi:10.3389/fimmu.2015.00422

Vilaseca, M., García-Calderó, H., Lafoz, E., Ruart, M., López-Sanjurjo, C. I., Murphy, M. P., et al. (2017). Mitochondria-targeted Antioxidant Mitoquinone Deactivates Human and Rat Hepatic Stellate Cells and Reduces portal Hypertension in Cirrhotic Rats. *Liver Int.* 37, 1002–1012. doi:10.1111/liv.13436

Wang, J., Simonavicius, N., Wu, X., Swaminath, G., Reagan, J., Tian, H., et al. (2006). Kynurenic Acid as a Ligand for Orphan G Protein-Coupled Receptor GPR35. *J. Biol. Chem.* 281, 22021–22028. doi:10.1074/jbc.m603503200

Wang, Z., Ying, Z., Bosy-Westphal, A., Zhang, J., Schautz, B., Later, W., et al. (2010). Specific Metabolic Rates of Major Organs and Tissues across Adulthood: Evaluation by Mechanistic Model of Resting Energy Expenditure. *Am. J. Clin. Nutr.* 92, 1369–1377. doi:10.3945/ajcn.2010.29885

Xu, J., Lamouille, S., and Derynck, R. (2009). TGF-β-induced Epithelial to Mesenchymal Transition. *Cell Res* 19, 156–172. doi:10.1038/cr.2009.5

Xu, Y., Kabba, J. A., Ruan, W., Wang, Y., Zhao, S., Song, X., et al. (2018). The PGC-1α Activator ZLN005 Ameliorates Ischemia-Induced Neuronal Injury *In Vitro* and *In Vivo*. *Cell Mol Neurobiol* 38, 929–939. doi:10.1007/s10571-017-0567-0

Yan, J.-J., Jung, J.-S., Lee, J.-E., Lee, J., Huh, S.-O., Kim, H.-S., et al. (2004). Therapeutic Effects of Lysophosphatidylcholine in Experimental Sepsis. *Nat. Med.* 10, 161–167. doi:10.1038/nm989

Zaccherini, G., Aguilar, F., Caraceni, P., Clària, J., Lozano, J. J., Fenaille, F., et al. (2021). Assessing the Role of Amino Acids in Systemic Inflammation and Organ Failure in Patients with ACLF. *J. Hepatol.* 74, 1117–1131. doi:10.1016/j.jhep.2020.11.035

Zhang, I. W., Curto, A., López-Vicario, C., Casulleras, M., Duran-Güell, M., Flores-Costa, R., et al. (2021). Mitochondrial Dysfunction Governs Immunometabolism in Leukocytes of Patients with Acute-On-Chronic Liver Failure. *J. Hepatol.* S0168-8278 (21), 02004-3. doi:10.1016/j.jhep.2021.08.009

Zhang, L.-N., Zhou, H.-Y., Fu, Y.-Y., Li, Y.-Y., Wu, F., Gu, M., et al. (2013). Novel Small-Molecule PGC-1 Transcriptional Regulator with Beneficial Effects on Diabetic Db/db Mice. *Diabetes* 62, 1297–1307. doi:10.2337/db12-0703

Zhong, Z., Liang, S., Sanchez-Lopez, E., He, F., Shalapour, S., Lin, X.-j., et al. (2018). New Mitochondrial DNA Synthesis Enables NLRP3 Inflammasome Activation. *Nature* 560, 198–203. doi:10.1038/s41586-018-0372-z

Zhou, R., Yazdi, A. S., Menu, P., and Tschopp, J. (2011). A Role for Mitochondria in NLRP3 Inflammasome Activation. *Nature* 469, 221–225. doi:10.1038/nature09663

Conflict of Interest: The authors declare that the research was conducted in the absence of any commercial or financial relationships that could be construed as a potential conflict of interest.

Publisher's Note: All claims expressed in this article are solely those of the authors and do not necessarily represent those of their affiliated organizations or those of the publisher, the editors and the reviewers. Any product that may be evaluated in this article, or claim that may be made by its manufacturer, is not guaranteed or endorsed by the publisher.

frontiers in Cell and Developmental Biology

REVIEW
published: 03 December 2021
doi: 10.3389/fcell.2021.795685

Protein Quality Control at the Mitochondrial Surface

*Fabian den Brave, Arushi Gupta and Thomas Becker**

Institute of Biochemistry and Molecular Biology, Faculty of Medicine, University of Bonn, Bonn, Germany

Mitochondria contain two membranes, the outer and inner membrane. The outer membrane fulfills crucial functions for the communication of mitochondria with the cellular environment like exchange of lipids via organelle contact sites, the transport of metabolites and the formation of a signaling platform in apoptosis and innate immunity. The translocase of the outer membrane (TOM complex) forms the entry gate for the vast majority of precursor proteins that are produced on cytosolic ribosomes. Surveillance of the functionality of outer membrane proteins is critical for mitochondrial functions and biogenesis. Quality control mechanisms remove defective and mistargeted proteins from the outer membrane as well as precursor proteins that clog the TOM complex. Selective degradation of single proteins is also an important mode to regulate mitochondrial dynamics and initiation of mitophagy pathways. Whereas inner mitochondrial compartments are equipped with specific proteases, the ubiquitin-proteasome system is a central player in protein surveillance on the mitochondrial surface. In this review, we summarize our current knowledge about the molecular mechanisms that govern quality control of proteins at the outer mitochondrial membrane.

Keywords: mitochondria, protein sorting, protein quality control, Cdc48, TOM complex

OPEN ACCESS

Edited by:
Sylvie Callegari,
Walter and Eliza Hall Institute of Medical Research, Australia

Reviewed by:
Piotr Bragoszewski,
Nencki Institute of Experimental Biology (PAS), Poland
Doron Rapaport,
University of Tübingen, Germany

****Correspondence:***
Thomas Becker
thbecker@uni-bonn.de

Specialty section:
This article was submitted to Cellular Biochemistry, a section of the journal Frontiers in Cell and Developmental Biology

Received: *15 October 2021*
Accepted: *05 November 2021*
Published: *03 December 2021*

Citation:
den Brave F, Gupta A and Becker T (2021) Protein Quality Control at the Mitochondrial Surface. Front. Cell Dev. Biol. 9:795685. doi: 10.3389/fcell.2021.795685

INTRODUCTION

Mitochondria are known as the powerhouse of the cell since they produce the bulk of energy for cellular processes. They also synthesize lipids and amino acids, form co-factors like iron-sulfur clusters and constitute a platform for cellular signaling in apoptosis and innate immunity (Spinelli and Haigis, 2018; Tiku et al., 2020). Mitochondria display specific features, which are due to their endosymbiotic origin. They contain their own genome, which encodes for eight proteins in the baker's yeast *Saccharomyces cerevisiae* and 13 proteins in human mitochondria. The vast majority of about 1,000 mitochondrial proteins are produced as precursors on cytosolic ribosomes and imported into the target organelle. Mitochondria contain two membranes, the outer membrane and the inner membrane, which create two aqueous compartments, the intermembrane space and the matrix. The inner membrane forms large invaginations, termed cristae, which harbor the respiratory chain complexes. These membrane-integrated protein complexes transport electrons from reducing agents to oxygen to form water. The released energy is used to establish a proton gradient across the inner membrane that drives the F_1F_O-ATP synthase to produce ATP (von Ballmoos et al., 2009; Spinelli and Haigis, 2018; Kuhlbrandt, 2019).

The outer membrane constitutes the border of mitochondria to their cellular environment and is therefore critical for the integration of mitochondria within the cell. The outer membrane contains a few dozen integral membrane proteins (Schmitt et al., 2006; Zahedi et al., 2006; Morgenstern et al., 2017; Vögtle et al., 2017). In yeast, five proteins are embedded into the membrane by a β-barrel, whereas the majority is anchored via a single or several α-helical transmembrane segments. The

voltage-dependent anion channel (VDAC or porin in yeast) mediates the exchange of small molecules and ions with the cellular environment (Colombini, 2012; Campo et al., 2017; Becker and Wagner, 2018). Protein translocases transport different types of precursor proteins that were produced on cytosolic ribosomes into and across the outer membrane (Dukanovic and Rapaport, 2011). Outer membrane proteins form contact sites to other cellular compartments. One example is the endoplasmic reticulum encounter structure (ERMES) in yeast that links mitochondria and the endoplasmic reticulum (ER) to facilitate lipid transfer (Kornmann et al., 2009; Ellenrieder et al., 2016). Finally, outer membrane localized proteins control fusion and fission of mitochondria (Escobar-Henriques and Anton, 2013; Kameoka et al., 2018; Tilokani et al., 2018).

Mitochondrial quality control mechanisms are critical to deal with the high load of incoming precursor proteins and to monitor their folding. The inner membrane and matrix are equipped with AAA proteases that remove misfolded or defective proteins: the *i*-AAA protease (Yme1/YME1L) of the inner membrane exposes its active site into the intermembrane space, the inner membrane embedded *m*-AAA protease (Yta10, Yta12/AFG3L2, paraplegin) exposes its catalytic center into the matrix and the soluble Pin1/LONP resides in the matrix (Gerdes et al., 2012; Deshwal et al., 2020; Song et al., 2021). The outer membrane lacks such specific AAA proteases. Instead, studies of the last few years uncovered that the ubiquitin proteasome system plays a central role in the degradation of aberrant proteins at the mitochondrial surface. We summarize here our current knowledge about surveillance of proteins on the mitochondrial surface.

OVERVIEW OF PROTEIN TRANSPORT INTO MITOCHONDRIA

Mitochondria have to import about 1,000 proteins in yeast and up to 1,500 proteins in humans that are produced on cytosolic ribosomes (Pagliarini et al., 2008; Morgenstern et al., 2017). Outer membrane proteins play a critical role in the import of precursor proteins into mitochondria (Endo and Yamano, 2009; Wiedemann and Pfanner, 2017; Hansen and Herrmann, 2019). The vast majority of mitochondrial proteins are synthesized by cytosolic ribosomes as precursors. Although co- and posttranslational import mechanisms have been reported, most mitochondrial precursor proteins are imported in a posttranslational manner (Becker et al., 2019; Bykov et al., 2020). Here, cytosolic chaperones like Hsp70 and Hsp90 guide these precursor proteins from ribosomes to the mitochondrial surface (Becker et al., 2019; Bykov et al., 2020). Receptors of the translocase of the outer membrane (TOM complex) recognize internal and cleavable mitochondrial targeting signals. The receptor protein Tom70 also binds to cytosolic Hsp70 and Hsp90 chaperones. The recruitment of chaperones to Tom70 is crucial to prevent proteotoxic stress due to aggregation of mitochondrial precursor proteins (Young et al., 2003; Backes et al., 2021). Alternatively, some hydrophobic precursor proteins are first guided to the ER and then transported to mitochondria (ER-SURF pathway) (Hansen et al., 2018). Here, the ER membrane serves as a scaffold to accommodate membrane proteins and thereby prevents their aggregation.

The TOM complex is the main entry gate for precursor proteins into mitochondria. The two peripheral TOM receptors, Tom20 and Tom70, bind to incoming precursor proteins. Proteins containing a cleavable presequence are primarily recognized by Tom20 (Abe et al., 2000; Yamano et al., 2008). Tom70 was previously thought to function as a receptor for integral membrane proteins, but several studies demonstrated that this receptor is also involved in the import of several presequence-containing proteins that contain internal mitochondrial targeting sequences (Hines et al., 1990; Brix et al., 1997; Young et al., 2003; Yamamoto et al., 2009; Backes et al., 2018; Backes et al., 2021). The central subunit of the TOM complex is the β-barrel protein Tom40, which forms the protein-conducting channel (Hill et al., 1998; Suzuki et al., 2004; Becker et al., 2005). High-resolution cryo-electron microscopic structures revealed that the TOM complex consists of two Tom40 lined by three small TOM subunits, Tom5, Tom6 and Tom7. Two Tom22 molecules link both Tom40-small Tom modules in the TOM complex. The overall dimeric structure is conserved from yeast to human (Bausewein et al., 2017; Araiso et al., 2019; Tucker and Park, 2019; Wang W. et al., 2020; Guan et al., 2021). Tom22 constitutes the docking site for Tom20 and Tom70 at the TOM complex to facilitate precursor transfer from the receptor proteins towards the translocation channel (van Wilpe et al., 1999).

After passage of the TOM channel, specific protein translocases sort the incoming precursor proteins to the mitochondrial subcompartments (**Figure 1**). The presequence translocase (TIM23 complex) transports precursor proteins into and across the inner membrane. The respiratory chain generates a membrane potential across the inner membrane that drives protein transport via the presequence pathways (Malhotra et al., 2013). Protein transport into the matrix additionally depends on the ATP consuming activity of the presequence translocase-associated motor (PAM). Multispanning inner membrane proteins like carriers lack a cleavable presequence. The small TIM chaperones of the intermembrane space transfer these hydrophobic proteins to a second protein translocase of the inner membrane, the carrier translocase (TIM22 complex). The TIM22 complex inserts carrier proteins in a membrane potential dependent manner into the inner membrane. The mitochondrial intermembrane space import and assembly (MIA) machinery imports cysteine-rich proteins such as the small TIM proteins into the intermembrane space and promotes their oxidative folding. Precursors of β-barrel proteins are first transported via the TOM complex across the outer membrane and subsequently guided by the small TIM chaperones to the sorting and assembly machinery (SAM complex), which integrates them into the outer membrane SAM complex. The mitochondrial import (MIM) machinery inserts proteins with an α-helical membrane anchor into the outer membrane. Remarkably, the majority of these precursor proteins is not transported via the TOM channel, but instead transferred to the MIM complex on the cytosolic side of the outer membrane.

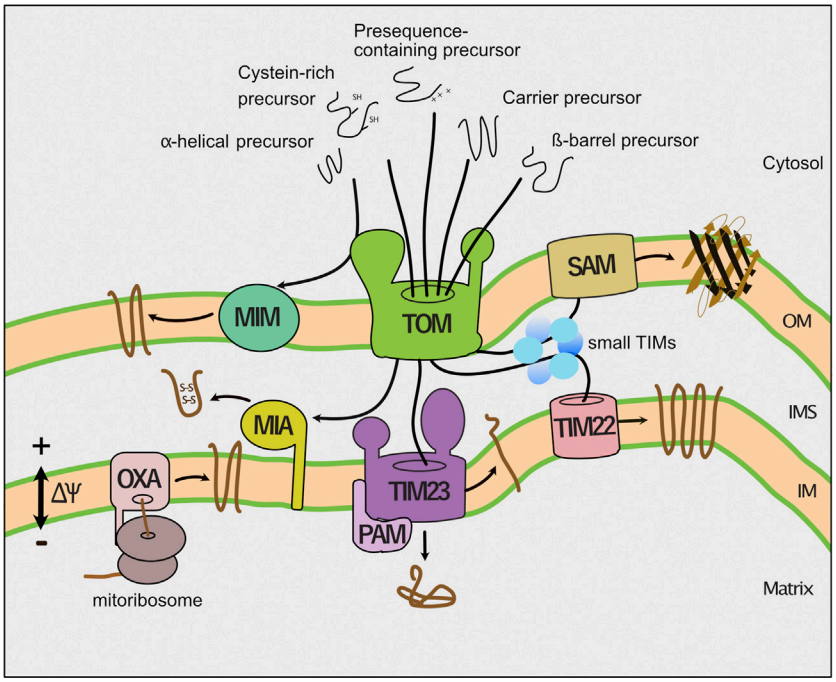

FIGURE 1 | Pathways of mitochondrial protein import. Dedicated protein translocases import precursor proteins into the mitochondrial subcompartments. First, the translocase of the outer membrane (TOM complex) transports precursor proteins across the outer membrane (OM). Second, the presequence translocase (TIM23 complex) sort precursors with a cleavable presequence into the inner membrane (IM) and matrix. The presequence translocase-associated motor (PAM) cooperates with the TIM23 complex to complete protein translocation into the matrix. Third, the carrier translocase (TIM22) inserts hydrophobic multispanning proteins into the inner membrane that are guided by small TIM chaperones through the intermembrane space. The membrane potential (Δψ) drives protein transport into the inner membrane and matrix. Fourth, the mitochondrial intermembrane space import and assembly (MIA) machinery mediates oxidative folding of proteins with a cysteine-rich targeting signal. Fifth, the sorting and assembly machinery (SAM complex) inserts β-barrel proteins into the outer membrane (OM). Sixth, the mitochondrial import (MIM) machinery integrates proteins with a single or multiple α-helical membrane spans into the outer membrane. Finally, the oxidase assembly (OXA) translocase inserts mitochondria-encoded proteins into the inner membrane.

Finally, the oxidase assembly (OXA) translocase integrates mitochondria-encoded proteins and some nuclear encoded proteins into the inner membrane (Endo and Yamano, 2009; Jores and Rapaport, 2017; Wiedemann and Pfanner, 2017; Hansen and Herrmann, 2019; Drwesh and Rapaport, 2020).

DEFECTIVE PROTEIN IMPORT INTO MITOCHONDRIA CAUSES CELLULAR STRESS

Cellular Stress Responses to Impaired Protein Import

Protein import into mitochondria is essential for cell viability and function. However, different scenarios could affect mitochondrial protein import. Precursor proteins have to be kept in a largely unfolded state to pass the Tom40 channel (Wiedemann et al., 2001; Shiota et al., 2015). Consequently, premature folding of precursor proteins blocks their passage of the TOM complex. If the N-terminal presequence of such prematurely folded precursor proteins already engages the presequence translocase of the inner membrane, the precursor protein will arrest within the protein translocon (Boos et al., 2019; Martensson et al., 2019). Particularly, precursor proteins that contain a bipartide targeting signal, which is composed of a mitochondrial presequence and an inner membrane sorting signal, are prone to clog the translocon (Weidberg and Amon, 2018). Moreover, mitochondrial dysfunction can affect the membrane potential across the inner membrane, which in turn impairs protein transport into mitochondria (Jin et al., 2010; Malhotra et al., 2013; Rolland et al., 2019).

Impaired protein transport into mitochondria causes cellular stress due to accumulation of mitochondrial precursor proteins (termed precursor overaccumulation stress (mPOS)) and induces a massive transcriptional reprogramming to deal with the proteotoxic stress (Wang and Chen, 2015; Boos et al., 2019). This stress response includes an increased expression and assembly of proteasomal subunits (termed the unfolded protein response activated by mistargeting of proteins (UPRam)) (Wrobel et al., 2015). As a result, the proteasomal activity in the cell is increased to degrade the precursor proteins. Precursor accumulation also induces the expression of chaperones and results in downregulation of general protein synthesis, including decreased expression of genes encoding for proteins involved in respiratory metabolism to reduce the protein load of the protein translocases (Wang and Chen, 2015;

Boos et al., 2019). If the proteotoxic stress persists it will eventually cause cell death (Wang and Chen, 2015). The induced stress responses reveal that the maintenance of full protein import competence of mitochondria is critical to balance cellular proteostasis. Thus, molecular mechanisms are required that prevent clogging of the TOM channel to ensure proper protein import into mitochondria.

Mislocalization of Mitochondrial Precursor Proteins

Non-imported mitochondrial precursor proteins can aggregate or mislocalize to different cellular compartments. Recent studies revealed that in yeast non-imported mitochondrial precursor proteins localize to the cytosol, the ER and the nucleus (den Brave et al., 2020; Doan et al., 2020; Shakya et al., 2021; Xiao et al., 2021). Several GFP-tagged and untagged matrix targeted precursor proteins have been found in the nucleus when protein import into mitochondria was impaired (den Brave et al., 2020; Shakya et al., 2021). The nucleus has a high concentration of proteasomes and is known to allow efficient degradation of aberrant proteins (Russell et al., 1999; Park et al., 2013; Enam et al., 2018; Frottin et al., 2019). Mitochondrial proteins accumulate in nuclear protein inclusions upon inhibition of proteasomal turnover (den Brave et al., 2020). Thus, transport to the nucleus could facilitate efficient degradation of non-imported mitochondrial precursor proteins. Outer and inner mitochondrial membrane proteins can mislocalize to the ER upon import failure (Doan et al., 2020; Shakya et al., 2021; Xiao et al., 2021). One possible reason is that the cytosolic protein targeting pathways to mitochondria and to the ER are closely linked to each other (Wang et al., 2010; Hansen et al., 2018; Becker et al., 2019; Bykov et al., 2020). For instance, some hydrophobic precursor proteins are transported via the ER surface to mitochondria (ER-SURF pathway; Hansen et al., 2018). The conserved P5A-ATPase (CATP-8 in *Caenorhabditis elegans*, Spf1 in yeast and ATP13A1 in humans) recognizes the transmembrane segment of mislocalized outer membrane proteins and dislocates them from the ER membrane (Krumpe et al., 2012; McKenna et al., 2020; Qin et al., 2020). In yeast, an interaction partner of Spf1, Ema19, binds to non-imported mitochondrial proteins and facilitates their degradation (Laborenz et al., 2021). Whether and how Ema19 cooperates with Spf1 remains to be investigated. Thus, non-imported mitochondrial precursor proteins are transported to different cellular compartments, where they challenge the compartment-specific quality control systems.

SURVEILLANCE OF PROTEIN ENTRY IN MITOCHONDRIA

Cytosolic Quality Control of Mitochondrial Proteins

Protein quality control of mitochondrial precursor proteins starts already in the cytosol. The ubiquitin-proteasome system plays a central role in the removal of non-imported precursor proteins. Upon failure of protein import, the precursor proteins are ubiquitylated and delivered for proteasomal degradation (Radke et al., 2008; Bragoszewski et al., 2013; Habich et al., 2018; Kowalski et al., 2018; Mohanraj et al., 2019; Finger et al., 2020). Ubiquitylated proteins cannot pass the TOM channel to enter mitochondria (Kowalski et al., 2018). Ubiquitin is a highly conserved small protein of 76 amino acids that marks substrate proteins for degradation by the 26S proteasome (Amm et al., 2014; Ciechanover and Stanhill, 2014; Finley et al., 2016; Chen et al., 2021). Ubiquitylation of client proteins is mediated by an enzymatic cascade comprising an ubiquitin-activating enzyme (E1), an ubiquitin-conjugating enzyme (E2) and a ubiquitin ligase (E3) (Kerscher et al., 2006; Komander and Rape, 2012; Clague et al., 2015; Cappadocia and Lima, 2018). The substrate specificity in the ubiquitin pathway is largely determined by the large set of E3 ubiquitin ligases. There are up to 100 in yeast and several hundred E3 ubiquitin ligases in mammalian cells (Deshaies and Joazeiro, 2009; Chaugule and Walden, 2016; Zheng and Shabek, 2017; Walden and Rittinger, 2018). Subsequently, specific factors like ubiquilins in mammalian cells deliver ubiquitylated proteins for proteasomal degradation. Ubiquilins bind to the transmembrane domain of mitochondrial precursor proteins to prevent their aggregation (Itakura et al., 2016). Upon import failure, ubiquilins deliver the bound client proteins for proteasomal degradation (Itakura et al., 2016). Ubiquilins contain a ubiquitin-associated (UBA) domains, as well as a ubiquitin-like (UBL) domain. The UBA and UBL domains interact with each other. Prolonged binding of the precursor to ubiquilin due to

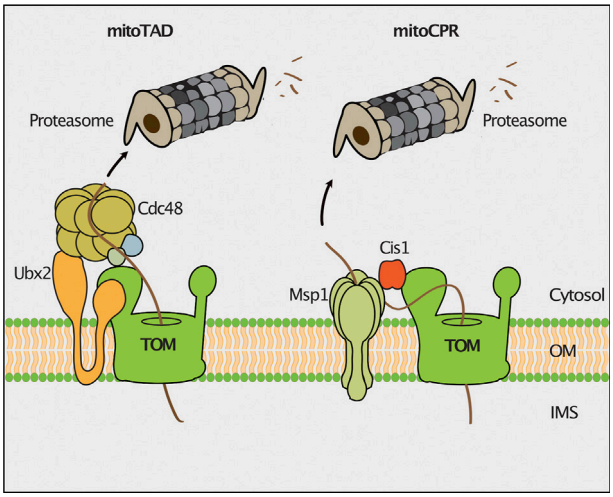

FIGURE 2 | Quality control of protein import. The mitochondrial protein translocation-associated degradation (mitoTAD) pathway removes precursor proteins from the TOM complex that arrest in the translocon during transport. Ubx2 recruits the AAA-ATPase Cdc48 for extraction of stalled precursor proteins from the TOM channel for proteasomal turnover. In the mitochondrial compromised protein import response (mitoCPR) the expression of the *CIS1* gene is induced upon mitochondrial import stress. Cis1 links the membrane bound AAA-ATPase Msp1 to Tom70 to facilitate the extraction and subsequent proteasomal turnover of stalled precursor proteins.

impaired import results in ubiquitylation of the attached client protein. The ubiquitylated client protein is then bound by the UBA domain, disrupting its interaction to the UBL domain. The released UBL domain mediates docking to the proteasome to transfer the client protein for degradation (Elsasser et al., 2002; Funakoshi et al., 2002).

Protein Quality Control at the Entry Gate of Mitochondria

Clogging of the TOM complex is deleterious for cell viability. Therefore, different molecular mechanisms operate at the translocase to remove precursor proteins that arrest during translocation in the TOM channel. The mitochondrial protein translocation-associated degradation (mitoTAD) pathway continuously monitors the TOM complex to prevent clogging of the translocation channel with precursor proteins (**Figure 2**; Martensson et al., 2019). A core subunit of this pathway is Ubx2, which was previously described to function in the endoplasmic reticulum associated degradation (ERAD) (Neuber et al., 2005; Schuberth and Buchberger, 2005). A fraction of Ubx2 is integrated into the mitochondrial outer membrane and binds to the TOM complex (Martensson et al., 2019). Ubx2 exposes a UBX domain, which is the docking site for the cytosolic AAA ATPase Cdc48 (p97/VCP in mammalian cells) at the TOM complex. Cdc48/p97 is a multifunctional protein that extracts proteins in different processes such as the ERAD, the ribosome-associated quality control (RQC) and the regulation of lipid droplet proteins (Olzmann et al., 2013; Franz et al., 2016; Wu and Rapoport, 2018; Joazeiro, 2019). Cdc48 harbors two ATPase domains and forms a hexameric structure with a central pore (DeLaBarre and Brunger, 2003). ATP hydrolysis drives the transport of the client protein through the central pore, thereby applying a pulling force on the substrate, which results in the extraction and unfolding of the bound protein (Bodnar and Rapoport, 2017). Cdc48 extracts translocation-arrested precursor proteins from the TOM channel and delivers them for proteasomal turnover (Martensson et al., 2019). The mechanism underlying substrate recognition and ubiquitylation in the mitoTAD pathway in yeast mitochondria is still unknown. In mammalian cells, the E3 ubiquitin ligase MARCH5 and the deubiquitylating enzyme USP30 have been shown to regulate the ubiquitylation of precursor proteins at the TOM complex (Ordureau et al., 2020; Phu et al., 2020). MARCH5-dependent ubiquitylation targets precursor proteins for degradation by the proteasome, whereas USP30 promotes import by removing ubiquitin from precursor proteins (Ordureau et al., 2020; Phu et al., 2020). It remains to be investigated whether also in mammalian cells the homologous proteins of Cdc48 (p97/VCP) and Ubx2 (UBXD8/FAF2) are involved in extraction of mitochondrial precursor proteins from the import channel.

The mitochondrial compromised protein import response (mitoCPR) is activated upon import failure in yeast cells (**Figure 2**). The accumulation of non-imported mitochondrial precursor proteins in the cell induces the expression of the cytosolic protein Cis1 (Weidberg and Amon, 2018; Boos et al., 2019). Cis1 in turn recruits the outer membrane bound AAA-ATPase Msp1 to the Tom70 receptor (Weidberg and Amon, 2018). Msp1 facilitates extraction of translocation-arrested precursor proteins from the TOM channel for their proteasomal degradation (Basch et al., 2020). How proteasomal targeting is achieved and whether Msp1 cooperates with components of the mitoTAD pathway in clearing proteins stalled in the TOM translocon, remains unclear.

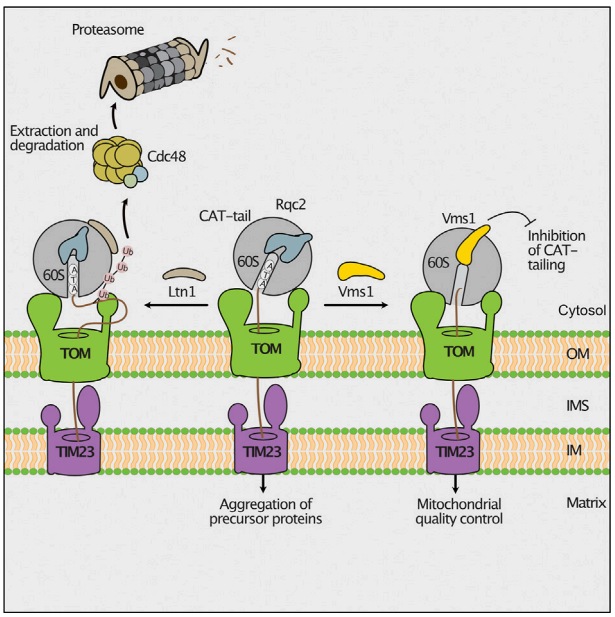

FIGURE 3 | Ribosomal protein quality control during import. Stalling during translation activates the mitochondrial ribosome-associated protein quality control (RQC). Nascent chains can be ubiquitylated by the ribosome bound E3 ubiquitin-ligase Ltn1, allowing their degradation by cytosolic proteasomes **(left).** If the lysine residues of the stalled polypeptide are not accessible for ubiquitylation, the RQC component Rqc2 will add C-terminal alanine and threonine residues (CAT-tails) to the nascent chain. Imported CAT-tailed proteins form toxic aggregates in the mitochondrial matrix **(middle).** The peptidyl-tRNA hydrolase Vms1 releases the nascent polypeptide from the ribosome and blocks the Rqc2-mediated CAT-tailing. Upon import, these unmodified proteins are degraded by mitochondrial proteases **(right).**

Nascent mitochondrial precursor proteins can stall at the ribosome during translation. Possible reasons are the lack of a STOP codon, strong secondary structures in the mRNA or deficiencies in the amounts of some amino acids or tRNAs (Brandman and Hegde, 2016). The ribosome-associated quality control (RQC) delivers such stalled nascent polypeptides to proteasomes for degradation (Joazeiro, 2019). In this pathway, the ribosomal subunits dissociate and the nascent protein remains bound to the 60S subunit. Subsequently, the E3 ubiquitin ligase Ltn1 ubiquitylates nascent polypeptides to mark them for proteasomal turnover (Bengtson and Joazeiro, 2010; Brandman et al., 2012). In case no lysine is accessible for ubiquitylation since they are buried in the ribosomal exit tunnel, Rqc2 binds to ribosomes and adds C-terminally alanine and threonine residues (CAT-tail) to the nascent chain. Thereby, additional lysine residues may exit the ribosomal tunnel and

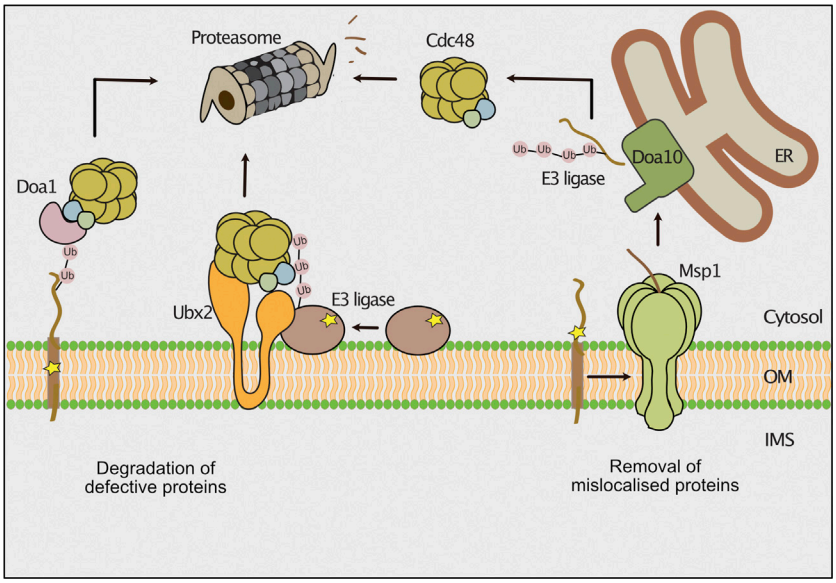

FIGURE 4 | Degradation pathways of outer membrane proteins. The cytosolic ubiquitin-proteasome system removes misfolded or mislocalized proteins from the outer mitochondrial membrane. Defective outer membrane proteins are ubiquitylated by different E3 ubiquitin ligases. The AAA-ATPase Cdc48 is recruited to the outer membrane by its ubiquitin binding co-factors Doa1 and Ubx2 and powers the extraction of substrate proteins for proteasomal turnover. The AAA-ATPase Msp1 extracts mislocalized tail-anchored proteins from the outer membrane. The ER localized E3 ubiquitin ligase Doa10 ubiquitylates these proteins and Cdc48 delivers them for proteasomal degradation.

be ubiquitylated by Ltn1 (Shen et al., 2015). During co-translational protein import into mitochondria, the nascent chain is directly transferred from the ribosome to the TOM channel. Consequently, lysine residues can escape ubiquitylation by Ltn1 although CAT-tailing occurs. Such CAT-tailed proteins can be imported into mitochondria, where they form toxic inclusions (**Figure 3**; Izawa et al., 2017). This detrimental import of CAT-tailed proteins is prevented by the conserved protein Vms1. Vms1 like its human homolog ANKZF1 functions as peptidyl-tRNA hydrolase and releases the nascent chain from the 60S ribosomal subunit (Izawa et al., 2017; Verma et al., 2018; Zurita Rendon et al., 2018). Furthermore, Vms1 hinders Rqc2 from binding to ribosomes and therefore prevents CAT-tailing (Izawa et al., 2017). The released nascent polypeptides are imported into mitochondria and degraded by mitochondrial proteases (**Figure 3**; Izawa et al., 2017).

REMOVAL OF MISLOCALIZED PROTEINS FROM THE OUTER MEMBRANE

An intertwined cytosolic chaperone network guides membrane proteins to the outer mitochondrial membrane, ER and peroxisomes (Guna and Hegde, 2018; Becker et al., 2019; Deuerling et al., 2019; Walter and Erdmann, 2019; Bykov et al., 2020). Defects in the targeting pathways can lead to mislocalization of ER- or peroxisome resident proteins to the outer mitochondrial membrane (Schuldiner et al., 2008; Jonikas et al., 2009; Chen et al., 2014; Okreglak and Walter, 2014; Vitali et al., 2018). To avoid overloading with mistargeted proteins, clearance pathways exist to recognize and remove such proteins. In the mitochondrial outer membrane, mistargeted proteins with a C-terminal membrane anchor (C-tail anchored) are removed by the conserved AAA ATPase Msp1 (ATAD1 in mammals) (**Figure 4**) that also functions in the mitoCPR pathway as described above (Chen et al., 2014; Okreglak and Walter, 2014; Wohlever et al., 2017; Weidberg and Amon, 2018). The protein has a dual localization to mitochondria and peroxisomes (Weir et al., 2017). Msp1 is N-terminally anchored to the membrane, exposing a single ATPase domain and forms a hexameric complex with a central pore (Wohlever et al., 2017; Castanzo et al., 2020; Wang et al., 2020). The cytosolic exposed AAA domain drives in an ATP-dependent manner the client protein through the central pore (Castanzo et al., 2020; Wang L. et al., 2020). Different modes of substrate binding by Msp1 have been reported (Wang and Walter, 2020; Dederer and Lemberg, 2021). The transmembrane domain of mislocalized proteins do not perfectly match the dimension of the outer membrane lipid bilayer, leading to exposure of hydrophobic domains, which are bound by Msp1 (Li et al., 2019; Castanzo et al., 2020; Wang L. et al., 2020). Furthermore, unassembled proteins expose regions that are normally covered by a partner protein. In this case, Msp1 recognizes such regions and dislocates the orphaned proteins (Weir et al., 2017; Dederer et al., 2019). Following extraction by Msp1 the tail-anchored proteins are first transferred to the ER, where they are ubiquitylated by the membrane bound E3-ubiquitin ligase Doa10 (Dederer et al., 2019; Matsumoto et al.,

2019). Subsequently, Cdc48 delivers these proteins for proteasomal degradation (Matsumoto et al., 2019). It is unclear why such proteins are not directly targeted from the mitochondrial surface to the proteasome for degradation. However, this mechanism might provide a second chance for mistargeted proteins to reach their correct destination.

QUALITY CONTROL OF MISFOLDED OUTER MEMBRANE PROTEINS

The ubiquitin-proteasome system removes aberrant or unassembled proteins form the outer membrane of mitochondria under constitutive or stress conditions (Taylor and Rutter, 2011; Bragoszewski et al., 2017; Ravanelli et al., 2020; Ruan et al., 2020; Song et al., 2021). Furthermore, selective removal of proteins is an important mode to regulate different mitochondrial processes like mitophagy, apoptosis and mitochondrial dynamics (Youle, 2019; Deshwal et al., 2020; Escobar-Henriques and Anton, 2020; Song et al., 2021). In analogy to the ERAD, the pathway for degrading mitochondrial outer membrane proteins by the proteasome was termed mitochondria-associated degradation (MAD). Degradation pathways of a few peripheral membrane proteins and proteins with α-helical membrane spans have been described (Wu et al., 2016; Chowdhury et al., 2018; Wu et al., 2018; Goodrum et al., 2019; Metzger et al., 2020; Nahar et al., 2020). How defective β-barrel proteins are removed from the outer membrane remains to be discovered.

A set of cytosolic E3 ubiquitin ligases has been reported to ubiquitylate outer membrane proteins. In yeast, the E3 ubiquitin ligases Rsp5 and Mdm30 mediate ubiquitylation of components of ER-mitochondria contact sites and the GTPase Fzo1 (fuzzy onion) that mediates mitochondrial fusion (Cohen et al., 2008; Wu et al., 2016; Belgareh-Touze et al., 2017; Goodrum et al., 2019). Mdm30 belongs to the F-box proteins, which determine substrate specificity of SCF (Skp, Cullin, F-box) ubiquitin ligase complexes (Skaar et al., 2013). The E3 ubiquitin ligase Rsp5 fulfills several functions in the cell such as regulation of the biosynthesis of unsaturated fatty acids, multivesicular body formation and protein degradation upon heat stress (Hoppe et al., 2000; Oestreich et al., 2007; Fang et al., 2014; Li et al., 2015). The proteasomal turnover of the mutant variants of Sam35 and Sen2 was shown to depend on the E3 ubiquitin ligases San1 and Ubr1 (**Figure 4**; Metzger et al., 2020). Both E3 ligases mediate the turnover of misfolded proteins from various cellular compartments including the nucleus, the ER, cytosol and mitochondria (Gardner et al., 2005; Heck et al., 2010; Nillegoda et al., 2010; Prasad et al., 2018; Szoradi et al., 2018; Shakya et al., 2021). Future work has to define how these E3 ubiquitin ligases are recruited to the outer membrane.

The removal of damaged outer membrane proteins by the proteasome requires a preceding membrane extraction step (**Figure 4**). Cdc48 in conjunction with multiple co-factors has been shown to mediate turnover of outer membrane proteins (Heo et al., 2010; Wu et al., 2016; Metzger et al., 2020). Different co-factors recruit Cdc48 to mitochondria. First, Ubx2 mediates the Cdc48-dependent turnover of peripheral proteins and of the integral membrane protein Fzo1 (Chowdhury et al., 2018; Metzger et al., 2020; Nahar et al., 2020). Second, Doa1 binds to Cdc48 in complex with Ufd1 and Npl4 (Rumpf and Jentsch, 2006). Several studies showed that Doa1 is involved in the turnover of mitochondrial outer membrane proteins (Wu et al., 2016; Goodrum et al., 2019; Metzger et al., 2020). Finally, Vms1 has a binding domain for Cdc48 and localizes to the mitochondrial outer membrane upon oxidative stress (Heo et al., 2010). The binding of Vms1 to mitochondria depends on oxidized ergosterol in the outer membrane and does not require additional interactions with membrane bound proteins (Nielson et al., 2017). The role of Vms1 in the degradation of outer membrane proteins is currently unclear. While it was initially reported that Vms1 targets Fzo1 for degradation (Heo et al., 2010), later studies found the degradation of Fzo1 to be independent of Vms1 (Esaki and Ogura, 2012; Wu et al., 2016).

It was reported that outer membrane proteins like Om45 and Tom22 that expose a soluble domain towards the intermembrane space can be degraded by the hexameric AAA-protease Yme1 (Wu et al., 2018). Yme1 is a multifunctional protease conserved from yeast to human that exposes its catalytic domain into the intermembrane space. It regulates mitochondrial fusion, lipid trafficking and protein transport to adjust mitochondrial biogenesis and function to cellular requirements (Baker et al., 2012; Schreiner et al., 2012; Rainbolt et al., 2013; Anand et al., 2014; MacVicar et al., 2019). Whether the ubiquitin-proteasome system is also involved in the degradation of these outer membrane proteins remains unclear. A recent study revealed that Yme1 and the ubiquitin-proteasome system can cooperate in protein degradation. The inner membrane-anchored NADH dehydrogenase Nde1 exists in two topomers. One topomer exposes the catalytic center into the intermembrane space, while the other topomer spans the outer membrane and is exposed to the cytosol. The ubiquitin-proteasome system degrades the cytosolic form, while the remaining part of the protein is removed by Yme1 (Saladi et al., 2020). Respiratory deficient cells accumulate the cytosol-exposed form of Nde1 that initiates cell death (Saladi et al., 2020).

SELECTIVE DEGRADATION OF OUTER MEMBRANE PROTEINS

Quality Control Regulates Mitochondrial Morphology

The role of ubiquitylation and proteasomal turnover on the regulation of mitochondrial dynamics have been extensively studied. Mitochondria form a tubular network, which is constantly remodeled by opposing fusion and fission events. Both processes are mediated by large dynamin-like GTPases mediating outer membrane fusion (Fzo1 in yeast, mitofusins Mfn1/Mfn2 in mammals), inner membrane fusion (Mgm1 in yeast, Opa1 in mammals) and mitochondrial fission (Dnm1 in yeast, Drp1 in mammals) (Bleazard et al., 1999; Escobar-Henriques and Anton, 2013; Tilokani et al., 2018; Murata

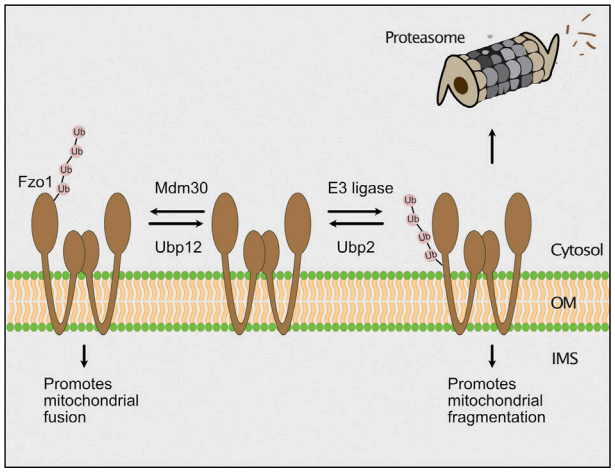

FIGURE 5 | The ubiquitin-proteasome system regulates mitochondrial fusion. In yeast, the GTPase Fzo1 (fuzzy onion) promotes fusion of mitochondria. The F-box protein Mdm30 mediates ubiquitylation of Fzo1 at specific lysines to stimulate mitochondrial fusion. Fusion-promoting ubiquitylation is reversed by the deubiquitylating enzyme Ubp12. Alternatively, an unknown E3 ubiquitin ligase ubiquitylates Fzo1 on different lysine residues, which leads to its proteasomal turnover. The degradation of Fzo1 inhibits fusion and results in mitochondrial fragmentation due to ongoing fission. Proteolytic ubiquitylation of Fzo1 is inhibited by the deubiquitylating enzyme Ubp2.

et al., 2020; Yapa et al., 2021). In particular turnover of Fzo1/mitofusins is a common mechanism to block fusion, thereby achieving mitochondrial fragmentation due to ongoing fission (Neutzner et al., 2007; Tanaka et al., 2010; Anton et al., 2013; Kim et al., 2013; Zhang et al., 2017; Goodrum et al., 2019). In yeast, the function of Fzo1 is fine-tuned by ubiquitylation and deubiquitylation (**Figure 5**; Cohen et al., 2008; Anton et al., 2013). Ubiquitylation of Fzo1 at specific lysine residues by Mdm30 promotes mitochondrial fusion (Fritz et al., 2003; Escobar-Henriques et al., 2006; Cohen et al., 2008; Anton et al., 2013), whereas ubiquitylation of alternative lysine residues of Fzo1 increases its degradation (Anton et al., 2013). The cytosolic deubiquitylase Ubp12 antagonizes Mdm30-mediated ubiquitylation and thereby inhibits mitochondrial fusion. Conversely, Ubp2 supports mitochondrial fusion by removing ubiquitylated species, which promote proteasomal turnover (Anton et al., 2013). In this process, Cdc48 functions as a regulatory hub, which is recruited by Fzo1 ubiquitylation and binds the deubiquitylating enzymes acting on Fzo1 (Simoes et al., 2018; Anton et al., 2019; Schuster et al., 2020). In contrast to its role in outer membrane quality control, Cdc48 appears to promote mitochondrial fusion by stabilizing ubiquitylated Fzo1 under non-stressed conditions (Simoes et al., 2018). Similarly, mammalian mitofusins are ubiquitylated by several E3 ubiquitin ligases (MARCH5, HUWE1, Parkin, Gp78), which regulate their degradation and function in fusion (Gegg et al., 2010; Tanaka et al., 2010; Leboucher et al., 2012; Fu et al., 2013; Yun et al., 2014; Tang et al., 2015; Mukherjee and Chakrabarti, 2016).

Regulation of Mitophagy by the Ubiquitin Proteosome System

The activity of the ubiquitin proteasome system on mitochondrial outer membrane proteins is linked to mitophagy in mammalian cells. Mitophagy is the removal of damaged mitochondria by selective autophagy (Harper et al., 2018; Pickles et al., 2018; Onishi et al., 2021). Central players of this pathway are the PTEN-induced kinase 1 (PINK1) and the E3 ubiquitin ligase Parkin. In healthy mitochondria, PINK1 is imported into mitochondria and processed by the mitochondrial processing peptidase and the inner membrane rhomboid protease PARL (Jin et al., 2010). The remaining soluble fragment retro-translocates into the cytosol, where it is degraded by the proteasome (Yamano and Youle, 2013). Upon mitochondrial dysfunction, the reduced membrane potential causes stalling of PINK1 at the TOM complex (Lazarou et al., 2012). PINK1 phosphorylates a second PINK1 protein, ubiquitin and Parkin, which results in recruitment and activation of Parkin (Geisler et al., 2010; Matsuda et al., 2010; Narendra et al., 2010; Ziviani et al., 2010; Okatsu et al., 2012; Shiba-Fukushima et al., 2014; Wauer et al., 2015; Rasool et al., 2018). Parkin in turn ubiquitylates several proteins at the outer membrane including the mitofusins (Gegg et al., 2010; Poole et al., 2010; Tanaka et al., 2010; Ziviani et al., 2010; Wang et al., 2011). The human homolog of Cdc48, p97/VCP extracts ubiquitylated mitofusins from the outer membrane to target them for proteasomal turnover (Tanaka et al., 2010; McLelland et al., 2018). Thereby, fusion of the damaged mitochondria is blocked to facilitate their removal by mitophagy. Moreover, ubiquitylated outer membrane proteins serve as a docking site for ubiquitin-binding autophagy receptors like p62, which initiate further steps in mitophagy (Geisler et al., 2010; Lazarou et al., 2015; Harper et al., 2018; Pickles et al., 2018; Onishi et al., 2021).

MITOCHONDRIAL-DERIVED VESICLES

An alternative process for the degradation of mitochondrial proteins is the formation of mitochondrial-derived vesicles (MDVs) in mammalian cells or mitochondrial-derived compartments (MDCs) in yeast (Suguira et al., 2014). Yeast MDCs contain only a small subset of mitochondrial proteins and show enrichment of the outer membrane protein Tom70. The separation of MDCs from mitochondria requires the dynamin-like GTPase Dnm1 (Hughes et al., 2016). The formation of MDCs was shown to maintain mitochondrial function during ageing in yeast (Hughes et al., 2016). Moreover, MDCs are formed upon toxic increase of amino acid levels, where they function in segregating amino acid carriers from the mitochondrial surface (Schuler et al., 2021). Different sub-populations of mammalian MDVs have been described containing the outer membrane or both mitochondrial membranes (Soubannier et al., 2012). They deliver cargo proteins to peroxisomes and multivesicular bodies/lysosomes for degradation as well as to mediate *de novo* biogenesis of peroxisomes (Neuspiel et al., 2008; Soubannier et al., 2012; Suguira et al., 2017). The formation of

MDVs occurs under basal growth conditions but is also triggered by cellular stress conditions such as oxidative stress or hypoxia (McLelland et al., 2014; Cadete et al., 2016; Matheoud et al., 2016; Li et al., 2020). In particular, MDVs function in targeting mitochondrial antigens for presentation by major histocompatibility complex class I (MHCI) on the cell surface in immune signaling (Matheoud et al., 2016). MDV-dependent antigen presentation is inhibited by PINK1 and Parkin (Matheoud et al., 2016), which however promote MDV formation under oxidative stress conditions (McLelland et al., 2014). MDCs and MDVs provide a safety mechanism that might be particularly important to rescue more bulky defects of mitochondria.

CONCLUSION

Protein quality control at the mitochondrial surface is essential for cell viability. Defects in quality control result in accumulation and mislocalization of mitochondrial proteins, which causes proteotoxic stress and eventually cell death. The ubiquitin-proteasome system monitors outer membrane proteins and protein import into mitochondria under constitutive and stress conditions. Two AAA ATPases, Cdc48 and Msp1, extract translocation-stalled precursor proteins from the TOM channel and aberrant or mislocalized proteins from the outer membrane for proteasomal turnover. Although several factors of these processes have been identified, our knowledge about key steps of these mechanisms such as substrate recognition and ubiquitylation are limited. Furthermore, the clearance mechanisms have only been described for a limited subset of proteins. It remains unknown whether the mitoTAD pathway specifically removes presequence-containing proteins or also other mitochondrial proteins that arrest in the TOM complex during translocation. While the removal of peripheral membrane proteins and proteins with an α-helical membrane anchor have been characterized, the degradation of damaged β-barrel proteins or protein complexes remains to be clarified. Strikingly, degradation of mislocalized proteins from the outer membrane involves the cooperation of mitochondria-associated, cytosolic and ER-localized factors (Dederer et al., 2019; Matsumoto et al., 2019). Further studies have to reveal how the interplay of the different components is coordinated across cellular compartments. Overall, the quality control mechanisms on the mitochondrial surface are an emerging field with many exciting discoveries within the past few years. Understanding these mechanisms will be crucial to understand how mitochondria are integrated into the cellular environment.

AUTHOR CONTRIBUTIONS

AG prepared the figures. FB and TB wrote the text. All authors discussed on the contents on the manuscript.

FUNDING

The work was funded by grants of the Deutsche Forschungsgemeinschaft to TB (BE 4679/2-2; SFB1218 project ID 269925409) and the BONFOR program of the University Hospital Bonn to FB.

ACKNOWLEDGMENTS

Work included in this article has been performed in partial fulfillment of the requirements for the doctoral thesis of AG.

REFERENCES

Abe, Y., Shodai, T., Muto, T., Mihara, K., Torii, H., Nishikawa, S.-i., et al. (2000). Structural Basis of Presequence Recognition by the Mitochondrial Protein Import Receptor Tom20. *Cell* 100, 551–560. doi:10.1016/s0092-8674(00)80691-1

Amm, I., Sommer, T., and Wolf, D. H. (2014). Protein Quality Control and Elimination of Protein Waste: The Role of the Ubiquitin-Proteasome System. *Biochim. Biophys. Acta Mol. Cell Res.* 1843, 182–196. doi:10.1016/j.bbamcr.2013.06.031

Anand, R., Wai, T., Baker, M. J., Kladt, N., Schauss, A. C., Rugarli, E., et al. (2014). The *i*-AAA Protease YME1L and OMA1 Cleave OPA1 to Balance Mitochondrial Fusion and Fission. *J. Cell Biol.* 204, 919–929. doi:10.1083/jcb.201308006

Anton, F., Dittmar, G., Langer, T., and Escobar-Henriques, M. (2013). Two Deubiquitylases Act on Mitofusin and Regulate Mitochondrial Fusion along Independent Pathways. *Mol. Cell* 49, 487–498. doi:10.1016/j.molcel.2012.12.003

Anton, V., Buntenbroich, I., Schuster, R., Babatz, F., Simões, T., Altin, S., et al. (2019). Plasticity in Salt Bridge Allows Fusion-Competent Ubiquitylation of Mitofusins and Cdc48 Recognition. *Life Sci. Alliance* 2, e201900491. doi:10.26508/lsa.201900491

Araiso, Y., Tsutsumi, A., Qiu, J., Imai, K., Shiota, T., Song, J., et al. (2019). Structure of the Mitochondrial Import Gate Reveals Distinct Preprotein Paths. *Nature* 575, 395–401. doi:10.1038/s41586-019-1680-7

Backes, S., Bykov, Y. S., Flohr, T., Räschle, M., Zhou, J., Lenhard, S., et al. (2021). The Chaperone-Binding Activity of the Mitochondrial Surface Receptor Tom70 Protects the Cytosol Against Mitoprotein-Induced Stress. *Cell Rep.* 35, 108936. doi:10.1016/j.celrep.2021.108936

Backes, S., Hess, S., Boos, F., Woellhaf, M. W., Gödel, S., Jung, M., et al. (2018). Tom70 Enhances Mitochondrial Preprotein Import Efficiency by Binding to Internal Targeting Sequences. *J. Cell Biol.* 217, 1369–1382. doi:10.1083/jcb.201708044

Baker, M. J., Mooga, V. P., Guiard, B., Langer, T., Ryan, M. T., and Stojanovski, D. (2012). Impaired Folding of the Mitochondrial Small TIM Chaperones Induces Clearance by the *i*-AAA Protease. *J. Mol. Biol.* 424, 227–239. doi:10.1016/j.jmb.2012.09.019

Basch, M., Wagner, M., Rolland, S., Carbonell, A., Zeng, R., Khosravi, S., et al. (2020). Msp1 Cooperates with the Proteasome for Extraction of Arrested Mitochondrial Import Intermediates. *Mol. Biol. Cell* 31, 753–767. doi:10.1091/mbc.e19-06-0329

Bausewein, T., Mills, D. J., Langer, J. D., Nitschke, B., Nussberger, S., and Kühlbrandt, W. (2017). Cryo-EM Structure of the TOM Core Complex from *Neurospora crassa*. *Cell* 170, 693–700. doi:10.1016/j.cell.2017.07.012

Becker, L., Bannwarth, M., Meisinger, C., Hill, K., Model, K., Krimmer, T., et al. (2005). Preprotein Translocase of the Outer Mitochondrial Membrane: Reconstituted Tom40 Forms a Characteristic TOM Pore. *J. Mol. Biol.* 353, 1011–1020. doi:10.1016/j.jmb.2005.09.019

Becker, T., Song, J., and Pfanner, N. (2019). Versatility of Preprotein Transfer from the Cytosol to Mitochondria. *Trends Cell Biol.* 29, 534–548. doi:10.1016/j.tcb.2019.03.007

Becker, T., and Wagner, R. (2018). Mitochondrial Outer Membrane Channels: Emerging Diversity in Transport Processes. *Bioessays* 40, 1800013. doi:10.1002/bies.201800013

Belgareh-Touzé, N., Cavellini, L., and Cohen, M. M. (2017). Ubiquitination of ERMES Components by the E3 Ligase Rsp5 is Involved in Mitophagy. *Autophagy* 13, 114–132. doi:10.1080/15548627.2016.1252889

Bengtson, M. H., and Joazeiro, C. A. P. (2010). Role of a Ribosome-Associated E3 Ubiquitin Ligase in Protein Quality Control. *Nature* 467, 470–473. doi:10.1038/nature09371

Bleazard, W., McCaffery, J. M., King, E. J., Bale, S., Mozdy, A., Tieu, Q., et al. (1999). The Dynamin-Related GTPase Dnm1 Regulates Mitochondrial Fission in Yeast. *Nat. Cell Biol.* 1, 298–304. doi:10.1038/13014

Bodnar, N. O., and Rapoport, T. A. (2017). Molecular Mechanism of Substrate Processing by the Cdc48 ATPase Complex. *Cell* 169, 722–735. doi:10.1016/j.cell.2017.04.020

Boos, F., Krämer, L., Groh, C., Jung, F., Haberkant, P., Stein, F., et al. (2019). Mitochondrial Protein-Induced Stress Triggers a Global Adaptive Transcriptional Programme. *Nat. Cell Biol.* 21, 442–451. doi:10.1038/s41556-019-0294-5

Bragoszewski, P., Gornicka, A., Sztolsztener, M. E., and Chacinska, A. (2013). The Ubiquitin-Proteasome System Regulates Mitochondrial Intermembrane Space Proteins. *Mol. Cell Biol.* 33, 2136–2148. doi:10.1128/mcb.01579-12

Bragoszewski, P., Turek, M., and Chacinska, A. (2017). Control of Mitochondrial Biogenesis and Function by the Ubiquitin-Proteasome System. *Open Biol.* 7, 170007. doi:10.1098/rsob.170007

Brandman, O., and Hegde, R. S. (2016). Ribosome-associated Protein Quality Control. *Nat. Struct. Mol. Biol.* 23, 7–15. doi:10.1038/nsmb.3147

Brandman, O., Stewart-Ornstein, J., Wong, D., Larson, A., Williams, C. C., Li, G.-W., et al. (2012). A Ribosome-Bound Quality Control Complex Triggers Degradation of Nascent Peptides and Signals Translation Stress. *Cell* 151, 1042–1054. doi:10.1016/j.cell.2012.10.044

Brix, J., Dietmeier, K., and Pfanner, N. (1997). Differential Recognition of Preproteins by the Purified Cytosolic Domains of the Mitochondrial Import Receptors Tom20, Tom22, and Tom70. *J. Biol. Chem.* 272, 20730–20735. doi:10.1074/jbc.272.33.20730

Bykov, Y. S., Rapaport, D., Herrmann, J. M., and Schuldiner, M. (2020). Cytosolic Events in the Biogenesis of Mitochondrial Proteins. *Trends Biochem. Sci.* 45, 650–667. doi:10.1016/j.tibs.2020.04.001

Cadete, V. J. J., Deschênes, S., Cuillerier, A., Brisebois, F., Sugiura, A., Vincent, A., et al. (2016). Formation of Mitochondrial-Derived Vesicles is an Active and Physiologically Relevant Mitochondrial Quality Control Process in the Cardiac System. *J. Physiol.* 594, 5343–5362. doi:10.1113/jp272703

Campo, M. L., Peixoto, P. M., and Martínez-Caballero, S. (2017). Revisiting Trends on Mitochondrial Mega-Channels for the Import of Proteins and Nucleic Acids. *J. Bioenerg. Biomembr.* 49, 75–99. doi:10.1007/s10863-016-9662-z

Cappadocia, L., and Lima, C. D. (2018). Ubiquitin-like Protein Conjugation: Structures, Chemistry, and Mechanism. *Chem. Rev.* 118, 889–918. doi:10.1021/acs.chemrev.6b00737

Castanzo, D. T., LaFrance, B., and Martin, A. (2020). The AAA+ ATPase Msp1 Is a Processive Protein Translocase With Robust Unfoldase Activity. *Proc. Natl. Acad. Sci. USA* 117, 14970–14977. doi:10.1073/pnas.1920109117

Chaugule, V. K., and Walden, H. (2016). Specificity and Disease in the Ubiquitin System. *Biochem. Soc. Trans.* 44, 212–227. doi:10.1042/bst20150209

Chen, X., Htet, Z. M., López-Alfonzo, E., Martin, A., and Walters, K. J. (2021). Proteasome Interaction with Ubiquitinated Substrates: From Mechanisms to Therapies. *FEBS J.* 288, 5231–5251. doi:10.1111/febs.15638

Chen, Y. C., Umanah, G. K. E., Dephoure, N., Andrabi, S. A., Gygi, S. P., Dawson, T. M., et al. (2014). M Sp1/ ATAD 1 Maintains Mitochondrial Function by Facilitating the Degradation of Mislocalized Tail-Anchored Proteins. *EMBO J.* 33, 1548–1564. doi:10.15252/embj.201487943

Chowdhury, A., Ogura, T., and Esaki, M. (2018). Two Cdc48 Cofactors Ubp3 and Ubx2 Regulate Mitochondrial Morphology and Protein Turnover. *J. Biochem.* 164, 349–358. doi:10.1093/jb/mvy057

Ciechanover, A., and Stanhill, A. (2014). The Complexity of Recognition of Ubiquitinated Substrates by the 26S Proteasome. *Biochim. Biophys. Acta Mol. Cell Res.* 1843, 86–96. doi:10.1016/j.bbamcr.2013.07.007

Clague, M. J., Heride, C., and Urbé, S. (2015). The Demographics of the Ubiquitin System. *Trends Cell Biol.* 25, 417–426. doi:10.1016/j.tcb.2015.03.002

Cohen, M. M. J., Leboucher, G. P., Livnat-Levanon, N., Glickman, M. H., and Weissman, A. M. (2008). Ubiquitin-Proteasome-Dependent Degradation of a Mitofusin, a Critical Regulator of Mitochondrial Fusion. *Mol. Biol. Cell* 19, 2457–2464. doi:10.1091/mbc.e08-02-0227

Colombini, M. (2012). VDAC Structure, Selectivity, and Dynamics. *Biochim. Biophys. Acta Biomembr.* 1818, 1457–1465. doi:10.1016/j.bbamem.2011.12.026

Dederer, V., Khmelinskii, A., Huhn, A. G., Okreglak, V., Knop, M., and Lemberg, M. K. (2019). Cooperation of Mitochondrial and ER Factors in Quality Control of Tail-Anchored Proteins. *eLife* 8, e45506. doi:10.7554/eLife.45506

Dederer, V., and Lemberg, M. K. (2021). Transmembrane Dislocases: a Second Chance for Protein Targeting. *Trends Cell Biol.* 31, 898–911. doi:10.1016/j.tcb.2021.05.007

DeLaBarre, B., and Brunger, A. T. (2003). Complete Structure of P97/valosin-Containing Protein Reveals Communication between Nucleotide Domains. *Nat. Struct. Mol. Biol.* 10, 856–863. doi:10.1038/nsb972

den Brave, F., Cairo, L. V., Jagadeesan, C., Ruger-Herreros, C., Mogk, A., Bukau, B., et al. (2020). Chaperone-Mediated Protein Disaggregation Triggers Proteolytic Clearance of Intra-Nuclear Protein Inclusions. *Cell Rep.* 31, 107680. doi:10.1016/j.celrep.2020.107680

Deshaies, R. J., and Joazeiro, C. A. P. (2009). RING Domain E3 Ubiquitin Ligases. *Annu. Rev. Biochem.* 78, 399–434. doi:10.1146/annurev.biochem.78.101807.093809

Deshwal, S., Fiedler, K. U., and Langer, T. (2020). Mitochondrial Proteases: Multifaceted Regulators of Mitochondrial Plasticity. *Annu. Rev. Biochem.* 89, 501–528. doi:10.1146/annurev-biochem-062917-012739

Deuerling, E., Gamerdinger, M., and Kreft, S. G. (2019). Chaperone Interactions at the Ribosome. *Cold Spring Harb. Perspect. Biol.* 11, a033977. doi:10.1101/cshperspect.a033977

Doan, K. N., Grevel, A., Mårtensson, C. U., Ellenrieder, L., Thornton, N., Wenz, L.-S., et al. (2020). The Mitochondrial Import Complex MIM Functions as Main Translocase for α-Helical Outer Membrane Proteins. *Cell Rep.* 31, 107567. doi:10.1016/j.celrep.2020.107567

Drwesh, L., and Rapaport, D. (2020). Biogenesis Pathways of α-helical Mitochondrial Outer Membrane Proteins. *Biol. Chem.* 401, 677–686. doi:10.1515/hsz-2019-0440

Dukanovic, J., and Rapaport, D. (2011). Multiple Pathways in the Integration of Proteins into the Mitochondrial Outer Membrane. *Biochim. Biophys. Acta Biomembr.* 1808, 971–980. doi:10.1016/j.bbamem.2010.06.021

Ellenrieder, L., Opaliński, Ł., Becker, L., Krüger, V., Mirus, O., Straub, S. P., et al. (2016). Separating Mitochondrial Protein Assembly and Endoplasmic Reticulum Tethering by Selective Coupling of Mdm10. *Nat. Commun.* 7, 13021. doi:10.1038/ncomms13021

Elsasser, S., Gali, R. R., Schwickart, M., Larsen, C. N., Leggett, D. S., Müller, B., et al. (2002). Proteasome Subunit Rpn1 Binds Ubiquitin-Like Protein Domains. *Nat. Cell Biol.* 4, 725–730. doi:10.1038/ncb845

Enam, C., Geffen, Y., Ravid, T., and Gardner, R. G. (2018). Protein Quality Control Degradation in the Nucleus. *Annu. Rev. Biochem.* 87, 725–749. doi:10.1146/annurev-biochem-062917-012730

Endo, T., and Yamano, K. (2009). Multiple Pathways for Mitochondrial Protein Traffic. *Biol. Chem.* 390, 723–730. doi:10.1515/BC.2009.087

Esaki, M., and Ogura, T. (2012). Cdc48p/p97-Mediated Regulation of Mitochondrial Morphology is Vms1p-independent. *J. Struct. Biol.* 179, 112–120. doi:10.1016/j.jsb.2012.04.017

Escobar-Henriques, M., and Anton, F. (2013). Mechanistic Perspective of Mitochondrial Fusion: Tubulation vs. Fragmentation. *Biochim. Biophys. Acta Mol. Cell Res.* 1833, 162–175. doi:10.1016/j.bbamcr.2012.07.016

Escobar-Henriques, M., and Anton, V. (2020). Mitochondrial Surveillance by Cdc48/p97: MAD vs. Membrane Fusion. *Int. J. Mol. Sci.* 21, 6841. doi:10.3390/ijms21186841

Escobar-Henriques, M., Westermann, B., and Langer, T. (2006). Regulation of Mitochondrial Fusion by the F-Box Protein Mdm30 Involves Proteasome-Independent Turnover of Fzo1. *J. Cell Biol.* 173, 645–650. doi:10.1083/jcb.200512079

Fang, N. N., Chan, G. T., Zhu, M., Comyn, S. A., Persaud, A., Deshaies, R. J., et al. (2014). Rsp5/Nedd4 is the Main Ubiquitin Ligase that Targets Cytosolic Misfolded Proteins Following Heat Stress. *Nat. Cell Biol.* 16, 1227–1237. doi:10.1038/ncb3054

Finger, Y., Habich, M., Gerlich, S., Urbanczyk, S., van de Logt, E., Koch, J., et al. (2020). Proteasomal Degradation Induced by DPP9-Mediated Processing

Competes with Mitochondrial Protein Import. *EMBO J.* 39, e103889. doi:10.15252/embj.2019103889

Finley, D., Chen, X., and Walters, K. J. (2016). Gates, Channels, and Switches: Elements of the Proteasome Machine. *Trends Biochem. Sci.* 41, 77–93. doi:10.1016/j.tibs.2015.10.009

Franz, A., Ackermann, L., and Hoppe, T. (2016). Ring of Change: CDC48/p97 Drives Protein Dynamics at Chromatin. *Front. Genet.* 7, 73. doi:10.3389/fgene.2016.00073

Fritz, S., Weinbach, N., and Westermann, B. (2003). Mdm30 Is an F-Box Protein Required for Maintenance of Fusion-Competent Mitochondria in Yeast. *Mol. Biol. Cell* 14, 2303–2313. doi:10.1091/mbc.e02-12-0831

Frottin, F., Schueder, F., Tiwary, S., Gupta, R., Körner, R., Schlichthaerle, T., et al. (2019). The Nucleolus Functions as a Phase-Separated Protein Quality Control Compartment. *Science* 365, 342–347. doi:10.1126/science.aaw9157

Fu, M., St-Pierre, P., Shankar, J., Wang, P. T. C., Joshi, B., and Nabi, I. R. (2013). Regulation of Mitophagy by the Gp78 E3 Ubiquitin Ligase. *Mol. Biol. Cell* 24, 1153–1162. doi:10.1091/mbc.e12-08-0607

Funakoshi, M., Sasaki, T., Nishimoto, T., and Kobayashi, H. (2002). Budding Yeast Dsk2p is a Polyubiquitin-Binding Protein that can Interact With the Proteasome. *Proc. Natl. Acad. Sci.* 99, 745–750. doi:10.1073/pnas.012585199

Gardner, R. G., Nelson, Z. W., and Gottschling, D. E. (2005). Degradation-mediated Protein Quality Control in the Nucleus. *Cell* 120, 803–815. doi:10.1016/j.cell.2005.01.016

Gegg, M. E., Cooper, J. M., Chau, K.-Y., Rojo, M., Schapira, A. H. V., and Taanman, J.-W. (2010). Mitofusin 1 and Mitofusin 2 are Ubiquitinated in a PINK1/Parkin-Dependent Manner Upon Induction of Mitophagy. *Hum. Mol. Genet.* 19, 4861–4870. doi:10.1093/hmg/ddq419

Geisler, S., Holmström, K. M., Skujat, D., Fiesel, F. C., Rothfuss, O. C., Kahle, P. J., et al. (2010). PINK1/Parkin-Mediated Mitophagy is Dependent on VDAC1 and p62/SQSTM1. *Nat. Cell Biol.* 12, 119–131. doi:10.1038/ncb2012

Gerdes, F., Tatsuta, T., and Langer, T. (2012). Mitochondrial AAA Proteases - Towards a Molecular Understanding of Membrane-Bound Proteolytic Machines. *Biochim. Biophys. Acta Mol. Cell Res.* 1823, 49–55. doi:10.1016/j.bbamcr.2011.09.015

Goodrum, J. M., Lever, A. R., Coody, T. K., Gottschling, D. E., and Hughes, A. L. (2019). Rsp5 and Mdm30 Reshape the Mitochondrial Network in Response to Age-Induced Vacuole Stress. *Mol. Biol. Cell* 30, 2141–2154. doi:10.1091/mbc.e19-02-0094

Guan, Z., Yan, L., Wang, Q., Qi, L., Hong, S., Gong, Z., et al. (2021). Structural Insights Into Assembly of Human Mitochondrial Translocase TOM Complex. *Cell Discov.* 7, 22. doi:10.1038/s41421-021-00252-7

Guna, A., and Hegde, R. S. (2018). Transmembrane Domain Recognition during Membrane Protein Biogenesis and Quality Control. *Curr. Biol.* 28, R498–R511. doi:10.1016/j.cub.2018.02.004

Habich, M., Salscheider, S. L., Murschall, L. M., Hoehne, M. N., Fischer, M., Schorn, F., et al. (2018). Vectorial Import via a Metastable Disulfide-Linked Complex Allows for a Quality Control Step and Import by the Mitochondrial Disulfide Relay. *Cell Rep.* 26, 759–e5. doi:10.1016/j.celrep.2018.12.092

Hansen, K. G., Aviram, N., Laborenz, J., Bibi, C., Meyer, M., Spang, A., et al. (2018). An ER Surface Retrieval Pathway Safeguards the Import of Mitochondrial Membrane Proteins in Yeast. *Science* 361, 1118–1122. doi:10.1126/science.aar8174

Hansen, K. G., and Herrmann, J. M. (2019). Transport of Proteins into Mitochondria. *Protein J.* 38, 330–342. doi:10.1007/s10930-019-09819-6

Harper, J. W., Ordureau, A., and Heo, J.-M. (2018). Building and Decoding Ubiquitin Chains for Mitophagy. *Nat. Rev. Mol. Cell Biol.* 19, 93–108. doi:10.1038/nrm.2017.129

Heck, J. W., Cheung, S. K., and Hampton, R. Y. (2010). Cytoplasmic Protein Quality Control Degradation Mediated by Parallel Actions of the E3 Ubiquitin Ligases Ubr1 and San1. *Proc. Natl. Acad. Sci.* 107, 1106–1111. doi:10.1073/pnas.0910591107

Heo, J.-M., Livnat-Levanon, N., Taylor, E. B., Jones, K. T., Dephoure, N., Ring, J., et al. (2010). A Stress-Responsive System for Mitochondrial Protein Degradation. *Mol. Cell* 40, 465–480. doi:10.1016/j.molcel.2010.10.021

Hill, K., Model, K., Ryan, M. T., Dietmeier, K., Martin, F., Wagner, R., et al. (1998). Tom40 Forms the Hydrophilic Channel of the Mitochondrial Import Pore for Preproteins. *Nature* 395, 516–521. doi:10.1038/26780

Hines, V., Brandt, A., Griffiths, G., Horstmann, H., Brütsch, H., and Schatz, G. (1990). Protein Import into Yeast Mitochondria is Accelerated by the Outer Membrane Protein MAS70. *EMBO J.* 9, 3191–3200. doi:10.1002/j.1460-2075.1990.tb07517.x

Hoppe, T., Matuschewski, K., Rape, M., Schlenker, S., Ulrich, H. D., and Jentsch, S. (2000). Activation of a Membrane-Bound Transcription Factor by Regulated Ubiquitin/Proteasome-Dependent Processing. *Cell* 102, 577–586. doi:10.1016/s0092-8674(00)00080-5

Hughes, A. L., Hughes, C. E., Henderson, K. A., Yazvenko, N., and Gottschling, D. E. (2016). Selective Sorting and Destruction of Mitochondrial Membrane Proteins in Aged Yeast. *eLife* 5, e13943. doi:10.7554/eLife.13943

Itakura, E., Zavodszky, E., Shao, S., Wohlever, M. L., Keenan, R. J., and Hegde, R. S. (2016). Ubiquilins Chaperone and Triage Mitochondrial Membrane Proteins for Degradation. *Mol. Cell* 63, 21–33. doi:10.1016/j.molcel.2016.05.020

Izawa, T., Park, S.-H., Zhao, L., Hartl, F. U., and Neupert, W. (2017). Cytosolic Protein Vms1 Links Ribosome Quality Control to Mitochondrial and Cellular Homeostasis. *Cell* 171, 890–903. doi:10.1016/j.cell.2017.10.002

Jin, S. M., Lazarou, M., Wang, C., Kane, L. A., Narendra, D. P., and Youle, R. J. (2010). Mitochondrial Membrane Potential Regulates PINK1 Import and Proteolytic Destabilization by PARL. *J. Cell Biol.* 191, 933–942. doi:10.1083/jcb.201008084

Joazeiro, C. A. P. (2019). Mechanisms and Functions of Ribosome-Associated Protein Quality Control. *Nat. Rev. Mol. Cell. Biol.* 20, 368–383. doi:10.1038/s41580-019-0118-2

Jonikas, M. C., Collins, S. R., Denic, V., Oh, E., Quan, E. M., Schmid, V., et al. (2009). Comprehensive Characterization of Genes Required for Protein Folding in the Endoplasmic Reticulum. *Science* 323, 1693–1697. doi:10.1126/science.1167983

Jores, T., and Rapaport, D. (2017). Early Stages in the Biogenesis of Eukaryotic β-barrel Proteins. *FEBS Lett.* 591, 2671–2681. doi:10.1002/1873-3468.12726

Kameoka, S., Adachi, Y., Okamoto, K., Iijima, M., and Sesaki, H. (2018). Phosphatidic Acid and Cardiolipin Coordinate Mitochondrial Dynamics. *Trends Cell Biol.* 28, 67–76. doi:10.1016/j.tcb.2017.08.011

Kerscher, O., Felberbaum, R., and Hochstrasser, M. (2006). Modification of Proteins by Ubiquitin and Ubiquitin-Like Proteins. *Annu. Rev. Cell Dev. Biol.* 22, 159–180. doi:10.1146/annurev.cellbio.22.010605.093503

Kim, N. C., Tresse, E., Kolaitis, R.-M., Molliex, A., Thomas, R. E., Alami, N. H., et al. (2013). VCP is Essential for Mitochondrial Quality Control by PINK1/Parkin and This Function is Impaired by VCP Mutations. *Neuron* 78, 65–80. doi:10.1016/j.neuron.2013.02.029

Komander, D., and Rape, M. (2012). The Ubiquitin Code. *Annu. Rev. Biochem.* 81, 203–229. doi:10.1146/annurev-biochem-060310-170328

Kornmann, B., Currie, E., Collins, S. R., Schuldiner, M., Nunnari, J., Weissman, J. S., et al. (2009). An ER-Mitochondria Tethering Complex Revealed by a Synthetic Biology Screen. *Science* 325, 477–481. doi:10.1126/science.1175088

Kowalski, L., Bragoszewski, P., Khmelinskii, A., Glow, E., Knop, M., and Chacinska, A. (2018). Determinants of the Cytosolic Turnover of Mitochondrial Intermembrane Space Proteins. *BMC Biol.* 16, 66. doi:10.1186/s12915-018-0536-1

Krumpe, K., Frumkin, I., Herzig, Y., Rimon, N., Özbalci, C., Brügger, B., et al. (2012). Ergosterol Content Specifies Targeting of Tail-Anchored Proteins to Mitochondrial Outer Membranes. *Mol. Biol. Cell* 23, 3927–3935. doi:10.1091/mbc.e11-12-0994

Kühlbrandt, W. (2019). Structure and Mechanisms of F-Type ATP Synthases. *Annu. Rev. Biochem.* 88, 515–549. doi:10.1146/annurev-biochem-013118-110903

Laborenz, J., Bykov, Y. S., Knöringer, K., Räschle, M., Filker, S., Prescianotto-Baschong, C., et al. (2021). The ER Protein Ema19 Facilitates the Degradation of Nonimported Mitochondrial Precursor Proteins. *Mol. Biol. Cell* 32, 664–674. doi:10.1091/mbc.e20-11-0748

Lazarou, M., Jin, S. M., Kane, L. A., and Youle, R. J. (2012). Role of PINK1 Binding to the TOM Complex and Alternate Intracellular Membranes in Recruitment and Activation of the E3 Ligase Parkin. *Dev. Cell* 22, 320–333. doi:10.1016/j.devcel.2011.12.014

Lazarou, M., Sliter, D. A., Kane, L. A., Sarraf, S. A., Wang, C., Burman, J. L., et al. (2015). The Ubiquitin Kinase PINK1 Recruits Autophagy Receptors to Induce Mitophagy. *Nature* 524, 309–314. doi:10.1038/nature14893

Leboucher, G. P., Tsai, Y. C., Yang, M., Shaw, K. C., Zhou, M., Veenstra, T. D., et al. (2012). Stress-induced Phosphorylation and Proteasomal Degradation of Mitofusin 2 Facilitates Mitochondrial Fragmentation and Apoptosis. *Mol. Cell* 47, 547–557. doi:10.1016/j.molcel.2012.05.041

Li, B., Zhao, H., Wu, Y., Zhu, Y., Zhang, J., Yang, G., et al. (2020). Mitochondrial-Derived Vesicles Protect Cardiomyocytes Against Hypoxic Damage. *Front. Cell Dev. Biol.* 8, 214. doi:10.3389/fcell.2020.00214

Li, L., Zheng, J., Wu, X., and Jiang, H. (2019). Mitochondrial AAA-ATPase Msp1 Detects Mislocalized Tail-Anchored Proteins through a Dual-Recognition Mechanism. *EMBO Rep.* 20, e46989. doi:10.15252/embr.201846989

Li, M., Rong, Y., Chuang, Y.-S., Peng, D., and Emr, S. D. (2015). Ubiquitin-Dependent Lysosomal Membrane Protein Sorting and Degradation. *Mol. Cell* 57, 467–478. doi:10.1016/j.molcel.2014.12.012

MacVicar, T., Ohba, Y., Nolte, H., Mayer, F. C., Tatsuta, T., Sprenger, H.-G., et al. (2019). Lipid Signalling Drives Proteolytic Rewiring of Mitochondria by YME1L. *Nature* 575, 361–365. doi:10.1038/s41586-019-1738-6

Malhotra, K., Sathappa, M., Landin, J. S., Johnson, A. E., and Alder, N. N. (2013). Structural Changes in the Mitochondrial Tim23 Channel are Coupled to the Proton-Motive Force. *Nat. Struct. Mol. Biol.* 20, 965–972. doi:10.1038/nsmb.2613

Mårtensson, C. U., Priesnitz, C., Song, J., Ellenrieder, L., Doan, K. N., Boos, F., et al. (2019). Mitochondrial Protein Translocation-Associated Degradation. *Nature* 569, 679–683. doi:10.1038/s41586-019-1227-y

Matheoud, D., Sugiura, A., Bellemare-Pelletier, A., Laplante, A., Rondeau, C., Chemali, M., et al. (2016). Parkinson's Disease-Related Proteins PINK1 and Parkin Repress Mitochondrial Antigen Presentation. *Cell* 166, 314–327. doi:10.1016/j.cell.2016.05.039

Matsuda, N., Sato, S., Shiba, K., Okatsu, K., Saisho, K., Gautier, C. A., et al. (2010). PINK1 Stabilized by Mitochondrial Depolarization Recruits Parkin to Damaged Mitochondria and Activates Latent Parkin for Mitophagy. *J. Cell Biol.* 189, 211–221. doi:10.1083/jcb.200910140

Matsumoto, S., Nakatsukasa, K., Kakuta, C., Tamura, Y., Esaki, M., and Endo, T. (2019). Msp1 Clears Mistargeted Proteins by Facilitating Their Transfer from Mitochondria to the ER. *Mol. Cell* 76, 191–205. doi:10.1016/j.molcel.2019.07.006

McKenna, M. J., Sim, S. I., Ordureau, A., Wei, L., Harper, J. W., Shao, S., et al. (2020). The Endoplasmic Reticulum P5A-ATPase is a Transmembrane Helix Dislocase. *Science* 369, eabc5809. doi:10.1126/science.abc5809

McLelland, G. L., Goiran, T., Yi, W., Dorval, G., Chen, C. X., Lauinger, N. D., et al. (2018). Mfn2 Ubiquitination by PINK1/Parkin Gates the p97-Dependent Release of ER from Mitochondria to Drive Mitophagy. *eLife* 7, e32866. doi:10.7554/eLife.32866

McLelland, G. L., Soubannier, V., Chen, C. X., McBride, H. M., and Fon, E. A. (2014). Parkin and PINK1 Function in a Vesicular Trafficking Pathway Regulating Mitochondrial Quality Control. *EMBO J.* 33, 282–295. doi:10.1002/embj.201385902

Metzger, M. B., Scales, J. L., Dunklebarger, M. F., Loncarek, J., and Weissman, A. M. (2020). A Protein Quality Control Pathway at the Mitochondrial Outer Membrane. *eLife* 9, e51065. doi:10.7554/eLife.51065

Mohanraj, K., Wasilewski, M., Benincá, C., Cysewski, D., Poznanski, J., Sakowska, P., et al. (2019). Inhibition of Proteasome Rescues a Pathogenic Variant of Respiratory Chain Assembly Factor COA7. *EMBO Mol. Med.* 11, e9561. doi:10.15252/emmm.201809561

Morgenstern, M., Stiller, S. B., Lübbert, P., Peikert, C. D., Dannenmaier, S., Drepper, F., et al. (2017). Definition of a High-Confidence Mitochondrial Proteome at Quantitative Scale. *Cell Rep.* 19, 2836–2852. doi:10.1016/j.celrep.2017.06.014

Mukherjee, R., and Chakrabarti, O. (2016). Regulation of Mitofusin1 by Mahogunin Ring Finger-1 and the Proteasome Modulates Mitochondrial Fusion. *Biochim. Biophys. Acta Mol. Cell Res.* 1863, 3065–3083. doi:10.1016/j.bbamcr.2016.09.022

Murata, D., Arai, K., Iijima, M., and Sesaki, H. (2020). Mitochondrial Division, Fusion and Degradation. *J. Biochem.* 167, 233–241. doi:10.1093/jb/mvz106

Nahar, S., Chowdhury, A., Ogura, T., and Esaki, M. (2020). A AAA ATPase Cdc48 With a Cofactor Ubx2 Facilitates Ubiquitylation of a Mitochondrial Fusion-Promoting Factor Fzo1 for Proteasomal Degradation. *J. Biochem.* 167, 279–286. doi:10.1093/jb/mvz104

Narendra, D. P., Jin, S. M., Tanaka, A., Suen, D.-F., Gautier, C. A., Shen, J., et al. (2010). PINK1 Is Selectively Stabilized on Impaired Mitochondria to Activate Parkin. *PLoS Biol.* 8, e1000298. doi:10.1371/journal.pbio.1000298

Neuber, O., Jarosch, E., Volkwein, C., Walter, J., and Sommer, T. (2005). Ubx2 Links the Cdc48 Complex to ER-Associated Protein Degradation. *Nat. Cell Biol.* 7, 993–998. doi:10.1038/ncb1298

Neuspiel, M., Schauss, A. C., Braschi, E., Zunino, R., Rippstein, P., Rachubinski, R. A., et al. (2008). Cargo-Selected Transport from the Mitochondria to Peroxisomes is Mediated by Vesicular Carriers. *Curr. Biol.* 18, 102–108. doi:10.1016/j.cub.2007.12.038

Neutzner, A., Youle, R. J., and Karbowski, M. (2007). Outer Mitochondrial Membrane Protein Degradation by the Proteasome. *Novartis Found. Symp.* 287, 4–20. doi:10.1002/9780470725207.ch2

Nielson, J. R., Fredrickson, E. K., Waller, T. C., Rendón, O. Z., Schubert, H. L., Lin, Z., et al. (2017). Sterol Oxidation Mediates Stress-Responsive Vms1 Translocation to Mitochondria. *Mol. Cell* 68, 673–685. doi:10.1016/j.molcel.2017.10.022

Nillegoda, N. B., Theodoraki, M. A., Mandal, A. K., Mayo, K. J., Ren, H. Y., Sultana, R., et al. (2010). Ubr1 and Ubr2 Function in a Quality Control Pathway for Degradation of Unfolded Cytosolic Proteins. *Mol. Biol. Cell* 21, 2102–2116. doi:10.1091/mbc.e10-02-0098

Oestreich, A. J., Aboian, M., Lee, J., Azmi, I., Payne, J., Issaka, R., et al. (2007). Characterization of Multiple Multivesicular Body Sorting Determinants within Sna3: A Role for the Ubiquitin Ligase Rsp5. *Mol. Biol. Cell* 18, 707–720. doi:10.1091/mbc.e06-08-0680

Okatsu, K., Oka, T., Iguchi, M., Imamura, K., Kosako, H., Tani, N., et al. (2012). PINK1 Autophosphorylation Upon Membrane Potential Dissipation Is Essential for Parkin Recruitment to Damaged Mitochondria. *Nat. Commun.* 3, 1016. doi:10.1038/ncomms2016

Okreglak, V., and Walter, P. (2014). The Conserved AAA-ATPase Msp1 Confers Organelle Specificity to Tail-Anchored Proteins. *Proc. Natl. Acad. Sci.* 111, 8019–8024. doi:10.1073/pnas.1405755111

Olzmann, J. A., Richter, C. M., and Kopito, R. R. (2013). Spatial Regulation of UBXD8 and P97/VCP Controls ATGL-Mediated Lipid Droplet Turnover. *Proc. Natl. Acad. Sci. USA* 110, 1345–1350. doi:10.1073/pnas.1213738110

Onishi, M., Yamano, K., Sato, M., Matsuda, N., and Okamoto, K. (2021). Molecular Mechanisms and Physiological Functions of Mitophagy. *EMBO J.* 40, e104705. doi:10.15252/embj.2020104705

Ordureau, A., Paulo, J. A., Zhang, J., An, H., Swatek, K. N., Cannon, J. R., et al. (2020). Global Landscape and Dynamics of Parkin and USP30-Dependent Ubiquitylomes in iNeurons During Mitophagic Signaling. *Mol. Cell* 77, 1124–1142. doi:10.1016/j.molcel.2019.11.013

Pagliarini, D. J., Calvo, S. E., Chang, B., Sheth, S. A., Vafai, S. B., Ong, S.-E., et al. (2008). A Mitochondrial Protein Compendium Elucidates Complex I Disease Biology. *Cell* 134, 112–123. doi:10.1016/j.cell.2008.06.016

Park, S.-H., Kukushkin, Y., Gupta, R., Chen, T., Konagai, A., Hipp, M. S., et al. (2013). PolyQ Proteins Interfere with Nuclear Degradation of Cytosolic Proteins by Sequestering the Sis1p Chaperone. *Cell* 154, 134–145. doi:10.1016/j.cell.2013.06.003

Phu, L., Rose, C. M., Tea, J. S., Wall, C. E., Verschueren, E., Cheung, T. K., et al. (2020). Dynamic Regulation of Mitochondrial Import by the Ubiquitin System. *Mol. Cell* 77, 1107–1123. doi:10.1016/j.molcel.2020.02.012

Pickles, S., Vigié, P., and Youle, R. J. (2018). Mitophagy and Quality Control Mechanisms in Mitochondrial Maintenance. *Curr. Biol.* 28, R170–R185. doi:10.1016/j.cub.2018.01.004

Poole, A. C., Thomas, R. E., Yu, S., Vincow, E. S., and Pallanck, L. (2010). The Mitochondrial Fusion-Promoting Factor Mitofusin is a Substrate of the PINK1/parkin Pathway. *PLoS One* 5, e10054. doi:10.1371/journal.pone.0010054

Prasad, R., Xu, C., and Ng, D. T. W. (2018). Hsp40/70/110 Chaperones Adapt Nuclear Protein Quality Control to Serve Cytosolic Clients. *J. Cell Biol.* 217, 2019–2032. doi:10.1083/jcb.201706091

Qin, Q., Zhao, T., Zou, W., Shen, K., and Wang, X. (2020). An Endoplasmic Reticulum ATPase Safeguards Endoplasmic Reticulum Identity by Removing Ectopically Localized Mitochondrial Proteins. *Cell Rep.* 33, 108363. doi:10.1016/j.celrep.2020.108363

Radke, S., Chander, H., Schäfer, P., Meiss, G., Krüger, R., Schulz, J. B., et al. (2008). Mitochondrial Protein Quality Control by the Proteasome Involves

Ubiquitination and the Protease Omi. *J. Biol. Chem.* 283, 12681–12685. doi:10.1074/jbc.c800036200

Rainbolt, T. K., Atanassova, N., Genereux, J. C., and Wiseman, R. L. (2013). Stress-Regulated Translational Attenuation Adapts Mitochondrial Protein Import through Tim17A Degradation. *Cell Metab.* 18, 908–919. doi:10.1016/j.cmet.2013.11.006

Rasool, S., Soya, N., Truong, L., Croteau, N., Lukacs, G. L., and Trempe, J. F. (2018). PINK1 Autophosphorylation is Required for Ubiquitin Recognition. *EMBO Rep.* 19, e44981. doi:10.15252/embr.201744981

Ravanelli, S., den Brave, F., and Hoppe, T. (2020). Mitochondrial Quality Control Governed by Ubiquitin. *Front. Cell Dev. Biol.* 8, 270. doi:10.3389/fcell.2020.00270

Rolland, S. G., Schneid, S., Schwarz, M., Rackles, E., Fischer, C., Haeussler, S., et al. (2019). Compromised Mitochondrial Protein Import Acts as a Signal for UPRmt. *Cell Rep.* 28, 1659–1669. doi:10.1016/j.celrep.2019.07.049

Ruan, L., Wang, Y., Zhang, X., Tomaszewski, A., McNamara, J. T., and Li, R. (2020). Mitochondria-Associated Proteostasis. *Annu. Rev. Biophys.* 49, 41–67. doi:10.1146/annurev-biophys-121219-081604

Rumpf, S., and Jentsch, S. (2006). Functional Division of Substrate Processing Cofactors of the Ubiquitin-Selective Cdc48 Chaperone. *Mol. Cell* 21, 261–269. doi:10.1016/j.molcel.2005.12.014

Russell, S. J., Steger, K. A., and Johnston, S. A. (1999). Subcellular Localization, Stoichiometry, and Protein Levels of 26 S Proteasome Subunits in Yeast. *J. Biol. Chem.* 274, 21943–21952. doi:10.1074/jbc.274.31.21943

Saladi, S., Boos, F., Poglitsch, M., Meyer, H., Sommer, F., Mühlhaus, T., et al. (2020). The NADH Dehydrogenase Nde1 Executes Cell Death After Integrating Signals from Metabolism and Proteostasis on the Mitochondrial Surface. *Mol. Cell* 77, 189–202. doi:10.1016/j.molcel.2019.09.027

Schmitt, S., Prokisch, H., Schlunck, T., Camp, D. G., 2nd, Ahting, U., Waizenegger, T., et al. (2006). Proteome Analysis of Mitochondrial Outer Membrane from *Neurospora crassa*. *Proteomics* 6, 72–80. doi:10.1002/pmic.200402084

Schreiner, B., Westerburg, H., Forné, I., Imhof, A., Neupert, W., and Mokranjac, D. (2012). Role of the AAA Protease Yme1 in Folding of Proteins in the Intermembrane Space of Mitochondria. *Mol. Biol. Cell* 23, 4335–4346. doi:10.1091/mbc.e12-05-0420

Schuberth, C., and Buchberger, A. (2005). Membrane-Bound Ubx2 Recruits Cdc48 to Ubiquitin Ligases and Their Substrates to Ensure Efficient ER-Associated Protein Degradation. *Nat. Cell Biol.* 7, 999–1006. doi:10.1038/ncb1299

Schuldiner, M., Metz, J., Schmid, V., Denic, V., Rakwalska, M., Schmitt, H. D., et al. (2008). The GET Complex Mediates Insertion of Tail-Anchored Proteins into the ER Membrane. *Cell* 134, 634–645. doi:10.1016/j.cell.2008.06.025

Schuler, M.-H., English, A. M., Xiao, T., Campbell, T. J., Shaw, J. M., and Hughes, A. L. (2021). Mitochondrial-derived Compartments Facilitate Cellular Adaptation to Amino Acid Stress. *Mol. Cell* 81, 3786–3802. doi:10.1016/j.molcel.2021.08.021

Schuster, R., Anton, V., Simões, T., Altin, S., den Brave, F., Hermanns, T., et al. (2020). Dual Role of a GTPase Conformational Switch for Membrane Fusion by Mitofusin Ubiquitylation. *Life Sci. Alliance* 3, e201900476. doi:10.26508/lsa.201900476

Shakya, V. P., Barbeau, W. A., Xiao, T., Knutson, C. S., Schuler, M. H., and Hughes, A. L. (2021). A Nuclear-Based Quality Control Pathway for Non-Imported Mitochondrial Proteins. *eLife* 10, e61230. doi:10.7554/elife.61230

Shen, P. S., Park, J., Qin, Y., Li, X., Parsawar, K., Larson, M. H., et al. (2015). Rqc2p and 60 S Ribosomal Subunits Mediate mRNA-Independent Elongation of Nascent Chains. *Science* 347, 75–78. doi:10.1126/science.1259724

Shiba-Fukushima, K., Arano, T., Matsumoto, G., Inoshita, T., Yoshida, S., Ishihama, Y., et al. (2014). Phosphorylation of Mitochondrial Polyubiquitin by PINK1 Promotes Parkin Mitochondrial Tethering. *PLoS Genet.* 10, e1004861. doi:10.1371/journal.pgen.1004861

Shiota, T., Imai, K., Qiu, J., Hewitt, V. L., Tan, K., Shen, H.-H., et al. (2015). Molecular Architecture of the Active Mitochondrial Protein Gate. *Science* 349, 1544–1548. doi:10.1126/science.aac6428

Simões, T., Schuster, R., den Brave, F., and Escobar-Henriques, M. (2018). Cdc48 Regulates a Deubiquitylase Cascade Critical for Mitochondrial Fusion. *eLife* 7, e30015. doi:10.7554/eLife.30015

Skaar, J. R., Pagan, J. K., and Pagano, M. (2013). Mechanisms and Function of Substrate Recruitment by F-Box Proteins. *Nat. Rev. Mol. Cell Biol.* 14, 369–381. doi:10.1038/nrm3582

Song, J., Herrmann, J. M., and Becker, T. (2021). Quality Control of the Mitochondrial Proteome. *Nat. Rev. Mol. Cell Biol.* 22, 54–70. doi:10.1038/s41580-020-00300-2

Soubannier, V., McLelland, G.-L., Zunino, R., Braschi, E., Rippstein, P., Fon, E. A., et al. (2012). A Vesicular Transport Pathway Shuttles Cargo from Mitochondria to Lysosomes. *Curr. Biol.* 22, 135–141. doi:10.1016/j.cub.2011.11.057

Spinelli, J. B., and Haigis, M. C. (2018). The Multifaceted Contributions of Mitochondria to Cellular Metabolism. *Nat. Cell Biol.* 20, 745–754. doi:10.1038/s41556-018-0124-1

Sugiura, A., Mattie, S., Prudent, J., and McBride, H. M. (2017). Newly Born Peroxisomes Are a Hybrid of Mitochondrial and ER-Derived Pre-Peroxisomes. *Nature* 542, 251–254. doi:10.1038/nature21375

Sugiura, A., McLelland, G. L., Fon, E. A., and McBride, H. M. (2014). A New Pathway for Mitochondrial Quality Control: Mitochondrial-Derived Vesicles. *EMBO J.* 33, 2142–2156. doi:10.15252/embj.201488104

Suzuki, H., Kadowaki, T., Maeda, M., Sasaki, H., Nabekura, J., Sakaguchi, M., et al. (2004). Membrane-Embedded C-Terminal Segment of Rat Mitochondrial TOM40 Constitutes Protein-Conducting Pore with Enriched β-Structure. *J. Biol. Chem.* 279, 50619–50629. doi:10.1074/jbc.m408604200

Szoradi, T., Schaeff, K., Garcia-Rivera, E. M., Itzhak, D. N., Schmidt, R. M., Bircham, P. W., et al. (2018). SHRED is a Regulatory Cascade That Reprograms Ubr1 Substrate Specificity for Enhanced Protein Quality Control During Stress. *Mol. Cell* 70, 1025–1037. doi:10.1016/j.molcel.2018.04.027

Tanaka, A., Cleland, M. M., Xu, S., Narendra, D. P., Suen, D.-F., Karbowski, M., et al. (2010). Proteasome and p97 Mediate Mitophagy and Degradation of Mitofusins Induced by Parkin. *J. Cell Biol.* 191, 1367–1380. doi:10.1083/jcb.201007013

Tang, F.-L., Liu, W., Hu, J.-X., Erion, J. R., Ye, J., Mei, L., et al. (2015). VPS35 Deficiency or Mutation Causes Dopaminergic Neuronal Loss by Impairing Mitochondrial Fusion and Function. *Cell Rep.* 12, 1631–1643. doi:10.1016/j.celrep.2015.08.001

Taylor, E. B., and Rutter, J. (2011). Mitochondrial Quality Control by the Ubiquitin-Proteasome System. *Biochem. Soc. Trans.* 39, 1509–1513. doi:10.1042/bst0391509

Tiku, V., Tan, M.-W., and Dikic, I. (2020). Mitochondrial Functions in Infection and Immunity. *Trends Cell Biol.* 30, 263–275. doi:10.1016/j.tcb.2020.01.006

Tilokani, L., Nagashima, S., Paupe, V., and Prudent, J. (2018). Mitochondrial Dynamics: Overview of Molecular Mechanisms. *Essays Biochem.* 62, 341–360. doi:10.1042/ebc20170104

Tucker, K., and Park, E. (2019). Cryo-EM Structure of the Mitochondrial Protein-Import Channel TOM Complex at Near-Atomic Resolution. *Nat. Struct. Mol. Biol.* 26, 1158–1166. doi:10.1038/s41594-019-0339-2

van Wilpe, S., Ryan, M. T., Hill, K., Maarse, A. C., Meisinger, C., Brix, J., et al. (1999). Tom22 is a Multifunctional Organizer of the Mitochondrial Preprotein Translocase. *Nature* 401, 485–489. doi:10.1038/46802

Verma, R., Reichermeier, K. M., Burroughs, A. M., Oania, R. S., Reitsma, J. M., Aravind, L., et al. (2018). Vms1 and ANKZF1 Peptidyl-tRNA Hydrolases Release Nascent Chains from Stalled Ribosomes. *Nature* 557, 446–451. doi:10.1038/s41586-018-0022-5

Vitali, D. G., Sinzel, M., Bulthuis, E. P., Kolb, A., Zabel, S., Mehlhorn, D. G., et al. (2018). The GET Pathway can Increase the Risk of Mitochondrial Outer Membrane Proteins to Be Mistargeted to the ER. *J. Cell Sci.* 131, jcs211110. doi:10.1242/jcs.211110

Vögtle, F.-N., Burkhart, J. M., Gonczarowska-Jorge, H., Kücükköse, C., Taskin, A. A., Kopczynski, D., et al. (2017). Landscape of Submitochondrial Protein Distribution. *Nat. Commun.* 8, 290. doi:10.1038/s41467-017-00359-0

von Ballmoos, C., Wiedenmann, A., and Dimroth, P. (2009). Essentials for ATP Synthesis by F1F0 ATP Synthases. *Annu. Rev. Biochem.* 78, 649–672. doi:10.1146/annurev.biochem.78.081307.104803

Walden, H., and Rittinger, K. (2018). RBR Ligase-Mediated Ubiquitin Transfer: A Tale With Many Twists and Turns. *Nat. Struct. Mol. Biol.* 25, 440–445. doi:10.1038/s41594-018-0063-3

Walter, T., and Erdmann, R. (2019). Current Advances in Protein Import into Peroxisomes. *Protein J.* 38, 351–362. doi:10.1007/s10930-019-09835-6

Wang, F., Brown, E. C., Mak, G., Zhuang, J., and Denic, V. (2010). A Chaperone Cascade Sorts Proteins for Posttranslational Membrane Insertion Into the Endoplasmic Reticulum. *Mol. Cell* 40, 159–171. doi:10.1016/j.molcel.2010.08.038

Wang, L., Myasnikov, A., Pan, X., and Walter, P. (2020). Structure of the AAA Protein Msp1 Reveals Mechanism of Mislocalized Membrane Protein Extraction. *eLife* 9, e54031. doi:10.7554/eLife.54031

Wang, L., and Walter, P. (2020). Msp1/ATAD1 in Protein Quality Control and Regulation of Synaptic Activities. *Annu. Rev. Cell Dev. Biol.* 36, 141–164. doi:10.1146/annurev-cellbio-031220-015840

Wang, W., Chen, X., Zhang, L., Yi, J., Ma, Q., Yin, J., et al. (2020). Atomic Structure of Human TOM Core Complex. *Cell Discov* 6, 67. doi:10.1038/s41421-020-00198-2

Wang, X., and Chen, X. J. (2015). A Cytosolic Network Suppressing Mitochondria-Mediated Proteostatic Stress and Cell Death. *Nature* 524, 481–484. doi:10.1038/nature14859

Wang, X., Winter, D., Ashrafi, G., Schlehe, J., Wong, Y. L., Selkoe, D., et al. (2011). PINK1 and Parkin Target Miro for Phosphorylation and Degradation to Arrest Mitochondrial Motility. *Cell* 147, 893–906. doi:10.1016/j.cell.2011.10.018

Wauer, T., Simicek, M., Schubert, A., and Komander, D. (2015). Mechanism of Phospho-Ubiquitin-Induced Parkin Activation. *Nature* 524, 370–374. doi:10.1038/nature14879

Weidberg, H., and Amon, A. (2018). MitoCPR-A Surveillance Pathway that Protects Mitochondria in Response to Protein Import Stress. *Science* 360, eaan4146. doi:10.1126/science.aan4146

Weir, N. R., Kamber, R. A., Martenson, J. S., and Denic, V. (2017). The AAA Protein Msp1 Mediates Clearance of Excess Tail-Anchored Proteins from the Peroxisomal Membrane. *eLife* 6, e28507. doi:10.7554/eLife.28507

Wiedemann, N., and Pfanner, N. (2017). Mitochondrial Machineries for Protein Import and Assembly. *Annu. Rev. Biochem.* 86, 685–714. doi:10.1146/annurev-biochem-060815-014352

Wiedemann, N., Pfanner, N., and Ryan, M. T. (2001). The Three Modules of ADP/ATP Carrier Cooperate in Receptor Recruitment and Translocation into Mitochondria. *EMBO J.* 20, 951–960. doi:10.1093/emboj/20.5.951

Wohlever, M. L., Mateja, A., McGilvray, P. T., Day, K. J., and Keenan, R. J. (2017). Msp1 is a Membrane Protein Dislocase for Tail-Anchored Proteins. *Mol. Cell* 67, 194–202. doi:10.1016/j.molcel.2017.06.019

Wrobel, L., Topf, U., Bragoszewski, P., Wiese, S., Sztolsztener, M. E., Oeljeklaus, S., et al. (2015). Mistargeted Mitochondrial Proteins Activate a Proteostatic Response in the Cytosol. *Nature* 524, 485–488. doi:10.1038/nature14951

Wu, X., Li, L., and Jiang, H. (2016). Doa1 Targets Ubiquitinated Substrates for Mitochondria-Associated Degradation. *J. Cell Biol.* 213, 49–63. doi:10.1083/jcb.201510098

Wu, X., Li, L., and Jiang, H. (2018). Mitochondrial Inner-Membrane Protease Yme1 Degrades Outer-Membrane Proteins Tom22 and Om45. *J. Cell Biol.* 217, 139–149. doi:10.1083/jcb.201702125

Wu, X., and Rapoport, T. A. (2018). Mechanistic Insights into ER-Associated Protein Degradation. *Curr. Opin. Cell Biol.* 53, 22–28. doi:10.1016/j.ceb.2018.04.004

Xiao, T., Shakya, V. P., and Hughes, A. L. (2021). ER Targeting of Non-imported Mitochondrial Carrier Proteins is Dependent on the GET Pathway. *Life Sci. Alliance* 4, e202000918. doi:10.26508/lsa.202000918

Yamamoto, H., Fukui, K., Takahashi, H., Kitamura, S., Shiota, T., Terao, K., et al. (2009). Roles of Tom70 in Import of Presequence-Containing Mitochondrial Proteins. *J. Biol. Chem.* 284, 31635–31646. doi:10.1074/jbc.m109.041756

Yamano, K., Yatsukawa, Y.-i., Esaki, M., Hobbs, A. E. A., Jensen, R. E., and Endo, T. (2008). Tom20 and Tom22 Share the Common Signal Recognition Pathway in Mitochondrial Protein Import. *J. Biol. Chem.* 283, 3799–3807. doi:10.1074/jbc.m708339200

Yamano, K., and Youle, R. J. (2013). PINK1 Is Degraded through the N-End Rule Pathway. *Autophagy* 9, 1758–1769. doi:10.4161/auto.24633

Yapa, N. M. B., Lisnyak, V., Reljic, B., and Ryan, M. T. (2021). Mitochondrial Dynamics in Health and Disease. *FEBS Lett.* 595, 1184–1204. doi:10.1002/1873-3468.14077

Youle, R. J. (2019). Mitochondria-Striking a Balance Between Host and Endosymbiont. *Science* 365, eaaw9855. doi:10.1126/science.aaw9855

Young, J. C., Hoogenraad, N. J., and Hartl, F. U. (2003). Molecular Chaperones Hsp90 and Hsp70 Deliver Preproteins to the Mitochondrial Import Receptor Tom70. *Cell* 112, 41–50. doi:10.1016/s0092-8674(02)01250-3

Yun, J., Puri, R., Yang, H., Lizzio, M. A., Wu, C., Sheng, Z. H., et al. (2014). MUL1 Acts in Parallel to the PINK1/Parkin Pathway in Regulating Mitofusin and Compensates for Loss of PINK1/Parkin. *eLife* 3, e01958. doi:10.7554/eLife.01958

Zahedi, R. P., Sickmann, A., Boehm, A. M., Winkler, C., Zufall, N., Schönfisch, B., et al. (2006). Proteomic Analysis of the Yeast Mitochondrial Outer Membrane Reveals Accumulation of a Subclass of Preproteins. *Mol. Biol. Cell* 17, 1436–1450. doi:10.1091/mbc.e05-08-0740

Zhang, T., Mishra, P., Hay, B. A., Chan, D., and Guo, M. (2017). Valosin-Containing Protein (VCP/p97) Inhibitors Relieve Mitofusin-dependent Mitochondrial Defects Due to VCP Disease Mutants. *eLife* 6, e17834. doi:10.7554/eLife.17834

Zheng, N., and Shabek, N. (2017). Ubiquitin Ligases: Structure, Function, and Regulation. *Annu. Rev. Biochem.* 86, 129–157. doi:10.1146/annurev-biochem-060815-014922

Ziviani, E., Tao, R. N., and Whitworth, A. J. (2010). Drosophila Parkin Requires PINK1 for Mitochondrial Translocation and Ubiquitinates Mitofusin. *Proc. Natl. Acad. Sci.* 107, 5018–5023. doi:10.1073/pnas.0913485107

Zurita Rendón, O., Fredrickson, E. K., Howard, C. J., Van Vranken, J., Fogarty, S., Tolley, N. D., et al. (2018). Vms1p is a Release Factor for the Ribosome-Associated Quality Control Complex. *Nat. Commun.* 9, 2197. doi:10.1038/s41467-018-04564-3

Conflict of Interest: The authors declare that the research was conducted in the absence of any commercial or financial relationships that could be construed as a potential conflict of interest.

Publisher's Note: All claims expressed in this article are solely those of the authors and do not necessarily represent those of their affiliated organizations, or those of the publisher, the editors and the reviewers. Any product that may be evaluated in this article, or claim that may be made by its manufacturer, is not guaranteed or endorsed by the publisher.

frontiers in Cell and Developmental Biology

MINI REVIEW
published: 21 December 2021
doi: 10.3389/fcell.2021.795838

Regulation of Mitochondrial Function by the Actin Cytoskeleton

María Illescas[1†], *Ana Peñas*[1†], *Joaquín Arenas*[1,2], *Miguel A. Martín*[1,2] *and Cristina Ugalde*[1,2*]

[1]*Instituto de Investigación Hospital 12 de Octubre, Madrid, Spain,* [2]*Centro de Investigación Biomédica en Red de Enfermedades Raras (CIBERER), Madrid, Spain*

The regulatory role of actin cytoskeleton on mitochondrial function is a growing research field, but the underlying molecular mechanisms remain poorly understood. Specific actin-binding proteins (ABPs), such as Gelsolin, have also been shown to participate in the pathophysiology of mitochondrial OXPHOS disorders through yet to be defined mechanisms. In this mini-review, we will summarize the experimental evidence supporting the fundamental roles of actin cytoskeleton and ABPs on mitochondrial trafficking, dynamics, biogenesis, metabolism and apoptosis, with a particular focus on Gelsolin involvement in mitochondrial disorders. The functional interplay between the actin cytoskeleton, ABPs and mitochondrial membranes for the regulation of cellular homeostasis thus emerges as a new exciting field for future research and therapeutic approaches.

Keywords: mitochondria, actin cytoskeleton, OXPHOS system, gelsolin, mitochondrial disease

OPEN ACCESS

Edited by:
David Pacheu-Grau,
University of Zaragoza, Spain

Reviewed by:
Seema Khurana,
University of Houston, United States
Ian Jame Holt,
Biodonostia Health Research Institute (IIS Biodonostia), Spain
Eva Carro,
Research Institute Hospital 12 de Octubre, Spain

***Correspondence:**
Cristina Ugalde
cugalde@h12o.es

†These authors have contributed equally to this work

Specialty section:
This article was submitted to Cellular Biochemistry, a section of the journal Frontiers in Cell and Developmental Biology

Received: *15 October 2021*
Accepted: *03 December 2021*
Published: *21 December 2021*

Citation:
Illescas M, Peñas A, Arenas J, Martín MA and Ugalde C (2021) Regulation of Mitochondrial Function by the Actin Cytoskeleton. Front. Cell Dev. Biol. 9:795838. doi: 10.3389/fcell.2021.795838

INTRODUCTION

As a major component of the cellular structural network, relevant biological processes like cell division, migration, intracellular transport and organelle organization extensively rely on the dynamics and organization of the actin cytoskeleton. Actin filaments (F-actin) are formed by the polymerization of globular actin monomers (G-actin) in a neat disposition that allows filaments to be polarized. Their remodeling is controlled by a repertoire of actin-binding proteins (ABPs), expressed in a tissue-dependent manner depending on where actin executes cell-specific functions (Lappalainen, 2016; Merino et al., 2020). These proteins regulate a wide spectrum of cellular processes, and are classified regarding their specific action mechanisms: maintenance of the G-actin monomers pool; G-actin nucleation and polymerization of actin filaments and branches; and filaments severing and depolymerization, mainly driven by cofilin and the gelsolin protein superfamily (Silacci et al., 2004).

ACTIN CYTOSKELETON INVOLVEMENT ON MITOCHONDRIAL FUNCTION

Mitochondria are present in eukaryotic cells and possess a characteristic architecture. The outer mitochondrial membrane (OMM) surrounds the inner mitochondrial membrane (IMM) creating two separate compartments: the internal matrix and intermembrane space (IMS). Mitochondria are fundamental for reactive oxygen species (ROS) production, calcium homeostasis, heat production, cell proliferation or apoptosis (Brookes et al., 2004), and are the main site to important metabolic reactions including the citric acid cycle, amino acids interconversion or β-oxidation of fatty acids (Nunnari and Suomalainen, 2012), and ATP synthesis through the oxidative phosphorylation (OXPHOS) system (Reid et al., 1966).

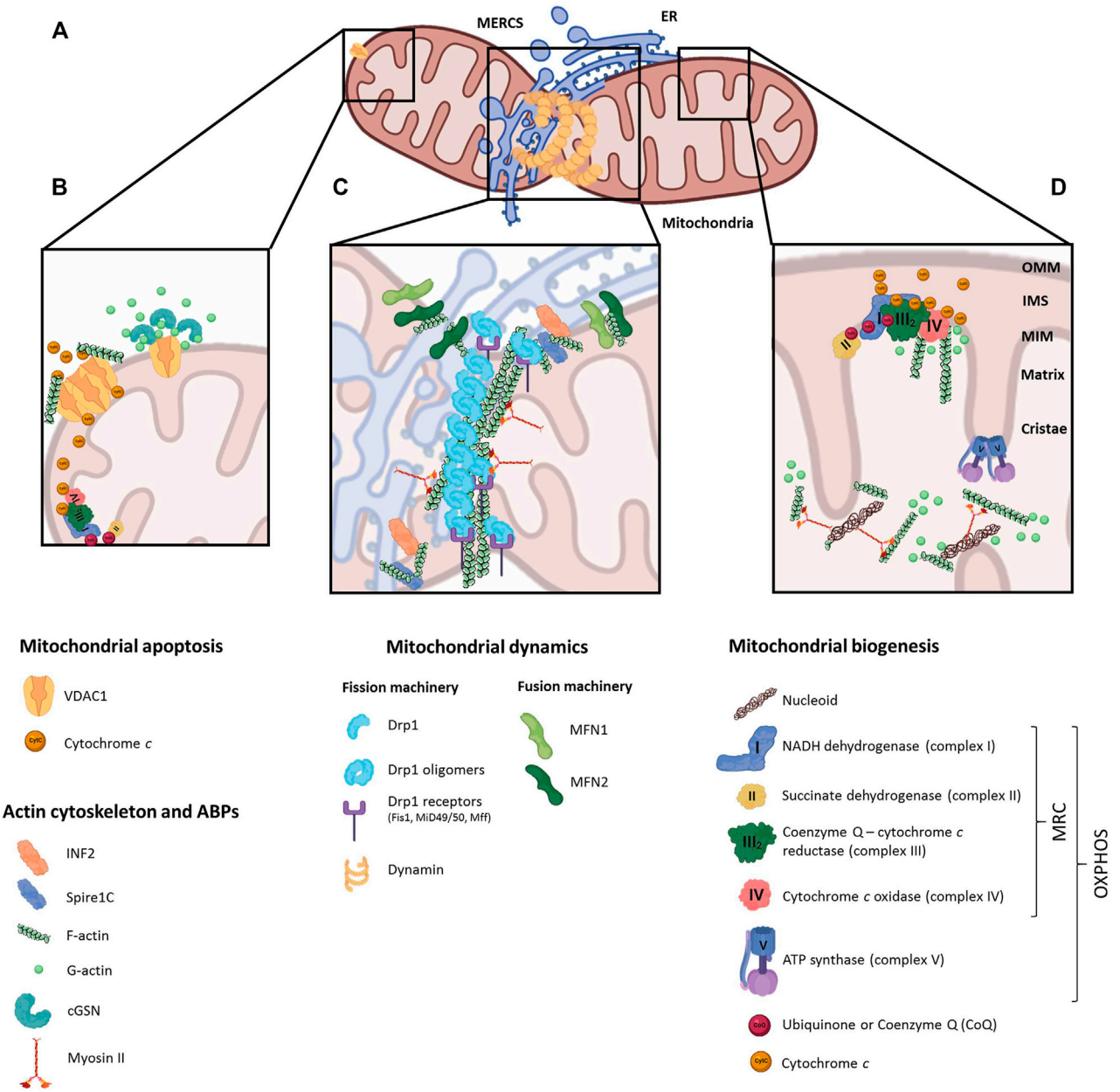

FIGURE 1 | Regulatory roles of actin cytoskeleton on mitochondrial function. **(A)** Schematic representation of a mitochondrion interacting with the endoplasmic reticulum (ER) at mitochondrial-endoplasmic reticulum contact sites (MERCS), where dynamin is recruited and fission events take place. **(B)** Under anti-apoptotic stimuli, actin-binding proteins interact with the voltage-dependent anion channel 1 (VDAC1) in the outer mitochondrial membrane (OMM), preventing actin filaments oligomerization and apoptosis; conversely, actin polymerization favors VDAC oligomerization and induces the apoptotic pathway. **(C)** Actin cytoskeleton is represented at MERCS, together with ABPs (INF2, Spire1C) and OMM proteins involved in mitochondrial dynamics (MFN1/2). Actin and myosin II localization at MERCSs initiates Drp1 recruitment, which binding to Drp1 receptors (Fis1, MUD49/50, MFF) leads to mitochondrial fission. **(D)** Actin interacts with mitochondrial respiratory chain (MRC) complexes III and IV in the matrix, controlling the association and dissociation of cytochrome *c*; and together with myosinII, actin regulates the distribution of mitochondrial nucleoids.

Actin is mainly located at the cell membrane, but also at specific mitochondrial subpopulations (Venit et al., 2021). Interactions between mitochondria and the actin cytoskeleton link the essential functions of this organelle to a plethora of cellular physiological processes. Actin filaments primarily modulate mitochondrial dynamics (Moore et al., 2016; Tilokani et al., 2018), trafficking and autophagy (Kast and Dominguez, 2017), but also mitochondrial biogenesis and metabolism (Fernie et al., 2020). The purpose of this review is to highlight the often overlooked regulatory roles of actin cytoskeleton and ABPs on mitochondrial function.

Actin Cytoskeleton on Mitochondrial Dynamics

Mitochondrial function directly depends on its correct morphology and distribution (Scott and Youle, 2010; Sheng, 2014; Chan, 2020), controlled by the balance between fission (division into two or more independent organelles), fusion (formation of a single structure) and mitophagy (clearance of damaged organelles) (Ni et al., 2015). Due to the importance of this system for the maintenance of the cellular metabolic state in mammals (Youle and Van Der Bliek, 2012), the fission and fusion forces require a high degree of regulation by specific molecules along with the actin cytoskeleton. In fact, the dynamic cycling of actin between mitochondrial subpopulations regulates mitochondrial motility and the fission–fusion balance within mitochondrial networks (Moore et al., 2016).

The main role of actin in mitochondrial dynamics is closely linked to the formation of mitochondria-endoplasmic reticulum contacts (MERCs), known as ERMES (ER-mitochondria encounter structure) in yeast (Kornmann and Walter, 2010) (**Figure 1A**). MERCs are involved in many biological processes like calcium signaling, autophagy, mtDNA replication and phospholipid trafficking (Bononi et al., 2012; Lewis et al., 2016; Xu et al., 2020), besides mitochondrial fission and fusion (Guo et al., 2018; Abrisch et al., 2020). The fusion of adjacent OMMs is orchestrated by mitofusins 1 and 2 (MFN1/2), outer mitochondrial membrane GTPases that form homo- and heterodimers (Friedman et al., 2011). MFN2 is known to tether MERCs, regulating mitochondrial calcium uptake from ER (Han et al., 2021). MERCs are formed before the recruitment of the fission machinery, defining the position of mitochondrial fission sites in a process called ERMD (ER-associated mitochondrial division) (Friedman et al., 2011). The ER-anchored formin INF2 binds to the OMM-located actin nucleator Spire1C, leading to the polymerization of F-actin at MERCs (Korobova et al., 2013; Manor et al., 2015). This leads to the pre-constriction of the OMM driven by the joint action of the ER, actin and non-muscular myosin II. Actin and myosin II ultimately recruit Drp1 (Dynamin Related Protein 1) from the cytosol to the OMM (De Vos et al., 2005), where it oligomerizes (Ji et al., 2015) and interacts with mitochondrial receptors (Mff, MiD49/51 or Fis1), shaping a ring that further constricts and splits the mitochondrion by GTP hydrolysis (Francy et al., 2015). Furthermore, INF2-mediated actin polymerization stimulates the mitochondrial calcium spike, enhancing the metabolic flux by the OXPHOS system and prompting IMM constriction at later stages (Chakrabarti et al., 2018). Interestingly, human cellular models depleted of ABPs, such as spire1C, myosin II or cofilin, showed abnormal mitochondrial motility and morphology, and altered Drp1 recruitment to the OMM (Korobova et al., 2013, 2014; Manor et al., 2015; Pagliuso et al., 2016; Rehklau et al., 2017), pointing to their dual role in OMM pre-constriction and recruitment of fission proteins to the MERCs (**Figure 1C**).

Actin Cytoskeleton on Mitochondrial Trafficking

Long-range mitochondrial transport has been primarily studied in neurons (Hirokawa and Takemura, 2005; Schwarz, 2013). This process is mediated by the coupling of mitochondria to microtubule motor proteins (kinesins and dyneins), forming a motor complex together with the OMM GTPase Miro and the adaptor protein Milton/TRAK that mediates mitochondrial transport (van Spronsen et al., 2013; Kruppa and Buss, 2021). Mitochondrial trafficking is closely regulated by intracellular calcium levels, whose increase inhibits both kinesin-dependent anterograde and dynein-dependent retrograde movements (Rintoul et al., 2003); by the PINK1/Parkin pathway, which regulates Miro turnover (Wang et al., 2011; Birsa et al., 2014); or by the nerve growth factor (NGF), responsible for mitochondrial accumulation at the axon region closest to the bead in a manner that involves PI3 kinase and actin (Verburg and Hollenbeck, 2008). The Miro proteins are also key adaptors for the recruitment and stabilization of the ABP myosin19 (Myo19) to the mitochondria (Shneyer et al., 2016; López-Doménech et al., 2018). In human cells, Myo19 has been proposed to regulate the equal segregation of mitochondria to daughter cells during mitosis (Rohn et al., 2014). In yeast, after mitochondrial fission and prior to cell division, mitochondrial populations suffer a poleward movement to both sides of the division plane, exhibiting similar patterns as chromosomes, to contribute to an equitable mitochondrial inheritance to both daughter cells under actin-dependent mechanisms (Boldogh and Pon, 2006; Scott and Youle, 2010). Based on the similarities with cytokinesis, this process was defined as "mitokinesis" (Hatch et al., 2014).

Actin Cytoskeleton on mtDNA Expression and Maintenance

The mammalian mitochondrial DNA genome (mtDNA) contains 37 genes organized in compact DNA:protein complexes called nucleoids (Clayton, 1991; Spelbrink, 2010), whose expression requires a high degree of coordination with the nuclear genome (Rampelt and Pfanner, 2016). In yeast, the ERMES complex regulates the stability and organization of mtDNA in nucleoids in an actin-dependent manner (Boldogh and Pon, 2006); in mammals, MERCs are spatially-linked to mitochondrial nucleoids, regulating their distribution, division and active transportation by the microtubules (Lewis et al., 2016). Although the presence of actin inside mitochondria and its functional connection with mtDNA was debated for decades (Venit et al., 2021), recent super-resolution microscopy-based studies probed the presence of β-actin-containing structures inside the mitochondrial matrix (Dadsena et al., 2021). Moreover, human cells lacking β-actin showed higher sensitivity to stress caused by loss of mitochondrial membrane potential ($\Delta\Psi$) plus perturbed mtDNA mass and nucleoid organization (Xie et al., 2018), suggesting a regulatory role in mtDNA transcription and quality control. Besides actin, myosin II is also associated with purified mitochondrial nucleoids, and its

silencing produces mtDNA abnormalities (Reyes et al., 2011). These evidences support the role of actin and ABPs in mitochondrial nucleoid segregation and mtDNA transcription and maintenance, likely through formation of a "mitoskeleton" network supporting mtDNA inheritance **(Figure 1D)**.

Actin Cytoskeleton on Mitochondrial Metabolism

Actin filaments are indispensable for the full activation of metabolic pathways that subsequently regulate mitochondrial function. For instance, activation of glycolytic enzymes such as aldolase or glyceraldehyde phosphate dehydrogenase, may occur through their direct binding to F-actin (Arnold and Pette, 1968). Aldolase is trapped by the actin cytoskeleton, whose release under PI3K activation increases aldolase activity, thus enhancing glycolysis (Hu et al., 2016). F-actin bundles may also sequester TRIM21 (Tripartite Motif-containing Protein 21), reducing the access of this E3 ubiquitin ligase to its substrates, such as the rate-limiting metabolic enzyme phosphofructokinase (PFK), thus maintaining high glycolytic rates (Park et al., 2020).

Interestingly, in brain mitochondria actin regulates the retention of cytochrome *c* between respiratory chain complexes III and IV by its direct association with both complexes, and inhibition of actin polymerization with cytochalasin *b* enhanced mitochondrial respiration through increased complex IV activity (Takahashi et al., 2018) **(Figure 1D)**.

Actin Cytoskeleton on Apoptosis

Mitochondria represent a major component in the cellular apoptotic machinery (Dadsena et al., 2021), influencing relevant processes like development, cell turnover or immune responses (Man, 2016). During the intrinsic pathway, increased OMM permeabilization and cristae disorganization initiate the release of pro-apoptotic factors (such as cytochrome *c* or AIF) from the IMS into the cytosol, prompting the formation of the apoptosome protein complex that activates caspases and subsequent chromatin fragmentation (Portt et al., 2011). Actin itself is a substrate of caspase-mediated cleavage (Kayalar et al., 1996), leading to a 15-kDa fragment that can be N-myristoylated and targeted to mitochondria (Utsumi et al., 2003). This interaction modulates ROS production through the regulation of OMM permeabilization by opening-closing membrane channels. In yeast, monomeric actin interacts with the voltage-dependent anion channel (VDAC), thus impacting on apoptosis modulation via interfering with the exchange of metabolites and energy between mitochondria and the cytosol (Xu et al., 2001; Roman et al., 2006). Disruption of actin dynamics causes a dramatic loss of mitochondrial $\Delta\Psi$, increased ROS and cell death (Gourlay and Ayscough, 2005). Studies in human cell lines treated with actin-disrupting drugs, affecting both actin stabilization and depolymerization, also reinforced the requirement of actin remodeling for the induction of the intrinsic apoptosis pathway (Odaka et al., 2000; Yamazaki et al., 2000) (**Figure 1B**).

Many ABPs are actively involved in apoptosis regulation in both yeast and mammals (Franklin-Tong and Gourlay, 2008). One well-studied ABP participating in this process is cofilin. During apoptosis induction in mammalian cells cofilin loses its actin-binding affinity, being translocated to the mitochondria prior to the permeability transition pore (mPTP) opening that promotes cytochrome *c* release and apoptosis progression (Chua et al., 2003; Roh et al., 2013). This process could be mediated by the interaction of cofilin with Drp1 (Hu et al., 2020), although the binding of cofilin to G-actin seems enough to induce its mitochondrial translocation (Rehklau et al., 2012). Under oxidative stress, oxidized cofilin is also translocated to the mitochondria, promoting mitochondrial fission and triggering the release of cytochrome *c* leading to apoptosis (Klamt et al., 2009; Lapeña-Luzón et al., 2021). Other relevant ABPs of the Gelsolin protein superfamily, like gelsolin itself and villin, modulate apoptosis induction in the gastrointestinal epithelium (Wang et al., 2012; Roy et al., 2018). Villin is a tissue-specific actin-modifying protein (Khurana and George, 2008), which together with gelsolin are targeted to the mitochondria on early steps of the apoptotic pathway (Roy et al., 2018). Their ability to associate with both actin and mitochondria suggest their role in cell survival through the preservation of actin cytoskeleton dynamics in mitochondrial regions controlling the trafficking of anti- and pro-apoptotic signals.

Given the relevance of gelsolin in several aspects of mitochondrial pathophysiology, we will henceforth focus the review on this particular ABP.

GELSOLIN

Gelsolin (GSN) is an abundant ABP that participates in actin-remodeling either by sequestering G-actin or by severing, capping, and nucleating F-actin (Yin and Stossel, 1979; Sun et al., 1999; Feng et al., 2001). This is mediated by calcium concentration, phosphatidylinositol-4,5-bisphosphate (PIP_2) and pH (Hu et al., 2016). In human, alternative splicing of *GSN* mRNA leads to two main isoforms with differentiated functions (Yin et al., 1984): the plasma (pGSN) and cytoplasmic (cGSN) isoforms (UniProtKB reference P06396). Structurally, both isoforms are composed by six gelsolin domains (G1-G6) (Kwiatkowski et al., 1986) divided in two homologous structures: the N-terminal fragment (G1-G3) is involved in actin severing, and the C-terminal fragment (G4-G6) coordinates calcium binding (Choe et al., 2002). Domains G3 and G4 are separated by a linker sequence of 70 amino acids that is prone to cleavage by caspase-3 (Kothakota et al., 1997; Kamada et al., 1998).

Plasma GSN

Secreted pGSN (86 kDa) differs from intracellular cGSN (81 kDa) in its N-terminal sequence, spanning a 51-amino acid secretory peptide, and in the presence of a disulphide bond between cysteine residues 188–201 that enhances its stability in the extracellular media (Kwiatkowski et al., 1988; Wen et al.,

1996). pGSN modulates bacterial immune response, acting as a buffering agent in inflammation (Bucki et al., 2008b; Cheng et al., 2017), and it is a part of the extracellular actin scavenger system (EASS) responsible for rapid severing and clearance of actin filaments released from dead cells into the bloodstream (Lind et al., 1986; Lee and Galbraith, 1992). In conditions of massive cell death, substantial actin release overwhelms the EASS, resulting in a decline of circulating pGSN levels. Consequently, pGSN has been proposed as a biomarker for multiple diseases (Li et al., 2012), ranging from cardiovascular pathologies (Khatri et al., 2014; Piktel et al., 2018; Feldt et al., 2019) to major trauma, diabetes, Alzheimer's disease, rheumatoid arthritis, sepsis, liver failure, or cancer, to the point that pGSN has been proposed as a general biomarker of health prognosis (Peddada et al., 2012).

Cytosolic GSN

Cytosolic GSN (cGSN) is ubiquitously expressed and, besides its main role in actin filament remodeling, it participates in regulatory signaling pathways that require a continuous rearrangement of the actin cytoskeleton, such as the phospholipase C (PLC) or phosphoinositide 3-kinase (PI3K) cascades (Singh et al., 1996; Sun et al., 1997); the epidermal growth factor receptor (EGFR) pathway (Chen et al., 1996; Azuma et al., 1998; De Corte et al., 2002); phagocytosis mediated by the Fc-receptor or integrins (Serrander et al., 2000; Witke et al., 2001; Arora et al., 2004); and also as a transcriptional coactivator of the thyroid (TR) and androgen (AR) receptors (Nishimura et al., 2003; Kim et al., 2007), and of the hypoxia inducible factor (HIF-1) to favor hypoxia-regulated genes expression, *GSN* itself among them (Greijer et al., 2005; Li Q. et al., 2009). Finally, cGSN also interacts with p53, inhibiting its nucleus translocation (An et al., 2011).

Besides, cGSN is associated to membrane regions of the cell rich in actin filaments such as the ER, vesicles or mitochondrial membranes (Cooper et al., 1988; Hartwig et al., 1989). cGSN co-purifies with isolated mitochondria, where it interacts with the major OMM channel protein VDAC to promote cell survival responses (**Figure 1B**) (Koya et al., 2000; Kusano et al., 2000; García-Bartolomé et al., 2017). In fact, cGSN is as a dual regulator of apoptotic cell death due to its cleavage by caspase-3 in two independent fragments (Kothakota et al., 1997). The C-terminal fragment, of 41 kDa, as well as full-length cGSN, may act as anti-apoptotic factors through VDAC blockage, thus avoiding Cyt c release into the cytosol (Koya et al., 2000; Kusano et al., 2000). Both can also bind to actin and DNaseI, forming a ternary complex that prevents the nuclear translocation of DNaseI. In contrast, the pro-apoptotic N-terminal fragment, of 39 kDa, may severe actin filaments in a calcium-independent manner (Kothakota et al., 1997; Geng et al., 1998; Kamada et al., 1998). It competes with actin for DNaseI binding, releasing it from the GSN:actin: DNaseI ternary complex and promoting its nuclear translocation, ultimately leading to nuclear DNA degradation and apoptosis (Chhabra et al., 2005; Li Q. et al., 2009). Furthermore, cGSN overexpression may inhibit the apoptotic pathway by sequestering and inactivating caspase3 in a GSN:PIP2:caspase3 complex (Ohtsu et al., 1997), and by precluding nuclear translocation of p53 (An et al., 2011). This protective role of cGSN was also demonstrated in mouse models of Alzheimer´s disease, where cGSN overexpression prevented the cytotoxic effect induced by accumulation of the amyloid beta (Aβ) peptide on mitochondrial function and cell death (Qiao et al., 2005; Antequera et al., 2009). High levels of cGSN were also reported in experimental models mainly exhibiting oxidative stress, such as upon hydrogen peroxide treatment, (Chauhan et al., 2008; Ji et al., 2010), as a consequence of intracellular calcium alterations (Bucki et al., 2008a), under HIF-1-modulated hypoxia (Nishimura et al., 2003), and in pathophysiological alterations like ageing and senescence (Ahn, 2003), Down syndrome (Ji et al., 2009), and heart failure (Li G. H. et al., 2009; Patel et al., 2018).

GSN and Mitochondrial Disease

The relative abundance of cGSN also increases in primary fibroblasts from patients and cellular models of OXPHOS system deficiency (Marín-Buera et al., 2015; García-Bartolomé et al., 2017; García-Bartolomé et al., 2020), suggesting its protective role through the regulation of cell survival responses. In these models, there was a reverse correlation between increased cGSN and decreased pGSN levels, resulting in a significantly high cGSN:pGSN protein ratio as a novel hallmark of OXPHOS dysfunction (García-Bartolomé et al., 2020). Interestingly, pGSN levels significantly decreased in OXPHOS-deficient patients, which reinforced the diagnosis accuracy for these disorders of the formerly reported biomarkers GDF-15 and FGF-21 (Peñas et al., 2021). These data suggest a tightly regulated coordination of both GSN isoforms, whose relevance in mitochondrial pathophysiology remains unknown.

CONCLUSIONS AND PERSPECTIVES

We have emphasized the importance of the actin cytoskeleton-mediated regulation on several aspects of mitochondrial (dys) function, and detailed the so-far known role of one of the most abundant ABPs, Gelsolin, in these processes. It remains unknown whether the apparently protective role of GSN, like other ABPs, directly impacts on mitochondrial function or whether it indirectly functions through regulation of actin cytoskeleton dynamics. Either way, the functional interplay between GSN isoforms in health and disease, as well as that between the actin cytoskeleton, ABPs and mitochondrial membranes for the regulation of cellular homeostasis and metabolism, open new exciting possibilities for future research.

AUTHOR CONTRIBUTIONS

Conceptualization and Investigation, MI, AP and CU; Writing – Original Draft, MI and AP; Writing – Review and Editing, CU; Visualization, MI; Supervision, JA, MAM and CU; Project

Administration, JA, MAM and CU; Funding Acquisition, MAM and CU.

FUNDING

Research was funded by Instituto de Salud Carlos III-MINECO/European FEDER Funds Grants PI17-00048 and PI20-00057 (to CU) and PI18-01374 (to MAM), and by Comunidad Autónoma de Madrid/ERDF-ESF Grant P2018/BAA-4403 (to CU).

ACKNOWLEDGMENTS

We thank all lab members for constructive discussions.

REFERENCES

Abrisch, R. G., Gumbin, S. C., Wisniewski, B. T., Lackner, L. L., and Voeltz, G. K. (2020). Fission and Fusion Machineries Converge at ER Contact Sites to Regulate Mitochondrial Morphology. *J. Cel Biol.* 219, e201911122. doi:10.1083/jcb.201911122

Ahn, J. S., Jang, I.-S., Rhim, J. H., Kim, K., Yeo, E.-J., and Park, S. C. (2003). Gelsolin for Senescence-Associated Resistance to Apoptosis. *Ann. N. Y. Acad. Sci.* 1010, 493–495. doi:10.1196/annals.1299.090

An, J.-H., Kim, J.-W., Jang, S.-M., Kim, C.-H., Kang, E.-J., and Choi, K.-H. (2011). Gelsolin Negatively Regulates the Activity of Tumor Suppressor P53 through Their Physical Interaction in Hepatocarcinoma HepG2 Cells. *Biochem. Biophysical Res. Commun.* 412, 44–49. doi:10.1016/j.bbrc.2011.07.034

Antequera, D., Vargas, T., Ugalde, C., Spuch, C., Molina, J. A., Ferrer, I., et al. (2009). Cytoplasmic Gelsolin Increases Mitochondrial Activity and Reduces Aβ burden in a Mouse Model of Alzheimer's Disease. *Neurobiol. Dis.* 36, 42–50. doi:10.1016/j.nbd.2009.06.018

Arnold, H., and Pette, D. (1968). Binding of Glycolytic Enzymes to Structure Proteins of the Muscle. *Eur. J. Biochem.* 6, 163–171. doi:10.1111/j.1432-1033.1968.tb00434.x

Arora, P. D., Glogauer, M., Kapus, A., Kwiatkowski, D. J., and McCulloch, C. A. (2004). Gelsolin Mediates Collagen Phagocytosis through a Rac-dependent Step. *MBoC* 15, 588–599. doi:10.1091/mbc.e03-07-0468

Azuma, T., Witke, W., Stossel, T. P., Hartwig, J. H., and Kwiatkowski, D. J. (1998). Gelsolin Is a Downstream Effector of Rac for Fibroblast Motility. *EMBO J.* 17, 1362–1370. doi:10.1093/emboj/17.5.1362

Birsa, N., Norkett, R., Wauer, T., Mevissen, T. E. T., Wu, H.-C., Foltynie, T., et al. (2014). Lysine 27 Ubiquitination of the Mitochondrial Transport Protein Miro Is Dependent on Serine 65 of the Parkin Ubiquitin Ligase. *J. Biol. Chem.* 289, 14569–14582. doi:10.1074/jbc.M114.563031

Boldogh, I. R., and Pon, L. A. (2006). Interactions of Mitochondria with the Actin Cytoskeleton. *Biochim. Biophys. Acta (Bba) - Mol. Cel Res.* 1763, 450–462. doi:10.1016/j.bbamcr.2006.02.014

Bononi, A., Missiroli, S., Poletti, F., Suski, J. M., Agnoletto, C., Bonora, M., et al. (2012). Mitochondria-Associated Membranes (MAMs) as Hotspot Ca2+ Signaling Units. *Adv. Exp. Med. Biol.* 740, 411–437. doi:10.1007/978-94-007-2888-2_17

Brookes, P. S., Yoon, Y., Robotham, J. L., Anders, M. W., and Sheu, S.-S. (2004). Calcium, ATP, and ROS: a Mitochondrial Love-Hate triangle. *Am. J. Physiology-Cell Physiol.* 287, C817–C833. doi:10.1152/ajpcell.00139.2004

Bucki, R., Byfield, F. J., Kulakowska, A., McCormick, M. E., Drozdowski, W., Namiot, Z., et al. (2008a). Extracellular Gelsolin Binds Lipoteichoic Acid and Modulates Cellular Response to Proinflammatory Bacterial Wall Components. *J. Immunol.* 181, 4936–4944. doi:10.4049/jimmunol.181.7.4936

Bucki, R., Levental, I., Kulakowska, A., and Janmey, P. (2008b). Plasma Gelsolin: Function, Prognostic Value, and Potential Therapeutic Use. *Cpps* 9, 541–551. doi:10.2174/138920308786733912

Chakrabarti, R., Ji, W.-K., Stan, R. V., Sanz, J., de Juan Sanz, T. A., and Higgs, H. N. (2018). INF2-mediated Actin Polymerization at the ER Stimulates Mitochondrial Calcium Uptake, Inner Membrane Constriction, and Division. *J. Cel Biol.* 217, 251–268. doi:10.1083/jcb.201709111

Chan, D. C. (2020). Mitochondrial Dynamics and its Involvement in Disease. *Annu. Rev. Pathol. Mech. Dis.* 15, 235–259. doi:10.1146/annurev-pathmechdis-012419-032711

Chauhan, V., Ji, L., and Chauhan, A. (2008). Anti-amyloidogenic, Anti-oxidant and Anti-apoptotic Role of Gelsolin in Alzheimer's Disease. *Biogerontology* 9, 381–389. doi:10.1007/s10522-008-9169-z

Chen, P., Murphy-Ullrich, J. E., and Wells, A. (1996). A Role for Gelsolin in Actuating Epidermal Growth Factor Receptor-Mediated Cell Motility. *J. Cel Biol.* 134, 689–698. doi:10.1083/jcb.134.3.689

Cheng, Y., Hu, X., Liu, C., Chen, M., Wang, J., Wang, M., et al. (2017). Gelsolin Inhibits the Inflammatory Process Induced by LPS. *Cell. Physiol. Biochem.* 41, 205–212. doi:10.1159/000456043

Chhabra, D., Nosworthy, N. J., and Dos Remedios, C. G. (2005). TheN-terminal Fragment of Gelsolin Inhibits the Interaction of DNase I with Isolated Actin, but Not with the Cofilin-Actin Complex. *Proteomics* 5, 3131–3136. doi:10.1002/pmic.200401127

Choe, H., Burtnick, L. D., Mejillano, M., Yin, H. L., Robinson, R. C., and Choe, S. (2002). The Calcium Activation of Gelsolin: Insights from the 3Å Structure of the G4-G6/Actin Complex. *J. Mol. Biol.* 324, 691–702. doi:10.1016/S0022-2836(02)01131-2

Chua, B. T., Volbracht, C., Tan, K. O., Li, R., Yu, V. C., and Li, P. (2003). Mitochondrial Translocation of Cofilin Is an Early Step in Apoptosis Induction. *Nat. Cel Biol.* 5, 1083–1089. doi:10.1038/ncb1070

Clayton, D. A. (1991). Replication and Transcription of Vertebrate Mitochondrial DNA. *Annu. Rev. Cel. Biol.* 7, 453–478. doi:10.1146/annurev.cb.07.110191.002321

Cooper, J. A., Loftus, D. J., Frieden, C., Bryan, J., and Elson, E. L. (1988). Localization and Mobility of Gelsolin in Cells. *J. Cel Biol.* 106, 1229–1240. doi:10.1083/jcb.106.4.1229

Dadsena, S., King, L. E., and García-Sáez, A. J. (2021). Apoptosis Regulation at the Mitochondria Membrane Level. *Biochim. Biophys. Acta (Bba) - Biomembranes* 1863, 183716–10. doi:10.1016/j.bbamem.2021.183716

De Corte, V., Bruyneel, E., Boucherie, C., Mareel, M., Vandekerckhove, J., and Gettemans, J. (2002). Gelsolin-induced Epithelial Cell Invasion Is Dependent on Ras-Rac Signaling. *EMBO J.* 21, 6781–6790. doi:10.1093/emboj/cdf680

De Vos, K. J., Allan, V. J., Grierson, A. J., and Sheetz, M. P. (2005). Mitochondrial Function and Actin Regulate Dynamin-Related Protein 1-dependent Mitochondrial Fission. *Curr. Biol.* 15, 678–683. doi:10.1016/j.cub.2005.02.064

Feldt, J., Schicht, M., Garreis, F., Welss, J., Schneider, U. W., and Paulsen, F. (2019). Structure, Regulation and Related Diseases of the Actin-Binding Protein Gelsolin. *Expert Rev. Mol. Med.* 20, e7. doi:10.1017/erm.2018.7

Feng, L., Mejillano, M., Yin, H. L., Chen, J., and Prestwich, G. D. (2001). Full-contact Domain Labeling: Identification of a Novel Phosphoinositide Binding Site on Gelsolin that Requires the Complete Protein. *Biochemistry* 40, 904–913. doi:10.1021/bi000996q

Fernie, A. R., Zhang, Y., and Sampathkumar, A. (2020). Cytoskeleton Architecture Regulates Glycolysis Coupling Cellular Metabolism to Mechanical Cues. *Trends Biochem. Sci.* 45, 637–638. doi:10.1016/j.tibs.2020.04.003

Francy, C. A., Alvarez, F. J. D., Zhou, L., Ramachandran, R., and Mears, J. A. (2015). The Mechanoenzymatic Core of Dynamin-Related Protein 1 Comprises the Minimal Machinery Required for Membrane Constriction. *J. Biol. Chem.* 290, 11692–11703. doi:10.1074/jbc.M114.610881

Franklin-Tong, V. E., and Gourlay, C. W. (2008). A Role for Actin in Regulating Apoptosis/programmed Cell Death: Evidence Spanning Yeast, Plants and Animals. *Biochem. J.* 413, 389–404. doi:10.1042/BJ20080320

Friedman, J. R., Lackner, L. L., West, M., DiBenedetto, J. R., Nunnari, J., and Voeltz, G. K. (2011). ER Tubules Mark Sites of Mitochondrial Division. *Science* 334, 358–362. doi:10.1126/science.1207385

García-Bartolomé, A., Peñas, A., Illescas, M., Bermejo, V., López-Calcerrada, S., Pérez-Pérez, R., et al. (2020). Altered Expression Ratio of Actin-Binding

Gelsolin Isoforms Is a Novel Hallmark of Mitochondrial OXPHOS Dysfunction. *Cells* 9, 1922–21. doi:10.3390/cells9091922

García-Bartolomé, A., Peñas, A., Marín-Buera, L., Lobo-Jarne, T., Pérez-Pérez, R., Morán, M., et al. (2017). Respiratory Chain Enzyme Deficiency Induces Mitochondrial Location of Actin-Binding Gelsolin to Modulate the Oligomerization of VDAC Complexes and Cell Survival. *Hum. Mol. Genet.* 26, 2493–2506. doi:10.1093/hmg/ddx144

Geng, Y.-J., Azuma, T., Tang, J. X., Hartwig, J. H., Muszynski, M., Wu, Q., et al. (1998). Caspase-3-induced Gelsolin Fragmentation Contributes to Actin Cytoskeletal Collapse, Nucleolysis, and Apoptosis of Vascular Smooth Muscle Cells Exposed to Proinflammatory Cytokines. *Eur. J. Cel Biol.* 77, 294–302. doi:10.1016/S0171-9335(98)80088-5

Gourlay, C. W., and Ayscough, K. R. (2005). The Actin Cytoskeleton: A Key Regulator of Apoptosis and Ageing? *Nat. Rev. Mol. Cel Biol.* 6, 583–589. doi:10.1038/nrm1682

Greijer, A., van der Groep, P., Kemming, D., Shvarts, A., Semenza, G., Meijer, G., et al. (2005). Up-regulation of Gene Expression by Hypoxia Is Mediated Predominantly by Hypoxia-Inducible Factor 1 (HIF-1). *J. Pathol.* 206, 291–304. doi:10.1002/path.1778

Guo, Y., Li, D., Zhang, S., Yang, Y., Liu, J.-J., Wang, X., et al. (2018). Visualizing Intracellular Organelle and Cytoskeletal Interactions at Nanoscale Resolution on Millisecond Timescales. *Cell* 175, 1430–1442. doi:10.1016/j.cell.2018.09.057

Han, S., Zhao, F., Hsia, J., Ma, X., Liu, Y., Torres, S., et al. (2021). The Role of Mfn2 in the Structure and Function of Endoplasmic Reticulum-Mitochondrial Tethering *In Vivo*. *J. Cel Sci.* 134, jcs253443. doi:10.1242/jcs.253443

Hartwig, J. H., Chambers, K. A., and Stossel, T. P. (1989). Association of Gelsolin with Actin Filaments and Cell Membranes of Macrophages and Platelets. *J. Cel Biol.* 108, 467–479. doi:10.1083/jcb.108.2.467

Hatch, A. L., Gurel, P. S., and Higgs, H. N. (2014). Novel Roles for Actin in Mitochondrial Fission. *J. Cel Sci.* 127, 4549–4560. doi:10.1242/jcs.153791

Hirokawa, N., and Takemura, R. (2005). Molecular Motors and Mechanisms of Directional Transport in Neurons. *Nat. Rev. Neurosci.* 6, 201–214. doi:10.1038/nrn1624

Hu, H., Juvekar, A., Lyssiotis, C. A., Lien, E. C., Albeck, J. G., Oh, D., et al. (2016). Phosphoinositide 3-Kinase Regulates Glycolysis through Mobilization of Aldolase from the Actin Cytoskeleton. *Cell* 164, 433–446. doi:10.1016/j.cell.2015.12.042

Hu, J., Zhang, H., Li, J., Jiang, X., Zhang, Y., Wu, Q., et al. (2020). ROCK1 Activation-Mediated Mitochondrial Translocation of Drp1 and Cofilin Are Required for Arnidiol-Induced Mitochondrial Fission and Apoptosis. *J. Exp. Clin. Cancer Res.* 39, 1–16. doi:10.1186/s13046-020-01545-7

Ji, L., Chauhan, A., and Chauhan, V. (2010). Upregulation of Cytoplasmic Gelsolin, an Amyloid-β-Binding Protein, under Oxidative Stress Conditions: Involvement of Protein Kinase C. *Jad* 19, 829–838. doi:10.3233/JAD-2010-1281

Ji, L., Chauhan, A., Muthaiyah, B., Wegiel, J., and Chauhan, V. (2009). Gelsolin Levels Are Increased in the Brain as a Function of Age During Normal Development in Children that Are Further Increased in Down Syndrome. *Alzheimer Dis. Assoc. Disord.* 23, 319–322. doi:10.1097/WAD.0b013e31819d494e

Ji, W.-k., Hatch, A. L., Merrill, R. A., Strack, S., and Higgs, H. N. (2015). Actin Filaments Target the Oligomeric Maturation of the Dynamin GTPase Drp1 to Mitochondrial Fission Sites. *Elife* 4, 1–25. doi:10.7554/eLife.11553

Kamada, S., Kusano, H., Fujita, H., Ohtsu, M., Koya, R. C., Kuzumaki, N., et al. (1998). A Cloning Method for Caspase Substrates that Uses the Yeast Two-Hybrid System: Cloning of the Antiapoptotic Gene Gelsolin. *Proc. Natl. Acad. Sci.* 95, 8532–8537. doi:10.1073/pnas.95.15.8532

Kast, D. J., and Dominguez, R. (2017). The Cytoskeleton-Autophagy Connection. *Curr. Biol.* 27, R318–R326. doi:10.1016/j.cub.2017.02.061

Kayalar, C., Örd, T., Testa, M. P., Zhong, L. T., and Bredesen, D. E. (1996). Cleavage of Actin by Interleukin 1 Beta-Converting Enzyme to Reverse DNase I Inhibition. *Proc. Natl. Acad. Sci.* 93, 2234–2238. doi:10.1073/pnas.93.5.2234

Khatri, N., Sagar, A., Peddada, N., Choudhary, V., Chopra, B. S., Garg, V., et al. (2014). Plasma Gelsolin Levels Decrease in Diabetic State and Increase upon Treatment with F-Actin Depolymerizing Versions of Gelsolin. *J. Diabetes Res.* 2014, 1–8. doi:10.1155/2014/152075

Khurana, S., and George, S. P. (2008). Regulation of Cell Structure and Function by Actin-Binding Proteins: Villin's Perspective. *FEBS Lett.* 582, 2128–2139. doi:10.1016/j.febslet.2008.02.040

Kim, C. S., Furuya, F., Ying, H., Kato, Y., Hanover, J. A., and Cheng, S.-y. (2007). Gelsolin: A Novel Thyroid Hormone Receptor-β Interacting Protein that Modulates Tumor Progression in a Mouse Model of Follicular Thyroid Cancer. *Endocrinology* 148, 1306–1312. doi:10.1210/en.2006-0923

Klamt, F., Zdanov, S., Levine, R. L., Pariser, A., Zhang, Y., Zhang, B., et al. (2009). Oxidant-induced Apoptosis Is Mediated by Oxidation of the Actin-Regulatory Protein Cofilin. *Nat. Cel Biol* 11, 1241–1246. doi:10.1038/ncb1968

Kornmann, B., and Walter, P. (2010). ERMES-mediated ER-Mitochondria Contacts: Molecular Hubs for the Regulation of Mitochondrial Biology. *J. Cel Sci.* 123, 1389–1393. doi:10.1242/jcs.058636

Korobova, F., Gauvin, T. J., and Higgs, H. N. (2014). A Role for Myosin II in Mammalian Mitochondrial Fission. *Curr. Biol.* 24, 409–414. doi:10.1016/j.cub.2013.12.032

Korobova, F., Ramabhadran, V., and Higgs, H. N. (2013). An Actin-Dependent Step in Mitochondrial Fission Mediated by the ER-Associated Formin INF2. *Science* 339, 464–467. doi:10.1126/science.1228360

Kothakota, S., Azuma, T., Reinhard, C., Klippel, A., Tang, J., Chu, K., et al. (1997). Caspase-3-generated Fragment of Gelsolin: Effector of Morphological Change in Apoptosis. *Science* 278, 294–298. doi:10.1126/science.278.5336.294

Koya, R. C., Fujita, H., Shimizu, S., Ohtsu, M., Takimoto, M., Tsujimoto, Y., et al. (2000). Gelsolin Inhibits Apoptosis by Blocking Mitochondrial Membrane Potential Loss and Cytochrome C Release. *J. Biol. Chem.* 275, 15343–15349. doi:10.1074/jbc.275.20.15343

Kruppa, A. J., and Buss, F. (2021). Motor Proteins at the Mitochondria-Cytoskeleton Interface. *J. Cel Sci.* 134, jcs226084. doi:10.1242/jcs.226084

Kusano, H., Shimizu, S., Koya, R. C., Fujita, H., Kamada, S., Kuzumaki, N., et al. (2000). Human Gelsolin Prevents Apoptosis by Inhibiting Apoptotic Mitochondrial Changes via Closing VDAC. *Oncogene* 19, 4807–4814. doi:10.1038/sj.onc.1203868

Kwiatkowski, D. J., Stossel, T. P., Orkin, S. H., Mole, J. E., Coltens, H. R., and Yin, H. L. (1986). Plasma and Cytoplasmic Gelsolins Are Encoded by a Single Gene and Contain a Duplicated Actin-Binding Domain. *Nature* 323, 455–458. doi:10.1038/323455a0

Kwiatkowski, D., Mehl, R., and Yin, H. (1988). Genomic Organization and Biosynthesis of Secreted and Cytoplasmic Forms of Gelsolin. *J. Cel Biol.* 106, 375–384. doi:10.1083/jcb.106.2.375

Lapeña-Luzón, T., Rodríguez, L. R., Beltran-Beltran, V., Benetó, N., Pallardó, F. V., and Gonzalez-Cabo, P. (2021). Cofilin and Neurodegeneration: New Functions for an Old but Gold Protein. *Brain Sci.* 11, 954. doi:10.3390/brainsci11070954

Lappalainen, P. (2016). Actin-binding Proteins: the Long Road to Understanding the Dynamic Landscape of Cellular Actin Networks. *MBoC* 27, 2519–2522. doi:10.1091/mbc.e15-10-0728

Lee, W. M., and Galbraith, R. M. (1992). The Extracellular Actin-Scavenger System and Actin Toxicity. *N. Engl. J. Med.* 326, 1335–1341. doi:10.1056/NEJM199205143262006

Lewis, S. C., Uchiyama, L. F., and Nunnari, J. (2016). ER-mitochondria Contacts Couple mtDNA Synthesis with Mitochondrial Division in Human Cells. *Science* 353, aaf5549. doi:10.1126/science.aaf5549

Li, G. H., Arora, P. D., Chen, Y., McCulloch, C. A., and Liu, P. (2012). Multifunctional Roles of Gelsolin in Health and Diseases. *Med. Res. Rev.* 32, 999–1025. doi:10.1002/med.20231

Li, G. H., Shi, Y., Chen, Y., Sun, M., Sader, S., Maekawa, Y., et al. (2009a). Gelsolin Regulates Cardiac Remodeling after Myocardial Infarction through DNase I-Mediated Apoptosis. *Circ. Res.* 104, 896–904. doi:10.1161/CIRCRESAHA.108.172882

Li, Q., Ye, Z., Wen, J., Ma, L., He, Y., Lian, G., et al. (2009b). Gelsolin, but Not its Cleavage, Is Required for TNF-Induced ROS Generation and Apoptosis in MCF-7 Cells. *Biochem. Biophysical Res. Commun.* 385, 284–289. doi:10.1016/j.bbrc.2009.05.078

Lind, S. E., Smith, D. B., Janmey, P. A., and Stossel, T. P. (1986). Role of Plasma Gelsolin and the Vitamin D-Binding Protein in Clearing Actin from the Circulation. *J. Clin. Invest.* 78, 736–742. doi:10.1172/JCI112634

López-Doménech, G., Covill-Cooke, C., Ivankovic, D., Halff, E. F., Sheehan, D. F., Norkett, R., et al. (2018). Miro Proteins Coordinate Microtubule- and Actin-

dependent Mitochondrial Transport and Distribution. *EMBO J.* 37, 321–336. doi:10.15252/embj.201696380

Man, S. M., and Kanneganti, T.-D. (2016). Converging Roles of Caspases in Inflammasome Activation, Cell Death and Innate Immunity. *Nat. Rev. Immunol.* 16, 7–21. doi:10.1038/nri.2015.7

Manor, U., Bartholomew, S., Golani, G., Christenson, E., Kozlov, M., Higgs, H., et al. (2015). A Mitochondria-Anchored Isoform of the Actin-Nucleating Spire Protein Regulates Mitochondrial Division. *Elife* 4, 1–27. doi:10.7554/eLife.08828

Marín-Buera, L., García-Bartolomé, A., Morán, M., López-Bernardo, E., Cadenas, S., Hidalgo, B., et al. (2015). Differential Proteomic Profiling Unveils New Molecular Mechanisms Associated with Mitochondrial Complex III Deficiency. *J. Proteomics* 113, 38–56. doi:10.1016/j.jprot.2014.09.007

Merino, F., Pospich, S., and Raunser, S. (2020). Towards a Structural Understanding of the Remodeling of the Actin Cytoskeleton. *Semin. Cel Dev. Biol.* 102, 51–64. doi:10.1016/j.semcdb.2019.11.018

Moore, A. S., Wong, Y. C., Simpson, C. L., and Holzbaur, E. L. F. (2016). Dynamic Actin Cycling through Mitochondrial Subpopulations Locally Regulates the Fission-Fusion Balance within Mitochondrial Networks. *Nat. Commun.* 7, 12886. doi:10.1038/ncomms12886

Ni, H.-M., Williams, J. A., and Ding, W.-X. (2015). Mitochondrial Dynamics and Mitochondrial Quality Control. *Redox Biol.* 4, 6–13. doi:10.1016/j.redox.2014.11.006

Nishimura, K., Ting, H. J., Harada, Y., Tokizane, T., Nonomura, N., Kang, H. Y., et al. (2003). Modulation of Androgen Receptor Transactivation by Gelsolin: a Newly Identified Androgen Receptor Coregulator. *Cancer Res.* 63, 4888–4894. PMID: 12941811.

Nunnari, J., and Suomalainen, A. (2012). Mitochondria: In Sickness and in Health. *Cell* 148, 1145–1159. doi:10.1016/j.cell.2012.02.035

Odaka, C., Sanders, M. L., and Crews, P. (2000). Jasplakinolide Induces Apoptosis in Various Transformed Cell Lines by a Caspase-3-like Protease-dependent Pathway. *Clin. Diagn. Lab. Immunol.* 7, 947–952. doi:10.1128/CDLI.7.6.947-952.2000

Ohtsu, M., Sakai, N., Fujita, H., Kashiwagi, M., Gasa, S., Shimizu, S., et al. (1997). Inhibition of Apoptosis by the Actin-Regulatory Protein Gelsolin. *EMBO J.* 16, 4650–4656. doi:10.1093/emboj/16.15.4650

Pagliuso, A., Tham, T. N., Stevens, J. K., Lagache, T., Persson, R., Salles, A., et al. (2016). A Role for Septin 2 in Drp1-mediated Mitochondrial Fission. *EMBO Rep.* 17, 858–873. doi:10.15252/embr.201541612

Park, J. S., Burckhardt, C. J., Lazcano, R., Solis, L. M., Isogai, T., Li, L., et al. (2020). Mechanical Regulation of Glycolysis via Cytoskeleton Architecture. *Nature* 578, 621–626. doi:10.1038/s41586-020-1998-1

Patel, V. B., Zhabyeyev, P., Chen, X., Wang, F., Paul, M., Fan, D., et al. (2018). PI3Kα-regulated Gelsolin Activity Is a Critical Determinant of Cardiac Cytoskeletal Remodeling and Heart Disease. *Nat. Commun.* 9, 5390. doi:10.1038/s41467-018-07812-8

Peddada, N., Sagar, A., Ashishand Garg, R. (2012). Plasma Gelsolin: A General Prognostic Marker of Health. *Med. Hypotheses* 78, 203–210. doi:10.1016/j.mehy.2011.10.024

Peñas, A., Fernández-De la Torre, M., Laine-Menéndez, S., Lora, D., Illescas, M., García-Bartolomé, A., et al. (2021). Plasma Gelsolin Reinforces the Diagnostic Value of FGF-21 and GDF-15 for Mitochondrial Disorders. *Ijms* 22, 6396. doi:10.3390/ijms22126396

Piktel, E., Levental, I., Durnaś, B., Janmey, P., and Bucki, R. (2018). Plasma Gelsolin: Indicator of Inflammation and its Potential as a Diagnostic Tool and Therapeutic Target. *Ijms* 19, 2516. doi:10.3390/ijms19092516

Portt, L., Norman, G., Clapp, C., Greenwood, M., and Greenwood, M. T. (2011). Anti-apoptosis and Cell Survival: A Review. *Biochim. Biophys. Acta (Bba) - Mol. Cel Res.* 1813, 238–259. doi:10.1016/j.bbamcr.2010.10.010

Qiao, H., Koya, R. C., Nakagawa, K., Tanaka, H., Fujita, H., Takimoto, M., et al. (2005). Inhibition of Alzheimer's Amyloid-β Peptide-Induced Reduction of Mitochondrial Membrane Potential and Neurotoxicity by Gelsolin. *Neurobiol. Aging* 26, 849–855. doi:10.1016/j.neurobiolaging.2004.08.003

Rampelt, H., and Pfanner, N. (2016). Coordination of Two Genomes by Mitochondrial Translational Plasticity. *Cell* 167, 308–310. doi:10.1016/j.cell.2016.09.042

Rehklau, K., Gurniak, C. B., Conrad, M., Friauf, E., Ott, M., and Rust, M. B. (2012). ADF/cofilin Proteins Translocate to Mitochondria during Apoptosis but Are Not Generally Required for Cell Death Signaling. *Cell Death Differ* 19, 958–967. doi:10.1038/cdd.2011.180

Rehklau, K., Hoffmann, L., Gurniak, C. B., Ott, M., Witke, W., Scorrano, L., et al. (2017). Cofilin1-dependent Actin Dynamics Control DRP1-Mediated Mitochondrial Fission. *Cell Death Dis* 8, e3063. doi:10.1038/cddis.2017.448

Reid, R. A., Moyle, J., and Mitchell, P. (1966). Synthesis of Adenosine Triphosphate by a Protonmotive Force in Rat Liver Mitochondria. *Nature* 212, 257–258. doi:10.1038/212257a0

Reyes, A., He, J., Mao, C. C., Bailey, L. J., Di Re, M., Sembongi, H., et al. (2011). Actin and Myosin Contribute to Mammalian Mitochondrial DNA Maintenance. *Nucleic Acids Res.* 39, 5098–5108. doi:10.1093/nar/gkr052

Rintoul, G. L., Filiano, A. J., Brocard, J. B., Kress, G. J., and Reynolds, I. J. (2003). Glutamate Decreases Mitochondrial Size and Movement in Primary Forebrain Neurons. *J. Neurosci.* 23, 7881–7888. doi:10.1523/jneurosci.23-21-07881.2003

Roh, S. E., Woo, J. A., Lakshmana, M. K., Uhlar, C., Ankala, V., Boggess, T., et al. (2013). Mitochondrial Dysfunction and Calcium Deregulation by the RanBP9-cofilin Pathway. *FASEB j.* 27, 4776–4789. doi:10.1096/fj.13-234765

Rohn, J. L., Patel, J. V., Neumann, B., Bulkescher, J., McHedlishvili, N., McMullan, R. C., et al. (2014). Myo19 Ensures Symmetric Partitioning of Mitochondria and Coupling of Mitochondrial Segregation to Cell Division. *Curr. Biol.* 24, 2598–2605. doi:10.1016/j.cub.2014.09.045

Roman, I., Figys, J., Steurs, G., and Zizi, M. (2006). Direct Measurement of VDAC-Actin Interaction by Surface Plasmon Resonance. *Biochim. Biophys. Acta (Bba) - Biomembranes* 1758, 479–486. doi:10.1016/j.bbamem.2006.03.019

Roy, S., Esmaeilniakooshkghazi, A., Patnaik, S., Wang, Y., George, S. P., Ahrorov, A., et al. (2018). Villin-1 and Gelsolin Regulate Changes in Actin Dynamics that Affect Cell Survival Signaling Pathways and Intestinal Inflammation. *Gastroenterology* 154, 1405–1420. doi:10.1053/j.gastro.2017.12.016

Schwarz, T. L. (2013). Mitochondrial Trafficking in Neurons. *Cold Spring Harbor Perspect. Biol.* 5, a011304. doi:10.1101/cshperspect.a011304

Scott, I., and Youle, R. J. (2010). Mitochondrial Fission and Fusion. *Essays Biochem.* 47, 85–98. doi:10.1042/bse0470085

Serrander, L., Skarman, P., Rasmussen, B., Witke, W., Lew, D. P., Krause, K.-H., et al. (2000). Selective Inhibition of IgG-Mediated Phagocytosis in Gelsolin-Deficient Murine Neutrophils. *J. Immunol.* 165, 2451–2457. doi:10.4049/jimmunol.165.5.2451

Sheng, Z.-H. (2014). Mitochondrial Trafficking and Anchoring in Neurons: New Insight and Implications. *J. Cel Biol.* 204, 1087–1098. doi:10.1083/jcb.201312123

Shneyer, B. I., Usaj, M., and Henn, A. (2016). Myo19 Is an Outer Mitochondrial Membrane Motor and Effector of Starvation Induced Filopodia, *J. Cell Sci.* , 543–556. doi:10.1242/jcs.175349

Silacci, P., Mazzolai, L., Gauci, C., Stergiopulos, N., Yin, H. L., and Hayoz, D. (2004). Gelsolin Superfamily Proteins: Key Regulators of Cellular Functions. *CMLS, Cell. Mol. Life Sci.* 61, 2614–2623. doi:10.1007/s00018-004-4225-6

Singh, S. S., Chauhan, A., Murakami, N., and Chauhan, V. P. S. (1996). Profilin and Gelsolin Stimulate Phosphatidylinositol 3-kinase Activity. *Biochemistry* 35, 16544–16549. doi:10.1021/bi9609634

Spelbrink, J. N. (2009). Functional Organization of Mammalian Mitochondrial DNA in Nucleoids: History, Recent Developments, and Future Challenges. *IUBMB Life* 62, a–n. doi:10.1002/iub.282

Sun, H.-q., Lin, K.-m., and Yin, H. L. (1997). Gelsolin Modulates Phospholipase C Activity *In Vivo* through Phospholipid Binding. *J. Cel Biol.* 138, 811–820. doi:10.1083/jcb.138.4.811

Sun, H. Q., Yamamoto, M., Mejillano, M., Yin, H. L., Yamamoto, M., Mejillano, M., et al. (1999). Gelsolin, a Multifunctional Actin Regulatory Protein. *J. Biol. Chem.* 274, 33179–33182. doi:10.1074/jbc.274.47.33179

Takahashi, K., Miura, Y., Ohsawa, I., Shirasawa, T., and Takahashi, M. (2018). *In Vitro* rejuvenation of Brain Mitochondria by the Inhibition of Actin Polymerization. *Sci. Rep.* 8, 2–11. doi:10.1038/s41598-018-34006-5

Tilokani, L., Nagashima, S., Paupe, V., and Prudent, J. (2018). Mitochondrial Dynamics: Overview of Molecular Mechanisms. *Essays Biochem.* 62, 341–360. doi:10.1042/EBC20170104

Utsumi, T., Sakurai, N., Nakano, K., and Ishisaka, R. (2003). C-terminal 15 kDa Fragment of Cytoskeletal Actin Is posttranslationallyN-Myristoylated upon Caspase-Mediated Cleavage and Targeted to Mitochondria. *FEBS Lett.* 539, 37–44. doi:10.1016/S0014-5793(03)00180-7

van Spronsen, M., Mikhaylova, M., Lipka, J., Schlager, M. A., van den Heuvel, D. J., Kuijpers, M., et al. (2013). TRAK/Milton Motor-Adaptor Proteins Steer Mitochondrial Trafficking to Axons and Dendrites. *Neuron* 77, 485–502. doi:10.1016/j.neuron.2012.11.027

Venit, T., El Said, N. H., Mahmood, S. R., and Percipalle, P. (2021). A Dynamic Actin-dependent Nucleoskeleton and Cell Identity. *J. Biochem.* 169, 243–257. doi:10.1093/jb/mvaa133

Verburg, J., and Hollenbeck, P. J. (2008). Mitochondrial Membrane Potential in Axons Increases with Local Nerve Growth Factor or Semaphorin Signaling. *J. Neurosci.* 28, 8306–8315. doi:10.1523/JNEUROSCI.2614-08.2008

Wang, X., Winter, D., Ashrafi, G., Schlehe, J., Wong, Y. L., Selkoe, D., et al. (2011). PINK1 and Parkin Target Miro for Phosphorylation and Degradation to Arrest Mitochondrial Motility. *Cell* 147, 893–906. doi:10.1016/j.cell.2011.10.018

Wang, Y., George, S. P., Srinivasan, K., Patnaik, S., and Khurana, S. (2012). Actin Reorganization as the Molecular Basis for the Regulation of Apoptosis in Gastrointestinal Epithelial Cells. *Cel Death Differ* 19, 1514–1524. doi:10.1038/cdd.2012.28

Wen, D., Corina, K., Chow, E. P., Miller, S., Janmey, P. A., and Pepinsky, R. B. (1996). The Plasma and Cytoplasmic Forms of Human Gelsolin Differ in Disulfide Structure. *Biochemistry* 35, 9700–9709. doi:10.1021/bi960920n

Witke, W., Li, W., Kwiatkowski, D. J., and Southwick, F. S. (2001). Comparisons of CapG and Gelsolin-Null Macrophages. *J. Cel Biol.* 154, 775–784. doi:10.1083/jcb.200101113

Xie, X., Venit, T., Drou, N., and Percipalle, P. (2018). In Mitochondria β-Actin Regulates mtDNA Transcription and Is Required for Mitochondrial Quality Control. *iScience*, 3, 226–237. doi:10.1016/j.isci.2018.04.021

Xu, L., Wang, X., and Tong, C. (2020). Endoplasmic Reticulum-Mitochondria Contact Sites and Neurodegeneration. *Front. Cel Dev. Biol.* 8, 428. doi:10.3389/fcell.2020.00428

Xu, X., Forbes, J. G., and Colombini, M. (2001). Actin Modulates the Gating of Neurospora Crassa VDAC. *J. Membr. Biol.* 180, 73–81. doi:10.1007/s002320010060

Yamazaki, Y., Tsuruga, M., Zhou, D., Fujita, Y., Shang, X., Dang, Y., et al. (2000). Cytoskeletal Disruption Accelerates Caspase-3 Activation and Alters the Intracellular Membrane Reorganization in DNA Damage-Induced Apoptosis. *Exp. Cel Res.* 259, 64–78. doi:10.1006/excr.2000.4970

Yin, H. L., Kwiatkowski, D. J., Mole, J. E., and Cole, F. S. (1984). Structure and Biosynthesis of Cytoplasmic and Secreted Variants of Gelsolin. *J. Biol. Chem.* 259, 5271–5276. doi:10.1016/s0021-9258(17)42985-1

Yin, H. L., and Stossel, T. P. (1979). Control of Cytoplasmic Actin Gel-Sol Transformation by Gelsolin, a Calcium-dependent Regulatory Protein. *Nature* 281, 583–586. doi:10.1038/281583a0

Youle, R. J., and Van Der Bliek, A. M. (2012). Mitochondrial Fission, Fusion, and Stress. *Science* 337, 1062–1065. doi:10.1126/science.1219855

Conflict of Interest: The authors declare that the research was conducted in the absence of any commercial or financial relationships that could be construed as a potential conflict of interest.

The reviewer EC declared a shared affiliation with the authors to the handling Editor.

Publisher's Note: All claims expressed in this article are solely those of the authors and do not necessarily represent those of their affiliated organizations, or those of the publisher, the editors and the reviewers. Any product that may be evaluated in this article, or claim that may be made by its manufacturer, is not guaranteed or endorsed by the publisher.

frontiers in Cell and Developmental Biology

REVIEW
published: 24 December 2021
doi: 10.3389/fcell.2021.803205

Targeting and Insertion of Membrane Proteins in Mitochondria

Ross Eaglesfield and Kostas Tokatlidis*

Institute of Molecular Cell and Systems Biology, College of Medical, Veterinary and Life Sciences, University of Glasgow, University Avenue, Scotland, United Kingdom

Mitochondrial membrane proteins play an essential role in all major mitochondrial functions. The respiratory complexes of the inner membrane are key for the generation of energy. The carrier proteins for the influx/efflux of essential metabolites to/from the matrix. Many other inner membrane proteins play critical roles in the import and processing of nuclear encoded proteins (~99% of all mitochondrial proteins). The outer membrane provides another lipidic barrier to nuclear-encoded protein translocation and is home to many proteins involved in the import process, maintenance of ionic balance, as well as the assembly of outer membrane components. While many aspects of the import and assembly pathways of mitochondrial membrane proteins have been elucidated, many open questions remain, especially surrounding the assembly of the respiratory complexes where certain highly hydrophobic subunits are encoded by the mitochondrial DNA and synthesised and inserted into the membrane from the matrix side. This review will examine the various assembly pathways for inner and outer mitochondrial membrane proteins while discussing the most recent structural and biochemical data examining the biogenesis process.

Keywords: mitochondria, membrane proteins, assembly, mitochondrial chaperones, translocons

OPEN ACCESS

Edited by:
David Pacheu-Grau,
University of Zaragoza, Spain

Reviewed by:
Michał Wasilewski,
The International Institute of Molecular Mechanisms and Machines Polish Academy of Sciences (IMol), Poland
Ridhima Gomkale,
University Medical Center Göttingen, Germany

****Correspondence:***
Ross Eaglesfield
Ross.Eaglesfield@glasgow.ac.uk

Specialty section:
This article was submitted to Cellular Biochemistry, a section of the journal Frontiers in Cell and Developmental Biology

Received: *27 October 2021*
Accepted: *09 December 2021*
Published: *24 December 2021*

Citation:
Eaglesfield R and Tokatlidis K (2021) Targeting and Insertion of Membrane Proteins in Mitochondria. Front. Cell Dev. Biol. 9:803205. doi: 10.3389/fcell.2021.803205

INTRODUCTION

Mitochondria are critically important for metabolism and a whole range of cellular functions, while they also play an essential role in programmed cell death. The mitochondrial proteome is made up of around 1,500 different proteins in humans and around 1,000 proteins in simpler eukaryotic organisms like *Saccharomyces cerevisiae* (Rath et al., 2021; Song et al., 2021). From these proteins, only 13 are encoded by mitochondrial DNA (mtDNA) in humans and 8 in *S. cerevisiae* (7 of which encode subunits of the oxidative phosphorylation complexes). Therefore, the majority of the mitochondrial proteins (about 99% of them) are nuclear-encoded, synthesised in the cytosol and then imported into their correct location within the organelle. The protein import system is very elaborate and depends on multiprotein complexes called translocons that reside in each one of the mitochondrial sub-compartments (Schmidt et al., 2010; Pfanner et al., 2019). The main pathway for mitochondrial proteins is the presequence pathway that guides soluble proteins into the mitochondrial matrix and accounts for almost two thirds of all mitochondrial protein import. On the other hand, the mitochondrial membrane proteins that reside in the inner or the outer membranes follow their own dedicated import routes that not only target the proteins to the correct mitochondrial membrane but also specifically insert them stably within the lipid bilayer (Wiedemann and Pfanner, 2017).

The mitochondrial β-barrel membrane proteins are found only in the outer membrane (OM), whilst α-helical membrane proteins (with either a single or multiple transmembrane domains) are present in both the outer (OM) and inner (IM) mitochondrial membranes (**Figure 1**). Insertion of all β-barrel proteins into the OM is thought to occur post-translationally (Lee et al., 2014), whilst insertion of the very few, highly

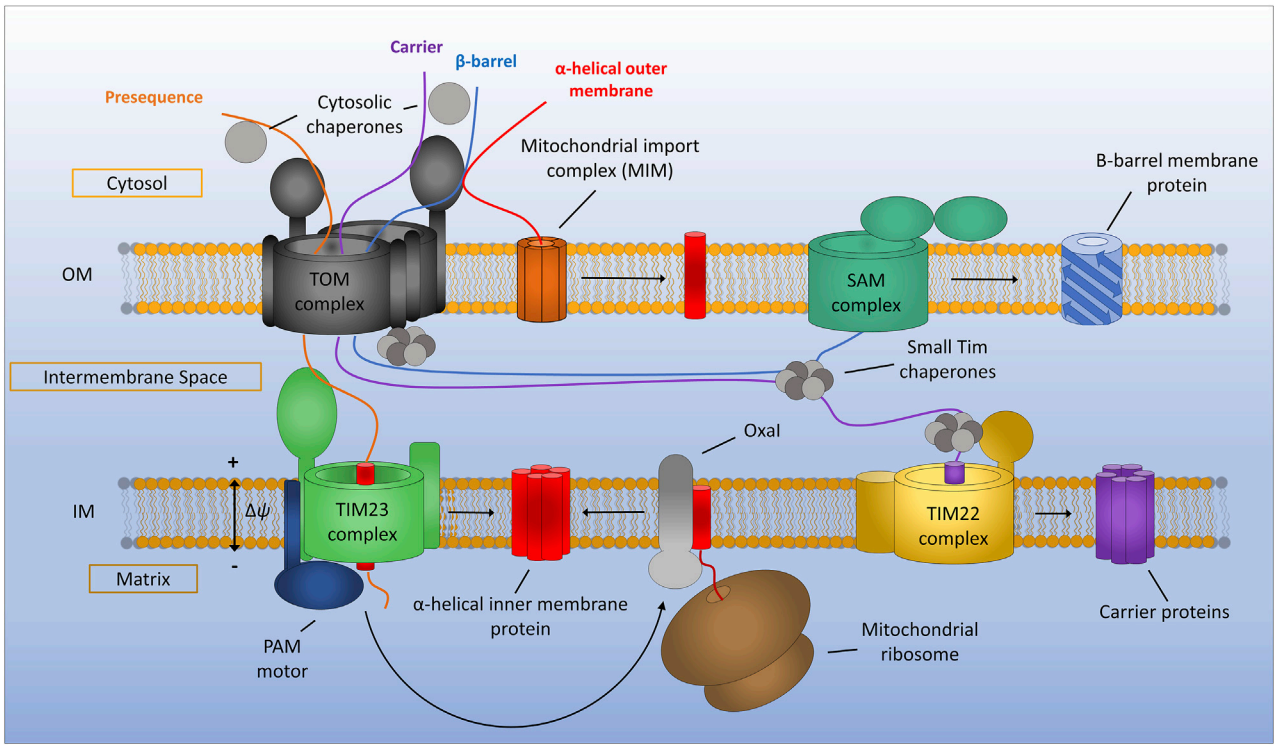

FIGURE 1 | General assembly pathways for mitochondrial membrane proteins. Presequence containing proteins are recognised by the translocon of the outer membrane (TOM) complex and translocated across the outer membrane before being assembled *via* the translocon of the inner membrane (TIM23) complex. TIM23 requires a potential gradient across the inner membrane and can either laterally diffuse stop-transfer hydrophobic α-helices directly into the inner membrane or translocate proteins all the way to the matrix *via* the PAM motor, which can be subsequently inserted into the inner membrane by the Oxa1 insertase. Mitochondrial carrier proteins are maintained in an import competent state by cytosolic chaperones before being translocated across the outer membrane by the TOM complex. Once in the IMS carrier precursors are chaperoned by the small TIMs to the TIM22 complex where insertion into the inner membrane occurs. Beta-barrel proteins of the outer membrane are first translocated into the IMS *via* the TOM complex. The small TIM chaperones then transfer β-barrel precursors from the TOM to the sorting and assembly machinery (SAM) complex where insertion and assembly of the β-barrels takes place. Alpha-helical outer membrane proteins are most often inserted into the membrane directly from the cytosol *via* the mitochondrial import machinery (MIM) complex.

hydrophobic IM proteins that are encoded by the mtDNA occurs in the close vicinity of the mitoribosome (Zorkau et al., 2021). The mitochondrial membrane protein insertion routes seem to diversify from others like the bacterial and the endoplasmic reticulum insertion pathways, which are largely co-translational (Hegde and Keenan, 2021). In the following sections of this review we will first detail the structural features of the translocon of the OM (the TOM complex), which is the main entry gate for all mitochondrial proteins, and we will then discuss the mechanism and structural basis for the import of proteins into the OM and IM of mitochondria.

THE TRANSLOCON OF THE OUTER MEMBRANE COMPLEX: THE MAIN GATEWAY FOR PROTEINS TO CROSS THE OUTER MEMBRANE

Nearly all mitochondrial membrane proteins are encoded in the nuclear genome and are synthesised by cytosolic ribosomes (Schmidt et al., 2010). The outer membrane therefore represents a significant barrier for these proteins which they must cross in order to be correctly assembled into both the inner and outer mitochondrial membranes. The entry gate that controls this import process is known as the TOM complex and is composed of a β-barrel pore forming protein (Tom40), a number of accessory/scaffolding proteins (Tom5, Tom6 and Tom7) and two receptor proteins (Tom20 and Tom70) that recognise mitochondrial targeting signals within protein sequences (Bolliger et al., 1995; Dietmeier et al., 1997; Rapaport and Neupert, 1999; Model et al., 2001; Gabriel et al., 2003; Mokranjac and Neupert, 2015; Pfanner et al., 2019; Wang et al., 2021). Additionally, the TOM complex contains a protein called Tom22, which appears to act as both a receptor and a scaffolding protein helping to control the number of pore-forming subunits associated to each fully assembled TOM complex as well as facilitating protein import (Lithgow et al., 1994; Bolliger et al., 1995; Moczko et al., 1997; Yano et al., 2000).

The proteinaceous components of the TOM complex described above were identified and assigned many years ago

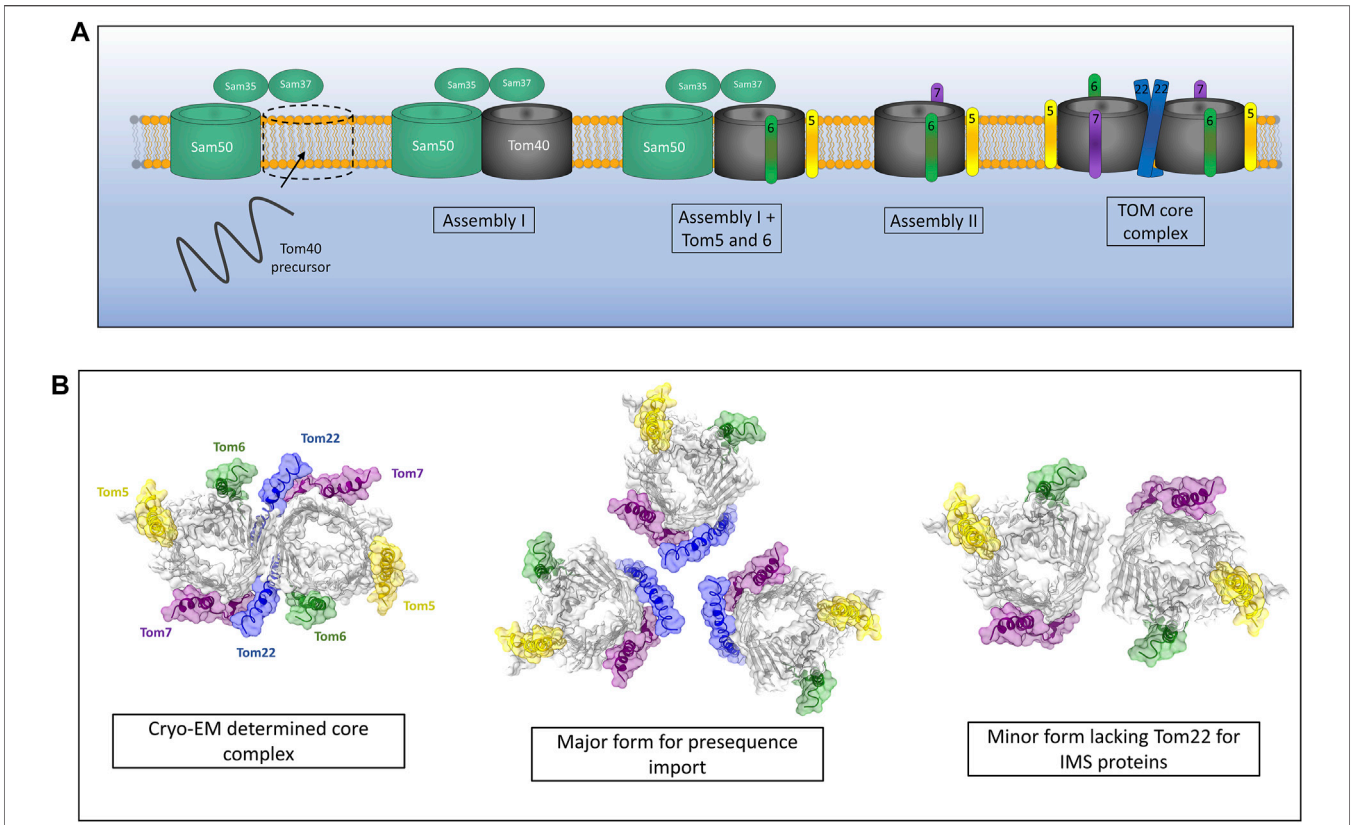

FIGURE 2 | Assembly of the TOM complex. **(A)** The TOM complex is assembled sequentially in the outer membrane. First, a Tom40 precursor from the IMS is assembled into the outer membrane by the SAM complex (Assembly I). Subsequently, the small TOMs Tom5 and Tom6 are assembled with Tom40 while still associated with Sam50. The addition of Tom7 leads to dissociation of the TOM-SAM complex (Assembly II) allowing the final assembly of the TOM core complex *via* the introduction of Tom22. **(B)** Cryo-EM experiments identify a dimeric form of TOM containing Tom22. *In vivo* crosslinking data suggest that TOM actually exists as a trimer containing Tom22 and a dimer lacking Tom22 but containing Tom5, 6 and 7. The trimer makes up the majority of the population and is the predominant form for presequence import. The dimeric form lacking Tom22 facilitates the import of soluble IMS proteins. Models generated using PDB ID 6JNF.

(Kiebler et al., 1990), however it is only with recent advances in techniques such as cryo-EM that the assembly pathway of the TOM complex has become clearer. The assembly of the TOM complex is separated into three distinct stages known as assembly I, assembly II and TOM core assembly (Wang et al., 2021) (**Figure 2A**). Assembly I involves the integration of the Tom40 β-barrel protein into the outer membrane from the intermembrane space (IMS) side of the outer membrane *via* the sorting and assembly machinery (SAM) complex (this process will be discussed in detail later) (Wiedemann et al., 2003). This initial assembly stage requires a fully assembled and functional TOM complex for the initial translocation of Tom40 precursors across the outer membrane. Tom5 and Tom6 are subsequently inserted and assembled with Tom40 while it is still associated with the SAM complex (Dietmeier et al., 1997; Model et al., 2001; Becker et al., 2010; Thornton et al., 2010). The subsequent addition of Tom7 leads to dissociation of the growing TOM complex from SAM and constitutes assembly II (Yamano et al., 2010; Becker et al., 2011b; Wang et al., 2021). The addition of Tom22 to the complex leads to the assembly of the TOM core complex containing multiple fully assembled TOM complexes with Tom22 acting as a scaffold holding them together (Araiso et al., 2019; Tucker and Park, 2019; Wang et al., 2020b; Wang et al., 2021).

While the cryo-EM structures of the TOM core complex are an invaluable source of molecular detail and give us many clues as to the function of TOM as a protein import gate, they invariably show a dimer containing two Tom40 pores and two copies of Tom22 (Araiso et al., 2019; Tucker and Park, 2019). The multimeric state of the TOM complex in intact mitochondria seems to differ from these cryo-EM snapshots. Crosslinking studies have shown that the TOM complex is likely to exist predominantly as a trimer containing three β-barrel Tom40 subunits held together by three Tom22 subunits (Shiota et al., 2011). A minor dimeric form of the TOM complex was observed using cysteine-cysteine crosslinking and was found to contain two Tom40 β-barrels but no Tom22 (Shiota et al., 2015) (**Figure 2B**). It should be noted that both the trimeric and dimeric forms of the TOM complex contained the other accessory TOM components Tom5, Tom6 and Tom7. Interestingly, the trimeric form seems to be indispensable for import of pre-proteins into the mitochondria due to the presence of Tom20 and Tom22, both of which are required for presequence recognition and transport (Model et al., 2001). The dimeric form of Tom40 lacking Tom22 acts as an

assembly intermediate allowing the dynamic exchange of new TOM subunits with the trimeric complex containing older subunits (Shiota et al., 2015; Araiso et al., 2021). Alongside this role, dimeric Tom40 can import several soluble MIA40 substrates into the IMS of mitochondria, specifically Tim9 and Cox17 (Gornicka et al., 2014; Sakaue et al., 2019). Larger TOM assemblies have also been observed via crosslinking analyses (Tucker and Park, 2019), although the physiological relevance of these larger oligomeric complexes remains to be discovered.

OUTER MEMBRANE PROTEIN BIOGENESIS

Aside from the vital role of the TOM complex in protein import, the outer membrane of mitochondria is also essential for maintaining the ionic balance of the organelle through the essential metabolite channel Porin/VDAC (Young et al., 2007), while also providing sites of contact between the endoplasmic reticulum (ER) and the mitochondria through mitochondrial distribution and morphology protein 10 (Mdm10) (Kühlbrandt, 2015; Ellenrieder et al., 2016). Given the vital nature of these functions the biogenesis of outer membrane proteins is a tightly regulated process requiring further essential components of the outer membrane. Membrane proteins of the outer mitochondrial membrane can be split into two distinct classes, the α-helical and β-barrel proteins.

Alpha-helical proteins are inserted directly into the outer membrane from the cytosol *via* the mitochondrial import machinery (MIM) complex in most cases (Doan et al., 2020). MIM is an oligomeric complex composed of two membrane spanning alpha-helical proteins, Mim1 and Mim2, with Mim1 being the major constituent of the complex (Becker et al., 2008; Hulett et al., 2008; Popov-Čeleketić et al., 2008; Dimmer et al., 2012). Mim1 is able to form pores in planar lipid membranes, while co-reconstitution with Mim2 does not substantially affect pore formation but may allow the recognition of positively charged residues in precursor proteins (Krüger et al., 2017). Mim1 (also known as Tom13), was originally characterised as a TOM complex assembly factor (Waizenegger et al., 2005; Lueder and Lithgow, 2009; Becker et al., 2011a). Given that the TOM complex contains a number of single-pass transmembrane alpha-helical proteins (Tom5, Tom6, Tom20 and Tom70) this is not surprising. Since these initial studies on TOM complex assembly, MIM has been identified as a key regulator for the assembly of outer membrane proteins Ugo1 and Fzo1, multi-spanning proteins involved in mitochondrial fusion (Becker et al., 2011a; Papić et al., 2011; Dimmer et al., 2012); as well as the multi-spanning protein Ubx2 (Mårtensson et al., 2019). Ubx2 is a dually localised protein resident in both the ER membrane, where it functions in the ER-associated degradation (ERAD) pathway, and the outer mitochondrial membrane where it performs a similar quality control function by removing stalled precursors from the TOM complex (Mårtensson et al., 2019).

Two interesting examples have also been found for MIM inserting proteins from the IMS as well as the cytosol (Song et al., 2014; Wenz et al., 2014). Outer membrane proteins Mcp3 and OM45 have both been identified as substrates of the MIM assembly pathway. What is interesting however is that initially these proteins are imported into the IMS via the presequence pathway involving the TOM complex. Prior to their insertion at the outer membrane by MIM they have also been found to interact with the TIM23 complex (Song et al., 2014; Wenz et al., 2014). This novel import route is interesting given the unknown functions of both of these proteins. A recent study has identified that the MIM complex exists in three distinct sub-populations (**Figure 3A**). As a lone insertase MIM acts on single spanning and tail anchored outer membrane proteins. MIM is also found in complex with the TOM and the SAM where it functions in multi-spanning outer membrane protein assembly and TOM assembly respectively (Doan et al., 2020). A protein complex performing the function of MIM has yet to be identified in mammalian cells, however a recent study was able to identify a functional equivalent to the MIM complex in trypanosomes (Vitali et al., 2018).

The proteins mentioned above represent a limited subset of outer membrane α-helical proteins and the insertion mechanism for many tail-anchored proteins remains to be properly elucidated. It has been suggested that some tail-anchored proteins are actually able to insert into the outer membrane without the assistance of any known insertase (Setoguchi et al., 2006; Kemper et al., 2008). This suggests that a spontaneous, thermodynamically driven mechanism may facilitate the insertion of these proteins, or there may be an as yet undiscovered pathway similar to the Get pathway of the ER (Asseck et al., 2021). It has also been postulated that the lipid composition of the outer membrane, specifically the presence of ergosterols, acts as a targeting factor for tail-anchored proteins (Krumpe et al., 2012).

The second class of outer membrane proteins are the β-barrel proteins, which form pores in the outer membrane for the transport of proteins and ions (Paschen et al., 2005). β-barrel precursors synthesised in the cytosol must first translocate across the outer membrane before being assembled from within the IMS by the SAM complex (**Figure 3B**) (Pfanner et al., 2004). Emerging precursors are stabilised in an unfolded state by the chaperones Hsp70 and Hsp40 proteins which recognise β-hairpins present in the precursors (Jores et al., 2018). Unfolded precursors are then trafficked to the mitochondrial outer membrane where they come into contact with the TOM complex *via* specific interactions between their β-hairpin structures and the receptor protein Tom20 (Jores et al., 2016). Unfolded proteins then pass through the outer membrane via the Tom40 channel, which is itself a β -barrel outer membrane protein required for its own import (Rapaport and Neupert, 1999).

As precursors emerge from Tom40 on the IMS side of the outer membrane they are able to interact with the small TIM proteins, IMS resident chaperones that protect the highly hydrophobic portions of membrane proteins from aggregation prior to correct assembly (Vial et al., 2002; Hoppins and Nargang, 2004; Wiedemann et al., 2004; Milenkovic et al., 2009; Weinhäupl et al., 2018).

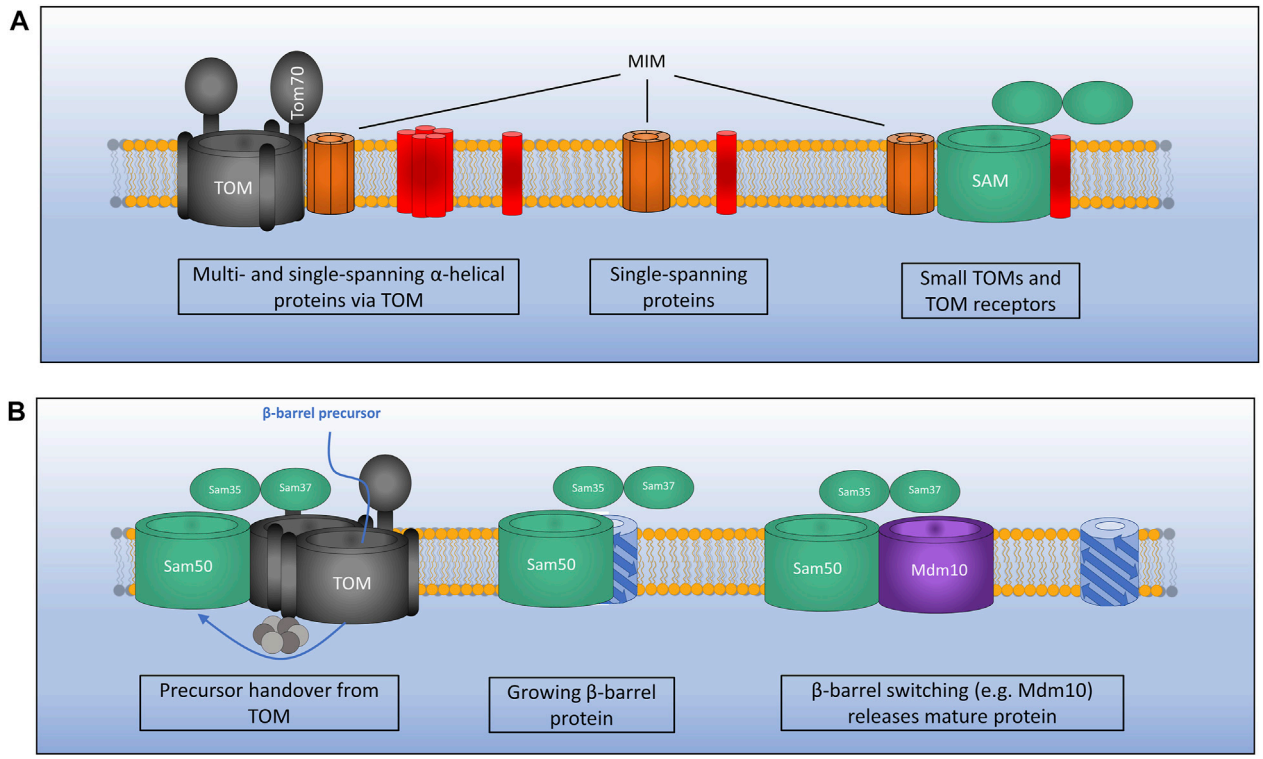

FIGURE 3 | Mechanisms of outer membrane protein biogenesis. **(A)** The MIM complex exists in three distinct conformations: 1). In complex with TOM for the assembly of certain multi- and single-spanning α-helical membrane proteins which interact via the receptor Tom70.2). As a lone insertase for the assembly of certain single-spanning and tail anchored α-helical proteins. 3). In complex with SAM where MIM functions during assembly of TOM by inserting small TOM components into the growing structure. **(B)** The SAM complex inserts β-barrel outer membrane proteins *via* the IMS. Precursors pass through the TOM which is bound to SAM *via* Sam37 and the small TIMs in the IMS. TOM is then displaced as a growing β-barrel protein emerges from SAM. A switching mechanism is then required whereby a mature β-barrel protein (e.g., Mdm10) displaces the newly formed β-barrel allowing it to be released from the SAM complex.

Beta-barrel precursors can then be assembled into the outer membrane by the SAM complex, an outer membrane protein complex consisting of a 16-stranded β-barrel protein Sam50 and two peripherally associated subunits Sam35 and Sam37 facing the cytosol (Kozjak et al., 2003; Milenkovic et al., 2004; Habib et al., 2005). Sam50 bears striking similarity to the bacterial outer membrane assembly protein BamA and indeed the assembly mechanism is also well conserved given that bacterial outer membrane proteins can be successfully imported and assembled into the mitochondrial outer membrane (Walther et al., 2009; Kozjak-Pavlovic et al., 2011; Ulrich et al., 2014).

Both Sam50 and Sam35 are essential proteins and have been found to interact with precursors through a motif known as the β-signal (Jores et al., 2016; Höhr et al., 2018). This motif (Polar-X-Gly-X-X-Hydrophobic-X-Hydrophobic) is present in the most C-terminal β-strand of precursor proteins and is required for membrane insertion. Sam50, being a β-barrel protein, also contains a β-signal in strand 16 (Imai et al., 2011). Recent crosslinking evidence suggests that an incoming β-signal is able to displace the endogenous Sam50 signal at a lateral opening in the Sam50 pore (Höhr et al., 2018). A β-barrel precursor associated with Sam50 through this β-signal interaction may then be able to grow and insert subsequent β-strands leading to a large assembly still associated with Sam50 in a similar manner as the recently proposed model for BAM insertion of β-barrel proteins in bacteria (Doyle and Bernstein, 2019). The role of Sam35 is yet to be fully elucidated, however some evidence indicates that Sam35 is required for protein insertion by Sam50 and interacts with the β-signal of precursors (Kutik et al., 2008). Sam35 is thought to be peripherally associated with the SAM complex facing the cytosol which is counterintuitive to a mechanistic understanding given that β-barrel proteins are inserted from the IMS side of the outer membrane. There is some evidence that Sam35 is actually embedded within the outer membrane through close interactions with Sam50 (Kutik et al., 2008), possibly within the pore of Sam50, although recent structural data do not support this hypothesis (Takeda et al., 2021; Wang et al., 2021).

The non-essential subunit Sam37 aids in the assembly of a SAM-TOM supercomplex through interactions with Sam35 and the cytosolic domain of Tom22 (Qiu et al., 2013; Wenz et al., 2015). These interactions, along with interactions with the small TIMs of the IMS, are thought to aid in precursor transfer from the TOM to the SAM during outer membrane protein biogenesis.

More recently, the outer membrane β-barrel mitochondrial distribution and morphology protein 10 (Mdm10) was identified as a transient component of the SAM complex important for the efficient assembly of the TOM complex (Meisinger et al., 2004,

2006). Mdm10 is dually localised to both the SAM complex and the ER mitochondria encounter structure (ERMES) which physically connects the mitochondrial outer membrane with the ER membrane and is thought to aid in lipid transfer between the two membranes (Kornmann et al., 2009; Flinner et al., 2013; Bohnert et al., 2015). Mdm10 acts as a membrane anchor for the rest of the ERMES complex subunits (Mdm34 and Mdm12) which connect to the ER through interactions with the ER protein Mmm1 (Kornmann and Walter, 2010).

The Mdm10 interaction with the SAM complex is mediated through Sam37 but also interestingly through Tom7, one of the small α-helical components of the TOM complex. Tom7 has an inhibitory effect on TOM complex assembly due to this dual interaction with both the TOM complex and Mdm10. Tom7 is able to interact with free Mdm10 which in turn favours Mdm10-ERMES assembly (Meisinger et al., 2006; Yamano et al., 2010). This has the effect of limiting the amount of Mdm10 which is able to bind to the SAM complex thus inhibiting TOM complex assembly. Cryo-EM experiments have recently generated high resolution structures of the SAM complex from *M. thermophila* and *S. cerevisiae* in complex with various substrates providing more evidence to support the mechanisms of outer membrane protein insertion discussed above (Diederichs et al., 2020; Takeda et al., 2021; Wang et al., 2021). The structural data clearly show a lateral opening in Sam50 between the β-signal in strand 16 and strand 1. Interestingly two of these studies were able to identify the SAM complex in association with Mdm10 (Takeda et al., 2021) and Tom40 (Wang et al., 2021). These structures have led to the β-barrel switching hypothesis which suggests that in order for a fully assembled β-barrel to be released by SAM into the outer membrane a dynamic switching event must take place with another β-barrel protein for this release to take place. It seems that for Tom40 this dynamic switching event is mediated by Mdm10 (Takeda et al., 2021; Wang et al., 2021), however for Porin this event seems to be mediated by a second monomer of Sam50 (Takeda et al., 2021). This SAM dimer complex will then dissociate to allow the start of the assembly process again. Further structural data are required to confirm this hypothesis however, as only fully assembled β-barrels have been visualised to date an assembly intermediate is missing. Such an intermediate has been observed in the bacterial BAM complex however which confirms the growth and release from the lateral opening (Tomasek et al., 2020). More work is also needed to understand SAM-mediated outer membrane assembly in humans given that yeast TOM cannot be assembled by human SAM (Wang et al., 2021).

PROTEIN ASSEMBLY BY THE TRANSLOCON OF THE INNER MEMBRANE

After passing through the TOM at the outer membrane, proteins containing a presequence that are destined for assembly at the inner membrane are transferred to the translocon of the inner membrane (TIM23) complex (**Figure 4**). TIM23 is a dynamic complex which adopts different conformations for the transport of proteins into the matrix and for partitioning certain membrane proteins into the inner membrane directly (Wiedemann and Pfanner, 2017).

Presequence containing precursors passing through the TOM complex will first interact with the receptor protein Tim50 which has a large receptor domain exposed to the IMS (Meinecke et al., 2006; Waegemann et al., 2015). In the absence of a bound precursor, Tim50 also acts as a plug for the Tim23 channel in order to maintain the permeability barrier of the inner membrane which is so crucial for the generation and maintenance of the proton gradient (Meinecke et al., 2006). Tim50 acts in concert with both the regulatory subunit Tim21 and the main channel forming polytopic membrane protein Tim23 to transfer precursors across the inner membrane and partition certain hydrophobic proteins into the inner membrane. Another membrane embedded subunit Tim17, which is a paralog of Tim23, is involved in maintenance of complex stability (Demishtein-Zohary et al., 2015).

Distinct conformations of the TIM23 complex have been identified that aid either the translocation of large hydrophilic domains across the inner membrane to the matrix, or the lateral diffusion of transmembrane α-helices into the lipid bilayer (Schendzielorz et al., 2018; Edwards et al., 2021). Key to these differing conformations are the TIM23 accessory proteins Pam18 and Mgr2. When Pam18 is bound to TIM23 (designated $TIM23_{MOTOR}$), as is the case during precursor translocation, the lateral release of membrane proteins is inhibited. When TIM23 is associated with the subunits Tim21 and Mgr2 (designated $TIM23_{SORT}$) hydrophobic protein sequences can be partitioned into the inner membrane in a process known as stop transfer (Chacinska et al., 2005, 2010; van der Laan et al., 2007; Bohnert et al., 2010; Schendzielorz et al., 2018). Mgr2 seems to act as a gatekeeper for protein lateral release due to its close association with the predicted lateral gate of Tim23 and its quality control-type effect on the lateral release process (Ieva et al., 2014; Matta et al., 2020). Following translocation or lateral release into the inner membrane, the presequence, which will have invariably been translocated into the matrix, is cleaved by the matrix processing peptidase (MPP). Interestingly, the TIM23 complex of yeast has been shown to interact with respiratory chain complexes in both the $TIM23_{SORT}$ and $TIM23_{MOTOR}$ conformations, indicating that a physical interaction keeping the translocase close to the site of proton motive force generation may be essential to the function of TIM23 in both the translocation and release of IM proteins and the translocation of soluble matrix proteins (van der Laan et al., 2006; Wiedemann et al., 2007).

In humans the TIM23 subunit TIM21 plays a distinct and important role in respiratory chain biogenesis. TIM21 was discovered as a component of an early cytochrome C oxidase assembly intermediate known as mitochondrial translation regulation assembly intermediate of cytochrome c oxidase (MITRAC) complex (Mick et al., 2012; Wang et al., 2020a). Knockdown of TIM21 also lead to complex IV assembly defects, while overexpression of TIM21 relieved ATP synthase assembly defects in yeast and improved the viability of human cell lines generated from patients with ATP synthase defects (Aiyar et al., 2014).

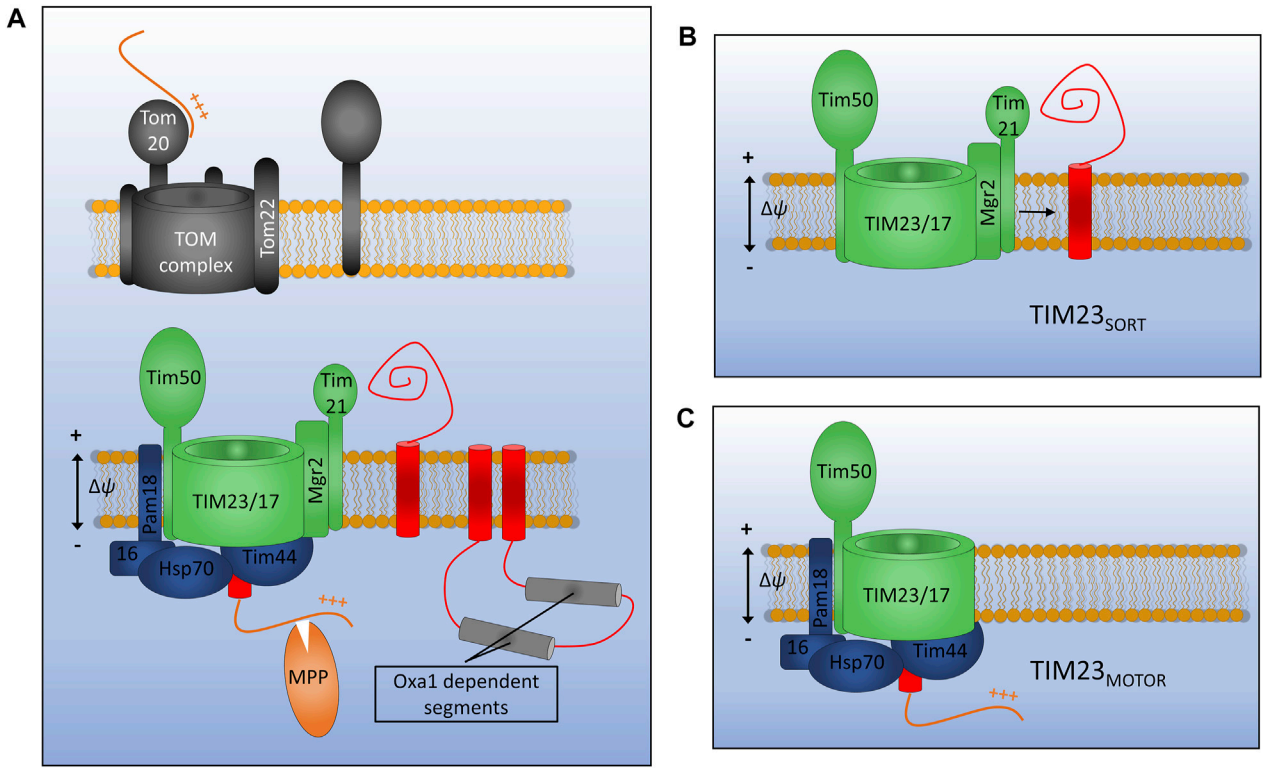

FIGURE 4 | Assembly of inner membrane proteins by TIM23. **(A)** Presequence containing membrane proteins are recognised at the outer membrane by the Tom20 receptor and translocated across the outer membrane *via* Tom22 and Tom40. Once in the IMS presequences are recognised by the TIM23 subunit Tim50 and moved into the Tim23 channel. TIM23 can either laterally release stop-transfer segments into the membrane *via* the lateral gatekeeper Mgr2 associated with Tim21 **(B)**, or can translocate entire domains into the matrix via the PAM motor **(C)**. Motor function requires an inner membrane potential and ATP hydrolysis by mtHsp70. Once in the matrix the presequence will be cleaved by matrix processing peptidase (MPP). Certain multi-spanning proteins utilise both lateral diffusion directly from Tim23 and translocation for subsequent insertion *via* the Oxa1 insertase.

In order for TIM23 to transfer large protein domains into the matrix two things are essential: the mitochondrial membrane potential ($\Delta\psi$) and the ATP-driven import motor PAM (Li et al., 2004; Van Der Laan et al., 2013). The major component of the import motor is the ATP-driven chaperone mitochondrial heat shock protein 70 (mtHsp70) which is connected to Tim23 *via* the peripheral subunit Tim44 which also aids in precursor transfer from Tim23 to mtHsp70 (Hutu et al., 2008; Banerjee et al., 2015). The co-chaperones Pam18 and Pam16 enable ATP hydrolysis by mtHsp70 while the nucleotide exchange factor Mge1 promotes the exchange of ADP for ATP and thus the recycling of the motor (Miao et al., 1997; Sakuragi et al., 1999; Wiedemann and Pfanner, 2017). The exact mechanistic details of how the motor operates and imports proteins into the matrix remains to be elucidated. Interestingly, a direct physical link has been found between Pam16 and Pam18 and the respiratory complex III-IV supercomplex (Wiedemann et al., 2007). This interaction is thought to facilitate the assembly of the PAM motor and may provide a key energetic environment to enhance protein translocation to the matrix.

The two distinct Tim23 pathways discussed above are most often used independently, however there is an example of a protein that utilises both mechanisms for its assembly in the inner membrane. Mdl1, a six transmembrane segment member of the ABC transporter superfamily, utilises both lateral diffusion and motor-driven translocation prior to its final assembly at the inner membrane (Bohnert et al., 2010). This study identified that of the six transmembrane helices of Mdl1, the first and last two diffuse directly into the inner membrane from $TIM23_{SORT}$ while the two helices located in the middle of the protein sequence are fully translocated into the matrix by $TIM23_{MOTOR}$ before being assembled into the inner membrane by the oxidase assembly protein 1 (Oxa1, whose function will be described later). Since this initial discovery further examples of proteins utilising a combination of stop-transfer and conservative (PAM-driven) mechanisms for assembly have been identified, for example Sdh4 (Park et al., 2013) and the Tim18-Sdh3 module of the TIM22 translocon (Stiller et al., 2016).

A high-resolution structure of the TIM23 complex is yet to be reported although given the speed of advancement of cryo-EM techniques a molecular structure will likely be available in the near future.

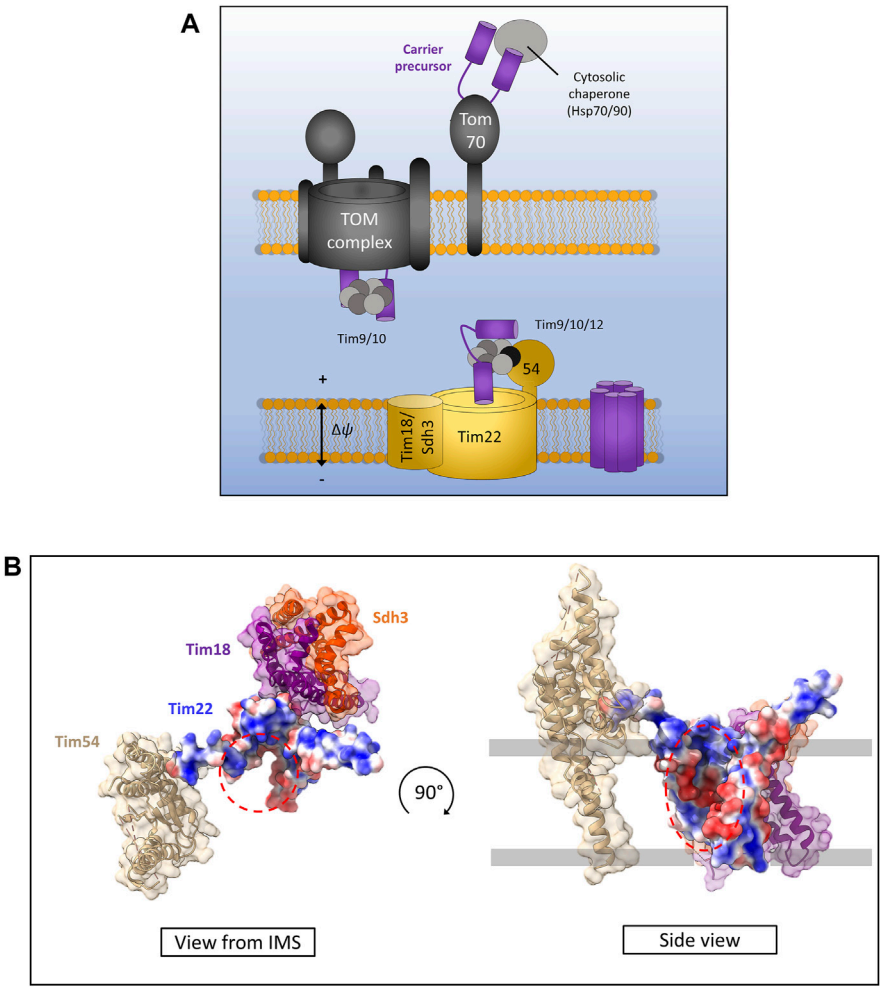

FIGURE 5 | The carrier pathway for insertion at the inner membrane by TIM22. **(A)** Carrier precursors are recognised by cytosolic chaperones which move the precursor to the mitochondrial outer membrane via interactions with the receptor Tom70. Precursors are then translocated *via* the TOM to the IMS where they are met by the Tim9-Tim10 complex which maintains the hydrophobic precursor in an insertion-competent state. The precursor is then handed to the TIM22 complex via the membrane bound Tim9-Tim10-Tim12 complex which is bound to Tim22 via Tim54. Tim22 then inserts α-helical modules into the inner membrane in a membrane potential dependent manner. The Tim18/Sdh3 module associated with Tim22 is required to maintain complex stability. **(B)** Yeast Tim22 appears to contain a lateral gate exposing the hydrophilic core of the channel to the surrounding lipid suggesting a method of lateral diffusion directly from the channel. Lateral gate highlighted by red dashed areas. Models generated using PDB ID 6LO8.

MITOCHONDRIAL CARRIER PROTEINS AND THE TIM22 COMPLEX

The mitochondrial carrier proteins are a superfamily of 6 transmembrane α-helical proteins localised to the inner membrane of mitochondria (**Figure 5A**) and are essential for the transport of essential metabolites into and out of the mitochondrial matrix (Horten et al., 2020). The carrier proteins are synthesised without N-terminal presequences, and instead have internal targeting signals which can be recognised by the Tom70 receptor at the cytosolic face of the outer membrane (Sirrenberg et al., 1998; Diekert et al., 1999; Wiedemann et al., 2001; Kreimendahl et al., 2020). However, recent evidence suggests that Tom70 acts more like a recruitment factor for cytosolic chaperones such as Hsp70 and Hsp90 which are able to maintain the highly hydrophobic carrier proteins in an import-competent state and avoid unwanted aggregation (Backes et al., 2021).

Following translocation across the outer membrane through the Tom40 pore, carrier precursors interact with the small TIM chaperones in the IMS. Specifically, they bind the Tim9-Tim10 (Tim9 and Tim10a in humans) complex first at the IMS side of TOM (Luciano et al., 2001; Truscott et al., 2002; Vial et al., 2002) which forms a ring or doughnut-like structure that shields the hydrophobic domains of carrier substrates from the aqueous medium of the IMS (Weinhäupl et al., 2018). From here carrier precursors are handed to a second small TIM complex associated with the TIM22 translocon containing Tim9-Tim10-Tim12 in yeast and Tim9-Tim10a-Tim10b in humans (Sirrenberg et al., 1998; Lionaki et al., 2008; Qi et al., 2021).

Interestingly, the outer membrane metabolite channel porin was recently identified to have a role in carrier protein biogenesis and bound directly to carrier protein precursors as well as directly recruiting TIM22 (Ellenrieder et al., 2019). The exact mechanism by which porin aids carrier insertion remains unknown but may involve physically linking the inner and outer membranes through these protein-protein interactions given that a direct TOM-TIM22 supercomplex does not appear to exist (Edwards and Tokatlidis, 2019; Ellenrieder et al., 2019; Horten et al., 2020).

Following outer membrane translocation and passage through the IMS chaperoned by the small TIMs, carrier precursors arrive at the TIM22 complex for their final insertion and assembly in the inner membrane. The TIM22 complex is composed of the main translocon protein Tim22 (Sirrenberg et al., 1996; Bauer et al., 1999) and a number of accessory proteins that are starkly different in yeast and humans. In yeast, the accessory proteins are Tim54, Sdh3 (which is also part of complex II), and Tim18. Tim54 contains a large IMS exposed domain which acts as a recruitment site for the Tim9-Tim10-Tim12 complex (Rehling et al., 2003, 2004). Tim18 and Sdh3 form a membrane integral module which is involved in the assembly of the TIM22 complex and is dependent on Oxa1 (Kerscher et al., 2000; Koehler et al., 2000; Gebert et al., 2011). In humans the accessory proteins are Tim29 and acylglycerol kinase (AGK) (Qi et al., 2021). Tim29 performs a similar function to yeast Tim54. It contains an IMS facing domain and is involved in interactions with the small TIMs and TIM22 complex assembly (Kang et al., 2016). AGK was only identified as a TIM22 complex subunit recently. Its role in carrier protein assembly is independent of its equally crucial role as a lipid kinase, however how it aids carrier protein biogenesis is not yet known (Kang et al., 2017; Vukotic et al., 2017).

The core component of the TIM22 complex in both yeast and humans is the translocase protein Tim22. The mitochondrial membrane potential is essential for precursor transfer from the small TIMs to Tim22 where carriers are laterally released as consecutive α-helical hairpin pairs into the inner membrane and adopt their functional fold (Wiedemann et al., 2001; Rehling et al., 2003). The mechanism of assembly and lateral release by Tim22 remains unknown, however recent structural analysis of both the human and yeast TIM22 complexes seems to indicate a cavity within Tim22 exposed to the lipid bilayer (**Figure 5B**) (Qi et al., 2021; Zhang et al., 2021). However, further structural data with bound precursors undergoing insertion are required to fully elucidate the carrier insertion mechanism.

As mentioned above, carrier proteins contain three modules each containing hairpin α-helical structures which are required for assembly by TIM22 (Wiedemann et al., 2001). Recently, a number of unconventional TIM22 substrates have been identified containing odd numbers of transmembrane helices in both yeast (Gomkale et al., 2020; Rampelt et al., 2020) and human (Acoba et al., 2021; Jackson et al., 2021) mitochondria. In yeast, the mitochondrial pyruvate carrier (MPC) proteins Mpc2 and Mpc3, both of which are predicted to have odd numbers of transmembrane α-helices (Bender et al., 2015), show a dependence on TIM22 for their assembly (Gomkale et al., 2020; Rampelt et al., 2020). TIM22 is also required for the assembly of MPC proteins in human cells (Gomkale et al., 2020). Furthermore, human cells also require TIM22 for the correct assembly of a number of sideroflexin (SFXN) proteins. These proteins are predicted to contain odd numbers of transmembrane α-helices and are essential as amino acid transporters in mitochondria that in turn affect mitochondrial one-carbon metabolism and respiratory complex III integrity (Kory et al., 2018; Acoba et al., 2021; Jackson et al., 2021). Taken together these recent studies suggest that the substrate spectrum of the TIM22 complex is much wider than previously thought, and biogenesis by TIM22 does not necessarily require modules of α-helical hairpin structures as originally thought.

OXA1 AND RESPIRATORY CHAIN ASSEMBLY

Mitochondria maintain fully functional transcription and translation machineries, however many of the proteins making up these systems are encoded by nuclear DNA. The mitochondrial DNA (mtDNA) of eukaryotes codes for a small subset of highly hydrophobic membrane proteins that are subunits of the complexes of the oxidative phosphorylation (OXPHOS) respiratory electron transport chain (Taanman, 1999). Yeast mitochondrial genomes encode for 30–40 genes that include ribosomal RNAs, tRNAs and subunits of the OXPHOS machinery; specifically three subunits of ATP synthase (atp6, atp8 and atp9), three subunits of complex IV (cox1, cox2 and cox3) and a single subunit of Complex III (cytb) (Freel et al., 2015). Human mitochondria encode a total of 37 genes including, like yeast, ribosomal RNAs, tRNAs and OXPHOS subunits. Human mtDNA encodes 13 protein subunits of the OXPHOS machinery, two subunits of ATP synthase (atp6 and atp8), three subunits of complex IV (cox1, cox2 and cox3), one subunit of complex III (cytb) and 7 subunits of complex I which is not present in yeast (nd1, nd2, nd3, nd4L, nd4, nd5 and nd6) (**Figure 6A**) (Chocron et al., 2019). The inner mitochondrial membrane protein Oxa1 is essential for the correct insertion and assembly of many of these proteins and is therefore required for oxidative phosphorylation and cell viability (**Figure 6B**) (Thompson et al., 2018). Oxa1 was first identified in yeast and shares structural and functional homology with the bacterial insertase YidC (Bonnefoy et al., 1994; Altamura et al., 1996; Scotti et al., 2000). Like YidC, Oxa1 has a membrane spanning core of five α-helices that is absolutely essential for its insertase function (Kuhn et al., 2003; Hennon et al., 2015). The major difference between Oxa1 and YidC is the presence of a large C-terminal hydrophilic domain in Oxa1 located in the mitochondrial matrix. Removal of this C-terminal domain resulted in a loss of cell viability due to incomplete assembly of respiratory complexes, with the most drastic defects being present in complex IV (Szyrach et al., 2003). Furthermore, the C-terminal domain of Oxa1 was found to act as a binding site for the mitochondrial ribosome (Szyrach et al., 2003) suggesting that localising the translation of certain hydrophobic proteins to the membrane in close proximity to Oxa1 is key to their correct insertion and assembly. The membrane proximity of translation was also recently shown to be crucial for the thermodynamically

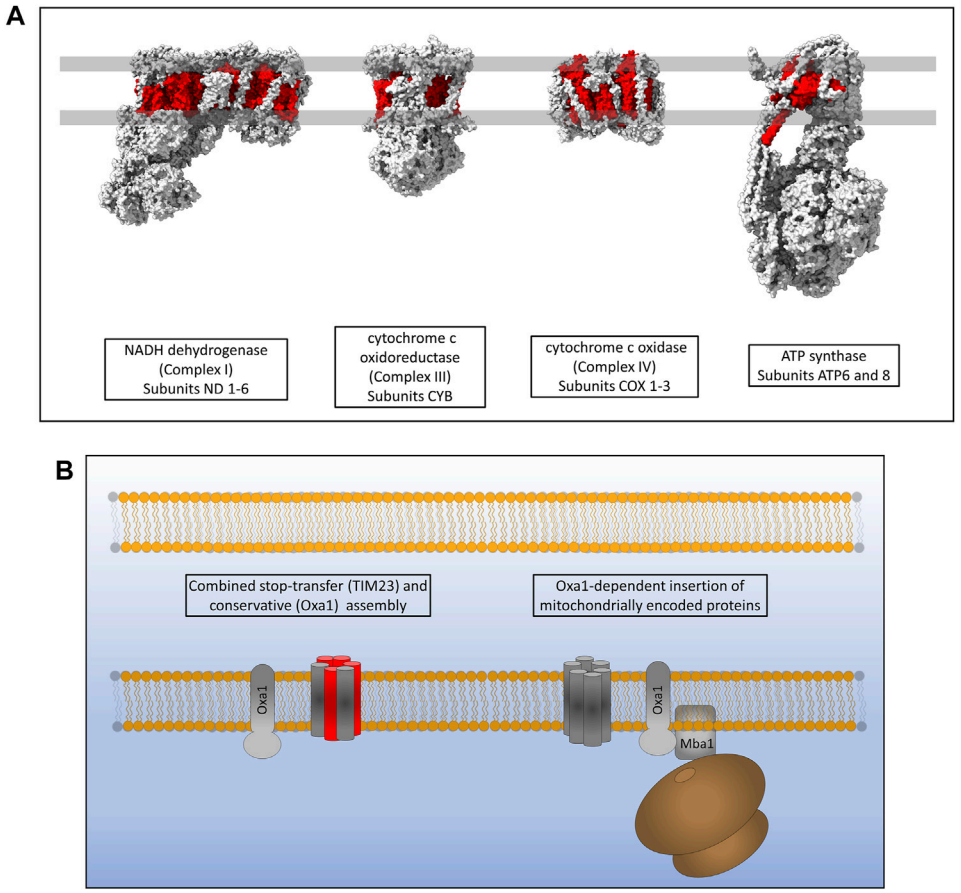

FIGURE 6 | Inner membrane protein assembly by Oxa1. **(A)** Hydrophobic proteins of the human respiratory complexes that are synthesised on mitoribosomes are highlighted in red. **(B)** Oxa1 is able to insert proteins from two origins. Some proteins that are synthesised in the cytosol, passed through TOM and partially assembled by TIM23 require Oxa1 for the assembly of some of their transmembrane α-helices. Oxa1 also acts as the main, and only, insertase for mitochondrially encoded membrane proteins. The mitoribosome is physically associated with Oxa1 *via* Mba1 in yeast (mL45 in humans) whereby respiratory subunits are inserted and assembled into the inner membrane co-translationally.

driven assembly of a bacterial α-helical membrane protein in an entirely *in vitro* artificial system (Eaglesfield et al., 2021). The yeast protein Mba1 was also initially identified as a component of the respiratory chain assembly pathway acting independently of Oxa1 for the insertion of Cox2, cytochrome b and Cox1 (Preuss et al., 2001). Subsequent study of Mba1 identified it as a secondary mitoribosome receptor whose function seems to be both the anchoring of translation to the membrane through interactions with the mitoribosome and facilitating a tight interaction between Oxa1 and the mitoribosome (Ott et al., 2006; Keil et al., 2012). Knockdown of Oxa1 in humans results in a similar phenotype to yeast knockdowns, with the assembly of the respiratory chain being affected, specifically complexes I, IV and V (Stiburek et al., 2007; Thompson et al., 2018). Mba1 in humans is not freely associated with the membrane and Oxa1 as it is in yeast. It is instead a proteinaceous component of the human mitoribosome known as mL45 which still functions in attachment of the ribosome to Oxa1 when the mitoribosome is actively translating (Kummer et al., 2018; Itoh et al., 2021). Human Oxa1 also contains a long C-terminal hydrophilic domain which as a contact site for the mitoribosome (Itoh et al., 2021). Recent microscopic evidence has shown that the majority of translation in human mitochondria occurs at the cristae membrane close to the site of OXPHOS assembly by Oxa1 (Zorkau et al., 2021) and not at the nucleoid or RNA granules where mRNA is processed (Rey et al., 2020). Interestingly, the submitochondrial distribution of Oxa1 in yeast is altered depending on the energy demands of the cell. Under respiratory conditions Oxa1 is located mainly in the cristae due to the requirement for assembly of the OXPHOS machinery, however under fermentative conditions where OXPHOS is not generally required, Oxa1 is redistributed to the boundary membrane (Stoldt et al., 2012). An explanation for this may be that Oxa1 is also required for the assembly of Tim22 in the inner membrane and thus has a knock-on effect on the assembly of many carrier proteins which are still required under fermentative conditions (Hildenbeutel et al., 2012; Stiller et al., 2016).

While the function of Oxa1 as a membrane protein insertase is clear, a direct mechanistic understanding of its function remains

elusive. It does appear to form voltage-gated ion channels when reconstituted in lipid membranes however the *in vivo* oligomeric structure as well as the mechanism allowing membrane protein lateral diffusion remain unclear (Krüger et al., 2012). No high-resolution structure for Oxa1 exists and would be a prerequisite to further our understanding of the role of Oxa1 in membrane protein biogenesis.

OUTLOOK

The field of mitochondrial membrane protein biogenesis has burgeoned in recent years. Advances in technologies such as cryo-EM have led to important discoveries enhancing our mechanistic understanding of this remarkably complex process. One thing that has become increasingly clear in recent years is the variety of membrane insertase and translocase complexes that exist within the mitochondria and appear to be highly adaptive, and most often act in concert with each other in dynamic ways to facilitate membrane protein biogenesis.

Even the relatively well understood presequence and carrier insertion pathways have revealed some new and exciting features recently. For example, the fact that the presequence (stop-transfer) pathway of TIM23 is able to work in conjunction with the Oxa1 insertase for the biogenesis of a number of inner membrane proteins, as well as the recent discovery of unconventional TIM22 substrates which suggests the recognition and insertion mechanism used by this insertase is more complex than previously thought.

A relatively unexplored avenue to date has been the involvement of the import and assembly protein Mia40 in oxidative folding required for membrane protein assembly. Mia40-dependent disulfide formation within transmembrane helices has however been identified in the essential proteins Tim22 and Tim17 (Wrobel et al., 2013, 2016). These disulfides may well stabilise transmembrane helical structure and could be important for other mitochondrial membrane proteins.

Despite all of these recent advances, there are still a number of key areas that require work to develop a full mechanistic understanding of the mitochondrial membrane protein biogenesis process. As discussed in this review, it is assumed that all of the known insertase complexes are able to laterally diffuse growing membrane proteins into the lipid environment through a "lateral-gate" type mechanism. While there is support for this theory based on the most recent structural data, what remains lacking for all of the mitochondrial insertases is a structural snapshot of this lateral diffusion process occurring. This has been shown for certain related bacterial insertases, but certainly an independent verification of this process by mitochondrial insertases would be incredibly valuable.

High-resolution structural data is still lacking for both the TIM23 complex and the Oxa1 insertase, while the recent structures of the TIM22 complex of both yeast and humans need further work to provide mechanistic details of insertion. It seems likely that the remarkable improvements in cryo-EM techniques will lead to structural data for these complexes being available in the near future and will likely provide us with further clues as to the insertion process. It will be very interesting to see structural snapshots of precursor protein translocation and biogenesis through all of the mitochondrial insertase complexes and to analyse these in conjunction with previously published cross-linking data to further elucidate the translocation and insertion process in mitochondria.

AUTHOR CONTRIBUTIONS

RE and KT wrote the manuscript. RE prepared the figures. All authors contributed to revision of the manuscript and read the final version before submission. KT obtained funding.

FUNDING

Work in our laboratory is supported by UKRI-BBSRC (Grants BB/R009031/1 and BB/T003804/1), an MRC Confidence in Concept grant and a Wellcome Trust early concept development grant (University of Glasgow). Structural biology work in our laboratory benefited from access to the Solution NMR, CERM/CIRMMP, Florence, Italy, an Instruct-ERIC centre.

REFERENCES

Acoba, M. G., Alpergin, E. S. S., Renuse, S., Fernández-del-Río, L., Lu, Y.-W., Khalimonchuk, O., et al. (2021). The Mitochondrial Carrier SFXN1 Is Critical for Complex III Integrity and Cellular Metabolism. *Cel Rep.* 34, 108869. doi:10.1016/j.celrep.2021.108869

Aiyar, R. S., Bohnert, M., Duvezin-Caubet, S., Voisset, C., Gagneur, J., Fritsch, E. S., et al. (2014). Mitochondrial Protein Sorting as a Therapeutic Target for ATP Synthase Disorders. *Nat. Commun.* 5, 5585. doi:10.1038/ncomms6585

Altamura, N., Capitanio, N., Bonnefoy, N., Papa, S., and Dujardin, G. (1996). The Saccharomyces cerevisiae OXA1 Gene Is Required for the Correct Assembly of Cytochrome C Oxidase and Oligomycin-Sensitive ATP Synthase. *FEBS Lett.* 382, 111–115. doi:10.1016/0014-5793(96)00165-2

Araiso, Y., Imai, K., and Endo, T. (2021). Structural Snapshot of the Mitochondrial Protein Import Gate. *FEBS J.* 288, 5300–5310. doi:10.1111/febs.15661

Araiso, Y., Tsutsumi, A., Qiu, J., Imai, K., Shiota, T., Song, J., et al. (2019). Structure of the Mitochondrial Import Gate Reveals Distinct Preprotein Paths. *Nature* 575, 395–401. doi:10.1038/s41586-019-1680-7

Asseck, L. Y., Mehlhorn, D. G., Monroy, J. R., Ricardi, M. M., Breuninger, H., Wallmeroth, N., et al. (2021). Endoplasmic Reticulum Membrane Receptors of the GET Pathway Are Conserved throughout Eukaryotes. *Proc. Natl. Acad. Sci. USA* 118, e2017636118. doi:10.1073/pnas.2017636118

Backes, S., Bykov, Y. S., Flohr, T., Räschle, M., Zhou, J., Lenhard, S., et al. (2021). The Chaperone-Binding Activity of the Mitochondrial Surface Receptor Tom70 Protects the Cytosol against Mitoprotein-Induced Stress. *Cel Rep.* 35, 108936. doi:10.1016/j.celrep.2021.108936

Banerjee, R., Gladkova, C., Mapa, K., Witte, G., and Mokranjac, D. (2015). Protein Translocation Channel of Mitochondrial Inner Membrane and Matrix-Exposed Import Motor Communicate via Two-Domain Coupling Protein. *Elife* 4, e11897. doi:10.7554/eLife.11897

Bauer, M. F., Rothbauer, U., Mühlenbein, N., Smith, R. J., Gerbitz, K., Neupert, W., et al. (1999). The Mitochondrial TIM22 Preprotein Translocase Is Highly

Conserved throughout the Eukaryotic Kingdom. *FEBS Lett.* 464, 41–47. doi:10.1016/S0014-5793(99)01665-8

Becker, T., Guiard, B., Thornton, N., Zufall, N., Stroud, D. A., Wiedemann, N., et al. (2010). Assembly of the Mitochondrial Protein Import Channel. *Mol. Biol. Cel* 21, 3106–3113. doi:10.1091/mbc.E10-06-0518

Becker, T., Pfannschmidt, S., Guiard, B., Stojanovski, D., Milenkovic, D., Kutik, S., et al. (2008). Biogenesis of the Mitochondrial TOM Complex. *J. Biol. Chem.* 283, 120–127. doi:10.1074/jbc.M706997200

Becker, T., Wenz, L.-S., Krüger, V., Lehmann, W., Müller, J. M., Goroncy, L., et al. (2011a). The Mitochondrial Import Protein Mim1 Promotes Biogenesis of Multispanning Outer Membrane Proteins. *J. Cel Biol.* 194, 387–395. doi:10.1083/jcb.201102044

Becker, T., Wenz, L.-S., Thornton, N., Stroud, D., Meisinger, C., Wiedemann, N., et al. (2011b). Biogenesis of Mitochondria: Dual Role of Tom7 in Modulating Assembly of the Preprotein Translocase of the Outer Membrane. *J. Mol. Biol.* 405, 113–124. doi:10.1016/j.jmb.2010.11.002

Bender, T., Pena, G., and Martinou, J. C. (2015). Regulation of Mitochondrial Pyruvate Uptake by Alternative Pyruvate Carrier Complexes. *EMBO J.* 34, 911–924. doi:10.15252/embj.201490197

Bohnert, M., Pfanner, N., and van der Laan, M. (2015). Mitochondrial Machineries for Insertion of Membrane Proteins. *Curr. Opin. Struct. Biol.* 33, 92–102. doi:10.1016/j.sbi.2015.07.013

Bohnert, M., Rehling, P., Guiard, B., Herrmann, J. M., Pfanner, N., and Van Der Laan, M. (2010). Cooperation of Stop-Transfer and Conservative Sorting Mechanisms in Mitochondrial Protein Transport. *Curr. Biol.* 20, 1227–1232. doi:10.1016/j.cub.2010.05.058

Bolliger, L., Junne, T., Schatz, G., and Lithgow, T. (1995). Acidic Receptor Domains on Both Sides of the Outer Membrane Mediate Translocation of Precursor Proteins into Yeast Mitochondria. *EMBO J.* 14, 6318–6326. doi:10.1002/j.1460-2075.1995.tb00322.x

Bonnefoy, N., Chalvet, F., Hamel, P., Slonimski, P. P., and Dujardin, G. (1994). OXA1, a Saccharomyces cerevisiae Nuclear Gene Whose Sequence Is Conserved Form Prokaryotes to Eukaryotes Controls Cytochrome Oxidase Biogenesis. *J. Mol. Biol.* 239, 201–212. doi:10.1006/jmbi.1994.1363

Chacinska, A., Lind, M., Frazier, A. E., Dudek, J., Meisinger, C., Geissler, A., et al. (2005). Mitochondrial Presequence Translocase: Switching between TOM Tethering and Motor Recruitment Involves Tim21 and Tim17. *Cell* 120, 817–829. doi:10.1016/j.cell.2005.01.011

Chacinska, A., van der Laan, M., Mehnert, C. S., Guiard, B., Mick, D. U., Hutu, D. P., et al. (2010). Distinct Forms of Mitochondrial TOM-TIM Supercomplexes Define Signal-dependent States of Preprotein Sorting. *Mol. Cel. Biol.* 30, 307–318. doi:10.1128/mcb.00749-09

Chocron, E. S., Munkácsy, E., and Pickering, A. M. (2019). Cause or Casualty: The Role of Mitochondrial DNA in Aging and Age-Associated Disease. *Biochim. Biophys. Acta (Bba) - Mol. Basis Dis.* 1865, 285–297. doi:10.1016/j.bbadis.2018.09.035

Demishtein-Zohary, K., Marom, M., Neupert, W., Mokranjac, D., and Azem, A. (2015). GxxxG Motifs Hold the TIM23 Complex Together. *FEBS J.* 282, 2178–2186. doi:10.1111/febs.13266

Diederichs, K. A., Ni, X., Rollauer, S. E., Botos, I., Tan, X., King, M. S., et al. (2020). Structural Insight into Mitochondrial β-barrel Outer Membrane Protein Biogenesis. *Nat. Commun.* 11: 3290. doi:10.1038/s41467-020-17144-1

Diekert, K., Kispal, G., Guiard, B., and Lill, R. (1999). An Internal Targeting Signal Directing Proteins into the Mitochondrial Intermembrane Space. *Proc. Natl. Acad. Sci.* 96, 11752–11757. doi:10.1073/pnas.96.21.11752

Dietmeier, K., Hönlinger, A., Bömer, U., Dekker, P. J. T., Eckerskorn, C., Lottspeich, F., et al. (1997). Tom5 Functionally Links Mitochondrial Preprotein Receptors to the General Import Pore. *Nature* 388, 195–200. doi:10.1038/40663

Dimmer, K. S., Papić, D., Schumann, B., Sperl, D., Krumpe, K., Walther, D. M., et al. (2012). A Crucial Role of Mim2 in the Biogenesis of Mitochondrial Outer Membrane Proteins. *J. Cel Sci.* 125, 3464–3473. doi:10.1242/jcs.103804

Doan, K. N., Grevel, A., Mårtensson, C. U., Ellenrieder, L., Thornton, N., Wenz, L.-S., et al. (2020). The Mitochondrial Import Complex MIM Functions as Main Translocase for α-Helical Outer Membrane Proteins. *Cel Rep.* 31, 107567. doi:10.1016/j.celrep.2020.107567

Doyle, M. T., and Bernstein, H. D. (2019). Bacterial Outer Membrane Proteins Assemble via Asymmetric Interactions with the BamA β-barrel. *Nat. Commun.* 10, 3358. doi:10.1038/s41467-019-11230-9

Eaglesfield, R., Madsen, M. A., Sanyal, S., Reboud, J., and Amtmann, A. (2021). Cotranslational Recruitment of Ribosomes in Protocells Recreates a Translocon-independent Mechanism of Proteorhodopsin Biogenesis. *iScience* 24, 102429. doi:10.1016/j.isci.2021.102429

Edwards, R., Eaglesfield, R., and Tokatlidis, K. (2021). The Mitochondrial Intermembrane Space: The Most Constricted Mitochondrial Sub-compartment with the Largest Variety of Protein Import Pathways. *Open Biol.* 11, 210002. doi:10.1098/rsob.210002

Edwards, R., and Tokatlidis, K. (2019). The Yeast Voltage-dependent Anion Channel Porin: More IMPORTant Than Just Metabolite Transport. *Mol. Cel.* 73, 861–862. doi:10.1016/J.MOLCEL.2019.02.028

Ellenrieder, L., Dieterle, M. P., Doan, K. N., Mårtensson, C. U., Floerchinger, A., Campo, M. L., et al. (2019). Dual Role of Mitochondrial Porin in Metabolite Transport across the Outer Membrane and Protein Transfer to the Inner Membrane. *Mol. Cel.* 73, 1056–1065. doi:10.1016/j.molcel.2018.12.014

Ellenrieder, L., Opaliński, Ł., Becker, L., Krüger, V., Mirus, O., Straub, S. P., et al. (2016). Separating Mitochondrial Protein Assembly and Endoplasmic Reticulum Tethering by Selective Coupling of Mdm10. *Nat. Commun.* 7, 13021. doi:10.1038/ncomms13021

Flinner, N., Ellenrieder, L., Stiller, S. B., Becker, T., Schleiff, E., and Mirus, O. (2013). Mdm10 Is an Ancient Eukaryotic Porin Co-occurring with the ERMES Complex. *Biochim. Biophys. Acta (Bba) - Mol. Cel Res.* 1833, 3314–3325. doi:10.1016/j.bbamcr.2013.10.006

Freel, K. C., Friedrich, A., and Schacherer, J. (2015). Mitochondrial Genome Evolution in Yeasts: An All-Encompassing View. *FEMS Yeast Res.* 15, fov023. doi:10.1093/femsyr/fov023

Gabriel, K., Egan, B., and Lithgow, T. (2003). Tom40, the Import Channel of the Mitochondrial Outer Membrane, Plays an Active Role in Sorting Imported Proteins. *EMBO J.* 22, 2380–2386. doi:10.1093/emboj/cdg229

Gebert, N., Gebert, M., Oeljeklaus, S., von der Malsburg, K., Stroud, D. A., Kulawiak, B., et al. (2011). Dual Function of Sdh3 in the Respiratory Chain and TIM22 Protein Translocase of the Mitochondrial Inner Membrane. *Mol. Cel.* 44, 811–818. doi:10.1016/j.molcel.2011.09.025

Gomkale, R., Cruz-Zaragoza, L. D., Suppanz, I., Guiard, B., Montoya, J., Callegari, S., et al. (2020). Defining the Substrate Spectrum of the TIM22 Complex Identifies Pyruvate Carrier Subunits as Unconventional Cargos. *Curr. Biol.* 30, 1119–1127. doi:10.1016/j.cub.2020.01.024

Gornicka, A., Bragoszewski, P., Chroscicki, P., Wenz, L.-S., Schulz, C., Rehling, P., et al. (2014). A Discrete Pathway for the Transfer of Intermembrane Space Proteins across the Outer Membrane of Mitochondria. *Mol. Biol. Cel.* 25, 3999–4009. doi:10.1091/mbc.E14-06-1155

Habib, S. J., Waizenegger, T., Lech, M., Neupert, W., and Rapaport, D. (2005). Assembly of the TOB Complex of Mitochondria. *J. Biol. Chem.* 280, 6434–6440. doi:10.1074/jbc.M411510200

Hegde, R. S., and Keenan, R. J. (2021). The Mechanisms of Integral Membrane Protein Biogenesis. *Nat. Rev. Mol. Cel Biol.* 28, 1–18. doi:10.1038/s41580-021-00413-2

Hennon, S. W., Soman, R., Zhu, L., and Dalbey, R. E. (2015). YidC/Alb3/Oxa1 Family of Insertases. *J. Biol. Chem.* 290, 14866–14874. doi:10.1074/jbc.R115.638171

Hildenbeutel, M., Theis, M., Geier, M., Haferkamp, I., Neuhaus, H. E., Herrmann, J. M., et al. (2012). The Membrane Insertase Oxa1 Is Required for Efficient Import of Carrier Proteins into Mitochondria. *J. Mol. Biol.* 423, 590–599. doi:10.1016/j.jmb.2012.07.018

Höhr, A. I. C., Lindau, C., Wirth, C., Qiu, J., Stroud, D. A., Kutik, S., et al. (2018). Membrane Protein Insertion through a Mitochondrial β-barrel Gate. *Science* 359, eaah6834. doi:10.1126/science.aah6834

Hoppins, S. C., and Nargang, F. E. (2004). The Tim8-Tim13 Complex of Neurospora Crassa Functions in the Assembly of Proteins into Both Mitochondrial Membranes. *J. Biol. Chem.* 279, 12396–12405. doi:10.1074/jbc.M313037200

Horten, P., Colina-Tenorio, L., and Rampelt, H. (2020). Biogenesis of Mitochondrial Metabolite Carriers. *Biomolecules* 10, 1008. doi:10.3390/biom10071008

Hulett, J. M., Lueder, F., Chan, N. C., Perry, A. J., Wolynec, P., Likić, V. A., et al. (2008). The Transmembrane Segment of Tom20 Is Recognized by Mim1 for

Docking to the Mitochondrial TOM Complex. *J. Mol. Biol.* 376, 694–704. doi:10.1016/j.jmb.2007.12.021

Hutu, D. P., Guiard, B., Chacinska, A., Becker, D., Pfanner, N., Rehling, P., et al. (2008). Mitochondrial Protein Import Motor: Differential Role of Tim44 in the Recruitment of Pam17 and J-Complex to the Presequence Translocase. *Mol. Biol. Cel.* 19, 2642–2649. doi:10.1091/mbc.E07-12-1226

Ieva, R., Schrempp, S. G., Opaliński, Ł., Wollweber, F., Höß, P., Heisswolf, A. K., et al. (2014). Mgr2 Functions as Lateral Gatekeeper for Preprotein Sorting in the Mitochondrial Inner Membrane. *Mol. Cel.* 56, 641–652. doi:10.1016/j.molcel.2014.10.010

Imai, K., Fujita, N., Gromiha, M. M., and Horton, P. (2011). Eukaryote-wide Sequence Analysis of Mitochondrial β-barrel Outer Membrane Proteins. *BMC Genomics* 12, 79. doi:10.1186/1471-2164-12-79

Itoh, Y., Andréll, J., Choi, A., Richter, U., Maiti, P., Best, R. B., et al. (2021). Mechanism of Membrane-Tethered Mitochondrial Protein Synthesis. *Science* 371, 846–849. doi:10.1126/science.abe0763

Jackson, T. D., Hock, D. H., Fujihara, K. M., Palmer, C. S., Frazier, A. E., Low, Y. C., et al. (2021). The TIM22 Complex Mediates the Import of Sideroflexins and Is Required for Efficient Mitochondrial One-Carbon Metabolism. *Mol. Biol. Cel.* 32, 475–491. doi:10.1091/MBC.E20-06-0390

Jores, T., Klinger, A., Groß, L. E., Kawano, S., Flinner, N., Duchardt-Ferner, E., et al. (2016). Characterization of the Targeting Signal in Mitochondrial β-barrel Proteins. *Nat. Commun.* 7, 12036. doi:10.1038/ncomms12036

Jores, T., Lawatscheck, J., Beke, V., Franz-Wachtel, M., Yunoki, K., Fitzgerald, J. C., et al. (2018). Cytosolic Hsp70 and Hsp40 Chaperones Enable the Biogenesis of Mitochondrial β-barrel Proteins. *J. Cel Biol.* 217, 3091–3108. doi:10.1083/jcb.201712029

Kang, Y., Baker, M. J., Liem, M., Louber, J., McKenzie, M., Atukorala, I., et al. (2016). Tim29 Is a Novel Subunit of the Human TIM22 Translocase and Is Involved in Complex Assembly and Stability. *Elife* 5, e17463. doi:10.7554/eLife.17463

Kang, Y., Stroud, D. A., Baker, M. J., De Souza, D. P., Frazier, A. E., Liem, M., et al. (2017). Sengers Syndrome-Associated Mitochondrial Acylglycerol Kinase Is a Subunit of the Human TIM22 Protein Import Complex. *Mol. Cel.* 67, 457–470. doi:10.1016/j.molcel.2017.06.014

Keil, M., Bareth, B., Woellhaf, M. W., Peleh, V., Prestele, M., Rehling, P., et al. (2012). Oxa1-ribosome Complexes Coordinate the Assembly of Cytochrome C Oxidase in Mitochondria. *J. Biol. Chem.* 287, 34484–34493. doi:10.1074/jbc.M112.382630

Kemper, C., Habib, S. J., Engl, G., Heckmeyer, P., Dimmer, K. S., and Rapaport, D. (2008). Integration of Tail-Anchored Proteins into the Mitochondrial Outer Membrane Does Not Require Any Known Import Components. *J. Cel Sci.* 121, 1990–1998. doi:10.1242/jcs.024034

Kerscher, O., Sepuri, N. B., and Jensen, R. E. (2000). Tim18p Is a New Component of the Tim54p-Tim22p Translocon in the Mitochondrial Inner Membrane. *Mol. Biol. Cel.* 11, 103–116. doi:10.1091/mbc.11.1.103

Kiebler, M., Pfaller, R., Söllner, T., Griffiths, G., Horstmann, H., Pfanner, N., et al. (1990). Identification of a Mitochondrial Receptor Complex Required for Recognition and Membrane Insertion of Precursor Proteins. *Nature* 348, 610–616. doi:10.1038/348610a0

Koehler, C. M., Murphy, M. P., Bally, N. A., Leuenberger, D., Oppliger, W., Dolfini, L., et al. (2000). Tim18p, a New Subunit of the TIM22 Complex that Mediates Insertion of Imported Proteins into the Yeast Mitochondrial Inner Membrane. *Mol. Cel. Biol.* 20, 1187–1193. doi:10.1128/mcb.20.4.1187-1193.2000

Kornmann, B., Currie, E., Collins, S. R., Schuldiner, M., Nunnari, J., Weissman, J. S., et al. (2009). An ER-Mitochondria Tethering Complex Revealed by a Synthetic Biology Screen. *Science* 325, 477–481. doi:10.1126/science.1175088

Kornmann, B., and Walter, P. (2010). ERMES-mediated ER-Mitochondria Contacts: Molecular Hubs for the Regulation of Mitochondrial Biology. *J. Cel Sci.* 123, 1389–1393. doi:10.1242/jcs.058636

Kory, N., Wyant, G. A., Prakash, G., uit de Bos, J., Bottanelli, F., Pacold, M. E., et al. (2018). SFXN1 Is a Mitochondrial Serine Transporter Required for One-Carbon Metabolism. *Science* 362, eaat9528. doi:10.1126/science.aat9528

Kozjak, V., Wiedemann, N., Milenkovic, D., Lohaus, C., Meyer, H. E., Guiard, B., et al. (2003). An Essential Role of Sam50 in the Protein Sorting and Assembly Machinery of the Mitochondrial Outer Membrane. *J. Biol. Chem.* 278, 48520–48523. doi:10.1074/jbc.C300442200

Kozjak-Pavlovic, V., Ott, C., Götz, M., and Rudel, T. (2011). Neisserial Omp85 Protein Is Selectively Recognized and Assembled into Functional Complexes in the Outer Membrane of Human Mitochondria. *J. Biol. Chem.* 286, 27019–27026. doi:10.1074/jbc.M111.232249

Kreimendahl, S., Schwichtenberg, J., Günnewig, K., Brandherm, L., and Rassow, J. (2020). The Selectivity Filter of the Mitochondrial Protein Import Machinery. *BMC Biol.* 18, 156. doi:10.1186/s12915-020-00888-z

Krüger, V., Becker, T., Becker, L., Montilla-Martinez, M., Ellenrieder, L., Vögtle, F.-N., et al. (2017). Identification of New Channels by Systematic Analysis of the Mitochondrial Outer Membrane. *J. Cel Biol.* 216, 3485–3495. doi:10.1083/jcb.201706043

Krüger, V., Deckers, M., Hildenbeutel, M., Van Der Laan, M., Hellmers, M., Dreker, C., et al. (2012). The Mitochondrial Oxidase Assembly Protein1 (Oxa1) Insertase Forms a Membrane Pore in Lipid Bilayers. *J. Biol. Chem.* 287, 33314–33326. doi:10.1074/jbc.M112.387563

Krumpe, K., Frumkin, I., Herzig, Y., Rimon, N., Özbalci, C., Brügger, B., et al. (2012). Ergosterol Content Specifies Targeting of Tail-Anchored Proteins to Mitochondrial Outer Membranes. *Mol. Biol. Cel.* 23, 3927–3935. doi:10.1091/mbc.E11-12-0994

Kühlbrandt, W. (2015). Structure and Function of Mitochondrial Membrane Protein Complexes. *BMC Biol.* 13, 89. doi:10.1186/s12915-015-0201-x

Kuhn, A., Stuart, R., Henry, R., and Dalbey, R. E. (2003). The Alb3/Oxa1/YidC Protein Family: Membrane-Localized Chaperones Facilitating Membrane Protein Insertion. *Trends Cel Biol.* 13, 510–516. doi:10.1016/j.tcb.2003.08.005

Kummer, E., Leibundgut, M., Rackham, O., Lee, R. G., Boehringer, D., Filipovska, A., et al. (2018). Unique Features of Mammalian Mitochondrial Translation Initiation Revealed by Cryo-EM. *Nature* 560, 263–267. doi:10.1038/s41586-018-0373-y

Kutik, S., Stojanovski, D., Becker, L., Becker, T., Meinecke, M., Krüger, V., et al. (2008). Dissecting Membrane Insertion of Mitochondrial β-Barrel Proteins. *Cell* 132, 1011–1024. doi:10.1016/j.cell.2008.01.028

Lee, J., Kim, D. H., and Hwang, I. (2014). Specific Targeting of Proteins to Outer Envelope Membranes of Endosymbiotic Organelles, Chloroplasts, and Mitochondria. *Front. Plant Sci.* 5, 173. doi:10.3389/fpls.2014.00173

Li, Y., Dudek, J., Guiard, B., Pfanner, N., Rehling, P., and Voos, W. (2004). The Presequence Translocase-Associated Protein Import Motor of Mitochondria. *J. Biol. Chem.* 279, 38047–38054. doi:10.1074/jbc.M404319200

Lionaki, E., de Marcos Lousa, C., Baud, C., Vougioukalaki, M., Panayotou, G., and Tokatlidis, K. (2008). The Essential Function of Tim12 *In Vivo* Is Ensured by the Assembly Interactions of its C-Terminal Domain. *J. Biol. Chem.* 283, 15747–15753. doi:10.1074/jbc.M800350200

Lithgow, T., Junne, T., Suda, K., Gratzer, S., and Schatz, G. (1994). The Mitochondrial Outer Membrane Protein Mas22p Is Essential for Protein Import and Viability of Yeast. *Proc. Natl. Acad. Sci.* 91, 11973–11977. doi:10.1073/pnas.91.25.11973

Luciano, P., Vial, S., Vergnolle, M. A. S., Dyall, S. D., Robinson, D. R., and Tokatlidis, K. (2001). Functional Reconstitution of the Import of the Yeast ADP/ATP Carrier Mediated by the TIM10 Complex. *EMBO J.* 20, 4099–4106. doi:10.1093/emboj/20.15.4099

Lueder, F., and Lithgow, T. (2009). The Three Domains of the Mitochondrial Outer Membrane Protein Mim1 Have Discrete Functions in Assembly of the TOM Complex. *FEBS Lett.* 583, 1475–1480. doi:10.1016/j.febslet.2009.03.064

Mårtensson, C. U., Priesnitz, C., Song, J., Ellenrieder, L., Doan, K. N., Boos, F., et al. (2019). Mitochondrial Protein Translocation-Associated Degradation. *Nature* 569, 679–683. doi:10.1038/s41586-019-1227-y

Matta, S. K., Kumar, A., and D'Silva, P. (2020). Mgr2 Regulates Mitochondrial Preprotein Import by Associating with Channel-Forming Tim23 Subunit. *Mol. Biol. Cel.* 31, 1112–1123. doi:10.1091/mbc.E19-12-0677

Meinecke, M., Wagner, R., Kovermann, P., Guiard, B., Mick, D. U., Hutu, D. P., et al. (2006). Tim50 Maintains the Permeability Barrier of the Mitochondrial Inner Membrane. *Science* 312, 1523–1526. doi:10.1126/science.1127628

Meisinger, C., Rissler, M., Chacinska, A., Szklarz, L. K. S., Milenkovic, D., Kozjak, V., et al. (2004). The Mitochondrial Morphology Protein Mdm10 Functions in Assembly of the Preprotein Translocase of the Outer Membrane. *Develop. Cel.* 7, 61–71. doi:10.1016/j.devcel.2004.06.003

Meisinger, C., Wiedemann, N., Rissler, M., Strub, A., Milenkovic, D., Schönfisch, B., et al. (2006). Mitochondrial Protein Sorting. *J. Biol. Chem.* 281, 22819–22826. doi:10.1074/jbc.M602679200

Miao, B., Davis, J. E., and Craig, E. A. (1997). Mge1 Functions as a Nucleotide Release Factor for Ssc1, a Mitochondrial Hsp70 of Saccharomyces cerevisiae. *J. Mol. Biol.* 265, 541–552. doi:10.1006/jmbi.1996.0762

Mick, D. U., Dennerlein, S., Wiese, H., Reinhold, R., Pacheu-Grau, D., Lorenzi, I., et al. (2012). MITRAC Links Mitochondrial Protein Translocation to Respiratory-Chain Assembly and Translational Regulation. *Cell* 151, 1528–1541. doi:10.1016/j.cell.2012.11.053

Milenkovic, D., Kozjak, V., Wiedemann, N., Lohaus, C., Meyer, H. E., Guiard, B., et al. (2004). Sam35 of the Mitochondrial Protein Sorting and Assembly Machinery Is a Peripheral Outer Membrane Protein Essential for Cell Viability. *J. Biol. Chem.* 279, 22781–22785. doi:10.1074/jbc.C400120200

Milenkovic, D., Ramming, T., Müller, J. M., Wenz, L.-S., Gebert, N., Schulze-Specking, A., et al. (2009). Identification of the Signal Directing Tim9 and Tim10 into the Intermembrane Space of Mitochondria. *Mol. Biol. Cel.* 20, 2530–2539. doi:10.1091/mbc.E08-11-1108

Moczko, M., Bömer, U., Kübrich, M., Zufall, N., Hönlinger, A., and Pfanner, N. (1997). The Intermembrane Space Domain of Mitochondrial Tom22 Functions as a Trans Binding Site for Preproteins with N-Terminal Targeting Sequences. *Mol. Cel. Biol.* 17, 6574–6584. doi:10.1128/mcb.17.11.6574

Model, K., Meisinger, C., Prinz, T., Wiedemann, N., Truscott, K. N., Pfanner, N., et al. (2001). Multistep Assembly of the Protein Import Channel of the Mitochondrial Outer Membrane. *Nat. Struct. Biol.* 8, 361–370. doi:10.1038/86253

Mokranjac, D., and Neupert, W. (2015). Architecture of a Protein Entry Gate. *Nature* 528, 201–202. doi:10.1038/nature16318

Ott, M., Prestele, M., Bauerschmitt, H., Funes, S., Bonnefoy, N., and Herrmann, J. M. (2006). Mba1, a Membrane-Associated Ribosome Receptor in Mitochondria. *Embo J.* 25, 1603–1610. doi:10.1038/sj.emboj.7601070

Papić, D., Krumpe, K., Dukanovic, J., Dimmer, K. S., and Rapaport, D. (2011). Multispan Mitochondrial Outer Membrane Protein Ugo1 Follows a Unique Mim1-dependent Import Pathway. *J. Cel Biol.* 194, 397–405. doi:10.1083/jcb.201102041

Park, K., Botelho, S. C., Hong, J., Österberg, M., and Kim, H. (2013). Dissecting Stop Transfer versus Conservative Sorting Pathways for Mitochondrial Inner Membrane Proteins *In Vivo*. *J. Biol. Chem.* 288, 1521–1532. doi:10.1074/jbc.M112.409748

Paschen, S. A., Neupert, W., and Rapaport, D. (2005). Biogenesis of β-barrel Membrane Proteins of Mitochondria. *Trends Biochem. Sci.* 30, 575–582. doi:10.1016/j.tibs.2005.08.009

Pfanner, N., Warscheid, B., and Wiedemann, N. (2019). Mitochondrial Proteins: from Biogenesis to Functional Networks. *Nat. Rev. Mol. Cel Biol.* 20, 267–284. doi:10.1038/s41580-018-0092-0

Pfanner, N., Wiedemann, N., Meisinger, C., and Lithgow, T. (2004). Assembling the Mitochondrial Outer Membrane. *Nat. Struct. Mol. Biol.* 11, 1044–1048. doi:10.1038/nsmb852

Popov-Čeleketić, J., Waizenegger, T., and Rapaport, D. (2008). Mim1 Functions in an Oligomeric Form to Facilitate the Integration of Tom20 into the Mitochondrial Outer Membrane. *J. Mol. Biol.* 376, 671–680. doi:10.1016/j.jmb.2007.12.006

Preuss, M., Leonhard, K., Hell, K., Stuart, R. A., Neupert, W., and Herrmann, J. M. (2001). Mba1, a Novel Component of the Mitochondrial Protein export Machinery of the Yeast Saccharomyces cerevisiae. *J. Cel Biol.* 153, 1085–1096. doi:10.1083/jcb.153.5.1085

Qi, L., Wang, Q., Guan, Z., Wu, Y., Shen, C., Hong, S., et al. (2021). Cryo-EM Structure of the Human Mitochondrial Translocase TIM22 Complex. *Cell Res.* 31, 369–372. doi:10.1038/s41422-020-00400-w

Qiu, J., Wenz, L.-S., Zerbes, R. M., Oeljeklaus, S., Bohnert, M., Stroud, D. A., et al. (2013). Coupling of Mitochondrial Import and Export Translocases by Receptor-Mediated Supercomplex Formation. *Cell* 154, 596–608. doi:10.1016/j.cell.2013.06.033

Rampelt, H., Sucec, I., Bersch, B., Horten, P., Perschil, I., Martinou, J.-C., et al. (2020). The Mitochondrial Carrier Pathway Transports Non-canonical Substrates with an Odd Number of Transmembrane Segments. *BMC Biol.* 18, 2. doi:10.1186/s12915-019-0733-6

Rapaport, D., and Neupert, W. (1999). Biogenesis of Tom40, Core Component of the TOM Complex of Mitochondria. *J. Cel Biol.* 146, 321–332. doi:10.1083/jcb.146.2.321

Rath, S., Sharma, R., Gupta, R., Ast, T., Chan, C., Durham, T. J., et al. (2021). MitoCarta3.0: An Updated Mitochondrial Proteome Now with Sub-organelle Localization and Pathway Annotations. *Nucleic Acids Res.* 49, D1541–D1547. doi:10.1093/nar/gkaa1011

Rehling, P., Brandner, K., and Pfanner, N. (2004). Mitochondrial Import and the Twin-Pore Translocase. *Nat. Rev. Mol. Cel Biol.* 5, 519–530. doi:10.1038/nrm1426

Rehling, P., Model, K., Brandner, K., Kovermann, P., Sickmann, A., Meyer, H. E., et al. (2003). Protein Insertion into the Mitochondrial Inner Membrane by a Twin-Pore Translocase. *Science* 299, 1747–1751. doi:10.1126/science.1080945

Rey, T., Zaganelli, S., Cuillery, E., Vartholomaiou, E., Croisier, M., Martinou, J.-C., et al. (2020). Mitochondrial RNA Granules Are Fluid Condensates Positioned by Membrane Dynamics. *Nat. Cel Biol.* 22, 1180–1186. doi:10.1038/s41556-020-00584-8

Sakaue, H., Shiota, T., Ishizaka, N., Kawano, S., Tamura, Y., Tan, K. S., et al. (2019). Porin Associates with Tom22 to Regulate the Mitochondrial Protein Gate Assembly. *Mol. Cel.* 73, 1044–1055. e8. doi:10.1016/j.molcel.2019.01.003

Sakuragi, S., Liu, Q., and Craig, E. (1999). Interaction between the Nucleotide Exchange Factor Mge1 and the Mitochondrial Hsp70 Ssc1. *J. Biol. Chem.* 274, 11275–11282. doi:10.1074/jbc.274.16.11275

Schendzielorz, A. B., Bragoszewski, P., Naumenko, N., Gomkale, R., Schulz, C., Guiard, B., et al. (2018). Motor Recruitment to the TIM23 Channel's Lateral Gate Restricts Polypeptide Release into the Inner Membrane. *Nat. Commun.* 9, 4028. doi:10.1038/s41467-018-06492-8

Schmidt, O., Pfanner, N., and Meisinger, C. (2010). Mitochondrial Protein Import: From Proteomics to Functional Mechanisms. *Nat. Rev. Mol. Cel Biol.* 11, 655–667. doi:10.1038/nrm2959

Scotti, P. A., Urbanus, M. L., Brunner, J., de Gier, J.-W. L., von Heijne, G., van der Does, C., et al. (2000). YidC, the Escherichia coli Homologue of Mitochondrial Oxa1p, Is a Component of the Sec Translocase. *Embo J.* 19, 542–549. doi:10.1093/emboj/19.4.542

Setoguchi, K., Otera, H., and Mihara, K. (2006). Cytosolic Factor- and TOM-independent Import of C-Tail-Anchored Mitochondrial Outer Membrane Proteins. *EMBO J.* 25, 5635–5647. doi:10.1038/sj.emboj.7601438

Shiota, T., Imai, K., Qiu, J., Hewitt, V. L., Tan, K., Shen, H.-H., et al. (2015). Molecular Architecture of the Active Mitochondrial Protein Gate. *Science* 349, 1544–1548. doi:10.1126/science.aac6428

Shiota, T., Mabuchi, H., Tanaka-Yamano, S., Yamano, K., and Endo, T. (2011). *In Vivo* protein-interaction Mapping of a Mitochondrial Translocator Protein Tom22 at Work. *Proc. Natl. Acad. Sci.* 108, 15179–15183. doi:10.1073/pnas.1105921108

Sirrenberg, C., Bauer, M. F., Guiard, B., Neupert, W., and Brunner, M. (1996). Import of Carrier Proteins into the Mitochondrial Inner Membrane Mediated by Tim22. *Nature* 384, 582–585. doi:10.1038/384582a0

Sirrenberg, C., Endres, M., Fölsch, H., Stuart, R. A., Neupert, W., and Brunner, M. (1998). Carrier Protein Import into Mitochondria Mediated by the Intermembrane Proteins Tim10/Mrs11 and Tim12/Mrs5. *Nature* 391, 912–915. doi:10.1038/36136

Song, J., Herrmann, J. M., and Becker, T. (2021). Quality Control of the Mitochondrial Proteome. *Nat. Rev. Mol. Cel Biol.* 22, 54–70. doi:10.1038/s41580-020-00300-2

Song, J., Tamura, Y., Yoshihisa, T., and Endo, T. (2014). A Novel Import Route for an N-Anchor Mitochondrial Outer Membrane Protein Aided by the TIM23 Complex. *EMBO Rep.* 15, 670–677. doi:10.1002/embr.201338142

Stiburek, L., Fornuskova, D., Wenchich, L., Pejznochova, M., Hansikova, H., and Zeman, J. (2007). Knockdown of Human Oxa1l Impairs the Biogenesis of F1Fo-ATP Synthase and NADH:Ubiquinone Oxidoreductase. *J. Mol. Biol.* 374, 506–516. doi:10.1016/j.jmb.2007.09.044

Stiller, S. B., Höpker, J., Oeljeklaus, S., Schütze, C., Schrempp, S. G., Vent-Schmidt, J., et al. (2016). Mitochondrial OXA Translocase Plays a Major Role in Biogenesis of Inner-Membrane Proteins. *Cel Metab.* 23, 901–908. doi:10.1016/j.cmet.2016.04.005

Stoldt, S., Wenzel, D., Hildenbeutel, M., Wurm, C. A., Herrmann, J. M., and Jakobs, S. (2012). The Inner-Mitochondrial Distribution of Oxa1 Depends on the Growth Conditions and on the Availability of Substrates. *Mol. Biol. Cel.* 23, 2292–2301. doi:10.1091/mbc.E11-06-0538

Szyrach, G., Ott, M., Bonnefoy, N., Neupert, W., and Herrmann, J. M. (2003). Ribosome Binding to the Oxa1 Complex Facilitates Co-translational Protein Insertion in Mitochondria. *EMBO J.* 22, 6448–6457. doi:10.1093/emboj/cdg623

Taanman, J. W. (1999). The Mitochondrial Genome: Structure, Transcription, Translation and Replication. *Biochim. Biophys. Acta.* 1410, 103–123. doi:10.1016/S0005-2728(98)00161-3

Takeda, H., Tsutsumi, A., Nishizawa, T., Lindau, C., Busto, J. V., Wenz, L.-S., et al. (2021). Mitochondrial Sorting and Assembly Machinery Operates by β-barrel Switching. *Nature* 590, 163–169. doi:10.1038/s41586-020-03113-7

Thompson, K., Mai, N., Oláhová, M., Scialó, F., Formosa, L. E., Stroud, D. A., et al. (2018). OXA 1L Mutations Cause Mitochondrial Encephalopathy and a Combined Oxidative Phosphorylation Defect. *EMBO Mol. Med.* 10, e9060. doi:10.15252/emmm.201809060

Thornton, N., Stroud, D. A., Milenkovic, D., Guiard, B., Pfanner, N., and Becker, T. (2010). Two Modular Forms of the Mitochondrial Sorting and Assembly Machinery Are Involved in Biogenesis of α-Helical Outer Membrane Proteins. *J. Mol. Biol.* 396, 540–549. doi:10.1016/j.jmb.2009.12.026

Tomasek, D., Rawson, S., Lee, J., Wzorek, J. S., Harrison, S. C., Li, Z., et al. (2020). Structure of a Nascent Membrane Protein as it Folds on the BAM Complex. *Nature* 583, 473–478. doi:10.1038/s41586-020-2370-1

Truscott, K. N., Wiedemann, N., Rehling, P., Muller, H., Meisinger, C., Pfanner, N., et al. (2002). Mitochondrial Import of the ADP/ATP Carrier: the Essential TIM Complex of the Intermembrane Space Is Required for Precursor Release from the TOM Complex. *Mol. Cel. Biol.* 22, 7780–7789. doi:10.1128/mcb.22.22.7780-7789.2002

Tucker, K., and Park, E. (2019). Cryo-EM Structure of the Mitochondrial Protein-Import Channel TOM Complex at Near-Atomic Resolution. *Nat. Struct. Mol. Biol.* 26, 1158–1166. doi:10.1038/s41594-019-0339-2

Ulrich, T., Oberhettinger, P., Schütz, M., Holzer, K., Ramms, A. S., Linke, D., et al. (2014). Evolutionary Conservation in Biogenesis of β-Barrel Proteins Allows Mitochondria to Assemble a Functional Bacterial Trimeric Autotransporter Protein. *J. Biol. Chem.* 289, 29457–29470. doi:10.1074/jbc.M114.565655

van der Laan, M., Meinecke, M., Dudek, J., Hutu, D. P., Lind, M., Perschil, I., et al. (2007). Motor-free Mitochondrial Presequence Translocase Drives Membrane Integration of Preproteins. *Nat. Cel Biol.* 9, 1152–1159. doi:10.1038/ncb1635

Van Der Laan, M., Schrempp, S. G., and Pfanner, N. (2013). Voltage-coupled Conformational Dynamics of Mitochondrial Protein-Import Channel. *Nat. Struct. Mol. Biol.* 20, 915–917. doi:10.1038/nsmb.2643

van der Laan, M., Wiedemann, N., Mick, D. U., Guiard, B., Rehling, P., and Pfanner, N. (2006). A Role for Tim21 in Membrane-potential-dependent Preprotein Sorting in Mitochondria. *Curr. Biol.* 16, 2271–2276. doi:10.1016/j.cub.2006.10.025

Vial, S., Lu, H., Allen, S., Savory, P., Thornton, D., Sheehan, J., et al. (2002). Assembly of TIM9 and TIM10 into a Functional Chaperone. *J. Biol. Chem.* 277, 36100–36108. doi:10.1074/jbc.M202310200

Vitali, D. G., Käser, S., Kolb, A., Dimmer, K. S., Schneider, A., and Rapaport, D. (2018). Independent Evolution of Functionally Exchangeable Mitochondrial Outer Membrane Import Complexes. *Elife* 7:e34488. doi:10.7554/eLife.34488

Vukotic, M., Nolte, H., König, T., Saita, S., Ananjew, M., Krüger, M., et al. (2017). Acylglycerol Kinase Mutated in Sengers Syndrome Is a Subunit of the TIM22 Protein Translocase in Mitochondria. *Mol. Cel.* 67, 471–483. doi:10.1016/j.molcel.2017.06.013

Waegemann, K., Popov-Čeleketić, D., Neupert, W., Azem, A., and Mokranjac, D. (2015). Cooperation of TOM and TIM23 Complexes during Translocation of Proteins into Mitochondria. *J. Mol. Biol.* 427, 1075–1084. doi:10.1016/j.jmb.2014.07.015

Waizenegger, T., Schmitt, S., Zivkovic, J., Neupert, W., and Rapaport, D. (2005). Mim1, a Protein Required for the Assembly of the TOM Complex of Mitochondria. *EMBO Rep.* 6, 57–62. doi:10.1038/sj.embor.7400318

Walther, D. M., Papic, D., Bos, M. P., Tommassen, J., and Rapaport, D. (2009). Signals in Bacterial β-barrel Proteins Are Functional in Eukaryotic Cells for Targeting to and Assembly in Mitochondria. *Proceedings of the National Academy of Sciences* 106, 2531–2536. doi:10.1073/pnas.0807830106

Wang, C., Richter-Dennerlein, R., Pacheu-Grau, D., Liu, F., Zhu, Y., Dennerlein, S., et al. (2020a). MITRAC15/COA1 Promotes Mitochondrial Translation in a ND2 Ribosome-Nascent Chain Complex. *EMBO Rep.* 21, e48833. doi:10.15252/embr.201948833

Wang, Q., Guan, Z., Qi, L., Zhuang, J., Wang, C., Hong, S., et al. (2021). Structural Insight into the SAM-Mediated Assembly of the Mitochondrial TOM Core Complex. *Science* 373, 1377–1381. doi:10.1126/science.abh0704

Wang, W., Chen, X., Zhang, L., Yi, J., Ma, Q., Yin, J., et al. (2020b). Atomic Structure of Human TOM Core Complex. *Cell Discov.* 6, 67. doi:10.1038/s41421-020-00198-2

Weinhäupl, K., Lindau, C., Hessel, A., Wang, Y., Schütze, C., Jores, T., et al. (2018). Structural Basis of Membrane Protein Chaperoning through the Mitochondrial Intermembrane Space. *Cell* 175, 1365–1379. doi:10.1016/j.cell.2018.10.039

Wenz, L.-S., Ellenrieder, L., Qiu, J., Bohnert, M., Zufall, N., van der Laan, M., et al. (2015). Sam37 Is Crucial for Formation of the Mitochondrial TOM-SAM Supercomplex, Thereby Promoting β-barrel Biogenesis. *J. Cel Biol.* 210, 1047–1054. doi:10.1083/jcb.201504119

Wenz, L.-S., Opalinski, u., Schuler, M.-H., Ellenrieder, L., Ieva, R., Bottinger, L., et al. (2014). The Presequence Pathway Is Involved in Protein Sorting to the Mitochondrial Outer Membrane. *EMBO Rep.* 15, 678–685. doi:10.1002/embr.201338144

Wiedemann, N., Kozjak, V., Chacinska, A., Schönfisch, B., Rospert, S., Ryan, M. T., et al. (2003). Machinery for Protein Sorting and Assembly in the Mitochondrial Outer Membrane. *Nature* 424, 565–571. doi:10.1038/nature01753

Wiedemann, N., and Pfanner, N. (2017). Mitochondrial Machineries for Protein Import and Assembly. *Annu. Rev. Biochem.* 86, 685–714. doi:10.1146/annurev-biochem-060815-014352

Wiedemann, N., Pfanner, N., and Ryan, M. T. (2001). The Three Modules of ADP/ATP Carrier Cooperate in Receptor Recruitment and Translocation into Mitochondria. *EMBO J.* 20, 951–960. doi:10.1093/emboj/20.5.951

Wiedemann, N., Truscott, K. N., Pfannschmidt, S., Guiard, B., Meisinger, C., and Pfanner, N. (2004). Biogenesis of the Protein Import Channel Tom40 of the Mitochondrial Outer Membrane. *J. Biol. Chem.* 279, 18188–18194. doi:10.1074/jbc.M400050200

Wiedemann, N., Van Der Laan, M., Hutu, D. P., Rehling, P., and Pfanner, N. (2007). Sorting Switch of Mitochondrial Presequence Translocase Involves Coupling of Motor Module to Respiratory Chain. *J. Cel Biol.* 179, 1115–1122. doi:10.1083/jcb.200709087

Wrobel, L., Sokol, A. M., Chojnacka, M., and Chacinska, A. (2016). The Presence of Disulfide Bonds Reveals an Evolutionarily Conserved Mechanism Involved in Mitochondrial Protein Translocase Assembly. *Sci. Rep.* 6. doi:10.1038/srep27484

Wrobel, L., Trojanowska, A., Sztolsztener, M. E., and Chacinska, A. (2013). Mitochondrial Protein Import: Mia40 Facilitates Tim22 Translocation into the Inner Membrane of Mitochondria. *Mol. Biol. Cel.* 24, 543–554. doi:10.1091/mbc.E12-09-0649

Yamano, K., Tanaka-Yamano, S., and Endo, T. (2010). Tom7 Regulates Mdm10-Mediated Assembly of the Mitochondrial Import Channel Protein TOM40. *J. Biol. Chem.* 285, 41222–41231. doi:10.1074/jbc.M110.163238

Yano, M., Hoogenraad, N., Terada, K., and Mori, M. (2000). Identification and Functional Analysis of Human Tom22 for Protein Import into Mitochondria. *Mol. Cel. Biol.* 20, 7205–7213. doi:10.1128/mcb.20.19.7205-7213.2000

Young, M. J., Bay, D. C., Hausner, G., and Court, D. A. (2007). The Evolutionary History of Mitochondrial Porins. *BMC Evol. Biol.* 7, 31. doi:10.1186/1471-2148-7-31

Zhang, Y., Ou, X., Wang, X., Sun, D., Zhou, X., Wu, X., et al. (2021). Structure of the Mitochondrial TIM22 Complex from Yeast. *Cel Res.* 31, 366–368. doi:10.1038/s41422-020-00399-0

Zorkau, M., Albus, C. A., Berlinguer-Palmini, R., Chrzanowska-Lightowlers, Z. M. A., and Lightowlers, R. N. (2021). High-resolution Imaging Reveals Compartmentalization of Mitochondrial Protein Synthesis in Cultured Human Cells. *Proc. Natl. Acad. Sci. USA.* 118, e2008778118. doi:10.1073/pnas.2008778118

Conflict of Interest: The authors declare that the research was conducted in the absence of any commercial or financial relationships that could be construed as a potential conflict of interest.

Publisher's Note: All claims expressed in this article are solely those of the authors and do not necessarily represent those of their affiliated organizations, or those of the publisher, the editors and the reviewers. Any product that may be evaluated in this article, or claim that may be made by its manufacturer, is not guaranteed or endorsed by the publisher.

frontiers in Molecular Biosciences

REVIEW
published: 03 January 2022
doi: 10.3389/fmolb.2021.798353

The Mysterious Multitude: Structural Perspective on the Accessory Subunits of Respiratory Complex I

*Abhilash Padavannil, Maria G. Ayala-Hernandez, Eimy A. Castellanos-Silva and James A. Letts**

Department of Molecular and Cellular Biology, University of California, Davis, Davis, CA, United States

Complex I (CI) is the largest protein complex in the mitochondrial oxidative phosphorylation electron transport chain of the inner mitochondrial membrane and plays a key role in the transport of electrons from reduced substrates to molecular oxygen. CI is composed of 14 core subunits that are conserved across species and an increasing number of accessory subunits from bacteria to mammals. The fact that adding accessory subunits incurs costs of protein production and import suggests that these subunits play important physiological roles. Accordingly, knockout studies have demonstrated that accessory subunits are essential for CI assembly and function. Furthermore, clinical studies have shown that amino acid substitutions in accessory subunits lead to several debilitating and fatal CI deficiencies. Nevertheless, the specific roles of CI's accessory subunits have remained mysterious. In this review, we explore the possible roles of each of mammalian CI's 31 accessory subunits by integrating recent high-resolution CI structures with knockout, assembly, and clinical studies. Thus, we develop a framework of experimentally testable hypotheses for the function of the accessory subunits. We believe that this framework will provide inroads towards the complete understanding of mitochondrial CI physiology and help to develop strategies for the treatment of CI deficiencies.

Keywords: mitochondrial complex I, oxidative phosphorylation (OXPHOS), accessory subunits, mitochondrial diseases, electron transport chain

OPEN ACCESS

Edited by:
Erika Fernandez-Vizarra, University of Glasgow, United Kingdom

Reviewed by:
Jamie Blaza, University of York, United Kingdom
Cristina Ugalde, Research Institute Hospital 12 de Octubre, Spain
David Stroud, The University of Melbourne, Australia

****Correspondence:***
James A. Letts
jaletts@ucdavis.edu

Specialty section:
This article was submitted to Cellular Biochemistry, a section of the journal Frontiers in Molecular Biosciences

Received: *20 October 2021*
Accepted: *25 November 2021*
Published: *03 January 2022*

Citation:
Padavannil A, Ayala-Hernandez MG, Castellanos-Silva EA and Letts JA (2022) The Mysterious Multitude: Structural Perspective on the Accessory Subunits of Respiratory Complex I. Front. Mol. Biosci. 8:798353. doi: 10.3389/fmolb.2021.798353

INTRODUCTION

Mitochondria are the nexus of energy metabolism in eukaryotic cells and play important roles in cellular signaling and apoptosis (Pagliarini and Rutter, 2013). The inner mitochondrial membrane (IMM) harbors the respiratory electron transport chain (ETC) which carries out the final stages of cellular respiration. The ETC is composed of four multi-subunit protein complexes (complex I to complex IV) that couple electron transfers to the pumping of protons across the IMM. The electrochemical proton gradient thus generated is used by ATP synthase (complex V) to generate ATP. Mutations of genes encoding subunits of ETC complexes that result in decreased activity (i.e., ETC deficiencies) are unable to meet the energy demands of muscle and neurons, resulting in severe and often fatal pediatric myopathies and neuropathies (Koene et al., 2012). Dysfunction in complex I (CI) accounts for one third of ETC deficiencies like Leber's hereditary optic neuropathy, Leigh syndrome and mitochondrial encephalomyopathy (Fiedorczuk and Sazanov, 2018; Ma et al., 2018). The outsized role of CI in mitochondrial disease stems in part from its large number of required subunits and complex assembly pathway (Guerrero-Castillo et al., 2017a). Whereas prokaryotic CI is composed of 14 subunits—7 in the cytoplasm and 7 in the plasma

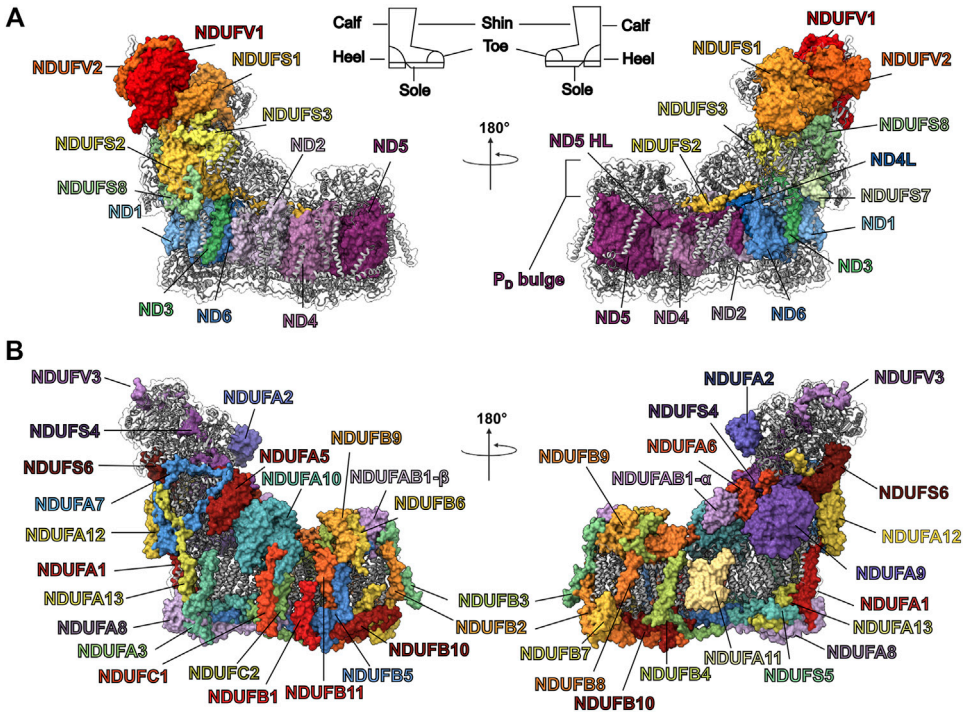

FIGURE 1 | Structure of mammalian CI from *O. aries* (PDB: 6ZKC). **(A)** The 14 core subunits are shown as colored surfaces. The accessory subunits are shown as grey cartoons. The CI boot-shape analogy is indicated at the top of the panel. **(B)** The 31 accessory subunits are shown as colored surfaces while the core subunits are shown as grey cartoons.

membrane (Brindefalk et al., 2011; Martijn et al., 2018)—mammalian mitochondrial CI is composed of 45 subunits – the 14 "core" subunits conserved from bacteria (**Figure 1A**) and an additional 31 accessory subunits that have been added during the evolution of eukaryotes (**Figure 1B**) (Letts and Sazanov, 2015). CI has a boot-shaped structure consisting of a proton-pumping membrane arm that is embedded in the IMM and an electron-transferring peripheral arm extending into the mitochondrial matrix (**Figure 1A**) (Baradaran et al., 2013; Berrisford et al., 2016). The seven core subunits of the CI membrane arm are encoded by the mitochondrial genome and are conserved across species. The core subunits of the peripheral arm as well as the accessory subunits are encoded by the nuclear genome, expressed in the cytoplasm and imported into the mitochondria. The CI assembly process occurs *via* the successive association of several distinct subassemblies (**Figure 2**) (Sánchez-Caballero et al., 2016) *via* the action of many essential assembly factors (Guerrero-Castillo et al., 2017a; Formosa et al., 2018). This modular assembly process may provide the organism with additional inputs for regulation and quality control.

Although the core subunits harbor all the substrate binding sites and cofactors needed for catalysis (Baradaran et al., 2013; Berrisford et al., 2016), mutagenesis, knockdown and knockout experiments demonstrate that in eukaryotes the core subunits alone are insufficient for CI assembly and function (Stroud et al., 2013, 2016; Garcia et al., 2017). Given that bacterial CI functions in the absence of accessory subunits, the appearance of essential accessory subunits in eukaryotes suggests changes in the core subunits that make them incapable of operating on their own. However, the roles of each accessory subunit in CI stability, regulation, and function remain unclear. Nonetheless, given that many disease-causing mutations are in the accessory subunits (Fiedorczuk and Sazanov, 2018), it is essential to understand the roles of the accessory subunits to develop treatment strategies for CI deficiencies. Recent advances in membrane-protein biochemistry and cryogenic electron microscopy have led to several high-resolution structures of bacterial and eukaryotic CI (Baradaran et al., 2013; Parey et al., 2019; Bridges et al., 2020; Galemou Yoga et al., 2020; Grba and Hirst, 2020; Kampjut and Sazanov, 2020; Chung et al., 2021; Kolata and Efremov, 2021). CI structures have been observed predominantly in two states: a closed state and an open state which differ in the angle between the peripheral arm and the membrane arm (Fiedorczuk et al., 2016; Zhu et al., 2016; Letts et al., 2019). The open state is characterized by the unfolding of several loops, within the quinone binding cavity and corresponds to the catalytically inert deactive (D) state of CI (Maklashina et al., 2003; Blaza et al., 2018). The closed state corresponds to the active (A) state of the complex (Agip et al., 2018; Letts et al., 2019). In addition, these structures defined the locations of the accessory subunits and advanced our understanding of the mechanism by which CI couples electron transfer to proton pumping (Kampjut and Sazanov, 2020; Parey et al., 2021). However, how the different accessory subunits contribute to CIs assembly and activity, including the

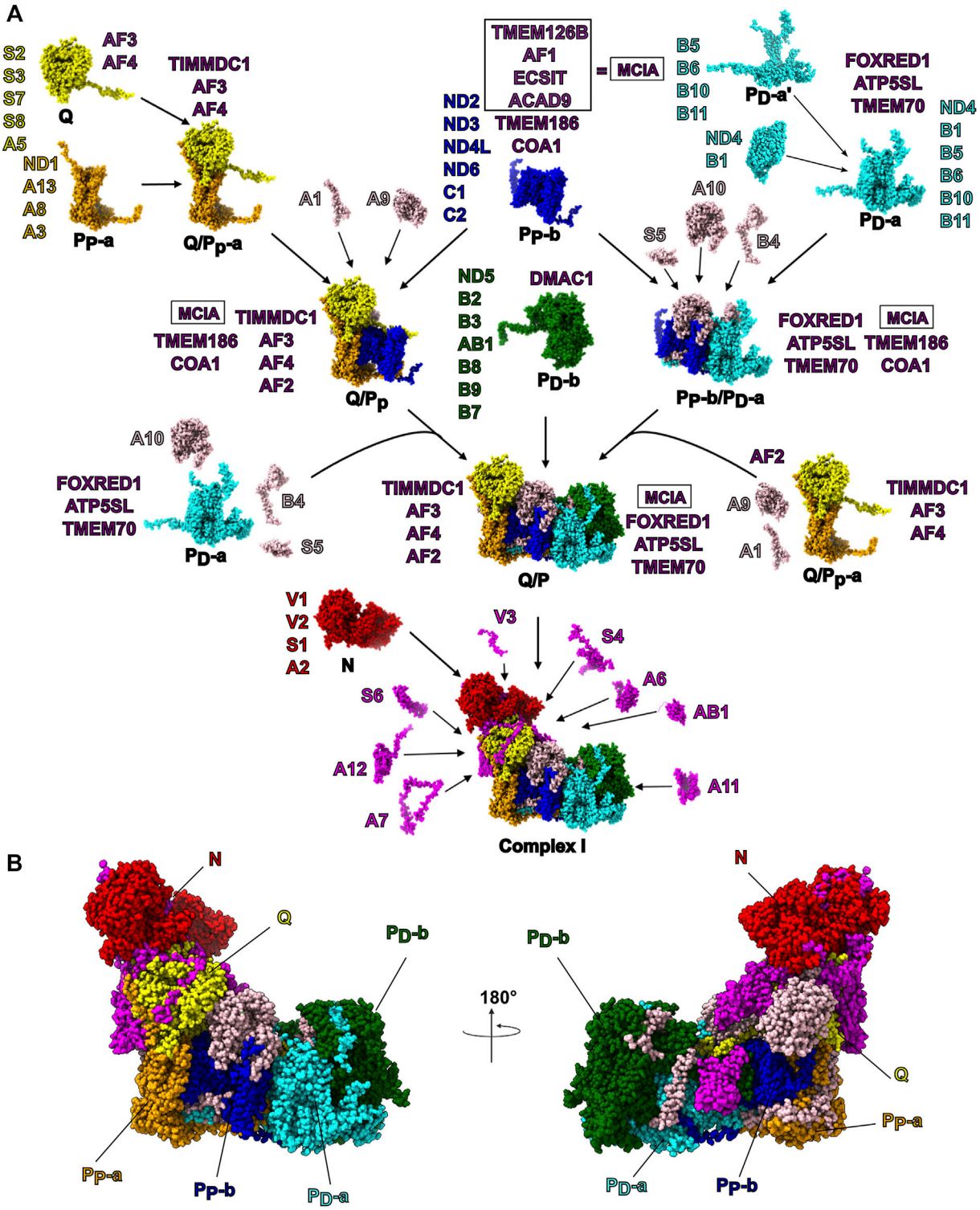

FIGURE 2 | Mammalian CI Assembly. **(A)** The modular assembly pathway of mammalian mitochondrial CI as proposed by Guerrero-Castillo et al. (2017a). The structures of CI subunits within each subassembly are shown as atomic spheres and colored by subassembly. The subunits constituting each subassembly are indicated in shorthand notation (e.g., NDUFS1 is shortened to S1). The assembly factors found associated with each subassembly are indicated in purple. Subunits that associate with intermediate assemblies (e.g., the Q/P_P subassembly) are shown in beige. The terminally associated subunits are shown in magenta. **(B)** CI structure shown as atomic spheres with subunits colored by their subassembly as in panel **(A)**. Subunits that associate with intermediate assemblies independent of the modules are shown in beige and terminally associated subunits are shown in magenta.

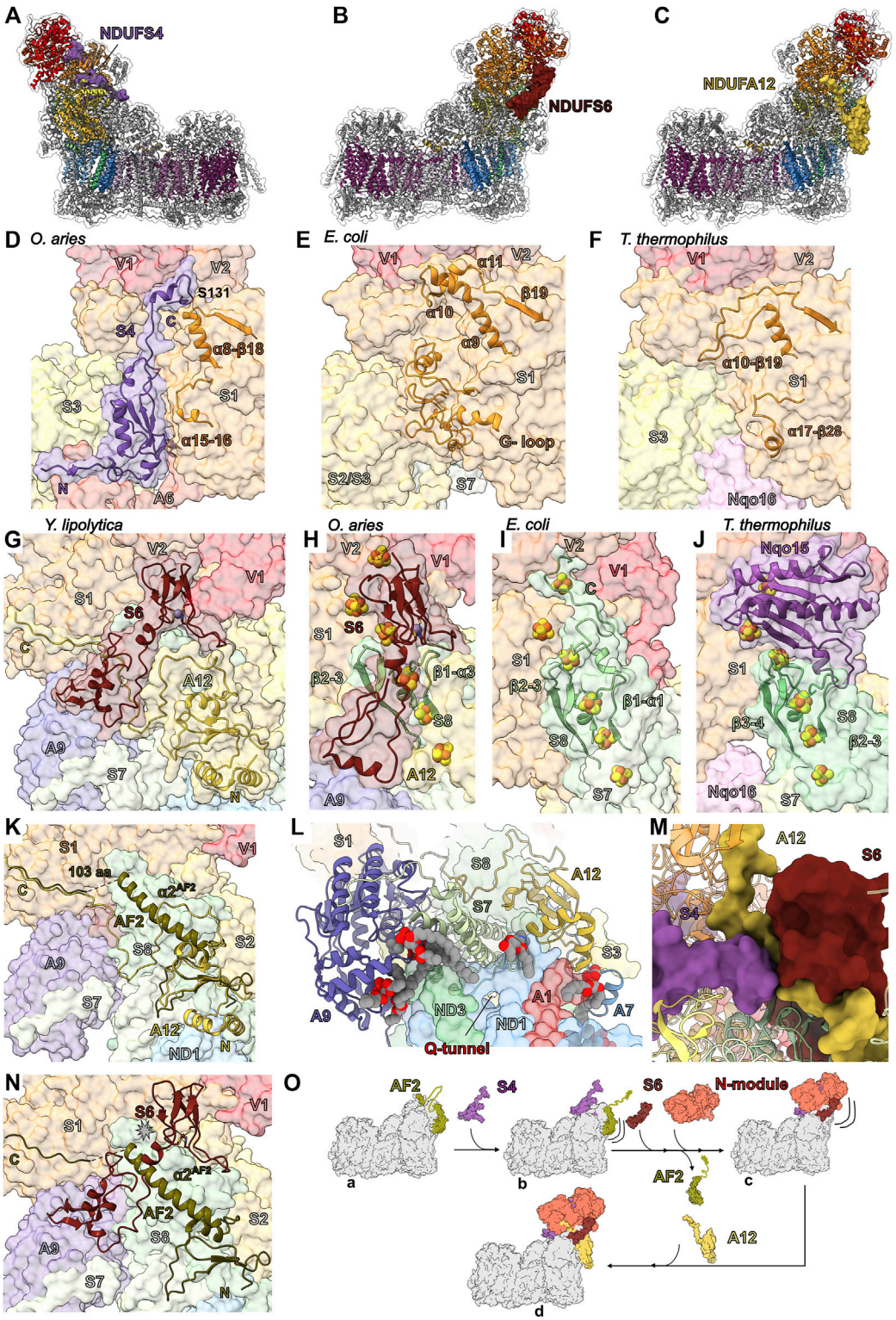

FIGURE 3 | Ancient accessory subunits of CI. **(A)** NDUFS4 (berry), **(B)** NDUFS6 (plum) and **(C)** NDUFA12 (gold) are shown as colored surfaces on CI, the core subunits are shown as colored cartoons and other accessory subunits are shown as grey cartoons. Shin view of **(D)** mammalian (*O. aries* PDB: 6ZKC throughout), **(E)** *E. coli* (PDB: 7NZ1 throughout) and **(F)** *T. thermophilus* (PDB: 4HEA throughout) CI structures shown as transparent surfaces. NDUFS4 and the NDUFS1 loops (orange) that differ between the structures are shown as cartoons. **(G)** Calf view of *Y. lipolytica* CI structure (PDB ID: 6YJ4) shown as transparent surfaces with NDUFS6 (NUMM) and NDUFA12 (N7BM) shown as cartoons with the Zn^{2+} ion shown as atomic sphere and coordinating residues shown as sticks colored by element. Calf view

(*Continued*)

FIGURE 3 | of **(H)** mammalian, **(I)** *E. coli* and **(J)** *T. thermophilus* CI structures shown as transparent surfaces with NDUFS6 and the NDUFS8 (sea green) loops that differ between the structures labeled and shown as cartoons. The FeS clusters and Zn^{2+} ions are shown as atomic spheres and colored by element. **(K)** Structural differences between assembly factor NDUFAF2 and accessory subunit NDUFA12. Calf view of CI showing assembly factor NDUFAF2 from *Y. lipolytica* (PDB: 6RFQ) superposed on NDUFA12 (N7BM) (PDB: 6RFR). The transparent surface of CI is shown with NDUFA12 as cartoon in gold and NDUFAF2 shown as cartoon colored in dark olive. **(L)** Lipid binding around the Q-tunnel. Looking up from the *Y. lipolytica* (PDB: 6YJ4) CI heel showing the accessory subunits NDUFA9 (NUEM) (lavender), NDUFA12 (N7BM) and core subunit NDUFS7 (NUKM) (tea green) as cartoon. Other subunits are shown as transparent surfaces. Lipids are shown as spheres colored by element. **(M)** The interface between NDUFS4 (NUYM), NDUFA12 (N7BM) and NDUFS6 (NUMM) of *Y. lipolytica* CI (PDB: 6RFR). NDUFS4, NDUFA12 and NDUFS6 are shown as surfaces and all other CI subunits are shown as cartoon. **(N)** Clash between NDUFS6 and NDUFAF2. *Y. lipolytica* NDUFAF2 (PDB: 6RFQ) superposed on to NDUFA12 (N7BM) (PDB: 6RFR). NDUFS6 (NUMM) and NDUFAF2 are shown as cartoon. NDUFA12 (N7BM) is not shown for clarity. **(O)** Schematic diagram showing the role of ancient accessory subunits in the "checkpoint" hypothesis of the CI assembly pathway. NDUFS4 binds to CI Q/P subassembly bound to NDUFAF2 and disengages the C-terminal unstructured region of NDUFAF2. Addition of NDUFS6 and N-module to the subassembly results in the release of NDUFAF2 and frees up the NDUFA12 binding site. NDUFA12 binds to the subassembly at the site of NDUFAF2 and completes the assembly. Subunits are colored as in **Figure 1** throughout unless stated otherwise. NDUFS4: berry, NDUFS6: plum, NDUFA12: gold, NDUFS1: orange, NDUFS8: sea green, NDUFAF2: dark olive, NDUFA9: lavender, NDUFS7: tea green.

transition between the A and D states, remains poorly understood.

In this review, we draw from the recent CI structures, as well as from knockout (Stroud et al., 2013; Stroud et al., 2016; Garcia et al., 2017), assembly (Ugalde et al., 2004; Sánchez-Caballero et al., 2016; Guerrero-Castillo et al., 2017a) and clinical studies (Mimaki et al., 2012; Rodenburg, 2016; Fiedorczuk and Sazanov, 2018) to determine the roles of mammalian CI's accessory subunits. By comparing structures of the bacteria and eukaryotic core subunits we identify changes that may make the eukaryotic core subunits no longer able to function in the absence of the accessory subunits. Furthermore, by comparing conserved and divergent features of the accessory subunits in mammals, fungi and plants we ascertain the essential structural and functional features of the accessory subunits. We also discuss the structural consequences of disease-causing mutations occurring in the accessory subunits and how they may affect CI function. Overall, we provide a structural and evolutionary framework for understanding the roles of the accessory subunits and propose several experimentally testable hypotheses on their function that we hope will help propel the field towards a full understanding of CI deficiencies and new potential treatments.

Throughout the text we use the human gene names (e.g., NDUFS1, NDUFV1) of the CI subunits, rather than the biochemical names (e.g., 75 kDa subunit, 51 kDa subunit). We also use the full numbering of residues starting from the initiator methionine of the canonical isoform, rather than from the first residue of the mature processed protein. Although the biochemical names have a long and important history in the study of CI, we chose the nomenclature and numbering described above to allow the medical community studying CI deficiencies to make full use of the plethora of structural data without the need for conversion tables. For this review, the accessory subunits were grouped based on their functional implications and discussed roughly starting from the tip of the peripheral arm to the heel of the complex, then from the heel to the tip of the membrane arm along the NDUFA10 side of the complex and finally down the ND5 lateral helix (ND5-HL) side of the membrane arm.

The Ancient Accessory Subunits of the Peripheral Arm—NDUFS4, NDUFS6 and NDUFA12

NDUFS6, NDUFA12 and NDUFS4 are ancient accessory subunits present in α-proteobacterial CI (Yip et al., 2011). The α-proteobacteria is the most closely related extant class of bacteria to the mitochondrial ancestor (Martijn et al., 2018), hence, these accessory subunits predate eukaryogenesis (Kahlhöfer et al., 2017) and are conserved throughout eukaryotes. NDUFS4, NDUFS6 and NDUFA12 are assembled at the N/Q interface (**Figures 3A–C**) during the final stages of CI assembly in mammals (**Figure 2A**) (Guerrero-Castillo et al., 2017a). Each of these three subunits are important for the activity of CI with many associated disease-causing mutations [recently reviewed by (Kahlhöfer et al., 2021)].

NDUFS4—In fully assembled CI NDUFS4 is located on the "shin" of the CI boot (**Figure 1** and **Figure 3A**). In eukaryotic CI NDUFS4's C-terminus binds in a groove between domains A and B of NDUFS1 (**Figure 3D** and **Figure 4G**). It is composed of a N-terminal coil, a folded N-terminal domain made up of three β-strands, four short α-helices, an extended loop (between $\beta2^{S4}$ and $\alpha3^{S4}$) and a C-terminal coil that reaches to the N-module and contains a short helix (**Figure 3D**). NDUFS4's N-terminal coil interacts with NDUFS3 and NDUFA6 (**Figure 3D**). The folded N-terminal domain bridges between NDUFS1 in the N-module and NDUFS3 in the Q-module (**Figure 3D**). The extended $\beta2$-$\alpha3^{S4}$ loop reaches across the peripheral arm of the complex interacting with NDUFS1, NDUFS3, NDUFS8, NDUFS6, NDUFA9, NDUFA6 and NDUFA12. NDUFS4's C-terminal coil interacts with NDUFV1, NDUFV2, NDUFS1 and NDUFV3 (**Figure 3D**). In mammalian and human cell cultures cAMP promotes the phosphorylation of the NDUFS4 protein at $S131^{S4}$ (Papa, 2002), which is located on NDUFS4's C-terminal tail. $S131^{S4}$ is buried in a pocket between NDUFS1, NDUFV1 and NDUFV2 that is insufficient to accommodate a phosphate group (**Figure 3D**). Hence phosphorylation of $S131^{S4}$, which has been proposed to enhance the functional capacity of CI (Papa, 2002), would require a conformational change in this region.

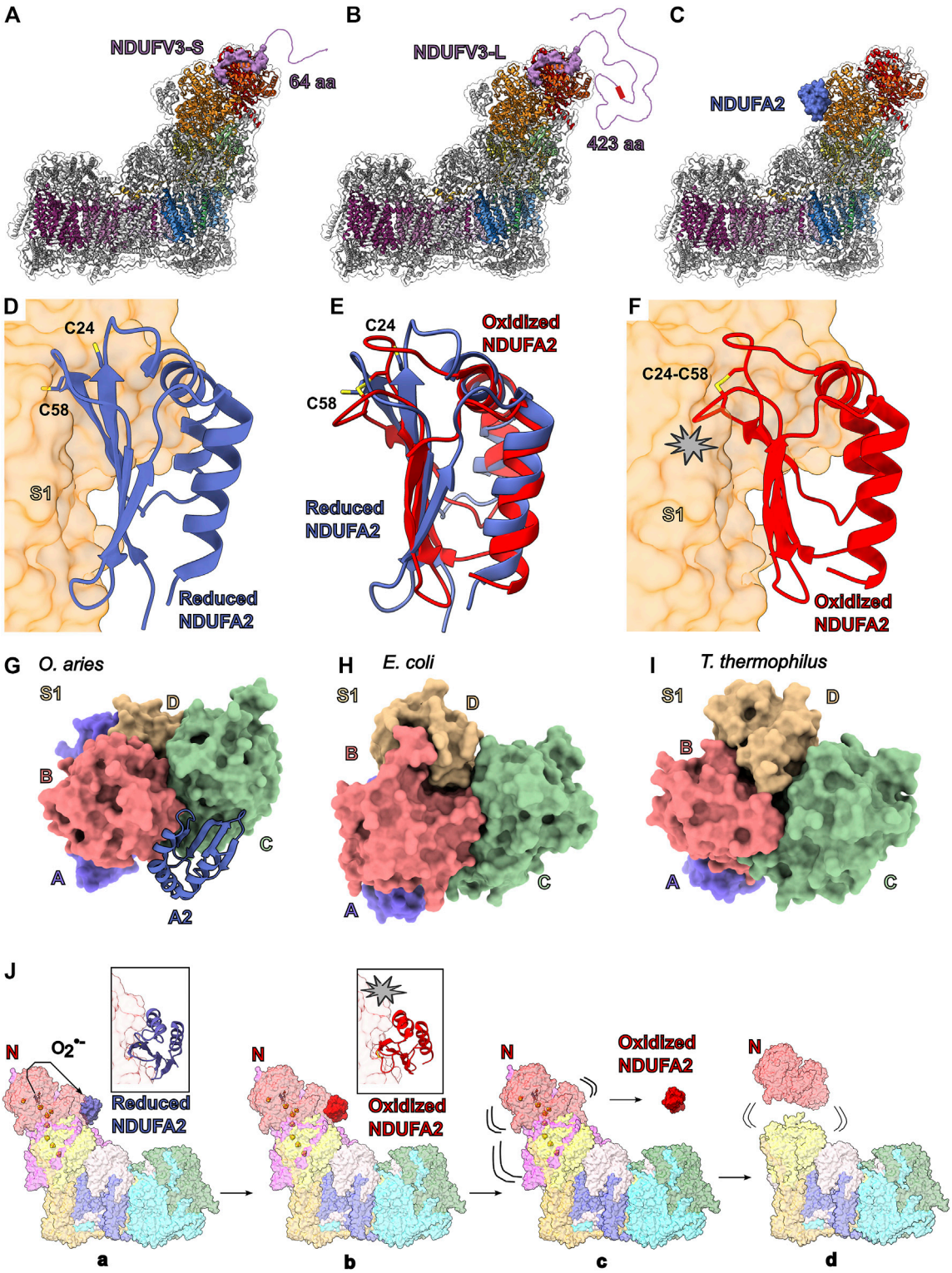

FIGURE 4 | Accessory subunits NDUFV3 and NDUFA2. NDUFV3-S (short isoform) (purple) **(A)**, NDUFV3-L (long isoform) (purple) **(B)** and NDUFA2 (blue) **(C)** are shown as colored surface on CI (PDB: 6ZKC). Disordered N-terminal of the **(A)** short isoform (64 aa) and **(B)** long isoforms (423 aa) are represented by the purple line. Red square in **(B)** represents the conserved string of serine residues. The core subunits are shown as cartoons colored as in **Figure 1A** and the other accessory subunits are shown as grey cartoon. **(D)** The mammalian reduced NDUFA2 structure shown as cartoon. The cysteines are shown in stick representation and colored by element (PDB: 6ZKC). **(E)** NMR solution structure of oxidized human NDUFA2 (PDB: 1S3A) superposed onto reduced NDUFA2 found in mammalian CI (PDB: 6ZKC). Reduced

(*Continued*)

FIGURE 4 | NDUFA2 is shown in blue cartoon and the oxidized NDUFA2 is shown in red cartoon. **(F)** NMR solution structure of human NDUFA2 (PDB: 1S3A) superposed onto reduced NDUFA2 seen in mammalian CI. The clash caused due to rearrangement of loops [β1-α1^{A2} (aa 23–29) and β2-3^{A2} (aa 57–63)] is shown by the star. **(G-I)** NDUFA2 compensates for the loss of NDUFS1 domain D. Domain architecture of NDUFS1 **(G)** mammalian (*O. aries*) (PDB:5LNK), **(H)** *E. coli* (PDB: 7NZ1) **(I)** *T. thermophilus* (PDB:4HEA) is shown as surfaces colored and labeled according to the domains. **(J)** Schematic representation of the partial dissociation of CI due to oxidation of cysteines in NDUFA2. ROS generated at the FMN site oxidizes the cysteines in NDUFA2 resulting in the formation of a disulfide bond. The rearranged NDUFA2 loop clashes with NDUFS1 resulting in the dissociation of NDUFA2. The dissociation of NDUFA2 destabilizes NDUFS1 and the N-module. This destabilization eventually results in the N-module dissociating. Subunits are colored as in **Figure 1** in all the structure figures unless stated otherwise. NDUFV3: purple, reduced NDUFA2: blue, oxidized NDUFA2: red.

The recent *E. coli* CI structure shows that the groove between A and B domains of NDUFS1 (NuoG) is filled by a large extension from NDUFS1 containing two short helices (α10/α11) (**Figure 3E**) (Kolata and Efremov, 2021). *E. coli* NDUFS1 also contains a large loop, coined the G-loop, which occupies the equivalent location of NDUFS4's N-terminal domain in eukaryotes (**Figure 3E**) (Kolata and Efremov, 2021). In *T. thermophilus*, like in *E. coli*, the NDUFS1 (Nqo3) groove is partly filled with an extended loop (α10-β19 loop) and the accessory subunit Nqo16, not present in *E. coli* or eukaryotes, wedges between NDUFS1, NDUFS3 and NDUFS7 providing additional structural support to this region (**Figure 3F**) (Baradaran et al., 2013; Berrisford et al., 2016; Kampjut and Sazanov, 2020). As pointed out by Kolata and Efremov (Kolata and Efremov, 2021), these different structural features suggest there is an evolutionary pressure for the stabilization of NDUFS1 by "filling in" this groove. The need for this stabilization has been addressed with three different solutions in the three different CI lineages for which we have structures: the NDUFS4 subunit in the α-proteobacteria/eukaryotes (**Figure 3D**); the α10/α11 extension and G-loop in the *γ*-proteobacteria (e.g., *E. coli*) (**Figure 3E**); and the α10-β19 loop and Nqo16 in the deinococci (e.g., *T. thermophilus*) (**Figure 3F**). This suggests that in eukaryotes NDUFS4 is needed for the structural integrity of the peripheral arm (Kolata and Efremov, 2021). Consistent with this hypothesis, deletion of NDUFS4 (NUYM) in *Y. lipolytica* (ΔNDUFS4) results in conformational changes in NDUFV1, NDUFV2 and NDUFS1, decreased CI activity and an increase in ROS formation (Kahlhöfer et al., 2017; Parey et al., 2019). Additionally, NDUFS4 is required to protect NDUFS1's N1b iron-sulfur cluster and ΔNDUFS4 in *Y. lipolytica* exposes this cluster resulting in an altered electron paramagnetic resonance (EPR) signal, likely contributing to the reduction in CI activity (Parey et al., 2019). In the bacterial structures this cluster is protected by the extensions and loops.

NDUFS6—In fully assembled CI NDUFS6 is located on the "calf" of the CI boot (**Figure 1** and **Figure 3B**). It is composed of an N-terminal domain with minimal secondary structure and whose fold varies between fungi and mammals (**Figures 3G,H**) (Parey et al., 2019; Grba and Hirst, 2020; Kampjut and Sazanov, 2020), followed by a coil and short α-helix (α1^{S6}) that connects to a C-terminal domain formed by five β-strands forming two small β-sheets (**Figure 3H**). NDUFS6's N-terminal domain interacts with NDUFA9, NDUFS4, NDUFA12 and NDUFS8 (**Figure 3H**). The interdomain coil and the short helix of NDUFS6 lodge in a cleft on the surface of NDUFS8 formed by the β1-α3^{S8} and β2-3^{S8} loops (**Figure 3H**). The C-terminal domain binds a Zn^{2+} ion and sits in a pocket formed by core subunits NDUFS1, NDUFV1, NDUFV2 and NDUFS8 (**Figure 3H**). In the structures of plant and algal CI (Maldonado et al., 2020; Soufari et al., 2020; Klusch et al., 2021), NDUFS6 lacks the N-terminal domain altogether and the sequence for the N-terminal domain is missing from the α-proteobacterial CI, indicating that this domain evolved later in specific eukaryotic lineages.

On the "calf" side of CI where NDUFS6 is located in mammals, the *T. thermophilus* and *E. coli* CIs have extended loops/coils—the NDUFS8 (Nqo9) β3-4^{S8} loop in *T. thermophilus* and the extended C-terminal coils of NDUFS8 (NuoI), NDUFS7 (NuoB) and NDUFV1 (NuoF) in *E. coli* – bind overtop of the NDUFS1 (NuoG) FeS clusters (**Figures 3I,J**) (Baradaran et al., 2013; Berrisford et al., 2016; Kolata and Efremov, 2021). In mammalian CI, the corresponding loops are shorter and the extended loops in the bacterial structures would conflict with the location of NDUFS6 (**Figure 3H**). This suggests that NDUFS6 replaces these bacterial sequences and acts to stabilize the NDUFS1 FeS clusters. Indeed, NDUFS6 (NUMM) deletion (ΔNDUFS6) or mutation of a NDUFS6 Zn^{2+} coordinating cysteine in *Y. lipolytica*, showed loss of EPR signal for nearby cluster N4, indicating severe disruption (Kmita et al., 2015). In humans, the mutation of one of the Zn^{2+} coordinating cysteines (C115Y^{S6}) results in fatal neo-natal lactic acidosis (Kmita et al., 2015) indicating the importance of NDUFS6's Zn^{2+} coordination in stabilizing its interaction with CI. It has been noted (Kmita et al., 2015) that two other Zn^{2+} containing proteins, IscU (Markley et al., 2013) and mito-NEET (Zuris et al., 2011), with the same Zn^{2+} coordination pattern as NDUFS6 (three-cysteine/one-histidine), are involved in FeS biogenesis. This suggests that NDUFS6 may have initially started as an assembly factor for the FeS clusters of the peripheral arm that became permanently associated with the complex as a stabilizing subunit.

NDUFA12—Located on the "calf" of the CI boot below NDUFS6, NDUFA12 sits at the interface of the matrix and IMM (**Figure 1** and **Figures 3C,G**). It is composed of a structured N-terminal domain that binds to the Q-module adjacent to the membrane and a C-terminal coil which extends to the N-module forming an extensive interface with the NDUFS8 and crossing under the N-terminal domain of NDUFS6 (**Figure 3G**). This suggests that either NDUFA12 binds the complex first, that NDUFS6 and NDUFA12 pre-assemble and bind together or that conformational changes in NDUFS6 are needed for NDUFA12 binding (Parey et al., 2019). The N-terminal domain consists of two amphipathic α-helices that interact with lipid, followed by a three stranded *β*-sheet, and an α-helix and interacts with NDUFS8, NDUFA7, NDUFS2 and NDUFS7 (**Figures 3G,K**). The amphipathic helices play a role,

along with NDUFA9 and NDUFS7, in distorting the membrane in the region of the CoQ-tunnel (**Figure 3L**) (Parey et al., 2019).

In *Y. lipolytica*, deletion of NDUFS6 (ΔNDUFS6) results in the assembly factor NDUFAF2 remaining bound to the enzyme and a decrease in the bound quinone content of the complex relative to wildtype (Parey et al., 2019). NDUFA12 and NDUFAF2 are paralogs and occupy the same binding site on CI (Parey et al., 2019), thus, NDUFAF2 must be removed from the assembly intermediate before NDUFA12 can bind (Vogel et al., 2007). Importantly, NDUFAF2 lacks the amphipathic helices seen in NDUFA12 (**Figure 3K**) and therefore fewer bound lipids are seen at the interface in the ΔNDUFS6 structure (Parey et al., 2019). The observation of decreased CoQ-content is consistent with the hypothesis that deformation of the membrane by NDUFA12, NDUFA9 and NDUFS7 promotes CoQ access to the CoQ-tunnel (**Figure 3L**) (Parey et al., 2019). Reduced CI activity seen in the NDUFA12^{KO} (Stroud et al., 2016) and a naturally occurring NDUFA12 nonsense mutation (Ostergaard et al., 2011) may be due in part to less efficient CoQ access to the active site. The inability of NDUFAF2 to deform the membrane may help prevent reverse electron transport (RET), which can generate significant reactive oxygen species (ROS) (Chouchani et al., 2014), before complete assembly of the complex at which point NDUFAF2 is replaced by NDUFA12 and CI is activated.

Roles of NDUFS4, NDUFS6 and NDUFA12 in CI assembly—Together NDUFS4, NDUFS6 and NDUFA12 play an important role in the attachment of the N-module during CI assembly. Patients with deletion or substitution mutations in the *NDUFS4* gene show an abnormal assembly profile with a complete loss of the fully assembled CI (Assouline et al., 2012). NDUFS4^{KO} studies in mice suggest that CI is unstable or fails to assemble properly in the absence of NDUFS4 (Kruse et al., 2008). In HEK293T cells, although, NDUFS4 only interacts with the C-terminal coil of NDUFA12 over a short sequence (**Figure 3M**), NDUFS4^{KO} results in poor incorporation of NDUFA12 but overall only mild assembly defects (Calvaruso et al., 2012; Stroud et al., 2016). The dependence on NDUFS4 for the incorporation of NDUFA12 was not seen in *Y. lipolytica* ΔNDUFS4 as this structure showed clear incorporation of NDUFA12 (Parey et al., 2019). However, although assembly goes to completion and NDUFA12 is incorporated into the complex, ΔNDUFS4 resulted in an increase of bound assembly factor NDUFAF2 (Parey et al., 2019; Kahlhöfer et al., 2021) indicating that the deletion introduces a bottleneck in the final stages of assembly (Kahlhöfer et al., 2021).

In HEK293T cells, NDUFS6^{KO} prevents attachment of the N-module, stalling CI assembly at the Q/P subassembly (**Figure 2A**) (Stroud et al., 2016; Guo et al., 2017). In *Y. lipolytica*, ΔNDUFS6 leads to accumulation of a CI intermediate with the assembly factor NDUFAF2 bound, lacking both NDUFS6 and NDUFA12 but with the N-module attached (Kmita et al., 2015; Parey et al., 2019). NDUFAF2 lacks the N-terminal amphipathic α-helices seen in NDUFA12, but has a similar central domain followed by a NDUFAF2 specific α-helix (α2^{AF2}) (**Figure 3K**) (Parey et al., 2019). The C-terminal region of NDUFAF2 contains a disordered region of 103 amino acid residues followed by a coil that binds in a similar position as the C-terminal coil of NDUFA12 (**Figure 3K**). The α2^{AF2} helix binds to the surface of NDUFS8 where NDUFS6 would normally bind, indicating that when bound to CI, NDUFAF2 would prevent NDUFS6 binding (**Figure 3N**) (Kmita et al., 2015; Parey et al., 2019). Given that the *NDUFA12* gene is wild type in the ΔNDUFS6 *Y. lipolytica* strain, but NDUFA12 is not seen on CI, NDUFA12 alone is not sufficient to remove NDUFAF2 and NDUFS6 must play an important role in the removal of NDUFAF2 during the final stages of CI assembly. The difference in N-module attachment between NDUFS6^{KO} in HEK293T cells and ΔNDUFS6 in *Y. lipolytica* indicate a more severe impact of loss of NDUFS6 on CI assembly in mammals compared to yeast.

In HEK293T cells, NDUFA12^{KO} increases the abundance of CI subassemblies and decreases CI activity, however, fully assembled CI is still observed (Stroud et al., 2016). In humans, a NDUFA12 nonsense mutation leads to a similar phenotype, i.e., although CI appears fully assembled in patients with the mutation, they have reduced CI activity resulting in Leigh syndrome (Ostergaard et al., 2011). These data indicate that, in contrast to the loss of NDUFS6, the loss of NDUFA12 does not prevent the full assembly of the complex but negatively impacts CI turnover.

From the wild type and mutant CI studies, the hypothesis arises that NDUFAF2 acts in concert with NDUFS4, NDUFS6 and NDUFA12 as an assembly checkpoint, blocking the full assembly of the peripheral arm until the rest of the complex is fully assembled. In this scenario, the formation of the Q/P subassembly (**Figure 2A**), which contains the full membrane arm and Q-module along with NDUFAF2, promotes the association of NDUFS4, which in turn recruits the N-module and NDUFS6. As pointed out by Parey et al., (2019) NDUFS4 binding also likely promotes exchange of NDUFAF2 for NDUFA12 *via* its extended β2-3^{S4} loop (**Figure 3M**).

This "checkpoint" hypothesis differs from the model proposed by Parey et al., (2019), in which NDUFAF2 recruits the N-module to the Q/P subassembly, in two major ways. 1) Given the inability of smaller NDUFAF2 containing assembly intermediates to recruit the N-module, NDUFAF2 alone is insufficient for N-module recruitment. Thus, NDUFS4 and potentially NDUFS6 are required to help bind the N-module (**Figure 3O**). Importantly, in mammals NDUFS4 and NDUFS6 do not associate with the complex until after formation of the Q/P subassembly preventing premature attachment of the N-module (**Figure 2A**). 2) Given that NDUFS6 is required for the removal of NDUFAF2, interaction of NDUFS6 with the complex likely precedes that of NDUFA12, whose binding site is only available after NDUFAF2 is removed (**Figure 3O**). This necessitates a more complicated "dance" in which the C-terminus of NDUFA12 works its way under the N-terminal domain of NDUFS6 and likely involves additional intermediate conformations (**Figure 3O**).

Notably, in plant mitochondrial CI, NDUFS6 lacks the N-terminal domain (Maldonado et al., 2020; Soufari et al., 2020; Klusch et al., 2021). This would simplify the assembly process for the peripheral arm, as the NDUFA12 C-terminal coil no longer passes under NDUFS6 (Maldonado et al., 2020).

Consistent with the interactions of these subunits regulating the association of the N-module, plant CI assembles by a distinct pathway, in which the N-module is connected to the complex before the P_D-module, forming the plant specific assembly intermediate CI* (Ligas et al., 2019; Maldonado et al., 2020). Although possible genes for NDUFAF2 have been identified in plants, biochemical studies of CI assembly in plant have yet to identify NDUFAF2 as a plant CI assembly factor (Meyer et al., 2019). Nonetheless, if overcoming the checkpoint for N-module attachment is initiated by NDUFS4 binding, the major difference between plants and opisthokonts could be the dependence of NDUFS4 binding on the attachment of the P_D-module.

The variety in assembly pathways suggests that the specific roles of NDUFS4, NDUFS6 and NDUFA12 in regulating CI assembly may have evolved later and that the original physiological roles of these subunits are structural. In α-proteobacteria the NDUFS6 gene lacks the sequence for an N-terminal domain and assembly of CI in *E. coli* follows a more "plant-like" pathway (though *E. coli* lacks the accessory subunits) (Friedrich et al., 2016). Further studies on CI assembly and structure in the α-proteobacteria would shed more light on these issues (Jarman et al., 2021).

The Subunit at the Tip of the Peripheral Arm: NDUFV3

NDUFV3 lies on the tip of the N-module and joins the complex in the final stage of assembly (**Figure 2A** and **Figure 4A**). NDUFV3 is composed of a N-terminal coil, an α-helix and a C-terminal coil that bind in the cleft between NDUFV1 and NDUFV2. The C-terminal coil of NDUFV3 reaches to NDUFS1 where it interacts with the C-terminal coil of NDUFS4. NDUFV3 is known to be present on CI in two isoforms (**Figures 4A,B**) (Bridges et al., 2017; Dibley et al., 2017; Guerrero-Castillo et al., 2017b). The 10 kDa "short" isoform (NDUFV3-S) is found in heart tissue while the 50 kDa "long" isoform (NDUFV3-L), generated by alternative splicing of the *NDUFV3* gene, appears to be dominant in other tissues (liver and brain) and in HEK293T cells (Bridges et al., 2017; Dibley et al., 2017). $NDUFV3^{KO}$ in HEK293T cells showed that lack of both NDUFV3 isoforms led to only minor defects in the assembly and function of CI suggesting its presence in CI is not essential (Stroud et al., 2016; Dibley et al., 2017). In addition, it was found that NDUFV3-S alone is sufficient for CI assembly (Dibley et al., 2017). The N-terminal 64 amino acid residues of NDUFV3-S are disordered and the region of NDUFV3-S that is bound to NDUFV1 and NDUFV2 and clearly resolved in the structure is conserved in NDUFV3-L, suggesting they bind similarly to CI (**Figures 4A,B**). Therefore, the main difference between the isoforms is not in their interaction with CI but that NDUFV3-L has an additional 423 amino acid residues on its N-terminus that are also predicted to be disordered (**Figures 4A,B**) (Guerrero-Castillo et al., 2017b; Bridges et al., 2017; Dibley et al., 2017).

Phylogenic tree analysis has shown that NDUFV3 is absent in jawless fish, insects, nematodes, and fungi suggesting it has evolved within the vertebrates (Bridges et al., 2017). Further, a sequence alignments show conservation in the C-terminal structured region of both NDUFV3 isoforms as well as in a string of 10 serine residues only present in NDUFV3-L (**Figure 4B**). Phospho-proteome analyses have identified three serine residues, from the string of 10, to be phosphorylated in various conditions which is consistent with the previous identification of NDUFV3-L as a mitochondrial phosphoprotein (Bridges et al., 2017).

Interestingly, as noted by Bridges et al. (2017), the size, lack of secondary structure and binding site of NDUFV3-L resembles the 68 kDa fragment of the atypical cadherin (Ft4) which has been shown to regulate CI activity in *Drosophila melanogaster* (Sing et al., 2014). Fat (Ft) cadherins are cell adhesion molecules that control tissue growth and organization (Tanoue and Takeichi, 2005). In *Drosophila*, Ft regulates ETC integrity and promotes OXPHOS by release of a soluble 68 kDa fragment by proteolytic cleavage of its intracellular domain, which is imported into mitochondria and binds to CI at NDUFV2 (Sing et al., 2014). Loss of Ft in *Drosophila* leads to loss of CI and increases ROS (Sing et al., 2014). This led Bridges et al. (2017) to propose that NDUFV3-L may play a similar role in mammals. Given that the unstructured regions of the intracellular domains of cadherins are known to associate with a variety of adaptors and signaling proteins (Maître and Heisenberg, 2013) and that unstructured regions of proteins are commonly involved in protein-protein interactions (Dyson and Wright, 2005), it is reasonable to speculate that NDUFV3-L has additional interaction partners and that the physiological impact of the NDUFV3 isoforms may have more to do with those additional interactions than with possible changes in the behavior of CI itself. In this scenario, CI is used as a scaffold for the localization of NDUFV3 to the matrix surface of the cristae. More work is needed to identify any additional NDUFV3 interaction partners and determine what role it may be playing at the cristae surface.

The Thioredoxin Fold Subunit NDUFA2

NDUFA2 is assembled into the N-module subassembly along with NDUFV1, NDUFV2 and NDUFS1 prior to attachment to CI (**Figure 2A** and **Figure 4C**) (Sánchez-Caballero et al., 2016; Guerrero-Castillo et al., 2017a). NDUFA2 has a thioredoxin fold consisting of a β-sheet with four anti-parallel β-strands and three α-helices (**Figure 4D**). Despite the structural homology to thioredoxins, the two vicinal cysteines of the canonical thioredoxin CXXC motif are not conserved, instead NDUFA2 has two different cysteines ($Cys24^{A2}$ and $Cys58^{A2}$ in humans) conserved across eukaryotes (with a notable exception of $Ala47^{A2(NI8M)}$ in *Y. lipolytica*).

In all current structures of eukaryotic CI, NDUFA2 interacts solely with core subunit NDUFS1 (**Figures 4C,D**) in a reduced form i.e., there is no disulfide bond between the conserved cysteine residues (**Figure 4D**). Nonetheless, the structure of isolated human NDUFA2 in the oxidized state, containing a disulfide linkage between $Cys24^{A2}$ and $Cys58^{A2}$, has been solved by NMR (**Figure 4E**) (Brockmann et al., 2004). In the oxidized state NDUFA2 adopts a distinct conformation compared to the

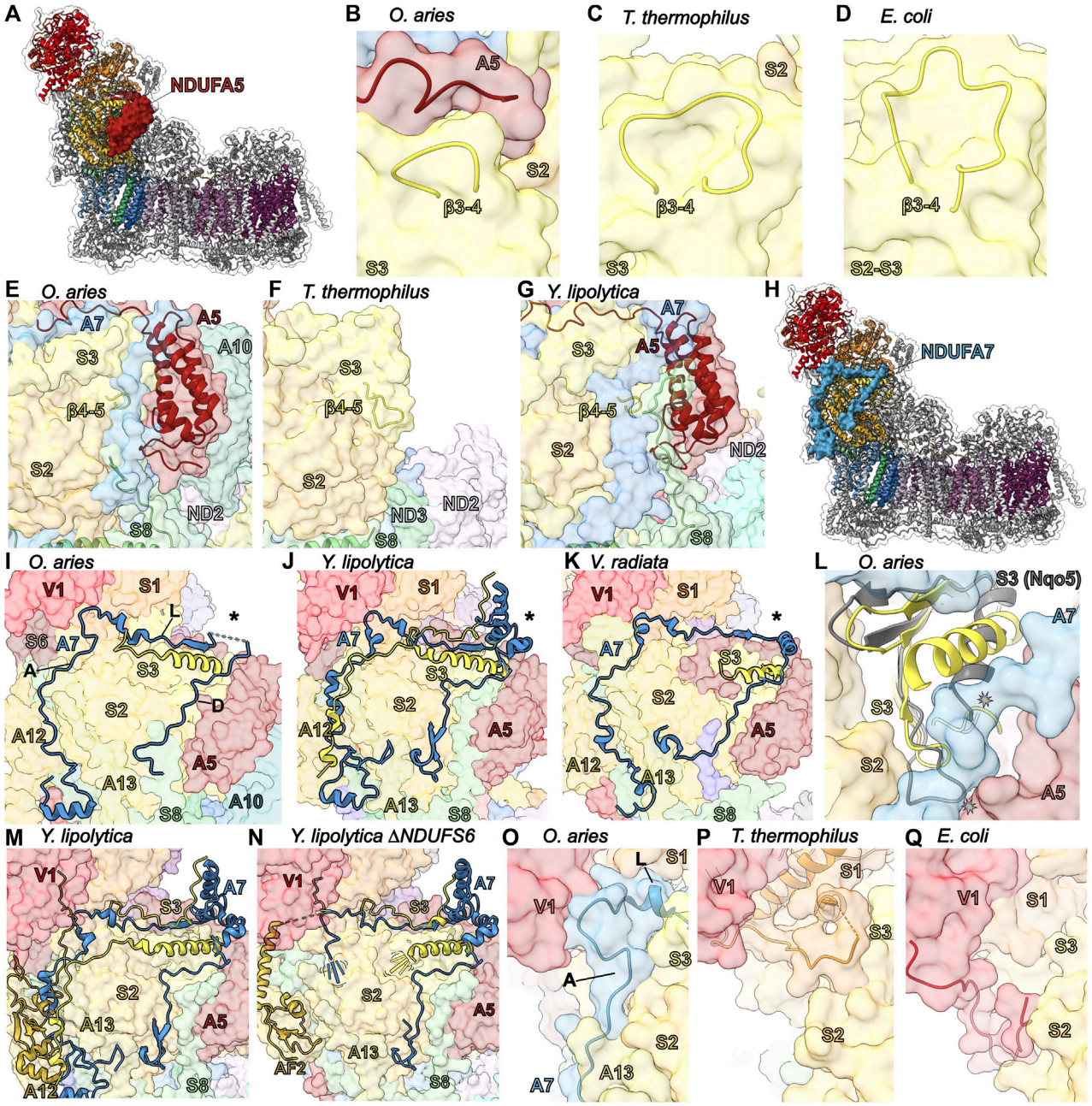

FIGURE 5 | Accessory subunits NDUFA5 and NDUFA7. **(A)** The structure of CI (PDB: 6ZKC) in cartoon with the surface of NDUFA5 (auburn) shown, the core subunits colored as in **Figure 1A** and the accessory subunits grey. **(B–D)** The NDUFA5 C-terminus compensates for a shorter NDUFS3 (corn yellow) β3-4^{S3} loop. **(B)** Mammalian (PDB: 6ZKC), **(C)** *T. thermophilus* (PDB: 4HEA) and **(D)** *E. coli* (PDB: 7NZ1). CI structures shown in transparent surface with NDUFA5 and the NDUFS3 β3-4^{S3} loop in cartoon. **(E–G)** NDUFA5 may compensate for a shorter NDUFS3 β4-5^{S3} loop. **(E)** *O. aries* cartoon of NDUFS3 β4-5^{S3} loop (aa 99–102), NDUFA5, and NDUFS8 (sea green) on the CI surface (PDB: 6ZKC). The β4-5^{S3} loop is shorter in *O. aries* than in bacteria. **(F)** *T. thermophilus* cartoon of the β4-5^{S3} loop (aa 76–86) and NDUFS8 (Nqo9) on the CI surface (PDB: 4HEA). **(G)** *Y. lipolytica* cartoon of the NDUFS3 β4-5^{S3} (NUGM) loop (aa 147–150), NDUFA5 (NUFM) and NDUFS8 (NUPM) on the CI surface (PDB: 6YJ4). *Y. lipolytica* has an extended NDUFS8 coil compared to *O. aries* and *T. thermophilus*. **(H)** The structure of CI (PDB: 6ZKC) shown in cartoon with the surface of NDUFA7 (azzure blue), the core subunits colored as in **Figure 1** and the accessory subunits grey. **(I–K)** Differences in NDUFA7 between eukaryotes. **(I)** *O. aries* NDUFA7 shown as cartoon on the CI (PDB: 6ZKC) surface with the variable region indicated (*) and the N-terminal coil and helix of NDUFS3 shown as cartoon. A: ascending coil, L: lateral coil, D: descending coil. **(J)** *Y. lipolytica* NDUFA7 (NUZM) shown as cartoon on the CI (PDB: 4HEA) surface with the variable region indicated (*) and the N-terminal coil and helix and C-terminal coil of NDUFS3 (NUGM) shown as cartoon. **(K)** *V. radiata* NDUFA7 (NDUA7) shown as cartoon on the CI (PDB: 6X89) surface with the variable region indicated (*) and the N-terminal coil and helix of NDUFS3 (NDUS3) shown as cartoon. **(L)** A conformation change is needed in the N-terminal helix of NDUFS3 relative to that from *T. thermophilus* to accommodate NDUFA7. Cartoon of NDUFS3 in *O. aries* (PDB: 6ZKC) and NDUFS3 (Nqo5; grey) in *T. thermophilus* (PDB: 4HEA) on the *O. aries* CI surface. **(M,N)** NDUFA7 participates in NDUFA12 (gold) binding. **(M)** Cartoon of NDUFA7 (NUZM), the N-terminal and

(*Continued*)

FIGURE 5 | C-terminal loop of NDUFS3 (NUGM) and NDUFA12 (N7BM) on the CI surface (PDB: 6YJ4). **(N)** Cartoon of NDUFA7, NDUFS3 and NDUFAF2 (N7BML) (gold) on the CI surface (PDB: 6RFQ). The N-terminal regions of NDUFA7 and NDUFS3 are disordered. **(O–Q)** Stabilizing role for NDUFA7 at the interface of the N and Q modules. **(O)** *O. aries* cartoon of NDUFA7 on CI surface (PDB:6ZKC). NDUFA7 stabilizing interactions are replaced by core subunits in bacteria. A: ascending coil, L: lateral coil. **(P)** *T. thermophilus* cartoon of NDUFS1 (orange) (Nqo1) on CI surface (PDB: 4HEA). **(Q)** *E. coli* cartoon of C-terminal coil of NDUFV1 (NuoF) on CI surface (PDB: 7NZ1). Subunits are colored as in **Figure 1** throughout unless stated otherwise. NDUFA5: auburn, NDUFS3: corn yellow, NDUFS8: sea green, NDUFA7: azzure blue, NDUFA12: gold, NDUFS1: orange.

reduced state (**Figure 4E**). When docked onto the structure of CI the oxidized conformation of NDUFA2 loops clashes with the surface of NDUFS1 (**Figure 4F**). This indicates that change in reduction state of NDUFA2 would impact NDUFA2's interaction with NDUFS1.

In bacteria, NDUFS1 (Nqo3 in *T. thermophilus* and NuoG in *E. coli*) is composed of four large domains A-D (**Figures 4H,I**). However, in eukaryotes, NDUFS1 lacks a significant domain D, and thus is composed of domains A-C alone and a short C-terminal helix (**Figure 4G**). In bacteria, domain D binds at the interface of domains B and C and likely stabilizes the overall domain architecture of NDUFS1 (**Figures 4H,I**). NDUFA2 in eukaryotes binds on the opposite face of NDUFS1 relative to domain D in bacteria, but like domain D in bacteria, NDUFA2 bridges domains B and C (**Figure 4G**). Thus, it is reasonable to hypothesize that, like domain D of bacteria, NDUFA2 stabilizes the overall domain architecture of NDUFS1, thereby compensating for the lack of domain D. Thus, the stability of eukaryotic NDUFS1 may depend on the presence of NDUFA2, thereby making the eukaryotic CI N-module dependent on this accessory subunit. Consistent with this NDUFA2^{KO} in HEK293T cells results in the accumulation of a CI intermediate lacking the N-module and severe defects in CI activity and respiration (Stroud et al., 2016).

These observations lead to the hypothesis that NDUFA2 may act as a ROS sensor that works to "shut off" CI activity under conditions of high ROS production. In this scenario, molecules of superoxide or hydrogen peroxide produced at the FMN site of CI could react with the conserved cysteines of NDUFA2, stripping electrons from them and resulting in the formation of a disulfide bond (**Figure 4J**). This would result in the conformational rearrangement of the NDUFA2 loops causing it to clash with NDUFS1 and unbind (**Figure 4J**). Loss of NDUFA2 would destabilize the NDUFS1 structure by removing the bridging interactions between domains B and C impacting NDUFS1's interaction with other N- and Q-module subunits (**Figure 4J**). In short, reaction of NDUFA2 with ROS may be an initiating factor resulting in the observed partial degradation of CI under RET conditions (Guarás et al., 2016). If correct, this hypothesis makes several experimentally testable predictions. First, treatment of isolated CI with oxidizing agents should result in loss of NDUFA2 followed by loss of the N-module. Second, *Y. lipolytica* CI, due to its lack of one of the conserved NDUFA2 cysteines, should be more resistant to oxidizing agents.

The Lone Accessory Subunit of the Q Subassembly: NDUFA5

NDUFA5 binds at the interface of core subunits NDUFS2 and NDUFS3 and is composed of a short N-terminal coil, a three-helix bundle, and a long C-terminal coil (**Figures 5A,E**). Along with NDUFS2, NDUFS3, NDUFS7 and NDUFS8, NDUFA5 forms the Q subassembly (**Figure 2A**). In the fully assembled complex, the N-terminal coil and three-helix bundle of NDUFA5 interacts with NDUFS2, NDUFS3 and NDUFA7 (**Figure 5E**). The three-helix bundle also interacts with NDUFA10 in a state-dependent manner (discussed in the section on NDUFA10). The C-terminal loop of NDUFA5 interacts with NDUFS2, NDUFS3 and NDUFS4. In HEK293T cells, NDUFA5^{KO} results in incomplete assembly of CI with the accumulation of a 460 kDa subcomplex composed of membrane arm subunits but lacking any Q- or N-module subunits (Stroud et al., 2016). In addition, HEK293T cells with NDUFA5 depleted by RNA interference showed a significant decrease in CI activity compared to other complexes (Rak and Rustin, 2014). *Ndufa5* deletion in mice is embryonic lethal and conditional neuronal-specific KO in mice yielded mild chronic encephalopathy with concomitant decreases in the levels of fully assembled CI and CI activity (Peralta et al., 2014). Together, these data indicate that NDUFA5 is required for the stability of the Q-module and the formation of a functional CI.

Bacterial CI structures, both *T. thermophilus* and *E. coli*, contain extended loops in NDUFS3 (Nqo5 and NuoCD, respectively), that would conflict with the position of NDUFA5 in eukaryotes (**Figures 5B–F**). Importantly, in *E. coli*, but not in *T. thermophilus*, the NDUFS2 and NDUFS3 subunits are a single polypeptide (NuoCD). Nonetheless, in both bacterial structures, an extended β3-4^{S3} loop (β3-4^{Nqo5} and β3-4^{NuoCD}) conflicts with the position of the NDUFA5 C-terminal coil in the mitochondrial CI structures (**Figures 5B–D**). This extended loop provides additional contacts between NDUFS3 and NDUFS2 in *T. thermophilus* and would stabilize the overall NuoCD fold in *E. coli*. Thus, NDUFA5 in mammals would replace these lost bacterial stabilizing interactions between NDUFS2 and NDUFS3. Additionally, the loop corresponding to β4-5^{S3} in *T. thermophilus* (β4-5^{Nqo5}) is also longer with an extended interaction interface between NDUFS3 and NDUFS2 (**Figure 5F**). This extended β4-5^{S3} loop would also conflict with the position of NDUFA5 in mitochondrial CI (**Figures 5E,G**). In *Y. lipolytica*, an additional stabilizing interaction involving the N-terminal coil of NDUFS8 is seen in this region, bridging NDUFA5 and NDUFS3 (**Figure 5G**). Overall, the differences of the NDUFS2 and NDUFS3 interfaces between the bacteria and

mitochondrial structures indicate that different strategies have evolved to support the association of these subunits. On one extreme there is *E. coli* that uses a fused NuoCD subunit and on the other is eukaryotes that have recruited NDUFA5 to facilitate interaction between NDUFS2 and NDUFS3. In the middle is *T. thermophilus* that has extended loops that help facilitate the interaction and occupy the equivalent position of NDUFA5 in eukaryotes.

Nonetheless, differences in the interaction interface between NDUFS2 and NDUFS3 in mammalian and *T. thermophilus* CIs alone cannot explain the dependency on NDUFA5 for Q-module assembly. In human CI the interface between NDUFS2 and NDUFS3 is larger (2,747.1 $Å^2$ vs. 2,613.5 $Å^2$) and more energetically favorable (-20.2 kcal/mol vs. -16.6 kcal/mol) than that of *T. thermophilus* (Krissinel and Henrick, 2007). This suggests that NDUFA5 binding, in addition to providing stabilizing interactions between the subunits, may also allosterically regulate their interaction, promoting necessary conformational changes that allow for Q-module assembly. Interaction studies between isolated NDUFS2 and NDUFS3 in the presence and absence of NDUFA5 are needed to address this hypothesis.

The Square Coil of the Peripheral Arm: NDUFA7

NDUFA7 forms part of the Q-module and it is believed to be among the last subunits added as no intermediates containing this subunit have been observed (**Figure 2A**) (Sánchez-Caballero et al., 2016). Except for the N-terminal amphipathic helix, which binds at the interface of the matrix and IMM adjacent to NDUFS8, NDUFA1 and NDUFA12, most of NDUFA7 is an extended coil without secondary structure that ascends from the membrane to the N-module, continues laterally along the N/Q-module interface then descends back towards the membrane (**Figures 5H,I**). NDUFS8, NDUFA12 and NDUFS2 create a binding surface for the NDUFA7 "ascending" coil (**Figure 5I**). The NDUFA7 "lateral" coil interacts with NDUFV1, NDUFS1 and NDUFS2 (**Figure 5I**). The lateral coil is followed by a variable region that is disordered in mammals (residues 72–89), a small α-helical domain in *Y. lipolytica* and a short α-helix in plants (**Figures 5I–K**) (Guo et al., 2017; Grba and Hirst, 2020; Kampjut and Sazanov, 2020; Maldonado et al., 2020). This variable region interacts with NDUFS3 and NDUFA5. The C-terminal NDUFA7 "descending" coil extends towards the N-terminus of NDUFS8 interacting with NDUFS2, NDUFS3 and NDUFA5 (**Figure 5I**). Adjacent to the variable region the lateral and descending coils sandwich the N-terminal α-helix of NDUFS3 resulting in a significant reorientation of the NDUFS3 helix in eukaryotic CI relative to its position in the bacterial structures (**Figure 5L**).

In HEK293T cells, NDUFA7^{KO} has negligible to moderate reductions in CI activity and stability. However, in any accessory subunit KO that results in the reduction of N-module incorporation, e.g., NDUFS6^{KO}, NDUFA2^{KO} and NDUFA6^{KO}, leads to a reduction of NDUFA7 (Stroud et al., 2016). This suggests that although NDUFA7 interacts mostly with Q-module subunits it requires the N-module for binding and has resulted in the proposal that NDUFA7 should be considered a N-module, as opposed to Q-module, subunit (Formosa et al., 2018). In cardiac cells, depletion of NDUFA7 promotes ROS generation and calcineurin signaling activation that results in the expression of cardiac hypertrophy genes (Shi et al., 2020).

Interestingly, in the *Y. lipolytica* ΔNDUFS6 CI structure – in which the assembly factor NDUFAF2 is bound instead of NDUFA12—the NDUFA7 amphipathic helix and ascending coil along with the N-terminal coil of NDUFS3—which binds overtop of the NDUFA7 ascending coil in *Y. lipolytica*—are disordered (**Figures 5M,N**). This indicates that full binding of NDUFA7 likely requires the exchange of NDUFAF2 for NDUFA12 during attachment of the N-module. However, in *Y. lipolytica* the C-terminal coils of NDUFA7 are held in place by the interaction between the small α-helical domain of the variable region and the C-terminal coil of NDUFS3 that wraps over the lateral coil, as well as additional interactions with the N-terminus of NDUFS8 (**Figures 5G,J,M,N**). These interactions are missing in mammals—which lack the α-helical domain and have shorter NDUFS3 C-terminal and NDUFS8 N-terminal coils (**Figure 5I**)—suggesting that NDUFA7 binding may be more sensitive to the exchange of NDUFAF2 and NDUFA12 in mammals.

Outside of the N-terminal amphipathic helix the most conserved region of NDUFA7 is the "corner" between the ascending and lateral coils which binds at the interface of NDUFV1 and NDUFS1 of the N-module and NDUFS2 and NDUFS3 of the Q-module (**Figure 5O**). In *T. thermophilus* and *E. coli* CIs this interface is filled with the NDUFS1 α3-β6^{S1} loop and the N-terminal coil of NDUFV1, respectively, which are much longer than their eukaryotic counterparts (**Figures 5P,Q**) (Baradaran et al., 2013; Kolata and Efremov, 2021). Like in the case of NDUFS4, these different interactions represent three different strategies for stabilizing this interface in the three different CI lineages (**Figures 5O–Q**). In mammals, it has also been shown that NDUFA7 is a target for phosphorylation by cAMP-dependent protein kinase (mtPKA) at Ser95^{A7} located at the interface of NDUFS3 and NDUFA5 (Rak and Rustin, 2014). Analogous to the interaction with the NDUFS3 C-terminal coil in *Y. lipolytica*, phosphorylation may promote NDUFA7 binding in this region and hence could play a part in regulating CI assembly (Palmisano et al., 2007). This leads to the hypothesis that NDUFA7, although not essential, functions to stabilize the attachment of the N-module and may aid in the replacement of NDUFAF2 with NDUFA12 during assembly.

The LYR/Acyl Carrier Protein Pairs: NDUFA6/NDUFAB1-α and NDUFB9/NDUFAB1-β

The NDUFAB1 subunit of mammalian CI is an acyl carrier protein (ACP) involved in transporting and extending fatty acid chains during fatty acid synthesis. ACPs interact closely with leucine-tyrosine-arginine (LYR) motif proteins (Dibley et al., 2020). The LYR family of proteins are involved with mitoribosome biogenesis (MIEF1-MP) (Brown et al., 2017;

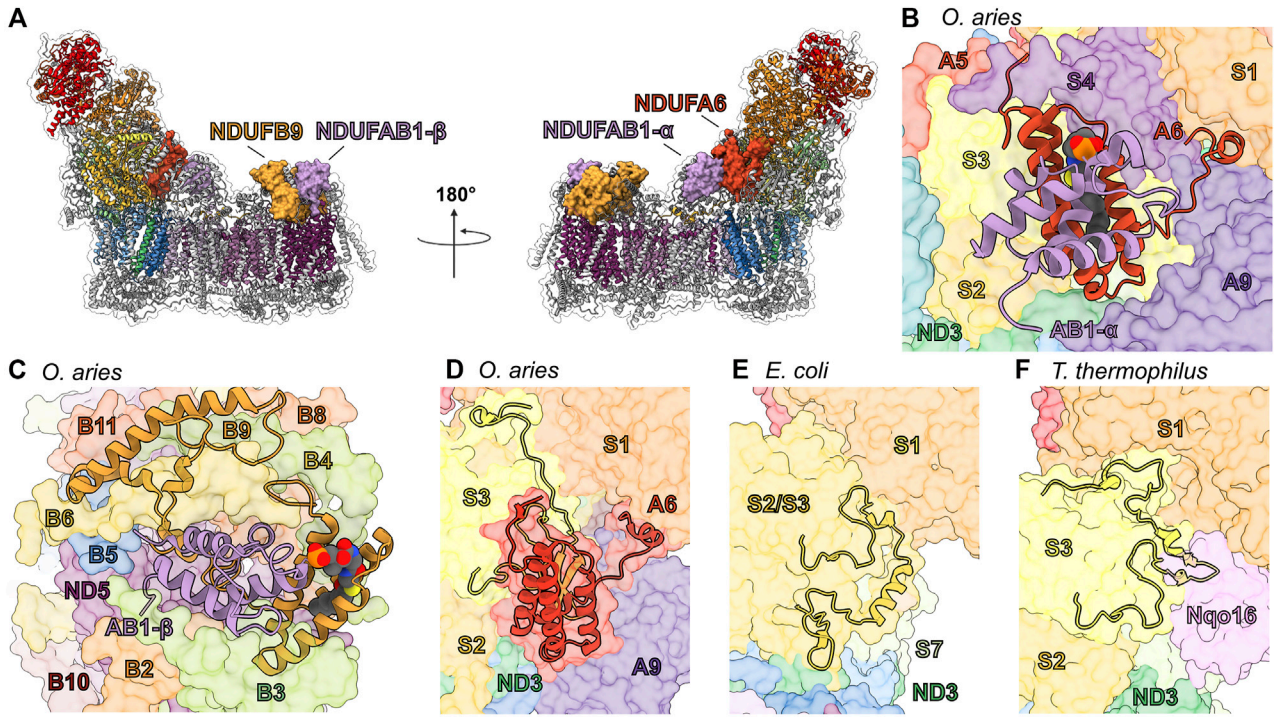

FIGURE 6 | Accessory subunits NDUFA6, NDUFAB1-α, NDUFB9, and NDUFAB1-β in mammalian CI. **(A)** The structure of CI in cartoon with the surfaces of NDUFA6 (cinnabar red)/NDUFAB1-α (violet) and NDUFB9 (yellow orange)/NDUFAB1-β (violet) shown, the core subunits colored as in **Figure 1A** and the accessory subunits grey. **(B)** Shin view CI showing the NDUFA6/NDUFAB1-β pair in cartoon and other CI subunits as transparent surfaces. The acylated 4′-phosphopantetheine group is shown in spheres (PDB: 5LNK). **(C)** Looking down on the toe of CI (PDB: 6ZKC) showing the NDUFB9/NDUFAB1-β pair in cartoon and the other CI subunits as transparent surfaces. **(D–F)** NDUFA6 replaces structural elements of bacterial CI. Shin view of **(D)** mammalian (PDB: 5LNK), **(E)** *E. coli* (PDB: 7NYR) and **(F)** *T. thermophilus* CI shown as transparent surface with NDUFA6, the NDUFS2/S3 (NuoCD) (corn yellow) linker and NDUFS3 C-termini shown in cartoon. Accessory subunits that are not important for the discussion are omitted from panel **(D)** for clarity. The NDUFS2/S3 (NuoCD) linker in *E. coli* and Nqo16 (pink) subunit in *T. thermophilus* conflict with the position of NDUFA6 in mammals. NDUFA6: cinnabar red, NDUFAB1-α: violet, NDUFB9: yellow orange, NDUFAB1-β: violet/violet, NDUFS2/S3: corn yellow, Nqo16: pink.

Rathore et al., 2018), CII assembly (SDHAF1) (Ghezzi et al., 2009), $CIII_2$ assembly (LYRM7) (Maio et al., 2017), and iron-sulfur cluster biogenesis (LYRM4) (Atkinson et al., 2011). These interactions link these different processes to fatty acid biosynthesis and/or are responsible for recruitment of downstream factors (Brown et al., 2017). Mitochondrial CI contains two LYR protein subunits, NDUFA6 and NDUFB9, both of which are found in association with a copy of NDUFAB1 in the intact complex (**Figure 6A**). Therefore, two copies of NDUFAB1 are present in mitochondrial CI. NDUFAB1-α binds to NDUFA6 on the "shin" side of the Q-module whereas NDUFAB1-β binds to NDUFB9 on the mitochondrial matrix side of the P_D-module forming part of the P_D-bulge (**Figure 1A** and **Figure 6A**).

NDUFAB1 is a small globular protein composed of four α-helices and a 4′-phosphopantetheine (4PP) group at Ser44 which serves as a prosthetic group for the attachment of fatty acids and which can exist in two conformations: buried, for fatty acid transport; or flipped-out, for interaction with fatty acid modifying enzymes (Cronan, 2014). The interaction between ACPs and LYR proteins *via* the flipped-out 4PP group and acyl chain extending into the core of the LYR protein (**Figures 6B,C**), was first observed in the structure of ovine CI (Fiedorczuk et al., 2016). The same flipped-out mode of interaction has since been seen for all ACP/LYR protein pairs (Boniecki et al., 2017; Brown et al., 2017). Unlike the case in mammals, *Y. lipolytica* CI does not harbor two identical copies of NDUFAB1 but two distinct homologues, ACMP1 and ACMP2, bound in the analogous positions of NDUFAB1-α and β respectively.

NDUFA6/NDUFAB1-α—In fully assembled CI NDUFAB1-α interacts solely with NDUFA6 and joins the complex in the final stages of CI assembly (**Figure 2A**) (Guerrero-Castillo et al., 2017a). Therefore, NDUFAB1-α is one of only two accessory subunits that does not interact directly with any core subunits (the other being NDUFC1). NDUFA6 is situated in the Q-module interacting with NDUFS3, NDUFS4 and ND3 bridging the peripheral and membrane arms of the complex (**Figure 6B**). NDUFA6's C-terminal coil extends toward the N-module and interacts with NDUFS3, NDUFA9 and NDUFS1 (**Figure 6B**). In *E. coli* the binding site of NDUFA6 conflicts with the loop connecting the fused NDUFS2/NDUFS3 single subunit NuoCD (**Figures 6D,E**). Whereas, in *T. thermophilus*, the binding site of NDUFA6 conflicts with the accessory subunit Nqo16, which is not present in other species (**Figure 6F**). Also, in

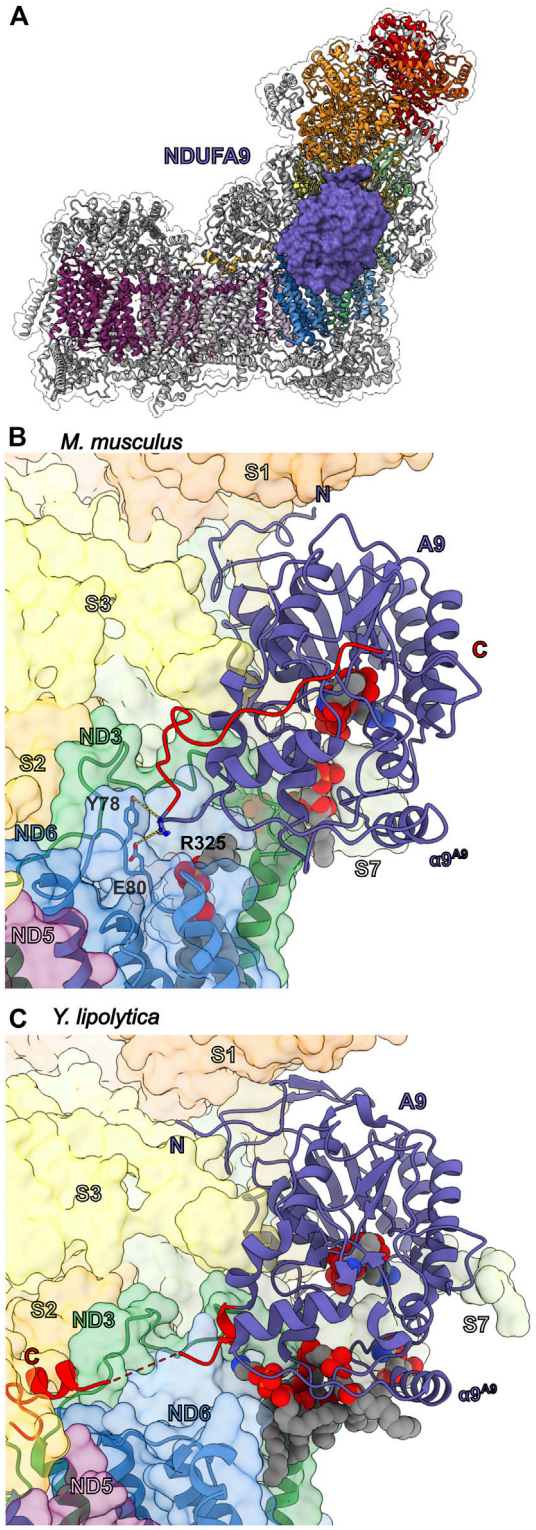

FIGURE 7 | Accessory subunit NDUFA9. **(A)** The structure of CI (PDB: 6ZKC) in cartoon with the surface of NDUFA9 (lavender) shown, the core subunits colored as in **Figure 1A** and the accessory subunits grey. **(B)** *M. musculus* CI (PDB: 6G2J) and **(C)** *Y. lipolytica* CI (PDB: 6RFR) shown as transparent surfaces with NDUFA9 (NUEM), ND3 (sea green) and ND6 (cyan-blue) shown in cartoon. NADPH and lipids are shown as spheres. The C-terminal coils of NDUFA9 are colored red. The key residues interacting with ND6 are shown in stick representation. Accessory subunits that are not important for the discussion are omitted from the figures for clarity. Subunits are colored as in **Figure 1** in all the structure figures unless stated otherwise. NDUFA9: lavender, ND3: sea green, ND6: cyan-blue.

this region differences can be seen between the C-terminal loops of NDUFS3 in mammals and *T. thermophilus* (Nqo5) which have adapted to interact with the distinct accessory subunits NDUFA9 and Nqo16 respectively (**Figures 6D,F**).

NDUFB9/NDUFAB1-β—In contrast to the NDUFA6/NDUFAB1-α pair, NDUFB9/NDUFAB1-β participates early in CI assembly, interacting with core subunit ND5 and accessory subunits NDUFB2, NDUFB3, NDUFB6 and NDUFB8 to form the P_D-b subassembly (**Figure 2** and **Figure 6C**) (Guerrero-Castillo et al., 2017a). Unlike NDUFA6, no structural elements of the bacterial core subunits conflict with the position of the NDUFB9/NDUFAB1-β pair, suggesting that NDUFB9 simply used the surface of ND5 as a platform without replacing any pre-existing functionality.

Roles of LYR/ACP pairs in CI assembly and activity—Given its role in fatty acid metabolism it is not surprising that NDUFAB1 is the only accessory subunit essential for overall HEK293T viability (Stroud et al., 2016). Complementation of $NDUFAB1^{KO}$ HEK293T cells with a yeast ACP rescued cell growth, but not CI assembly (Stroud et al., 2016). This demonstrates that although NDUFAB1 is essential for CI assembly, the essential role of NDUFAB1 in cell viability is independent of CI. $NDUFA6^{KO}$ in HEK293T or NDUFA6 (LYRM6) deletion in *Y. lipolytica* (ΔNDUFA6) results in a subassembly of CI lacking the N-module or a fully assembled (only lacking the NDUFA6/NDUFAB1-α pair), but catalytically incompetent CI, respectively (Stroud et al., 2016; Guerrero-Castillo et al., 2017a). This indicates the NDUFA6/NDUFAB1-α pair is essential for activity (Guerrero-Castillo et al., 2017a). More recently, point mutations of NDUFA6, generated in *Y. lipolytica*, at its interface with core membrane subunits ND1 and ND3 (**Figure 6B**) demonstrated that NDUFA6's essential role in CI activity is mediated by contacts at this site (Angerer et al., 2014) (Galemou Yoga et al., 2020). Structural analysis of the functionally impaired $F89A^{A6(LYRM6)}$ mutant revealed that this mutation influences the structures of the $TMH1\text{-}2^{ND3}$ loop, $TMH5\text{-}6^{ND1}$ loop, and NDUFA9; this network of loops is proposed to provide needed conformational flexibility during ubiquinone reduction (Galemou Yoga et al., 2020). Conversely, $NDUFB9^{KO}$ in HEK293T cells more closely recapitulates, though with lesser severity, the $NDUFAB1^{KO}$ phenotype in which the assembly of CI is abrogated (Stroud et al., 2016). This demonstrates the importance of the NDUFB9/NDUFAB1-β pair in the early stages of CI assembly.

The above indicates that CI assembly and activity are dependent on the presence of acylated ACPs and leads to the hypothesis that the LYR/ACP pairs connect CI assembly and activity to fatty acid metabolism. The NDUFB9/NDUFAB1-β and NDUFA6/NDUFAB1-α pairs ensures that new CI is not

assembled, and that CI activity is "switched off" in the absence of sufficient levels of fatty acid fuel, i.e., low levels of acylated ACP. In metazoans that rely solely on respiration for energy production, the dependence of CI on the presence of sufficient fatty acids is likely moot, as the organism would be unlikely survive such severe starvation conditions. However, during the evolution of eukaryotes dependence of CI assembly and activity on the presence of sufficient levels of fatty acid may have aided in switching between different metabolic strategies. The fact that *Y. lipolytica* CI harbors two distinct ACP homologues, ACMP1 and ACMP2, may provide additional flexibility in regulating CI assembly vs. activity. This combined with its powerful genetic tools makes *Y. lipolytica* a powerful system in which to test the distinct roles of the ACPs in CI assembly and activity.

The NADPH Containing Subunit NDUFA9

NDUFA9 is part of the Q-module adjacent to the membrane at the Q/P interface (**Figure 1B** and **Figure 7A**). Along with NDUFA1 and assembly factor NDUFAF2, NDUFA9 is incorporated after formation of the Q/P_P subassembly (**Figure 2A**) (Sánchez-Caballero et al., 2016; Guerrero-Castillo et al., 2017a). NDUFA9 belongs to the family of short-chain dehydrogenase/reductases and contains a conserved nucleotide binding Rossmann fold motif that binds a NADPH cofactor (**Figure 7B**). NDUFA9 forms an extensive interface with the core-subunits NDUFS1, NDUFS3, NDUFS7 and NDUFS8, as well as ND1, ND3 and ND6 (**Figure 7B**). NDUFA9 binds on the surface of membrane overhanging the opening of CoQ tunnel in ND1 (**Figure 3L**). The short amphipathic helix of NDUFA9 ($\alpha9^{A9}$) along with those of NDUFS7 ($\alpha1^{S7}$ and $\alpha6^{S7}$) and NDUFA12 ($\alpha2^{A12}$) pull the membrane lipids in the region out of the membrane plane by ~10 Å (**Figure 3L**) (Parey et al., 2019). Additionally, the C-terminal amphipathic helix of NDUFS7 ($\alpha6^{S7}$) approaches NDUFA9's NADPH binding pocket and may contact the NADPH directly (Fiedorczuk et al., 2016). Distortion of the membrane at the entry site of the hydrophobic CoQ substrate has been suggested to help promote CoQ entry and exit from the CoQ tunnel (Parey et al., 2019).

Despite its homology to dehydrogenase enzymes, NDUFA9 has not be shown to have any catalytic activity and the bound NADPH cofactor most likely plays a structural role as demonstrated by mutations that block NADPH binding in *Y. lipolytica* only affecting CI assembly but not activity (Abdrakhmanova et al., 2006; Ciano et al., 2013; Torraco et al., 2017). Deletion of NDUFA9 in *Y. lipolytica* (NUEM) or *Neurospora crassa* (Nuo-40) abolished CI activity and severely decreased the total amount of CI reflecting a severe assembly defect (Schulte et al., 1999; Abdrakhmanova et al., 2006). In HEK293T cells, $NDUFA9^{KO}$ results in loss of CI activity and the appearance of a novel ~600-kDa subassembly lacking the N-module as well as components of the Q-module (Stroud et al., 2013). NDUFA9 missense mutations $R321P^{A9}$ and $R360C^{A9}$ are associated with human mitochondrial disease (van den Bosch et al., 2012; Baertling et al., 2018). $R321^{A9}$ is in the core of the Rossmann fold and forms a salt bridge with Asp/$Glu133^{A9}$ (Asp in humans, Glu in other mammals) adjacent to the NADPH binding site. Therefore, like the NADPH disrupting mutations, mutation of $R321^{A9}$ to proline likely disrupts the stability of NDUFA9 and its interaction with CI. However, $R360^{A9}$ (R325 in *M. musculus*) is not located in the core of the protein but on the C-terminal loop where it packs against $Tyr78^{ND6}$ of the TMH3-4^{ND6} loop, suggesting an important role for the interaction between NDUFA9 and the core TM subunits (**Figure 7B**).

Cross-linking studies have shown that in the deactive (D)-form of CI, ND3 crosslinked to NDUFA9 but not in the active (A)-form (Ciano et al., 2013). The order to disorder transitions seen in the TMH1-2^{ND3} loop and the TMH 3-4^{ND6} loop between the A- and D-forms of the enzyme are also reflected in a structurally conserved short amphipathic helix of NDUFA9 (human $\alpha9^{A9}$), which is ordered in the A-form but disordered in the D-form (Kampjut and Sazanov, 2020). In *Y. lipolytica* mutations in NDUFA6 (LYR6M) adjacent to the TMH1-2^{ND3} loop ($F89A^{A6(LYRM6)}$) result in disorder of the Q-site loops of the core subunits (the TMH1-2^{ND3}, TMH5-6^{ND1} and $\beta1$-$\beta2^{S2}$ loops), as well as the C-terminal loop of NDUFA9 propagating over 50 Å away from the mutation site (Galemou Yoga et al., 2020). The disorder of NDUFA9 also results in the loss of density for several NDUFA9 associated lipid molecules adjacent to the CoQ tunnel entry (Galemou Yoga et al., 2020).

Importantly, the above demonstrates that the interactions between NDUFA9 and the core TM subunits are key to CI activity in both mammals and yeast. However, significant structural differences exist in the interactions of the NDUFA9 C-terminus in mammals and yeast (**Figures 7B,C**). In mammals, the C-terminus of NDUFA9 interacts closely with both ND3 and ND6 but then folds back onto the core of the Rossman fold (**Figure 7B**). Conversely, in *Y. lipolytica*, the NDUFA9 C-terminus extends across the surface of the membrane arm and buries an α-helix adjacent to ND4L and the NDUFS2 N-terminal coil (**Figure 7C**). Despite these differences the hypothesis emerges that NDUFA9, due to its close interaction with the Q-site loops and role in distorting the membrane around the Q-tunnel, may help regulate substrate access to the CoQ-tunnel by altering the membrane environment in response to changes in the conformation of the Q-site loops. The order to disorder transitions of the NDUFA9 C-terminus, seen in the A- and D-forms of the mammalian enzyme and in the *Y. lipolytica* NDUFA6 mutant, propagate to the membrane and likely disrupt the lipid environment generated by NDUFA9, NDUFS7 and NDUFA12 (**Figure 3L**). Therefore, NDUFA9 may regulate access to the CoQ site in the A/D transitions and during early stages of CI assembly.

Transmembrane Accessory Subunits of the Heel: NDUFA13, NDUFA3 and NDUFA1

The heel of CI is the site of CoQ reduction. This region is composed of the core subunits ND1, which harbors the entry site of the CoQ tunnel, three accessory transmembrane subunits NDUFA13, NDUFA3 and NDUFA1 (**Figures**

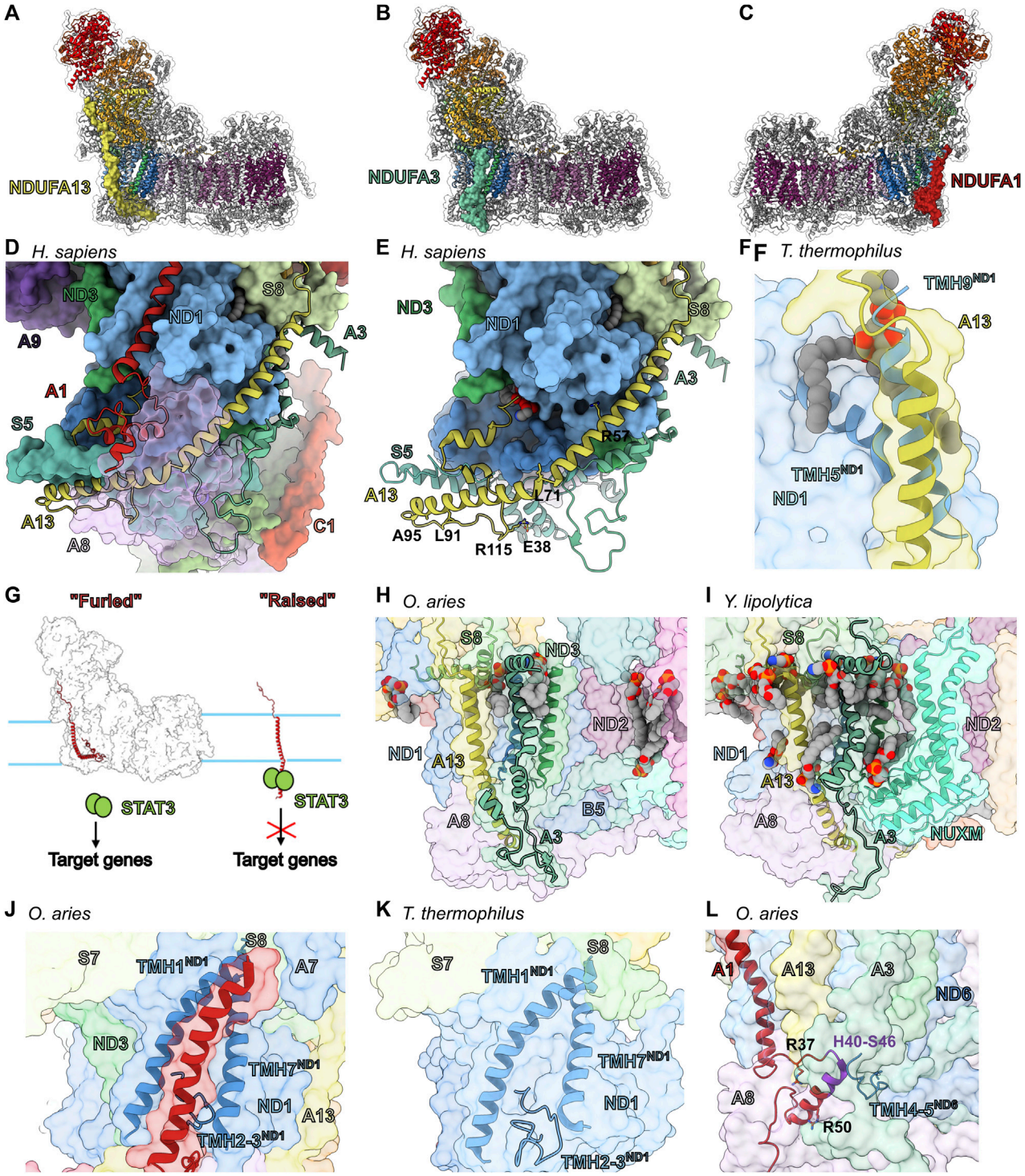

FIGURE 8 | Accessory subunits of the CI heel. The structure of CI (PDB: 6ZKC used throughout) in cartoon with the surface of NDUFA13 (light yellow) **(A)**, NDUFA3 (pine green) (**B**) and NDUFA1 (firebrick red) **(C)** shown, the core subunits colored as in **Figure 1A** and the accessory subunits grey. **(D)** Looking up from the CI heel showing NDUFA13, NDUFA3, and NDUFA1 of *H. sapiens* CI structure (PDB: 5XTD) as cartoons. NDUFA8 (lilac purple) is shown as a transparent surface for clarity. **(E)** Accessory subunit NDUFA13 of *H. sapiens* CI structure (PDB: 5XTD) is shown as cartoon. The residues mentioned in the text are shown in stick representation. **(F)** NDUFA13 compensates for the lost transmembrane helix $TMH9^{ND1}$ (cobalt blue) of *T. thermophilus*. *T. thermophilus* ND1 (Nqo8) (PDB: 4HEA used throughout) is superposed on ND1 of mammalian (*O. aries*) CI structure shown as transparent surface. $TMH5^{ND1(Nqo8)}$ and $TMH9^{ND1(Nqo8)}$ are shown as cartoons. NDUFA13 surface and cartoon are shown. **(G)** Schematic representation of the "Flag post model." NDUFA13 of healthy CI is furled and incapable of binding to STAT3. NDUFA13 alone is raised exposing the STAT3 interacting site to the IMS. **(H,I)** Assembly vs. lipid binding roles of NDUFA3. **(H)** Mammalian CI shown as transparent surface with NDUFA3, (*Continued*)

FIGURE 8 | NDUFA13, $\alpha1^{ND1}$ (cobalt blue), and $\alpha3^{ND3}$ (sea green) shown as cartoons. **(I)** *Y. lipolytica* CI (PDB: 6YJ4) shown as transparent surface with NDUFA3 (NI9M), NDUFA13 (NB6M), NUXM (light cyan), $\alpha1^{ND1}$ (NU1M), and $\alpha3^{ND3}$ (NU3M) (sea green) shown as cartoons. **(J,K)** NDUFA1 compensates for the shorter TMH2-3^{ND1} loop. **(J)** Mammalian CI structure shown as transparent surface with NDUFA1, $TMH1^{ND1}$, $TMH7^{ND1}$ and the TMH2-3^{ND1} loop shown as cartoons. **(K)** *T. thermophilus* CI shown as transparent surface with $TMH1^{ND1(Nqo8)}$, $TMH7^{ND1(Nqo8)}$ and the TMH2-$3^{ND1(Nqo8)}$ loop shown as cartoon. **(L)** NDUFA1 connects the P_P-a and P_P-b subassemblies. Mammalian CI a transparent surface with NDUFA1 and the ND6 TMH4-5^{ND6} (cyan-blue) loop shown as cartoon. Residues mentioned in the text are shown as sticks. Key H40-S46 sequence shown in purple. Subunits are colored as in **Figure 1** in all panels unless stated otherwise. NDUFA13: light yellow, NDUFA3: pine, NDUFA1: firebrick red, NDUFA8: lilac purple, ND1: cobalt blue, ND3: sea green, ND6: cyan-blue, NUXM (light cyan).

8A–C), as well as the quadruple-CX_9C motif containing subunit NDUFA8 (discussed below) (**Figure 8D**).

NDUFA13—Along with ND1, NDUFA3 and NDUFA8, NDUFA13 forms the P_P-a subassembly (**Figure 2**). NDUFA13 has an N-terminal coil that binds along the Q-module, a single TMH that extends into the intermembrane space (IMS) followed by a coil and two short α-helices at the C-terminus in a helix-turn-helix motif (**Figures 8A,E**). The N-terminal coil of NDUFA13 binds atop the ascending coil of NDUFA7 near the interface of the N- and Q-modules (**Figure 8A**) and follows a groove along NDUFS2 towards the membrane (**Figure 5I**). At the interface of the matrix and IMM, NDUFA13 interacts with NDUFS8 and a lipid molecule (**Figure 8D**). The NDUFA13 TMH binds to ND1 in the membrane and continues into the IMS where it interacts with ND3, NDUFA3 and NDUFA8 (**Figure 8D**). Although not completely vertical in the membrane the interaction with NDUFA8 bends the NDUFA13 TMH sharply, making it run nearly parallel to the surface of the membrane (**Figures 8D,E**). Thus, the NDUFA13 TMH extends across the IMS side of the complex interacting with ND6, NDUFB5, NDUFA1, NDUFS5 and NDUFA8 (**Figures 8D,E**). After crossing the complex, NDUFA13 turns back interacting with NDUFS5, NDUFA8, NDUFB5, ND6, ND3 and NDUFA1 (**Figures 8D,E**). The NDUFA13 C-terminal coil also participates in the binding of a lipid molecule between ND1, ND3 and ND6 (**Figure 8E**). In *T. thermophilus* CI, ND1 (Nqo8) has an additional C-terminal TMH (TMH9$^{ND1(Nqo8)}$) that occupies the same position as the NDUFA13 TMH in eukaryotes (**Figure 8F**), however, this additional TMH is not seen in the *E. coli* CI structure (Baradaran et al., 2013; Kolata and Efremov, 2021). Nonetheless, the presence of the additional helix in *T. thermophilus* ND1 suggests that the position of NDUFA13 binding at the N-terminus of the tilted $TMH5^{ND1}$ may confer additional stability to ND1 (**Figure 8F**).

In HEK293T cells, $NDUFA13^{KO}$ results in loss of the N-module, NDUFA10 and NDUFB5 indicating that, although it is added early in assembly, NDUFA13 is necessary for the final stages of CI assembly (Stroud et al., 2016). NDUFA13 mutations $K5N^{A13}$ and $R115P^{A13}$ have been implicated in Oxyphil or Hurthle cell tumors (Máximo et al., 2005). The side chain of $K5^{A13}$ is solvent exposed and does not make any specific interaction with other residues, hence mutation of this residue is unlikely to affect the structural integrity of CI directly but may affect mitochondrial targeting and import. $R115^{A13}$ is on the TMH1-$\alpha1^{A13}$ loop and forms a salt bridge with NDUFS5 conserved residue $E38^{S5}$ (**Figure 8E**). This salt bridge likely helps to stabilize the kinked structure of the NDUFA13 TMH and the $R115P^{A13}$ mutation would remove this stabilizing interaction. Germline mutation $R57H^{A13}$ leads to early onset of hypotonia, dyskinesia and sensorial deficiencies (Angebault et al., 2015). $R57^{A13}$ is buried in a pocket at the interface with ND1 (**Figure 8E**) and mutation would disrupt this interaction and weaken the association of NDUFA13 with CI.

NDUFA13 is also known as GRIM-19 and was independently discovered as part of an apoptosis/cell proliferation pathway involving the cytoplasmic transcription factor STAT3 (Lufei et al., 2003). Through its interaction with STAT3, NDUFA13 represses STAT3 dependent transcription and thus has an anti-proliferative pro-apoptotic effect and plays a role in tumor suppression (Lufei et al., 2003). The interaction between NDUFA13 and STAT3 was narrowed down to the DNA binding domain and linker region of STAT3 and residues 36–72 of NDUFA13 (Lufei et al., 2003), however, given that residues 29–51 of NDUFA13 are buried in the membrane, the most likely interaction site would be between residues 52–72 which extend into the IMS. Consistent with this, mutations in the IMS portion of the NDUFA13 TMH (L71P, L91P and A95T in human) disrupt STAT3 binding and promote oncogenesis (Nallar et al., 2013). When associated with CI, this region of NDUFA13 (residues 52–72) is inaccessible due to interactions with NDUFA8 and NDUFA3 (**Figure 8D**). Hence, NDUFA13 can only interact with STAT3 when it is not bound to CI. These observations lead to a "flagpole" hypothesis in which NDUFA13 acts as a sensor that ties mitochondrial and ETC health to cell proliferation and apoptosis (**Figure 8G**). In conditions that block CI assembly or promote CI disassembly the NDUFA13 "flag" is raised allowing it to interact with STAT3 suppressing proliferation and promoting apoptosis (**Figure 8G**). Conversely, in healthy mitochondria, NDUFA13 is "furled," i.e., interacting with CI, and thus sequestered away from interaction with STAT3 thereby promoting proliferation (**Figure 8G**).

NDUFA3—Along with NDUFA13, NDUFA8 and ND1, NDUFA3 is a member of the P_P-a subassembly (**Figure 2A**) (Sánchez-Caballero et al., 2016). NDUFA3 is made up of an amphipathic helix that lies at the matrix-membrane interface, a single TMH, and an α-helix followed by a C-terminal coil in the IMS (**Figures 8B,H**). The NDUFA3 amphipathic helix interacts with the N-terminal NDUFS8 amphipathic helix and helps to trap two lipids, one against ND1 and the other against ND3 (**Figure 8H**). In the membrane and IMS, NDUFA3 interacts with ND3 and ND1 *via* a short α-helix and NDUFA13, ND6, NDUFS5, NDUFB5 and NDUFA8 *via* a C-terminal coil. Thus, NDUFA3's interactions bridge components of the Q, P_P-a and P_P-b subassemblies within the matrix and IMS (**Figure 8H**).

In HEK293T cells, $NDUFA3^{KO}$ blocks CI assembly and leads to a decrease in the level of subunits in the N- and P_P-b

subassemblies, as well as subunits in the P_D-a subassembly (Stroud et al., 2016). NDUFA3 knockdown in human cell lines also showed that NDUFA3 is required for the assembly and stability of the Q-module (Rak and Rustin, 2014). In the structure of *Y. lipolytica* CI (Grba and Hirst, 2020) the amphipathic helix of NDUFA3 (NI9M), along with subunit NUXM, trap several lipids against ND3 and ND2 (**Figure 8I**). However, in mammals the loss of the first three TMHs of ND2, which form the binding site of NUXM, results in the lack of a homolog for NUXM and fewer structured lipids in this region (**Figure 8H**). Interestingly, a NUXM homologue is also seen in plants (coined NDUX1) emphasizing this metazoan specific deletion in ND2 (Maldonado et al., 2020).

This leads to the hypothesis that one of the original functions of NDUFA3 was to stabilize lipid binding at the interface of ND1, ND3 and ND2, however with the truncation of ND2 and loss of NUXM, this function may be minimized in metazoans. The importance of NDUFA3 in CI assembly likely stems from interactions at two interfaces. 1) At the interface of the matrix and IMM, the NDUFA3 amphipathic helix, along with NDUFA13, sandwich the N-terminal amphipathic helix of NDUFS8, anchoring the Q subassembly to the Pp-a subassembly (**Figure 8H**). 2) In the IMS NDUFA3's helix binds between ND1 and ND3, thereby stabilizing the association of the Pp-a and Pp-b subassemblies. This interaction involving ND1 and ND3 is much diminished in *Y.lipolytica* CI where NDUFA3 (NI9M) lacks the IMS α-helix but binds several additional lipids not seen in mammalian structures (**Figure 8I**), suggesting the possibility of different primary roles, lipid biding vs. assembly, in different organisms.

NDUFA1—The single TMH accessory subunit NDUFA1 is not found in the P_P-a or P_P-a/Q subassemblies but joins along with NDUFA9 upon connection of the P_P-a/Q and P_P-b subassemblies forming the Q/P_P or Q/P intermediates (**Figure 2A**) (Sánchez-Caballero et al., 2016). NDUFA1 does not have an N-terminal coil but begins at the interface of the matrix and IMM with its TMH (**Figures 8C,J**). In the IMS, NDUFA1 has a small domain comprised of a loop, α-helix ($\alpha1^{A1}$) and C-terminal coil. At the interface of the matrix and IMM, the NDUFA1 N-terminus interacts with NDUFS8 and NDUFA7 (**Figure 8J**). Also, at the matrix/IMM interface the amphipathic helix of NDUFA12 binds atop NDUFA1 trapping a cardiolipin onto the NDUFA1 TMH (**Figure 3L**). In the membrane, NDUFA1 interacts with ND1 filling a groove formed between $TMH1^{ND1}$ and $TMH7^{ND1}$ (**Figure 8J**). In the IMS, NDUFA1 interacts with NDUFA8, ND1, ND6, NDUFS5 and NDUFA13. In *T. thermophilus* the ND1 (Nqo8) groove that houses NDUFA1 in eukaryotes is partially filled by the TMH2-$3^{ND1(Nqo8)}$ loop which is 10 residues longer relative to that seen in eukaryotes (**Figure 8K**). In the *E. coli* CI structure, $TMH1^{ND1(NuoH)}$ is disordered and the TMH2-$3^{ND1(NuoH)}$ loop is of intermediate length (5 amino acid residues longer than the eukaryotic loop), suggesting that the TMH2-3^{ND1} loop is important for the stability of $TMH1^{ND1}$.

NDUFA1 has been shown to play an essential role in the assembly pathway and function of CI in mammals (Fernandez-Moreira et al., 2007). $NDUFA1^{KO}$ in HEK293T cells prevents the full assembly of the complex and leads to a drop in the levels of subunits associated with the N- and P_P-b subassemblies (Stroud et al., 2016). The promoter region of the *NDUFA1* gene contains a cAMP response element suggesting it is linked to cAMP signaling pathways that regulate cellular energy metabolism (Palmisano et al., 2007). Studies in Chinese hamster cells identified several important functional residues and regions of NDUFA1 (Breen and Scheffler, 1979; Au et al., 1999; Yadava et al., 2002). For example, the conservative mutation $R50K^{A1}$ results in a severe loss of CI activity (Yadava et al., 2002). The structure shows that $R50^{A1}$ forms an inter-subunit salt bridge with $E77^{A13}$ buried in an otherwise relatively hydrophobic pocket (**Figure 8L**). The inability of the $R50K^{A1}$ to maintain this interaction speaks to the specificity and importance of the interaction between NDUFA1 and NDUFA13. Furthermore, sequence differences between rodent and primate NDUFA1 in the region from $H40\text{-}S46^{A1}$ in humans was also shown to prevent complementation between the NDUFA1 sequences from the different species (Yadava et al., 2002). Swapping just a few residues between the hamster and the human sequence results in CI assembly defects (Yadava et al., 2002). This region of the NDUFA1 interacts most closely with ND6 highlighting the importance of this interaction for CI assembly (**Figure 8L**). Additionally, mutations of highly conserved residues ($G8R^{A1}$ and $R37S^{A1}$) were found in two patients with Leigh's syndrome and with myoclonic epilepsy and developmental delay (Fernandez-Moreira et al., 2007). $G8^{A1}$ lies within the first 28 amino acids required for mitochondrial targeting, import, and orientation of NDUFA1 but also packs tightly against ND1 indicating either an import defect or assembly defect due to impaired interaction of NDUFA1 and ND1 (Fernandez-Moreira et al., 2007). $R37^{A1}$ forms inter-subunit salt bridges with $D89^{A8}$ and $E94^{A8}$ of NDUFA8 (**Figure 8L**).

The above leads to the hypothesis that NDUFA1 through its interaction with ND1, ND6, NDUFA8 and NDUFA13, is required for the stable connection of the P_P-a and P_P-b subassemblies during CI biogenesis. Given that none of the Q/P_P-a subassembly subunits are directly blocking NDUFA1 binding, it is unclear from the structure of the intact complex what prevents association of NDUFA1 to the Q/P_P-a subassembly. This suggests a conformation change upon association of the P_P-b subassembly that would expose the NDUFA1 binding site. Notably, $TMH1^{ND1}$, which is flexible in the *E. coli* structure (Kolata and Efremov, 2021), interacts closely with ND3 which arrives as part of the P_P-b subassembly. Altogether, this suggests that NDUFA1 compensates for the shortened TMH2-3^{ND1} loop as a "wedge" that stabilizes the position of $TMH1^{ND1}$ and whose binding site is not fully available until the position of $TMH1^{ND1}$ is established through interaction with ND3. Thus, NDUFA1 would only bind after association of the Q/P_P-a and P_P-b subassemblies and further stabilizes their association *via* a network of interactions (**Figure 8L**). Furthermore, the addition of NDUFA12 in the final stages of CI biogenesis, which binds overtop of NDUFA1 at the interface of the matrix and IMM, would act to lock NDUFA1 in place further stabilizing its association.

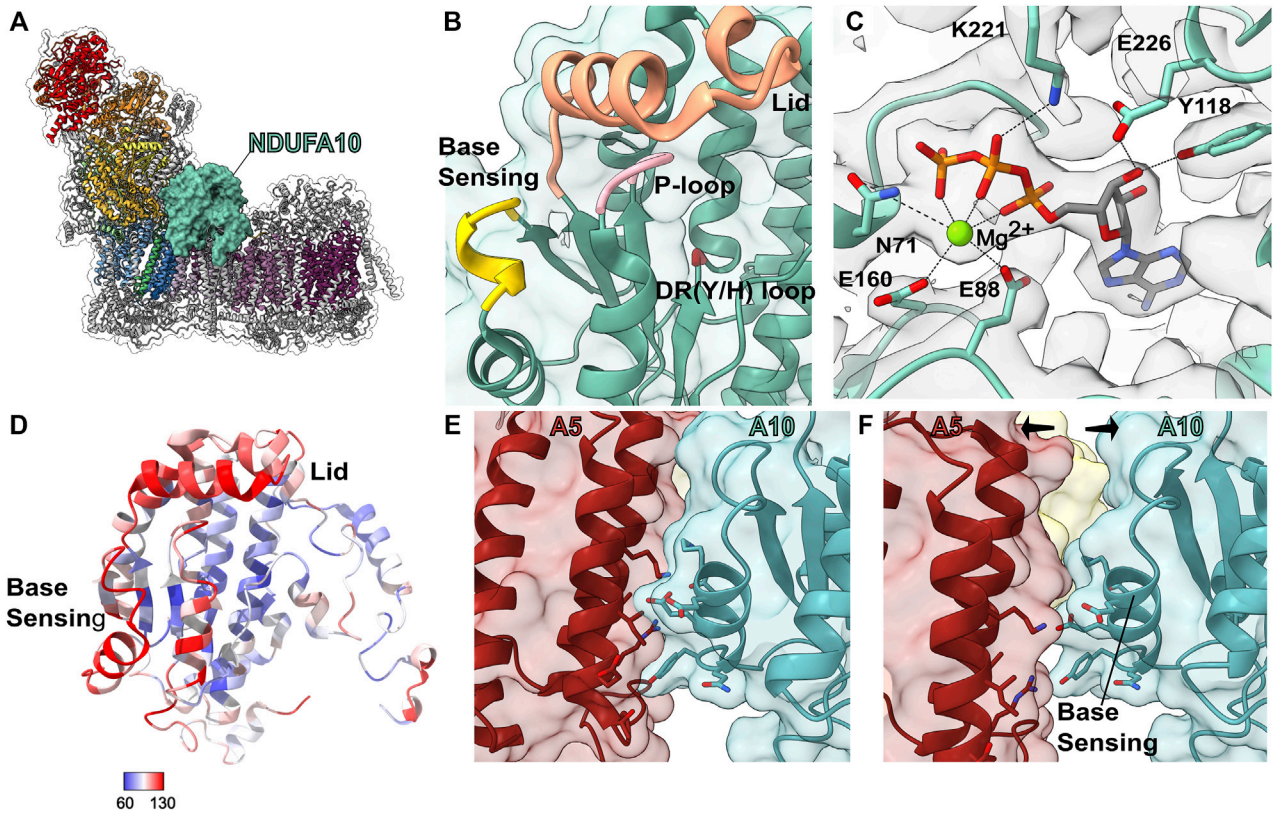

FIGURE 9 | Accessory subunit NDUFA10. **(A)** The structure of CI (PDB: 6ZKC) in cartoon with the surface of NDUFA10 (cadet blue) shown, the core subunits colored as in **Figure 1A** and the accessory subunits grey. **(B)** Transparent surface and cartoon of *O. aries* NDUFA10 (PDB: 6ZKC). The P-loop (pink), DR (Y/H) motif (red), lid region (orange) and base sensing loop (yellow) are shown as thickened cartoon. **(C)** Cartoon of NDUFA10 with the density map (grey) from *M. musculus* CI bound to the Q-site inhibitor piericidin (PDB: 7B93). Mg^{2+} ATP and key binding residues are shown as sticks and colored by element. **(D)** Cartoon of NDUFA10 colored by atomic displacement parameter (ADP) in CI (PDB: 6ZKO). Red: most flexible, Blue: least flexible. **(E,F)** State dependent interactions between NDUFA5 and NDUFA10 involve the base-sensing loop. **(E)** Transparent surface of closed A-state CI showing NDUFA10 and NDUFA5 (auburn) as cartoons (PDB: 6ZKC). **(F)** Transparent surface of open D-state CI showing NDUFA10 and NDUFA5 as cartoons (PDB: 6ZKD). Key residues involved in the interaction are shown as sticks and colored by element. NDUFA10: cadet blue, NDUFA5: auburn.

The Nucleoside Kinase Subunit: NDUFA10

NDUFA10 is a globular protein of the nucleoside kinase family (Steeg et al., 2011) that lies on the matrix side of ND2 (**Figure 9A**). It is one of the last assembled subunits of the P_P-b subassembly joining along with NDUFS5, NDUFB4 and the P_D-a subassembly to make either the P_P-b/P_D-a or Q/P subassemblies (**Figure 2A**) (Sánchez-Caballero et al., 2016). Addition of NDUFA10 as a subunit of CI occurred in metazoans and no structural homolog for NDUFA10 is seen in fungi or plants (Elurbe and Huynen, 2016). NDUFA10 interacts with accessory subunits NDUFC1, NDUFA5, NDUFB11 and NDUFC2 and core subunits ND2 and NDUFS2. The N-terminal coil of NDUFA10 occupies space at the interface of the matrix and IMM that is occupied by the first three ND2 TMH in bacteria, fungi, and plants. In HEK293T cells, $NDUFA10^{KO}$ leads to the loss of the N-module as well as NDUFB4 which is added to the complex in the same step as NDUFA10 (**Figure 2A**) (Stroud et al., 2016). This suggests that in the absence of NDUFA10 the assembly of the complex stalls at the Q/P intermediate.

NDUFA10 is related to deoxyguanosine (dG) kinases, which catalyze phospho-transfer reactions between a donor ATP and a dG acceptor, generating ADP and dGMP. Theses enzymes have two substrate binding sites, a deep pocket for binding the acceptor nucleoside and a more exposed binding site for the donor ATP nucleotide (Ostermann et al., 2000; Sabini et al., 2008). However, it has also been shown that ATP nucleotide can bind to the acceptor nucleoside pocket acting as a feedback inhibitor of the phospho-transfer reaction (Welin et al., 2007). Four loops are important for substrate binding and catalysis in dG kinases: the P-loop ($\beta1$-$\alpha1^{A10}$ loop), the DR(Y/H) motif containing loop (^{160}ERS^{162} in human NDUFA10); the "lid" region (D173-I194^{A10}); and the base-sensing loop that recognizes the donor nucleotide base (S224-E229) (**Figure 9B**) (Ostermann et al., 2000; Sabini et al., 2008). It is known that in dG and related nucleoside kinases the lid region and base-sensing loops undergo conformational change upon binding of substrate (Vonrhein et al., 1995; Sabini et al., 2008).

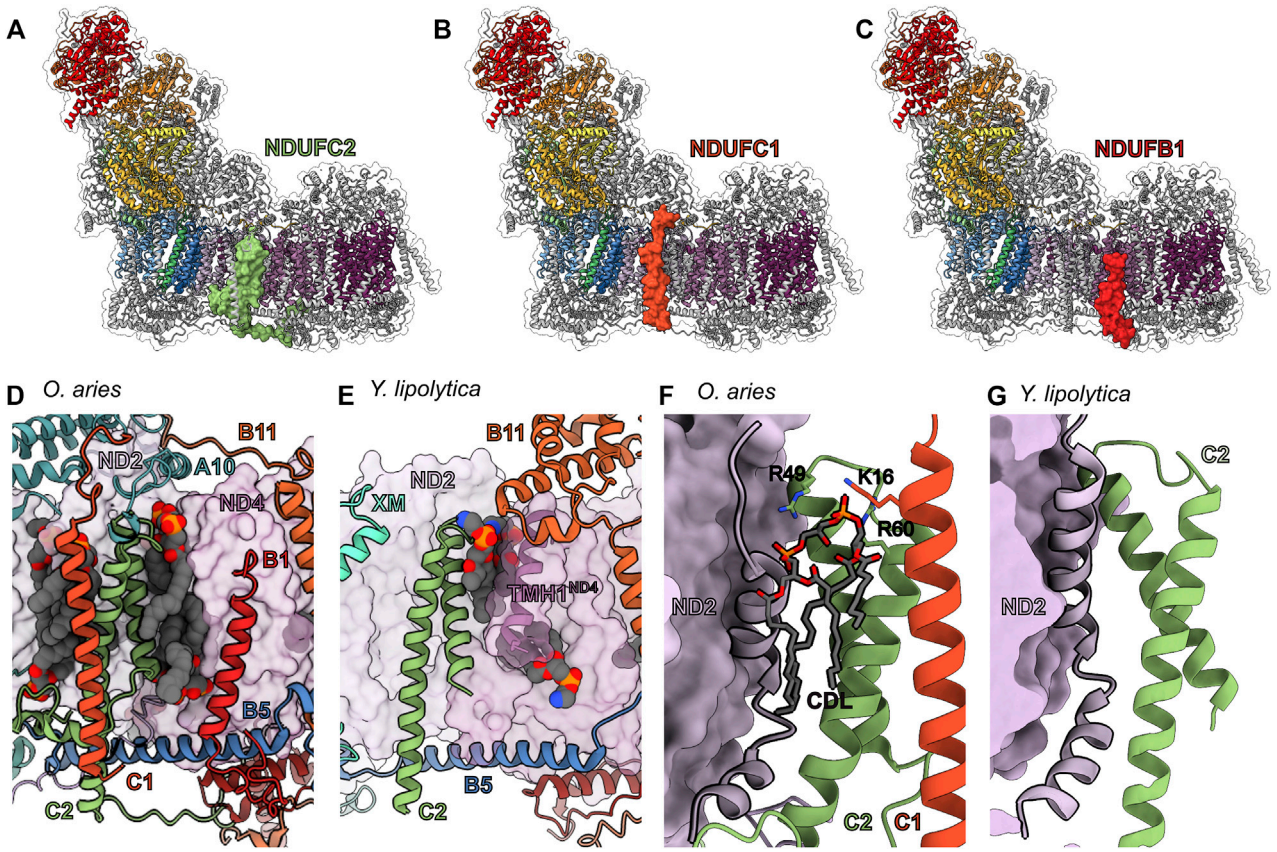

FIGURE 10 | TM accessory subunits of the ND2 and ND4 interface. The structure of mammalian CI (PDB: 6ZKC throughout) in cartoon and the surface of **(A)** NDUFC2 (green), **(B)** NDUFC1 (deep orange) and **(C)** NDUFB1 (red) shown, the core subunits colored as in **Figure 1A** and the accessory subunits grey. **(D)** Lipid binding pocket in the mammalian ND2 (thistle purple)/ND4 (pearly purple) interface with the accessory subunits in cartoon and lipids in spheres. **(E)** Lipid binding in the *Y. lipolytica* (PDB: 6YJ4) ND2/ND4 interface with the accessory subunits in cartoon and lipids in spheres. **(F,G)** NDUFC1 alters the structure of ND2 through lipid binding. **(F)** NDUFC2 and NDUFC1 form a cardiolipin binding pocket with the final TMH^{ND2} in *O. aries*, $TMH11^{ND2}$ (PDB: 6ZKC). Positive residues that interact with the cardiolipin, as well as the cardiolipin, are represented as sticks. **(G)** The cardiolipin pocket is not present in *Y. lipolytica* which lacks NDUFC1 (PDB: 6YJ4). NDUFC2: green, NDUFC1: deep orange, ND2: thistle purple, ND4: pearly purple, NDUFB11: carrot orange, NDUFB5: cyan azure, NUXM: light cyan.

As has been noted previously (Elurbe and Huynen, 2016), many of the residues for binding nucleoside in the acceptor pocket are conserved in NDUFA10. Although the quality of density for bound substrate varies significantly, mammalian CI structures have been modeled either empty or with ATP, ADP or AMP in the NDUFA10 acceptor binding pocket (Fiedorczuk et al., 2016; Wu et al., 2016; Guo et al., 2017; Agip et al., 2018; Bridges et al., 2020; Kampjut and Sazanov, 2020; Chung et al., 2021; Yin et al., 2021). Most CI density maps obtained thus far have been at 3–4 Å resolution and this medium resolution can lead to difficulty in the modeling and interpretation of bound ligands. Therefore, when analyzing the presence of bound ligands at medium resolution it is important to examine cryoEM maps directly. The cryoEM map with the clearest density for the bound substrate is the mouse CI bound to the Q-site inhibitor Piericidin A at 3.0 Å (Bridges et al., 2020). Although substrate bound to NDUFA10 is modeled as ATP, the density is most consistent with Mg^{2+} ATP or potentially Mg^{2+} deoxyATP (dATP) (**Figure 9C**). The Mg^{2+} ion is coordinated by $E88^{A10}$ and $E160^{A10}$. $E160^{A10}$ is part of the DR(Y/H) motif loop and the equivalent residue in thymidylate kinase has also been shown to coordinate a Mg^{2+} ion (Whittingham et al., 2010). In the different CI structures solved to date the lid region and base-sensing loop are more flexible, with weaker cryoEM density and higher atomic displacement parameters (ADPs) than the other regions of NDUFA10 (**Figure 9D**). The clearest cryoEM density for these loops appears in the mouse structures with nucleotide bound (Bridges et al., 2020), suggesting a role for substrate in stabilizing these loops, *via* interactions between $K221^{A10}$ and $D191^{A10}$ of the lid region and the β-phosphate and 3′-hydroxyl of the bound nucleotide, respectively (**Figure 9C**), similar to what is seen in other nucleoside kinases (Vonrhein et al., 1995; Sabini et al., 2008). The 'base-sensing' loop of NDUFA10 (mainly via $α9^{A10}$) participates in a state-dependent interaction with NDUFA5 (**Figures 9E,F**). The peripheral arm of CI rotates between the D-state and the A-state and brings NDUFA5 into contact with the base-sensing loop of NDUFA10 only in the A-state (**Figure 9E**).

The above leads to the hypothesis that NDUFA10 is a nucleotide receptor that may influence the A-to-D state

transition. Flexibility in the lid and base-sensing loops may impose an entropic barrier weakening the interaction between NDUFA10 and NDUFA5. If so, binding of nucleotide in the acceptor site may remove that barrier and hence help to promote the active state of the complex. Conversely, as has been proposed previously from cryoEM map local resolution analysis (Letts et al., 2019), flexibility within NDUFA10 may allow for conformational changes to be transmitted from the peripheral arm into the membrane arm. In this scenario, nucleotide binding may limit conformational coupling across NDUFA10. In either case, evolution would have transformed an enzyme that recognizes nucleotide substrate through a series of conformational changes into a nucleotide sensor that influences CI activity. This hypothesis generates several experimentally testable predictions, the major one being that the CI activity or A-to-D transition would be sensitive to nucleotide concentration.

Transmembrane Subunits at the Interface of ND2 and ND4: NDUFC2, NDUFC1 and NDUFB1

The interface of core antiporter-like subunits ND2 and ND4 on the side opposite to the ND5 lateral helix (ND5-HL) is defined by a deep lipid filled pocket bordered by the accessory TM subunits NDUFC2, NDUFC1 and NDUFB1 (**Figures 10A–D**) and capped by NDUFA10.

NDUFC2—Along with NDUFC1, NDUFC2 joins ND2, ND3, ND4L, and ND6 to form the P_P-b subassembly (**Figure 2A**) (Sánchez-Caballero et al., 2016). NDUFC2 is composed of a N-terminal coil followed by two TMHs bound to ND2 and a C-terminal coil that reaches to ND4 (**Figures 10A,D**). In the IMS, the N-terminal coil of NDUFC2 occupies space at the interface of the IMS and IMM that is occupied by the first three ND2 TMH's in non-metazoans. This coil interacts with ND2, NDUFB5, NDUFS5, NDUFA8, and NDUFC1. In the membrane, $TMH1^{C2}$ interacts with ND2 *via* $TMH11^{ND2}$ and $TMH9^{ND2}$, as well as stabilizes several lipid molecules at the interface of ND2 and ND4 (**Figure 10D**). In the matrix, the $TMH1\text{-}2^{C2}$ loop interacts with ND2 and NDUFA10 as well as binds several lipids. $TMH2^{C2}$ interacts with NDUFC1 and NDUFA8. In the IMS, the C-terminal coil of NDUFC2 interacts with NDUFB5, NDUFB10, NDUFB11, and ND4. In HEK293T cells, $NDUFC2^{KO}$ blocks CI assembly and results in a decrease in the abundance of subunits associated with the P_P-b subassembly and the N-module (Stroud et al., 2016). A heterozygous $NDUFC2^{KO}$ in rats causes an increase in ROS and mitochondrial dysfunction (Raffa et al., 2017). A similar phenotype was observed in another rat model where the reduction of *Ndufc2* expression induced CI dysfunction and promoted stroke-like episodes (Rubattu et al., 2016). These data demonstrate that NDUFC2 is vital for proper CI assembly and activity.

Across species there are notable differences in the structure of NDUFC2's N- and C-terminal coils. The N- and C-termini in plants and yeast are truncated relative to mammals without any extended coil structures (**Figures 10D,E**) (Parey et al., 2019; Maldonado et al., 2020). Although the coil structures vary between mammalian species, the presence of the extended termini is conserved in mammals. Notably, the extended C-terminus of NDUFC2 in mammals bridges the P_P- and P_D-modules, stabilizing the membrane arm of the complex. A universal feature of NDUFC2 seen in plants, yeast and mammals is the stabilization of lipids both on the surface of ND2 and in a deep pocket at the interface between ND2 and ND4 (**Figures 10D,E**). This suggests that the main function of NDUFC2 is the stabilization of structured lipids at the interface of ND2 and ND4 and that NDUFC2's role in bridging between the P_P-b and P_D-a subassemblies *via* the extended C-terminal coil evolved later in metazoans.

NDUFC1—Similar to NDUFC2, NDUFC1 is part of the P_P-b subassembly (**Figure 2A**) (Sánchez-Caballero et al., 2016). NDUFC1 consists of a single TMH that is bound to CI mainly via interaction with NDUFC2 and NDUFA10 (**Figures 10B,D**). NDUFC1 is one of the two accessory subunits that does not make direct contact with any of the core subunits (NDUFAB1-α is the other). In the mitochondrial matrix, the N-terminal coil of NDUFC1 binds NDUFA10 (**Figure 10D**). In the membrane NDUFC1 interacts with NDUFC2 and, along with NDUFC2 and ND2, NDUFC1 forms a cardiolipin binding pocket (**Figure 10F**). In HEK293T cells, $NDUFC1^{KO}$ blocks CI assembly and results in the buildup of an intermediate lacking the N-module (Stroud et al., 2016). Similar to NDUFC2, $NDUFC1^{KO}$ results in a decrease in the abundance of P_P-b subassembly and N-module subunits (Stroud et al., 2016). This suggests that both NDUFC2 and NDUFC1 are required for the formation or stability of the P_P-b subassembly.

Subunits analogous to NDUFC1 are absent in *Y. lipolytica* and plant CI (Wirth et al., 2016; Parey et al., 2019; Grba and Hirst, 2020; Maldonado et al., 2020; Klusch et al., 2021), making it, along with NDUFA10, a metazoan specific subunit. The other major metazoan specific difference in this region is the deletion of the first three helices of ND2 and the loss of subunit NDUX1 (NUXM in *Y. lipolytica*). A less prominent difference between the mammalian and yeast/plant structures in this region is that the final TMH of ND2 in mammals ($TMH11^{ND2}$) is shorter on its N-terminal matrix side by two turns compared to that of *Y. lipolytica* and plants ($TMH14^{ND2}$) (**Figures 10F,G**). This results in the first turn of the helix in mammals being within the membrane with the positive helix dipole capped by the phosphate of the cardiolipin which is held to the complex by NDUFC1 and NDUFC2 (**Figure 10F**). The position of this cardiolipin conflicts with the additional helical turns of $TMH14^{ND2}$ in *Y. lipolytica* and plants (**Figures 10F,G**). Importantly, the $TMH10\text{-}11^{ND2}$ loop forms a major interaction interface with NDUFA10 and unwinding of $TMH11^{ND2}$ may influence the position of this loop and hence interaction with NDUFA10. Thus, NDUFC1 may work to recruit a cardiolipin molecule that impacts the structure of ND2 which in turn influences the binding of NDUFA10. In this way, although it does not interact directly with any core subunit, NDUFC1 would influence the assembly of the entire complex.

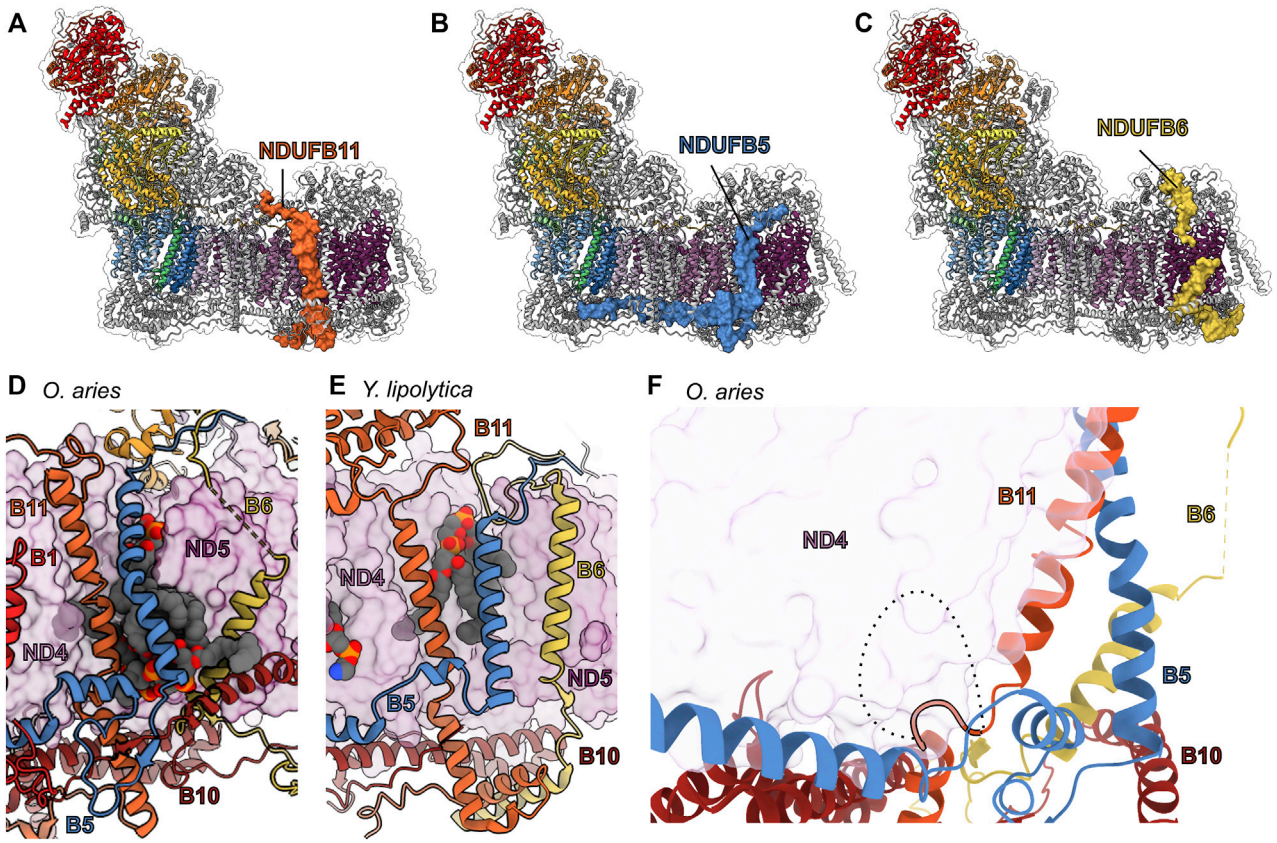

FIGURE 11 | TM accessory subunits of the ND4 and ND5 interface. The structure of mammalian CI (PDB: 6ZKC throughout) in cartoon with the surface of **(A)** NDUFB11 (carrot orange), **(B)** NDUFB5 (cyan azure), and **(C)** NDUFB6 (old gold), the core subunits colored as in **Figure 1A** and the accessory subunits grey. **(D)** Lipid binding pocket in the mammalian ND4 (pearly purple)/ND5 (boysenberry purple) interface with the accessory subunits in cartoon and lipids in spheres. **(E)** Lipid binding in the *Y. lipoyltica* (PDB: 6YJ4) ND4/ND5 interface with the accessory subunits in cartoon and lipids in spheres. **(F)** The NDUFB11-S (short isoform) is shown in carrot orange cartoon. The additional 10 amino acids of the NDUFB11-L (long isoform, represented as dashed line) clash with core subunit ND4 but may be accommodated in the P_D-a′ assembly with accessory subunits NDUFB6, NDUFB10 (vivid auburn) and NDUFB11 shown in cartoon. NDUFB11: carrot orange, NDUFB5: cyan azure, NDUFB6: old gold, ND4: pearly purple, ND5: boysenberry purple, NDUFB10: vivid auburn.

NDUFB1—Along with ND4, NDUFB5, NDUFB6, and NDUFB10, NDUFB1 forms part of the P_D-a subassembly (**Figure 2A**) (Sánchez-Caballero et al., 2016). NDUFB1 is composed of a single TMH with a C-terminal loop extending into the IMS (**Figures 10C,D**). The NDUFB1 TMH contacts ND4 and binds two lipid molecules (**Figure 10D**). The C-terminal loop of NDUFB1 contacts NDUFB5 and NDUFB10 (**Figure 10D**). In HEK293T cells, NDUFB1^{KO} blocks CI assembly and decreases the abundance of subunits associated with the P_P-b, P_D-a and N subassemblies, with only minor impact on subunits associated with the P_P-a/Q and P_P-b subassemblies (Stroud et al., 2016). This indicates that NDUFB1 is needed for the stabilization of the P_P-b/P_D-a subassembly and thus NDUFB1^{KO} blocks formation of the full Q/P intermediate required for the addition of the N-module in mammals (Guerrero-Castillo et al., 2017a).

It is important to note that a subunit called MNLL, which is a synonym for NDUFB1, was assigned in the recent full length structures of plant and algal CI (Soufari et al., 2020; Klusch et al., 2021). However, this subunit is not a NDUFB1 (MNLL) homolog, nor does it bind in the equivalent position of NDUFB1. Instead, this plant subunit is a structural homolog of the *Y. lipolytica* subunit NUXM, which does not have a homolog in mammals. For this reason, Maldonado et al. (2020) coined this subunit NDUX1, an important distinction, as NDUFB1 appears to be metazoan specific not having homologs in either fungi or plants.

The structures of mammalian and *Y. lipolytica* CI indicate that NDUFB1's main function may be to stabilize structural lipids at the interface of ND2 and ND4 (**Figure 10D**). An evolutionary pressure for trapping lipids at this interface becomes apparent in the *Y. lipolytica* structure, which lacks a NDUFB1 homolog, but instead the first TMH of ND4 is pulled away from the rest of subunit occupying an equivalent position to that of NDUFB1 in mammals (**Figure 10E**). The repositioning of TMH1^{ND4} in *Y. lipolytica* is likely aided through interaction with the matrix domain of NDUFB11 (NESM) and traps several lipids at the interface of ND2 and ND4 (**Figure 10E**). The evolution of these two distinct strategies for trapping lipids at this interface indicate the importance of these lipids for CI.

Transmembrane Subunits at the Interface of ND4 and ND5: NDUFB11, NDUFB5, and NDUFB6

Like the interface of ND2 and ND4 discussed above, the interface of the antiporter-like subunits ND4 and ND5 on the side opposite the ND5-HL is also defined by a deep lipid filled pocket. This pocket is bordered by the accessory TM subunits NDUFB11, NDUFB5 and NDUFB6 (**Figures 11A–C**).

NDUFB11—Dynamic complexome profiling of CI assembly indicates NDUFB11 preassembles with subunits NDUFB5, NDUFB6, and NDUFB10 forming what we coin the P_D-a′ subassembly, before joining ND4 and NDUFB1 to form the P_D-a subassembly (**Figure 2A**) (Guerrero-Castillo et al., 2017a). NDUFB11 is a single TMH subunit with a long N-terminal coil in the matrix and a C-terminal α-helix and coil in the IMS (**Figures 11A,D**). In the matrix NDUFB11's N-terminal 50 amino acids are disordered. The resolved residues of the N-terminal coil bind across the matrix side of the membrane arm interacting with NDUFA10, NDUFS2, NDUFB4 and NDUFB9. The NDUFB11 TMH predominantly binds ND4 directly, but also on the IMS side of the membrane pins a lipid molecule to the surface of ND4 (**Figure 11D**). In both mammals and *Y. lipolytica*, NDUFB11 helps to form the side of the lipid filled cavity between ND4 and ND5 (**Figures 11D,E**). In the IMS NDUFB11 interacts with NDUFB5, ND4, NDUFB10, ND5 and NDUFC2.

In HEK293T cells, NDUFB11^{KO} disrupts CI assembly with a decrease in the abundance of subunits associated with the P_P-b, P_D-a, P_D-b and N subassemblies (Stroud et al., 2016). Mutations in the *Ndufb11* gene, including an in frame deletion of F93^{B11} located in the NDUFB11 TMH that would impact its interaction with ND4, compromise CI stability and have been associated with various diseases such as congenital sideroblastic anemia, microphthalmia with linear skin defects, and lactic acidosis (Van Rahden et al., 2015; Lichtenstein et al., 2016; Torraco et al., 2017). Thus, NDUFB11 is important for CI assembly and activity. Additionally, NDUFB11 is one of the few supernumerary subunits to have isoforms produced by alternative splicing (Panelli et al., 2013). The short 153 amino acid isoform is the structurally resolved CI subunit and is expressed at higher levels than its longer 163 amino acid isoform (Panelli et al., 2013). The isoforms utilize two different 5′ splice sites and the longer 163 amino acid isoform includes an additional 30 nucleotides in the second exon of *Ndufb11* (Panelli et al., 2013) thereby producing a NDUFB11 isoform with an additional 10 amino acid residues inserted into the loop between the TMH and the IMS α-helix (α1^{B11}) (**Figure 11F**). In the fully assembled complex, the TMH-α1^{B11} loop packs closely against ND4 and major conformational changes would be needed to accommodate the additional residues of the splice variant (**Figure 11F**). Nonetheless, the location of the insertion and the fact that it is predicted to be an unstructured coil may not prevent the formation of the P_D-a′ subassembly between NDUFB5, NDUFB6, NDUFB10 and NDUFB11 (**Figure 11F**). In this way, the long NDUFB11 isoform may regulate CI assembly by sequestering the P_D-a′ interaction partners while blocking association of ND4. Interestingly, treatment of human SH-SY5Y neuroblastoma cells with the specific CI inhibitor rotenone enhances the expression of the long isoform while also triggering apoptosis suggesting a regulatory response to mitochondrial stress or cell death (Panelli et al., 2013). More work is needed to fully understand the role of the NDUFB11 isoforms.

NDUFB5—In the fully assembled complex, NDUFB5 spans the membrane arm of the complex with its TMH situated between ND4 and ND5 and two α-helices in the IMS parallel to the membrane (**Figure 11B**). In the matrix, the N-terminal coil of NDUFB5 contacts NDUFB3, NDUFAB1-β, NDUFB6, NDUFB9, and ND5. In the membrane, NDUFB5 contacts ND4, NDUFB11 and several well resolved lipid molecules. The NDUFB5 TMH pins NDUFB11 and the lipid molecules onto the surfaces of ND4 and ND5. In the IMS, NDUFB5 wraps around NDUFB10 with a coil of NDUFB10 threading through an eyelet formed by a coil of NDUFB5 (**Figures 11D,F**). This eyelet is not present in the *Y. lipolytica* structure and both NDUFB10 and the NDUFB5 loop (TMH-α1^{B5} loop) are shorter in yeast CI (**Figures 11D,E**). This interaction is directly followed by a short α-helix (α1^{B5}) which binds overtop NDUFB11 and contacts ND4, then a long α-helix (α2^{B5}) which contacts NDUFB1, ND4, NDUFB10, NDUFA8, NDUFC2, NDUFA11, and ND2. Finally, the C-terminal coil of NDUFB5 contacts NDUFC2, ND2, NDUFS5, NDUFA8, NDUFA3, and NDUFA13 (**Figure 8H**). Given this extensive network of interactions that span the membrane arm, it is not surprising that in HEK293T cells NDUFB5^{KO} blocks CI assembly with a larger impact in the abundance of subunits in the P_P-b and P_D-a subassemblies (Stroud et al., 2016) compared to the Q or P_D-b subassemblies. This indicates that NDUFB5 is essential for establishing the P_D-a subassembly and formation of the P_P-b/P_D-a subassembly (Stroud et al., 2016). NDUFB5's long α2^{B5} which binds along the IMS side of the membrane arm likely plays the major role in the connection between the P_D-a and P_P-b modules (**Figure 11B**).

In both mammals and *Y. lipolytica* the NDUFB5 (NUUM in *Y. lipolytica*) TMHs cap a lipid filled cavity trapping several lipids at the interface between ND4 and ND5. This indicates an important role for NDUFB5 in trapping lipids at the interface of ND4 and ND5 in addition to its role in assembly. Interestingly, in plants the accessory subunit P2 is structurally analogous to the long IMS helix of NDUFB5 (α2^{B5}) but lacks the TMH (Soufari et al., 2020; Klusch et al., 2021). This indicates that the roles of NDUFB5 in assembly and lipid binding may be separable, with plants using this subunit only to aid complex assembly and stability and opisthokonts using it additionally for lipid sequestration.

NDUFB6—Despite its low sequence conservation, NDUFB6 is structurally conserved across eukaryotes. NDUFB6 is a single TMH subunit that has an N-terminal matrix domain containing an α-helix (α1^{B6}) which forms part of the matrix P_D-bulge (**Figure 1A**), a highly tilted TMH which is partially disordered in mammals, indicating flexibility, and an IMS C-terminal coil (**Figure 11C**). Although in mature CI NDUFB6 mostly interacts with the subunits of the P_D-b subassembly, during assembly it

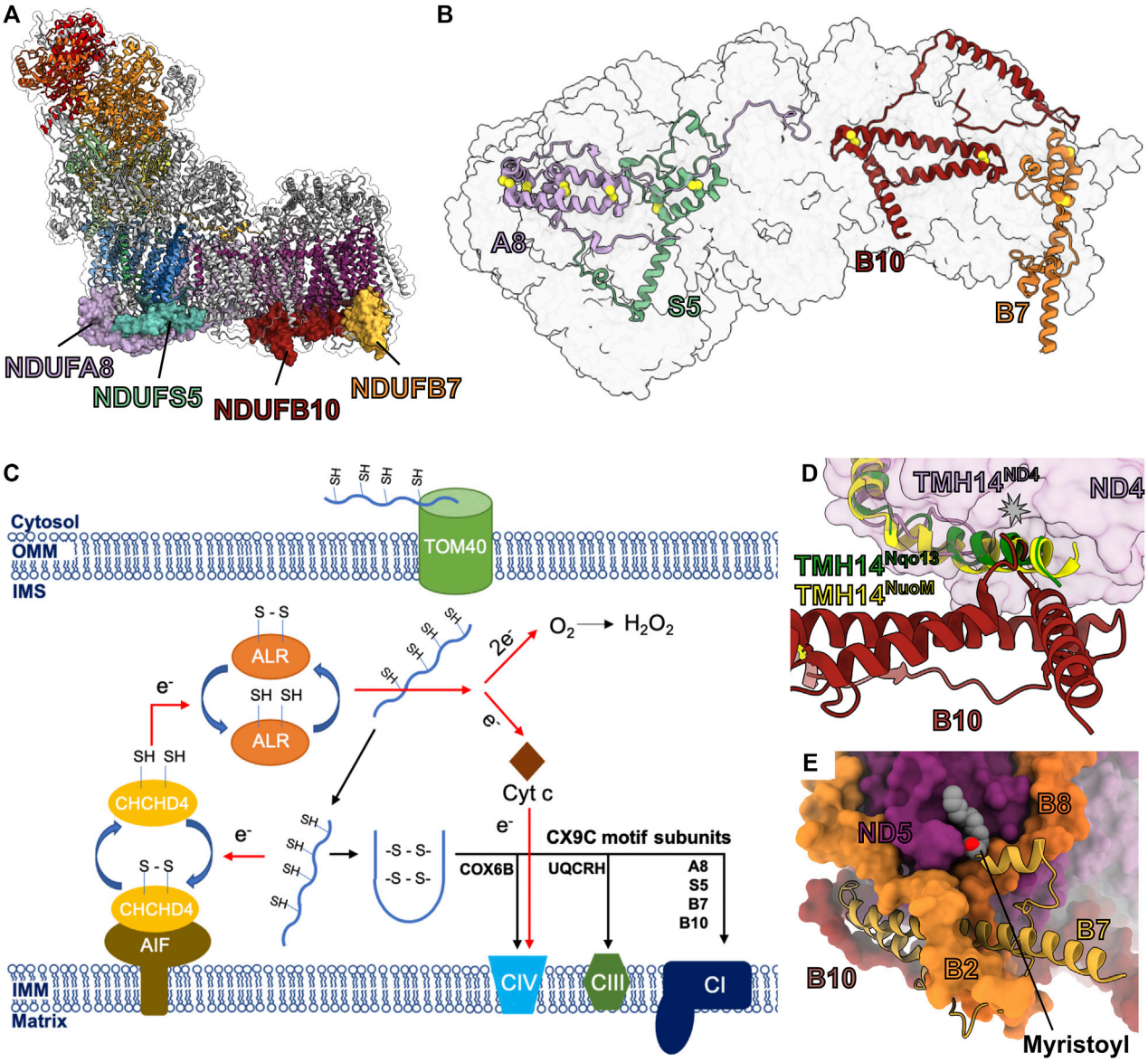

FIGURE 12 | The CX_9C motif containing accessory subunits. **(A)** The structure of mammalian CI (PDB: 6ZKC throughout unless stated otherwise) in cartoon with the surface of NDUFA8 (lilac purple), NDUFS5 (cadet blue), NDUFB10 (vivid auburn) and NDUFB7 (gold) shown, the core subunits colored as in **Figure 1A** and the other accessory subunits grey. **(B)** IMS view of the CI sole showing the CX_9C motif containing subunits. CI is shown as a transparent surface. The CX_9C subunits are shown as cartoons colored as in **Figure 1** with the disulfide bonding residues shown as spheres. **(C)** Schematic diagram showing the import of CX_9C motif subunits into the IMS and assembly onto CI. CX_9C motif subunits are imported from the cytosol into the IMS via outer membrane protein TOM40. CX_9C subunits are oxidized by CHCHD4 protein bound to the AIF protein in its NADH bound state. The folded CX_9C subunits are assembled on their destined ETC complex. The electrons are transferred from CHCHD4 protein to CIV *via* the ALR protein and cyt *c* or are transferred from ALR protein to molecular O_2. **(D)** NDUFB10 interacts with the surface of ND4 (pearly purple) and compensates for the loss of the extended helical region of $TMH14^{ND4}$ present in bacteria. ND4 (NuoM) of *E. coli* CI (PDB: 7NZ1) and ND4 (Nqo13) of *T. thermophilus* (PDB: 4HEA) are superposed onto ND4 of mammalian (*O. aries*) CI structure. NDUFB10 and $TMH14^{ND4}$ are shown as cartoons. **(E)** NDUFB7 is myristoylated. Mammalian NDUFB7 (PDB: 6ZKO) of CI is shown as cartoon and other subunits are shown as colored surface. The myristoyl group is shown as spheres. NDUFA8: lilac purple, NDUFS5: cadet blue, NDUFB10: vivid auburn, NDUFB7: gold, ND4: pearly purple, ND5: boysenberry purple.

joins the P_D-a′ subassembly and then the P_D-a subassembly (**Figure 2A**) (Sánchez-Caballero et al., 2016). In the fully assembled complex, NDUFB6 interacts with NDUFAB1-β, NDUFB9 and NDUFB5 as part of the matrix P_D-bulge (**Figure 6C**). The matrix side of the NDUFB6 TMH is disordered in mammals with only the IMS half of the TMH having clearly defined density, indicating a flexibility in the matrix half of the TMH not seen for any other TM accessory subunit. The IMS half of NDUFB6's TMH interacts with ND5 and NDUFB10. Together with NDUFB5 and NDUFB11, NDUFB6's TMH^{B6} forms the boundary of a lipid filled cavity at the interface between ND4 and ND5 (**Figure 11D**). In the IMS

the C-terminal coil of NDUFB6 interacts with ND5, NDUFB10, and NDUFB7.

In HEK293T cells, NDUFB6^{KO} prevents full assembly of the complex and reduces the abundance of subunits of the N-, Q-, and P_D-b modules (Stroud et al., 2016) and NDUFB6 depletion in HEK293T Flp-In cells displayed an 80% decrease in CI activity (Loublier et al., 2011) indicating that NDUFB6 is necessary for CI assembly and hence activity. Moreover, NDUFB6 expression may play a regulatory role in CI activity. Patients with type 2 diabetes mellitus experience a decrease in NDUFB6 expression in muscle cells (Ling et al., 2007). DNA methylation in the NDUFB6 promoter present in elderly patients was observed to reduce NDUFB6 expression, suggesting an epigenetic-basis of NDUFB6 regulation (Ling et al., 2007).

Given that NDUFB6 forms part of the P_D-a subassembly but that it interacts mostly with P_D-b subassembly subunits in the final CI structure and NDUFB6^{KO} results in decreased levels of subunits associated with the P_D-b subassembly, it is clear that a major role of NDUFB6 is to bridge the P_D-a and P_D-b subassemblies during CI biogenesis in mammals. As NDUFB6 does not directly interact with ND4, this bridging interaction would be facilitated through the interactions with the P_D-bulge in the matrix and the P_D-a′ subassembly subunits, specifically NDUFB10, in the IMS.

The Sole of CI—Intermembrane Space CX_9C Motif Subunits

NDUFA8, NDUFS5, NDUFB10, and NDUFB7 are members of the coiled-coil-helix-coiled-coil-helix domain-containing family that carry CX_9C motifs, and all reside on the IMS surface of the CI membrane arm (**Figures 12A,B**). NDUFA8 is a subunit of the P_P-a subassembly added to ND1 along with NDUFA3 and NDUFA13 (**Figure 2A**). NDUFS5 is a subunit of the P_P-b/P_D-a subassembly and assembles along with NDUFA10 and NDUFB4 upon connection of P_D-b and P_D-a (**Figure 2A**). NDUFB10 is part of the P_D-a′ subassembly with NDUFB11, NDUFB5 and NDUFB6 and goes on to form the P_D-a subassembly along with the addition of ND4 and NDUFB1 (**Figure 2A**). NDUFB7 is a subunit of the P_D-b subassembly, it assembles with ND5, NDUFB2, NDUFB3, NDUFB7, NDUFB8, NDUFB9, and NDUFAB1-β (**Figure 2A**) (Guerrero-Castillo et al., 2017a). Thus, during assembly each of the membrane arm subassemblies has an associated CX_9C motif subunit: P_P-a has NDUFA8, P_P-b has NDUFS5, P_D-a has NDUFB10, and P_D-b has NDUFB7 (**Figure 2A**).

The CX_9C motifs of these subunits form disulfide bonds that stabilize the helix-turn-helix structure of the subunits (**Figure 12B**) (Ugalde et al., 2004; Longen et al., 2009; Szklarczyk et al., 2011). These subunits are imported into the IMS in an unfolded reduced form and subsequently folded and oxidized via the disulfide relay-dependent Mitochondrial Import and Assembly (MIA) pathway (**Figure 12C**) (Mesecke et al., 2005; Fischer et al., 2013; Modjtahedi et al., 2016; Dickson-Murray et al., 2021). The electrons thus released during the oxidation are fed to CIV of the ETC via cytochrome *c* (cyt *c*) or released as reactive oxygen species (ROS) (**Figure 12C**) (Allen et al., 2005; Bihlmaier et al., 2007). The MIA pathway is regulated by the redox environment of the cell and interacts with several antioxidant systems (Nakao et al., 2015; Kritsiligkou et al., 2017), as well as small molecule regulators (Dickson-Murray et al., 2021).

NDUFA8—In the fully assembled complex NDUFA8 binds overtop NDUFA13 forming the base of CI's heel (**Figure 8D** and **Figure 12A**). NDUFA8 has an N-terminal coil, followed by six α-helices folded into an L-shape containing two disulfide cross-linked helix-turn-helix motifs (**Figure 12B**) and a long C-terminal coil. The N-terminal region of NDUFA8 interacts with NDUFA13, NDUFS5 and NDUFA1. The first NDUFA8 disulfide cross-linked helix-turn-helix motif (α3-α4^{A8}) interacts with NDUFA13, NDUFB5 and NDUFA3. The second NDUFA8 disulfide cross-linked helix-turn-helix motif (α5-α6^{A8}) interacts with NDUFA1, ND1 and NDUFA13. The C-terminal coil of NDUFA8 reaches halfway down the membrane arm interacting with NDUFA3, NDUFA13, NDUFS5, NDUFB5, NDUFC2, ND2 and ND4. The C-terminus of NDUFA8 also interacts with lipid molecules bound at the interface of ND2 and ND4.

NDUFS5—Spanning the IMS side of the P_P-b module, NDUFS5 interacts with core subunits ND6, ND4L and ND2 (**Figures 12A,B**). In mammals NDUFS5's N-terminal coil occupies space at the interface of the IMS and IMM that is occupied by the first three ND2 TMHs in other species. This is followed by the disulfide cross-linked helix-turn-helix motif (α1-α2^{S5}), a α-helix (α3^{S5}) and a C-terminal coil (**Figure 12B**). The N-terminal coil of NDUFS5 interacts with ND2, NDUFC2, NDUFB5, ND4L, ND6 and NDUFA3. The disulfide cross-linked NDUFS5 helix-turn-helix motif interacts with NDUFA8, NDUFB5, ND2 and ND4L. NDUFS5's α3^{S5} interacts with ND4L, ND6 and NDUFA13. The C-terminal coil of NDUFS5 interacts with NDUFA13, NDUFA1, and NDUFA8.

NDUFB10—During CI assembly NDUFB10 associates with NDUFB5, NDUFB6 and NDUFB11 to form the P_D-a′ subassembly before interacting with any core subunits (**Figure 2A**). In the fully assembled complex NDUFB10 zigzags between ND5 and ND4 interacting with both core subunits and several accessory subunits (**Figures 12A,B**). NDUFB10's N-terminal coil and helix interact with NDUFB11, NDUFB6, NDUFB7, ND5 and NDUFB5. The long α1-2^{B10} loop passes through an eyelet formed by NDUFB5 and interacts with NDUFB11, NDUFB1, and NDUFC2. The disulfide cross-linked NDUFB10 helix-turn-helix motif interacts with ND4, NDUFB11, ND5, NDUFB6, NDUFB7, NDUFB8 and NDUFB4. The C-terminal region of NDUFB10 interacts with ND4, NDUFC2 and NDUFB11. NDUFB10 occupies a binding site on the bottom of ND4 that in both *T. thermophilus* and *E. coli* CI structures is occupied by extensions of ND4 TMH^{14}, suggesting that interactions in the pocket formed by the TMH8-9^{ND4}, TMH10-11^{ND4}, and TMH11-12^{ND4} loops may be important for stability of the complex (**Figure 12D**).

NDUFB7—Located under the CI toe, NDUFB7 has a long N-terminal coil with two short α-helices (α1^{B7} and α2^{B7}) followed by the disulfide cross-linked helix-turn-helix motif (α3-α4^{B7}) (**Figures 12A,B**). The N-terminal glycine of NDUFB7 is

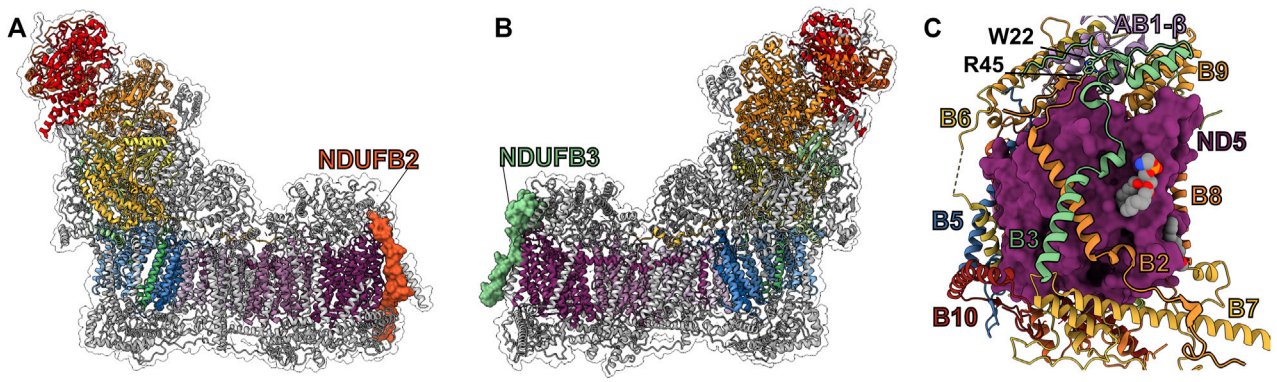

FIGURE 13 | TM accessory subunits at the CI toe. The structure of mammalian CI (PDB: 6ZKC) in cartoon with the surface of **(A)** NDUFB2 (yellow orange) and **(B)** NDUFB3 (iguana green) shown, the core subunits colored as in **Figure 1A** and the other accessory subunits grey. **(C)** Cartoon of accessory subunits on surface of ND5 (boysenberry purple). Key residue mentioned in the text are shown. Lipid and NDUFB7 myristoyl group are shown as spheres. NDUFB2: yellow orange, NDUFB3: iguana green, ND5: boysenberry purple.

myristoylated anchoring it to IMS leaflet of the membrane (**Figure 12E**) (Carroll et al., 2005). NDUFB7 is the only CI subunit that is known to be lipid modified. The myristoyl group is bound in a groove on ND5 formed by $TMH12^{ND5}$, $TMH13^{ND5}$ and $TMH15^{ND5}$ (**Figure 12E**) (Kampjut and Sazanov, 2020). The N-terminal coil of NDUFB7 interacts with ND5, NDUFB8, NDUFB2, NDUFB6 and NDUFB10. The NDUFB7 disulfide cross-linked helix-turn-helix motif interacts with ND5, NDUFB10, NDUFB6 and NDUFB2.

Roles of NDUFA8, NDUFS5, NDUFB10 and NDUFB7 in CI assembly—In HEK293T cells, $NDUFA8^{KO}$, $NDUFS5^{KO}$, $NDUFB10^{KO}$ or $NDUFB7^{KO}$ results CI assembly defects and reductions in subunits associated with the P_P-a, P_P-b, P_D-a and P_D-b subassemblies respectively as well as N-module subunits (Stroud et al., 2016). Accordingly, CI activity and basal mitochondrial respiration are reduced drastically in all four KOs (Stroud et al., 2016). NDUFS5 (Nuo-11.5) and NDUFA8 (Nuo-20.8) deletion in *N. crassa* prevents full assembly of CI and results in the accumulation of membrane arm intermediates (Vieira Da Silva et al., 1996; Marques et al., 2007). A missense mutation in NDUFB10 ($C107S^{B10}$) was discovered in patients with CI deficiency (Friederich et al., 2017). The substitution of the highly conserved $C107^{B10}$, which is involved in disulfide crosslinking, blocks import of the mutated protein into the IMS due to its failure to act as a CHCHD4 substrate (**Figure 12C**) (Friederich et al., 2017). These results indicate that NDUFA8, NDUFS5, NDUFB10 and NDUFB7 are each essential for CI assembly and stability.

The dependence on CX_9C motif containing subunits ties CI assembly to the functioning of the MIA pathway which in turn depends upon pre-existence of a functional ETC, namely sufficient CIV to act as an electron sink in the disulfide relay (**Figure 12C**). Additionally, the MIA pathway is highly regulated through redox signaling (Dickson-Murray et al., 2021). Hence, the evolution of essential CX_9C motif containing subunits has multiple applications: 1) they enhance CI stability through rigid disulfide linked structures, 2) they ensure that CI assembly only occurs in healthy respiring mitochondria and 3) they allow for additional regulation of CI assembly by the overall redox status of the cell. It is important to note that both CIII and CIV also have CX_9C motif containing subunits (UQCRH and COX6B respectively) indicating that this is a general strategy used for the entire ETC (**Figure 12C**).

Transmembrane Subunits at the Tip of the Toe: NDUFB2 and NDUFB3

NDUFB2 and NDUFB3 are single TMH subunits bound to the toe of the CI membrane arm (**Figures 13A,B**). During assembly they are incorporated together as part of the P_D-b subassembly with core subunit ND5 and accessory subunits NDUFAB1-β, NDUFB7, NDUFB8, and NDUFB9 (**Figure 2A**) (Stroud et al., 2016; Guerrero-Castillo et al., 2017a).

NDUFB2—In the matrix, NDUFB2's N-terminal coil interacts with NDUFAB1-β, NDUFB3 and ND5 (**Figure 13C**). On the matrix side of the membrane, NDUFB2's TMH binds between $TMH12^{ND5}$ and $TMH14^{ND5}$ interacting with the extended loop of the broken $THM12^{ND5}$. In the IMS, NDUFB2's C-terminal coil interacts with ND5 and NDUFB7 (**Figure 13C**).

NDUFB3—The N-terminal matrix domain of NDUFB3 interacts with NDUFAB1-β, NDUFB9, NDUFB2, and ND5 (**Figure 13C**). In the membrane, the N-terminus of NDUFB3's TMH binds in a pocket on ND5 formed by $TMH12^{ND5}$, $TMH13^{ND5}$ and $TMH15^{ND5}$ then as it encounters NDUFB2 it kinks sharply and extends outward from the tip of the membrane arm with no visible structure extending into the IMS (**Figures 13B,C**). Thus, NDUFB3 pins NDUFB2 to the surface of ND5. The N-terminal tilted region of NDUFB3's TMH creates a lipid binding site on the surface of ND5 in which the lipid is pulled down relative to the plane of the membrane indicating thinning of the membrane in this region (**Figure 13C**).

Roles of NDUFB2 and NDUFB3 in CI assembly—In HEK293T cells, $NDUFB2^{KO}$ or $NDUFB3^{KO}$ results in a severe CI assembly defect with a decrease in the abundance of P_D-b and N subassembly subunits (Stroud et al., 2016). The NDUFB2 gene contains a highly conserved CHOP element in its promoter

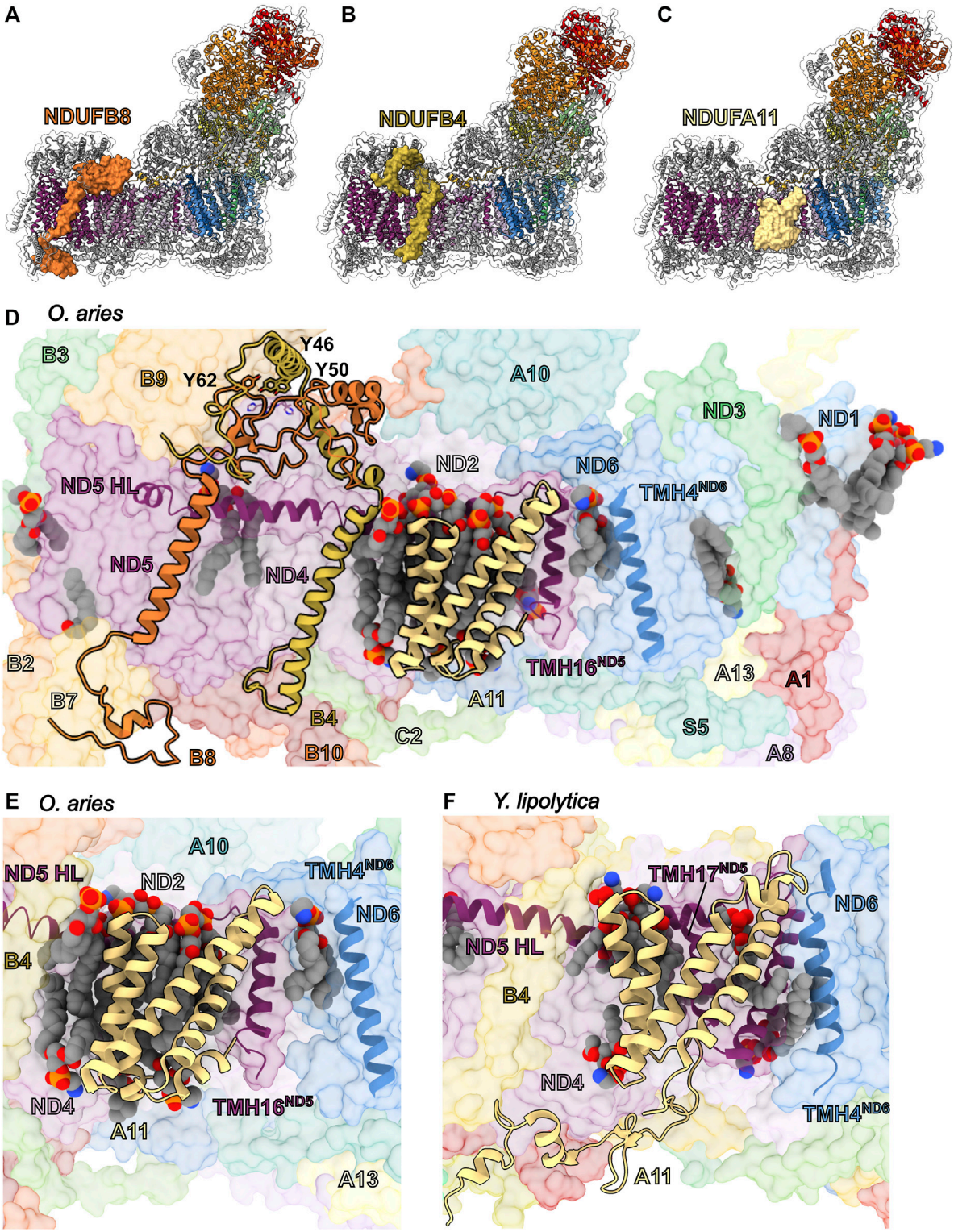

FIGURE 14 | TM accessory subunits of the ND5 lateral helix (ND5 HL). The structure of mammalian CI (PDB: 6ZKC throughout unless stated otherwise) in cartoon with the surface of **(A)** NDUFB8 (vivid tangelo), **(B)** NDUFB4 (old gold) and **(C)** NDUFA11 (wheat) shown, the core subunits colored as in **Figure 1A** and the other accessory subunits grey. **(D)** Mammalian NDUFB8, NDUFB4 and NDUFA11 subunits are shown as cartoons on the surface of CI. Residues that are discussed in the text are shown as sticks. ND5 HL, $TMH16^{ND5}$ and $TMH4^{ND6}$ are shown as cartoon. Lipids are shown as spheres. **(E)** Zoom in on mammalian NDUFA11 shown as cartoon. ND5 HL, $TMH16^{ND5}$ and $TMH4^{ND6}$ are shown as cartoon. Lipids are shown as spheres. **(F)** *Y. lipolytica* NDUFA11 (NUJM; PDB: 6RFR) shown as cartoon. The ND5 (NU5M) HL (ND5 HL), $TMH16^{ND5(NU5M)}$, $TMH17^{ND5(NU5M}$ and $TMH14^{ND6(NU6M)}$ are shown as cartoons. The lipids are shows as spheres. Subunits are colored as in **Figure 1** unless stated otherwise. NDUFB8: vivid tangelo, NDUFB4: old gold, NDUFA11: wheat, ND5: boysenberry purple, ND6: cyan-blue.

(Aldridge et al., 2007). Transcription of CHOP element containing genes is upregulated in response to the accumulation of unfolded proteins and induce the mitochondrial unfolded protein response (Aldridge et al., 2007). A point mutation in NDUFB3 ($W22R^{B3}$) is associated with CI deficiency (Calvo et al., 2012; Haack et al., 2012) as well as with a distinctive facial appearance and short stature (Alston et al., 2016). W22 is located on the N-terminal matrix loop of NDUFB3, and binds overtop of NDUFB2 $R45^{B2}$, the $W22R^{B3}$ mutation would introduce unfavorable electrostatics likely disrupting the interactions in this region (**Figure 13C**). Therefore, the $W22R^{B3}$ mutation reveals the importance of the NDUFB2 and NDUFB3 interactions in the mitochondrial matrix for overall CI activity.

NDUFB3 is also involved with supercomplex formation as it contacts CIV (via COX8B) in the tight conformation of the respirasome (Letts et al., 2016b). Deformation of the lipid bilayer by NDUFB2 at this interface may promote interaction with CIV. Altogether, due to their many interactions with accessory subunits on both sides of the membrane, NDUFB2 and NDUFB3 are required for the assembly of the P_D-b subassembly and are hence essential to CI biogenesis.

Transmembrane Subunits of the Lateral Helix: NDUFB8, NDUFB4 and NDUFA11

The lateral helix of ND5 (ND5 HL) is an amphipathic helix that stretches between $TMH15^{ND5}$ at the tip of the membrane arm and $TMH16^{ND5}$ adjacent to ND2 and ND4L (**Figure 1A**). Along its length ND5-HL is bound by three accessory transmembrane subunits, NDUFB8, NDUFB4 and NDUFA11 (**Figures 14A–C**). These subunits all bind overtop of ND5-HL and help anchor it to the complex.

NDUFB8—Together with ND5, NDUFB2, NDUFB3, NDUFB7, NDUFB9, and NDUFAB1-β, NDUFB8 forms the P_D-b subassembly (**Figure 2A**) (Guerrero-Castillo et al., 2017a). NDUFB8 is a single TMH accessory subunit with an N-terminal domain in the matrix and a short C-terminal coil in the IMS. Despite structural variability in the N- and C-terminal regions, the position of NDUFB8 is conserved in mammals, yeast and plants (Parey et al., 2019; Kampjut and Sazanov, 2020; Klusch et al., 2021). In mammals, the N-terminal domain interacts with NDUFB4, ND4, ND5, NDUFB9 and NDUFAB1-β, as well as with the head group of a lipid that is trapped by the ND5-HL at the ND5/ND4 interface (**Figure 14D**). In the membrane NDUFB8 interacts solely with ND5. In the IMS the C-terminal coil of NDUFB8 interacts with ND5, NDUFB7, NDUFB10 and NDUFB2.

In HEK293T cells, $NDUFB8^{KO}$ prevents proper assembly of CI and results in a decreased abundance of subunits associated with the N-module (Stroud et al., 2016). NDUFB8 mutations $Y62H^{B8}$, $E63D^{B8}$, $P76Q^{B8}$, $C144W^{B8}$ or deletion of the region $M105\text{-}V156^{B8}$ cause CI deficiency with symptoms ranging from fatal infantile lactic acidosis to Leigh-like syndrome (Piekutowska-Abramczuk et al., 2018). In humans, $C144^{B8}$ (not conserved in other *sps*.) is positioned to form a possible inter-subunit disulfide bond with core subunit ND5 residue $C279^{ND5}$. The larger tryptophan sidechain in $C144W^{B8}$ mutation would disrupt the close interaction between NDUFB4 and ND5 in this region. The other mutations are in the matrix domain of the complex and would disrupt the stability of the P_D-bulge.

NDUFB4—During assembly of CI NDUFB4 does not form part of the individual membrane arm subassemblies but has been proposed to join during formation of the P_P-b/P_D-a subassembly or the Q/P subassembly (**Figure 2A**) (Guerrero-Castillo et al., 2017a). In the fully assembled complex the N-terminal matrix domain of NDUFB4 is composed of a coil and two helices ($\alpha1^{B4}$ and $\alpha2^{B4}$) that zigzag over the matrix side of the complex forming part of the P_D-bulge and interacting with NDUFB9, NDUFB8, ND5, NDUFB11 and ND4 (**Figures 14B,D**). In the membrane, NDUFB4 interacts with ND5 via ND5-HL, and ND4. NDUFB4 along with NDUFA11 also traps lipids to the surface of the complex (**Figure 14D**). In the IMS, NDUFB4 interacts with NDUFC2, NDUFB10, ND5 and ND4.

The position of NDUFB4 binding overtop of ND5-HL raises questions about the proposed assembly pathway (Guerrero-Castillo et al., 2017a). If NDUFB4 binds to the P_P-b/P_D-a subassembly, unless its interaction with ND4 is very different than what is observed in the structure of the full complex, it would block the binding of the ND5-HL preventing the addition of the P_D-b subassembly. Thus, the structure indicates that NDUFB4 would need to be added only after the connection of the P_D-a and P_D-b subassemblies, which occurs upon formation of the Q/P subassembly (**Figure 2A**). This also explains why NDUFB4 is not part of any of the individual membrane arm subassemblies but is only added to the complex later. Together with NDUFB9, NDUFB4 forms one of the most extensive contacts with $CIII_2$ in the supercomplex, binding to a loop extended from the UQCRC1 subunit of $CIII_2$ (Letts et al., 2019).

In HEK293T cells, $NDUFB4^{KO}$ results in incomplete assembly of the complex with a reduction in the levels of subunits in the P_D-b subassembly and N-module (Stroud et al., 2016). NDUFB4 can be modified by peroxynitrite resulting in 3-nitrotyrosine at $Tyr46^{B4}$, $Tyr50^{B4}$ and $Tyr51^{B4}$ in *B. taurus* (Murray et al., 2003). Tyr46 and Tyr50 are conserved in humans and in *O. aries* on $\alpha1^{B4}$ in the matrix (**Figure 14D**). In *O. aries* Tyr46 and Tyr50 contact ND4 (*via* $His421^{ND4}$, $His422^{ND4}$ of the $TMH13\text{-}14^{ND4}$ loop), NDUFB9 (*via* $His168^{B9}$) and NDUFB8 (*via* $Asp65^{B8}$ and $Trp73^{B8}$). Tyr46 and Tyr50 are hypothesized to contribute to the altered function of CI and perhaps play a role in the onset of Parkinson's disease (Murray et al., 2003). Overall, this suggests an important role for the NDUFB4 P_D-bulge interactions in CI assembly and stability and leads to the hypothesis that NDUFB4 acts to cement the interaction between the P_D-a and P_D-b subassemblies during CI biogenesis. This is achieved by NDUFB4 "clamping" over ND5-HL, intertwining with the P_D-bulge in the matrix and binding ND4, ND5 and NDUFB10 in the IMS (**Figure 14D**).

NDUFA11—The four TMH subunit NDUFA11 binds overtop of ND5-HL adjacent to the final $TMH16^{ND5}$ at the interface of ND2 and ND4 (**Figure 14C**). During CI assembly

NDUFA11 joins the complex only after formation of the Q/P-subassembly making it the final membrane arm subunit to join the complex (**Figure 2A**) (Sánchez-Caballero et al., 2016). NDUFA11 is structurally conserved across eukaryotes and is homologous to Tim17, Tim22, and Tim23, which are involved in protein translocation across the inner membrane (Carroll et al., 2002). NDUFA11's four TMHs form an "arch" shape with the feet of the arch contacting CI and the central cavity of the arch filled with lipids (**Figure 14D**). It interacts with core subunits ND2, ND4 and ND5 with most of these interactions mediated *via* lipids trapped between NDUFA11 and the core subunits. The C-terminal coil of NDUFA11 interacts with ND2, ND4 and NDUFB5. In addition to the lipids trapped between NDUFA11 and ND2, ND4 and ND5, NDUFA11 also binds lipids adjacent to NDUFB4 and ND6 $TMH4^{ND6}$ (**Figure 14D**).

Suppression of NDUFA11 expression in human osteosarcoma 143B cells results in reduced oxygen consumption, a fragmented mitochondrial network, a reduction in intact CI and accumulation of subassemblies associated with assembly factors NDUFAF1-4, ACAD9, ECSIT, FOXRED1 and TMEM126B (Andrews et al., 2013). In HEK293T cells, $NDUFA11^{KO}$ results in incomplete assembly of CI with a decrease in the levels of subunits associated with the N-module (Stroud et al., 2016) indicating that NDUFA11 is needed for the final stages of CI biogenesis.

In *Y. lipolytica* ND5 has two TMHs after ND5-HL ($TMH16^{ND5}$ and $TMH17^{ND5}$) whereas mammalian ND5 on has one ($TMH16^{ND5}$) (**Figures 14E,F**). The additional $TMH17^{ND5}$ binds within the central cavity of the NDUFA11 arch displacing some of the lipids seen in the mammalian structures (**Figures 14E,F**). Also, *Y. lipolytica* NDUFA11 has a longer C-terminal coil relative to mammals, that extends along the IMS side of the complex interacting with ND4, NDUFB10, NDUFB4, NDUFB11, and NDUFB6 (**Figure 14F**). In *Y. lipolytica* and bacterial CI structures (*E. coli* and *T. thermophilus*) $TMH4^{ND6}$ binds at the interface of $TMH16^{ND5}$, $TMH1^{ND4L}$ and $TMH6^{ND2}$, forming additional contacts with NDUFA11 in *Y. lipolytica* (**Figure 14F**). In mammals, $TMH4^{ND6}$ is displaced from this position binding adjacent to $TMH1^{ND6}$ and not directly interacting with ND2 or NDUFA11 (**Figure 14E**). These additional NDUFA11 interactions in *Y. lipolytica* are likely why dissolution of CI using the harsh detergent lauryl dimethylamine oxide (LDAO) results in a different pattern of subcomplexes in *Y. lipolytica* vs. mammals (reviewed by Letts and Sazanov 2015) (Sazanov et al., 2000; Angerer et al., 2011; Letts and Sazanov, 2015; Letts et al., 2016a). In *Y. lipolytica* the P_D-module remains associated with the Q- and N-modules even after the loss of P_P-module subunits whereas in mammalian CI the P_D-module is more easily dissociated (Sazanov et al., 2000; Angerer et al., 2011; Letts et al., 2016a). These data indicate that NDUFA11 plays an important role in stabilizing the interaction between the P_D- and P_P-modules and that this role has been diminished in mammals. The predominantly lipid-mediated contacts between CI and NDUFA11 in mammals, is also likely the reason why NDUFA11 is easily lost or disordered by detergent when mammalian CI is extracted from the membrane (Letts et al., 2019).

In the mammalian supercomplex I + III_2 structure, NDUFA11 forms the only interface between CI and CIII in the membrane. The interface is largely formed by interactions between NDUFA11, UQCRB, and UQCRQ (Letts et al., 2019). NDUFA11 therefore plays a role in stabilizing supercomplex I + III_2 (Letts et al., 2019) and conversely $CIII_2$ helps to stabilize NDUFA11 onto the surface of CI (Letts and Sazanov, 2017). The fact that in mammals NDUFA11's stabilizing role at the interface of the P_P and P_D modules is diminished relative to *Y. lipolytica*, and that NDUFA11 plays an important role in the formation of supercomplex I + III_2, leads to the hypothesis that NDUFA11 has been coopted to promote supercomplex formation in mammals. In this scenario CI stability would depend in part on interaction with $CIII_2$ through the stabilization of NDUFA11 onto the CI core subunits.

CONCLUSION

The functional roles of the multitude of CI accessory subunits have remained mysterious. However, the recent trove of CI structures across bacteria and eukaryotes provides a wealth of information to explore possible functional roles. Comparing the available structures and integrating information from assembly, knockout, knockdown, mutagenesis and clinical studies have allowed us to propose new functional hypotheses for most accessory subunits that can now be experimentally tested. Overall, we hypothesize that CI accessory subunits have roles in 1) coordinating CI assembly, e.g., preventing the association of the N-module until the membrane arm is fully assembled (NDUFS4, NDUFS6, and NDUFA12); 2) providing a scaffold to localize proteins to the inner surface of the cristae (NDUFV3); 3) allowing CI to alter its activity in response to ROS (NDUFA2); 4) integrating information about upstream energy supplies (LYR/ACP pairs) and downstream energy output (NDUFA10); 5) regulating access to the Q-tunnel in an assembly or state dependent manner (NDUFA12, NDUFA9, and NDUFA1); 6) linking CI assembly to cell proliferation (NDUFA13); 7) linking CI assembly mitochondria health (e.g. the CX_9C motif subunits NDUFA8, NDUFS5, NDUFB10 and NDUFB7, as well as all the TM and matrix subunits that require membrane potential for import into or across the IMM); 8) coupling CI assembly to the redox state of the cell (CX_9C motif subunits); 9) regulating CI biogenesis via the unfolded protein response (NDUFB2) or alternative splicing (NDUFB11); 10) regulating supercomplex formation (NDUFB3, NDUFB4, NDUFB9, and NDUFA11); and 11) stabilizing the association of lipids at key subunit interfaces (NDUFA3, NDUFC2, NDUFC1, NDUFB1, NDUFB11, NDUFB5, and NDUFB6). We anticipate that this framework for the potential functions of CI's accessory subunits will contribute to an experimental roadmap to build on the structural, cellular, genetic and biochemical work of the last

decades to fully understand the roles of this mysterious multitude in health and disease.

AUTHOR CONTRIBUTIONS

JL conceived of and designed the study. JL, AP, MA-H and EC-S searched and examined the literature. JL, AP, MA-H and EC-S wrote the manuscript. AP, MA-H and EC-S prepared the figures. All authors have read and approved the manuscript.

FUNDING

This work was supported by National Institute of General Medical Sciences (NIGMS) Award number R35GM137929.

ACKNOWLEDGMENTS

We thank Dr. María Maldonado for critical reading of the manuscript.

REFERENCES

Abdrakhmanova, A., Zwicker, K., Kerscher, S., Zickermann, V., and Brandt, U. (2006). Tight Binding of NADPH to the 39-kDa Subunit of Complex I Is Not Required for Catalytic Activity but Stabilizes the Multiprotein Complex. *Biochim. Biophys. Acta (Bba) - Bioenerg.* 1757, 1676–1682. doi:10.1016/j.bbabio.2006.09.003

Agip, A.-N. A., Blaza, J. N., Bridges, H. R., Viscomi, C., Rawson, S., Muench, S. P., et al. (2018). Cryo-em Structures of Complex I from Mouse Heart Mitochondria in Two Biochemically Defined States. *Nat. Struct. Mol. Biol.* 25, 548–556. doi:10.1038/s41594-018-0073-1

Aldridge, J. E., Horibe, T., and Hoogenraad, N. J. (2007). Discovery of Genes Activated by the Mitochondrial Unfolded Protein Response (mtUPR) and Cognate Promoter Elements. *PLoS One* 2, e874. doi:10.1371/journal.pone.0000874

Allen, S., Balabanidou, V., Sideris, D. P., Lisowsky, T., and Tokatlidis, K. (2005). Erv1 Mediates the Mia40-dependent Protein Import Pathway and Provides a Functional Link to the Respiratory Chain by Shuttling Electrons to Cytochrome C. *J. Mol. Biol.* 353, 937–944. doi:10.1016/j.jmb.2005.08.049

Alston, C. L., Howard, C., Oláhová, M., Hardy, S. A., He, L., Murray, P. G., et al. (2016). A Recurrent Mitochondrial p.Trp22ArgNDUFB3variant Causes a Distinctive Facial Appearance, Short Stature and a Mild Biochemical and Clinical Phenotype. *J. Med. Genet.* 53, 634–641. doi:10.1136/jmedgenet-2015-103576

Andrews, B., Carroll, J., Ding, S., Fearnley, I. M., and Walker, J. E. (2013). Assembly Factors for the Membrane Arm of Human Complex I. *Proc. Natl. Acad. Sci.* 110, 18934–18939. doi:10.1073/pnas.1319247110

Angebault, C., Charif, M., Guegen, N., Piro-Megy, C., Mousson de camaret, B., Procaccio, V., et al. (2015). Mutation in NDUFA13/GRIM19 Leads to Early Onset Hypotonia, Dyskinesia and Sensorial Deficiencies, and Mitochondrial Complex I Instability. *Hum. Mol. Genet.* 24, 3948–3955. doi:10.1093/hmg/ddv133

Angerer, H., Radermacher, M., Ma kowska, M., Steger, M., Zwicker, K., Heide, H., et al. (2014). The LYR Protein Subunit NB4M/NDUFA6 of Mitochondrial Complex I Anchors an Acyl Carrier Protein and Is Essential for Catalytic Activity. *Proc. Natl. Acad. Sci.* 111, 5207–5212. doi:10.1073/pnas.1322438111

Angerer, H., Zwicker, K., Wumaier, Z., Sokolova, L., Heide, H., Steger, M., et al. (2011). A Scaffold of Accessory Subunits Links the Peripheral Arm and the Distal Proton-Pumping Module of Mitochondrial Complex I. *Biochem. J.* 437, 279–288. doi:10.1042/BJ20110359

Assouline, Z., Jambou, M., Rio, M., Bole-Feysot, C., de Lonlay, P., Barnerias, C., et al. (2012). A Constant and Similar Assembly Defect of Mitochondrial Respiratory Chain Complex I Allows Rapid Identification of NDUFS4 Mutations in Patients with Leigh Syndrome. *Biochim. Biophys. Acta (Bba) - Mol. Basis Dis.* 1822, 1062–1069. doi:10.1016/j.bbadis.2012.01.013

Atkinson, A., Smith, P., Fox, J. L., Cui, T.-Z., Khalimonchuk, O., and Winge, D. R. (2011). The LYR Protein Mzm1 Functions in the Insertion of the Rieske Fe/S Protein in Yeast Mitochondria. *Mol. Cell Biol.* 31, 3988–3996. doi:10.1128/mcb.05673-11

Au, H. C., Seo, B. B., Matsuno-Yagi, A., Yagi, T., and Scheffler, I. E. (1999). The NDUFA1 Gene Product (MWFE Protein) Is Essential for Activity of Complex I in Mammalian Mitochondria. *Proc. Natl. Acad. Sci.* 96, 4354–4359. doi:10.1073/pnas.96.8.4354

Baertling, F., Sánchez-Caballero, L., van den Brand, M. A. M., Fung, C.-W., Chan, S. H.-S., Wong, V. C.-N., et al. (2018). NDUFA9 point Mutations Cause a Variable Mitochondrial Complex I Assembly Defect. *Clin. Genet.* 93, 111–118. doi:10.1111/cge.13089

Baradaran, R., Berrisford, J. M., Minhas, G. S., and Sazanov, L. A. (2013). Crystal Structure of the Entire Respiratory Complex I. *Nature* 494, 443–448. doi:10.1038/nature11871

Berrisford, J. M., Baradaran, R., and Sazanov, L. A. (2016). Structure of Bacterial Respiratory Complex I. *Biochim. Biophys. Acta (Bba) - Bioenerg.* 1857, 892–901. doi:10.1016/j.bbabio.2016.01.012

Bihlmaier, K., Mesecke, N., Terziyska, N., Bien, M., Hell, K., and Herrmann, J. M. (2007). The Disulfide Relay System of Mitochondria Is Connected to the Respiratory Chain. *J. Cel Biol.* 179, 389–395. doi:10.1083/jcb.200707123

Blaza, J. N., Vinothkumar, K. R., and Hirst, J. (2018). Structure of the Deactive State of Mammalian Respiratory Complex I. *Structure* 26, 312–319. e3. doi:10.1016/j.str.2017.12.014

Boniecki, M. T., Freibert, S. A., Mühlenhoff, U., Lill, R., and Cygler, M. (2017). Structure and Functional Dynamics of the Mitochondrial Fe/S Cluster Synthesis Complex. *Nat. Commun.* 8. doi:10.1038/s41467-017-01497-1

Breen, G. A. M., and Scheffler, I. E. (1979). Respiration-deficient Chinese Hamster Cell Mutants: Biochemical Characterization. *Somat Cel Mol Genet* 5, 441–451. doi:10.1007/BF01538879

Bridges, H. R., Fedor, J. G., Blaza, J. N., Di Luca, A., Jussupow, A., Jarman, O. D., et al. (2020). Structure of Inhibitor-Bound Mammalian Complex I. *Nat. Commun.* 11, 1–11. doi:10.1038/s41467-020-18950-3

Bridges, H. R., Mohammed, K., Harbour, M. E., and Hirst, J. (2017). Subunit NDUFV3 Is Present in Two Distinct Isoforms in Mammalian Complex I. *Biochim. Biophys. Acta (Bba) - Bioenerg.* 1858, 197–207. doi:10.1016/j.bbabio.2016.12.001

Brindefalk, B., Ettema, T. J. G., Viklund, J., Thollesson, M., and Andersson, S. G. E. (2011). A Phylometagenomic Exploration of Oceanic Alphaproteobacteria Reveals Mitochondrial Relatives Unrelated to the SAR11 Clade. *PLoS One* 6, e24457. doi:10.1371/journal.pone.0024457

Brockmann, C., Diehl, A., Rehbein, K., Strauss, H., Schmieder, P., Korn, B., et al. (2004). The Oxidized Subunit B8 from Human Complex I Adopts a Thioredoxin Fold. *Structure* 12, 1645–1654. doi:10.1016/j.str.2004.06.021

Brown, A., Rathore, S., Kimanius, D., Aibara, S., Bai, X.-c., Rorbach, J., et al. (2017). Structures of the Human Mitochondrial Ribosome in Native States of Assembly. *Nat. Struct. Mol. Biol.* 24, 866–869. doi:10.1038/nsmb.3464

Calvaruso, M. A., Willems, P., Van den brand, M., Valsecchi, F., Kruse, S., Palmiter, R., et al. (2012). Mitochondrial Complex III Stabilizes Complex I in the Absence of NDUFS4 to Provide Partial Activity. *Hum. Mol. Genet.* 21, 115–120. doi:10.1093/hmg/ddr446

Calvo, S. E., Compton, A. G., Hershman, S. G., Lim, S. C., Lieber, D. S., Tucker, E. J., et al. (2012). Molecular Diagnosis of Infantile Mitochondrial Disease with Targeted Next-Generation Sequencing. *Sci. Transl. Med.* 4. doi:10.1126/scitranslmed.3003310

Carroll, J., Fearnley, I. M., Skehel, J. M., Runswick, M. J., Shannon, R. J., Hirst, J., et al. (2005). The post-translational Modifications of the Nuclear Encoded Subunits of Complex I from Bovine Heart Mitochondria. *Mol. Cell Proteomics* 4, 693–699. doi:10.1074/mcp.M500014-MCP200

Carroll, J., Shannon, R. J., Fearnley, I. M., Walker, J. E., and Hirst, J. (2002). Definition of the Nuclear Encoded Protein Composition of Bovine Heart

Mitochondrial Complex I. *J. Biol. Chem.* 277, 50311–50317. doi:10.1074/jbc.M209166200

Chouchani, E. T., Pell, V. R., Gaude, E., Aksentijević, D., Sundier, S. Y., Robb, E. L., et al. (2014). Ischaemic Accumulation of Succinate Controls Reperfusion Injury through Mitochondrial ROS. *Nature* 515, 431–435. doi:10.1038/nature13909

Chung, I., Serreli, R., Cross, J. B., Di Francesco, M. E., Marszalek, J. R., and Hirst, J. (2021). Cork-in-bottle Mechanism of Inhibitor Binding to Mammalian Complex I. *Sci. Adv.* 7. doi:10.1126/sciadv.abg4000

Ciano, M., Fuszard, M., Heide, H., Botting, C. H., and Galkin, A. (2013). Conformation-specific Crosslinking of Mitochondrial Complex I. *FEBS Lett.* 587, 867–872. doi:10.1016/j.febslet.2013.02.039

Cronan, J. E. (2014). The Chain-Flipping Mechanism of ACP (Acyl Carrier Protein)-dependent Enzymes Appears Universal. *Biochem. J.* 460, 157–163. doi:10.1042/BJ20140239

da Silva, M. V., Alves, P. C., Duarte, M., Mota, N., Lobo-Da-Cunha, A., Videira, A., et al. (1996). Disruption of the Nuclear Gene Encoding the 20.8-kDa Subunit of NADH:ubiquinone Reductase ofNeurospora Mitochondria. *Mol. Gen. Genet.* 252, 177–183. doi:10.1007/s00438967002010.1007/bf02173218

Dibley, M. G., Formosa, L. E., Lyu, B., Reljic, B., McGann, D., Muellner-Wong, L., et al. (2020). The Mitochondrial Acyl-Carrier Protein Interaction Network Highlights Important Roles for LYRM Family Members in Complex I and Mitoribosome Assembly. *Mol. Cell Proteomics* 19, 65–77. doi:10.1074/mcp.RA119.001784

Dibley, M. G., Ryan, M. T., and Stroud, D. A. (2017). A Novel Isoform of the Human Mitochondrial Complex I Subunit NDUFV3. *FEBS Lett.* 591, 109–117. doi:10.1002/1873-3468.12527

Dickson-Murray, E., Nedara, K., Modjtahedi, N., and Tokatlidis, K. (2021). The Mia40/chchd4 Oxidative Folding System: Redox Regulation and Signaling in the Mitochondrial Intermembrane Space. *Antioxidants* 10, 592. doi:10.3390/antiox10040592

Dyson, H. J., and Wright, P. E. (2005). Intrinsically Unstructured Proteins and Their Functions. *Nat. Rev. Mol. Cel Biol.* 6, 197–208. doi:10.1038/nrm1589

Elurbe, D. M., and Huynen, M. A. (2016). The Origin of the Supernumerary Subunits and Assembly Factors of Complex I: A Treasure Trove of Pathway Evolution. *Biochim. Biophys. Acta (Bba) - Bioenerg.* 1857, 971–979. doi:10.1016/j.bbabio.2016.03.027

Fernandez-Moreira, D., Ugalde, C., Smeets, R., Rodenburg, R. J. T., Lopez-Laso, E., Ruiz-Falco, M. L., et al. (2007). X-linkedNDUFA1gene Mutations Associated with Mitochondrial Encephalomyopathy. *Ann. Neurol.* 61, 73–83. doi:10.1002/ana.21036

Fiedorczuk, K., Letts, J. A., Degliesposti, G., Kaszuba, K., Skehel, M., and Sazanov, L. A. (2016). Atomic Structure of the Entire Mammalian Mitochondrial Complex I. *Nature* 538, 406–410. doi:10.1038/nature19794

Fiedorczuk, K., and Sazanov, L. A. (2018). Mammalian Mitochondrial Complex I Structure and Disease-Causing Mutations. *Trends Cel Biol.* 28, 835–867. doi:10.1016/j.tcb.2018.06.006

Fischer, M., Horn, S., Belkacemi, A., Kojer, K., Petrungaro, C., Habich, M., et al. (2013). Protein Import and Oxidative Folding in the Mitochondrial Intermembrane Space of Intact Mammalian Cells. *Mol. Biol. Cell* 24, 2160–2170. doi:10.1091/mbc.E12-12-0862

Formosa, L. E., Dibley, M. G., Stroud, D. A., and Ryan, M. T. (2018). Building a Complex Complex: Assembly of Mitochondrial Respiratory Chain Complex I. *Semin. Cel Developmental Biol.* 76, 154–162. doi:10.1016/j.semcdb.2017.08.011

Friederich, M. W., Erdogan, A. J., Coughlin, C. R., Elos, M. T., Jiang, H., O'Rourke, C. P., et al. (2017). Mutations in the Accessory subunitNDUFB10result in Isolated Complex I Deficiency and Illustrate the Critical Role of Intermembrane Space Import for Complex I Holoenzyme Assembly. *Hum. Mol. Genet.* 26, ddw431–716. doi:10.1093/hmg/ddw431

Friedrich, T., Dekovic, D. K., and Burschel, S. (2016). Assembly of the *Escherichia coli* NADH:ubiquinone Oxidoreductase (Respiratory Complex I). *Biochim. Biophys. Acta (Bba) - Bioenerg.* 1857, 214–223. doi:10.1016/j.bbabio.2015.12.004

Galemou Yoga, E., Parey, K., Djurabekova, A., Haapanen, O., Siegmund, K., Zwicker, K., et al. (2020). Essential Role of Accessory Subunit LYRM6 in the Mechanism of Mitochondrial Complex I. *Nat. Commun.* 11, 1–8. doi:10.1038/s41467-020-19778-7

Garcia, C. J., Khajeh, J., Coulanges, E., Chen, E. I.-j., and Owusu-Ansah, E. (2017). Regulation of Mitochondrial Complex I Biogenesis in Drosophila Flight Muscles. *Cel Rep.* 20, 264–278. doi:10.1016/j.celrep.2017.06.015

Ghezzi, D., Goffrini, P., Uziel, G., Horvath, R., Klopstock, T., Lochmüller, H., et al. (2009). SDHAF1, Encoding a LYR Complex-II Specific Assembly Factor, Is Mutated in SDH-Defective Infantile Leukoencephalopathy. *Nat. Genet.* 41, 654–656. doi:10.1038/ng.378

Grba, D. N., and Hirst, J. (2020). Mitochondrial Complex I Structure Reveals Ordered Water Molecules for Catalysis and Proton Translocation. *Nat. Struct. Mol. Biol.* 27, 892–900. doi:10.1038/s41594-020-0473-x

Guarás, A., Perales-Clemente, E., Calvo, E., Acín-Pérez, R., Loureiro-Lopez, M., Pujol, C., et al. (2016). The CoQH2/CoQ Ratio Serves as a Sensor of Respiratory Chain Efficiency. *Cel Rep.* 15, 197–209. doi:10.1016/j.celrep.2016.03.009

Guerrero-Castillo, S., Baertling, F., Kownatzki, D., Wessels, H. J., Arnold, S., Brandt, U., et al. (2017a). The Assembly Pathway of Mitochondrial Respiratory Chain Complex I. *Cel Metab.* 25, 128–139. doi:10.1016/j.cmet.2016.09.002

Guerrero-Castillo, S., Cabrera-Orefice, A., Huynen, M. A., and Arnold, S. (2017b). Identification and Evolutionary Analysis of Tissue-specific Isoforms of Mitochondrial Complex I Subunit NDUFV3. *Biochim. Biophys. Acta (Bba) - Bioenerg.* 1858, 208–217. doi:10.1016/j.bbabio.2016.12.004

Guo, R., Zong, S., Wu, M., Gu, J., and Yang, M. (2017). Architecture of Human Mitochondrial Respiratory Megacomplex I2III2IV2. *Cell* 170, 1247–1257. e12. doi:10.1016/j.cell.2017.07.050

Haack, T. B., Madignier, F., Herzer, M., Lamantea, E., Danhauser, K., Invernizzi, F., et al. (2012). Mutation Screening of 75 Candidate Genes in 152 Complex I Deficiency Cases Identifies Pathogenic Variants in 16 Genes includingNDUFB9. *J. Med. Genet.* 49, 83–89. doi:10.1136/jmedgenet-2011-100577

Jarman, O. D., Biner, O., Wright, J. J., and Hirst, J. (2021). Paracoccus Denitrificans: a Genetically Tractable Model System for Studying Respiratory Complex I. *Sci. Rep.* 11. doi:10.1038/s41598-021-89575-9

Kahlhöfer, F., Gansen, M., and Zickermann, V. (2021). Accessory Subunits of the Matrix Arm of Mitochondrial Complex I with a Focus on Subunit Ndufs4 and its Role in Complex I Function and Assembly. *Life* 11, 455. doi:10.3390/life11050455

Kahlhöfer, F., Kmita, K., Wittig, I., Zwicker, K., and Zickermann, V. (2017). Accessory Subunit NUYM (NDUFS4) Is Required for Stability of the Electron Input Module and Activity of Mitochondrial Complex I. *Biochim. Biophys. Acta (Bba) - Bioenerg.* 1858, 175–181. doi:10.1016/j.bbabio.2016.11.010

Kampjut, D., and Sazanov, L. A. (2020). The Coupling Mechanism of Mammalian Respiratory Complex I. *Science* 370, 370. doi:10.1126/SCIENCE.ABC4209

Klusch, N., Senkler, J., Yildiz, Ö., Kühlbrandt, W., and Braun, H.-P. (2021). A Ferredoxin Bridge Connects the Two Arms of Plant Mitochondrial Complex I. *Plant Cell* 33, 2072–2091. doi:10.1093/plcell/koab092

Kmita, K., Wirth, C., Warnau, J., Guerrero-Castillo, S., Hunte, C., Hummer, G., et al. (2015). Accessory NUMM (NDUFS6) Subunit Harbors a Zn-Binding Site and Is Essential for Biogenesis of Mitochondrial Complex I. *Proc. Natl. Acad. Sci. USA* 112, 5685–5690. doi:10.1073/pnas.1424353112

Koene, S., Rodenburg, R. J., Van Der Knaap, M. S., Willemsen, M. A. A. P., Sperl, W., Laugel, V., et al. (2012). Natural Disease Course and Genotype-Phenotype Correlations in Complex I Deficiency Caused by Nuclear Gene Defects: What We Learned from 130 Cases. *J. Inherit. Metab. Dis.* 35, 737–747. doi:10.1007/s10545-012-9492-z

Kolata, P., and Efremov, R. G. (2021). Structure of *Escherichia coli* Respiratory Complex I Reconstituted into Lipid Nanodiscs Reveals an Uncoupled Conformation. *bioRxiv*. doi:10.1101/2021.04.09.439197

Krissinel, E., and Henrick, K. (2007). Inference of Macromolecular Assemblies from Crystalline State. *J. Mol. Biol.* 372, 774–797. doi:10.1016/j.jmb.2007.05.022

Kritsiligkou, P., Chatzi, A., Charalampous, G., Mironov, A., Grant, C. M., and Tokatlidis, K. (2017). Unconventional Targeting of a Thiol Peroxidase to the Mitochondrial Intermembrane Space Facilitates Oxidative Protein Folding. *Cel Rep.* 18, 2729–2741. doi:10.1016/j.celrep.2017.02.053

Kruse, S. E., Watt, W. C., Marcinek, D. J., Kapur, R. P., Schenkman, K. A., and Palmiter, R. D. (2008). Mice with Mitochondrial Complex I Deficiency Develop a Fatal Encephalomyopathy. *Cel Metab.* 7, 312–320. doi:10.1016/j.cmet.2008.02.004

Letts, J. A., Degliesposti, G., Fiedorczuk, K., Skehel, M., and Sazanov, L. A. (2016a). Purification of Ovine Respiratory Complex I Results in a Highly Active and Stable Preparation. *J. Biol. Chem.* 291, 24657–24675. doi:10.1074/jbc.M116.735142

Letts, J. A., Fiedorczuk, K., Degliesposti, G., Skehel, M., and Sazanov, L. A. (2019). Structures of Respiratory Supercomplex I+III2 Reveal Functional and Conformational Crosstalk. *Mol. Cel* 75, 1131–1146. e6. doi:10.1016/j.molcel.2019.07.022

Letts, J. A., Fiedorczuk, K., and Sazanov, L. A. (2016b). The Architecture of Respiratory Supercomplexes. *Nature* 537, 644–648. doi:10.1038/nature19774

Letts, J. A., and Sazanov, L. A. (2017). Clarifying the Supercomplex: The Higher-Order Organization of the Mitochondrial Electron Transport Chain. *Nat. Struct. Mol. Biol.* 24, 800–808. doi:10.1038/nsmb.3460

Letts, J. A., and Sazanov, L. A. (2015). Gaining Mass: The Structure of Respiratory Complex I-From Bacterial towards Mitochondrial Versions. *Curr. Opin. Struct. Biol.* 33, 135–145. doi:10.1016/j.sbi.2015.08.008

Lichtenstein, D. A., Crispin, A. W., Sendamarai, A. K., Campagna, D. R., Schmitz-Abe, K., Sousa, C. M., et al. (2016). A Recurring Mutation in the Respiratory Complex 1 Protein NDUFB11 Is Responsible for a Novel Form of X-Linked Sideroblastic Anemia. *Blood* 128, 1913–1917. doi:10.1182/blood-2016-05-719062

Ligas, J., Pineau, E., Bock, R., Huynen, M. A., and Meyer, E. H. (2019). The Assembly Pathway of Complex I in *Arabidopsis thaliana*. *Plant J.* 97, 447–459. doi:10.1111/tpj.14133

Ling, C., Poulsen, P., Simonsson, S., Rönn, T., Holmkvist, J., Almgren, P., et al. (2007). Genetic and Epigenetic Factors Are Associated with Expression of Respiratory Chain Component NDUFB6 in Human Skeletal Muscle. *J. Clin. Invest.* 117, 3427–3435. doi:10.1172/JCI30938

Longen, S., Bien, M., Bihlmaier, K., Kloeppel, C., Kauff, F., Hammermeister, M., et al. (2009). Systematic Analysis of the Twin Cx9C Protein Family. *J. Mol. Biol.* 393, 356–368. doi:10.1016/j.jmb.2009.08.041

Loublier, S., Bayot, A., Rak, M., El-Khoury, R., Bénit, P., and Rustin, P. (2011). The NDUFB6 Subunit of the Mitochondrial Respiratory Chain Complex I Is Required for Electron Transfer Activity: A Proof of Principle Study on Stable and Controlled RNA Interference in Human Cell Lines. *Biochem. Biophysical Res. Commun.* 414, 367–372. doi:10.1016/j.bbrc.2011.09.078

Lufei, C., Ma, J., Huang, G., Zhang, T., Novotny-Diermayr, V., Ong, C. T., et al. (2003). GRIM-19, a Death-Regulatory Gene Product, Suppresses Stat3 Activity via Functional Interaction. *EMBO J.* 22, 1325–1335. doi:10.1093/emboj/cdg135

Ma, Y.-Y., Li, X.-Y., Li, Z.-Q., Song, J.-Q., Hou, J., Li, J.-H., et al. (2018). Clinical, Biochemical, and Genetic Analysis of the Mitochondrial Respiratory Chain Complex I Deficiency. *Med. (United States* 97, e11606–34. doi:10.1097/MD.0000000000011606

Maio, N., Kim, K. S., Singh, A., and Rouault, T. A. (2017). A Single Adaptable Cochaperone-Scaffold Complex Delivers Nascent Iron-Sulfur Clusters to Mammalian Respiratory Chain Complexes I-III. *Cel Metab.* 25, 945–953. e6. doi:10.1016/j.cmet.2017.03.010

Maître, J.-L., and Heisenberg, C.-P. (2013). Three Functions of Cadherins in Cell Adhesion. *Curr. Biol.* 23, R626–R633. doi:10.1016/j.cub.2013.06.019

Maklashina, E., Kotlyar, A. B., and Cecchini, G. (2003). Active/de-active Transition of Respiratory Complex I in Bacteria, Fungi, and Animals. *Biochim. Biophys. Acta (Bba) - Bioenerg.* 1606, 95–103. doi:10.1016/S0005-2728(03)00087-2

Maldonado, M., Padavannil, A., Zhou, L., Guo, F., and Letts, J. A. (2020). Atomic Structure of a Mitochondrial Complex I Intermediate from Vascular Plants. *Elife* 9, 1–36. doi:10.7554/ELIFE.56664

Markley, J. L., Kim, J. H., Dai, Z., Bothe, J. R., Cai, K., Frederick, R. O., et al. (2013). Metamorphic Protein IscU Alternates Conformations in the Course of its Role as the Scaffold Protein for Iron-Sulfur Cluster Biosynthesis and Delivery. *FEBS Lett.* 587, 1172–1179. doi:10.1016/j.febslet.2013.01.003

Marques, I., Ushakova, A. V., Duarte, M., and Videira, A. (2007). Role of the Conserved Cysteine Residues of the 11.5 kDa Subunit in Complex I Catalytic Properties. *J. Biochem.* 141, 489–493. doi:10.1093/jb/mvm049

Martijn, J., Vosseberg, J., Guy, L., Offre, P., and Ettema, T. J. G. (2018). Deep Mitochondrial Origin outside the Sampled Alphaproteobacteria. *Nature* 557, 101–105. doi:10.1038/s41586-018-0059-5

Máximo, V., Botelho, T., Capela, J., Soares, P., Lima, J., Taveira, A., et al. (2005). Somatic and Germline Mutation in GRIM-19, a Dual Function Gene Involved in Mitochondrial Metabolism and Cell Death, Is Linked to Mitochondrion-Rich (Hürthle Cell) Tumours of the Thyroid. *Br. J. Cancer* 92, 1892–1898. doi:10.1038/sj.bjc.6602547

Mesecke, N., Terziyska, N., Kozany, C., Baumann, F., Neupert, W., Hell, K., et al. (2005). A Disulfide Relay System in the Intermembrane Space of Mitochondria that Mediates Protein Import. *Cell* 121, 1059–1069. doi:10.1016/j.cell.2005.04.011

Meyer, E. H., Welchen, E., and Carrie, C. (2019). Assembly of the Complexes of the Oxidative Phosphorylation System in Land Plant Mitochondria. *Annu. Rev. Plant Biol.* 70, 23–50. doi:10.1146/annurev-arplant-050718-100412

Mimaki, M., Wang, X., McKenzie, M., Thorburn, D. R., and Ryan, M. T. (2012). Understanding Mitochondrial Complex I Assembly in Health and Disease. *Biochim. Biophys. Acta (Bba) - Bioenerg.* 1817, 851–862. doi:10.1016/j.bbabio.2011.08.010

Modjtahedi, N., Tokatlidis, K., Dessen, P., and Kroemer, G. (2016). Mitochondrial Proteins Containing Coiled-Coil-Helix-Coiled-Coil-Helix (CHCH) Domains in Health and Disease. *Trends Biochem. Sci.* 41, 245–260. doi:10.1016/j.tibs.2015.12.004

Murray, J., Taylor, S. W., Zhang, B., Ghosh, S. S., and Capaldi, R. A. (2003). Oxidative Damage to Mitochondrial Complex I Due to Peroxynitrite. *J. Biol. Chem.* 278, 37223–37230. doi:10.1074/jbc.M305694200

Nakao, L. S., Everley, R. A., Marino, S. M., Lo, S. M., De Souza, L. E., Gygi, S. P., et al. (2015). Mechanism-based Proteomic Screening Identifies Targets of Thioredoxin-like Proteins. *J. Biol. Chem.* 290, 5685–5695. doi:10.1074/jbc.M114.597245

Nallar, S. C., Kalakonda, S., Lindner, D. J., Lorenz, R. R., Lamarre, E., Weihua, X., et al. (2013). Tumor-derived Mutations in the Gene Associated with Retinoid Interferon-Induced Mortality (GRIM-19) Disrupt its Anti-signal Transducer and Activator of Transcription 3 (STAT3) Activity and Promote Oncogenesis. *J. Biol. Chem.* 288, 7930–7941. doi:10.1074/jbc.M112.440610

Ostergaard, E., Rodenburg, R. J., van den Brand, M., Thomsen, L. L., Duno, M., Batbayli, M., et al. (2011). Respiratory Chain Complex I Deficiency Due to NDUFA12 Mutations as a New Cause of Leigh Syndrome. *J. Med. Genet.* 48, 737–740. doi:10.1136/jmg.2011.088856

Ostermann, N., Schlichting, I., Brundiers, R., Konrad, M., Reinstein, J., Veit, T., et al. (2000). Insights into the Phosphoryltransfer Mechanism of Human Thymidylate Kinase Gained from crystal Structures of Enzyme Complexes along the Reaction Coordinate. *Structure* 8, 629–642. doi:10.1016/S0969-2126(00)00149-0

Pagliarini, D. J., and Rutter, J. (2013). Hallmarks of a new era in Mitochondrial Biochemistry. *Genes Dev.* 27, 2615–2627. doi:10.1101/gad.229724.113

Palmisano, G., Sardanelli, A. M., Signorile, A., Papa, S., and Larsen, M. R. (2007). The Phosphorylation Pattern of Bovine Heart Complex I Subunits. *Proteomics* 7, 1575–1583. doi:10.1002/pmic.200600801

Panelli, D., Lorusso, F. P., Papa, F., Panelli, P., Stella, A., Caputi, M., et al. (2013). The Mechanism of Alternative Splicing of the X-Linked NDUFB11 Gene of the Respiratory Chain Complex I, Impact of Rotenone Treatment in Neuroblastoma Cells. *Biochim. Biophys. Acta (Bba) - Gene Regul. Mech.* 1829, 211–218. doi:10.1016/j.bbagrm.2012.12.001

Papa, S. (2002). The NDUFS4 Nuclear Gene of Complex I of Mitochondria and the cAMP cascade. *Biochim. Biophys. Acta (Bba) - Bioenerg.* 1555, 147–153. doi:10.1016/S0005-2728(02)00270-0

Parey, K., Haapanen, O., Sharma, V., Köfeler, H., Züllig, T., Prinz, S., et al. (2019). High-resolution Cryo-EM Structures of Respiratory Complex I: Mechanism, Assembly, and Disease. *Sci. Adv.* 5, 1–10. doi:10.1126/sciadv.aax9484

Parey, K., Lasham, J., Mills, D. J., Djurabekova, A., Haapanen, O., Galemou Yoga, E., et al. (2021). High-resolution Structure and Dynamics of Mitochondrial Complex I – Insights into the Proton Pumping Mechanism. *bioRxiv*. Available at:http://biorxiv.org/content/early/2021/04/16/2021.04.16.440187.abstract.

Peralta, S., Torraco, A., Wenz, T., Garcia, S., Diaz, F., and Moraes, C. T. (2014). Partial Complex I Deficiency Due to the CNS Conditional Ablation of Ndufa5 Results in a Mild Chronic Encephalopathy but No Increase in Oxidative Damage. *Hum. Mol. Genet.* 23, 1399–1412. doi:10.1093/hmg/ddt526

Piekutowska-Abramczuk, D., Assouline, Z., Mataković, L., Feichtinger, R. G., Koňařiková, E., Jurkiewicz, E., et al. (2018). NDUFB8 Mutations Cause Mitochondrial Complex I Deficiency in Individuals with Leigh-like Encephalomyopathy. *Am. J. Hum. Genet.* 102, 460–467. doi:10.1016/j.ajhg.2018.01.008

Raffa, S., Scrofani, C., Valente, S., Micaloni, A., Forte, M., Bianchi, F., et al. (2017). *In Vitro* characterization of Mitochondrial Function and Structure in Rat and

Human Cells with a Deficiency of the NADH: Ubiquinone Oxidoreductase Ndufc2 Subunit. *Hum. Mol. Genet.* 26, 4541–4555. doi:10.1093/hmg/ddx333

Rak, M., and Rustin, P. (2014). Supernumerary Subunits NDUFA3, NDUFA5 and NDUFA12 Are Required for the Formation of the Extramembrane Arm of Human Mitochondrial Complex I. *FEBS Lett.* 588, 1832–1838. doi:10.1016/j.febslet.2014.03.046

Rathore, A., Chu, Q., Tan, D., Martinez, T. F., Donaldson, C. J., Diedrich, J. K., et al. (2018). MIEF1 Microprotein Regulates Mitochondrial Translation. *Biochemistry* 57, 5564–5575. doi:10.1021/acs.biochem.8b00726

Rodenburg, R. J. (2016). Mitochondrial Complex I-Linked Disease. *Biochim. Biophys. Acta (Bba) - Bioenerg.* 1857, 938–945. doi:10.1016/j.bbabio.2016.02.012

Rubattu, S., Di Castro, S., Schulz, H., Geurts, A. M., Cotugno, M., Bianchi, F., et al. (2016). Ndufc2 Gene Inhibition Is Associated with Mitochondrial Dysfunction and Increased Stroke Susceptibility in an Animal Model of Complex Human Disease. *Jaha* 5, 1–26. doi:10.1161/JAHA.115.002701

Sabini, E., Hazra, S., Ort, S., Konrad, M., and Lavie, A. (2008). Structural Basis for Substrate Promiscuity of dCK. *J. Mol. Biol.* 378, 607–621. doi:10.1016/j.jmb.2008.02.061

Sánchez-Caballero, L., Guerrero-Castillo, S., and Nijtmans, L. (2016). Unraveling the Complexity of Mitochondrial Complex I Assembly: A Dynamic Process. *Biochim. Biophys. Acta (Bba) - Bioenerg.* 1857, 980–990. doi:10.1016/j.bbabio.2016.03.031

Sazanov, L. A., Peak-Chew, S. Y., Fearnley, I. M., and Walker, J. E. (2000). Resolution of the Membrane Domain of Bovine Complex I into Subcomplexes: Implications for the Structural Organization of the Enzyme. *Biochemistry* 39, 7229–7235. doi:10.1021/bi000335t

Schulte, U., Haupt, V., Abelmann, A., Fecke, W., Brors, B., Rasmussen, T., et al. (1999). A Reductase/isomerase Subunit of Mitochondrial NADH:ubiquinone Oxidoreductase (Complex I) Carries an NADPH and Is Involved in the Biogenesis of the Complex. *J. Mol. Biol.* 292, 569–580. doi:10.1006/jmbi.1999.3096

Shi, X., Zhang, Y., Chen, R., Gong, Y., Zhang, M., Guan, R., et al. (2020). Ndufa7 Plays a Critical Role in Cardiac Hypertrophy. *J. Cel. Mol. Med.* 24, 13151–13162. doi:10.1111/jcmm.15921

Sing, A., Tsatskis, Y., Fabian, L., Hester, I., Rosenfeld, R., Serricchio, M., et al. (2014). The Atypical Cadherin Fat Directly Regulates Mitochondrial Function and Metabolic State. *Cell* 158, 1293–1308. doi:10.1016/j.cell.2014.07.036

Soufari, H., Parrot, C., Kuhn, L., Waltz, F., and Hashem, Y. (2020). Specific Features and Assembly of the Plant Mitochondrial Complex I Revealed by Cryo-EM. *Nat. Commun.* 11. doi:10.1038/s41467-020-18814-w

Steeg, P. S., Zollo, M., and Wieland, T. (2011). A Critical Evaluation of Biochemical Activities Reported for the Nucleoside Diphosphate kinase/Nm23/Awd Family Proteins: Opportunities and Missteps in Understanding Their Biological Functions. *Naunyn-schmiedeberg's Arch. Pharmacol.* 384, 331–339. doi:10.1007/s00210-011-0651-9

Stroud, D. A., Formosa, L. E., Wijeyeratne, X. W., Nguyen, T. N., and Ryan, M. T. (2013). Gene Knockout Using Transcription Activator-like Effector Nucleases (TALENs) Reveals that Human Ndufa9 Protein Is Essential for Stabilizing the junction between Membrane and Matrix Arms of Complex I. *J. Biol. Chem.* 288, 1685–1690. doi:10.1074/jbc.C112.436766

Stroud, D. A., Surgenor, E. E., Formosa, L. E., Reljic, B., Frazier, A. E., Dibley, M. G., et al. (2016). Accessory Subunits Are Integral for Assembly and Function of Human Mitochondrial Complex I. *Nature* 538, 123–126. doi:10.1038/nature19754

Szklarczyk, R., Wanschers, B. F. J., Nabuurs, S. B., Nouws, J., Nijtmans, L. G., and Huynen, M. A. (2011). NDUFB7 and NDUFA8 Are Located at the Intermembrane Surface of Complex I. *FEBS Lett.* 585, 737–743. doi:10.1016/j.febslet.2011.01.046

Tanoue, T., and Takeichi, M. (2005). New Insights into Fat Cadherins. *J. Cel Sci.* 118, 2347–2353. doi:10.1242/jcs.02398

Torraco, A., Bianchi, M., Verrigni, D., Gelmetti, V., Riley, L., Niceta, M., et al. (2017). A Novel Mutation in NDUFB11 Unveils a New Clinical Phenotype Associated with Lactic Acidosis and Sideroblastic Anemia. *Clin. Genet.* 91, 441–447. doi:10.1111/cge.12790

Ugalde, C., Vogel, R., Huijbens, R., van den Heuvel, B., Smeitink, J., and Nijtmans, L. (2004). Human Mitochondrial Complex I Assembles through the Combination of Evolutionary Conserved Modules: A Framework to Interpret Complex I Deficiencies. *Hum. Mol. Genet.* 13, 2461–2472. doi:10.1093/hmg/ddh262

van den Bosch, B. J. C., Gerards, M., Sluiter, W., Stegmann, A. P. A., Jongen, E. L. C., Hellebrekers, D. M. E. I., et al. (2012). Defective NDUFA9 as a Novel Cause of Neonatally Fatal Complex I Disease. *J. Med. Genet.* 49, 10–15. doi:10.1136/jmedgenet-2011-100466

van Rahden, V. A., Fernandez-Vizarra, E., Alawi, M., Brand, K., Fellmann, F., Horn, D., et al. (2015). Mutations in NDUFB11, Encoding a Complex I Component of the Mitochondrial Respiratory Chain, Cause Microphthalmia with Linear Skin Defects Syndrome. *Am. J. Hum. Genet.* 96, 640–650. doi:10.1016/j.ajhg.2015.02.002

Vogel, R. O., van den Brand, M. A. M., Rodenburg, R. J., van den Heuvel, L. P. W. J., Tsuneoka, M., Smeitink, J. A. M., et al. (2007). Investigation of the Complex I Assembly Chaperones B17.2L and NDUFAF1 in a Cohort of CI Deficient Patients. *Mol. Genet. Metab.* 91, 176–182. doi:10.1016/j.ymgme.2007.02.007

Vonrhein, C., Schlauderer, G. J., and Schulz, G. E. (1995). Movie of the Structural Changes during a Catalytic Cycle of Nucleoside Monophosphate Kinases. *Structure* 3, 483–490. doi:10.1016/S0969-2126(01)00181-2

Welin, M., Wang, L., Eriksson, S., and Eklund, H. (2007). Structure-function Analysis of a Bacterial Deoxyadenosine Kinase Reveals the Basis for Substrate Specificity. *J. Mol. Biol.* 366, 1615–1623. doi:10.1016/j.jmb.2006.12.010

Whittingham, J. L., Carrero-Lerida, J., Brannigan, J. A., Ruiz-Perez, L. M., Silva, A. P. G., Fogg, M. J., et al. (2010). Structural Basis for the Efficient Phosphorylation of AZT-MP (3′-Azido-3′-Deoxythymidine Monophosphate) and dGMP by Plasmodium Falciparum Type I Thymidylate Kinase. *Biochem. J.* 428, 499–509. doi:10.1042/BJ20091880

Wirth, C., Brandt, U., Hunte, C., and Zickermann, V. (2016). Structure and Function of Mitochondrial Complex I. *Biochim. Biophys. Acta (Bba) - Bioenerg.* 1857, 902–914. doi:10.1016/j.bbabio.2016.02.013

Wu, M., Gu, J., Guo, R., Huang, Y., and Yang, M. (2016). Structure of Mammalian Respiratory Supercomplex I 1 III 2 IV 1. *Cell* 167, 1598–1609. e10. doi:10.1016/j.cell.2016.11.012

Yadava, N., Potluri, P., Smith, E. N., Bisevac, A., and Scheffler, I. E. (2002). Species-specific and Mutant MWFE Proteins. *J. Biol. Chem.* 277, 21221–21230. doi:10.1074/jbc.M202016200

Yin, Z., Burger, N., Kula-Alwar, D., Aksentijević, D., Bridges, H. R., Prag, H. A., et al. (2021). Structural Basis for a Complex I Mutation that Blocks Pathological ROS Production. *Nat. Commun.* 12, 1–12. doi:10.1038/s41467-021-20942-w

Yip, C.-y., Harbour, M. E., Jayawardena, K., Fearnley, I. M., and Sazanov, L. A. (2011). Evolution of Respiratory Complex I. *J. Biol. Chem.* 286, 5023–5033. doi:10.1074/jbc.M110.194993

Zhu, J., Vinothkumar, K. R., and Hirst, J. (2016). Structure of Mammalian Respiratory Complex I. *Nature* 536, 354–358. doi:10.1038/nature19095

Zuris, J. A., Harir, Y., Conlan, A. R., Shvartsman, M., Michaeli, D., Tamir, S., et al. (2011). Facile Transfer of [2Fe-2S] Clusters from the Diabetes Drug Target mitoNEET to an Apo-Acceptor Protein. *Proc. Natl. Acad. Sci. USA* 108, 13047–13052. doi:10.1073/pnas.1109986108

Author Disclaimer: The content is solely the responsibility of the authors and does not necessarily represent the official views of the National Institutes of Health.

Conflict of Interest: The authors declare that the research was conducted in the absence of any commercial or financial relationships that could be construed as a potential conflict of interest.

Publisher's Note: All claims expressed in this article are solely those of the authors and do not necessarily represent those of their affiliated organizations, or those of the publisher, the editors and the reviewers. Any product that may be evaluated in this article, or claim that may be made by its manufacturer, is not guaranteed or endorsed by the publisher.

frontiers in Cell and Developmental Biology

REVIEW
published: 10 January 2022
doi: 10.3389/fcell.2021.800529

Recent Advances in Modeling Mitochondrial Cardiomyopathy Using Human Induced Pluripotent Stem Cells

Mario G. Pavez-Giani[1,2] *and Lukas Cyganek*[1,2,3]*

[1]Stem Cell Unit, Clinic for Cardiology and Pneumology, University Medical Center Göttingen, Göttingen, Germany, [2]German Center for Cardiovascular Research (DZHK), Partner Site Göttingen, Göttingen, Germany, [3]Cluster of Excellence "Multiscale Bioimaging: From Molecular Machines to Networks of Excitable Cells", University of Göttingen, Göttingen, Germany

OPEN ACCESS

Edited by:
Sylvie Callegari,
Walter and Eliza Hall Institute of Medical Research, Australia

Reviewed by:
Ann Frazier,
Royal Children's Hospital, Australia
Iain P. Hargreaves,
Liverpool John Moores University, United Kingdom

***Correspondence:**
Lukas Cyganek
lukas.cyganek@gwdg.de

Specialty section:
This article was submitted to Cellular Biochemistry, a section of the journal Frontiers in Cell and Developmental Biology

Received: *23 October 2021*
Accepted: *20 December 2021*
Published: *10 January 2022*

Citation:
Pavez-Giani MG and Cyganek L (2022) Recent Advances in Modeling Mitochondrial Cardiomyopathy Using Human Induced Pluripotent Stem Cells. Front. Cell Dev. Biol. 9:800529. doi: 10.3389/fcell.2021.800529

Around one third of patients with mitochondrial disorders develop a kind of cardiomyopathy. In these cases, severity is quite variable ranging from asymptomatic status to severe manifestations including heart failure, arrhythmias, and sudden cardiac death. ATP is primarily generated in the mitochondrial respiratory chain via oxidative phosphorylation by utilizing fatty acids and carbohydrates. Genes in both the nuclear and the mitochondrial DNA encode components of this metabolic route and, although mutations in these genes are extremely rare, the risk to develop cardiac symptoms is significantly higher in this patient cohort. Additionally, infants with cardiovascular compromise in mitochondrial deficiency display a worse late survival compared to patients without cardiac symptoms. At this point, the mechanisms behind cardiac disease progression related to mitochondrial gene mutations are poorly understood and current therapies are unable to substantially restore the cardiac performance and to reduce the disease burden. Therefore, new strategies are needed to uncover the pathophysiological mechanisms and to identify new therapeutic options for mitochondrial cardiomyopathies. Here, human induced pluripotent stem cell (iPSC) technology has emerged to provide a suitable patient-specific model system by recapitulating major characteristics of the disease *in vitro*, as well as to offer a powerful platform for pre-clinical drug development and for the testing of novel therapeutic options. In the present review, we summarize recent advances in iPSC-based disease modeling of mitochondrial cardiomyopathies and explore the patho-mechanistic insights as well as new therapeutic approaches that were uncovered with this experimental platform. Further, we discuss the challenges and limitations of this technology and provide an overview of the latest techniques to promote metabolic and functional maturation of iPSC-derived cardiomyocytes that might be necessary for modeling of mitochondrial disorders.

Keywords: mitochondrial cardiomyopathy, mitochondrial disease, mtDNA, heteroplasmy, induced pluripotent stem cells (hiPSCs), iPSC-derived cardiomyocytes

INTRODUCTION

Mitochondrial diseases comprise a multisystemic group of metabolic disorders characterized by early- or late-onset progressive neurodegenerative and cardiac symptoms, likely associated with a psychomotor regression, encephalopathy, myopathy and cardiomyopathy (DiMauro and Schon, 2013). Around 20–40% of children with a mitochondrial disease develop a kind of cardiac symptoms (Brambilla et al., 2020; Mazzaccara et al., 2021). In such cases, severity is quite variable ranging from asymptomatic status to severe manifestations including heart failure, arrhythmias, and sudden cardiac death. The highest prevalence in these patients is to develop a hypertrophic cardiomyopathy (HCM), nonetheless, there are also reports about cases with mitochondrial-caused restrictive, dilated and left ventricular non-compaction cardiomyopathies (Finsterer and Kothari, 2014). As a result of its continuous contractile work, the heart is an extremely oxidative organ which demands a high amount of energy. To sustain this task, the adult human heart consumes 6 kg of adenosine triphosphate (ATP) each day (Taegtmeyer, 1994; Bottomley et al., 1996). ATP is primarily generated in the mitochondrial respiratory chain (MRC) by the oxidative phosphorylation system (OXPHOS) by utilizing fatty acids and carbohydrates (Kolwicz et al., 2013). If the energy production in the heart is inhibited, the cardiac capacity to store ATP is only sufficient to sustain three heart beats, making the heart extremely vulnerable to mitochondrial insufficiency (Ingwall, 2009). Indeed, a deleterious mitochondrial function can detrimentally impact the contraction or relaxation capacity of the heart (Brown et al., 2017).

Mitochondria is a ubiquitous double membrane organelle that contains its own genome, which is maternally inherit and presents in multiple copies in every eukaryotic cell. Around 95% of the ATP production in cardiomyocytes is produced by substrate oxidation in the mitochondria (Doenst et al. 2013; Rosca and Hoppel, 2010). The OXPHOS is localized in the inner mitochondrial membrane where several metabolic pathways converge, with β-oxidation and Krebs cycle (citric acid cycle) being the most relevant in cardiomyocytes (Lai et al., 2014). Subsequently, both routes deliver nucleotides to Complex I (NADH-ubiquinone oxidoreductase) and Complex II (succinate dehydrogenase) in the MRC; nicotinamide-adenine-dinucleotide (NADH) delivered by Krebs cycle, and flavin-adenin-dinucleotide ($FADH_2$) from β-oxidation, respectively (Brandt, 2006; Cecchini, 2003; Gu et al., 2016). Complex III (ubiquinol-cytochrome c oxidoreductase) represents the central core for the MRC, reducing cytochrome c from coenzyme Q oxidation. Here, the so-called Q-cycle mechanism takes place, which ensures a continuing proton pumping from the matrix to the intermembrane space (Slater, 1983). Finally, each cytochrome c molecule delivers one electron into the Complex IV (cytochrome c oxidase), which transfers them to one dioxygen molecule, converting the molecular oxygen into two molecules of water (Turrens, 2003). Consequently, three proton translocating complexes (Complex I, Complex III and Complex IV), connected by the mobile electron carrier ubiquinone and cytochrome c, catalyze the electron transfer from NADH to O_2, thereby promoting an electrochemical gradient among the inner space membrane and the mitochondrial matrix. This gradient is used by Complex V (or adenosine triphosphate synthase; ATP synthase), to generate ATP from ADP conversion (Neupane et al., 2019). Notably, the MRC can exist as distinct enzymes or associate in supercomplexes that may facilitate its stabilization as well as the provision of greater spatiotemporal control of respiration (Vercellino and Sazanov, 2021).

OXPHOS is encoded by genes in both the mitochondrial (mtDNA) and the nuclear genome, and in fact, genes on both genomes are critical in controlling the bioenergetic mitochondrial function (Smeitink et al., 2001). Maternally inherited mtDNA is circular and relatively small (over 16,000 base pairs) and encodes 37 genes: 13 proteins, 22 transfer-RNAs and two ribosomal RNAs (**Figure 1**). Although this group of genes represents only 1% of mitochondrial proteins, it is critical for a proper OXPHOS function (Anderson et al., 1981; Schon et al., 2012). mtDNA is localized in the mitochondrial matrix, closely to the MRC, one of the major sources for reactive oxygen species (ROS) (Bogenhagen, 2012). Hence, the mitochondrial genome is highly susceptible for spontaneous mutations. In fact, epidemiological studies demonstrated that mutations in mitochondria-related genes including single-nucleotide variants to large-scale deletions, affect 1 in 4,500 individuals (Chinnery et al., 2000), and the risk to develop cardiac symptoms is significantly higher in this patient cohort. Furthermore, a clinical study showed that 36% of patients with mitochondrial disorders harboring mutations in nuclear DNA- or mtDNA-encoded genes developed a kind of cardiomyopathy (Brambilla et al., 2020), probably due to the high bioenergetic demand required by the heart. At the same time, infants with cardiovascular compromise in mitochondrial deficiency display a worse late survival compared to patients without cardiac compromise and current therapies are unable to substantially mitigate the disease burden (Wahbi et al., 2015; Brambilla et al., 2020). The genotype-phenotype correlation in patients with mitochondrial cardiomyopathies as well as the underlying pathophysiological mechanisms associated to mitochondrial gene mutations are still poorly understood. This is particularly true when it comes to understanding the impact of mtDNA gene mutations, mainly because the variable amount of pathogenic mtDNA variant load (heteroplasmy) represents an additional level of complexity in the interpretation of clinical and genetic findings.

In the present review, we will explore the advantages and challenges of human induced pluripotent stem cell (iPSC) technology applied for mitochondrial cardiomyopathies, describing novel findings in modeling mtDNA and nuclear DNA mitochondrial gene mutations, as well as its potential scopes for biomedical research and therapeutic approaches.

HUMAN INDUCED PLURIPOTENT STEM CELLS AS CARDIOMYOPATHY MODEL

Cardiomyopathy is a clinically heterogeneous group of cardiac disorders that can be classified in congenital (or inherited),

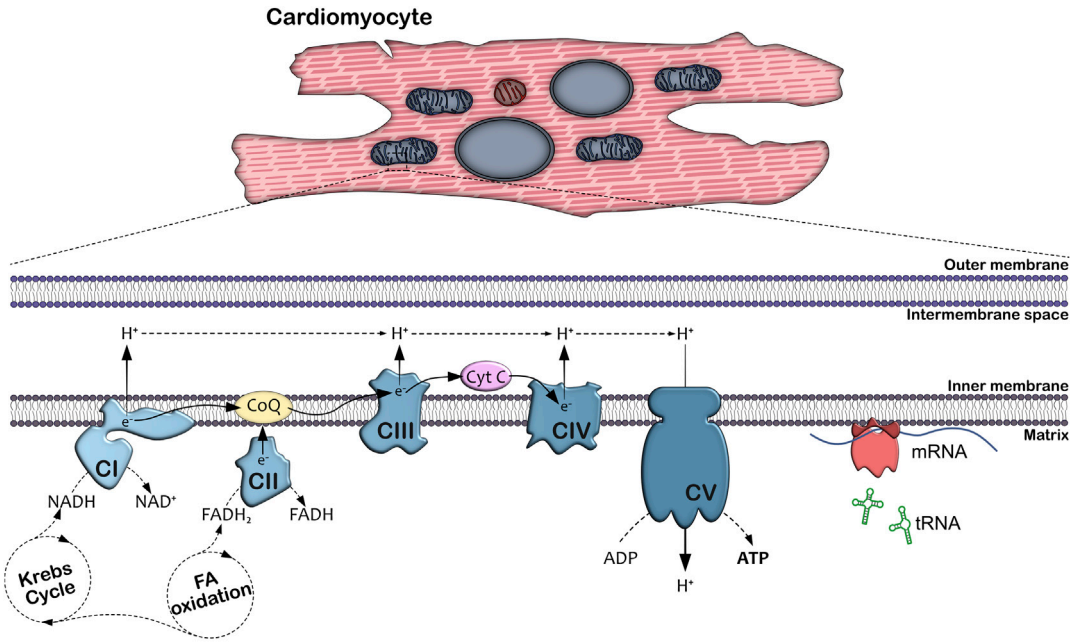

	OXPHOS proteins					rRNA	tRNA
	Complex I	Complex II	Complex III	Complex IV	Complex V		
mtDNA	MT-ND1 MT-ND2 MT-ND3 MT-ND4 MT-ND4L MT-ND5 MT-ND6		MT-CYB	MT-CO1 MT-CO2 MT-CO3	MT-ATP6 MT-ATP8	MT-RNR1 MT-RNR2	MT-TA MT-TI MT-TR MT-TL1 MT-TN MT-TL2 MT-TD MT-TK MT-TC MT-TM MT-TE MT-TF MT-TQ MT-TP MT-TG MT-TS1 MT-TH MT-TS2 MT-TT MT-TY MT-TW MT-TV
nuclear DNA	NDUFA1 NDUFA2 NDUFA3 NDUFA5 NDUFA6 NDUFA7 NDUFA8 NDUFA9 NDUFA10 NDUFA11 NDUFA12 NDUFA13 NDUFAB1 NDUFB1 NDUFB2 NDUFB3 NDUFB4 NDUFB5 NDUFB6 NDUFB7 NDUFB8 NDUFB9 NDUFB10 NDUFB11 NDUFC1 NDUFC2 NDUFS1 NDUFS2 NDUFS3 NDUFS4 NDUFS5 NDUFS6 NDUFS7 NDUFS8 NDUFV1 NDUFV2 NDUFV3	SDHA SDHB SDHC SDHD	CYC1 CYCS UQCRB UQCRC1 UQCRC2 UQCRFS1 UQCRH UQCRQ UQCR10 UQCR11	COX4I1 COX4I2 COX5A COX5B COX6A1 COX6A2 COX6B1 COX6B2 COX6C COX7A1 COX7A2 COX7B COX7C COX8A COX8BP NDUFA4	ATP5F1A ATP5F1B ATP5F1C ATP5F1D ATP5F1E ATP5PB ATP5MC1 ATP5PD ATP5ME ATP5MF ATP5MG ATP5MJ ATP5MK ATP5PO OSCP1	Associated proteins **Transcriptional machinery** POLG TFAM PPARGC1A **Mitochondrial dynamics** DNM1L MFF MFN2 OPA1 **Mitophagy** PINK1 PRKN **Others** TAZ FXN ...	
	OXPHOS assembly proteins						
	ACAD9 COA1 DMAC1 DMAC2 ECSIT FOXRED1 NDUFAF1 NDUFAF2 NDUFAF3 NDUFAF4 NDUFAF5 NDUFAF6 NDUFAF7 NUBPL TIMMDC1 TMEM70 TMEM126A TMEM126B TMEM186	SDHAF1 SDHAF2 SDHAF3 SDHAF4	BCS1L UQCC1 UQCC2 UQCC3 HIGD1A LYRM7 TTC19 BRAWNIN	CEP89 COA1 OMA1 CMC1 COA3 OXA1L CMC2 COA5 PET100 COX10 COA6 PET117 COX11 COA7 PNKD COX14 COA8 SCO1 COX15 FASTKD2 SCO2 COX16 HIGD1A SMIM20 COX17 HIGD2A SURF1 COX18 IMMP1L TACO1 COX19 IMMP2L TMEM177 COX20 LRPPRC ...	ATPAF1 ATPAF2 FMC1 TMEM70 TMEM242		

FIGURE 1 | Schematic representation of mitochondria-associated genes involved in protein synthesis and complex formation of the oxidative phosphorylation and ATP synthesis. The table summarizes the most important OXPHOS subunit and assembly proteins in human cells. mtDNA indicates mitochondrial DNA; nDNA, nuclear DNA; rRNA, ribosomal RNA; tRNA, transfer RNA; FA, fatty acids; CI, Complex I or NADH ubiquinone oxidoreductase; CII, Complex II or succinate dehydrogenase; CIII, Complex III or ubiquinol-cytochrome c oxidoreductase; CIV, Complex IV or cytochrome c oxidase; CV, Complex V or ATP synthase; CoQ, coenzyme Q10 and Cyt C, cytochrome c.

acquired or mixed subtypes, with the latter one accounting for individuals that carry distinct genetic risk factors that might provoke cardiac symptoms under certain environmental circumstances (Elliott et al., 2014). Historically, cardiomyopathies have been classified in hypertrophic cardiomyopathy (HCM), dilated cardiomyopathy (DCM), and arrhythmogenic right ventricular cardiomyopathy (ARVC), nonetheless, due the upgrade of genetic and molecular assays, a better understanding has been gained in terms of etiology and phenotypic expression (Brieler et al., 2017). Congenital cardiomyopathy is caused by genetic mutations that affect the heart and/or the cardiovascular system. Whereas a certain correlation exists between the clinical features of cardiomyopathies and an autosomal dominant inheritance of gene mutations—as it is for instance known for MYH7 gene mutations causing HCM or titin truncating variants leading to DCM (Herman et al., 2012; Marian and Braunwald, 2017)—the etiology of around 40% of the cases with cardiac symptoms remains unknown (Campuzano et al., 2014).

Over the last years, the vast development of iPSC technology allows to study human diseases by using patient-specific cells *in vitro*. By activation of four essential transcriptional factors (such as OCT4, SOX2, C-MYC, and KLF4), isolated somatic cells from skin biopsies or blood samples from donors can be reprogrammed into iPSCs that harbor the identical genome of the donor including genetic variants/defects (Robinton and Daley, 2012). Significant progress has been made in developing efficient protocols for the directed differentiation of iPSCs into functional cardiomyocytes (iPSC-CMs), thus we are now able to generate defined cardiac subtypes in high quantity and purity. Substantial evidence shows that iPSC-CMs derived from patients with congenital cardiomyopathies represent the phenotype of the disease, thereby providing a unique and powerful platform for modeling genetic diseases as well as investigating the underlying pathological mechanisms.

Nowadays, iPSC-derived cardiomyocytes have been applied to gain insights into channelopathies (such as Long-QT and Brugada syndrome) (Garg et al., 2018), sarcomeric cardiomyopathies (such as HCM and DCM) (Eschenhagen et al., 2015), syndromic cardiomyopathies (such as Noonan syndrome or Duchenne muscular dystrophy) (Long et al., 2018; Hanses et al., 2020), or polygenetic cardiac diseases (Borchert et al., 2017). However, although many phenotypic properties can be recapitulated in patients' iPSC-CMs, a higher 'adult-like' maturation state and appropriate physiological conditions might to be required to comprehensively mimic all aspects of the disease in the dish. Therefore, pursuing efforts are being made to accomplish suitable mature conditions, which involve, among others, energetic substrates delivered in culture medium (Yang et al., 2019), growth factors (Yang et al., 2014), metabolic pathway modulators (Gentillon et al., 2019; Sarikhani et al., 2020) and engineered 3D cardiac tissue (Tiburcy et al., 2017). Further, this technology is now gradually entering into preclinical and clinical phase by testing of novel therapeutic options, such as screening of chemical compounds or evaluating gene therapy approaches (Musunuru et al., 2018).

In the following sections, we summarized the promises and challenges of iPSC-based modeling of mitochondrial cardiomyopathies, involving both nuclear and mitochondrial genome mutations, as well as the analysis of bioenergetic disturbances as a consequence of heart failure via iPSC-CMs.

MODELING MITOCHONDRIAL CARDIOMYOPATHIES USING IPSC-DERIVED CARDIOMYOCYTES

Mitochondrial disorders triggered by both nuclear DNA- and mtDNA-encoded mutated genes might cause a kind of cardiomyopathy. For a long time, the absence of robust and reliable mitochondrial disease models hindered to explore the underlying pathomechanisms and to find new treatment options for this rare condition, principally due to the genetic heterogeneity of patients and challenges to recapitulate the disease phenotypes in animal models due to the interspecies discrepancy in cardiac physiology (Chanana et al., 2016; Ulmer and Eschenhagen, 2020). Here, modeling of mitochondrial DNA-encoded gene mutations represents a particular difficulty, as it is virtually impossible to introduce a desired gene variant in a multitude of copies of the mitochondrial genome. Most of the strategies to generate a disease models with mtDNA variants involved transgenic animals in combination with cytoplasmic transplantation (so-called cybrids) (Wilkins et al., 2014). Although these models might display some of the metabolic features, they are not able to fully recapitulate the patients' genetic context and therefore cannot represent the entire picture of the disease.

Recent reports exploited iPSC-CMs as platform to overcome this challenge by reprogramming patients' somatic cells. Throughout this approach, novel investigations were made possible in analyzing the key molecular and functional features of patients' cardiomyocytes and revealing novel insights in cardiac disease progression of mitochondrial disorders. Herein, we will highlight some of the major findings obtained using iPSC-CMs and we will explore the pathophysiological causality of both mtDNA and nuclear DNA gene mutations in causing mitochondrial cardiomyopathy.

mtDNA Disorders

The involvement of mitochondrial dysfunction as a result of mutations in mtDNA-encoded genes was first observed more than 3 decades ago. Wallace et al. (1988) provided the first approximation through identifying a point mutation in the mtDNA gene for subunit 4 of the NADH dehydrogenase complex (MT-ND4) to be associated with maternally inherited Leber's hereditary optic neuropathy. Since then, a completely new genomic mitochondrial era was pioneered, describing many other syndromes related to this gene. In eukaryotic cells, nuclear DNA and mtDNA co-exist, based on the cell type, in a ratio of 1:10 in sperm, over 1:100–300 in stem cells/iPSCs up to 1:1,000–10,000 in terminally differentiated cells such as cardiomyocytes, in line with an increased organelle biogenesis upon differentiation (Kelly et al., 2012; Kelly et al., 2013) Due to spontaneous variations in

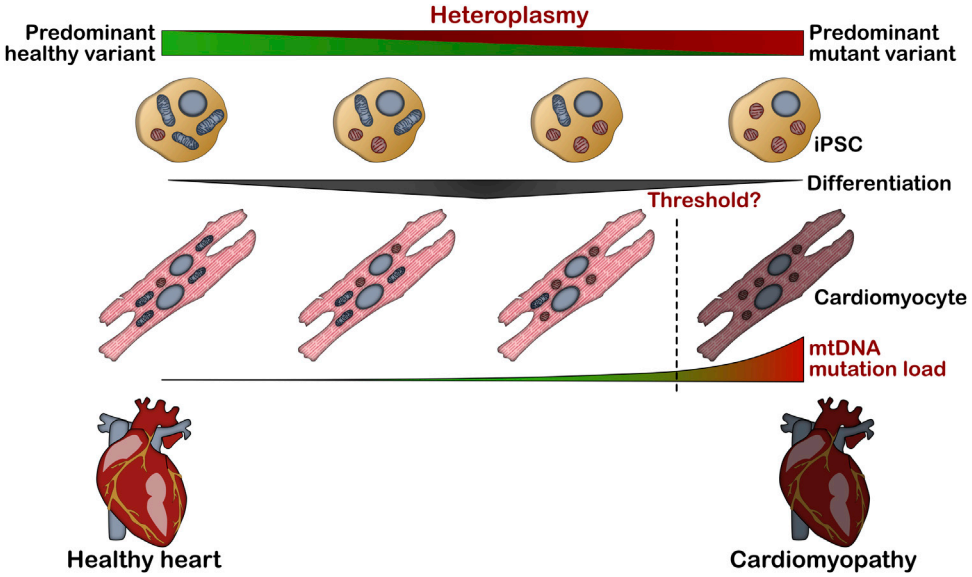

FIGURE 2 | Impact of mtDNA heteroplasmy levels on cardiomyocyte pathology. mtDNA heteroplasmy associated to pathogenic variant load in iPSCs is typically preserved during cardiomyocyte differentiation, promoting poor mitochondrial performance and cardiac remodeling when mtDNA variant load exceeds a certain.

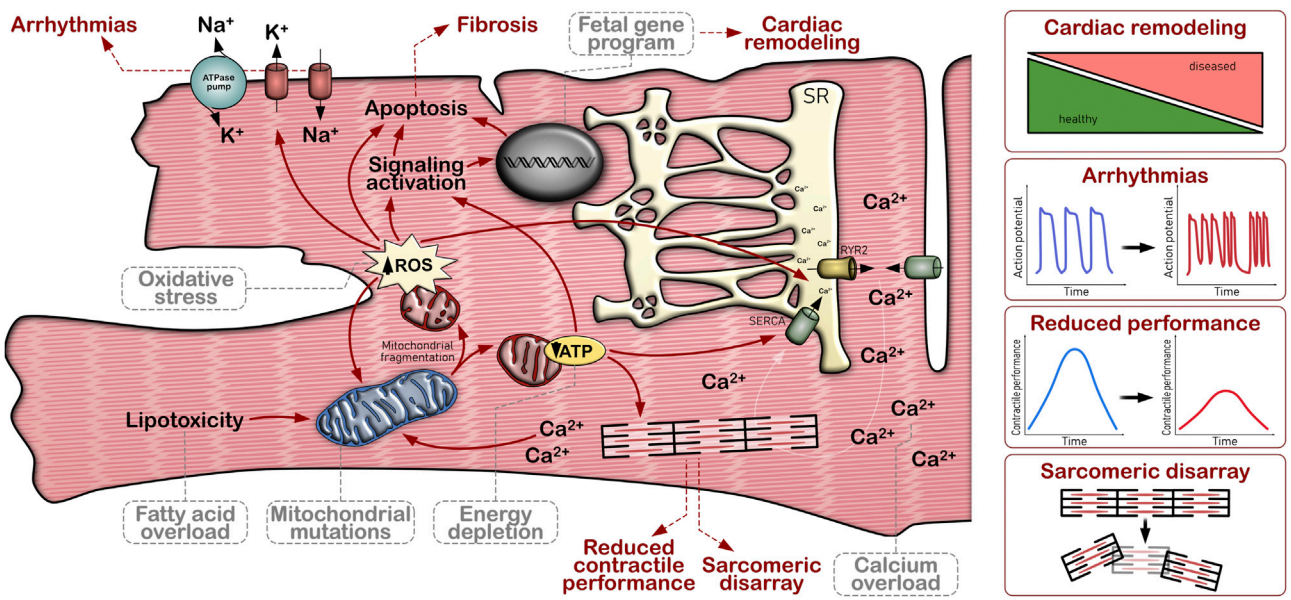

FIGURE 3 | Impact of mitochondrial dysfunction on cardiomyocyte pathology. Mitochondrial dysfunction, either caused by gene mutations in mitochondrial genes (primary mitochondrial cardiomyopathy) or as a consequence of other cellular disturbances (such as calcium overload or lipotoxicity), promotes an energy depletion as well as increased ROS production. Poor bioenergetic capacity and oxidative stress provoke, among others, changes in cytosolic calcium handling, electrophysiological defects, reduced contractile performance, sarcomeric re-arrangements, re-expression of fetal genes, cardiac remodeling and apoptosis.

the mitochondrial genome, mtDNA within one cell might be mixture of different mtDNA genomes, and this event is called heteroplasmy (Stewart and Chinnery, 2015). When a mixture of normal and mutated mtDNA is present, the cell may randomly deliver these variations to daughter cells (Stewart and Chinnery, 2021). As a consequence of this event, daughter cells can receive a

different load of mutant mtDNA, generating diverse levels of heteroplasmic mutations (Durham et al., 2007). Considering that 1) this event occurs during every cell division, and 2) mtDNA copy number from less than 300 copies in undifferentiated cells significantly increases as cells differentiate into mature functional cells the percentage of mutant mtDNA load might highly differ between tissues and organs (**Figure 2**). However, when mtDNA variant load exceeds a certain threshold (which might highly differ between individual gene mutations), some clinical manifestations in certain tissues may occur (Yu-Wai-Man et al., 2010). This phenomenon, in addition to the unique patient's genetic background, explains the high range of signs and symptoms that are depicted in mtDNA disorder patients.

An additional challenge represents the variable heteroplasmy levels in biopsy material used for iPSC generation (Perales-Clemente et al., 2016). However, the variable amount of mutant mtDNA load in somatic cells (such as dermal fibroblasts) allows to generate patient-specific iPSC lines with high and low heteroplasmic levels in parallel during one reprogramming procedure (Kodaira et al., 2015; Ma et al., 2015). Further, once a iPSC line is established, mtDNA heteroplasmy levels are not significantly altered during *in vitro* differentiation, so that higher and lower percentage of heteroplasmy is preserved in fully differentiated cells (Folmes et al., 2013; Klein Gunnewiek et al., 2020). In-depth genetic screening methods nowadays allow a detailed estimation of the heteroplasmy levels in patients, further enhancing our knowledge of the impact of mtDNA variants in mitochondrial disorders. However, there is still little knowledge about the consequences of mtDNA mutations in the manifestation of disease symptoms and, so far, only few studies investigated the cardiac phenotype of mtDNA mutations via patient-specific iPSC-CMs.

For instance, Leigh syndrome is a multi-systemic disease characterized by a progressive neurodegenerative disorder, as a result of OXPHOS gene mutations encoded either by the mitochondrial or nuclear genome (Sofou et al., 2018). The mitochondrial gene mutation m.13513G>A within the MT-ND5 gene, encoding the core subunit of Complex I, has been reported as a frequent cause of Leigh syndrome and is commonly associated with cardiac defects (Ruiter et al., 2007). Galera-Monge et al. (2019) generated iPSCs from patients' fibroblasts with high (>40%) and low (<20%) mutation load of the respective m.13513G>A variant. Surprisingly, high mutation load iPSCs displayed a highly impaired cardiac differentiation, probably due to an ineffective epithelial-mesenchymal transition at the first days of differentiation. Nevertheless, when using iPSCs with a mtDNA mutation load below the threshold of 30%, dysfunctional iPSC-CMs could be obtained which presented aberrant pattern of beating strength and rate and higher apoptosis levels compared to the control group in a mutant-load dependent way (Galera-Monge et al., 2019).

A similar outcome was obtained from in an iPSC model from a patient with mitochondrial encephalomyopathy and stroke-like episodes (MELAS) (Yokota et al., 2017). Patient-specific iPSCs with high (>90%), intermediate (80–90%) and low (40–50%) mutation load were employed to explore the cardiac and neurological consequences caused by the heteroplasmic mitochondrial gene mutation m.3243A>G within MT-TL1 (encoding a mitochondrial transfer RNA). By analyzing skin fibroblasts collected from MELAS patients, the molecular pathogenic threshold for this particular mutation with regard to mitochondrial respiratory function was expected to be around 90% (Yokota et al., 2015). In contrast to intermediate and low mutation load, and in line with the neuronal differentiation of these lines, the mitochondrial dysfunction promoted by high-load m.3243A>G disturbed cardiac lineage commitment during iPSC differentiation, suggesting that the mitochondrial protein synthesis machinery is central for triggering cardiomyocyte differentiation (Yokota et al., 2017). In line, iPSC-CMs from two patients with myoclonic epilepsy with ragged red fiber (MERRF) syndrome harboring a mutation in a different mitochondrial transfer RNA, namely the mitochondrial gene mutation m.8344A>G in MT-TK, and here with a mutation load around 50%, revealed an impaired mitochondrial respiration, an abnormal ultrastructure of mitochondria, elevated levels of ROS, as well as upregulation of antioxidant genes (Chou et al., 2016).

A different study demonstrated that iPSC-CMs derived from patients with a family history of maternally inherited HCM, who harbor the homoplasmic mitochondrial gene mutation m.2336T>C in MT-RNR2 (100% mutated mtDNA load), encoding the large subunit of the mitochondrial ribosomal RNA, resulted in mitochondrial dysfunction and ultrastructural defects by decreasing the stability of the 16S ribosomal RNA, which consequently led to reduced levels of mitochondrial proteins. Furthermore, mtDNA variants can lead to energetic depletion through impaired OXPHOS and mitochondrial Ca^{2+} regulation, which are central for excitation–contraction coupling in cardiac cells (Sommakia et al., 2017). Indeed, iPSC-CMs that harbor the m.2336T>C variant also presented disturbances in cytosolic Ca^{2+} handling and a deleterious electrophysiological pattern, thereby possibly triggering the manifestation of HCM in these patients (Li et al., 2018). Interestingly, by combining mtDNA sequencing data from a cellular iPSC-CM model of HCM with genetic screens from multiple unrelated HCM patients, novel potentially HCM-protective and HCM-deteriorating mtDNA variants were identified, mostly not overlapping with common ones in mitochondrial diseases (Kargaran et al., 2020).

The number of iPSC-based reports within the last decade underlines the challenges that are associated with the modeling of mtDNA gene mutations and the impact of heteroplasmy. Given the advantage of iPSC-CMs over other model systems, e.g. by allowing to precisely investigate the genotype-phenotype correlation in cardiac cells with different heteroplasmic load, iPSC-CM disease modeling might be considered a highly suitable model to uncover novel insights in the underlying pathomechanisms related to mtDNA gene variants.

Nuclear DNA Disorders

Nuclear DNA-encoded proteins represent around 99% of the total mitochondrial proteome and due the diversity of function that mitochondria exhibit, variations in this gene group extend beyond bioenergetic perturbations. Proteomic studies have

revealed that mitochondria harbor almost 1,500 different proteins (Prokisch et al., 2004; Morgenstern et al., 2017; Pfanner et al., 2019), that are related, among others, to biosynthesis of amino acids, lipids, heme and Fe–S clusters, cellular signaling pathways, regulation of Ca^{2+} levels, quality control and programmed cell death.

The generation of iPSC-based models for mitochondrial disorders such as Leigh syndrome is not dissimilar to any other iPSC model when it comes to nuclear DNA mutations. However, the majority of studies have focused on the neurological phenotyping of these patient lines, probably since neuro-related symptoms are a major hallmark of mitochondrial disorders (Zhao et al., 2018; Liang et al., 2020; Inak et al., 2021). Most of the iPSC-CM studies related to nuclear-encoded gene mutations in OXPHOS have been focused in Complex IV deficiency, which has been involved in certain forms of inherited cardiomyopathies (Jaksch et al., 2000). Briefly, the main function of Complex IV is to oxidize cytochrome c and to transfer electrons to molecular oxygen. Here, the mitochondria-encoded COX1 and COX2 provide the essential sites for oxygen reduction, by housing the redox-active heme and copper centers (Capaldi, 1990; Khalimonchuk et al., 2010). Further, nuclear-encoded SCO1, SCO2, and COA6 are required for copper center formation (Leary et al., 2014; Soma et al., 2019). A loss of function of these chaperones and the concomitant cytochrome c oxidase deficiency causes severe human disorders (Brischigliaro and Zeviani, 2021). SCO2 encodes a 266 amino acid metallochaperone that participate in copper delivery to COX, and its mutations represent the most common cause of COX or Complex IV deficiency, often leading to cardiomyopathies (Jaksch et al., 2000). The first study using iPSC-CMs to model COX deficiency was conducted by Hallas et al. (2018) by generating iPSCs from two Leigh syndrome patients with HCM harboring the homozygous variant $SCO2^{G193S}$ (c.577G>A) and the compound-heterozygous variant $SCO2^{E140K}$ (c.418G>A) in combination with an early truncating variant (c.17ins19), respectively. In the study, the SCO2-associated COX deficiency resulted in ultrastructural abnormalities of the mitochondria, a reduced mitochondrial oxidative ATP production capacity, as well as aberrant Ca^{2+} handling and an arrhythmic contractility pattern in the patients' iPSC-CMs.

Meanwhile, new reports have proven evidence of mitochondrial disease models harboring gene mutations in accessorial components of OXPHOS. Friedreich's ataxia is autosomal recessive genetic condition that causes a neuro-degenerative movement disorder, with a typical age of onset between 10 and 15 years (Koeppen, 2011), and HCM is quite prevalent in this patient cohort (Weidemann et al., 2013). The condition is caused by expanded GAA repeats within the first intron of the nuclear-allocated gene frataxin, a protein that is involved in the biosynthesis of iron-sulfur co-factors required by multiple mitochondrial and extra-mitochondrial proteins (Castro et al., 2019). One of the first publications investigating the cardiac consequences of the Friedreich's ataxia syndrome via patients' iPSCs was described in 2013 (Hick et al., 2013). In the aforementioned work, the group applied iPSCs from two patients and registered partially degenerated mitochondria with abnormal structures—in line with mitochondrial damages observed in cardiac tissues from Friedreich's ataxia patients—suggesting a functional defect in cellular respiration in these cells. Lee et al. (2016) revealed increased ROS levels, intracellular iron accumulation, as well as electrophysiological and Ca^{2+} handling abnormalities in patients' iPSC-CMs . Another report provided evidence for the presence of an HCM-dependent transcriptional profile in cells from Friedreich's ataxia patients (Li et al., 2019). Furthermore, a recent study proved that the contractile capacity from both patient-derived and frataxin-knockdown iPSC-CMs showed a poor performance using human engineered tissue modeling (Wong et al., 2019). In depth, frataxin-deficient cardiac tissues displayed attenuated force development compared to healthy controls with a correlation between frataxin gene expression and contractility. In addition, an aberrant electrophysiological pattern was detected (depicted as prolongation of the action potential duration and reduction of the maximum capture rate), thereby recapitulating some major clinical findings (Wong et al., 2019).

Similar efforts had been conducted in modeling Barth syndrome, a rare X-linked genetic disorder characterized by cardiomyopathy, skeletal myopathy, growth delay, neutropenia and increased urinary excretion of 3-methylglutaconic acid (Clarke et al., 2013). This disease has been mainly described by mutations in the nuclear-encoded tafazzin (Bione et al., 1996). Barth syndrome presents a unique pathophysiological mechanism: in detail, mutated tafazzin primary promotes an aberrant cardiolipin maturation process due its role in the transacylation process showing preference for the transfer of a linoleic acid group from phosphatidylcholine to monolysocardiolipin, resulting in depletion of mature cardiolipin and accumulation of an immature form and thereby in a deleterious mitochondrial metabolism (Garlid et al., 2020). Cardiolipin is an important component of the inner mitochondrial membrane, where it constitutes about 20% of the total lipid composition and affects many aspects of mitochondrial structure and function, including MRC complex formation/interaction, mitochondrial dynamics, and apoptosis (Dudek, 2017). In an extensive study, Wang et al. (2014) generated patient-specific iPSC lines with a tafazzin frameshift mutation (c.517delG) and a missense mutation TAZ^{S110P} (c.328T>C), respectively, as well as different CRISPR/Cas9-engineered tafazzin-deficient iPSC lines, in order to investigate the mitochondrial cardiomyopathy *in vitro*. Barth syndrome cells recapitulated the expected muscle-selective phenotype with an impaired cardiolipin biogenesis (by exceeding the monolysocardiolipin-to-cardiolipin ratio), smaller and fragmented mitochondria, deficits in the oxygen consumption rate, a decreased efficiency in ATP generation, as well as higher levels of ROS. Further, by analyzing iPSC-CM-based engineered cardiac tissues, tafazzin deficiency revealed impaired sarcomere assembly and defects in contractility that occurred independently of ATP depletion, thereby suggesting that both proper mitochondrial function and reduced ROS production is crucial for sarcomerogenesis and contractile performance (Wang et al.,

2014). In a subsequent study, the group identified aberrant Ca^{2+} handling as major cause for the contractile deficits in the patients' cells, most probably due to ROS-dependent activation of Ca^{2+}/calmodulin-dependent protein kinase II and subsequent phosphorylation of the ryanodine receptor 2 (Liu et al., 2021). The identical patient line with the frameshift mutation was further used to identify an accumulation of cellular long chain acylcarnitines, as well as alterations in metabolic pathways related to energy production in iPSC-CMs (Fatica et al., 2019). In agreement with the previous reports, Dudek et al. reported a significant downregulation in the mitochondrial bioenergetic capacity in iPSC-CMs from a patient harboring the missense mutation TAZ^{G197V} (c.590G>T) (Dudek et al., 2016). Interestingly, the detrimental mitochondrial respiration coincided with dramatic structural remodeling of MRC supercomplexes and a deficiency in succinate dehydrogenase. Further, cardiolipin remodeling impaired NF-κB signaling and affected the HIF-1α response to hypoxic conditions (Chowdhury et al., 2018).

Moreover, a homozygous intronic variant (IVS3-1G>C) in DNAJC19 (also called TIM14), affecting splicing and resulting in gene loss-of-function, has been described to cause dilated cardiomyopathy with ataxia syndrome (Davey et al., 2006). Due to its similarities in abnormal metabolism, it has been linked to Barth syndrome. TIM14 is predicted to function as a part of the mitochondrial import complex facilitating the import of nuclear-encoded proteins into the mitochondria (Mokranjac et al., 2006), but also to regulate cardiolipin remodeling by tafazzin (Davey et al., 2006). However, by investigating iPSC-CMs from two patients with the respective homozygous variant, no differences in the cardiolipin content were observed (Rohani et al., 2020). Instead, fragmented and abnormally shaped mitochondria were recorded together with an isoform imbalance of OPA1, an important regulator of mitochondrial fusion that has been linked to heart failure.

Lastly, patients with autosomal recessive gene mutations in ACADVL, an inner-mitochondrial membrane localized enzyme that catalyzes the first step of the mitochondrial long-chain fatty acid β-oxidation pathway, possess a very long-chain acyl-CoA dehydrogenase deficiency and possess a high risk for developing cardiac arrhythmias. Consequently, patient-derived iPSC-CMs with a homozygous frameshift variant $ACADVL^{P35Lfs*26}$ (c.104delC) or compound-heterozygous gene mutations $ACADVL^{V283A}$/$ACADVL^{E381del}$ (c.848T>C/c.1141_1143delGAG), respectively, revealed accumulation of potentially toxic intermediates of long-chain fatty acid oxidation (Knottnerus et al., 2020). Further, the cells displayed electrophysiological abnormalities (such as short action potentials), disturbances in Ca^{2+} handling) and presented delayed afterdepolarizations, thereby providing a mechanistic link for the cardiac arrhythmia risk in these patients (Knottnerus et al., 2020; Verkerk et al., 2020).

In summary, nuclear DNA-encoded mitochondrial genes represent 99% of the total mitochondrial proteome and functionality of many of these genes is still unknown. Patient-specific iPSCs could unmask the pathophysiologic mechanisms of several of them. Moreover, since mitochondrial function is involved in many different cellular processes, iPSC-based disease modeling has helped to explore the role of these proteins in other signaling hubs, beyond their importance in energetic homeostasis.

Mitochondrial Dysfunction as a Consequence of Cardiomyopathies

Metabolic imbalances and bioenergetic perturbations are not only observed in primary mitochondrial disorders but might also be a consequence in other cardiomyopathies related to specific genetic conditions. As an example, phospholamban is a sarco/endoplasmic reticulum Ca^{2+}-ATPase pump regulator and an active player in the cytosolic Ca^{2+} handling and contractility (Frank and Kranias, 2000). Carriers with the recurrent mutation PLN^{R14del} (c.40_42delAGA), which is commonly reported in cardiomyopathy patients from Europe and USA (Haghighi et al., 2006; Kayvanpour et al., 2017), present a significantly higher risk to suffer from DCM and arrhythmogenic episodes associated to aberrant Ca^{2+} handling and pathological cardiac remodeling (Posch et al., 2009). A recent study by Cuello and co-workers described a tight correlation between phospholamban gene mutations and mitochondrial dysfunction. Particularly, patients' iPSC-CMs harboring the PLN^{R14del} variant depicted a detrimental mitochondrial function by displaying a low oxygen consumption rate as well as elevated mitochondrial ROS production (Cuello et al., 2021). Notably, whereas sarcoplasmic reticulum function remained unaltered, impairments of the endoplasmic reticulum to mitochondria crosstalk were detected resulting in lipid accumulation, mitochondrial dysfunction and degeneration, suggesting a cause-consequence correlation provided by a deleterious cytoplasmic Ca^{2+} signaling (Cuello et al., 2021).

In a different study, by generating multiple CRISPR-engineered iPSC lines harboring the HCM-associated gene mutation $MYH7^{R453C}$ (c.9123C>T), Mosqueira et al. (2018) not only recapitulated the classical hallmarks of HCM (such as cellular hypertrophy, sarcomeric disarray or Ca^{2+} handling disturbances), but also identified increased oxygen consumption rates in affected iPSC-CMs. Hence, the authors could show that the mutation-induced sarcomeric disarray caused an inefficient sarcomeric ATP utilization and energy depletion by maintaining the mitochondrial contents unchanged, thereby improving our mechanistic understanding in HCM.

Duchenne muscular dystrophy (DMD) is another genetic condition that causes a severe cardiomyopathy, particularly DCM, due to a loss of dystrophin (Kamdar and Garry, 2016). Patient-derived iPSC-CMs from two patients with out-of-frame deletions in dystrophin exon 45–52 recapitulated the expected dystrophin deficiency (Lin et al., 2015). In addition, mitochondrial damage and increased levels of cell death were detected in the patients' cells. Strikingly, Lin et al. (2015) were able to underpin this findings by identifying a mitochondria-mediated signaling network that linked damaged mitochondria with caspase-3 mediated apoptosis, thereby uncovering a potential new disease mechanism in DMD.

The iPSC-CM model has been also applied to examine the cardio-metabolic remodeling in type 2 diabetes. Modulation of the insulin signaling involves the tyrosine kinase receptor which activates insulin receptor substrate family proteins (IRS-1/2), phosphoinositide 3-kinase (PI3K) and AKT. In the heart, AKT activation promotes intracellular glucose import through translocation of the glucose transporter type 4 to the plasma membrane, thereby stimulating glycolysis and mitochondrial substrate oxidation (Abel, 2021). As a hallmark of type 2 diabetes mellitus, PI3K/AKT signaling is disrupted as a result of the insulin resistance, promoting a fatty acid oversupply (Wende and Abel, 2010). However, elevated intracellular fatty acid levels increase ROS production, thereby inducing cellular and mitochondrial damage, decreasing energy production and promoting lipid accumulation in a positive feedback loop (van de Weijer et al., 2011; Westermeier et al., 2016). In consequence, triglycerides, sphingolipids and ceramides accumulate in peroxisomes and liposomes, resulting in cellular oxidative stress and poor cardiac performance; a process called lipotoxicity (D'Souza et al., 2016). In fact, a large community-based sample study demonstrated a potential association of elevated circulating ceramide with lower left ventricle function, suggesting a tight correlation between cardiac performance and lipotoxicity (Nwabuo et al., 2019). A recent report demonstrated the impact of ceramide overload on the cellular physiology using iPSC-CMs (Bekhite et al., 2021). Herein, both diabetic-like culture conditions as well as SPTLC1 overexpression, which promotes *de novo* synthesis of ceramides, resulted in increased intracellular ceramide levels and lipid accumulation (Bekhite et al., 2021). Interestingly, these changes were associated with impaired PI3K/AKT signaling, transcriptional changes in metabolic enzymes, abnormal bioenergetic capacity, as well as an increase in ROS production and apoptosis. Further, cardiac lipotoxicity and oxidative stress induced mitochondrial fission (indicated by increased levels of DRP1 and MFF) as well as mitophagy (indicated by upregulation of PINK1 and LC3B) in iPSC-CMs, thereby providing novel insights in the pathological mechanisms underlying lipotoxic cardiomyopathy. Aligned to this findings, Drawnel and co-workers recapitulated the type 2 diabetes associated cardiomyopathy using a selective medium composition (Drawnel et al., 2014). Briefly, the group incubated iPSC-CMs with two different culture conditions: one group was cultured in standard maintenance medium, whereas the other one was exposed to glucose-free medium with addition of insulin and fatty acids (maturation media). Thereby, iPSC-CM cultures were forced to exclusively utilize fatty acids through a persistent insulin signaling modulation. After administration of diabetic factors that are typically found in blood plasma of diabetic patients (endothelin-1 and cortisol), a clear DCM phenotype in the patients' iPSC-CMs was observed when incubated in a diabetogenic environment including sarcomeric disarrangements, lipid peroxidation, and decreased expression of Krebs cycle-associated enzymes (Drawnel et al., 2014).

Besides, primarily neurological diseases might have an impact on cardiac physiology, as it is the case in Huntington's disease (Critchley et al., 2018). In order to understand the role of neuronal function and mitochondrial metabolism, neuronal stem cells with increasing polyglutamine (polyQ) repeat length in the huntingtin gene were engineered (Ghosh et al., 2020). Here, the expression of huntingtin exon 1 fragments with polyQ-expansions inducing a deleterious mitochondrial function, such as a lower mitochondrial respiration promoted by decreased Complex I and III activity. Interestingly, similar effects were described by Joshi and co-workers in iPSC-CMs (Joshi et al., 2019). In their study, iPSC-CMs with polyQ-expansions showed an aberrant mitochondrial network due hyperactivation of the mitochondrial fission complex, uncovering a potential phenotype correlation in Huntington's disease.

Summarizing, these examples highlight that maladaptive metabolic remodeling is not an exclusive pattern in mitochondrial cardiomyopathies **Figure 3**. Considering the high impact of mitochondrial function in multiple cellular processes, the bioenergetic modifications as a consequence of other forms of inherited cardiomyopathies should be taken into account in cardiovascular disease modeling.

DRUG SCREENING AND PRECLINICAL GENE THERAPY APPROACHES FOR MITOCHONDRIAL CARDIOMYOPATHIES

Although several therapeutic strategies using iPSC-CMs has been raised over the past decade, the limited number of disease models for mitochondrial disorders hampers drug screening approaches and represents one of the major hurdles in the development of novel treatments for mitochondrial cardiomyopathies. Nevertheless, recent efforts in iPSC-based drug screening had been reported. Further, significant breakthroughs in genome editing technologies enabling genetic correction of underlying gene mutations show great promise for the therapy of mitochondrial disorders.

A major upgrade that the iPSC technology offers is to screen selective therapeutics under more physiological conditions in patient-derived and disease-relevant cells, tissues or even organ-like cultures. For instance, to assess the efficacy of treatment for Friedreich's ataxia, a pool of different antioxidants (an iron chelating agent deferiprone and an ubiquinone-derived analog idebenone) were tested in frataxin-deficient iPSC-CMs mimicking the cardiac stress stimulation (Lee et al., 2016). In their study, ROS production was evaluated after antioxidants administration in presence and absence of iron. Interestingly, deferiprone significantly decreased the intracellular ROS levels promoted by iron overload, and restored some aspects of deleterious Ca^{2+} handling in the patients' iPSC-CMs, suggesting a tight correlation between iron overload-induced mitochondrial oxidative stress and cardiomyocyte contractility (Lee et al., 2016).

A drug screening approach in patients' iPSC-CMs had been also performed for DCM as a result of TIM14 gene loss-of-function; the respective disease model had been introduced in the previous chapter (Rohani et al., 2020). Although, a severe disruption of the mitochondrial morphology was observed in TIM14-deficient cells, most of the deleterious effects could be

restored by elamipretide treatment that resulted in a profound reduction of the proteolytic cleavage of the short OPA1 isoform, in lower levels of fragmentation of the mitochondrial network, as well as in an improved mitochondrial ultrastructure (Rohani et al., 2020). This inner mitochondrial membrane-targeting peptide is currently used in clinical trials for patients with primary mitochondrial myopathies (Karaa et al., 2020; Reid Thompson et al., 2021).

Further, iPSC models for type 2 diabetes were also utilized for compound screening. An impressive library of 480 compounds was tested in patient-specific iPSC-CMs and 10 out of these small molecules were able to restore the pathological phenotype. Here, thapsigaragin and fluspirilene presented the most-effective impact in cells under diabetic stress (Drawnel et al., 2014). Bekhite and co-workers explored the potential role of myriocin (a potent sphingosine biosynthesis inhibitor) in their SPTLC1 overexpression iPSC-CM model. Interestingly, most of the deleterious effects observed by ceramide accumulation—predominantly, fission morphology and mitochondrial/lysosome co-localization—was restored by myriocin. Moreover, mitochondrial respiration was significantly upregulated after SP1 inhibitor treatment (Bekhite et al., 2021). These examples demonstrate that iPSCs can be widely used for high-content phenotypic screenings for the estimation of drug effectiveness, toxicology and drug metabolism, thereby taken in consideration the patients' genetic background as well as external pathophysiological factors.

On the opposite side, gene therapy as a consequence of the rapidly developing programmable genome editing tools may offer a promising resource to bypass the hurdles in the treatment of mitochondrial disorders. Particularly, huge progress in CRISPR/Cas9 genome editing and base editing for genetic correction of nuclear DNA gene mutations—such as for DMD (Amoasii et al., 2018) or for the Hutchinson-Gilford syndrome (Koblan et al., 2021)—can be transferred practically one-to-one to nuclear DNA-associated mitochondrial disorders. To name a few: Friedreich's ataxia and coenzyme Q10 deficiency were successfully corrected by genome editing *in vitro*. For the former, Li and co-workers utilized two zinc finger nucleases specifically targeting the intronic region of GAA repeats in the frataxin gene (Li et al., 2019). As a result, the repeat expansion sequence was reduced by ~1.2 kbps and total protein levels of full-length functional frataxin were doubled. In consequence, lipid droplets accumulation and expression of cardiac stress markers typically observed in untreated patients' iPSC-CMs were restored after zinc finger nuclease-based treatment (Li et al., 2019).

For coenzyme Q10 deficiency, Nakamoto and co-workers applied a site-specific CRISPR/Cas9-mediated gene correction and evaluated its subsequent molecular and functional characteristics (Nakamoto et al., 2018). In detail, coenzyme Q10 represents one of the major antioxidant factors for the MRC, and its synthesis is commanded by coenzyme Q2 (polyprenyltransferase; COQ2) which catalyzes the second step of coenzyme Q10 biosynthesis (Forsgren et al., 2004; Quinzii et al., 2006). In the present study, the group generated iPSCs from a patient that harbors compound heterozygous mutations in the COQ2 gene (p.R387*/V393A) and observed an aberrant mitochondrial respiration, an elevated ROS production and increased apoptotic levels in iPSC-derived neuronal cells. Interestingly, after CRISPR/Cas9-based correction of both gene mutations on both alleles, the pathological parameters were fully restored, highlighting the promise of the genome editing technologies for future clinical translation.

In strong contrast, CRISPR/Cas9-based genome editing of mtDNA represents a significantly bigger challenge, mainly because of the absence of efficient endogenous RNA import mechanisms that would be required to introduce the CRISPR guide RNA into the mitochondrial matrix (Gammage et al., 2018a). This disadvantage motivated to develop alternative protein-only genome editing tools fused to a mitochondrial targeting signal, which enable to selectively modify mtDNA. Although these mitochondrial-specific transcription activator-like effector nucleases (mitoTALEN), zinc finger nucleases (mtZFN) and meganucleases (mitoARCUS) have not yet been tested in the human cardiac setting, these systems demonstrated certain success in selective degradation of mutant mtDNA by nuclease-mediated cleavage of mtDNA in both patients' iPSCs (Yahata et al., 2017; Yang et al., 2018) as well as *in vivo* (Gammage et al., 2018b; Zekonyte et al., 2021), thereby resulting in heteroplasmic shifts by decreasing the pathological heteroplasmy levels. Importantly, classical DNA repair mechanisms are limited in mitochondria (Fu et al., 2020), which promotes major effects in edited cells, such as: 1) mitochondrial repair pathways of introduced double stand breaks in the mtDNA typically result in deletions that can manifest in a pathological phenotype, 2) nuclease-induced mtDNA linearization is rapidly recognized leading to rapid degradation of mtDNA and depletion of mitochondria (Peeva et al., 2018), and 3) ineffective mtDNA repair may trigger a toxic accumulation of mitochondrial content in host cells, therefore, might enhance intrinsic immune surveillance mechanisms (Tigano et al., 2021). This major hurdle can be overcome by precise base editing without induction of double strand breaks. Very recently, Mok and co-workers engineered a mitochondrial RNA-free base editor DdCBE by fusion of transcription activator-like effector proteins with split versions of a double-stranded deaminase $DddA_{tox}$ to induce selective C to T conversion in mtDNA with high target specificity and product purity (Mok et al., 2020). Strikingly, the authors confirmed that base editing (tested in HEK293T cells) was almost exclusively observed on the target sites at various mtDNA-encoded gene loci with an efficiency of up to 27%, becoming a promising approach in the future to precisely correct mtDNA variants and to decrease the mtDNA heteroplasmy (Mok et al., 2020). However, as it is true for the majority of gene therapy approaches, efficient delivery of the genome editing components into target organs, target cells and mitochondria remains currently one of the biggest challenges for clinical translation.

Finally, although not applicable as therapy for patients with mtDNA disorders, it should be mentioned that mitochondrial DNA replacement technologies aiming to transfer nuclear DNA from a zygote containing disease-causing mtDNA variants to a corresponding zygote with healthy mitochondria, offer a huge

therapeutic benefit for assisted reproductive medicine to avoid pathogenic mtDNA transmission between generations (Greenfield et al., 2017).

In summary, the high versatility of iPSC-CMs have proven a powerful pre-clinical platform in the screening of drugs and genome editing tools in a patient context and might support the translation of these approaches into clinical practice by bridging the gap between preclinical and clinical research.

CHALLENGES AND LIMITATIONS OF IPSC-CMS FOR MITOCHONDRIAL CARDIOMYOPATHY RESEARCH

Mature cardiomyocytes reflect a very particular set of properties that involve myofibril re-arrangements, characteristic electrophysiological patterns, increased contractility, decreased cell cycle progression and a metabolic shift (Guo and Pu, 2020). The metabolic state is central in cardiac development and multiple studies demonstrated that a distinct substrate oxidation is present during the process of cardiac maturation (Lopaschuk and Jaswal, 2010; Dorn et al., 2015). The fetal heart exhibits a high glycolytic metabolism, accompanied by expression of different glucose transports and distinct transcriptional factors that maintain the glycolytic program in immature cardiomyocytes (Taegtmeyer et al., 2010). In a remarkable shift during postnatal development, around 80% of ATP production in the adult heart is generated from fatty acids oxidation and OXPHOS activity (Wisneski et al., 1987; Koff and Schimmel, 1993). This massive change in metabolic supply is mainly explained as a consequence of substrates availability, metabolic pathway activity and differential transcriptional factor induction (Lopaschuk and Kelly, 2008). Indeed, the metabolic transition from immature cardiomyocytes to mature cardiomyocytes is driven by the activation of transcriptional regulators including PGC-1α/β and NRF1/2, resulting in upregulation of metabolic genes that are involved in fatty acid transport and oxidation, OXPHOS as well as mitochondrial biogenesis (Lai et al., 2008; Leone and Kelly, 2011; Vega and Kelly, 2017). Simultaneously, a downregulation in glycolytic genes, among others, mediated by HIF-1α inactivation, enhances the switch towards mitochondrial metabolism (Menendez-Montes et al., 2016). A considerable rearrangement in mitochondrial morphology orchestrated by fusion/fission proteins is necessary for an optimal mitochondrial bioenergetic adaptation. As an example, mitofusion 1/2 and OPA1 that regulate the fusion of external and internal mitochondrial membranes, are increased in mature cardiomyocytes, promoting an effective ATP generation (Martin et al., 2014). Furthermore, an increased coordination among sarcoplasmic reticulum, sarcomeres and mitochondria has been described during cardiac maturation (Seppet et al., 2001; Guo et al., 2021). In depth, adult cardiomyocytes show a highly structured sarcomere pattern associated with an abundant mitochondrial network, which, in turn, presents several contact sites with the sarcoplasmic reticulum. This close interaction leads to efficient ATP transport from mitochondria to ATPases that participate in excitation-contraction coupling (Seppet et al., 2001).

Although recent studies have reported iPSC-CMs as a suitable experimental model for mitochondrial disease (see section three), one of the major limitations of these cells is their fetal-like properties compared to adult cardiac tissue, specifically their poor mitochondrial bioenergetic capacity (Guo and Pu, 2020). This limitation might have remarkable relevance in disease modeling particularly of mitochondrial disorders, since less-mature (glycolytic) iPSC-CMs might not reproduce the expected pathological disease phenotype. Regarding this issue, numerous methods have been developed in order to facilitate iPSC-CM maturation to generate an "adult-like" phenotype. Most of these attempts can be grouped in delivery of energy sources (e.g. fatty acids versus glucose), biochemical cues, transcriptional factor modulation, physical/electrical stimulation and 3D tissue engineering. Herein, we aim to summarize some of these strategies with particular emphasis on cardiac metabolism and mitochondrial function. One of the first studies that proposed fatty acid-based conditioned medium to induce cardiomyocyte maturation was provided by Correia and co-workers using a mixture of fatty acids (oleic acid, palmitate, and galactose) (Correia et al., 2017). After approximately 2 weeks of incubation, iPSC-CMs showed elevated mitochondrial respiration attended by elongated cell morphology, higher organized sarcomeric structures and an increased action potential upstroke velocity, comparable to adult cardiomyocytes (Correia et al., 2017). A subsequent study demonstrated that iPSC-CMs incubated in fatty acid-based medium showed an increased ATP generation as a consequence of elevated mitochondrial OXPHOS activity, resulting in increased force generation and contractility (Yang et al., 2019). Since then, many other studies have used this approach to evaluate different aspects of cardiomyocyte differentiation. For instance, Knight and co-workers used a similar conditioned medium combined with substrate patterning and could confirm that iPSC-CMs displayed an elongated morphology, a higher sarcomeric alignment and an elevated contraction force, equivalent with donor heart tissue (Knight et al., 2021). Besides, a differential and more robust pathological hypertrophic phenotype could be observed using the aforementioned setting. In line, fatty acid-based media also allowed a phenotypic resemblance of different inherent cardiomyopathies with more-mature iPSC-CMs, such as arrhythmogenic episodes described in Long QT syndrome, dilated cardiomyopathy or Danon disease (Feyen et al., 2020; Knight et al., 2021). Collectively, considering the high impact of substrate oxidation in mitochondrial function, the selective composition of culture media should be taken into consideration when studying the wide spectrum of phenotypic changes induced by mitochondrial disorders.

Considering the high prevalence that glycolytic metabolism plays at embryonic stage, an alternative cardiomyocyte maturation strategy involved the downregulation of glycolysis-associated components by inactivation of the hypoxia-inducible factor 1-alpha (HIF-1α) and the lactate dehydrogenase A

(LDHA) during cardiac differentiation of iPSCs (Hu et al., 2018). Whereas HIF-1α controls glycolytic gene expression during hypoxic conditions and suppresses mitochondrial metabolism, LDHA mediates the conversion of pyruvate into lactate, thereby decreasing pyruvate oxidation in the mitochondria (Kim et al., 2006; Semenza, 2007). Hu and coworkers used small molecule inhibitors and small interfering RNAs (siRNAs) against HIF-1α and LDHA and observed reduced glycolytic activity and enhanced mitochondrial metabolism that was accompanied by increased mtDNA levels and mitochondrial content (Hu et al., 2018). Strikingly, HIF-1α/LDHA inhibition in iPSC-CMs did not only provided metabolic maturation, it also improved structural and functional maturation (Hu et al., 2018). Although this setting has not yet been tested in pathological conditions using iPSC-CMs, the metabolic shift from aerobic glycolysis to mitochondrial OXPHOS may be useful to understand the cardiac remodeling associated with mitochondrial insufficiencies.

Simultaneously, circulating factors and drugs have been tested as potential inductors of iPSC-CM maturation. Triiodothyronine (T3) is one of the most relevant metabolic hormones controlling the mitochondrial biogenesis and metabolism through its regulation via the thyroid hormone receptor-mediated pathway (Goldenthal et al., 2005). T3 has a preponderant effect on cardiomyocyte development, supported by the fact that cardiac defects have been described in congenital hypothyroidism patients (Wędrychowicz et al., 2019). Yang et al. (2014) showed that iPSC-CM cultures treated with T3 for over 1 week presented an augmentation of cellular size and sarcomere length and increased force generation. Interestingly, T3 treatment decreased cell cycle activity, an attribute also described in adult cardiomyocytes. Additionally, all these changes were aligned with a significant enhancement of mitochondrial function Yang et al. (2014). Thereafter, Parikh et al. (2017) demonstrated that combined treatment with T3 and glucocorticoids during cardiac differentiation resulted in an increase of cellular size and improved contractility. Surprisingly, iPSC-CMs also developed an extensive T-tubule network when using a Matrigel mattress. Although, the T-tubules were less structured compared to adult human myocardium, the distribution of junctophilin-2, which is mainly associated with T-tubule maturation, was significantly increased after T3 and dexamethasone treatment (Parikh et al., 2017). At the same time, iPSC-CMs showed a uniform Ca^{2+} release, a characteristic of maturated "adult-like" cardiomyocytes. In line, an iPSC-CM disease model based on a MYBPC3 gene mutation causing HCM revealed a robust disease phenotype only in maturation medium containing T3, IGF-1 and dexamethasone (Birket et al., 2015). In analogy to hormones, drug-based targeting of the AMP-activated protein kinase (AMPK), one of the master metabolic regulators of the cell (Garcia and Shaw, 2017), have also been tested to enhance mitochondrial respiration and to induce maturation. AMPK subunit gamma acts a sensor for adenosine monophosphate (AMP) and participates in the catalytic activation of the enzyme. Thus, when AMP/ATP ratio is high, AMPK is activated, thereby increasing the energy production through modulation of various signaling cascades (Garcia and Shaw, 2017). Two recent independent reports probed that AMPK modulation induced maturation of iPSC-CMs (Sarikhani et al., 2020; Ye et al., 2021). Long-term incubation of cultures with AMPK activator AICAR increased the expression of mitochondrial biogenesis-related markers such as PGC-1α and ERRα, increased fatty acid β-oxidation, and displayed an elevated mitochondrial density as well as an extended mitochondrial network. Besides, these changes were accompanied by increased expression of sarcomeric proteins including cardiac troponin T and cardiac troponin I as a consequence of long-term AICAR treatment.

Finally, 3D-engineered cardiac tissue, composed of iPSC-CMs and non-myocytes embedded in a hydrogel, has been considered the gold standard with respect to structural and functional maturation by more closely reflecting the native physiological conditions of the human heart muscle (Tiburcy et al., 2017). Indeed, the improved contractile properties of these cardiac tissues also contributed to a metabolic maturation of iPSC-CMs with higher abundance of mitochondria, less anaerobic glycolysis and an improved oxidative metabolism (Ulmer et al., 2018). In an extensive work performed by Ronaldson-Bouchard et al. (2018) addressing the maturity aspects of iPSC-CMs, they could demonstrate a robust sarcomeric re-arrangement, T-tubule maturation, increased contractility, and enhanced mitochondrial energy production upon early-stage biophysical pacing of cardiac tissues, highly recapitulating an "adult-like" cardiac phenotype.

Collectively, the physiologically immature state of iPSC-CMs might be a critical limitation in cardiac disease modeling by masking disease-relevant phenotypes/symptoms such as the disease-associated bioenergetic mitochondrial function. An improved maturation of iPSC-CM cultures accompanied with a shift from aerobic glycolysis to OXPHOS metabolism (e.g. by using one of the aforementioned approaches) might significantly improve evaluation of the cardiac pathology *in vitro* and should be taken into account in iPSC-based disease modeling of mitochondrial disorders.

CONCLUSION

Mitochondrial diseases can promote multi-organ insufficiency during early or late state. Around one third of these patients present a type of cardiac involvement by showing the poorest prognosis in the childhood. However, the lack of suitable disease models and the challenges associated with the different levels of heteroplasmy have been one of the major hurdles in the discovery of therapeutic targets. Our knowledge of iPSC biology has advanced to the point where we now can generate the majority of disease-relevant cell types of the human body in a culture dish, promoting iPSC technology as a suitable tool to overtake these challenges. The great variability of cardiac symptoms associated to mitochondrial disorders can by now be recapitulated and modelled more precisely, helping to evaluate tissue-specific threshold of mtDNA mutation load for individual genes or gene variants as well as to elucidate the tentative mechanisms behind the metabolic perturbations promoted as a consequence of mitochondrial disorders. Considering the high impact of maturity of iPSC-CMs in mitochondrial metabolism, it

becomes crucial to not only study the pathology in traditional 2D culture systems, but to also incorporate improved maturation methods in order to get the most representative cardiac phenotype-genotype correlation. These efforts might be central to develop novel and personalized therapeutic approaches.

AUTHOR CONTRIBUTIONS

Conceptualization and structure, MPG and LC; writing—original draft preparation, MPG; writing—review and editing, LC; figure preparation, MPG; both authors have read and agreed to the published version of the manuscript.

FUNDING

This work was supported by the German Federal Ministry of Education and Research (BMBF)/German Center for Cardiovascular Research (DZHK) (to LC) and by the German Research Foundation (DFG) (EXC 2067/1-390729940, CY 90/1-1 and SFB1002 S01 to LC).

REFERENCES

Abel, E. D. (2021). Insulin Signaling in the Heart. *Am. J. Physiology-Endocrinology Metab.* 321, E130–E145. doi:10.1152/ajpendo.00158.2021

Amoasii, L., Hildyard, J. C. W., Li, H., Sanchez-Ortiz, E., Mireault, A., Caballero, D., et al. (2018). Gene Editing Restores Dystrophin Expression in a Canine Model of Duchenne Muscular Dystrophy. *Science* 362, 86–91. doi:10.1126/science.aau1549

Anderson, S., Bankier, A. T., Barrell, B. G., de Bruijn, M. H. L., Coulson, A. R., Drouin, J., et al. (1981). Sequence and Organization of the Human Mitochondrial Genome. *Nature* 290, 457–465. doi:10.1038/290457a0

Bekhite, M., González-Delgado, A., Hübner, S., Haxhikadrija, P., Kretzschmar, T., Müller, T., et al. (2021). The Role of Ceramide Accumulation in Human Induced Pluripotent Stem Cell-Derived Cardiomyocytes on Mitochondrial Oxidative Stress and Mitophagy. *Free Radic. Biol. Med.* 167, 66–80. doi:10.1016/j.freeradbiomed.2021.02.016

Bione, S., D'Adamo, P., Maestrini, E., Gedeon, A. K., Bolhuis, P. A., and Toniolo, D. (1996). A Novel X-Linked Gene, G4.5. Is Responsible for Barth Syndrome. *Nat. Genet.* 12, 385–389. doi:10.1038/ng0496-385

Birket, M. J., Ribeiro, M. C., Kosmidis, G., Ward, D., Leitoguinho, A. R., van de Pol, V., et al. (2015). Contractile Defect Caused by Mutation in MYBPC3 Revealed under Conditions Optimized for Human PSC-Cardiomyocyte Function. *Cel Rep.* 13, 733–745. doi:10.1016/j.celrep.2015.09.025

Bogenhagen, D. F. (2012). Mitochondrial DNA Nucleoid Structure. *Biochim. Biophys. Acta (Bba) - Gene Regul. Mech.* 1819, 914–920. doi:10.1016/j.bbagrm.2011.11.005

Borchert, T., Hübscher, D., Guessoum, C. I., Lam, T.-D. D., Ghadri, J. R., Schellinger, I. N., et al. (2017). Catecholamine-Dependent β-Adrenergic Signaling in a Pluripotent Stem Cell Model of Takotsubo Cardiomyopathy. *J. Am. Coll. Cardiol.* 70, 975–991. doi:10.1016/j.jacc.2017.06.061

Bottomley, P. A., Atalar, E., and Weiss, R. G. (1996). Human Cardiac High-Energy Phosphate Metabolite Concentrations by 1D-Resolved NMR Spectroscopy. *Magn. Reson. Med.* 35, 664–670. doi:10.1002/mrm.1910350507

Brambilla, A., Olivotto, I., Favilli, S., Spaziani, G., Passantino, S., Procopio, E., et al. (2020). Impact of Cardiovascular Involvement on the Clinical Course of Paediatric Mitochondrial Disorders. *Orphanet J. Rare Dis.* 15, 196. doi:10.1186/s13023-020-01466-w

Brandt, U. (2006). Energy Converting NADH: Quinone Oxidoreductase (Complex I). *Annu. Rev. Biochem.* 75, 69–92. doi:10.1146/annurev.biochem.75.103004.142539

Brieler, J., Breeden, M. A., and Tucker, J. (2017). Cardiomyopathy: An Overview. *Am. Fam. Physician* 96, 640–646.

Brischigliaro, M., and Zeviani, M. (2021). Cytochrome C Oxidase Deficiency. *Biochim. Biophys. Acta (Bba) - Bioenerg.* 1862, 148335. doi:10.1016/j.bbabio.2020.148335

Brown, D. A., Perry, J. B., Allen, M. E., Sabbah, H. N., Stauffer, B. L., Shaikh, S. R., et al. (2017). Mitochondrial Function as a Therapeutic Target in Heart Failure. *Nat. Rev. Cardiol.* 14, 238–250. doi:10.1038/nrcardio.2016.203

Campuzano, O., Sanchez-Molero, O., Allegue, C., Coll, M., Mademont-Soler, I., Selga, E., et al. (2014). Post-mortem Genetic Analysis in Juvenile Cases of Sudden Cardiac Death. *Forensic Sci. Int.* 245, 30–37. doi:10.1016/j.forsciint.2014.10.004

Capaldi, R. A. (1990). Structure and Function of Cytochrome C Oxidase. *Annu. Rev. Biochem.* 59, 569–596. doi:10.1146/annurev.bi.59.070190.003033

Castro, I. H., Pignataro, M. F., Sewell, K. E., Espeche, L. D., Herrera, M. G., Noguera, M. E., et al. (2019). Frataxin Structure and Function. *Subcell Biochem.* 93, 393–438. doi:10.1007/978-3-030-28151-9_13

Cecchini, Gary (2003). Function and structure of complex II of the respiratory chain. In *Annual review of biochemistry* 72, pp. 77–109. doi:10.1146/annurev.biochem.72.121801.161700

Chanana, A. M., Rhee, J. W., and Wu, J. C. (2016). Human-Induced Pluripotent Stem Cell Approaches to Model Inborn and Acquired Metabolic Heart Diseases. *Curr Opin Cardiol.* 31, 266–274. doi:10.1097/HCO.0000000000000277

Chinnery, P. F., Johnson, M. A., Wardell, T. M., Singh-Kler, R., Hayes, C., Brown, D. T., et al. (2000). The Epidemiology of Pathogenic Mitochondrial DNA Mutations. *Ann. Neurol.* 48, 188–193. doi:10.1002/1531-8249(200008)48:2<188:aid-ana8>3.0.co;2-p

Chou, S.-J., Tseng, W.-L., Chen, C.-T., Lai, Y.-F., Chien, C.-S., Chang, Y.-L., et al. (2016). Impaired ROS Scavenging System in Human Induced Pluripotent Stem Cells Generated from Patients with MERRF Syndrome. *Sci. Rep.* 6, 23661. doi:10.1038/srep23661

Chowdhury, A., Aich, A., Jain, G., Wozny, K., Lüchtenborg, C., Hartmann, M., et al. (2018). Defective Mitochondrial Cardiolipin Remodeling Dampens HIF-1α Expression in Hypoxia. *Cel Rep.* 25, 561–570. e6. doi:10.1016/j.celrep.2018.09.057

Clarke, S. L., Bowron, A., Gonzalez, I. L., Groves, S. J., Newbury-Ecob, R., Clayton, N., et al. (2013). Barth Syndrome. *Orphanet J. Rare Dis.* 8, 23. doi:10.1186/1750-1172-8-23

Correia, C., Koshkin, A., Duarte, P., Hu, D., Teixeira, A., Domian, I., et al. (2017). Distinct Carbon Sources Affect Structural and Functional Maturation of Cardiomyocytes Derived from Human Pluripotent Stem Cells. *Sci. Rep.* 7, 8590. doi:10.1038/s41598-017-08713-4

Critchley, B. J., Isalan, M., and Mielcarek, M. (2018). Neuro-Cardio Mechanisms in Huntington's Disease and Other Neurodegenerative Disorders. *Front. Physiol.* 9, 559. doi:10.3389/fphys.2018.00559

Cuello, F., Knaust, A. E., Saleem, U., Loos, M., Raabe, J., Mosqueira, D., et al. (2021). Impairment of the ER/mitochondria compartment in human cardiomyocytes with PLN p.Arg14del mutation. *EMBO Mol. Med.* 13, e13074. doi:10.15252/emmm.202013074

D'Souza, K., Nzirorera, C., and Kienesberger, P. C. (2016). Lipid Metabolism and Signaling in Cardiac Lipotoxicity. *Biochim. Biophys. Acta (Bba) - Mol. Cel Biol. Lipids* 1861, 1513–1524. doi:10.1016/j.bbalip.2016.02.016

Davey, K. M., Parboosingh, J. S., McLeod, D. R., Chan, A., Casey, R., Ferreira, P., et al. (2006). Mutation of DNAJC19, a Human Homologue of Yeast Inner Mitochondrial Membrane Co-chaperones, Causes DCMA Syndrome, a Novel Autosomal Recessive Barth Syndrome-like Condition. *J. Med. Genet.* 43, 385–393. doi:10.1136/jmg.2005.036657

DiMauro, S., and Schon, Eric. A. (2003). Mitochondrial Respiratory-Chain Diseases. *In The New England journal of medicine* 348, 2656–2668. doi:10.1056/NEJMra022567

Dorn, G. W., Vega, R. B., and Kelly, D. P. (2015). Mitochondrial Biogenesis and Dynamics in the Developing and Diseased Heart. *Genes Dev.* 29, 1981–1991. doi:10.1101/gad.269894.115

Doenst, Torsten, Nguyen, Tien Dung, and Abel, E. Dale (2013). Cardiac metabolism in heart failure: implications beyond ATP production. In *Circulation research* 113 (6), pp. 709–724. doi:10.1161/CIRCRESAHA.113.300376

Drawnel, F. M., Boccardo, S., Prummer, M., Delobel, F., Graff, A., Weber, M., et al. (2014). Disease Modeling and Phenotypic Drug Screening for Diabetic Cardiomyopathy Using Human Induced Pluripotent Stem Cells. *Cel Rep.* 9, 810–820. doi:10.1016/j.celrep.2014.09.055

Dudek, J. (2017). Role of Cardiolipin in Mitochondrial Signaling Pathways. *Front. Cel Dev. Biol.* 5, 90. doi:10.3389/fcell.2017.00090

Dudek, J., Cheng, I. F., Chowdhury, A., Wozny, K., Balleininger, M., Reinhold, R., et al. (2016). Cardiac-Specific Succinate Dehydrogenase Deficiency in Barth Syndrome. *EMBO Mol Med.* 8, 139–154. doi:10.15252/emmm.201505644

Durham, S. E., Samuels, D. C., Cree, L. M., and Chinnery, P. F. (2007). Normal Levels of Wild-type Mitochondrial DNA Maintain Cytochrome C Oxidase Activity for Two Pathogenic Mitochondrial DNA Mutations but Not for m.3243A→G. *Am. J. Hum. Genet.* 81, 189–195. doi:10.1086/518901

Elliott, P. M., Anastasakis, A., Borger, M. A., Borggrefe, M., Cecchi, F., Charron, P., et al. (2014). 2014 ESC Guidelines on Diagnosis and Management of Hypertrophic Cardiomyopathy. *Eur. Heart J.* 35, 2733–2779. doi:10.1093/eurheartj/ehu284

Eschenhagen, T., Mummery, C., and Knollmann, B. C. (2015). Modelling Sarcomeric Cardiomyopathies in the Dish: from Human Heart Samples to iPSC Cardiomyocytes. *Cardiovasc. Res.* 105, 424–438. doi:10.1093/cvr/cvv017

Fatica, E. M., DeLeonibus, G. A., House, A., Kodger, J. V., Pearce, R. W., Shah, R. R., et al. (2019). Barth Syndrome: Exploring Cardiac Metabolism with Induced Pluripotent Stem Cell-Derived Cardiomyocytes. *Metabolites* 9, 306. doi:10.3390/metabo9120306

Feyen, D. A. M., McKeithan, W. L., Bruyneel, A. A. N., Spiering, S., Hörmann, L., Ulmer, B., et al. (2020). Metabolic Maturation Media Improve Physiological Function of Human iPSC-Derived Cardiomyocytes. *Cel Rep.* 32, 107925. doi:10.1016/j.celrep.2020.107925

Finsterer, J., and Kothari, S. (2014). Cardiac Manifestations of Primary Mitochondrial Disorders. *Int. J. Cardiol.* 177, 754–763. doi:10.1016/j.ijcard.2014.11.014

Folmes, C. D. L., Martinez-Fernandez, A., Perales-Clemente, E., Li, X., McDonald, A., Oglesbee, D., et al. (2013). Disease-Causing Mitochondrial Heteroplasmy Segregated within Induced Pluripotent Stem Cell Clones Derived from a Patient with MELAS. *Stem Cells* 31, 1298–1308. doi:10.1002/stem.1389

Forsgren, M., Attersand, A., Lake, S., Grünler, J., Swiezewska, E., Dallner, G., et al. (2004). Isolation and Functional Expression of Human COQ2, a Gene Encoding a Polyprenyl Transferase Involved in the Synthesis of CoQ. *Biochem. J.* 382, 519–526. doi:10.1042/BJ20040261

Frank, K., and Kranias, E. G. (2000). Phospholamban and Cardiac Contractility. *Ann. Med.* 32, 572–578. doi:10.3109/07853890008998837

Fu, Y., Tigano, M., and Sfeir, A. (2020). Safeguarding Mitochondrial Genomes in Higher Eukaryotes. *Nat. Struct. Mol. Biol.* 27, 687–695. doi:10.1038/s41594-020-0474-9

Galera-Monge, T., Zurita-Díaz, F., Garesse, R., and Gallardo, M. E. (2019). The Mutation m.13513G>A Impairs Cardiac Function, Favoring a Neuroectoderm Commitment, in a Mutant-load Dependent Way. *J. Cel Physiol* 234, 19511–19522. doi:10.1002/jcp.28549

Gammage, P. A., Moraes, C. T., and Minczuk, M. (2018a). Mitochondrial Genome Engineering: The Revolution May Not Be CRISPR-Ized. *Trends Genet.* 34, 101–110. doi:10.1016/j.tig.2017.11.001

Gammage, P. A., Viscomi, C., Simard, M.-L., Costa, A. S. H., Gaude, E., Powell, C. A., et al. (2018b). Genome Editing in Mitochondria Corrects a Pathogenic mtDNA Mutation *In Vivo*. *Nat. Med.* 24, 1691–1695. doi:10.1038/s41591-018-0165-9

Garcia, D., and Shaw, R. J. (2017). AMPK: Mechanisms of Cellular Energy Sensing and Restoration of Metabolic Balance. *Mol. Cel* 66, 789–800. doi:10.1016/j.molcel.2017.05.032

Garg, P., Garg, V., Shrestha, R., Sanguinetti, M. C., Kamp, T. J., and Wu, J. C. (2018). Human Induced Pluripotent Stem Cell-Derived Cardiomyocytes as Models for Cardiac Channelopathies. *Circ. Res.* 123, 224–243. doi:10.1161/CIRCRESAHA.118.311209

Garlid, A. O., Schaffer, C. T., Kim, J., Bhatt, H., Guevara-Gonzalez, V., and Ping, P. (2020). TAZ Encodes Tafazzin, a Transacylase Essential for Cardiolipin Formation and central to the Etiology of Barth Syndrome. *Gene* 726, 144148. doi:10.1016/j.gene.2019.144148

Gentillon, C., Li, D., Duan, M., Yu, W.-M., Preininger, M. K., Jha, R., et al. (2019). Targeting HIF-1α in Combination with PPARα Activation and Postnatal Factors Promotes the Metabolic Maturation of Human Induced Pluripotent Stem Cell-Derived Cardiomyocytes. *J. Mol. Cell Cardiol.* 132, 120–135. doi:10.1016/j.yjmcc.2019.05.003

Ghosh, R., Wood-Kaczmar, A., Dobson, L., Smith, E. J., Sirinathsinghji, E. C., Kriston-Vizi, J., et al. (2020). Expression of Mutant Exon 1 Huntingtin Fragments in Human Neural Stem Cells and Neurons Causes Inclusion Formation and Mitochondrial Dysfunction. *FASEB j.* 34, 8139–8154. doi:10.1096/fj.201902277RR

Goldenthal, M., Ananthakrishnan, R., and Maringarcia, J. (2005). Nuclear-mitochondrial Cross-Talk in Cardiomyocyte T3 Signaling: a Time-Course Analysis. *J. Mol. Cell Cardiol.* 39, 319–326. doi:10.1016/j.yjmcc.2005.03.016

Greenfield, A., Braude, P., Flinter, F., Lovell-Badge, R., Ogilvie, C., and Perry, A. C. F. (2017). Assisted Reproductive Technologies to Prevent Human Mitochondrial Disease Transmission. *Nat. Biotechnol.* 35, 1059–1068. doi:10.1038/nbt.3997

Gu, J., Wu, M., Guo, R., Yan, K., Lei, J., Gao, N., et al. (2016). The Architecture of the Mammalian Respirasome. *Nature* 537, 639–643. doi:10.1038/nature19359

Guo, Y., Cao, Y., Jardin, B. D., Sethi, I., Ma, Q., Moghadaszadeh, B., et al. (2021). Sarcomeres Regulate Murine Cardiomyocyte Maturation through MRTF-SRF Signaling. *Proc. Natl. Acad. Sci. USA* 118, e2008861118. doi:10.1073/pnas.2008861118

Guo, Y., and Pu, W. T. (2020). Cardiomyocyte Maturation. *Circ. Res.* 126, 1086–1106. doi:10.1161/CIRCRESAHA.119.315862

Haghighi, K., Kolokathis, F., Gramolini, A. O., Waggoner, J. R., Pater, L., Lynch, R. A., et al. (2006). A Mutation in the Human Phospholamban Gene, Deleting Arginine 14, Results in Lethal, Hereditary Cardiomyopathy. *Proc. Natl. Acad. Sci.* 103, 1388–1393. doi:10.1073/pnas.0510519103

Hallas, T., Eisen, B., Shemer, Y., Ben Jehuda, R., Mekies, L. N., Naor, S., et al. (2018). Investigating the Cardiac Pathology of SCO2-Mediated Hypertrophic Cardiomyopathy Using Patients Induced Pluripotent Stem Cell-Derived Cardiomyocytes. *J. Cel. Mol. Med.* 22, 913–925. doi:10.1111/jcmm.13392

Hanses, U., Kleinsorge, M., Roos, L., Yigit, G., Li, Y., Barbarics, B., et al. (2020). Intronic CRISPR Repair in a Preclinical Model of Noonan Syndrome-Associated Cardiomyopathy. *Circulation* 142, 1059–1076. doi:10.1161/CIRCULATIONAHA.119.044794

Herman, D. S., Lam, L., Taylor, M. R. G., Wang, L., Teekakirikul, P., Christodoulou, D., et al. (2012). Truncations of Titin Causing Dilated Cardiomyopathy. *N. Engl. J. Med.* 366, 619–628. doi:10.1056/NEJMoa1110186

Hick, A., Wattenhofer-Donzé, M., Chintawar, S., Tropel, P., Simard, J. P., Vaucamps, N., et al. (2013). Neurons and Cardiomyocytes Derived from Induced Pluripotent Stem Cells as a Model for Mitochondrial Defects in Friedreich's Ataxia. *Dis. Model. Mech.* 6, 608–621. doi:10.1242/dmm.010900

Hu, D., Linders, A., Yamak, A., Correia, C., Kijlstra, J. D., Garakani, A., et al. (2018). Metabolic Maturation of Human Pluripotent Stem Cell-Derived Cardiomyocytes by Inhibition of HIF1α and LDHA. *Circ. Res.* 123, 1066–1079. doi:10.1161/CIRCRESAHA.118.313249

Inak, G., Rybak-Wolf, A., Lisowski, P., Pentimalli, T. M., Jüttner, R., Glažar, P., et al. (2021). Defective Metabolic Programming Impairs Early Neuronal Morphogenesis in Neural Cultures and an Organoid Model of Leigh Syndrome. *Nat. Commun.* 12, 1929. doi:10.1038/s41467-021-22117-z

Ingwall, J. S. (2009). Energy Metabolism in Heart Failure and Remodelling. *Cardiovasc. Res.* 81, 412–419. doi:10.1093/cvr/cvn301

Jaksch, M., Ogilvie, I., Yao, J., Kortenhaus, G., Bresser, H. G., Gerbitz, K. D., et al. (2000). Mutations in SCO2 Are Associated with a Distinct Form of Hypertrophic Cardiomyopathy and Cytochrome C Oxidase Deficiency. *Hum. Mol. Genet.* 9, 795–801. doi:10.1093/hmg/9.5.795

Joshi, A. U., Ebert, A. E., Haileselassie, B., and Mochly-Rosen, D. (2019). Drp1/Fis1-mediated Mitochondrial Fragmentation Leads to Lysosomal Dysfunction in Cardiac Models of Huntington's Disease. *J. Mol. Cell Cardiol.* 127, 125–133. doi:10.1016/j.yjmcc.2018.12.004

Kamdar, F., and Garry, D. J. (2016). Dystrophin-Deficient Cardiomyopathy. *J. Am. Coll. Cardiol.* 67, 2533–2546. doi:10.1016/j.jacc.2016.02.081

Karaa, A., Haas, R., Goldstein, A., Vockley, J., and Cohen, B. H. (2020). A Randomized Crossover Trial of Elamipretide in Adults with Primary Mitochondrial Myopathy. *J. Cachexia, Sarcopenia Muscle* 11, 909–918. doi:10.1002/jcsm.12559

Kargaran, P. K., Evans, J. M., Bodbin, S. E., Smith, J. G. W., Nelson, T. J., Denning, C., et al. (2020). Mitochondrial DNA: Hotspot for Potential Gene Modifiers Regulating Hypertrophic Cardiomyopathy. *Jcm* 9, 2349. doi:10.3390/jcm9082349

Kayvanpour, E., Sedaghat-Hamedani, F., Amr, A., Lai, A., Haas, J., Holzer, D. B., et al. (2017). Genotype-phenotype Associations in Dilated Cardiomyopathy:

Meta-Analysis on More Than 8000 Individuals. *Clin. Res. Cardiol.* 106, 127–139. doi:10.1007/s00392-016-1033-6

Kelly, R. D. W., Mahmud, A., McKenzie, M., Trounce, I. A., and St John, J. C. (2012). Mitochondrial DNA Copy Number Is Regulated in a Tissue Specific Manner by DNA Methylation of the Nuclear-Encoded DNA Polymerase Gamma A. *Nucleic Acids Res.* 40, 10124–10138. doi:10.1093/nar/gks770

Kelly, R. D. W., Sumer, H., McKenzie, M., Facucho-Oliveira, J., Trounce, I. A., Verma, P. J., et al. (2013). The Effects of Nuclear Reprogramming on Mitochondrial DNA Replication. *Stem Cel Rev Rep* 9, 1–15. doi:10.1007/s12015-011-9318-7

Khalimonchuk, O., Bestwick, M., Meunier, B., Watts, T. C., and Winge, D. R. (2010). Formation of the Redox Cofactor Centers during Cox1 Maturation in Yeast Cytochrome Oxidase. *Mol. Cel Biol* 30, 1004–1017. doi:10.1128/MCB.00640-09

Kim, J.-w., Tchernyshyov, I., Semenza, G. L., and Dang, C. V. (2006). HIF-1-mediated Expression of Pyruvate Dehydrogenase Kinase: a Metabolic Switch Required for Cellular Adaptation to Hypoxia. *Cel Metab.* 3, 177–185. doi:10.1016/j.cmet.2006.02.002

Klein Gunnewiek, T. M., van Hugte, E. J. H., Frega, M., Guardia, G. S., Foreman, K., Panneman, D., et al. (2020). m.3243A > G-Induced Mitochondrial Dysfunction Impairs Human Neuronal Development and Reduces Neuronal Network Activity and Synchronicity. *Cel Rep.* 31, 107538. doi:10.1016/j.celrep.2020.107538

Knight, W. E., Cao, Y., Lin, Y.-H., Chi, C., Bai, B., Sparagna, G. C., et al. (2021). Maturation of Pluripotent Stem Cell-Derived Cardiomyocytes Enables Modeling of Human Hypertrophic Cardiomyopathy. *Stem Cel Rep.* 16, 519–533. doi:10.1016/j.stemcr.2021.01.018

Knottnerus, S. J. G., Mengarelli, I., Wüst, R. C. I., Baartscheer, A., Bleeker, J. C., Coronel, R., et al. (2020). Electrophysiological Abnormalities in VLCAD Deficient hiPSC-Cardiomyocytes Can Be Improved by Lowering Accumulation of Fatty Acid Oxidation Intermediates. *Ijms* 21, 2589. doi:10.3390/ijms21072589

Koblan, L. W., Erdos, M. R., Wilson, C., Cabral, W. A., Levy, J. M., Xiong, Z.-M., et al. (2021). *In Vivo* base Editing Rescues Hutchinson-Gilford Progeria Syndrome in Mice. *Nature* 589, 608–614. doi:10.1038/s41586-020-03086-7

Kodaira, M., Hatakeyama, H., Yuasa, S., Seki, T., Egashira, T., Tohyama, S., et al. (2015). Impaired Respiratory Function in MELAS-Induced Pluripotent Stem Cells with High Heteroplasmy Levels. *FEBS Open Bio* 5, 219–225. doi:10.1016/j.fob.2015.03.008

Koeppen, A. H. (2011). Friedreich's Ataxia: Pathology, Pathogenesis, and Molecular Genetics. *J. Neurol. Sci.* 303, 1–12. doi:10.1016/j.jns.2011.01.010

Koff, R. S., and Schimmel, E. M. (1993). in *Energy Metabolism: Tissue Determinants and Cellular Corollaries*. Editors J. M. Kinney and H. N. Tucker (New York: Raven Press), 562. 1992, $56. Hepatology 17, 347, 347. doi:10.1002/hep.1840170231

Kolwicz, S. C., Purohit, S., and Tian, R. (2013). Cardiac Metabolism and its Interactions with Contraction, Growth, and Survival of Cardiomyocytes. *Circ. Res.* 113, 603–616. doi:10.1161/CIRCRESAHA.113.302095

Lai, L., Leone, T. C., Keller, M. P., Martin, O. J., Broman, A. T., Nigro, J., et al. (2014). Energy Metabolic Reprogramming in the Hypertrophied and Early Stage Failing Heart. *Circ. Heart Fail.* 7, 1022–1031. doi:10.1161/CIRCHEARTFAILURE.114.001469

Lai, L., Leone, T. C., Zechner, C., Schaeffer, P. J., Kelly, S. M., Flanagan, D. P., et al. (2008). Transcriptional Coactivators PGC-1α and PGC-Lβ Control Overlapping Programs Required for Perinatal Maturation of the Heart. *Genes Dev.* 22, 1948–1961. doi:10.1101/gad.1661708

Leary, S. C., Kaufman, B. A., Pellecchia, G., Guercin, G.-H., Mattman, A., Jaksch, M., et al. (2004). Human SCO1 and SCO2 Have Independent, Cooperative Functions in Copper Delivery to Cytochrome C Oxidase. *Hum. Mol. Genet.* 13, 1839–1848. doi:10.1093/hmg/ddh197

Lee, Y.-K., Lau, Y.-M., Ng, K.-M., Lai, W.-H., Ho, S.-L., Tse, H.-F., et al. (2016). Efficient Attenuation of Friedreich's Ataxia (FRDA) Cardiomyopathy by Modulation of Iron Homeostasis-Human Induced Pluripotent Stem Cell (hiPSC) as a Drug Screening Platform for FRDA. *Int. J. Cardiol.* 203, 964–971. doi:10.1016/j.ijcard.2015.11.101

Leone, T. C., and Kelly, D. P. (2011). Transcriptional Control of Cardiac Fuel Metabolism and Mitochondrial Function. *Cold Spring Harbor Symposia Quantitative Biol.* 76, 175–182. doi:10.1101/sqb.2011.76.011965

Li, J., Rozwadowska, N., Clark, A., Fil, D., Napierala, J. S., and Napierala, M. (2019). Excision of the Expanded GAA Repeats Corrects Cardiomyopathy Phenotypes of iPSC-Derived Friedreich's Ataxia Cardiomyocytes. *Stem Cel Res.* 40, 101529. doi:10.1016/j.scr.2019.101529

Li, S., Pan, H., Tan, C., Sun, Y., Song, Y., Zhang, X., et al. (2018). Mitochondrial Dysfunctions Contribute to Hypertrophic Cardiomyopathy in Patient iPSC-Derived Cardiomyocytes with MT-RNR2 Mutation. *Stem Cel Rep.* 10, 808–821. doi:10.1016/j.stemcr.2018.01.013

Liang, K. X., Kristiansen, C. K., Mostafavi, S., Vatne, G. H., Zantingh, G. A., Kianian, A., et al. (2020). Disease-specific Phenotypes in iPSC -derived Neural Stem Cells with POLG Mutations. *EMBO Mol. Med.* 12, e12146. doi:10.15252/emmm.202012146

Lin, B., Li, Y., Han, L., Kaplan, A. D., Ao, Y., Kalra, S., et al. (2015). Modeling and Study of the Mechanism of Dilated Cardiomyopathy Using Induced Pluripotent Stem Cells Derived from Individuals with Duchenne Muscular Dystrophy. *Dis. Model. Mech.* 8, 457–466. doi:10.1242/dmm.019505

Liu, X., Wang, S., Guo, X., Li, Y., Ogurlu, R., Lu, F., et al. (2021). Increased Reactive Oxygen Species-Mediated Ca 2+/Calmodulin-dependent Protein Kinase II Activation Contributes to Calcium Handling Abnormalities and Impaired Contraction in Barth Syndrome. *Circulation* 143, 1894–1911. doi:10.1161/CIRCULATIONAHA.120.048698

Long, C., Li, H., Tiburcy, M., Rodriguez-Caycedo, C., Kyrychenko, V., Zhou, H., et al. (2018). Correction of Diverse Muscular Dystrophy Mutations in Human Engineered Heart Muscle by Single-Site Genome Editing. *Sci. Adv.* 4, eaap9004, 2018 . Energy metabolism: Tissue determinants and cellular corollaries. doi:10.1126/sciadv.aap9004

Lopaschuk, G. D., and Jaswal, J. S. (2010). Energy Metabolic Phenotype of the Cardiomyocyte during Development, Differentiation, and Postnatal Maturation. *J. Cardiovasc. Pharmacol.* 56, 130–140. doi:10.1097/FJC.0b013e3181e74a14

Lopaschuk, G. D., and Kelly, D. P. (2008). Signalling in Cardiac Metabolism. *Cardiovasc. Res.* 79, 205–207. doi:10.1093/cvr/cvn134

Ma, H., Folmes, C. D. L., Wu, J., Morey, R., Mora-Castilla, S., Ocampo, A., et al. (2015). Metabolic rescue in Pluripotent Cells from Patients with mtDNA Disease. *Nature* 524, 234–238. doi:10.1038/nature14546

Marian, A. J., and Braunwald, E. (2017). Hypertrophic Cardiomyopathy. *Circ. Res.* 121, 749–770. doi:10.1161/CIRCRESAHA.117.311059

Martin, O. J., Lai, L., Soundarapandian, M. M., Leone, T. C., Zorzano, A., Keller, M. P., et al. (2014). A Role for Peroxisome Proliferator-Activated Receptor γ Coactivator-1 in the Control of Mitochondrial Dynamics during Postnatal Cardiac Growth. *Circ. Res.* 114, 626–636. doi:10.1161/CIRCRESAHA.114.302562

Mazzaccara, C., Mirra, B., Barretta, F., Caiazza, M., Lombardo, B., Scudiero, O., et al. (2021). Molecular Epidemiology of Mitochondrial Cardiomyopathy: A Search Among Mitochondrial and Nuclear Genes. *Ijms* 22, 5742. doi:10.3390/ijms22115742

Menendez-Montes, I., Escobar, B., Palacios, B., Gómez, M. J., Izquierdo-Garcia, J. L., Flores, L., et al. (2016). Myocardial VHL-HIF Signaling Controls an Embryonic Metabolic Switch Essential for Cardiac Maturation. *Develop. Cel* 39, 724–739. doi:10.1016/j.devcel.2016.11.012

Mok, B. Y., de Moraes, M. H., Zeng, J., Bosch, D. E., Kotrys, A. V., Raguram, A., et al. (2020). A Bacterial Cytidine Deaminase Toxin Enables CRISPR-free Mitochondrial Base Editing. *Nature* 583, 631–637. doi:10.1038/s41586-020-2477-4

Mokranjac, D., Bourenkov, G., Hell, K., Neupert, W., and Groll, M. (2006). Structure and Function of Tim14 and Tim16, the J and J-like Components of the Mitochondrial Protein Import Motor. *EMBO J.* 25, 4675–4685. doi:10.1038/sj.emboj.7601334

Morgenstern, M., Stiller, S. B., Lübbert, P., Peikert, C. D., Dannenmaier, S., Drepper, F., et al. (2017). Definition of a High-Confidence Mitochondrial Proteome at Quantitative Scale. *Cel Rep.* 19, 2836–2852. doi:10.1016/j.celrep.2017.06.014

Mosqueira, D., Mannhardt, I., Bhagwan, J. R., Lis-Slimak, K., Katili, P., Scott, E., et al. (2018). CRISPR/Cas9 Editing in Human Pluripotent Stem Cell-Cardiomyocytes Highlights Arrhythmias, Hypocontractility, and Energy Depletion as Potential Therapeutic Targets for Hypertrophic Cardiomyopathy. *Eur. Heart J.* 39, 3879–3892. doi:10.1093/eurheartj/ehy249

Musunuru, K., Sheikh, F., Gupta, R. M., Houser, S. R., Maher, K. O., Milan, D. J., et al. (2018). Induced Pluripotent Stem Cells for Cardiovascular Disease Modeling and Precision Medicine: A Scientific Statement from the American Heart Association. *Circ. Genomic Precision Med.* 11, e000043. doi:10.1161/HCG.0000000000000043

Nakamoto, F. K., Okamoto, S., Mitsui, J., Sone, T., Ishikawa, M., Yamamoto, Y., et al. (2018). The Pathogenesis Linked to Coenzyme Q10 Insufficiency in iPSC-Derived Neurons from Patients with Multiple-System Atrophy. *Sci. Rep.* 8, 14215. doi:10.1038/s41598-018-32573-1

Neupane, P., Bhuju, S., Thapa, N., and Bhattarai, H. K. (2019). ATP Synthase: Structure, Function and Inhibition. *Biomol. Concepts* 10, 1–10. doi:10.1515/bmc-2019-0001

Nwabuo, C. C., Duncan, M., Xanthakis, V., Peterson, L. R., Mitchell, G. F., McManus, D., et al. (2019). Association of Circulating Ceramides with Cardiac Structure and Function in the Community: The Framingham Heart Study. *Jaha* 8, e013050. doi:10.1161/JAHA.119.013050

Parikh, S. S., Blackwell, D. J., Gomez-Hurtado, N., Frisk, M., Wang, L., Kim, K., et al. (2017). Thyroid and Glucocorticoid Hormones Promote Functional T-Tubule Development in Human-Induced Pluripotent Stem Cell-Derived Cardiomyocytes. *Circ. Res.* 121, 1323–1330. doi:10.1161/CIRCRESAHA.117.311920

Peeva, V., Blei, D., Trombly, G., Corsi, S., Szukszto, M. J., Rebelo-Guiomar, P., et al. (2018). Linear Mitochondrial DNA Is Rapidly Degraded by Components of the Replication Machinery. *Nat. Commun.* 9, 1727. doi:10.1038/s41467-018-04131-w

Perales-Clemente, E., Cook, A. N., Evans, J. M., Roellinger, S., Secreto, F., Emmanuele, V., et al. (2016). Natural Underlying Mt DNA Heteroplasmy as a Potential Source of Intra-person Hi PSC Variability. *EMBO J.* 35, 1979–1990. doi:10.15252/embj.201694892

Pfanner, N., Warscheid, B., and Wiedemann, N. (2019). Mitochondrial Proteins: from Biogenesis to Functional Networks. *Nat. Rev. Mol. Cel Biol* 20, 267–284. doi:10.1038/s41580-018-0092-0

Posch, M. G., Perrot, A., Geier, C., Boldt, L.-H., Schmidt, G., Lehmkuhl, H. B., et al. (2009). Genetic Deletion of Arginine 14 in Phospholamban Causes Dilated Cardiomyopathy with Attenuated Electrocardiographic R Amplitudes. *Heart Rhythm* 6, 480–486. doi:10.1016/j.hrthm.2009.01.016

Prokisch, H., Scharfe, C., Camp, D. G., Xiao, W., David, L., Andreoli, C., et al. (2004). Integrative Analysis of the Mitochondrial Proteome in Yeast. *Plos Biol.* 2, e160. doi:10.1371/journal.pbio.0020160

Quinzii, C., Naini, A., Salviati, L., Trevisson, E., Navas, P., DiMauro, S., et al. (2006). A Mutation in Para-Hydroxybenzoate-Polyprenyl Transferase (COQ2) Causes Primary Coenzyme Q10 Deficiency. *Am. J. Hum. Genet.* 78, 345–349. doi:10.1086/500092

Reid Thompson, W., Hornby, B., Manuel, R., Bradley, E., Laux, J., Carr, J., et al. (2021). A Phase 2/3 Randomized Clinical Trial Followed by an Open-Label Extension to Evaluate the Effectiveness of Elamipretide in Barth Syndrome, a Genetic Disorder of Mitochondrial Cardiolipin Metabolism. *Genet. Med.* 23, 471–478. doi:10.1038/s41436-020-01006-8

Robinton, D. A., and Daley, G. Q. (2012). The Promise of Induced Pluripotent Stem Cells in Research and Therapy. *Nature* 481, 295–305. doi:10.1038/nature10761

Rohani, L., Machiraju, P., Sabouny, R., Meng, G., Liu, S., Zhao, T., et al. (2020). Reversible Mitochondrial Fragmentation in iPSC-Derived Cardiomyocytes from Children with DCMA, a Mitochondrial Cardiomyopathy. *Can. J. Cardiol.* 36, 554–563. doi:10.1016/j.cjca.2019.09.021

Ronaldson-Bouchard, K., Ma, S. P., Yeager, K., Chen, T., Song, L., Sirabella, D., et al. (2018). Advanced Maturation of Human Cardiac Tissue Grown from Pluripotent Stem Cells. *Nature* 556, 239–243. doi:10.1038/s41586-018-0016-3

Rosca, M. G., and Hoppel, C. L. (2010). Mitochondria in Heart Failure. *Cardiovasc. Res.* 88, 40–50. doi:10.1093/cvr/cvq240

Ruiter, E. M., Siers, M. H., van den Elzen, C., van Engelen, B. G., Smeitink, J. A. M., Rodenburg, R. J., et al. (2007). The Mitochondrial 13513G>A Mutation Is Most Frequent in Leigh Syndrome Combined with Reduced Complex I Activity, Optic Atrophy And/or Wolff-Parkinson-White. *Eur. J. Hum. Genet.* 15, 155–161. doi:10.1038/sj.ejhg.5201735

Sarikhani, M., Garbern, J. C., Ma, S., Sereda, R., Conde, J., Krähenbühl, G., et al. (2020). Sustained Activation of AMPK Enhances Differentiation of Human iPSC-Derived Cardiomyocytes via Sirtuin Activation. *Stem Cel Rep.* 15, 498–514. doi:10.1016/j.stemcr.2020.06.012

Schon, E. A., DiMauro, S., and Hirano, M. (2012). Human Mitochondrial DNA: Roles of Inherited and Somatic Mutations. *Nat. Rev. Genet.* 13, 878–890. doi:10.1038/nrg3275

Semenza, G. L. (2007). Oxygen-dependent Regulation of Mitochondrial Respiration by Hypoxia-Inducible Factor 1. *Biochem. J.* 405, 1–9. doi:10.1042/BJ20070389

Seppet, E. K., Kaambre, T., Sikk, P., Tiivel, T., Vija, H., Tonkonogi, M., et al. (2001). Functional Complexes of Mitochondria with Ca,MgATPases of Myofibrils and Sarcoplasmic Reticulum in Muscle Cells. *Biochim. Biophys. Acta (Bba) - Bioenerg.* 1504, 379–395. doi:10.1016/S0005-2728(00)00269-3

Slater, E. C. (1983). The Q Cycle, an Ubiquitous Mechanism of Electron Transfer. *Trends Biochem. Sci.* 8, 239–242. doi:10.1016/0968-0004(83)90348-1

Smeitink, J., van den Heuvel, L., and DiMauro, S. (2001). The Genetics and Pathology of Oxidative Phosphorylation. *Nat. Rev. Genet.* 2, 342–352. doi:10.1038/35072063

Sofou, K., de Coo, I. F. M., Ostergaard, E., Isohanni, P., Naess, K., De Meirleir, L., et al. (2018). Phenotype-genotype Correlations in Leigh Syndrome: New Insights from a Multicentre Study of 96 Patients. *J. Med. Genet.* 55, 21–27. doi:10.1136/jmedgenet-2017-104891

Soma, S., Morgada, M. N., Naik, M. T., Boulet, A., Roesler, A. A., and Dziuba, N. (2019). COA6 Is Structurally Tuned to Function as a Thiol-Disulfide Oxidoreductase in Copper Delivery to Mitochondrial Cytochrome c Oxidase. *Cell Rep.* 29, 4114–4126. doi:10.1016/j.celrep.2019.11.054

Sommakia, S., Houlihan, P. R., Deane, S. S., Simcox, J. A., Torres, N. S., Jeong, M.-Y., et al. (2017). Mitochondrial Cardiomyopathies Feature Increased Uptake and Diminished Efflux of Mitochondrial Calcium. *J. Mol. Cell Cardiol.* 113, 22–32. doi:10.1016/j.yjmcc.2017.09.009

Stewart, J. B., and Chinnery, P. F. (2021). Extreme Heterogeneity of Human Mitochondrial DNA from Organelles to Populations. *Nat. Rev. Genet.* 22, 106–118. doi:10.1038/s41576-020-00284-x

Stewart, J. B., and Chinnery, P. F. (2015). The Dynamics of Mitochondrial DNA Heteroplasmy: Implications for Human Health and Disease. *Nat. Rev. Genet.* 16, 530–542. doi:10.1038/nrg3966

Taegtmeyer, H. (1994). Energy Metabolism of the Heart: From Basic Concepts to Clinical Applications Applications. *Curr. Probl. Cardiol.* 19, 61–86. doi:10.1016/0146-2806(94)90008-6

Taegtmeyer, H., Sen, S., and Vela, D. (2010). Return to the Fetal Gene Program. *Ann. N. Y Acad. Sci.* 1188, 191–198. doi:10.1111/j.1749-6632.2009.05100.x

Tiburcy, M., Hudson, J. E., Balfanz, P., Schlick, S., Meyer, T., Chang Liao, M.-L., et al. (2017). Defined Engineered Human Myocardium with Advanced Maturation for Applications in Heart Failure Modeling and Repair. *Circulation* 135, 1832–1847. doi:10.1161/CIRCULATIONAHA.116.024145

Tigano, M., Vargas, D. C., Tremblay-Belzile, S., Fu, Y., and Sfeir, A. (2021). Nuclear Sensing of Breaks in Mitochondrial DNA Enhances Immune Surveillance. *Nature* 591, 477–481. doi:10.1038/s41586-021-03269-w

Turrens, J. F. (2003). Mitochondrial Formation of Reactive Oxygen Species. *J. Physiol.* 552, 335–344. doi:10.1113/jphysiol.2003.049478

Ulmer, B. M., and Eschenhagen, T. (2020). Human Pluripotent Stem Cell-Derived Cardiomyocytes for Studying Energy Metabolism. *Biochim. Biophys. Acta (Bba) - Mol. Cel Res.* 1867, 118471. doi:10.1016/j.bbamcr.2019.04.001

Ulmer, B. M., Stoehr, A., Schulze, M. L., Patel, S., Gucek, M., Mannhardt, I., et al. (2018). Contractile Work Contributes to Maturation of Energy Metabolism in hiPSC-Derived Cardiomyocytes. *Stem Cel Rep.* 10, 834–847. doi:10.1016/j.stemcr.2018.01.039

van de Weijer, T., Schrauwen-Hinderling, V. B., and Schrauwen, P. (2011). Lipotoxicity in Type 2 Diabetic Cardiomyopathy. *Cardiovasc. Res.* 92, 10–18. doi:10.1093/cvr/cvr212

Vega, R. B., and Kelly, D. P. (2017). Cardiac Nuclear Receptors: Architects of Mitochondrial Structure and Function. *J. Clin. Invest.* 127, 1155–1164. doi:10.1172/JCI88888

Vercellino, I., and Sazanov, L. A. (2021). The Assembly, Regulation and Function of the Mitochondrial Respiratory Chain. *Nat. Rev. Mol. Cel Biol.* doi:10.1038/s41580-021-00415-0

Verkerk, A. O., Knottnerus, S. J. G., Portero, V., Bleeker, J. C., Ferdinandusse, S., Guan, K., et al. (2020). Electrophysiological Abnormalities in VLCAD Deficient

hiPSC-Cardiomyocytes Do Not Improve with Carnitine Supplementation. *Front. Pharmacol.* 11, 616834. doi:10.3389/fphar.2020.616834

Wahbi, K., Bougouin, W., Béhin, A., Stojkovic, T., Bécane, H. M., Jardel, C., et al. (2015). Long-term Cardiac Prognosis and Risk Stratification in 260 Adults Presenting with Mitochondrial Diseases. *Eur. Heart J.* 36, 2886–2893. doi:10.1093/eurheartj/ehv307

Wallace, D. C., Singh, G., Lott, M. T., Hodge, J. A., Schurr, T. G., Lezza, A. M. S., et al. (1988). Mitochondrial DNA Mutation Associated with Leber's Hereditary Optic Neuropathy. *Science* 242, 1427–1430. doi:10.1126/science.3201231

Wang, G., McCain, M. L., Yang, L., He, A., Pasqualini, F. S., Agarwal, A., et al. (2014). Modeling the Mitochondrial Cardiomyopathy of Barth Syndrome with Induced Pluripotent Stem Cell and Heart-On-Chip Technologies. *Nat. Med.* 20, 616–623. doi:10.1038/nm.3545

Wędrychowicz, A., Furtak, A., Prośniak, A., Żuberek, M., Szczerkowska, M., Pacut, P., et al. (2019). Extrathyroidal Congenital Defects in Children with Congenital Hypothyroidism - Observations from a Single Paediatric centre in Central Europe with a Review of Literature. *pedm* 25, 114–121. doi:10.5114/pedm.2019.87178

Weidemann, F., Störk, S., Liu, D., Hu, K., Herrmann, S., Ertl, G., et al. (2013). Cardiomyopathy of Friedreich Ataxia. *J. Neurochem.* 126 (Suppl. 1), 88–93. doi:10.1111/jnc.12217

Wende, A. R., and Abel, E. D. (2010). Lipotoxicity in the Heart. *Biochim. Biophys. Acta (Bba) - Mol. Cel Biol. Lipids* 1801, 311–319. doi:10.1016/j.bbalip.2009.09.023

Westermeier, F., Riquelme, J. A., Pavez, M., Garrido, V., Díaz, A., Verdejo, H. E., et al. (2016). New Molecular Insights of Insulin in Diabetic Cardiomyopathy. *Front. Physiol.* 7, 125. doi:10.3389/fphys.2016.00125

Wilkins, H. M., Carl, S. M., and Swerdlow, R. H. (2014). Cytoplasmic Hybrid (Cybrid) Cell Lines as a Practical Model for Mitochondriopathies. *Redox Biol.* 2, 619–631. doi:10.1016/j.redox.2014.03.006

Wisneski, J. A., Gertz, E. W., Neese, R. A., and Mayr, M. (1987). Myocardial Metabolism of Free Fatty Acids. Studies with 14C-Labeled Substrates in Humans. *J. Clin. Invest.* 79, 359–366. doi:10.1172/JCI112820

Wong, A. O.-T., Wong, G., Shen, M., Chow, M. Z.-Y., Tse, W. W., Gurung, B., et al. (2019). Correlation between Frataxin Expression and Contractility Revealed by *In Vitro* Friedreich's Ataxia Cardiac Tissue Models Engineered from Human Pluripotent Stem Cells. *Stem Cel Res Ther* 10, 203. doi:10.1186/s13287-019-1305-y

Yahata, N., Matsumoto, Y., Omi, M., Yamamoto, N., and Hata, R. (2017). TALEN-mediated Shift of Mitochondrial DNA Heteroplasmy in MELAS-iPSCs with m.13513G>A Mutation. *Sci. Rep.* 7, 15557. doi:10.1038/s41598-017-15871-y

Yang, X., Rodriguez, M. L., Leonard, A., Sun, L., Fischer, K. A., Wang, Y., et al. (2019). Fatty Acids Enhance the Maturation of Cardiomyocytes Derived from Human Pluripotent Stem Cells. *Stem Cel Rep.* 13, 657–668. doi:10.1016/j.stemcr.2019.08.013

Yang, X., Rodriguez, M., Pabon, L., Fischer, K. A., Reinecke, H., Regnier, M., et al. (2014). Tri-iodo-l-thyronine Promotes the Maturation of Human Cardiomyocytes-Derived from Induced Pluripotent Stem Cells. *J. Mol. Cell Cardiol.* 72, 296–304. doi:10.1016/j.yjmcc.2014.04.005

Yang, Y., Wu, H., Kang, X., Liang, Y., Lan, T., Li, T., et al. (2018). Targeted Elimination of Mutant Mitochondrial DNA in MELAS-iPSCs by mitoTALENs. *Protein Cell* 9, 283–297. doi:10.1007/s13238-017-0499-y

Ye, L., Zhang, X., Zhou, Q., Tan, B., Xu, H., Yi, Q., et al. (2021). Activation of AMPK Promotes Maturation of Cardiomyocytes Derived from Human Induced Pluripotent Stem Cells. *Front. Cel Dev. Biol.* 9, 644667. doi:10.3389/fcell.2021.644667

Yokota, M., Hatakeyama, H., Okabe, S., Ono, Y., and Goto, Y.-I. (2015). Mitochondrial Respiratory Dysfunction Caused by a Heteroplasmic Mitochondrial DNA Mutation Blocks Cellular Reprogramming. *Hum. Mol. Genet.* 24, 4698–4709. doi:10.1093/hmg/ddv201

Yokota, M., Hatakeyama, H., Ono, Y., Kanazawa, M., and Goto, Y.-I. (2017). Mitochondrial Respiratory Dysfunction Disturbs Neuronal and Cardiac Lineage Commitment of Human iPSCs. *Cell Death Dis* 8, e2551. doi:10.1038/cddis.2016.484

Yu-Wai-Man, P., Sitarz, K. S., Samuels, D. C., Griffiths, P. G., Reeve, A. K., Bindoff, L. A., et al. (2010). OPA1 Mutations Cause Cytochrome C Oxidase Deficiency Due to Loss of Wild-type mtDNA Molecules. *Hum. Mol. Genet.* 19, 3043–3052. doi:10.1093/hmg/ddq209

Zekonyte, U., Bacman, S. R., Smith, J., Shoop, W., Pereira, C. V., Tomberlin, G., et al. (2021). Mitochondrial Targeted Meganuclease as a Platform to Eliminate Mutant mtDNA in Vivo. *Nat Commun.* 12, 3210. doi:10.1038/s41467-021-23561-7

Zhao, H., Perkins, G., Yao, H., Callacondo, D., Appenzeller, O., Ellisman, M., et al. (2018). Mitochondrial Dysfunction in iPSC-Derived Neurons of Subjects with Chronic Mountain Sickness. *J. Appl. Physiol. (1985).* 125, 832–840. doi:10.1152/japplphysiol.00689.2017

Conflict of Interest: The authors declare that the research was conducted in the absence of any commercial or financial relationships that could be construed as a potential conflict of interest.

frontiers in Cell and Developmental Biology

REVIEW
published: 12 January 2022
doi: 10.3389/fcell.2021.796128

Complexome Profiling—Exploring Mitochondrial Protein Complexes in Health and Disease

Alfredo Cabrera-Orefice[1], Alisa Potter[2†], Felix Evers[3†], Johannes F. Hevler[4,5,6,7] and Sergio Guerrero-Castillo[8]**

[1]Center for Molecular and Biomolecular Informatics, Radboud Institute for Molecular Life Sciences, Radboud University Medical Center, Nijmegen, Netherlands, [2]Department of Pediatrics, Radboud Center for Mitochondrial Medicine, Radboud University Medical Center, Nijmegen, Netherlands, [3]Department of Medical Microbiology, Radboud Institute for Molecular Life Sciences, Radboud University Medical Center, Nijmegen, Netherlands, [4]Biomolecular Mass Spectrometry and Proteomics, University of Utrecht, Utrecht, Netherlands, [5]Bijvoet Center for Biomolecular Research, University of Utrecht, Utrecht, Netherlands, [6]Utrecht Institute for Pharmaceutical Sciences, University of Utrecht, Utrecht, Netherlands, [7]Netherlands Proteomics Center, Utrecht, Netherlands, [8]University Children's Research@Kinder-UKE, University Medical Center Hamburg-Eppendorf, Hamburg, Germany

OPEN ACCESS

Edited by:
Erika Fernandez-Vizarra, Veneto Institute of Molecular Medicine (VIMM), Italy

Reviewed by:
Ilka Wittig, Goethe University Frankfurt, Germany
Massimo Zeviani, University of Padua, Italy

***Correspondence:**
Alfredo Cabrera-Orefice
alfredbiomed@gmail.com
Sergio Guerrero-Castillo
s.guerrerocastillo@uke.de

[†]These authors have contributed equally to this work

Specialty section:
This article was submitted to Cellular Biochemistry, a section of the journal Frontiers in Cell and Developmental Biology

Received: *15 October 2021*
Accepted: *08 December 2021*
Published: *12 January 2022*

Citation:
Cabrera-Orefice A, Potter A, Evers F, Hevler JF and Guerrero-Castillo S (2022) Complexome Profiling—Exploring Mitochondrial Protein Complexes in Health and Disease. Front. Cell Dev. Biol. 9:796128. doi: 10.3389/fcell.2021.796128

Complexome profiling (CP) is a state-of-the-art approach that combines separation of native proteins by electrophoresis, size exclusion chromatography or density gradient centrifugation with tandem mass spectrometry identification and quantification. Resulting data are computationally clustered to visualize the inventory, abundance and arrangement of multiprotein complexes in a biological sample. Since its formal introduction a decade ago, this method has been mostly applied to explore not only the composition and abundance of mitochondrial oxidative phosphorylation (OXPHOS) complexes in several species but also to identify novel protein interactors involved in their assembly, maintenance and functions. Besides, complexome profiling has been utilized to study the dynamics of OXPHOS complexes, as well as the impact of an increasing number of mutations leading to mitochondrial disorders or rearrangements of the whole mitochondrial complexome. Here, we summarize the major findings obtained by this approach; emphasize its advantages and current limitations; discuss multiple examples on how this tool could be applied to further investigate pathophysiological mechanisms and comment on the latest advances and opportunity areas to keep developing this methodology.

Keywords: complexome profiling, mitochondria, protein complex, protein-protein interaction (PPI), oxidative phosphorylation, disease, proteomics, mass spectrometry

1 INTRODUCTION

Proteins, the so-called "workhorses" of life, are the tools that make living machines work (Adams, 2008). The vast majority of biological processes are thus structured, mediated and executed by these macromolecules. Even though many single proteins do perform specific functions by their own, most proteins habitually interact with other proteins, DNA, RNA and lipid molecules rather than acting individually for achieving their biological tasks. The resultant protein complexes can form transient or steady interactions, which also correlate with the type of biological processes they are involved in (De Las Rivas and Fontanillo, 2010). For example, housekeeping cell processes are likely performed by a large fraction of steady protein complexes, whereas in signaling, cell migration, membrane

trafficking, metabolic response and other highly dynamic processes, involvement of transient complexes is definitely required for rapid responses and adaptation. The entire set of multi-protein complexes in a cell or compartment is referred to as the complexome (Deshaies et al., 2002; Ceulemans et al., 2006; Lasserre et al., 2006).

In situations where impaired interaction of the elements of a protein complex affect its proper formation; e.g., due to genetic mutations, the related cell process(es) could be compromised and result in biological dysfunction. Higher complexity in multicellular organisms is of course accompanied by larger complexomes than those from unicellular species. Therefore, alterations in protein complexes may affect not only multiple cell processes, but also lead to severe pathophysiological issues at the tissue/organ level. An integral elucidation of both complexomes and protein interaction networks; i.e., interactome (Vidal et al., 2011) under different cellular scenarios, becomes crucial to fully comprehend the molecular mechanisms behind cell physiology and disease.

Numerous biochemical, biophysical, structural, genetic, microscopy and mass spectrometry (MS) approaches have been applied to characterize protein complexes. Although these methods have different principles, in most cases, they require experimental interventions, cell/tissue fractionation, protein extraction and/or time-consuming protocols prior to data collection and analyses. Besides, the amount of information obtained is often limited to one or a small set of protein complexes. The recent breakthrough in quantitative high-throughput technologies and bioinformatic tools has substantially increased the efficiency and quality of the large-scale identification of protein interactors (Iacobucci et al., 2021; Low et al., 2021). Accordingly, an outstanding volume of evidence on the composition, 3D structure, interactions and molecular roles of hundreds of protein complexes is now easily accessible through multiple repositories, such as RCSB PDB (Burley et al., 2021), STRING (Szklarczyk et al., 2021), CORUM (Giurgiu et al., 2019), BioGRID (Oughtred et al., 2021), Pfam (Mistry et al., 2021), Complex Portal (Meldal et al., 2021), NCBI (Coordinators, 2016) and UniProt (UniProt, 2021). Yet, a substantial fraction of the protein interactors reported in those databases still lack full validation of their occurrence *in vivo* by using novel and more reliable methods.

A systematic approach known as complexome profiling (CP) has recently been introduced as a straightforward and unbiased way to explore protein complexes (Heide et al., 2012; Wessels et al., 2013). CP combines fractionation of protein complexes under native conditions with digestion and quantitative tandem MS-based identification of the derived peptides. Resultant data are clustered to visualize the inventory, abundance and arrangement of multi-protein complexes in a biological sample. Since its formal introduction a decade ago, CP has been primarily used in mitochondrial research (Kiirika et al., 2013; Senkler et al., 2017; Giese et al., 2021; Guerrero-Castillo et al., 2021b; Wittig and Malacarne, 2021); albeit CP can be applied to any kind of cellular fraction.

2 COMPLEXOME PROFILING

2.1 General Overview

The first requisite to carry out a CP experiment is the collection of biological material; e.g., tissue pieces/biopsies, cultured cells, enriched cell fractions, purified organelles, etc. These materials might also come from previous experimental interventions. Homogenization and cell fractionation methods should aim to keep the native state of protein complexes. For solubilization of membrane proteins, it is recommended to use mild, non-ionic detergents; e.g., Triton X-100, NP-40, dodecyl-maltoside, octyl-glucoside or digitonin (Eubel et al., 2005; Wittig et al., 2006). Next, native protein extracts are separated by a so-called "untargeted" method (Iacobucci et al., 2021), such as native electrophoresis, size-exclusion chromatography or density gradient ultracentrifugation (**Figure 1**). Regardless of the type of protein separation, CP follows a well-defined protocol that slightly differs among variants. In all cases, protein complexes are separated by size, hence, by shape and molecular mass. Each fraction is further digested with high-purity and specific proteases (e.g., trypsin, chymotrypsin and endoproteinase Lys-C) followed by MS/MS identification of the resulting peptides (**Figure 1**); i.e., bottom-up proteomics strategy (Zhang et al., 2013).

Previous to MS analysis, peptides are usually separated based on their hydrophobicity by reversed-phase high-performance liquid chromatography (RP-HPLC) followed by electrospray ionization (ESI) to produce gas phase ions (Zhang et al., 2013). The majority of MS data for CP studies has been acquired in data-dependent mode (DDA); i.e., collection of a predefined number of precursor ions for fragmentation during the MS2 cycle is done according to their charge states and abundance (Hu et al., 2016). In conventional DDA modes, the possibility to identify low abundant peptides thus becomes significantly limited. To avoid this issue, acquisition strategies in data-independent mode (DIA) (Krasny and Huang, 2021), such as sequential window acquisition of all theoretical mass spectra (SWATH-MS) (Gillet et al., 2012), in which fragmentation of all precursor ions identified in the MS1 cycle can be analyzed in the MS2 cycle, have recently been introduced to CP-like workflows (Heusel et al., 2019; Bludau et al., 2020; Calvo et al., 2020).

MS spectra are routinely matched against a proteome database of the species of interest by using a variety of software/search engines (**Figure 1**), such as Mascot (Perkins et al., 1999), openMS (Rost et al., 2016), PEAKS DB (Zhang et al., 2012), Proteome discoverer (Orsburn, 2021), Protein Prospector (Chalkley et al., 2005) and MaxQuant (Tyanova et al., 2016a). In case that the proteome of the studied organism is not yet available or fully annotated, metagenome or transcriptome data are useful to generate a list of proteins and perform the search. Alternatively, peptide sequences might be deduced directly from tandem MS spectra by using database-independent computational approaches; i.e., *de novo* peptide sequencing (Tran et al., 2017).

Protein abundance profiles are further obtained by plotting, for example, label-free quantification (LFQ) (Cox et al., 2014) or

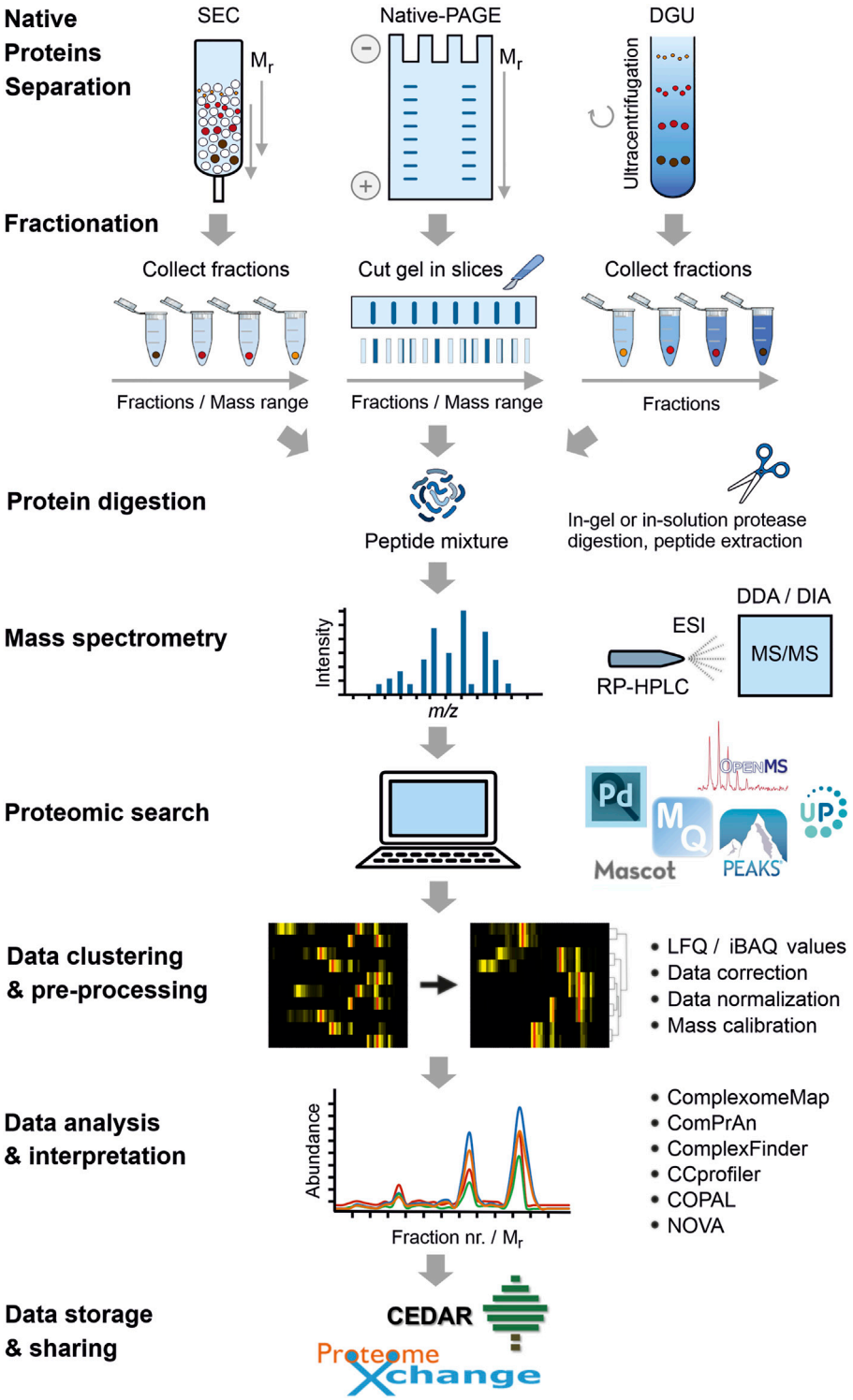

FIGURE 1 | Overall workflow of complexome profiling (CP). After collection, homogenization and fractionation of biological materials, proteins are separated by either native polyacrylamide gel electrophoresis (PAGE), size exclusion chromatography (SEC) or density gradient ultracentrifugation (DGU) for CP studies. The obtained protein-containing fractions are individually digested with specific proteases. Resultant peptides are extracted, cleaned and usually separated by reversed-phase high-performance liquid chromatography (RP-HPLC) followed by tandem mass spectrometry (MS/MS) analysis. MS data can be acquired in data-dependent or data-independent modes, DDA or DIA, respectively. Next, a proteomic search is performed to match obtained MS spectra against proteome databases using a variety of available software. Icons of the most popular tools used for CP studies are shown (see **Section 2.1** for details). Protein abundance profiles are further obtained by

(*Continued*)

FIGURE 1 | plotting LFQ/iBAQ values against the number of fractions. The list of identified protein groups is computationally sorted based on similarities of the abundance patterns across fractions; e.g., hierarchical clustering. Prior to analysis, complexome data are pre-processed to account for protein loading/MS sensitivity differences. Data correction and normalization between samples are regularly applied. In SEC- and native-PAGE-based CP, a mass calibration can be implemented for a more meaningful biological dimension. Data can be analyzed by using available bioinformatic tools specifically created for CP. Some of these programs are shown in the figure (see **Section 2.4** for details). For reusing and further analysis, large CP datasets can be deposited and publicly shared through PRIDE (Proteome Xchange consortium) or the new dedicated website for CP, CEDAR.

intensity-based absolute quantification (iBAQ) (Schwanhausser et al., 2011; Tyanova et al., 2016a) values against the number of fraction. While LFQ intensities are typically utilized for comparing relative amounts of proteins in multiple samples, iBAQ values offer a more stoichiometric impression of the identified protein groups as those are proportional to their molar quantities. iBAQ values are calculated as the sum of all individual peptide intensities of a given protein group divided by its number of theoretical identifiable peptides. It is thus not surprising that the majority of CP studies use iBAQ since it enables a fair comparison between different protein groups in the same and multiple samples. Additional information regarding LFQ and other alternative methods have been reviewed in Fabre et al. (2014) and Wittig and Malacarne (2021). Ultimately, the list of hundreds or even thousands of identified proteins is mainly sorted based on similarities of the abundance patterns across fractions by hierarchical clustering analysis (**Figure 1**). Proteins that are part of the same complex consistently cluster together since these show co-migration in the same fraction(s) and similar abundance profiles.

2.2 Different Complexome Profiling Setups, One Common Goal

As a ground-breaking "-omics" method, CP has been rapidly developing and spreading among the scientific community. It is thus not striking that in less than a decade, multiple strategies have complemented or even improved its scope. At the same time, several limitations of CP have been circumvented gradually by including novel MS-based strategies, specific adaptions in sample processing and new tools for data analysis. All variants of CP do share a common goal nonetheless: to unravel the composition of protein complexes, as well as their abundance, stabilities, apparent molecular masses and stoichiometries.

The most used CP workflow, currently referred to as "classic CP" (Wittig and Malacarne, 2021), uses Blue Native-polyacrylamide gel electrophoresis (BN-PAGE) followed by MS identification. The main advantages of BN-PAGE are the relatively low amounts of biological material required and high-resolution separation of native proteins. BN-PAGE conditions keep proteins in similar native states to those occurring *in vivo* (Wittig et al., 2006). However, if the presence of Coomassie blue dye affects the stability of one or more protein complexes of interest, milder dye-free versions of native-PAGE can easily be used instead; e.g., high-resolution clear native-PAGE (hrCN-PAGE) (Wittig et al., 2007; Ladig et al., 2011). Native-PAGE is suitable for separation of proteins between ~0.02–10 MDa. If the study requires interrogation of bigger protein complexes (>10 MDa), large pore BN-PAGE (LP-BN-PAGE) can be applied instead (Strecker et al., 2010; Heide et al., 2012).

After electrophoresis, entire gel strips are fixed and often cut into 32–70 slices followed by LC-MS/MS identification (Heide et al., 2012; Senkler et al., 2017; Vidoni et al., 2017; Giese et al., 2021). For CP analysis, slice numbers can be transformed into apparent molecular mass values by carrying out a calibration using standard proteins as exemplified in Wittig et al. (2010) and Heide et al. (2012). Molecular mass accuracy is optimized by using different sets of standard protein complexes, one for water-soluble proteins and the other for membrane proteins. On the whole, the more fractions collected the better resolution of the resultant profiles will be. In 2016, Müller and co-workers developed cryo-slicing Blue Native-Mass Spectrometry (csBN-MS), which helped increase the resolution, accuracy and quantification of the complexome profiles by slicing the BN-lanes in 230 pieces as well as optimizing MS analysis and protein identification (Muller et al., 2016). The resolution of complexome profiles obtained from ≤30 slices would not be suitable to unambiguously assign protein interactions.

Besides native-PAGE, size exclusion chromatography (SEC) and density gradient ultracentrifugation (DGU) have been implemented in different CP setups. Using SEC, native proteins are separated by filtration through a gel matrix (resin), which consists of spherical porous beads of different sizes depending on the desired range of molecular masses (Burgess, 2018). Elution of heavier proteins is faster than the lighter ones by this method. Apparent molecular masses of eluted fractions can be determined with proper standard mixes; although the mass calibration is more accurate for globular proteins (Hong et al., 2012; Korepanova and Matayoshi, 2012). SEC resins are suitable for separating proteins in a wide range of molecular masses; e.g., 1–700 kDa (Sephadex™, Superdex™); 5–5,000 kDa (Superose™) and 0.01–40 MDa (Sepharose™). The number of fractions that can be collected after SEC is comparable to those aforementioned. For example, in the recently introduced SEC-SWATH-MS approach (Heusel et al., 2019), 81 fractions were collected, subjected to MS identification and examined by complex-centric proteome analysis. This CP setup led to higher sensitivity and accuracy in protein quantification, less noise, and validation of protein interactions. SEC has been particularly useful in CP studies characterizing large protein complexes, such as nuclear components (Connelly et al., 2018). However, key limitations of SEC-involving CP setups would be the larger amounts of biological material required, loss of protein

interactions by dilution, formation of self-oligomers and inadequate identification of membrane and low abundant protein complexes (Burgess, 2018; Heusel et al., 2019; Iacobucci et al., 2021).

On the other hand, DGU uses solutions of different densities made of glycerol, sucrose, cesium chloride, iodixanol or Ficoll® through which protein complexes are separated based on their sedimentation rates, where heavier complexes sediment faster. DGU is an excellent technique for separating large protein complexes, ribosomes, membrane vesicles and subcellular organelles. DGU is also suitable to separate cleared cell lysates as well as immunoprecipitation (IP)-captured protein complexes (Lee and Skalnik, 2013; Caudron-Herger et al., 2019). After separation, most of resolved protein complexes remain in near-native states. In a recent study, a reliable DGU-based CP variant, referred to as quantitative density gradient analysis by mass spectrometry (qDGMS) has been developed to study the human mitoribosome (Palenikova et al., 2021a). qDGMS combines stable isotope labeling by amino acids in cell culture (SILAC) and DGU followed by fractionation and LC-MS/MS analysis. SILAC is a MS-based technique that quantifies the differences in protein abundance/expression among biological samples (Ong et al., 2002). In conventional SILAC, two different cell lines/strains are cultured using media supplemented with either "heavy" or "light" essential aminoacids that are labeled with non-radioactive isotopes (e.g., ^{13}C, ^{2}H, ^{18}O, ^{15}N) or unlabeled, respectively (Geiger et al., 2011). The specific labeled aminoacids are hence incorporated into all cell proteins during cell growth. Proteins of cell lysates/fractions obtained from the two samples are mixed (1:1), digested and analyzed together by LC-MS/MS. The isotope-labeled peptides appear in MS spectra as pairs with identic chemical composition but different masses. Ratios of intensities for the many identified peptide pairs thus denote the respective changes in protein abundance between samples. Incorporation of SILAC not only in qDGMS but also in classic CP allows duplexing, MS time-saving and, most important, higher accuracy of quantification in proteomic analysis of two experimental conditions (Palenikova et al., 2021a; Palenikova et al., 2021b).

A major challenge of DGU relies on retrieving of fractions without manual disturbance of the resolved layers. To account for this issue, several strategies and devices have been developed, including commercially available automatic fractionators and freezing the gradient after centrifugation followed by cryo-slicing to fractionate samples consistently (Yu et al., 2016). Location of resolved proteins by DGU is considerably more spread when compared to native-PAGE or SEC, which means that increasing the number of fractions does not necessarily lead to higher resolution. Furthermore, sedimentation rates do not only depend on molecular masses of protein particles but also on shape and densities from both the particles and fluid used for making the gradient (Cole et al., 2008). For these reasons, co-migration of identified proteins by this CP setup does not immediately represent actual associations rather than merely similar sedimentation rates.

2.3 Other Mass Spectrometry-Based Approaches Related to Complexome Profiling

Additional untargeted MS-based assays have been described in the literature, which share the same principles of a CP experiment. The group of Matthias Mann developed protein correlation profiling (PCP) by combining DGU and quantitative MS to identify and validate several components of the human centrosome (Andersen et al., 2003). A few years later, Harner and co-workers applied PCP to discover the mitochondrial contact site (MICOS) complex (Harner et al., 2011). The further inclusion of hierarchical clustering and bioinformatic analysis of PCP data improved substantially this method leading to a broader characterization of both organelle and cell complexomes (Foster et al., 2006; Havugimana et al., 2012). PCP has also been related to co-fractionation coupled to MS (CoFrac-MS) experiments (Bludau, 2021). In CoFrac-MS, ion-exchange chromatography (IEX) or SEC have however been used for a higher resolution separation of protein complexes by their charges or hydrodynamic radii, respectively (Bludau and Aebersold, 2020). The combination of PCP/CoFrac-MS with other techniques, such as SILAC or stable isotope labelling in mammals (SILAM) have been proven valuable in proteome-scale interactome studies across cells (Kristensen et al., 2012) and tissues (Skinnider et al., 2021).

CP-like approaches using BN-PAGE followed by MS analysis have also been applied in different studies. A systematic proteomic analysis of series of 15 protein bands excised from individual BN-gel lanes allowed the identification of subunits of the mitochondrial respiratory complexes and was helpful to correctly re-assign NDUFA4, previously misidentified as a complex I subunit, as a *bona fide* component of the cytochrome *c* oxidase (Balsa et al., 2012). Likewise, Cogliati and co-workers separated mitochondrial proteins from mice by BN-PAGE and cut the strips in 26 slices before MS identification (Cogliati et al., 2016a) using a data-independent scanning (DiS) method (Guaras et al., 2016). The latter workflow has recently been standardized and referred to as Blue-DiS (Calvo et al., 2020).

2.4 Complexome Profiling Data Analysis and Visualization

Huge output files are obtained in CP studies after protein searches, which usually contain all data necessary for further analysis, including identified protein groups, unique peptides, sequence coverage, MS/MS counts, scores, LFQ/iBAQ values from each fraction, etc. The most common visualizations of a complexome profile are heatmaps accompanied by line charts plotting the LFQ/iBAQ values throughout the fractions (**Figure 1**). Complexome profiles of a short set of proteins can be manually generated and analyzed. Yet, the large volume of protein identifications in CP datasets makes full manual inspection impractical. In the last years, several tools have been specifically designed for automated processing and exploration of CP datasets.

ComplexomeMap has been developed as an online public platform for mining the mitochondrial complexome of plants *Arabidopsis thaliana* and *Viscum album* (Senkler et al., 2017). NOVA is a user-friendly software to perform cluster analysis, mass calibration, normalization, visual inspection, links to protein databases and comparison of experimental conditions (Giese et al., 2015). The software COPAL has proven helpful for analyzing multiple CP datasets, aligning experimental replicates and detecting significantly affected protein complexes (Van Strien et al., 2019). It also generates files that can be directly used for gene set enrichment analysis. ComPrAn, a Shiny R app, has been developed for analyzing qDGMS data; this tool enables analysis of peptide-level data, normalization, clustering, visualization options and a graphical user interface (Palenikova et al., 2021a). In addition, ComPrAn is particularly useful to analyze proteomic data obtained from SILAC-treated samples. ComplexFinder, a Python-based software suit, has recently been released to analyze fractionation of native protein complexes, particularly from BN-PAGE- or SEC-based CP experiments (Nolte and Langer, 2021). This tool allows machine learning-based prediction of potential protein-protein interactions (PPIs) and high flexibility in CP data analysis. ComplexFinder also provides improved peak-centric quantification and kinetic modelling, protein connectivity networks and compatibility with different quantification strategies. CCprofiler is a robust R package for analyzing co-fractionation MS datasets, which has been originally designed for SEC-SWATH-MS (Heusel et al., 2019). CCprofiler and its web interface, SECexplorer, offer multiple functions, such as quality control and filtering for less erroneous assignment of protein interactors, usage of curated reference datasets, protein quantification, protein- and complex-centric data analysis and visualization.

Other software available for proteomic and interactome analysis can also be used for CP data processing. For instance, free tools such as Perseus (Tyanova et al., 2016b), PrInCE (Stacey et al., 2017) and EPIC (Hu et al., 2019) may provide suitable options for visualization, protein quantification, statistical analysis, prediction of PPIs from co-fractionation data, obtention of supporting info from public repositories and/or cross-omics comparisons.

2.5 Storage, Sharing and Examination of Complexome Profiling Data

Although CP datasets contain a long list of identified proteins, the majority of studies have focused only on a small subset of the identified protein complexes. Naturally, the amount of information contained in those datasets could be useful not only to unveil uncharacterized PPIs, but also to validate previously reported protein complexes. All these under-explored results thus represent a valuable source of information, which could be reused and further mined by other researchers. To achieve this purpose, the ComplexomE profiling DAta Resource (CEDAR) has recently been established as the first website for depositing and sharing CP data (van Strien et al., 2021). A standardized format containing the minimum information required for a CP experiment (MIACE) ensures compatibility and correct retrieval of data. CEDAR is able to link access to raw MS data and other files deposited parallelly in the known repository PRIDE (ProteomeXchange consortium) (Perez-Riverol et al., 2019). Additionally, CEDAR has a profile viewer tool that allows users to examine CP data directly on the website. Since its release in June 2020, 24 complete CP experiments encompassing a total of 146 samples have been submitted to CEDAR (web V1.1, accessed October 6, 2021). CP data from 11 species covering different life domains are already accessible (**Figure 2**).

It should be mentioned that the data available through CEDAR are just a fraction of the CP studies reported in the literature. At present, ~145 publications mentioning the term "complexome" (or complexomic/complexomics) have been found in PubMed (NCBI) records; ~62 publications correspond to CP-related studies, reviews, methods and software tools (**Figure 3**). In ~40 and ~18 publications, CP has been used for mitochondrial research or to study protein complexes involved in disease, respectively (**Figure 3**). As the number of CP publications continues accelerating, it is desirable that future studies using this approach would also share resultant CP datasets publicly through CEDAR to simplify their reuse by the scientific community and keep expanding its valuable offer.

3 COMPLEXOME PROFILING AS A TOOL TO INVESTIGATE MITOCHONDRIAL PROTEIN COMPLEXES

Mitochondria are traditionally known as the eukaryotes' "powerhouses" since they contain all the enzymes required to generate ATP via the oxidative phosphorylation (OXPHOS) pathway. This process is catalyzed canonically by four respiratory chain complexes (I, II, III and IV) and a F_1F_O-ATP synthase (complex V). Complexes I, III and IV couple the energy released during electron transfer to oxygen to the generation of an electrochemical gradient of protons across the inner mitochondrial membrane (IMM). The proton gradient not only drives the synthesis of ATP, but also other processes such as metabolite transport, protein import, redox and Ca^{2+} homeostasis, fusion/fission, signaling and cell death. These organelles do also contain their own genome, also known as mitochondrial DNA (mtDNA), which encodes for a few but essential subunits of OXPHOS complexes. The roles of mitochondria are thus not limited to their energy duties. These organelles are multi-functional "hubs" critical to almost every cell process.

Despite of the great progress in molecular characterization and structure elucidation of numerous mitochondrial protein complexes, mostly OXPHOS- and mitoribosome-related proteins, a large number of mitochondrial PPIs remain elusive. In the last years, however, CP has proven valuable for identifying novel protein interactors, validating previous results and shedding light on intricate assembly pathways. In this section, we summarize these findings and describe how CP has boosted the analysis of protein complexes in the mitochondrial research field. Expectedly, most of these findings are again related to

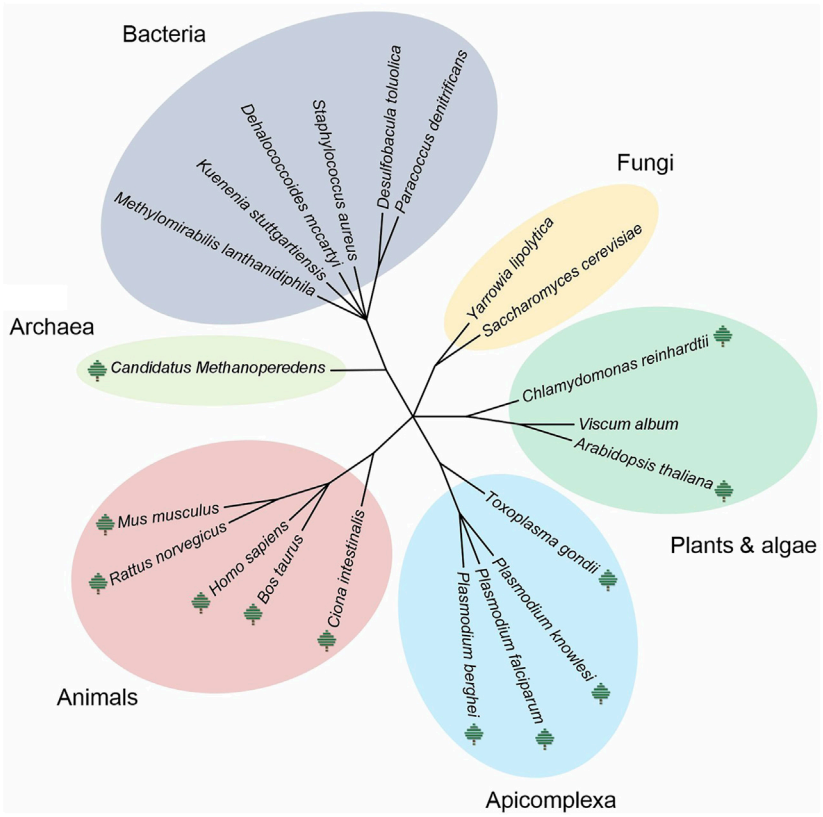

FIGURE 2 | Different species used in complexome profiling studies. Phylogenetic tree including all the species reported in complexome profiling (CP) studies until November 2021. As it can be seen, CP has been used to study multiple species covering the three different life domains. Where a tree-like icon is shown next to the species name, CP data are currently available on CEDAR (https://www3.cmbi.umcn.nl/cedar/browse/). The template of the tree was generated online using Interactive Tree of Life (iTOL) v6.3.3 (https://itol.embl.de/) and further edited manually.

components or mediators of the assembly of OXPHOS complexes, energy metabolism-linked proteins and mitoribosomes.

The first groups that established CP have also been interested in the many features of OXPHOS and in particular of complex I (CI). CI is the largest redox enzyme of the mitochondrial respiratory chain constituted by ~45 subunits depending on the species. CI generates proton-motive force driven by the transfer of electrons from NADH to ubiquinone (Hirst, 2013). Although the redox features and composition of mitochondrial CI in several species were already known by the start of the 2010s, major queries on this enzyme had yet unresolved: its entire 3D structure, its energy-conversion mechanism and how it assembles. To help tackle the last one, the formal introduction of CP by Heide and co-workers was useful to identify TMEM126B interacting with the known CI assembly factors NDUFAF1, ECSIT and ACAD9 (Heide et al., 2012). *TMEM126B* knockdown in 143B osteosarcoma cells led to ~95% specific decrease in CI-containing supercomplexes, i.e., supramolecular associations of complexes I, III and IV. These results thus proposed TMEM126B as a CI assembly factor. In an earlier report using HEK293 cells, Wessels and co-workers identified with a similar approach two other assembly factors of CI: C6ORF66 and C3ORF60 (Wessels et al., 2009), currently known as NDUFAF4 and NDUFAF3, respectively. In this study, mitochondrial proteins were separated by BN-PAGE followed by LC-MS/MS identification, but comparison of migration patterns was limited to the use of PCP.

A few years later, a dynamic CP strategy was successfully implemented to describe the step-by-step integration of the subunits, assembly factors and the different assembly intermediates of human CI (Guerrero-Castillo et al., 2017a). The authors used CP data from time-based mitochondrial translation recovery to describe a number of assembly intermediates of CI accumulating at various timepoints after removal of chloramphenicol, a reversible inhibitor of mitoribosomes (Ugalde et al., 2004). These data corroborated the long time proposed modular assembly pathway of CI, which basically involves the coordinated formation and pre-assembly of its functional modules, N, Q, P_P and P_D, before forming the entire enzyme. This study also provided insight into the specific involvement of earlier reported assembly factors and novel interactors. Complex IV (CIV) assembly-related chaperone COA1 and TMEM186 were clearly found associated with membrane arm intermediates that also interact with TMEM126B, NDUFAF1 and ECSIT. At present, all these

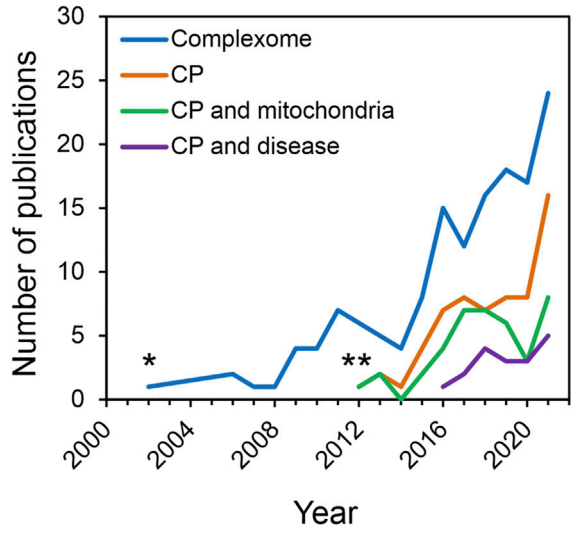

FIGURE 3 | Reported studies in the literature including the complexome profiling approach. Since the introduction of the term "complexome" back in 2002 (*), ~145 publications referring to this term have been reported in PubMed (NCBI) (blue line). Formal introduction of complexome profiling (CP) in 2012 (**). In less than 10 years, ~62 studies have applied CP (orange line), where ~40 and ~18 publications are related to mitochondrial research (green line) or to protein complexes involved in disease (purple line), respectively. The positive tendency of multiple groups around the world implementing CP to study protein-protein interactions in both fundamental- and disease-related studies as a standard method is incontrovertible.

proteins have been recognized as true components of the so-called mitochondrial CI assembly (MCIA) complex (Formosa et al., 2020). ATP5SL clustered with FOXRED1, another CI assembly factor. However, ATP5SL disruption did not lead to CI deficiency (Andrews et al., 2013) and its involvement in the assembly pathway is thereby unclear. Complex V assembly-involved protein TMEM70 was also identified in assembly intermediates of CI. To further explore the putative role of TMEM70 on CI assembly, Sánchez-Caballero and co-workers performed a study including proximity-dependent biotin identification (BioID), co-evolution analyses and CP (Sanchez-Caballero et al., 2020). In this study, TMEM70 was found in close contact with subunits of complexes I and V, as well as the small mitoribosome subunit. The absence of TMEM70 resulted in slight depletion of fully assembled CI and accumulation of assembly intermediates of the distal part of the membrane arm of CI, whereas mature complex V (CV) content was ~70% lower than in the control cell line. These authors showed TMEM70 as a non-essential assembly factor of complexes I and V, and proposed a possible role in tethering mitoribosomes to the IMM during translation.

Apart from studies in human cells, CP has also been used to study the role of several accessory subunits of CI in different models. For example, Kmita and co-workers analyzed the assembly of CI in a deletion strain of the yeast *Yarrowia lipolytica* lacking the Zn^{2+}-containing subunit NUMM/NDUFS6 (Kmita et al., 2015). Absence of this subunit did not prevent formation of the entire CI, since a lower enzyme content and higher fraction of peripheral arm subcomplexes were observed. Unexpectedly, the almost fully assembled CI contained the assembly factor N7BML/NDUFAF2 bound instead of accessory subunit N7BM/NDUFAF12. Moreover, Angerer et al. implemented CP in a study on the mitochondrial acyl carrier proteins (ACPM) 1 and 2, which are accessory subunits of CI and contain LYR motifs (Angerer et al., 2014). Although ACPM1/2 are predominantly associated to CI, ACPM1 was also found as a free protein in the matrix and forming a complex with LYRM4(ISD11)/NFS1 involved in iron-sulfur cluster biosynthesis. Furthermore, two different groups in parallel unveiled the existence of two isoforms of the peripheral arm subunit NDUFV3 of CI in mammals (Bridges et al., 2017; Guerrero-Castillo et al., 2017b). An extra exon present in gene *NDUFV3* can be alternative spliced, hence generating short and long isoforms of ~10 and ~50 kDa, respectively. CP helped find a different expression of these isoforms in different tissues of bovine, mouse and rat as well as in cultured human cells. The canonical short isoform was predominantly identified in heart and skeletal muscle, whereas the large isoform was the foremost isoform in liver, brain and lung tissues. Both NDUFV3 isoforms can also be expressed at the same time and correctly assembled onto CI in some tissues; yet, one isoform predominated in each case.

Other OXPHOS complexes and their chaperones have also been explored by CP. Singhal et al. identified the product of ORF *YDR381C-A* as an assembly factor of yeast complexes III and IV (Singhal et al., 2017). This protein was renamed as cytochrome *c* oxidase interacting protein 1 (Coi1), which occurs only in fungi. Deletion of Coi1 resulted in severe alteration of mitochondrial function, diminished amounts of CIV-associated heme, defective assembly of complexes III, IV and their supercomplexes, as well as accumulation of assembly intermediates. Vidoni and co-workers reported that the short isoform of myofibrillogenesis regulator 1 (MR-1S) associates with chaperones PET100 and PET117 to mediate human CIV assembly (Vidoni et al., 2017). Authors implemented not only CP to study assembly intermediates accumulated in control and *MT-CO3* mutant cybrids, but also SILAC and quantitative MS.

CP has been helpful to better understand the formation of supercomplexes or respirasomes. The specific factors for mediating this process remain unclear. COX7A2L, also known as SCAFI, has been shown critical for the association of complexes III and IV (Perez-Perez et al., 2016). Its putative involvement in larger respirasome formation has also been reported (Lapuente-Brun et al., 2013). To better understand the role of SCAFI, Férnandez-Vizarra et al. explored the mitochondrial complexome of a SCAFI knockout human cell line by SILAC-based CP (Fernández-Vizarra et al., 2021). Absence of SCAFI resulted in marked loss of supercomplex III_2-IV, whereas CI-containing respirasomes were not affected. In contrast, authors showed that ~70% of respirasomes contained COX7A2 in either human cell line analyzed. This discrepancy has apparently been related to a tissue-specific expression of the two isoforms (Lapuente-Brun et al., 2013). On the other hand, Protasoni and co-workers demonstrated that absence of a fully assembled complex III (CIII) in a MT-CYB-deficient human cell

line stalled CI biogenesis by preventing the integration of its N-module (Protasoni et al., 2020). Although substantial accumulation of partially assembled Q/P intermediate was observed by SILAC-based CP, a slight fraction of CI could still be detected. Reasonably, respirasome assembly was totally lost in the mutant. Besides, assembly of CIV was affected since several COX subunits were found associated with CIII sub-assemblies; hence interfering their correct assembly. It has thus been proposed that human complexes I, III and IV assemble in a cooperative fashion, where CIII seems to be central.

Mitochondria are characterized by a highly folded IMM. These folds, called cristae, have emerged as dynamic compartments whose shape and dimensions influence structure and functioning of the OXPHOS system (Cogliati et al., 2016b). A key player in shaping cristae appears to be the MICOS complex, which also interacts with the sorting and assembly machinery (SAM) complex from the outer mitochondrial membrane (OMM) (Huynen et al., 2016). Interaction of these two complexes constitutes the mitochondrial intermembrane space bridging (MIB) complex (Ott et al., 2015). Since its relatively recent discovery (Harner et al., 2011), much of what we know about the MICOS complex has been derived from CP-based studies.

For instance, Weber and co-workers identified apolipoprotein O (APOO/MIC26) and apolipoprotein O-like protein (APOOL/MIC27) as potential components of the human MIB complex (Weber et al., 2013). Huynen and co-workers described the composition and apparent masses of the fully assembled MIB complex (2.2–2.8 MDa) and other putative assembly intermediates, e.g., the free MICOS complex (~700 kDa) (Huynen et al., 2016). Anand et al. identified MIC13 (QIL1) as a novel MICOS complex subunit (Anand et al., 2016). Deletion of MIC13 resulted in a smaller albeit still assembled MICOS complex while having no effect on integrity of OXPHOS complexes. They also demonstrated a disruptive effect of MIC13 deletion on cristae morphology accompanied by reduced respiratory capacity. The same group used a similar approach to characterize MIC26 and MIC27 (Anand et al., 2020). They showed negative effects on CV stability as well as cristae morphology defects both of which were much more pronounced in the double knockout than either single knockout, suggesting overlapping roles. Assembly of other MICOS components was however unimpeded by MIC26/27 knockouts, proposing these proteins are not essential for its assembly or stability. The link of MICOS components to CV was further explored by Eydt et al. (2017), showing that MIC10 comigrates with CV dimers. Additionally, they presented evidence that MIC10 acts antagonistically to MIC27 in negatively controlling CV oligomerization, while MIC27 appears to be a positive regulator. A recent paper by Bock and co-workers reported the interaction of PGC-1- and ERR-induced regulator in muscle 1 (PERM1) with multiple components of the MICOS/MIB complex as well as vimentin and ankyrin B in skeletal muscle from mouse (Bock et al., 2021). These findings suggested a novel mechanism to help understand not only the interconnection of mitochondria and sarcolemma but also mitochondria-cytoskeleton associations as well as the organization of a functional mitochondrial network in this tissue. Taken together CP has greatly aided our understanding of MICOS/MIB complex composition, the role of individual subunits and its interaction with OXPHOS complexes.

The IMM contains other key protein complexes involved in proteolytic events, fusion/fission of mitochondrial membranes, regulation of cristae morphology and cell signaling. Some of these proteins belong to the SPFH (stomatin, prohibitin, flotillin and HflC/K) family and usually arrange as large scaffolds. To have a clearer picture, Wai and co-workers implemented CP to unveil the interaction partners of stomatin-like protein 2 (SLP2) and at least two proteases, PARL and YME1L, in immortalized embryonic fibroblasts mitochondria (Wai et al., 2016). SLP2 works as a regulator of PARL, which also modulates other proteins such as PGAM5, PINK1 and OMA1. These interactions were suggested to occur in defined sites of the IMM and related to mitochondrial proteostasis, dynamics and cell survival. Similarly, Konig and co-workers identified MAIP1 (C2Orf47) as a novel *m*-AAA protease-binding protein in complexome profiles (Konig et al., 2016). MAIP1 was shown essential for regulating the assembly of subunit EMRE into mitochondrial Ca^{2+} uniporter (MCU) complexes.

CP has also played an important role in the field of plant and parasite mitochondrial biology. Using CP, Senkler and co-workers performed a systematic characterization of mitochondrial complexes in the plant *A. thaliana* (Senkler et al., 2017). CP data were also useful to update the subunit composition of OXPHOS complexes and identifying respective assembly intermediates. This group then used the same approach on mitochondria from the mistletoe *V. album*, revealing a highly unusual OXPHOS system (Senkler et al., 2018). This species completely lacks CI, the only multicellular eukaryote to date with this distinction; instead, *V. album* contains alternative NAD(P)H oxidoreductases. This species also expresses an alternative oxidase and its complexes III and IV are firmly associated as supercomplexes. In comparison to *A. thaliana*, the abundance of complexes II and V was particularly low, suggesting a shift in stoichiometry of the OXPHOS complexes in the IMM of this plant. Rugen and co-workers took a more focused CP strategy to investigate the composition of the mitoribosome in *A. thaliana* (Rugen et al., 2019). Utilizing LP-BN-PAGE- and DGU-based CP setups, several non-conventional proteins were found attached to the mitoribosome, mostly from the class of pentatricopeptide repeat proteins that seem to be involved in RNA processing and protein maturation. Presence of these additional interactors results in a larger mitoribosome with unusual large and small subunits of ~3 and ~5.7 MDa, respectively. Additional functions are thus likely incorporated into the plant mitoribosome.

Due to their extreme divergence, apicomplexan parasites of the genera *Plasmodium* and *Toxoplasma* that cause the infectious diseases malaria and toxoplasmosis, respectively, remain poorly understood. In fact, more than one-third of their genes still lack any functional annotation (Aurrecoechea et al., 2009; Harb et al., 2020). To help narrow this gap, Evers et al. and Maclean et al. obtained evidence for highly divergent composition of the mitochondrial OXPHOS complexes in *Plasmodium falciparum* and *Toxoplasma gondii*, respectively (Evers et al., 2021; Maclean

TABLE 1 | Complexome profiling studies in biomedical research.

Gene	Disease/Impairment	OMIM[a]	Clinical features/Phenotype	Pathway/ Mechanism	Effect of mutation	Sample type	CEDAR/ PRIDE entry[b]	References
Mitochondrial CI deficiency								
TMEM126B	CI deficiency	# 618250	Muscle weakness, elevated lactate and alanine	Assembly of CI, peripheral arm, P-proximal ND2-module	Accumulation of assembly intermediates of CI	Patient fibroblasts	n.d.	Alston et al. (2016), Sánchez-Caballero et al. (2016b), Fuhrmann et al. (2018)
NDUFAF8	Leigh Syndrome, CI deficiency	# 618776	Encephalopathy, seizures, neuroradiologic features	Assembly of CI, Q-module (?)	Decreased CI activity and abundance, impaired assembly of the Q-module	Patient fibroblasts	CRX15	Alston et al. (2020)
NDUFC2	Leigh Syndrome, CI deficiency	# 619170	Developmental regression, lactic acidosis, neurologic deterioration	CI subunit, P-proximal ND2-module	Accumulation of assembly intermediates of CI	Patient fibroblasts	PXD014936	Alahmad et al. (2020)
NDUFA6	CI deficiency	# 618253	Delayed development, neurologic deterioration, optic atrophy	CI subunit, Q-module	Destabilization of the Q-module of CI	Patient fibroblasts	n.d.	Alston et al. (2018)
TMEM70	CV deficiency	# 614052	Mitochondrial encephalocardio-myopathy, 3-methylglutaconic aciduria, CV deficiency	Assembly of CI and CV	Decreased CI and CV activities, accumulation of subassemblies of CI and CV	HAP1, TMEM70-KO	CRX10	Sanchez-Caballero et al. (2020)
DNAJC30	LHON	# 619382	Bilateral vision loss	CI maintenance	Slower turnover of the N-module subunits	Patient fibroblasts, HEK293, DNAJC30-KO	PXD021385 PXD021386 PXD021500 PXD022340 PXD022339 PXD021548 PXD021499	Stenton et al. (2021)
CLPP	Perrault syndrome	# 614129	Sensorineural hearing loss, premature ovarian failure	CI turnover	—	HEK293-KO, MEF-KO, Mouse heart-KO	CRX12	Szczepanowska et al. (2020)
Mitochondrial CIII deficiency								
MT-CYB	LHON	* 516020	Weakness, ataxia, neurologic involvement; combined respiratory chain deficiency	CIII subunit	Decreased enzyme activities of CI, CIII and CIV	143B-derived cybrid cells	CRX19, CRX26	Protasoni et al. (2020), Palenikova et al. (2021b)
TTC19	Mitochondrial complex III deficiency nuclear type 2 (MC3DN2)	# 615157	Motor disability with ataxia, apraxia, dystonia and dysarthria. Cognitive impairment and axonal neuropathy	CIII maturation	Decreased CIII activity due to failure to remove inhibitory N-terminal fragments of UQCRFS1	Mouse brain mitochondria	n.d.	Bottani et al. (2017)
Mitochondrial CIV deficiency								
COX4I1	CIV deficiency	# 619060	Failure to thrive, neurologic involvement, hypotonia, seizures, cerebellar atrophy	CIV subunit	Impaired assembly of CIV and CI	HEK293-KO	CRX25	Cunatova et al. (2021)
COX4I2	Exocrine pancreatic insufficiency, dyserythropoietic anemia, and calvarial hyperostosis	# 612714	Steatorrhea, anemia, failure to thrive	CIV subunit	Impaired assembly of CIV and CI	HEK293-KO	CRX25	Cunatova et al. (2021)

(Continued on following page)

TABLE 1 | (*Continued*) Complexome profiling studies in biomedical research.

Gene	Disease/Impairment	OMIM[a]	Clinical features/Phenotype	Pathway/ Mechanism	Effect of mutation	Sample type	CEDAR/ PRIDE entry[b]	References
MT-CO1	LHON, Mitochondrially inherited non-syndromic sensorineural deafness	# 535000, # 500008, * 516030	Heterogeneous variety of neuromuscular disorders	CIV subunit	Loss of CIV holoenzyme; destabilization of CI-$CIII_2$ supercomplex (S_0)	143B-derived cybrid cells	CRX17	Lobo-Jarne et al. (2020)
MT-CO2	CIV deficiency	* 516040	Progressive gait ataxia, cognitive impairment, bilateral optic atrophy, pigmentary retinopathy	CIV subunit	Loss of CIV holoenzyme	143B-derived cybrid cells	CRX17	Lobo-Jarne et al. (2020)
COX7A2L	—	* 605771	—	Stabilization of SCs containing $CIII_2$ and CIV	Aberrant supercomplexes formation (?)	HEK293, SCAFI-KO	CRX28	Fernández-Vizarra et al. (2021)
Combined OXPHOS deficiency								
MRPS2	Combined OXPHOS complexes deficiency	# 617950	Mild multisystem disease; Sensorineural hearing loss, hypoglycemia; Mitochondrial dysfunction	Component of the 28S mitochondrial ribosomal subunit	Decreased abundance of OXPHOS complexes, and destabilization of the 28S mitochondrial ribosomal subunit	Patient fibroblasts	CRX22	Gardeitchik et al. (2018)
MRPS22	Combined OXPHOS complexes deficiency; ovarian dysgenesis	# 611719, # 618117	Cardiomyopathy, metabolic acidosis, reduced mitochondrial OXPHOS complexes activities	Component of the 28S mitochondrial ribosomal subunit	Decreased abundance of OXPHOS complexes, and destabilization of the 28S mitochondrial ribosomal subunit	Patient fibroblasts	CRX22	Gardeitchik et al. (2018)
TAZ	Barth syndrome	# 302060	3-methylglutaconic aciduria, neutropenia, dilated cardiomyopathy, skeletal myopathy	Cardiolipin remodeling/ Membrane curvature	Widespread reorganization of the mitochondrial complexome	Patient fibroblasts	CRX8	Chatzispyrou et al. (2018)
METTL15	—	* 618711	—	N4-methylcytidine methyltransferase	Decreased mitochondrial protein biosynthesis	HAP1-KO HeLa	CRX13	Van Haute et al. (2019)
ERAL1	Perrault syndrome	# 617565	sensorineural deafness, ovarian dysgenesis	28S mitochondrial ribosomal subunit assembly	Decreased 28S mitochondrial ribosomal subunit abundance	Patient fibroblasts	n.d.	Chatzispyrou et al. (2017)
mtDNA loss	—	—	—	OXPHOS complexes I, III, IV, V, and t- and rRNAs	Dysfunctional mitochondrial energy metabolism	Rho0 cells	CRX32	Guerrero-Castillo et al. (2021b)
Other								
CLPB	MEGCANN	# 616271	3-methylglutaconic aciduria, neutropenia, neurologic symptoms	Intermembrane space ATP-dependent dissagregase	Aberrant interaction between CLPB and HAX1	Patient fibroblasts	n.d.	Wortmann et al. (2021)
ATP6V1A	Cutis laxa, developmental and epileptic encephalopathy	# 617403, # 618012	Wrinkled skin, hypotonia, dysmorphic facial features, cardiovascular and neurologic involvement	V-type ATPase subunit, V_1 segment	Destabilization of V-type. ATPase holocomplex	Patient fibroblasts	CRX11	Van Damme et al. (2017)
ATP6V1E	Cutis laxa	# 617402	Wrinkled skin, hypotonia, cardiopulmonary involvement	V-type ATPase subunit, V_1 segment	Destabilization of V-type, ATPase holocomplex	Patient fibroblasts	CRX11	Van Damme et al. (2017)
ATP6V0A2	Cutis laxa	# 219200				Patient fibroblasts	CRX11	Van Damme et al. (2017)

(Continued on following page)

TABLE 1 | (*Continued*) Complexome profiling studies in biomedical research.

Gene	Disease/Impairment	OMIM[a]	Clinical features/Phenotype	Pathway/ Mechanism	Effect of mutation	Sample type	CEDAR/ PRIDE entry[b]	References
			Wrinkly skin syndrome; varying degrees of growth and developmental delay and neurologic abnormalities	V-type ATPase subunit, V_O segment	Decreased abundance of V-type ATPase holocomplex			
PI4K2A	Cutis laxa	* 609763	Wrinkled skin, choreoathetoid movement disorder, dysmorphic features and intellectual disability	Phosphoinositide lipids regulation	Impaired intracellular signaling and trafficking	Patient fibroblasts	n.d.	Mohamed et al. (2020)
PEX19	Zellweger syndrome	# 614886	Hypotonia, seizures, craniofacial anomalies, neuronal migration defects, hepatomegaly, chondrodysplasia punctate	Peroxisome biogenesis	Impaired import of peroxisomal membrane proteins	Wild-type yeast and single and double deletion strains for PEX19 and ATAD1 yeast orthologs, *pex19*Δ and *msp1*Δ, respectively	PXD024625	Nuebel et al. (2021)

[a]*Online Mendelian Inheritance in Man® (OMIM); #: Phenotype descriptive entries, *: Gene entries.*

[b]*CEDAR entries correspond to CRX codes, whereas PRIDE (ProteomeXchange) entries correspond to PXD codes.*

Mitochondrial OXPHOS complexes are shown as: CI, complex I; CIII or $CIII_2$, complex III; CIV, complex IV and CV, complex V. Abbreviations; KO, knockout; MEGCANN, 3-methylglutaconic aciduria, type VII, with cataracts, neurologic involvement and neutropenia; LHON, Leber hereditary optic neuropathy; n.d., not deposited.

et al., 2021). More than 30 novel subunits across complexes II, III, IV and V with no recognizable orthologs outside of the myzozoan phylum could be identified by CP. These novel subunits did not only replace subunits typically observed in standard models, but also increased the size of *P. falciparum* OXPHOS complexes by around 50, 50, 130 and 70% as compared to complexes II, III, IV and V from mammalian mitochondria, respectively. This was consistent with the observations in *T. gondii*, thus making apicomplexan OXPHOS complexes the largest described to date. Furthermore, abundance of OXPHOS complexes was ~32 fold increased in the transmissible gametocyte stages compared to the pathogenic asexual stages of *P. falciparum* (Evers et al., 2021). This finding offered protein-level support for the long-standing hypothesis that malaria parasites undergo a metabolic switch towards mitochondrial catabolism to facilitate their transmission back to the insect vector (MacRae et al., 2013). Despite its relatively recent introduction to the field of parasite research, CP has already provided valuable data for mapping a number of previously unknown interactors to protein complexes and biological processes. As these novel additions are unlike what is known from standard models, it opens the door for new discoveries, even in pathways as fundamental as respiration.

4 THE MITOCHONDRIAL COMPLEXOME AND HUMAN DISEASE

In the last years, several metabolic diseases have been characterized along with accompanying complexome studies of human subjects carrying mutations in subunits of the OXPHOS complexes, assembly factors or proteins required for efficient mitochondrial protein biosynthesis. Most of these studies involved patients with metabolic disorders that affect mitochondrial processes leading to heterogeneous clinical manifestations ranging from mild to severe phenotypes. These studies analyzed subcellular preparations from primary skin fibroblasts from patients and controls, or from cell lines with genetic mutations/deletions used as disease models. CP analysis revealed either changes in abundance of specific protein complexes, indicating alterations of their relative steady-state levels in comparison to the controls, or molecular mass shifts resulting from the loss of protein components or from destabilization of the complexes. Beyond the described main alteration of the complex directly involved with the respective genetic mutation, an enormous amount of information can be retrieved from the deposited complexome data of these studies that could potentially be re-analyzed and investigated, for instance, in relation to the clinical features of these patients. Such in-depth characterization of the mitochondrial proteome at the level of macromolecular complexes in disease states may conceivably help uncover molecular basis and consequences of metabolic disorders and, importantly, could serve to identify molecular targets for developing novel therapeutic strategies. In this section, we summarize studies of genetic defects causing metabolic diseases in human subjects and mutations in model organisms analyzed to date by CP (**Table 1**).

4.1 Complex I Deficiency

CI deficiencies may potentially originate from genetic defects in either the seven genes encoded in the mtDNA or in the 37 subunits and the increasing number of assembly factors encoded in the nuclear DNA (Fassone and Rahman, 2012; Sánchez-Caballero et al., 2016a). Pathogenic mutations in patients have been found in the majority of CI subunits and in many assembly factors (Rodenburg, 2016), and the number of mutations identified continuously grows. Since TMEM126B was the first assembly factor of CI identified by CP, it was not unexpected that the first complexomes from patient fibroblasts with genetic alterations described in the literature belonged to subjects harboring mutations in this gene. Independently, two research groups described six (Alston et al., 2016) and three (Sánchez-Caballero et al., 2016b) subjects, respectively, presenting isolated CI deficiency with muscle weakness in most cases and with recessive mutations, evidenced by whole exome sequencing, in the gene encoding TMEM126B. Complexome profiles of three subjects revealed aberrant migration patterns of CI subunits with decreased abundance of mature CI-containing supercomplexes at ~1.7 MDa and accumulation of assembly intermediates. In both studies, increased steady-state levels of subunits belonging to the Q-module plus assembly factors NDUFAF3 and NDUFAF4, and to the P-distal ND4 module indicated stalled assembly intermediates of these unaffected modules, suggesting that TMEM126B takes part, together with the other MCIA complex components, ACAD9, NDUFAF1 and ECSIT, in the assembly of the P-proximal ND2 module. Complementation of patient fibroblasts using lentiviral expression of wild-type TMEM126B partially restored the abundance of CI-containing supercomplexes and decreased the abundance of Q- and P-module assembly intermediates, validating its role as assembly factor. Notably, specific ubiquitination and further degradation of this assembly factor has been implicated in a regulatory mechanism to decrease CI content and consequently oxygen consumption under hypoxic conditions (Fuhrmann et al., 2018).

Complexome profiles of patient fibroblasts with mutations either in a subunit or in an assembly factor of the Q-module, NDUFA6 and NDUFAF8, respectively, proved useful to corroborate the pathogenicity of the respective mutation and for pointing out the stage in which CI assembly was stalled. Bi-allelic mutations in NDUFA6, a LYR-motif subunit important for proper functioning of ubiquinone redox chemistry (Galemou Yoga et al., 2020), were found responsible for defects in CI assembly (Alston et al., 2018). In one of the three subjects studied, it has been found a decrease not only in the subunits of the Q-module, NDUFA6, NDUFA7 and NDUFA12, but also in subunits belonging to the N-module, correlating with the more severe phenotype observed in this subject. Of note, in these three patients, assembly factor NDUFAF2, which is known to interchange for subunit NDUFA12 in a late assembly step (Pereira et al., 2013), remained to some extent bound to CI intermediates, indicating that also in the other two subjects N-module incorporation was inefficient. On the other hand, NDUFAF8 has been identified to physically interact with NDUFAF5 (Floyd et al., 2016), an assembly factor of CI required to hydroxylate an arginine residue of the Q-module subunit NDUFS7 (Rhein et al., 2016). Alston and co-workers identified three subjects presenting Leigh syndrome with bi-allelic mutations in NDUFAF8 causing isolated CI deficiency (Alston et al., 2020). Complexome profile of one of the patients revealed decrease abundance of CI-containing supercomplexes. Consistent with the role of this protein in early CI assembly, NDUFAF8-mutated patient fibroblasts showed incomplete formation of the Q-module since neither its signal nor the fraction of this module holding assembly factors NDUFAF3/4 were observed. These fractions are visible even in control cells where CI assembly process occurs normally; in particular the more prominent one including the assembly factors. In contrast, accumulation of the earliest Q-module sub-assembly formed only by subunits NDUFA5, NDUFS2 and NDUFS3 has been described. In addition, accumulation of the P-distal ND4 module has also been reported.

Extending the genotype of CI deficiency, pathogenic mutations in subunit NDUFC2 have been identified in two unrelated children presenting Leigh syndrome (Alahmad et al., 2020). CP analysis from both subjects indicated severe impairment of CI assembly since abundance of CI-containing supercomplexes decreased prominently. In addition, intermediates composed by subunits of the Q-module, the Q/P-proximal module and the P-distal ND4 module accumulated, suggesting that stalling of CI assembly in these patients occurred at the intermediate stage (Guerrero-Castillo et al., 2017a). Comparably, mutations in the gene encoding TMEM70 have been identified in patients with deficiencies in complexes I and V (Jonckheere et al., 2011). The importance of TMEM70 in CV assembly has become clear from many mutations identified in human subjects (Cízková et al., 2008; Honzík et al., 2010), but recently in-depth analyses of complexome profiles delineated the role of TMEM70 in the formation of the F_1-c intermediate (Sanchez-Caballero et al., 2020). In regard to CI however, accumulations of assembly intermediates corresponding to the Q/P-proximal module as well as to the P-distal ND5 module, evidenced by complexome profiling of TMEM70 knockout HAP1 cells, indicated stalling of CI assembly at the binding of P-distal ND4 module to these intermediates (Sanchez-Caballero et al., 2020).

CI deficiency may not exclusively originate from pathogenic mutations in structural components and assembly factors, but also from mutations in genes involved in the maintenance and repair of damaged subunits. In an exhaustive study including 29 families (Stenton et al., 2021), Stenton and co-workers identified mutations in DNAJC30 as a cause of LHON syndrome. Co-migration of DNAJC30 with OXPHOS supercomplexes was identified in the control but not in the patient complexome profile. The abundance of CI assembled into supercomplexes, slightly higher in the patient samples, excluded a role of DNAJC30 in the assembly of CI. Instead, turnover of subunits of the N-module of CI that are more frequently interchanged during optimal maintenance was slowed down, implicating DNAJC30 in a repair mechanism of CI still associated into the supercomplex. Interestingly, the ATP-dependent serine protease CLPP, whose mutations in humans are known to cause Perrault

syndrome (Jenkinson et al., 2013), has also been implicated in CI repair by selectively replacing subunits of the N-module that are exposed to oxidative damage (Szczepanowska et al., 2020).

4.2 Complex III Deficiency

Proper assembly of CIII is not only important for generation of proton-motive force driven by the enzymatic oxidation of ubiquinol molecules produced by multiple dehydrogenases localized in the IMM, but also, at the core of respiratory supercomplexes, for structural stabilization of complexes I and IV. This phenomenon has been observed in several CIII-deficient patients where the activity and content of CI and CIV were concomitantly decreased (recently reviewed by Vercellino and Sazanov, 2021). In addition, a SILAC-duplexed CP study of cells lacking subunit cytochrome *b* due to a 4-bp deletion in *MT-CYB* and therefore unable to form holo-complex III, was consistent with a role of CIII-containing supercomplexes in CI maturation, since a late assembly intermediate containing assembly factor NDUFAF2 accumulated in cells with mutated cytochrome *b* (Protasoni et al., 2020). In contrast, mutations that partially affect the enzymatic activity of CIII, but not its assembly, do not compromise the stability and activity of CI and CIV. For instance, using a mouse model of CIII deficiency by deletion of TTC19, a protein involved in the removal of inhibitory proteolytic fragments of the Rieske iron-sulfur protein from the holo-complex, Bottani and coworkers showed that while the activity of CIII decreased in the tissues tested, the content and activity of CI and CIV were hardly altered (Bottani et al., 2017).

4.3 Complex IV Deficiency

Respiratory complex IV is a terminal oxidase that transfers electrons from soluble cytochrome *c* to oxygen, which also generates proton-motive force. Although no complexomes from patients with mutations in subunits or assembly factors of CIV have been described so far, multiple cell lines representing disease models of its deficiency have lately been characterized by CP. A complexome study of COX4I1/2 double knockout using HEK293 cells illustrated the interdependency of OXPHOS complexes in terms of their assembly and stability (Cunatova et al., 2021). The lack of subunits COX4I1/2 completely abolished formation of CIV. This is consistent with the role of this subunit forming an early assembly intermediate with COX5. In the absence of CIV, a pronounced decrease in the abundance of the CIV-containing supercomplexes have certainly been evidenced, whereas supercomplex I-III_2 (S_0) and complexes II, III and V remained unaffected. Notably, even if complex V forms large macromolecular assemblies that are independent of respirasomes, its interconnection to other OXPHOS complexes became apparent by the accumulation in COX4I1/2 double knockout cells not only of the F_1 segment, but also of the early F_O intermediate containing subunits ATP5MF, ATP5PB, ATP5ME and ATP5MG.

Similarly, Lobo-Jarne and co-workers analyzed the effects of the lack of CIV holoenzyme on the stability of respiratory complexes and respirasomes using trans-mitochondrial cybrids of human osteosarcoma 143B cells harboring nonsense mutations in mitochondrial genes *MT-CO1* and *MT-CO2* that resulted in truncated versions of subunits COX1 or COX2, respectively (Lobo-Jarne et al., 2020). In contrast to control 143B cells that, besides monomeric CIV, contained larger assemblies of this complex corresponding to IV_2, III_2-IV and respirasome I-III_2-IV (S_1), in cybrids with truncated COX1 and COX2 no CIV was formed but S_0 remained stable. In the absence of COX1, the only detected assembly intermediate contained subunits COX4 and COX5, whereas the lack of signals of all other unassembled CIV subunits indicated their degradation. Conversely, cells lacking COX2 displayed, in addition to the heterodimer intermediate formed by COX4 and COX5, a larger intermediate containing also subunit COX1. Importantly, these authors described the formation of a heavier S_0 containing several subunits and assembly factors of CIV, which has also been corroborated by bidirectional co-IP assays. The association of this partially assembled unconventional intermediate of CIV bound to S_0 exemplified how alternative biogenesis of respirasomes could occur in disease-related conditions.

4.4 Combined Oxidative Phosphorylation Complexes Deficiency

The intricate assembly process of OXPHOS complexes requires not only expression and import of functional subunits as well as ancillary proteins produced by cytosolic ribosomes, but also proper expression and insertion of the mtDNA-encoded components. Therefore, diseases featured by energy metabolism alterations may also result from mitochondrial translation deficits. In mammals, the 13 mtDNA-encoded subunits of OXPHOS complexes are synthesized by the mitochondrial translation machinery (Hällberg and Larsson, 2014). This includes the small and large subunits of the mitoribosome [mt-SSU (28S) and mt-LSU (39S), respectively], a set of tRNAs and many regulatory proteins required for the proper functioning and fine tuning of this process (Kummer and Ban, 2021). Taking into account all the factors involved in mitochondrial translation, it is thus not surprising that an increasing number of genetic mutations causing multiple OXPHOS complex deficiencies due to impaired mitochondrial protein biosynthesis have been identified (Pearce et al., 2013).

Perrault syndrome is a rare genetic mitochondrial disorder with a relatively mild phenotype characterized by sensorineural deafness and ovarian dysgenesis. Genetic mutations in several genes encoding mitochondrial and peroxisomal proteins have been identified as direct causes for this disease, including CLPP, HSD17B4, LARS2, HARS2 and TWNK. Chatzispyrou et al. identified two unrelated female patients presenting Perrault syndrome symptoms where whole exome sequencing revealed no mutations in any of the enlisted genes causing this syndrome (Chatzispyrou et al., 2017). Instead, a predicted pathogenic mutation in ERAL1, a chaperone of the 12S mitochondrial rRNA was identified. Complexome profiles of the two patients evidenced a pronounced decrease in the abundance of the mt-SSU, while the mt-LSU remained unaffected; however, very slight changes in OXPHOS complexes intensities have been detected. This correlated with the milder phenotypes of Perrault syndrome

patients, contrary to the clinical features observed when the mutations occurred in structural components of the mitoribosome, where multiple OXPHOS complex deficiencies manifested (Gardeitchik et al., 2018).

A study of two subjects with mutations in MRPS2, a structural component of the mt-SSU, has linked these mutations to combined OXPHOS complex defects with sensorineural hearing loss (Gardeitchik et al., 2018). The complexome profile of one of the subjects has been analyzed in parallel with fibroblasts from a previously studied patient with mutations in MRPS22 exhibiting similar symptoms (Smits et al., 2011). Complexomes of both patients revealed a marked decrease in the mt-SSU, while the large subunit remained unaffected. Decrease of mt-SSU abundance was also reflected in the patterns of OXPHOS complexes, which, in both patients, showed largely decreased abundance, particularly for CI and CIV. The abundance of monomeric CV remained unaltered in fibroblasts with mutations in MRPS2 or MRPS22. However, accumulations of assembly intermediates of CV, corresponding to the F_1 segment and to F_O early subassemblies that are not detected in control cell lines also indicated mitochondrial translation impairment in these patients.

A comparable decrease in the abundance of the mt-SSU has been found in a knockout cell line of METTL15, a N4-methylcytidine methyltransferase responsible for modification of the 12S mitochondrial rRNA (Van Haute et al., 2019). The absence of METTL15 impaired the translation of OXPHOS complex subunits encoded in the mtDNA and decreased the steady-state levels subunits of complexes I, III and IV. The DGU-based complexome profiles showed an interaction of METTL15 with mitoribosome components. In contrast to the aforementioned genetic defects where only the mt-SSU was affected, deletion of METTL15 resulted in a parallel decrease of the mt-LSU as well.

Shifting the energy metabolism from oxidative to glycolytic involves remodeling of biochemical pathways and structural rearranges of protein complexes inside and outside mitochondria. In this regard, Rho 0 (ρ^0) cells, devoid of mtDNA, are incapable to respire due to the lack of essential subunits of OXPHOS complexes thus depend entirely on anaerobic ATP synthesis (King and Attardi, 1989). These cells represent an optimal system to study mtDNA-related defects and OXPHOS deficiencies. Beyond the impaired assembly of OXPHOS complexes I, III, IV and V, which did retain partially assembled intermediates formed by nuclear-encoded subunits, complexomes of ρ^0 cells displayed unexpected modifications in migration patterns of a wide range of membrane-embedded and water-soluble protein complexes (Guerrero-Castillo et al., 2021b). Changes in expression of, for example, mitochondrial inner membrane carrier proteins, TCA cycle enzymes, mtDNA maintenance proteins and protein translocases localized to both mitochondrial membranes were described. Moreover, the absence of the mtDNA-encoded 12S and 16S rRNAs hindered the formation of mitochondrial ribosomal subunits, from which only smaller parts, composed exclusively of proteins, were preserved. This extensive re-organization of the mitochondrial complexome greatly illustrated the adaptability of mitochondria to self-adjust and compensate the absence of aerobic energy metabolism.

4.5 Pathogenic Mutations of Mitochondrial Proteins Affecting Indirectly the Assembly or Stability of Oxidative Phosphorylation Complexes

Reorganization of the mitochondrial energy metabolism can be triggered not only by genetic defects in OXPHOS complexes, assembly factors, mitochondrial translation and/or import machineries, but also by changes in the lipid environment of the inner mitochondrial membrane. This is particularly evident in patients with Barth syndrome, an inherited disorder of cardiolipin remodeling characterized by cardiomyopathy, neutropenia, 3-methylglutaconic aciduria and growth retardation (Neustein et al., 1979; Barth et al., 1983). This syndrome is caused by mutations in *TAZ* (Bione et al., 1996), encoding a mitochondrial acyltransferase called tafazzin, responsible for a CoA-independent exchange of (poly) unsaturated acyl chains from phosphatidyl-choline or phosphatidyl-ethanolamine to cardiolipin (Xu et al., 2006). The polyunsaturated acyl chains shape cardiolipin into a conical form, required for stabilization of membrane curvatures that optimize bioenergetics functions and are especially abundant at the inner mitochondrial membrane of multiple tissues, including heart. Complexome profiles of four Barth syndrome patients with altered saturation patterns of cardiolipin acyl chains revealed marked destabilization of several protein complexes involved in different mitochondrial processes. Significant disruption of supercomplexes containing 2–4 copies of CIV (I-III_2-IV_{2-4}), but not supercomplexes S_0 and S_1, has been found as well as partial destabilization of the complexes α-ketoglutarate dehydrogenase and branched-chain α-keto acid dehydrogenase (Chatzispyrou et al., 2018). Importantly, protein complexes involved in maintenance of mitochondrial morphology (e.g., MICOS) and in protein-driven mitochondrial apoptosis were substantially increased in patient fibroblasts. Overall, more than 200 proteins displayed altered migration patterns as a consequence of the membrane curvature destabilization, indicating a widespread reorganization of the mitochondrial complexome. These changes have not been limited to components of the inner mitochondrial membrane; but unexpectedly also spread among complexes located in the other three mitochondrial compartments.

In-depth understanding of remodeling of the mitochondrial complexome might be helpful to explain the links between the biochemical and clinical features observed in patients. For example, to delineate the molecular mechanisms underlying 3-methylglutaconic aciduria or neutropenia. These two clinical signs are also present in subjects with MEGCANN (3-methylglutaconic aciduria with cataracts, neurologic involvement and neutropenia), which is caused by mutations in CLPB, an ATP-dependent refoldase (dissagregase) of the mitochondrial intermembrane space. In a recent study comparing two subjects with bi-allelic mutations in *CLPB* and three subjects with mono-allelic mutations, different patterns of

oligomeric CLPB and HAX1, whose genetics variants have been associated to neutropenia, were interpreted as a retention of HAX1 in inefficient CLPB oligomers in the patients (Wortmann et al., 2021). Besides this effect, aberrant migration patterns of multiple mitochondrial proteins were noticed. Comprehensively re-analysing these complexome datasets together with those from Barth syndrome patients and TMEM70 knockout cells, in which accumulation of 3-methylglutaconic acid is commonly observed, could potentially shed light into the causes and consequences of this type of aciduria.

5 COMPLEXOME PROFILING: PERSPECTIVES

The implementation of CP analysis to help tackle the many open questions regarding PPIs is not limited to mitochondrial biology. CP is swiftly spreading to other scientific fields and already utilized to investigate protein complexes from other cell compartments and different species. However, there are still key limitations in the current setups, which open the door for further development and expanding its reach. In this final section we discussed not only the most recent advances in CP, but also its application to study protein complexes beyond the mitochondrion.

5.1 Improving Separation of Protein Complexes, Mass Spectrometry Quantification and Data Acquisition Time

The biochemical native separation techniques used to date for complexome analysis cover wide molecular mass ranges. Although each of these methods can easily be adapted to enhance the separation resolution of a certain mass window of interest, alternative strategies or modifications to the currently applied methods are envisioned, especially to improve separation resolution of large complexes.

Replacement of detergents by amphiphilic polymers (amphipols) could also help improve the analysis of membrane protein complexes. Amphipol-enclosed transmembrane complexes are more stable during separation than the ones solubilized with detergents (Althoff et al., 2011). Moreover, field flow fractionation (FFF) is a method to separate large (>1 nm) protein complexes. Proteins in solution are passed through a long narrow channel without a stationary phase and separated by their mobility upon a hydraulic field applied perpendicularly (Reschiglian and Moon, 2008), where small particles migrate faster than the bigger ones due to their smaller hydrodynamic sizes and higher diffusion coefficients. This technique has proven effective for analyzing ribosome profiles of the plant *Nicothiana benthamiana* with a similar resolution to the one of density gradients to distinguish ribosomal subunits from monosomes and free proteins (Pitkanen et al., 2014). FFF could thus represent an alternative separation technique in future CP setups.

Resolution of complexome profiles might be significantly improved by increasing the number of fractions in native-PAGE- and SEC-based CP setups. The more fractions the more MS data acquisition time is required however. Hence, a major limitation of CP is LC-MS time; especially if analysis of multiple experimental conditions is intended. Duplexing and triplexing with conventional SILAC/SILAM as well as multiplexing using isobaric labeling compounds are promising strategies for increasing the throughput of CP while reducing MS measuring times (Guerrero-Castillo et al., 2021a; Palenikova et al., 2021b). Incorporation of these strategies in CP studies also offers a higher level of proteomic quantification.

On the one hand, SILAC/SILAM-based quantifications enable more precise comparisons between samples or conditions than label-free quantification methods, and software tools have already been developed to facilitate data analysis (Palenikova et al., 2021a). SILAC is a suitable, affordable and compatible method with practically any cell culture condition. Accuracy and reproducibility are not hampered in this method since there are no precursor interferences as it occurs in isobaric tagging strategies (Chen et al., 2015). Other related variants, such as pulsed (p)SILAC and neutron-encoding (NeuCode) SILAC/SILAM, may also expand the possibilities this strategy can be used for in combination with CP. In pSILAC, the labeled essential aminoacids are added only for a brief period of time during cell growth to monitor differences in newly synthesized proteins and their half-life (Schwanhausser et al., 2009). As aforesaid, pSILAC and CP have proven useful to study the roles of mitochondrial protease ClpXP in turnover of N-module subunits of CI (Szczepanowska et al., 2020) and the chaperone DNAJC30 in the repair mechanism of impaired CI (Stenton et al., 2021). Furthermore, NeuCode SILAC/SILAM allows higher sensitivity and multiplexing with metabolic labeling using heavy stable isotopologues with additional neutrons (Hebert et al., 2013; Merrill et al., 2014; Overmyer et al., 2018). The subtle mass differences caused by neutron-binding energy variations are revealed under ultrahigh-resolution analysis that is only offered by Fourier-transform (FT)-MS or orbitrap analyzer systems (Overmyer et al., 2018). Thereby, implementation of this strategy in CP setups seems plausible.

Multiplexed CP (MCP), on the other hand, employs a set of isobaric labeling compounds, such as tandem mass tags that allows pooling a higher number of samples together after tryptic digestion. With commercially available tags, it is now possible to combine peptide solutions from up to 16 samples together before LC-MS/MS analyses. The quantitative advantage of using multiplexing isobaric compounds is that these molecules contain a reporter ion that is cleaved off during high collision dissociation together with precursor ion fragmentation. Therefore, quantifications of the reporter ions are performed at the MS2 level in the same spectrum used for peptide identification. Nevertheless, state-of-the-art equipment capable of MS3 or quantifications based on complement reporter ions are required to avoid quantification distortion due to interfering co-isolated ions (McAlister et al., 2014; Sonnett et al., 2018).

5.2 Combined Approaches for Selective Structural Analysis of Protein Complexes

Cross-linking mass spectrometry (XL-MS) has emerged as a powerful technology for interactome and structural biology studies in mitochondria (Schweppe et al., 2017; Liu et al., 2018; Ryl et al., 2020; Hevler et al., 2021b). Chemical cross-linkers react covalently with residues of proteins that are in close proximity to stabilize native PPIs for further characterization (Gomes and Gozzo, 2010; Mintseris and Gygi, 2020). After scrutiny of the identified intra- or inter-cross-linked peptides, a list of protein interactors and distance restraints is generated. This information can be used to guide computational modeling of single proteins and complex interfaces, most often in combination with data derived by classical structural methods, such as X-ray crystallography, nuclear magnetic resonance (NMR) or cryogenic electron microscopy (cryo-EM) (Herzog et al., 2012; Kornberg et al., 2015; O'Reilly and Rappsilber, 2018; Steigenberger et al., 2020).

Before structure analysis, determination of the optimal concentrations of cross-linkers and protein is strictly required to abate artifacts. To help circumvent this, a hybrid workflow termed in-gel cross-linking (IGX-MS) has recently been developed (Hevler et al., 2021a). In this method, proteins are separated by BN-PAGE and the gel spots of interest are cut and incubated with a cross-linker, digested and further analyzed by LC-MS/MS.

IGX-MS not only makes time-consuming experimental optimization steps (e.g., determining concentration of cross-linkers, optimal buffer system, etc.) nearly obsolete but also decreases the required protein amounts as well as undesired over-length cross-links. In contrast to classical in-solution XL-MS workflows, IGX-MS allows the differentiation of conformation- and interaction-specific distance restraints as it has been shown for various protein complexes, among them complexes I and V from bovine heart mitochondria. IGX-MS seems specially promising for future modeling studies that aim at characterizing co-occurring protein complexes with different stoichiometries or assembly states.

It has lately been demonstrated that CP and XL-MS are highly complementary and could provide valuable insights into the macromolecular organization of, for instance, the mitochondrial complexome. By combining CP and XL-MS data, Hevler and co-workers build a detailed atomic model of bovine CIV associated with dimeric apoptosis-inducing factor 1 (AIFM1) (Hevler et al., 2021b). CP analysis was indeed helpful to determine the stoichiometry of such a complex and validating this interaction. Combination of both approaches offers the possibility to cross-validate PPIs and to identify protein complexes that could be overlooked otherwise. Although actual scalability and throughput have not yet been addressed, combination of CP and XL-MS holds a great potential not only to better define the composition and states of protein complexes but also to help stabilize transient PPIs.

XL-MS has also been used to validate another CP-like setup that includes protein separation by SEC, quantitative MS analysis, cryo-electron microscopy (EM) and computational modeling. This structural proteomics approach allowed simultaneous description of the abundance, PPIs and structure profiling of 1/3 of the proteome of *Chaetomium thermophilum* (Kastritis et al., 2017). These results were integrated in a network map comprising 48 protein complexes and communities. This approach was also suitable to resolve the structure of the fatty acid synthase complex and its arrangements. Recent inclusion of image-processing workflows based on machine-learning methods opens the door to a much more robust data analysis, improved identification of PPIs, higher resolution in structure models and multi-scale molecular description of protein communities *in situ* (Kyrilis et al., 2021).

5.3 Investigating DNA-/RNA-Protein Complexes by Complexome Profiling

CP has not been popular for the analysis of DNA-interacting protein complexes. These have been addressed with more targeted approaches like chromatin immunoprecipitation (ChIP) (Das et al., 2004), electrophoretic mobility shift assay (EMSA) (Hellman and Fried, 2007) and a variety of Co-IP techniques (Sahr and Buchrieser, 2013), which have been extensively reviewed by Ferraz et al. (2021). Although both genomic and mitochondrial DNA molecules that interact with proteins are too large to enter standard native gels and do not exist in populations separable by size, like RNPs, CP could be useful for decomposing DNA-associated protein complexes. For example, Munawar and co-workers studied the complexome of a chromatin-enriched fraction separated by BN-PAGE after enzymatic digestion of DNA (Munawar et al., 2015). The resulting profile contained >50% of known chromatin complexes represented by at least half their subunits and contained information about assemblies for some of the complexes, such as PRC2 and NuRD. This illustrated the potential of CP for massive characterization of DNA-associated complexes. This fact is also corroborated by appearance of a variety of DNA-related complexes in existing CP datasets, such as histones, DNA repairing, replication and transcription factors.

Two research groups aiming to characterize the protein composition of chromatin complexes have made use of separation of protein complexes by size and LC-MS/MS analysis followed by correlation profiling. One utilized sucrose density gradients for separation of complexes containing chromatin-associated protein Wdr82 (Lee and Skalnik, 2013). The other used BN-PAGE to separate different populations of a chromatin remodeling complex NuRD derived from mouse embryonic stem cells. This approach led, among other things, to discovery of a new subunit of NuRD-associated protein, Wdr5 (Bode et al., 2016). Although these works were performed using affinity-purified complexes, they illustrated the potential of CP for characterization of chromatin-associated protein complexes as both allowed identification of different populations and assemblies in native state in contrast to pull-down techniques.

Conversely, CP variants to study RNA-protein complexes have been developed. Yet, these approaches have been particularly used for studying ribonucleoproteins (RNPs).

Applications of RNP complexomics are generously reviewed in Gerovac et al. (2021). Complexomics studies based on protein co-migration profiles obtained from density gradients are commonly used to investigate ribosomal protein components and associated factors (Yu et al., 2005; Aviner et al., 2017; Van Haute et al., 2019; Palenikova et al., 2021a). Besides ribosomes, other RNPs are likely to have specific sedimentation patterns on density gradients due to their complex composition (Caudron-Herger et al., 2019). The simplicity and gentleness of fractionation by density gradient allows parallel identification of both proteins and RNA molecules by LC-MS/MS and RNA-seq, respectively. This setup has been established in a robust RNP complexomics method called Grad-seq that enabled global classification of stable RNA-protein complexes as well as identification of novel RNPs (Smirnov et al., 2016; Hor et al., 2020).

SEC is another method that has successfully been used for separation of RNPs from complex mixtures (Yoshikawa et al., 2018; Mallam et al., 2019). It provides fast and reproducible automated separation of particles with an impressive upper limit size of ~30–40 MDa. SEC has been applied to specifically separate human 80S monosomes (~4.3 MDa) and n-polysomes from HeLa cells (Yoshikawa et al., 2018). Moreover, hierarchical clustering revealed complexes involved in translation associated with ribosomal subunits, which makes this method a good alternative to the time-consuming and less specific DGU.

Classic CP has also been useful for dissecting protein composition of mitoribosomes as they enter regular BN-gels (Wessels et al., 2013; Chatzispyrou et al., 2017; Gardeitchik et al., 2018; Van Strien et al., 2019; Cunatova et al., 2021). For larger ribosomal species however, LP-native gels can be used (Strecker et al., 2010). As aforementioned, LP-BN-PAGE-based CP helped identify a RNP complex containing the mt-SSU associated with several translation and transcription factors at ~5.7 MDa (Rugen et al., 2019). LP-gels could thus be very useful for further dissection of larger RNPs or those that are associated with many other factors as it has been commonly reported for translation and RNA-processing machineries (Acestor et al., 2009; Hocine et al., 2010; Blombach et al., 2011; Doetsch et al., 2011; Sprink et al., 2016; Duss et al., 2019; Gopalakrishna et al., 2019; Hilander et al., 2021).

A potential issue for characterization of RNA-protein complexes may result from the poor stability of RNA molecules, which are also prone to degradation by RNases. In this case, RNA-protein interactions would be lost and leading to identification of not only sub-assemblies but also artifacts. To avoid this, prior to CP, separation of these complexes should be thus performed using RNase-free materials and RNase inhibitors to keep stable both the protein and RNA interactors (López De Heredia and Jansen, 2004; Mili and Steitz, 2004; Wang et al., 2016; Aarum et al., 2020). Alternatively, to stabilize weak interactions of fragile RNA-protein complexes during separation, cross-linking strategies can be implemented. Treatment with chemicals (Rugen et al., 2019; Herrmannova et al., 2020; Patton et al., 2020), such as formaldehyde or UV irradiation (Trendel et al., 2019; Urdaneta et al., 2019; Urdaneta and Beckmann, 2020; van Esveld and Spelbrink, 2021) create short cross-links between a nucleic acid and close-contact protein interactors. In contrast, different types of enzymatic digestion of RNA can be used purposely to affect structure and stability of RNA-protein complexes to build additional levels of information for CP analysis, which can enable identification of previously unknown RNA-binding proteins (Caudron-Herger et al., 2019; Mallam et al., 2019; Gerovac et al., 2021).

5.4 Filling the Void: Complexome Profiling as a Workflow to Identify Protein-Protein Interactions and Improve Functional Annotation of Protein Complexes Across Species

Many species still lack functional annotation for a large portion of their genomes despite their significance as pathogens or drivers of major ecological processes. This is often owed to poor conservation, missing orthologues and the additional pitfall that the most unique biology that is not found in standard models, remains enigmatic. Systematic knowledge of PPIs can allow us to place these proteins into pathways, compartments and interaction networks. CP represents a clear choice to help narrow this gap and has the added benefit that no genetic intervention is required, which allows immediate assessment of species without a well-developed toolkit.

For example, Hillier et al. applied CP to study schizont stages of three different *Plasmodium* species. Integration with machine-learning led to identification of ~20,000 putative PPIs arranged into ~600 protein clusters, which were used to map the interactome (Hillier et al., 2019). Next to creating a valuable resource for *Plasmodium* research, the authors shed light on the interaction network of a group of parasite-specific transcription factors as well as identifying novel parasite-specific interactors. The latter could serve as targets for drug development due to their divergence from host biology. These data are sorely needed in the face of emerging drug resistance that is threatening our attempts to eradicate malaria (Haldar et al., 2018).

Prokaryotes also deviate considerably from the standard protein complexes found in eukaryotes. These organisms cover virtually every ecological niche on earth and have adapted their protein complexes accordingly. This is indeed exemplified in energy metabolic pathways, where prokaryotes utilize a wide variety of electron donors and acceptors, each requiring their own adapted set of classical and alternative respiratory complexes (Poole and Cook, 2000; Kaila and Wikstrom, 2021), most of which remain undescribed. While genomic analyses led to the hypothetical annotation of many homologous proteins involved in prokaryotic respiration, this approach is ill suited to the identification of novel components and interactors. CP complements this shortcoming and stands up as a good approach for characterizing PPIs in these organisms. This was illustrated beautifully by de Almeida and co-workers who investigated the electron transport system of the anaerobic ammonium-oxidizing bacterium *Kuenenia stuttgartiensis* (de Almeida et al., 2016). These bacteria oxidize ammonium with nitrite to produce N_2 gas. It has been estimated that this process account for ~50% of all N_2 emitted into the atmosphere (Devol, 2015). Although this enormous ecological significance, the underlying respiratory complexes were largely theoretical (Kartal et al., 2013). By applying CP, these authors did not only confirm

the presence of nearly all predicted respiratory complexes but also found evidence for novel protein complexes. One striking finding was that this bacterium appears to assemble a set of respiratory complexes that utilize Na^+ besides the expected proton-pumping complexes, which suggested a role for a sodium-motive force to drive, for instance, the unfavorable reduction of ferredoxin. A set of three Rieske/cyt*b* complexes has also been found that shed light on how these bacteria can capture energy from hydrazine oxidation, challenging a previous hypothesis suggesting a quinone-reducing enzyme (Kartal et al., 2013). Similarly, CP has been used to analyze the nitrite-dependent methanotroph *Methylomirabilis lanthanidiphila* (Versantvoort et al., 2019). This species may potentially contribute to reduction of methane and nitrous oxide; i.e., potent greenhouse gases, by oxidizing methane to CO_2 and reducing nitrate without producing nitrous oxide. To explain this process, a metabolic model based on genomic information had previously been proposed (Ettwig et al., 2010). Versantvoort and co-workers could confirm this model by identifying all proposed underlying protein complexes. Interestingly, three protein complexes thought to be involved in nitrate reduction were also identified, suggesting metabolic capabilities which had not yet been described in *Methylomirabilis* species. On the other hand, application of CP to study the marine sulfate reducer *Desulfobacula toluolica*, also led to detection of not only the expected membrane complexes but also new assemblies, unexpected associations, multimeric states, redox complexes involved in Na^+-based bioenergetics and indications of respiratory supercomplexes (Wöhlbrand et al., 2016).

To shed more light on the biogenesis of thylakoid membrane complexes, CP was used to study auxiliary factors involved in the assembly of photosystem II (PSII) from the single-cell green alga *Chlamydomonas reinhardtii* (Spaniol et al., 2021). Authors demonstrated that the homolog for low PSII accumulation 2 (LPA2) protein is critical for PSII assembly and further supercomplex formation. Besides, novel interactors were found and possibly involved in regulation of PSII. This study exemplifies the great potential CP has for further studying photosynthesis-related protein complexes in algae, cyanobacteria and plants.

Finally, even in microorganisms that are not currently obtainable in axenic cultures, such as the archaeon *Candidatus Methanoperedens*, CP has proven invaluable (Berger et al., 2021). In this study, Berger et al. confirmed the presence of several predicted membrane-bound respiratory chain complexes as well as novel associations. Taken together these results demonstrated the suitability of CP to explore species previously inaccessible to most protein research. Overall, it is clear that CP complements (meta) genomic studies perfectly, by identifying in one experiment how these gene products assemble to form protein complexes, what subset of genome is really expressed and consequently update our understanding of metabolic capabilities and how these organisms achieve them.

5.5 Exploring Effects of Pathogenic Mutations in Non-Mitochondrial Proteins by Complexome Profiling

Although to date the vast majority of CP analyses in patients have been focused on disorders affecting mitochondria, its application is broadening nonetheless. The effects of pathogenic missense mutations in structural subunits of the V-type ATPase on the stability of the holoenzyme have been characterized by this method (Van Damme et al., 2017). By whole exome sequencing, predicted pathogenic mutations have been identified in genes *ATP6V1E1* and *ATP6V1A*, encoding subunits E and A from the V_1 segment of the V-type ATPase, respectively. Primary skin fibroblasts from three patients, one with a mutation in E1 and two with mutations in subunit A were compared to controls and to an earlier described subject presenting cutis laxa with a mutation in subunit ATP6V0A2 of the V_O segment. To further investigate this, enriched Golgi preparations have been analyzed by BN-PAGE-based CP. Migration patterns of healthy controls revealed three assembly intermediates of the V_1 segment, the V_O segment and a highly abundant, fully assembled V_1V_O-ATPase complex. In contrast, in patient fibroblasts with mutations in subunits of the V_1 segment, only the V_O intermediate and traces of the holo-complex have been detected. Comparably, the mutation in ATP6V0A2 decreased the abundance of intermediates of both domains as well as the holo-complex. The destabilization of the fully assembled V_1V_O-ATPase evidenced by CP contributed to detailing the molecular consequences and pathogenicity of these mutations.

In a recent CP study of peroxisome-deficient cells using peroxins deletion strains of *S. cerevisiae* as a model system and fibroblasts from a Zellweger syndrome patient, Nübel and co-workers linked accumulation of miss-targeted peroxisomal membrane proteins into mitochondria to metabolic and morphological abnormalities of this organelle (Nuebel et al., 2021). Complexome profiles of yeast strains lacking peroxisomes showed formation of the docking subassembly of the peroxisomal importomer complex in mitochondria, explaining also the incorporation of peroxisomal matrix proteins to this subcellular compartment. It would be interesting to also explore the complexome profiles of fibroblasts from patients with Zellweger spectrum disorder to investigate in detail the rearrangements of mitochondrial complexes caused by peroxisomes deficit in humans.

These two studies exemplified how CP offers a straightforward option to shed light on the pathophysiological roles of critical proteins located in cell compartments other than mitochondria and the specific consequences of impairments in protein complexes and PPIs resulting from genetic and/or biochemical defects. CP thus holds a great potential to help not only unveil the molecular mechanisms of diseases, but also develop novel treatments.

6 CONCLUDING REMARKS

In a very short time, CP has revolutionized the way we study mitochondrial protein complexes and significantly increased the amount of data collected from single unbiased experiments. Research findings obtained by this methodology include, for instance, identification of novel OXPHOS-related subunits and assembly factors; stepwise description of intricate assembly

pathways; molecular evidence on the role of accessory subunits and existence of tissue-specific subunit isoforms of CI; better insight on the formation of respirasomes and the supramolecular organization of the MICOS/MIB complexes as well as the unique composition of OXPHOS complexes and mitoribosomes in different species. Notably, CP has also been invaluable to better understand the effects of mutations found in mitochondrial genes from patients as well as in disease models. Recent developments in duplexing and multiplexing CP experiments not only enable accurate proteomic quantifications, but also greatly increase the feasibility of including this approach in future clinical diagnosis. We have also discussed innovative strategies exemplifying how CP easily complements other state-of-the-art methods such as XL-MS, RNAseq and cryo-EM. However, there is still a lot of room for improving this method and keep expanding its reach. It is projected that CP will further evolve with the advent of the next generation of LC-MS instruments and proteomic strategies as well as upcoming complexome data analysis software. Finally, we also encourage the scientific community to apply CP for studying protein complexes from cell compartments other than the mitochondrion and share publicly the resultant complexome datasets through CEDAR.

AUTHOR CONTRIBUTIONS

AC-O and SG-C contributed to the conception and design of this review. AC-O and SG-C wrote the first draft of the manuscript with contributions of AP, FE and JH in specific subsections. SG-C generated **Table 1**. AC-O and AP generated the set of figures. All authors contributed to discussion, literature revision, edition of figures as well as manuscript revision. All authors approved the submitted version.

FUNDING

AC-O is supported by the Netherlands Organization for Health Research and Development (ZonMW TOP-Grant 91217009); AP is supported by the European Union's Horizon 2020 research and innovation program under the Marie Sklodowska-Curie grant agreement 721757; FE is supported by the Netherlands Organization for Scientific Research (NWO-VIDI 864.13.009); JH is supported by the NWO funding the Netherlands Proteomics Centre through the X-omics Road Map program (Project 184.034.019), the TOP project 714.017.004 and the EU Horizon 2020 program Epic-XS (Project 823839). This work was also supported by the Else Kröner-Fresenius-Stiftung grant 2019_A135 to SG-C.

ACKNOWLEDGMENTS

Authors thank Prof. Ulrich Brandt for carefully revising this manuscript and helpful suggestions.

REFERENCES

Aarum, J., Cabrera, C. P., Jones, T. A., Rajendran, S., Adiutori, R., Giovannoni, G., et al. (2020). Enzymatic Degradation of RNA Causes Widespread Protein Aggregation in Cell and Tissue Lysates. *EMBO Rep.* 21. doi:10.15252/embr.201949585

Acestor, N., Panigrahi, A. K., Carnes, J., Zíková, A., and Stuart, K. D. (2009). The MRB1 Complex Functions in Kinetoplastid RNA Processing. *RNA* 15, 277–286. doi:10.1261/RNA.1353209

Adams, J. (2008). The Proteome: Discovering the Structure and Function of Proteins. *Nat. Education* 1, 6.

Alahmad, A., Nasca, A., Heidler, J., Thompson, K., Oláhová, M., Legati, A., et al. (2020). Bi-allelic Pathogenic Variants in NDUFC2 Cause Early-onset Leigh Syndrome and Stalled Biogenesis of Complex I. *EMBO Mol. Med.* 12, e12619. doi:10.15252/emmm.202012619

Alston, C. L., Compton, A. G., Formosa, L. E., Strecker, V., Oláhová, M., Haack, T. B., et al. (2016). Biallelic Mutations in TMEM126B Cause Severe Complex I Deficiency with a Variable Clinical Phenotype. *Am. J. Hum. Genet.* 99, 217–227. doi:10.1016/j.ajhg.2016.05.021

Alston, C. L., Heidler, J., Dibley, M. G., Kremer, L. S., Taylor, L. S., Fratter, C., et al. (2018). Bi-allelic Mutations in NDUFA6 Establish its Role in Early-Onset Isolated Mitochondrial Complex I Deficiency. *Am. J. Hum. Genet.* 103, 592–601. doi:10.1016/j.ajhg.2018.08.013

Alston, C. L., Veling, M. T., Heidler, J., Taylor, L. S., Alaimo, J. T., Sung, A. Y., et al. (2020). Pathogenic Bi-allelic Mutations in NDUFAF8 Cause Leigh Syndrome with an Isolated Complex I Deficiency. *Am. J. Hum. Genet.* 106, 92–101. doi:10.1016/j.ajhg.2019.12.001

Althoff, T., Mills, D. J., Popot, J.-L., and Kühlbrandt, W. (2011). Arrangement of Electron Transport Chain Components in Bovine Mitochondrial Supercomplex I1III2IV1. *EMBO J.* 30, 4652–4664. doi:10.1038/emboj.2011.324

Anand, R., Kondadi, A. K., Meisterknecht, J., Golombek, M., Nortmann, O., Riedel, J., et al. (2020). MIC26 and MIC27 Cooperate to Regulate Cardiolipin Levels and the Landscape of OXPHOS Complexes. *Life Sci. Alliance* 3, e202000711. doi:10.26508/lsa.202000711

Anand, R., Strecker, V., Urbach, J., Wittig, I., and Reichert, A. S. (2016). Mic13 Is Essential for Formation of Crista Junctions in Mammalian Cells. *PLOS ONE* 11, e0160258. doi:10.1371/journal.pone.0160258

Andersen, J. S., Wilkinson, C. J., Mayor, T., Mortensen, P., Nigg, E. A., and Mann, M. (2003). Proteomic Characterization of the Human Centrosome by Protein Correlation Profiling. *Nature* 426, 570–574. doi:10.1038/nature02166

Andrews, B., Carroll, J., Ding, S., Fearnley, I. M., and Walker, J. E. (2013). Assembly Factors for the Membrane Arm of Human Complex I. *Proc. Natl. Acad. Sci.* 110, 18934–18939. doi:10.1073/pnas.1319247110

Angerer, H., Radermacher, M., Ma kowska, M., Steger, M., Zwicker, K., Heide, H., et al. (2014). The LYR Protein Subunit NB4M/NDUFA6 of Mitochondrial Complex I Anchors an Acyl Carrier Protein and Is Essential for Catalytic Activity. *Proc. Natl. Acad. Sci.* 111, 5207–5212. doi:10.1073/pnas.1322438111

Aurrecoechea, C., Brestelli, J., Brunk, B. P., Dommer, J., Fischer, S., Gajria, B., et al. (2009). PlasmoDB: a Functional Genomic Database for Malaria Parasites. *Nucleic Acids Res.* 37, D539–D543. doi:10.1093/nar/gkn814

Aviner, R., Hofmann, S., Elman, T., Shenoy, A., Geiger, T., Elkon, R., et al. (2017). Proteomic Analysis of Polyribosomes Identifies Splicing Factors as Potential Regulators of Translation during Mitosis. *Nucleic Acids Res.* 45, 5945–5957. doi:10.1093/nar/gkx326

Balsa, E., Marco, R., Perales-Clemente, E., Szklarczyk, R., Calvo, E., Landázuri, M. O., et al. (2012). NDUFA4 Is a Subunit of Complex IV of the Mammalian Electron Transport Chain. *Cel Metab.* 16, 378–386. doi:10.1016/j.cmet.2012.07.015

Barth, P. G., Scholte, H. R., Berden, J. A., Van Der Klei-Van Moorsel, J. M., Luyt-Houwen, I. E. M., Van'T Veer-Korthof, E. T., et al. (1983). An X-Linked Mitochondrial Disease Affecting Cardiac Muscle, Skeletal Muscle and Neutrophil Leucocytes. *J. Neurol. Sci.* 62, 327–355. doi:10.1016/0022-510x(83)90209-5

Berger, S., Cabrera-Orefice, A., Jetten, M. S. M., Brandt, U., and Welte, C. U. (2021). Investigation of central Energy Metabolism-Related Protein Complexes of

ANME-2d Methanotrophic Archaea by Complexome Profiling. *Biochim. Biophys. Acta (Bba) - Bioenerg.* 1862, 148308. doi:10.1016/j.bbabio.2020.148308

Bione, S., D'adamo, P., Maestrini, E., Gedeon, A. K., Bolhuis, P. A., and Toniolo, D. (1996). A Novel X-Linked Gene, G4.5. Is Responsible for Barth Syndrome. *Nat. Genet.* 12, 385–389. doi:10.1038/ng0496-385

Blombach, F., Brouns, S. J. J., and van der Oost, J. (2011). Assembling the Archaeal Ribosome: Roles for Translation-Factor-Related GTPases. *Biochem. Soc. Trans.* 39, 45–50. doi:10.1042/BST0390045

Bludau, I., and Aebersold, R. (2020). Proteomic and Interactomic Insights into the Molecular Basis of Cell Functional Diversity. *Nat. Rev. Mol. Cel Biol* 21, 327–340. doi:10.1038/s41580-020-0231-2

Bludau, I. (2021). Discovery-Versus Hypothesis-Driven Detection of Protein-Protein Interactions and Complexes. *Ijms* 22, 4450. doi:10.3390/ijms22094450

Bludau, I., Heusel, M., Frank, M., Rosenberger, G., Hafen, R., Banaei-Esfahani, A., et al. (2020). Complex-centric Proteome Profiling by SEC-SWATH-MS for the Parallel Detection of Hundreds of Protein Complexes. *Nat. Protoc.* 15, 2341–2386. doi:10.1038/s41596-020-0332-6

Bock, T., Türk, C., Aravamudhan, S., Keufgens, L., Bloch, W., Rozsivalova, D. H., et al. (2021). PERM1 Interacts with the MICOS-MIB Complex to Connect the Mitochondria and Sarcolemma via Ankyrin B. *Nat. Commun.* 12, 4900. doi:10.1038/s41467-021-25185-3

Bode, D., Yu, L., Tate, P., Pardo, M., and Choudhary, J. (2016). Characterization of Two Distinct Nucleosome Remodeling and Deacetylase (NuRD) Complex Assemblies in Embryonic Stem Cells. *Mol. Cell Proteomics* 15, 878–891. doi:10.1074/mcp.M115.053207

Bottani, E., Cerutti, R., Harbour, M. E., Ravaglia, S., Dogan, S. A., Giordano, C., et al. (2017). TTC19 Plays a Husbandry Role on UQCRFS1 Turnover in the Biogenesis of Mitochondrial Respiratory Complex III. *Mol. Cel* 67, 96–105. doi:10.1016/j.molcel.2017.06.001

Bridges, H. R., Mohammed, K., Harbour, M. E., and Hirst, J. (2017). Subunit NDUFV3 Is Present in Two Distinct Isoforms in Mammalian Complex I. *Biochim. Biophys. Acta (Bba) - Bioenerg.* 1858, 197–207. doi:10.1016/j.bbabio.2016.12.001

Burgess, R. R. (2018). A Brief Practical Review of Size Exclusion Chromatography: Rules of Thumb, Limitations, and Troubleshooting. *Protein Expr. Purif.* 150, 81–85. doi:10.1016/j.pep.2018.05.007

Burley, S. K., Bhikadiya, C., Bi, C., Bittrich, S., Chen, L., Crichlow, G. V., et al. (2021). RCSB Protein Data Bank: Powerful New Tools for Exploring 3D Structures of Biological Macromolecules for Basic and Applied Research and Education in Fundamental Biology, Biomedicine, Biotechnology, Bioengineering and Energy Sciences. *Nucleic Acids Res.* 49, D437–D451. doi:10.1093/nar/gkaa1038

Calvo, E., Cogliati, S., Hernansanz-Agustín, P., Loureiro-López, M., Guarás, A., Casuso, R. A., et al. (2020). Functional Role of Respiratory Supercomplexes in Mice: SCAF1 Relevance and Segmentation of the Q Pool. *Sci. Adv.* 6, eaba7509. doi:10.1126/sciadv.aba7509

Caudron-Herger, M., Rusin, S. F., Adamo, M. E., Seiler, J., Schmid, V. K., Barreau, E., et al. (2019). R-DeeP: Proteome-wide and Quantitative Identification of RNA-dependent Proteins by Density Gradient Ultracentrifugation. *Mol. Cel* 75, 184–199. doi:10.1016/j.molcel.2019.04.018

Ceulemans, H., Beke, L., and Bollen, M. (2006). Approaches to Defining the Ancestral Eukaryotic Protein Complexome. *Bioessays* 28, 316–324. doi:10.1002/bies.20373

Chalkley, R. J., Baker, P. R., Huang, L., Hansen, K. C., Allen, N. P., Rexach, M., et al. (2005). Comprehensive Analysis of a Multidimensional Liquid Chromatography Mass Spectrometry Dataset Acquired on a Quadrupole Selecting, Quadrupole Collision Cell, Time-Of-Flight Mass Spectrometer. *Mol. Cell Proteomics* 4, 1194–1204. doi:10.1074/mcp.D500002-MCP200

Chatzispyrou, I. A., Alders, M., Guerrero-Castillo, S., Zapata Perez, R., Haagmans, M. A., Mouchiroud, L., et al. (2017). A Homozygous Missense Mutation in ERAL1, Encoding a Mitochondrial rRNA Chaperone, Causes Perrault Syndrome. *Hum. Mol. Genet.* 26, 2541–2550. doi:10.1093/hmg/ddx152

Chatzispyrou, I. A., Guerrero-Castillo, S., Held, N. M., Ruiter, J. P. N., Denis, S. W., Ijlst, L., et al. (2018). Barth Syndrome Cells Display Widespread Remodeling of Mitochondrial Complexes without Affecting Metabolic Flux Distribution. *Biochim. Biophys. Acta (Bba) - Mol. Basis Dis.* 1864, 3650–3658. doi:10.1016/j.bbadis.2018.08.041

Chen, X., Wei, S., Ji, Y., Guo, X., and Yang, F. (2015). Quantitative Proteomics Using SILAC: Principles, Applications, and Developments. *Proteomics* 15, 3175–3192. doi:10.1002/pmic.201500108

Čížková, A., Stránecký, V., Mayr, J. A., Tesařová, M., Havlíčková, V., Paul, J., et al. (2008). TMEM70 Mutations Cause Isolated ATP Synthase Deficiency and Neonatal Mitochondrial Encephalocardiomyopathy. *Nat. Genet.* 40, 1288–1290. doi:10.1038/ng.246

Cogliati, S., Calvo, E., Loureiro, M., Guaras, A. M., Nieto-Arellano, R., Garcia-Poyatos, C., et al. (2016a). Mechanism of Super-assembly of Respiratory Complexes III and IV. *Nature* 539, 579–582. doi:10.1038/nature20157

Cogliati, S., Enriquez, J. A., and Scorrano, L. (2016b). Mitochondrial Cristae: Where Beauty Meets Functionality. *Trends Biochem. Sci.* 41, 261–273. doi:10.1016/j.tibs.2016.01.001

Cole, J. L., Lary, J. W., P. Moody, T., and Laue, T. M. (2008). Analytical Ultracentrifugation: Sedimentation Velocity and Sedimentation Equilibrium. *Methods Cel Biol* 84, 143–179. doi:10.1016/S0091-679X(07)84006-4

Connelly, K. E., Hedrick, V., Paschoal Sobreira, T. J., Dykhuizen, E. C., and Aryal, U. K. (2018). Analysis of Human Nuclear Protein Complexes by Quantitative Mass Spectrometry Profiling. *Proteomics* 18, 1700427. doi:10.1002/pmic.201700427

Coordinators, N. R. (2016). Database Resources of the National Center for Biotechnology Information. *Nucleic Acids Res.* 44, D7–D19. doi:10.1093/nar/gkv1290

Cox, J., Hein, M. Y., Luber, C. A., Paron, I., Nagaraj, N., and Mann, M. (2014). Accurate Proteome-wide Label-free Quantification by Delayed Normalization and Maximal Peptide Ratio Extraction, Termed MaxLFQ. *Mol. Cell Proteomics* 13, 2513–2526. doi:10.1074/mcp.M113.031591

Čunátová, K., Reguera, D. P., Vrbacký, M., Fernández-Vizarra, E., Ding, S., Fearnley, I. M., et al. (2021). Loss of COX4I1 Leads to Combined Respiratory Chain Deficiency and Impaired Mitochondrial Protein Synthesis. *Cells* 10, 369. doi:10.3390/cells10020369

Das, P. M., Ramachandran, K., Vanwert, J., and Singal, R. (2004). "Chromatin Immunoprecipitation Assay," in BioTechniques. *Biotechniques)*. doi:10.2144/04376rv01

De Almeida, N. M., Wessels, H. J. C. T., De Graaf, R. M., Ferousi, C., Jetten, M. S. M., Keltjens, J. T., et al. (2016). Membrane-bound Electron Transport Systems of an Anammox Bacterium: A Complexome Analysis. *Biochim. Biophys. Acta (Bba) - Bioenerg.* 1857, 1694–1704. doi:10.1016/j.bbabio.2016.07.006

De Las Rivas, J., and Fontanillo, C. (2010). Protein-protein Interactions Essentials: Key Concepts to Building and Analyzing Interactome Networks. *Plos Comput. Biol.* 6, e1000807. doi:10.1371/journal.pcbi.1000807

Deshaies, R. J., Seol, J. H., Mcdonald, W. H., Cope, G., Lyapina, S., Shevchenko, A., et al. (2002). Charting the Protein Complexome in Yeast by Mass Spectrometry. *Mol. Cell Proteomics* 1, 3–10. doi:10.1074/mcp.r100001-mcp200

Devol, A. H. (2015). Denitrification, Anammox, and N2 Production in Marine Sediments. *Annu. Rev. Mar. Sci.* 7, 403–423. doi:10.1146/annurev-marine-010213-135040

Doetsch, M., Schroeder, R., and Fürtig, B. (2011). Transient RNA-Protein Interactions in RNA Folding. *Febs J.* 278, 1634–1642. doi:10.1111/J.1742-4658.2011.08094.X

Duss, O., Stepanyuk, G. A., Puglisi, J. D., and Williamson, J. R. (2019). Transient Protein-RNA Interactions Guide Nascent Ribosomal RNA Folding. *Cell* 179, 1357–1369. e1316. doi:10.1016/J.CELL.2019.10.035

Ettwig, K. F., Butler, M. K., Le Paslier, D., Pelletier, E., Mangenot, S., Kuypers, M. M. M., et al. (2010). Nitrite-driven Anaerobic Methane Oxidation by Oxygenic Bacteria. *Nature* 464, 543–548. doi:10.1038/nature08883

Eubel, H., Braun, H.-P., and Millar, A. (2005). Blue-native PAGE in Plants: a Tool in Analysis of Protein-Protein Interactions. *Plant Methods* 1, 11. doi:10.1186/1746-4811-1-11

Evers, F., Cabrera-Orefice, A., Elurbe, D. M., Kea-Te Lindert, M., Boltryk, S. D., Voss, T. S., et al. (2021). Composition and Stage Dynamics of Mitochondrial Complexes in Plasmodium Falciparum. *Nat. Commun.* 12, 3820. doi:10.1038/s41467-021-23919-x

Eydt, K., Davis, K. M., Behrendt, C., Wittig, I., and Reichert, A. S. (2017). Cristae Architecture Is Determined by an Interplay of the MICOS Complex and the F1Fo ATP Synthase via Mic27 and Mic10. *Microb. Cel* 4, 259–272. doi:10.15698/mic2017.08.585

Fabre, B., Lambour, T., Bouyssié, D., Menneteau, T., Monsarrat, B., Burlet-Schiltz, O., et al. (2014). Comparison of Label-free Quantification Methods for the Determination of Protein Complexes Subunits Stoichiometry. *EuPA Open Proteomics* 4, 82–86. doi:10.1016/j.euprot.2014.06.001

Fassone, E., and Rahman, S. (2012). Complex I Deficiency: Clinical Features, Biochemistry and Molecular Genetics. *J. Med. Genet.* 49, 578–590. doi:10.1136/jmedgenet-2012-101159

Fernández-Vizarra, E., López-Calcerrada, S., Formosa, L. E., Pérez-Pérez, R., Ding, S., Fearnley, I. M., et al. (2021). SILAC-based Complexome Profiling Dissects the Structural Organization of the Human Respiratory Supercomplexes in SCAFIKO Cells. *Biochim. Biophys. Acta (Bba) - Bioenerg.* 1862, 148414. doi:10.1016/j.bbabio.2021.148414

Ferraz, R. a. C., Lopes, A. L. G., Da Silva, J. a. F., Moreira, D. F. V., Ferreira, M. J. N., and De Almeida Coimbra, S. V. (2021). "DNA–protein Interaction Studies: a Historical and Comparative Analysis," in Plant Methods. *Plant Methods)*.

Floyd, B. J., Wilkerson, E. M., Veling, M. T., Minogue, C. E., Xia, C., Beebe, E. T., et al. (2016). Mitochondrial Protein Interaction Mapping Identifies Regulators of Respiratory Chain Function. *Mol. Cel* 63, 621–632. doi:10.1016/j.molcel.2016.06.033

Formosa, L. E., Muellner-Wong, L., Reljic, B., Sharpe, A. J., Jackson, T. D., Beilharz, T. H., et al. (2020). Dissecting the Roles of Mitochondrial Complex I Intermediate Assembly Complex Factors in the Biogenesis of Complex I. *Cel Rep.* 31, 107541. doi:10.1016/j.celrep.2020.107541

Foster, L. J., De Hoog, C. L., Zhang, Y., Zhang, Y., Xie, X., Mootha, V. K., et al. (2006). A Mammalian Organelle Map by Protein Correlation Profiling. *Cell* 125, 187–199. doi:10.1016/j.cell.2006.03.022

Fuhrmann, D. C., Wittig, I., Dröse, S., Schmid, T., Dehne, N., and Brüne, B. (2018). Degradation of the Mitochondrial Complex I Assembly Factor TMEM126B under Chronic Hypoxia. *Cell. Mol. Life Sci.* 75, 3051–3067. doi:10.1007/s00018-018-2779-y

Galemou Yoga, E., Parey, K., Djurabekova, A., Haapanen, O., Siegmund, K., Zwicker, K., et al. (2020). Essential Role of Accessory Subunit LYRM6 in the Mechanism of Mitochondrial Complex I. *Nat. Commun.* 11, 6008. doi:10.1038/s41467-020-19778-7

Gardeitchik, T., Mohamed, M., Ruzzenente, B., Karall, D., Guerrero-Castillo, S., Dalloyaux, D., et al. (2018). Bi-allelic Mutations in the Mitochondrial Ribosomal Protein MRPS2 Cause Sensorineural Hearing Loss, Hypoglycemia, and Multiple OXPHOS Complex Deficiencies. *Am. J. Hum. Genet.* 102, 685–695. doi:10.1016/j.ajhg.2018.02.012

Geiger, T., Wisniewski, J. R., Cox, J., Zanivan, S., Kruger, M., Ishihama, Y., et al. (2011). Use of Stable Isotope Labeling by Amino Acids in Cell Culture as a Spike-In Standard in Quantitative Proteomics. *Nat. Protoc.* 6, 147–157. doi:10.1038/nprot.2010.192

Gerovac, M., Vogel, J., and Smirnov, A. (2021). The World of Stable Ribonucleoproteins and its Mapping with Grad-Seq and Related Approaches. *Front. Mol. Biosci.* 8, 661448. doi:10.3389/fmolb.2021.661448

Giese, H., Ackermann, J., Heide, H., Bleier, L., Drose, S., Wittig, I., et al. (2015). NOVA: a Software to Analyze Complexome Profiling Data. *Bioinformatics* 31, 440–441. doi:10.1093/bioinformatics/btu623

Giese, H., Meisterknecht, J., Heidler, J., and Wittig, I. (2021). Mitochondrial Complexome Profiling. *Methods Mol. Biol.* 2192, 269–285. doi:10.1007/978-1-0716-0834-0_19

Gillet, L. C., Navarro, P., Tate, S., Röst, H., Selevsek, N., Reiter, L., et al. (2012). Targeted Data Extraction of the MS/MS Spectra Generated by Data-independent Acquisition: a New Concept for Consistent and Accurate Proteome Analysis. *Mol. Cell Proteomics* 11, O111. doi:10.1074/mcp.O111.016717

Giurgiu, M., Reinhard, J., Brauner, B., Dunger-Kaltenbach, I., Fobo, G., Frishman, G., et al. (2019). CORUM: the Comprehensive Resource of Mammalian Protein Complexes-2019. *Nucleic Acids Res.* 47, D559–D563. doi:10.1093/nar/gky973

Gomes, A. F., and Gozzo, F. C. (2010). Chemical Cross-Linking with a Diazirine Photoactivatable Cross-Linker Investigated by MALDI- and ESI-MS/MS. *J. Mass. Spectrom.* 45, 892–899. doi:10.1002/jms.1776

Gopalakrishna, S., Pearce, S. F., Dinan, A. M., Schober, F. A., Cipullo, M., Spåhr, H., et al. (2019). C6orf203 Is an RNA-Binding Protein Involved in Mitochondrial Protein Synthesis. *Nucleic Acids Res.* 47, 9386–9399. doi:10.1093/NAR/GKZ684

Guarás, A., Perales-Clemente, E., Calvo, E., Acín-Pérez, R., Loureiro-Lopez, M., Pujol, C., et al. (2016). The CoQH2/CoQ Ratio Serves as a Sensor of Respiratory Chain Efficiency. *Cel Rep.* 15, 197–209. doi:10.1016/j.celrep.2016.03.009

Guerrero-Castillo, S., Van Strien, J., Brandt, U., and Arnold, S. (2021b). Ablation of Mitochondrial DNA Results in Widespread Remodeling of the Mitochondrial Complexome. *EMBO J.* 40, e108648. doi:10.15252/embj.2021108648

Guerrero-Castillo, S., Baertling, F., Kownatzki, D., Wessels, H. J., Arnold, S., Brandt, U., et al. (2017a). The Assembly Pathway of Mitochondrial Respiratory Chain Complex I. *Cel Metab.* 25, 128–139. doi:10.1016/j.cmet.2016.09.002

Guerrero-Castillo, S., Cabrera-Orefice, A., Huynen, M. A., and Arnold, S. (2017b). Identification and Evolutionary Analysis of Tissue-specific Isoforms of Mitochondrial Complex I Subunit NDUFV3. *Biochim. Biophys. Acta (Bba) - Bioenerg.* 1858, 208–217. doi:10.1016/j.bbabio.2016.12.004

Guerrero-Castillo, S., Krisp, C., Küchler, K., Arnold, S., Schlüter, H., and Gersting, S. W. (2021a). Multiplexed Complexome Profiling Using Tandem Mass Tags. *Biochim. Biophys. Acta (Bba) - Bioenerg.* 1862, 148448. doi:10.1016/j.bbabio.2021.148448

Haldar, K., Bhattacharjee, S., and Safeukui, I. (2018). Drug Resistance in Plasmodium. *Nat. Rev. Microbiol.* 16, 156–170. doi:10.1038/nrmicro.2017.161

Hällberg, B. M., and Larsson, N.-G. (2014). Making Proteins in the Powerhouse. *Cel Metab.* 20, 226–240. doi:10.1016/j.cmet.2014.07.001

Harb, O. S., Kissinger, J. C., and Roos, D. S. (2020). "ToxoDB: the Functional Genomic Resource for Toxoplasma and Related Organisms," in *Toxoplasma Gondii* (Elsevier), 1021–1041. doi:10.1016/b978-0-12-815041-2.00023-2

Harner, M., Körner, C., Walther, D., Mokranjac, D., Kaesmacher, J., Welsch, U., et al. (2011). The Mitochondrial Contact Site Complex, a Determinant of Mitochondrial Architecture. *EMBO J.* 30, 4356–4370. doi:10.1038/emboj.2011.379

Haute, L. V., Hendrick, A. G., D'Souza, A. R., Powell, C. A., Rebelo-Guiomar, P., Harbour, M. E., et al. (2019). METTL15 Introduces N4-Methylcytidine into Human Mitochondrial 12S rRNA and Is Required for Mitoribosome Biogenesis. *Nucleic Acids Res.* 47, 10267–10281. doi:10.1093/nar/gkz735

Havugimana, P. C., Hart, G. T., Nepusz, T., Yang, H., Turinsky, A. L., Li, Z., et al. (2012). A Census of Human Soluble Protein Complexes. *Cell* 150, 1068–1081. doi:10.1016/j.cell.2012.08.011

Hebert, A. S., Merrill, A. E., Bailey, D. J., Still, A. J., Westphall, M. S., Strieter, E. R., et al. (2013). Neutron-encoded Mass Signatures for Multiplexed Proteome Quantification. *Nat. Methods* 10, 332–334. doi:10.1038/nmeth.2378

Heide, H., Bleier, L., Steger, M., Ackermann, J., Dröse, S., Schwamb, B., et al. (2012). Complexome Profiling Identifies TMEM126B as a Component of the Mitochondrial Complex I Assembly Complex. *Cel Metab.* 16, 538–549. doi:10.1016/j.cmet.2012.08.009

Hellman, L. M., and Fried, M. G. (2007). Electrophoretic Mobility Shift Assay (EMSA) for Detecting Protein-Nucleic Acid Interactions. *Nat. Protoc.* 2, 1849–1861. doi:10.1038/nprot.2007.249

Herrmannová, A., Prilepskaja, T., Wagner, S., Šikrová, D., Zeman, J., Poncová, K., et al. (2020). Adapted Formaldehyde Gradient Cross-Linking Protocol Implicates Human eIF3d and eIF3c, K and L Subunits in the 43S and 48S Pre-initiation Complex Assembly, Respectively. *Nucleic Acids Res.* 48, 1969–1984. doi:10.1093/nar/gkz1185

Herzog, F., Kahraman, A., Boehringer, D., Mak, R., Bracher, A., Walzthoeni, T., et al. (2012). Structural Probing of a Protein Phosphatase 2A Network by Chemical Cross-Linking and Mass Spectrometry. *Science* 337, 1348–1352. doi:10.1126/science.1221483

Heusel, M., Bludau, I., Rosenberger, G., Hafen, R., Frank, M., Banaei-Esfahani, A., et al. (2019). Complex-centric Proteome Profiling by SEC - SWATH - MS. *Mol. Syst. Biol.* 15, e8438. doi:10.15252/msb.20188438

Hevler, J. F., Lukassen, M. V., Cabrera-Orefice, A., Arnold, S., Pronker, M. F., Franc, V., et al. (2021a). Selective Cross-linking of Coinciding Protein Assemblies by In-gel Cross-linking Mass Spectrometry. *EMBO J.* 40, e106174. doi:10.15252/embj.2020106174

Hevler, J. F., Zenezeni Chiozzi, R., Cabrera-Orefice, A., Brandt, U., Arnold, S., and Heck, A. J. R. (2021b). Molecular Characterization of a Complex of Apoptosis-Inducing Factor 1 with Cytochrome C Oxidase of the Mitochondrial Respiratory Chain. *Proc. Natl. Acad. Sci. USA* 118, e2106950118. doi:10.1073/pnas.2106950118

Hilander, T., Jackson, C. B., Robciuc, M., Bashir, T., and Zhao, H. (2021). The Roles of Assembly Factors in Mammalian Mitoribosome Biogenesis. *Mitochondrion* 60, 70–84. doi:10.1016/J.MITO.2021.07.008

Hillier, C., Pardo, M., Yu, L., Bushell, E., Sanderson, T., Metcalf, T., et al. (2019). Landscape of the Plasmodium Interactome Reveals Both Conserved and Species-specific Functionality. *Cel Rep.* 28, 1635–1647. e1635. doi:10.1016/j.celrep.2019.07.019

Hirst, J. (2013). Mitochondrial Complex I. *Annu. Rev. Biochem.* 82, 551–575. doi:10.1146/annurev-biochem-070511-103700

Hocine, S., Singer, R. H., and Grünwald, D. (2010). RNA Processing and Export. *Cold Spring Harbor Perspect. Biol.* 2, a000752. doi:10.1101/CSHPERSPECT.A000752

Hong, P., Koza, S., and Bouvier, E. S. P. (2012). A Review Size-Exclusion Chromatography for the Analysis of Protein Biotherapeutics and Their Aggregates. *J. Liquid Chromatogr. Relat. Tech.* 35, 2923–2950. doi:10.1080/10826076.2012.743724

Honzík, T., Tesarová, M., Mayr, J. A., Hansíková, H., Jesina, P., Bodamer, O., et al. (2010). Mitochondrial Encephalocardio-Myopathy with Early Neonatal Onset Due to TMEM70 Mutation. *Arch. Dis. Child.* 95, 296–301. doi:10.1136/adc.2009.168096

Hör, J., Di Giorgio, S., Gerovac, M., Venturini, E., Förstner, K. U., and Vogel, J. (2020). Grad-seq Shines Light on Unrecognized RNA and Protein Complexes in the Model Bacterium *Escherichia coli*. *Nucleic Acids Res.* 48, 9301–9319. doi:10.1093/nar/gkaa676

Hu, A., Noble, W. S., and Wolf-Yadlin, A. (2016). Technical Advances in Proteomics: New Developments in Data-independent Acquisition. *F1000Res* 5, 419. doi:10.12688/f1000research.7042.1

Hu, L. Z., Goebels, F., Tan, J. H., Wolf, E., Kuzmanov, U., Wan, C., et al. (2019). EPIC: Software Toolkit for Elution Profile-Based Inference of Protein Complexes. *Nat. Methods* 16, 737–742. doi:10.1038/s41592-019-0461-4

Huynen, M. A., Mühlmeister, M., Gotthardt, K., Guerrero-Castillo, S., and Brandt, U. (2016). Evolution and Structural Organization of the Mitochondrial Contact Site (MICOS) Complex and the Mitochondrial Intermembrane Space Bridging (MIB) Complex. *Biochim. Biophys. Acta (Bba) - Mol. Cel Res.* 1863, 91–101. doi:10.1016/j.bbamcr.2015.10.009

Iacobucci, I., Monaco, V., Cozzolino, F., and Monti, M. (2021). From Classical to New Generation Approaches: An Excursus of -omics Methods for Investigation of Protein-Protein Interaction Networks. *J. Proteomics* 230, 103990. doi:10.1016/j.jprot.2020.103990

Jenkinson, E. M., Rehman, A. U., Walsh, T., Clayton-Smith, J., Lee, K., Morell, R. J., et al. (2013). Perrault Syndrome Is Caused by Recessive Mutations in CLPP, Encoding a Mitochondrial ATP-dependent Chambered Protease. *Am. J. Hum. Genet.* 92, 605–613. doi:10.1016/j.ajhg.2013.02.013

Jonckheere, A. I., Huigsloot, M., Lammens, M., Jansen, J., Van Den Heuvel, L. P., Spiekerkoetter, U., et al. (2011). Restoration of Complex V Deficiency Caused by a Novel Deletion in the Human TMEM70 Gene Normalizes Mitochondrial Morphology. *Mitochondrion* 11, 954–963. doi:10.1016/j.mito.2011.08.012

Kaila, V. R. I., and Wikström, M. (2021). Architecture of Bacterial Respiratory Chains. *Nat. Rev. Microbiol.* 19, 319–330. doi:10.1038/s41579-020-00486-4

Kartal, B., De Almeida, N. M., Maalcke, W. J., Op Den Camp, H. J. M., Jetten, M. S. M., and Keltjens, J. T. (2013). How to Make a Living from Anaerobic Ammonium Oxidation. *FEMS Microbiol. Rev.* 37, 428–461. doi:10.1111/1574-6976.12014

Kastritis, P. L., O'reilly, F. J., Bock, T., Li, Y., Rogon, M. Z., Buczak, K., et al. (2017). Capturing Protein Communities by Structural Proteomics in a Thermophilic Eukaryote. *Mol. Syst. Biol.* 13, 936. doi:10.15252/msb.20167412

Kiirika, L. M., Behrens, C., Braun, H.-P., and Colditz, F. (2013). The Mitochondrial Complexome of Medicago Truncatula. *Front. Plant Sci.* 4, 84. doi:10.3389/fpls.2013.00084

King, M. P., and Attardi, G. (1989). Human Cells Lacking mtDNA: Repopulation with Exogenous Mitochondria by Complementation. *Science* 246, 500–503. doi:10.1126/science.2814477

Kmita, K., Wirth, C., Warnau, J., Guerrero-Castillo, S., Hunte, C., Hummer, G., et al. (2015). Accessory NUMM (NDUFS6) Subunit Harbors a Zn-Binding Site and Is Essential for Biogenesis of Mitochondrial Complex I. *Proc. Natl. Acad. Sci. USA* 112, 5685–5690. doi:10.1073/pnas.1424353112

König, T., Tröder, S. E., Bakka, K., Korwitz, A., Richter-Dennerlein, R., Lampe, P. A., et al. (2016). The M -AAA Protease Associated with Neurodegeneration Limits MCU Activity in Mitochondria. *Mol. Cel* 64, 148–162. doi:10.1016/j.molcel.2016.08.020

Korepanova, A., and Matayoshi, E. D. (2012). HPLC-SEC Characterization of Membrane Protein-Detergent Complexes. *Curr. Protoc. Protein Sci.* 68–12. doi:10.1002/0471140864.ps2905s68

Krasny, L., and Huang, P. H. (2021). Data-independent Acquisition Mass Spectrometry (DIA-MS) for Proteomic Applications in Oncology. *Mol. Omics* 17, 29–42. doi:10.1039/d0mo00072h

Kristensen, A. R., Gsponer, J., and Foster, L. J. (2012). A High-Throughput Approach for Measuring Temporal Changes in the Interactome. *Nat. Methods* 9, 907–909. doi:10.1038/nmeth.2131

Kummer, E., and Ban, N. (2021). Mechanisms and Regulation of Protein Synthesis in Mitochondria. *Nat. Rev. Mol. Cel Biol* 22, 307–325. doi:10.1038/s41580-021-00332-2

Kyrilis, F. L., Belapure, J., and Kastritis, P. L. (2021). Detecting Protein Communities in Native Cell Extracts by Machine Learning: A Structural Biologist's Perspective. *Front. Mol. Biosci.* 8, 660542. doi:10.3389/fmolb.2021.660542

Ladig, R., Sommer, M. S., Hahn, A., Leisegang, M. S., Papasotiriou, D. G., Ibrahim, M., et al. (2011). A High-Definition Native Polyacrylamide Gel Electrophoresis System for the Analysis of Membrane Complexes. *Plant J.* 67, 181–194. doi:10.1111/j.1365-313X.2011.04577.x

Lapuente-Brun, E., Moreno-Loshuertos, R., Acín-Pérez, R., Latorre-Pellicer, A., Colás, C., Balsa, E., et al. (2013). Supercomplex Assembly Determines Electron Flux in the Mitochondrial Electron Transport Chain. *Science* 340, 1567–1570. doi:10.1126/science.1230381

Lasserre, J.-P., Beyne, E., Pyndiah, S., Lapaillerie, D., Claverol, S., and Bonneu, M. (2006). A Complexomic Study ofEscherichia Coli Using Two-Dimensional Blue Native/SDS Polyacrylamide Gel Electrophoresis. *Electrophoresis* 27, 3306–3321. doi:10.1002/elps.200500912

Lee, J.-H., and Skalnik, D. (2013). Simple and Efficient Identification of Chromatin Modifying Complexes and Characterization of Complex Composition. *Methods Mol. Biol.* 977, 289–298. doi:10.1007/978-1-62703-284-1_23

Liu, F., Lössl, P., Rabbitts, B. M., Balaban, R. S., and Heck, A. J. R. (2018). The Interactome of Intact Mitochondria by Cross-Linking Mass Spectrometry Provides Evidence for Coexisting Respiratory Supercomplexes. *Mol. Cell Proteomics* 17, 216–232. doi:10.1074/mcp.RA117.000470

Lobo-Jarne, T., Pérez-Pérez, R., Fontanesi, F., Timón-Gómez, A., Wittig, I., Peñas, A., et al. (2020). Multiple Pathways Coordinate Assembly of Human Mitochondrial Complex IV and Stabilization of Respiratory Supercomplexes. *EMBO J.* 39, e103912. doi:10.15252/embj.2019103912

López De Heredia, M., and Jansen, R. P. (2004). RNA Integrity as a Quality Indicator during the First Steps of RNP Purifications: A Comparison of Yeast Lysis Methods. *BMC Biochem.* 5, 14. doi:10.1186/1471-2091-5-14

Low, T. Y., Syafruddin, S. E., Mohtar, M. A., Vellaichamy, A., A Rahman, N. S., Pung, Y.-F., et al. (2021). Recent Progress in Mass Spectrometry-Based Strategies for Elucidating Protein-Protein Interactions. *Cell. Mol. Life Sci.* 78, 5325–5339. doi:10.1007/s00018-021-03856-0

Maclean, A. E., Bridges, H. R., Silva, M. F., Ding, S., Ovciarikova, J., Hirst, J., et al. (2021). Complexome Profile of Toxoplasma Gondii Mitochondria Identifies Divergent Subunits of Respiratory Chain Complexes Including New Subunits of Cytochrome Bc1 Complex. *Plos Pathog.* 17, e1009301. doi:10.1371/journal.ppat.1009301

Macrae, J. I., Dixon, M. W., Dearnley, M. K., Chua, H. H., Chambers, J. M., Kenny, S., et al. (2013). Mitochondrial Metabolism of Sexual and Asexual Blood Stages of the Malaria Parasite Plasmodium Falciparum. *BMC Biol.* 11, 67. doi:10.1186/1741-7007-11-67

Mallam, A. L., Sae-Lee, W., Schaub, J. M., Tu, F., Battenhouse, A., Jang, Y. J., et al. (2019). Systematic Discovery of Endogenous Human Ribonucleoprotein Complexes. *Cel Rep.* 29, 1351–1368. e1355. doi:10.1016/j.celrep.2019.09.060

Mcalister, G. C., Nusinow, D. P., Jedrychowski, M. P., Wühr, M., Huttlin, E. L., Erickson, B. K., et al. (2014). MultiNotch MS3 Enables Accurate, Sensitive, and Multiplexed Detection of Differential Expression across Cancer Cell Line Proteomes. *Anal. Chem.* 86, 7150–7158. doi:10.1021/ac502040v

Meldal, B. H. M., Perfetto, L., Combe, C., Lubiana, T., Ferreira Cavalcante, J. V., Bye-A-Jee, H., et al. (2021). Complex Portal 2022: New Curation Frontiers. *Nucleic Acids Res.*, gkab991. doi:10.1093/nar/gkab991

Merrill, A. E., Hebert, A. S., Macgilvray, M. E., Rose, C. M., Bailey, D. J., Bradley, J. C., et al. (2014). NeuCode Labels for Relative Protein Quantification. *Mol. Cell Proteomics* 13, 2503–2512. doi:10.1074/mcp.M114.040287

Mili, S., and Steitz, J. A. (2004). Evidence for Reassociation of RNA-Binding Proteins after Cell Lysis: Implications for the Interpretation of Immunoprecipitation Analyses. *RNA* 10, 1692–1694. doi:10.1261/rna.7151404

Mintseris, J., and Gygi, S. P. (2020). High-density Chemical Cross-Linking for Modeling Protein Interactions. *Proc. Natl. Acad. Sci. USA* 117, 93–102. doi:10.1073/pnas.1902931116

Mistry, J., Chuguransky, S., Williams, L., Qureshi, M., Salazar, G. A., Sonnhammer, E. L. L., et al. (2021). Pfam: The Protein Families Database in 2021. *Nucleic Acids Res.* 49, D412–D419. doi:10.1093/nar/gkaa913

Mohamed, M., Gardeitchik, T., Balasubramaniam, S., Guerrero-Castillo, S., Dalloyaux, D., Kraaij, S., et al. (2020). Novel Defect in Phosphatidylinositol 4-kinase Type 2-alpha (PI4K2A) at the Membrane-enzyme Interface Is Associated with Metabolic Cutis Laxa. *Jrnl Inher Metab. Disea* 43, 1382–1391. doi:10.1002/jimd.12255

Müller, C. S., Bildl, W., Haupt, A., Ellenrieder, L., Becker, T., Hunte, C., et al. (2016). Cryo-slicing Blue Native-Mass Spectrometry (csBN-MS), a Novel Technology for High Resolution Complexome Profiling. *Mol. Cell Proteomics* 15, 669–681. doi:10.1074/mcp.M115.054080

Munawar, N., Olivero, G., Jerman, E., Doyle, B., Streubel, G., Wynne, K., et al. (2015). Native Gel Analysis of Macromolecular Protein Complexes in Cultured Mammalian Cells. *Proteomics* 15, 3603–3612. doi:10.1002/pmic.201500045

Neustein, H. B., Lurie, P. R., Dahms, B., and Takahashi, M. (1979). An X-Linked Recessive Cardiomyopathy with Abnormal Mitochondria. *Pediatrics* 64, 24–29.

Nolte, H., and Langer, T. (2021). ComplexFinder: A Software Package for the Analysis of Native Protein Complex Fractionation Experiments. *Biochim. Biophys. Acta (Bba) - Bioenerg.* 1862, 148444. doi:10.1016/j.bbabio.2021.148444

Nuebel, E., Morgan, J. T., Fogarty, S., Winter, J. M., Lettlova, S., Berg, J. A., et al. (2021). The Biochemical Basis of Mitochondrial Dysfunction in Zellweger Spectrum Disorder. *EMBO Rep.* 22, e51991. doi:10.15252/embr.202051991

Ong, S.-E., Blagoev, B., Kratchmarova, I., Kristensen, D. B., Steen, H., Pandey, A., et al. (2002). Stable Isotope Labeling by Amino Acids in Cell Culture, SILAC, as a Simple and Accurate Approach to Expression Proteomics. *Mol. Cell Proteomics* 1, 376–386. doi:10.1074/mcp.m200025-mcp200

O'Reilly, F. J., and Rappsilber, J. (2018). Cross-linking Mass Spectrometry: Methods and Applications in Structural, Molecular and Systems Biology. *Nat. Struct. Mol. Biol.* 25, 1000–1008. doi:10.1038/s41594-018-0147-0

Orsburn, B. C. (2021). Proteome Discoverer-A Community Enhanced Data Processing Suite for Protein Informatics. *Proteomes* 9, 15. doi:10.3390/proteomes9010015

Ott, C., Dorsch, E., Fraunholz, M., Straub, S., and Kozjak-Pavlovic, V. (2015). Detailed Analysis of the Human Mitochondrial Contact Site Complex Indicate a Hierarchy of Subunits. *PLoS One* 10, e0120213. doi:10.1371/journal.pone.0120213

Oughtred, R., Rust, J., Chang, C., Breitkreutz, B. J., Stark, C., Willems, A., et al. (2021). TheBioGRIDdatabase: A Comprehensive Biomedical Resource of Curated Protein, Genetic, and Chemical Interactions. *Protein Sci.* 30, 187–200. doi:10.1002/pro.3978

Overmyer, K. A., Tyanova, S., Hebert, A. S., Westphall, M. S., Cox, J., and Coon, J. J. (2018). Multiplexed Proteome Analysis with Neutron-Encoded Stable Isotope Labeling in Cells and Mice. *Nat. Protoc.* 13, 293–306. doi:10.1038/nprot.2017.121

Páleníková, P., Harbour, M. E., Ding, S., Fearnley, I. M., Van Haute, L., Rorbach, J., et al. (2021a). Quantitative Density Gradient Analysis by Mass Spectrometry (qDGMS) and Complexome Profiling Analysis (ComPrAn) R Package for the Study of Macromolecular Complexes. *Biochim. Biophys. Acta (Bba) - Bioenerg.* 1862, 148399. doi:10.1016/j.bbabio.2021.148399

Páleníková, P., Harbour, M. E., Prodi, F., Minczuk, M., Zeviani, M., Ghelli, A., et al. (2021b). Duplexing Complexome Profiling with SILAC to Study Human Respiratory Chain Assembly Defects. *Biochim. Biophys. Acta (Bba) - Bioenerg.* 1862, 148395. doi:10.1016/j.bbabio.2021.148395

Patton, R. D., Sanjeev, M., Woodward, L. A., Mabin, J. W., Bundschuh, R., and Singh, G. (2020). Chemical Crosslinking Enhances RNA Immunoprecipitation for Efficient Identification of Binding Sites of Proteins that Photo-Crosslink Poorly with RNA. *RNA* 26, 1216–1233. doi:10.1261/rna.074856.120

Pearce, S., Nezich, C. L., and Spinazzola, A. (2013). Mitochondrial Diseases: Translation Matters. *Mol. Cell Neurosci.* 55, 1–12. doi:10.1016/j.mcn.2012.08.013

Pereira, B., Videira, A., and Duarte, M. (2013). Novel Insights into the Role of Neurospora Crassa NDUFAF2, an Evolutionarily Conserved Mitochondrial Complex I Assembly Factor. *Mol. Cel Biol* 33, 2623–2634. doi:10.1128/MCB.01476-12

Pérez-Pérez, R., Lobo-Jarne, T., Milenkovic, D., Mourier, A., Bratic, A., García-Bartolomé, A., et al. (2016). COX7A2L Is a Mitochondrial Complex III Binding Protein that Stabilizes the III2+IV Supercomplex without Affecting Respirasome Formation. *Cel Rep.* 16, 2387–2398. doi:10.1016/j.celrep.2016.07.081

Perez-Riverol, Y., Csordas, A., Bai, J., Bernal-Llinares, M., Hewapathirana, S., Kundu, D. J., et al. (2019). The PRIDE Database and Related Tools and Resources in 2019: Improving Support for Quantification Data. *Nucleic Acids Res.* 47, D442–D450. doi:10.1093/nar/gky1106

Perkins, D. N., Pappin, D. J. C., Creasy, D. M., and Cottrell, J. S. (1999). Probability-based Protein Identification by Searching Sequence Databases Using Mass Spectrometry Data. *Electrophoresis* 20, 3551–3567. doi:10.1002/(sici)1522-2683(19991201)20:18<3551::aid-elps3551>3.0.co;2-2

Pitkänen, L., Tuomainen, P., and Eskelin, K. (2014). Analysis of Plant Ribosomes with Asymmetric Flow Field-Flow Fractionation. *Anal. Bioanal. Chem.* 406, 1629–1637. doi:10.1007/s00216-013-7454-4

Poole, R. K., and Cook, G. M. (2000). Redundancy of Aerobic Respiratory Chains in Bacteria? Routes, Reasons and Regulation. *Adv. Microb. Physiol.* 43, 165–224. doi:10.1016/s0065-2911(00)43005-5

Protasoni, M., Pérez-Pérez, R., Lobo-Jarne, T., Harbour, M. E., Ding, S., Peñas, A., et al. (2020). Respiratory Supercomplexes Act as a Platform for Complex III -mediated Maturation of Human Mitochondrial Complexes I and IV. *EMBO J.* 39, e102817. doi:10.15252/embj.2019102817

Reschiglian, P., and Moon, M. H. (2008). Flow Field-Flow Fractionation: a Pre-analytical Method for Proteomics. *J. Proteomics* 71, 265–276. doi:10.1016/j.jprot.2008.06.002

Rhein, V. F., Carroll, J., Ding, S., Fearnley, I. M., and Walker, J. E. (2016). NDUFAF5 Hydroxylates NDUFS7 at an Early Stage in the Assembly of Human Complex I. *J. Biol. Chem.* 291, 14851–14860. doi:10.1074/jbc.M116.734970

Robinson, P. J., Trnka, M. J., Pellarin, R., Greenberg, C. H., Bushnell, D. A., Davis, R., et al. (2015). Molecular Architecture of the Yeast Mediator Complex. *Elife* 4, e08719. doi:10.7554/eLife.08719

Rodenburg, R. J. (2016). Mitochondrial Complex I-Linked Disease. *Biochim. Biophys. Acta (Bba) - Bioenerg.* 1857, 938–945. doi:10.1016/j.bbabio.2016.02.012

Röst, H. L., Sachsenberg, T., Aiche, S., Bielow, C., Weisser, H., Aicheler, F., et al. (2016). OpenMS: a Flexible Open-Source Software Platform for Mass Spectrometry Data Analysis. *Nat. Methods* 13, 741–748. doi:10.1038/nmeth.3959

Rugen, N., Straube, H., Franken, L. E., Braun, H.-P., and Eubel, H. (2019). Complexome Profiling Reveals Association of PPR Proteins with Ribosomes in the Mitochondria of Plants. *Mol. Cell Proteomics* 18, 1345–1362. doi:10.1074/mcp.RA119.001396

Ryl, P. S. J., Bohlke-Schneider, M., Lenz, S., Fischer, L., Budzinski, L., Stuiver, M., et al. (2020). *In Situ* Structural Restraints from Cross-Linking Mass Spectrometry in Human Mitochondria. *J. Proteome Res.* 19, 327–336. doi:10.1021/acs.jproteome.9b00541

Sahr, T., and Buchrieser, C. (2013). Co-immunoprecipitation: Protein-RNA and Protein-DNA Interaction. *Methods Mol. Biol.* 954, 583–593. doi:10.1007/978-1-62703-161-5_36

Sánchez-Caballero, L., Elurbe, D. M., Baertling, F., Guerrero-Castillo, S., Van Den Brand, M., Van Strien, J., et al. (2020). TMEM70 Functions in the Assembly of Complexes I and V. *Biochim. Biophys. Acta (Bba) - Bioenerg.* 1861, 148202. doi:10.1016/j.bbabio.2020.148202

Sánchez-Caballero, L., Guerrero-Castillo, S., and Nijtmans, L. (2016a). Unraveling the Complexity of Mitochondrial Complex I Assembly: A Dynamic Process. *Biochim. Biophys. Acta (Bba) - Bioenerg.* 1857, 980–990. doi:10.1016/j.bbabio.2016.03.031

Sánchez-Caballero, L., Ruzzenente, B., Bianchi, L., Assouline, Z., Barcia, G., Metodiev, M. D., et al. (2016b). Mutations in Complex I Assembly Factor

TMEM126B Result in Muscle Weakness and Isolated Complex I Deficiency. *Am. J. Hum. Genet.* 99, 208–216. doi:10.1016/j.ajhg.2016.05.022

Schwanhäusser, B., Busse, D., Li, N., Dittmar, G., Schuchhardt, J., Wolf, J., et al. (2011). Global Quantification of Mammalian Gene Expression Control. *Nature* 473, 337–342. doi:10.1038/nature10098

Schwanhäusser, B., Gossen, M., Dittmar, G., and Selbach, M. (2009). Global Analysis of Cellular Protein Translation by Pulsed SILAC. *Proteomics* 9, 205–209. doi:10.1002/pmic.200800275

Schweppe, D. K., Chavez, J. D., Lee, C. F., Caudal, A., Kruse, S. E., Stuppard, R., et al. (2017). Mitochondrial Protein Interactome Elucidated by Chemical Cross-Linking Mass Spectrometry. *Proc. Natl. Acad. Sci. USA* 114, 1732–1737. doi:10.1073/pnas.1617220114

Senkler, J., Rugen, N., Eubel, H., Hegermann, J., and Braun, H.-P. (2018). Absence of Complex I Implicates Rearrangement of the Respiratory Chain in European Mistletoe. *Curr. Biol.* 28, 1606–1613. e1604. doi:10.1016/j.cub.2018.03.050

Senkler, J., Senkler, M., Eubel, H., Hildebrandt, T., Lengwenus, C., Schertl, P., et al. (2017). The Mitochondrial Complexome of *Arabidopsis thaliana*. *Plant J.* 89, 1079–1092. doi:10.1111/tpj.13448

Singhal, R. K., Kruse, C., Heidler, J., Strecker, V., Zwicker, K., Düsterwald, L., et al. (2017). Coi1 Is a Novel Assembly Factor of the Yeast Complex III-Complex IV Supercomplex. *MBoC* 28, 2609–2622. doi:10.1091/mbc.E17-02-0093

Skinnider, M. A., Scott, N. E., Prudova, A., Kerr, C. H., Stoynov, N., Stacey, R. G., et al. (2021). An Atlas of Protein-Protein Interactions across Mouse Tissues. *Cell* 184, 4073–4089. e4017. doi:10.1016/j.cell.2021.06.003

Smirnov, A., Förstner, K. U., Holmqvist, E., Otto, A., Günster, R., Becher, D., et al. (2016). Grad-seq Guides the Discovery of ProQ as a Major Small RNA-Binding Protein. *Proc. Natl. Acad. Sci. USA* 113, 11591–11596. doi:10.1073/pnas.1609981113

Smits, P., Saada, A., Wortmann, S. B., Heister, A. J., Brink, M., Pfundt, R., et al. (2011). Mutation in mitochondrial ribosomal protein MRPS22 leads to Cornelia de Lange-like phenotype, brain abnormalities and hypertrophic cardiomyopathy. *Eur. J. Hum. Genet.* 19, 394–399. doi:10.1038/ejhg.2010.214

Sonnett, M., Yeung, E., and Wühr, M. (2018). Accurate, Sensitive, and Precise Multiplexed Proteomics Using the Complement Reporter Ion Cluster. *Anal. Chem.* 90, 5032–5039. doi:10.1021/acs.analchem.7b04713

Spaniol, B., Lang, J., Venn, B., Schake, L., Sommer, F., Mustas, M., et al. (2021). Complexome Profiling on the Chlamydomonas Lpa2 Mutant Reveals Insights into PSII Biogenesis and New PSII Associated Proteins. *J. Exp. Bot.*, erab390. doi:10.1093/jxb/erab390

Sprink, T., Ramrath, D. J. F., Yamamoto, H., Yamamoto, K., Loerke, J., Ismer, J., et al. (2016). Structures of Ribosome-Bound Initiation Factor 2 Reveal the Mechanism of Subunit Association. *Sci. Adv.* 2, e1501502. doi:10.1126/SCIADV.1501502

Stacey, R. G., Skinnider, M. A., Scott, N. E., and Foster, L. J. (2017). A Rapid and Accurate Approach for Prediction of Interactomes from Co-elution Data (PrInCE). *BMC Bioinformatics* 18, 457. doi:10.1186/s12859-017-1865-8

Steigenberger, B., Albanese, P., Heck, A. J. R., and Scheltema, R. A. (2020). To Cleave or Not to Cleave in XL-MS? *J. Am. Soc. Mass. Spectrom.* 31, 196–206. doi:10.1021/jasms.9b00085

Stenton, S. L., Sheremet, N. L., Catarino, C. B., Andreeva, N. A., Assouline, Z., Barboni, P., et al. (2021). Impaired Complex I Repair Causes Recessive Leber's Hereditary Optic Neuropathy. *J. Clin. Invest.* 131. doi:10.1172/JCI138267

Strecker, V., Wumaier, Z., Wittig, I., and Schägger, H. (2010). Large Pore Gels to Separate Mega Protein Complexes Larger Than 10 MDa by Blue Native Electrophoresis: Isolation of Putative Respiratory Strings or Patches. *Proteomics* 10, 3379–3387. doi:10.1002/pmic.201000343

Szczepanowska, K., Senft, K., Heidler, J., Herholz, M., Kukat, A., Höhne, M. N., et al. (2020). A Salvage Pathway Maintains Highly Functional Respiratory Complex I. *Nat. Commun.* 11, 1643. doi:10.1038/s41467-020-15467-7

Szklarczyk, D., Gable, A. L., Nastou, K. C., Lyon, D., Kirsch, R., Pyysalo, S., et al. (2021). The STRING Database in 2021: Customizable Protein-Protein Networks, and Functional Characterization of User-Uploaded Gene/measurement Sets. *Nucleic Acids Res.* 49, D605–D612. doi:10.1093/nar/gkaa1074

Tran, N. H., Zhang, X., Xin, L., Shan, B., and Li, M. (2017). De Novo peptide Sequencing by Deep Learning. *Proc. Natl. Acad. Sci. USA* 114, 8247–8252. doi:10.1073/pnas.1705691114

Trendel, J., Schwarzl, T., Horos, R., Prakash, A., Bateman, A., Hentze, M. W., et al. (2019). The Human RNA-Binding Proteome and its Dynamics during Translational Arrest. *Cell* 176, 391–403. e319. doi:10.1016/j.cell.2018.11.004

Tyanova, S., Temu, T., and Cox, J. (2016a). The MaxQuant Computational Platform for Mass Spectrometry-Based Shotgun Proteomics. *Nat. Protoc.* 11, 2301–2319. doi:10.1038/nprot.2016.136

Tyanova, S., Temu, T., Sinitcyn, P., Carlson, A., Hein, M. Y., Geiger, T., et al. (2016b). The Perseus Computational Platform for Comprehensive Analysis of (Prote)omics Data. *Nat. Methods* 13, 731–740. doi:10.1038/nmeth.3901

Ugalde, C., Vogel, R., Huijbens, R., Van Den Heuvel, B., Smeitink, J., and Nijtmans, L. (2004). Human Mitochondrial Complex I Assembles through the Combination of Evolutionary Conserved Modules: a Framework to Interpret Complex I Deficiencies. *Hum. Mol. Genet.* 13, 2461–2472. doi:10.1093/hmg/ddh262

Uniprot, C. (2021). UniProt: the Universal Protein Knowledgebase in 2021. *Nucleic Acids Res.* 49, D480–D489. doi:10.1093/nar/gkaa1100

Urdaneta, E. C., and Beckmann, B. M. (2020). Fast and Unbiased Purification of RNA-Protein Complexes after UV Cross-Linking. *Methods* 178, 72–82. doi:10.1016/J.YMETH.2019.09.013

Urdaneta, E. C., Vieira-Vieira, C. H., Hick, T., Wessels, H.-H., Figini, D., Moschall, R., et al. (2019). Purification of Cross-Linked RNA-Protein Complexes by Phenol-Toluol Extraction. *Nat. Commun.* 10, 990. doi:10.1038/s41467-019-08942-3

Van Damme, T., Gardeitchik, T., Mohamed, M., Guerrero-Castillo, S., Freisinger, P., Guillemyn, B., et al. (2017). Mutations in ATP6V1E1 or ATP6V1A Cause Autosomal-Recessive Cutis Laxa. *Am. J. Hum. Genet.* 100, 216–227. doi:10.1016/j.ajhg.2016.12.010

Van Esveld, S. L., and Spelbrink, J. N. (2021). RNA Crosslinking to Analyze the Mitochondrial RNA-Binding Proteome. *Methods Mol. Biol.* 2192, 147–158. doi:10.1007/978-1-0716-0834-0_12

Van Strien, J., Guerrero-Castillo, S., Chatzispyrou, I. A., Houtkooper, R. H., Brandt, U., and Huynen, M. A. (2019). COmplexome Profiling ALignment (COPAL) Reveals Remodeling of Mitochondrial Protein Complexes in Barth Syndrome. *Bioinformatics* 35, 3083–3091. doi:10.1093/bioinformatics/btz025

Van Strien, J., Haupt, A., Schulte, U., Braun, H.-P., Cabrera-Orefice, A., Choudhary, J. S., et al. (2021). CEDAR, an Online Resource for the Reporting and Exploration of Complexome Profiling Data. *Biochim. Biophys. Acta (Bba) - Bioenerg.* 1862, 148411. doi:10.1016/j.bbabio.2021.148411

Vercellino, I., and Sazanov, L. A. (2021). The Assembly, Regulation and Function of the Mitochondrial Respiratory Chain. *Nat. Rev. Mol. Cel Biol.* doi:10.1038/s41580-021-00415-0

Versantvoort, W., Guerrero-Castillo, S., Wessels, H. J. C. T., Van Niftrik, L., Jetten, M. S. M., Brandt, U., et al. (2019). Complexome Analysis of the Nitrite-dependent Methanotroph Methylomirabilis Lanthanidiphila. *Biochim. Biophys. Acta (Bba) - Bioenerg.* 1860, 734–744. doi:10.1016/j.bbabio.2019.07.011

Vidal, M., Cusick, M. E., and Barabási, A.-L. (2011). Interactome Networks and Human Disease. *Cell* 144, 986–998. doi:10.1016/j.cell.2011.02.016

Vidoni, S., Harbour, M. E., Guerrero-Castillo, S., Signes, A., Ding, S., Fearnley, I. M., et al. (2017). MR-1S Interacts with PET100 and PET117 in Module-Based Assembly of Human Cytochrome C Oxidase. *Cel Rep.* 18, 1727–1738. doi:10.1016/j.celrep.2017.01.044

Wai, T., Saita, S., Nolte, H., Müller, S., König, T., Richter-Dennerlein, R., et al. (2016). The Membrane Scaffold SLP2 Anchors a Proteolytic Hub in Mitochondria Containing PARL and the I -AAA Protease YME1L. *EMBO Rep.* 17, 1844–1856. doi:10.15252/embr.201642698

Wang, X., Teferedegne, B., Shatzkes, K., Tu, W., and Murata, H. (2016). Endogenous RNase Inhibitor Contributes to Stability of RNA in Crude Cell Lysates: Applicability to RT-qPCR. *Anal. Biochem.* 513, 21–27. doi:10.1016/J.AB.2016.08.011

Weber, T. A., Koob, S., Heide, H., Wittig, I., Head, B., Van Der Bliek, A., et al. (2013). APOOL Is a Cardiolipin-Binding Constituent of the Mitofilin/MINOS Protein Complex Determining Cristae Morphology in Mammalian Mitochondria. *PLoS One* 8, e63683. doi:10.1371/journal.pone.0063683

Wessels, H. J. C. T., Vogel, R. O., Lightowlers, R. N., Spelbrink, J. N., Rodenburg, R. J., Van Den Heuvel, L. P., et al. (2013). Analysis of 953 Human Proteins from a Mitochondrial HEK293 Fraction by Complexome Profiling. *PLoS One* 8, e68340. doi:10.1371/journal.pone.0068340

Wessels, H. J. C. T., Vogel, R. O., Van Den Heuvel, L., Smeitink, J. A., Rodenburg, R. J., Nijtmans, L. G., et al. (2009). LC-MS/MS as an Alternative for SDS-PAGE

in Blue Native Analysis of Protein Complexes. *Proteomics* 9, 4221–4228. doi:10.1002/pmic.200900157

Wittig, I., Beckhaus, T., Wumaier, Z., Karas, M., and Schägger, H. (2010). Mass Estimation of Native Proteins by Blue Native Electrophoresis. *Mol. Cell Proteomics* 9, 2149–2161. doi:10.1074/mcp.M900526-MCP200

Wittig, I., Braun, H.-P., and Schägger, H. (2006). Blue Native PAGE. *Nat. Protoc.* 1, 418–428. doi:10.1038/nprot.2006.62

Wittig, I., Karas, M., and Schägger, H. (2007). High Resolution clear Native Electrophoresis for In-Gel Functional Assays and Fluorescence Studies of Membrane Protein Complexes. *Mol. Cell Proteomics* 6, 1215–1225. doi:10.1074/mcp.M700076-MCP200

Wittig, I., and Malacarne, P. F. (2021). Complexome Profiling: Assembly and Remodeling of Protein Complexes. *Ijms* 22, 7809. doi:10.3390/ijms22157809

Wöhlbrand, L., Ruppersberg, H. S., Feenders, C., Blasius, B., Braun, H.-P., and Rabus, R. (2016). Analysis of Membrane-Protein Complexes of the marine Sulfate Reducer Desulfobacula Toluolica Tol2 by 1D Blue Native-PAGE Complexome Profiling and 2D Blue Native-/SDS-PAGE. *PROTEOMICS* 16, 973–988. doi:10.1002/pmic.201500360

Wortmann, S. B., Ziętkiewicz, S., Guerrero-Castillo, S., Feichtinger, R. G., Wagner, M., Russell, J., et al. (2021). Neutropenia and Intellectual Disability Are Hallmarks of Biallelic and De Novo CLPB Deficiency. *Genet. Med.* 23, 1705–1714. doi:10.1038/s41436-021-01194-x

Xu, Y., Malhotra, A., Ren, M., and Schlame, M. (2006). The Enzymatic Function of Tafazzin. *J. Biol. Chem.* 281, 39217–39224. doi:10.1074/jbc.M606100200

Yoshikawa, H., Larance, M., Harney, D. J., Sundaramoorthy, R., Ly, T., Owen-Hughes, T., et al. (2018). Efficient Analysis of Mammalian Polysomes in Cells and Tissues Using Ribo Mega-SEC. *Elife* 7. doi:10.7554/eLife.36530

Yu, H., Lu, J. J., Rao, W., and Liu, S. (20162016). Capitalizing Resolving Power of Density Gradient Ultracentrifugation by Freezing and Precisely Slicing Centrifuged Solution: Enabling Identification of Complex Proteins from Mitochondria by Matrix Assisted Laser Desorption/Ionization Time-Of-Flight Mass Spectrometry. *J. Anal. Methods Chem.* 2016, 1–7. doi:10.1155/2016/8183656

Yu, Y., Ji, H., Doudna, J. A., and Leary, J. A. (2005). Mass Spectrometric Analysis of the Human 40S Ribosomal Subunit: Native and HCV IRES-Bound Complexes. *Protein Sci.* 14, 1438–1446. doi:10.1110/ps.041293005

Zhang, J., Xin, L., Shan, B., Chen, W., Xie, M., Yuen, D., et al. (2012). PEAKS DB: De Novo Sequencing Assisted Database Search for Sensitive and Accurate Peptide Identification. *Mol. Cell Proteomics* 11, M111. doi:10.1074/mcp.M111.010587

Zhang, Y., Fonslow, B. R., Shan, B., Baek, M.-C., and Yates, J. R., 3rd (2013). Protein Analysis by Shotgun/bottom-Up Proteomics. *Chem. Rev.* 113, 2343–2394. doi:10.1021/cr3003533

Conflict of Interest: The authors declare that the research was conducted in the absence of any commercial or financial relationships that could be construed as a potential conflict of interest.

Publisher's Note: All claims expressed in this article are solely those of the authors and do not necessarily represent those of their affiliated organizations, or those of the publisher, the editors and the reviewers. Any product that may be evaluated in this article, or claim that may be made by its manufacturer, is not guaranteed or endorsed by the publisher.

frontiers in Cell and Developmental Biology

REVIEW
published: 11 February 2022
doi: 10.3389/fcell.2022.796066

Role of Mitochondrial Nucleic Acid Sensing Pathways in Health and Patho-Physiology

Arpita Chowdhury[1], *Steffen Witte*[1] *and Abhishek Aich*[1,2]*

[1]Department of Cellular Biochemistry, University Medical Center, Göttingen, Germany, [2]Cluster of Excellence "Multiscale Bioimaging, from Molecular Machines to Networks of Excitable Cells" (MBExC), University of Göttingen, Göttingen, Germany

Mitochondria, in symbiosis with the host cell, carry out a wide variety of functions from generating energy, regulating the metabolic processes, cell death to inflammation. The most prominent function of mitochondria relies on the oxidative phosphorylation (OXPHOS) system. OXPHOS heavily influences the mitochondrial-nuclear communication through a plethora of interconnected signaling pathways. Additionally, owing to the bacterial ancestry, mitochondria also harbor a large number of Damage Associated Molecular Patterns (DAMPs). These molecules relay the information about the state of the mitochondrial health and dysfunction to the innate immune system. Consequently, depending on the intracellular or extracellular nature of detection, different inflammatory pathways are elicited. One group of DAMPs, the mitochondrial nucleic acids, hijack the antiviral DNA or RNA sensing mechanisms such as the cGAS/STING and RIG-1/MAVS pathways. A pro-inflammatory response is invoked by these signals predominantly through type I interferon (T1-IFN) cytokines. This affects a wide range of organ systems which exhibit clinical presentations of auto-immune disorders. Interestingly, tumor cells too, have devised ingenious ways to use the mitochondrial DNA mediated cGAS-STING-IRF3 response to promote neoplastic transformations and develop tumor micro-environments. Thus, mitochondrial nucleic acid-sensing pathways are fundamental in understanding the source and nature of disease initiation and development. Apart from the pathological interest, recent studies also attempt to delineate the structural considerations for the release of nucleic acids across the mitochondrial membranes. Hence, this review presents a comprehensive overview of the different aspects of mitochondrial nucleic acid-sensing. It attempts to summarize the nature of the molecular patterns involved, their release and recognition in the cytoplasm and signaling. Finally, a major emphasis is given to elaborate the resulting patho-physiologies.

Keywords: mitochondrion, disease, innate immunity, signaling, mitochondrial—nuclear exchange

OPEN ACCESS

Edited by:
Erika Fernandez-Vizarra, Veneto Institute of Molecular Medicine (VIMM), Italy

Reviewed by:
Tomàs Pinós, Vall d'Hebron Research Institute (VHIR), Spain
Carlo Fiore Viscomi, University of Padua, Italy

***Correspondence:**
Abhishek Aich
abhishek.aich@med.uni-goettingen.de

Specialty section:
This article was submitted to Cellular Biochemistry, a section of the journal Frontiers in Cell and Developmental Biology

Received: *15 October 2021*
Accepted: *14 January 2022*
Published: *11 February 2022*

Citation:
Chowdhury A, Witte S and Aich A (2022) Role of Mitochondrial Nucleic Acid Sensing Pathways in Health and Patho-Physiology. Front. Cell Dev. Biol. 10:796066. doi: 10.3389/fcell.2022.796066

INTRODUCTION

Mitochondria play an essential role in generating cellular energy and contain the oxidative phosphorylation (OXPHOS) system. Primary mitochondrial disorders are a complex group of metabolic impairments caused by flaws or deficiencies in one or more components of the OXPHOS. All these defects manifest in mitochondrial dysfunction which is sensed and communicated through

a plethora of mitochondrial-nuclear signaling pathways (Mottis et al., 2019). However, in recent years, interferon-dependent innate immune responses have been shown to affect OXPHOS machinery and vice versa (Kiritsy et al., 2020; Buang et al., 2021). Defects in OXPHOS metabolism also result in the trigger of mitochondrial nucleic acid sensing pathways (Lei et al., 2021; Sprenger et al., 2021). Thus, to unravel this complex interaction, it is necessary to decipher how mitochondria communicate with the immune system.

FOREIGN NATURE OF MITOCHONDRIA

The eukaryotic way of life is principally maintained by energy-transducing organelles, the mitochondria. An endosymbiotic event around two billion years ago led to the acquisition of this organelle. (Gray et al., 1999; Osteryoung and Nunnari, 2003). According to the widely accepted theory, a host cell engulfed an α-proteobacterium *via* endocytosis, which led to a double-membrane-bound organelle harboring its independent genetic material. Thus the host cell acquired the ability to couple catabolism of carbon fuels to ATP synthesis through OXPHOS. In course of evolution, functional redundancy led to the loss of the original proteobacterial genetic material. The rest which was essential was transferred to the nuclear genome (nDNA) of the host cell (Gray et al., 1999). In modern-day mammals, around 1,200 mitochondrial proteins are encoded by the nDNA (Pagliarini et al., 2008; Rath et al., 2020). These proteins are translated on the cytosolic ribosomes and subsequently imported into mitochondria through a dedicated mitochondrial protein import system (Dudek et al., 2013). However, mitochondria still retains a small fraction of the original proteobacterial genome within its matrix—mitochondrial DNA (mtDNA). In vertebrates, mtDNA contains intronless, polycistronic genes that encode only 13 mitochondrial proteins, 22 transfer RNAs and two ribosomal RNAs (Shadel and Clayton, 1997).

Mitochondrial Organization and Dynamics

Like other organelles, mitochondria are maintained within the cell where they undergo biogenesis and turnover. They are also distributed among daughter cells following mitosis. Thus, the dynamic nature of mitochondria—fission, fusion and distribution—is responsible for its function and inheritance. Among the mitochondria in each cell, there are intricate networks of threads and smaller fragmented bodies depending on its health and function. Smaller mitochondrial organelles are generated when mitochondria divide, permitting efficient movement, organisation around the cell and inheritance. Mitochondrial fusion ensures that functionally and structurally homogeneous networks are formed by mixing material between organelles. Consequently, mitochondrial dynamics govern many aspects of the network, including organelle turnover, metabolism, cell stress and disease (Kraus et al., 2021).

Furthermore, mitochondrial state also contributes to continuous nucleo-mitochondrial communication, such as the retrograde signaling, anterograde signaling, integrated stress response and mito-nuclear crosstalk (**Figure 1**). It is the complex signaling cascade that involves nuclear genes encoding transcription factors for mitochondrial maintenance. This directly affects OXPHOS structural heterogeneity and metabolic plasticity (Ryan and Hoogenraad, 2007). Furthermore, during stress conditions such as starvation or cell growth, contact sites among organelles can spatially regulate lipid synthesis, protein turnover and molecular trafficking. Moreover, the mitochondria associated membranes (MAMs), which are contact sites between the endoplasmic reticulum (ER) and the mitochondria, are responsible for the regulation of ROS generation, calcium homeostasis and autophagy (Quirós et al., 2016). Thus, to maintain the balance between cellular and mitochondrial health, several quality control mechanisms have evolved. Notably, the most studied ones are autophagy, mitophagy, translation attenuation processes and mitochondrial unfolded protein response (mtUPR) (Lechuga-Vieco et al., 2021). In recent years, a new paradigm of mitochondrial stress signaling is being uncovered. In this review, we would like to highlight this equally important pathway of mitochondrial nucleic acid sensing induced stress signaling.

Mitochondrial Derived Damage Associated Molecular Patterns

Innate immunity is body's first line of defense against pathogens and other invaders. It relies on sensing of two kinds of stimuli, Pathogen Associated Molecular Patterns (PAMPs) or Damage Associated Molecular Patterns (DAMPs) (Zindel and Kubes, 2019). PAMPs are foreign, pathogen-exclusive molecules meant to alert the immune system of an invader it needs to clear. DAMPs, on the other hand, are host produced molecules—usually sequestered away from the surveillance of the immune system in cellular compartments. But upon stress or cellular damage, these are released from their compartments and sensed as foreign, eliciting a similar innate immune response one would see against pathogens. The sensing of these molecules could be through intrinsic pathway or extrinsic pathway. In the intrinsic pathway they are sensed in the cytoplasm of the cells undergoing the damage, while in the extrinsic pathway the sensing occurs outside in the plasma by other cells such as the dendritic cells or monocytes (**Figure 2**). The chemical properties of the DAMPs decide its ability to trigger either of the pathways. Thus, it is important to look at some of the key mitochondria derived DAMPs (mtDs) and their mode of action.

Adenosine triphosphate (ATP) is the most prominent product of mitochondria, associated as the currency of energy in the cell. It is synthesized in the matrix of the mitochondria by ATP synthase coupled to the OXPHOS. Depending upon the demand it is translocated to the cytoplasm of the cell through the adenine nucleotide translocator (Ruprecht et al., 2019). Thus, under normal heathy physiology, ATP mostly stays intracellular. ATP exit the cells upon cellular damage, exocytosis and through ATP release channels (Taruno, 2018). Extracellular ATP associated with stress or damage is mostly pro-inflammatory (Faas et al., 2017). Through the activation of

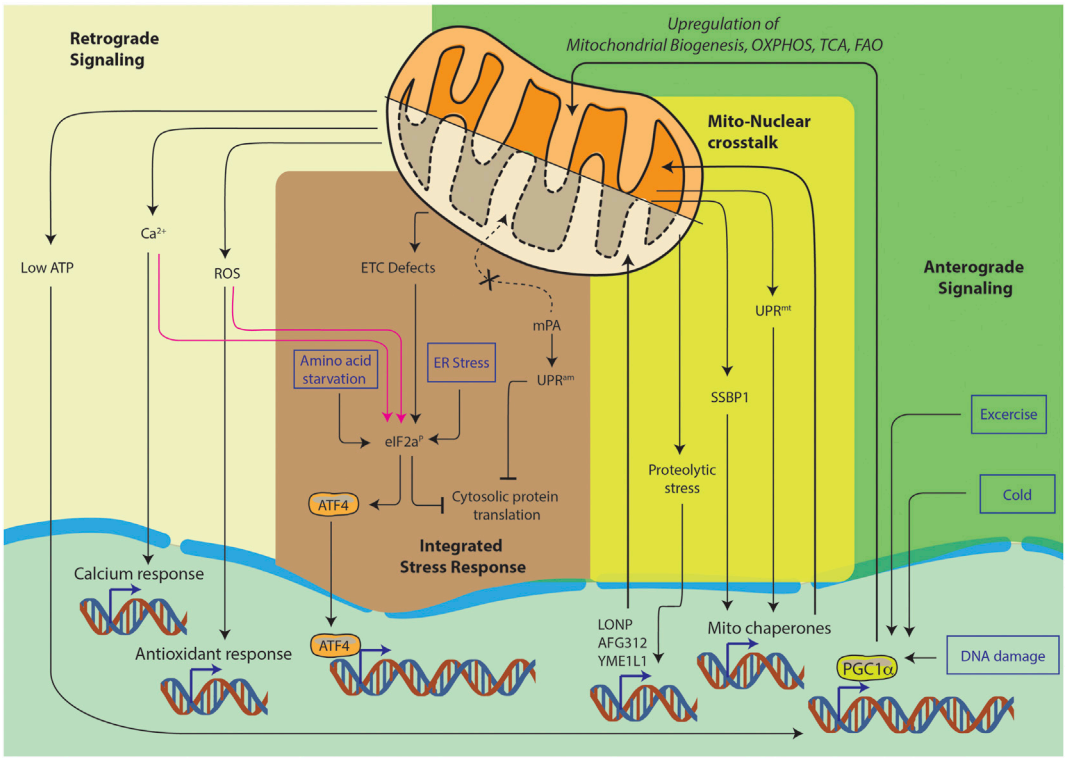

FIGURE 1 | Pathways of nucleo-mitochondrial communication. Nucleus-to-mitochondrion signals make up anterograde signaling. Signals from the mitochondria constitute the retrograde signaling. The integrated stress response is a general cellular stress pathway which can be triggered in ER, mitochondria or cytosol. Lastly, mito-nuclear crosstalk is the ability to orchestrate bidirectional feedback responses, they usually originate in mitochondria and result in nuclear responses.

P2X ligand-gated ion channels and P2Y G protein-coupled receptors, extracellular ATP is able to act on virtually all subsets of immune cells (Cekic and Linden, 2016).

Another mtDs, succinate, is generated in the in mitochondria during energy metabolism *via* the tricarboxylic acid cycle (TCA). It may be released to the extracellular space through plasma membrane transporters of the SLC13 family (Willmes and Birkenfeld, 2013). Here, it is sensed by G protein-coupled receptors, GPR91/SUCNR1—which are expressed across a wide variety of tissues (Gilissen et al., 2016). Succinate has dual roles during inflammatory responses. It has either a pro- or anti-inflammatory role depending on the cellular context (Grimolizzi and Arranz, 2018). Studies on uncoupling protein 1 (UCP1) using the UCP1KO mice, show that UCP1-succinate–SUCNR1 axis is crucial for liver immune cell infiltration and pathology (Mills et al., 2021). On the other hand, it has been shown to hyperpolarize macrophages towards the M2 phenotype (Trauelsen et al., 2021).

The next mtDs, cardiolipin (CL), is a phospholipid which happens to be an important component of the inner mitochondrial membrane (IMM). Upon apoptotic signals, cellular infections and inflammatory diseases, it is translocated to the outer mitochondrial membrane (OMM) (Pizzuto and Pelegrin, 2020). Mitochondrial function and the inflammatory response to translocated cardiolipin depend on its saturation and oxidation status. Similar to succinate, it can have both pro- or anti-inflammatory roles. In addition to its direct sensing by CD1d on T-cells (Dieudé et al., 2011) and NLRP3 inflammasome (Iyer et al., 2013), it can also promote inflammation by blocking IL-10 production as shown in mice infected with *Klebsiella pneumoniae* (Chakraborty et al., 2017).

Another archaic remnant in the mitochondria is the process of N-formylation. The mitochondria still use N-formyl-methionyl-tRNA as an initiator of protein synthesis (Ayyub and Varshney, 2019). This process is also observed in bacteria and chloroplasts. Thus, damaged and dying mitochondria secrete N-formyl peptides which are picked up as chemotactic tails by polymorphonuclear cells (Wenceslau et al., 2014). These are recognized by FPR1 receptors (He and Ye, 2017). The outcome of FPR1 receptor engagement depends on the pathogen and disease. It either acts pro- or anti-inflammatory. This contrast can be seen in two different bacterial infections. In case of *Escherichia coli and Listeria monocytogenes*, FPR1 causes chemotactic recruitment of neutrophils, whereas contrarily it helps in the dissemination of *Yersinia pestis* (Vacchelli et al., 2020).

Mitochondrial transcription factor A (TFAM) is another mtDs, which is a protein that binds nonspecifically in large number of copies to the mtDNA. It is responsible for the spatial organization and biogenesis of the same. Upon mitochondrial damage and dysfunction, extramitochondrial protein localization of TFAM increases significantly.

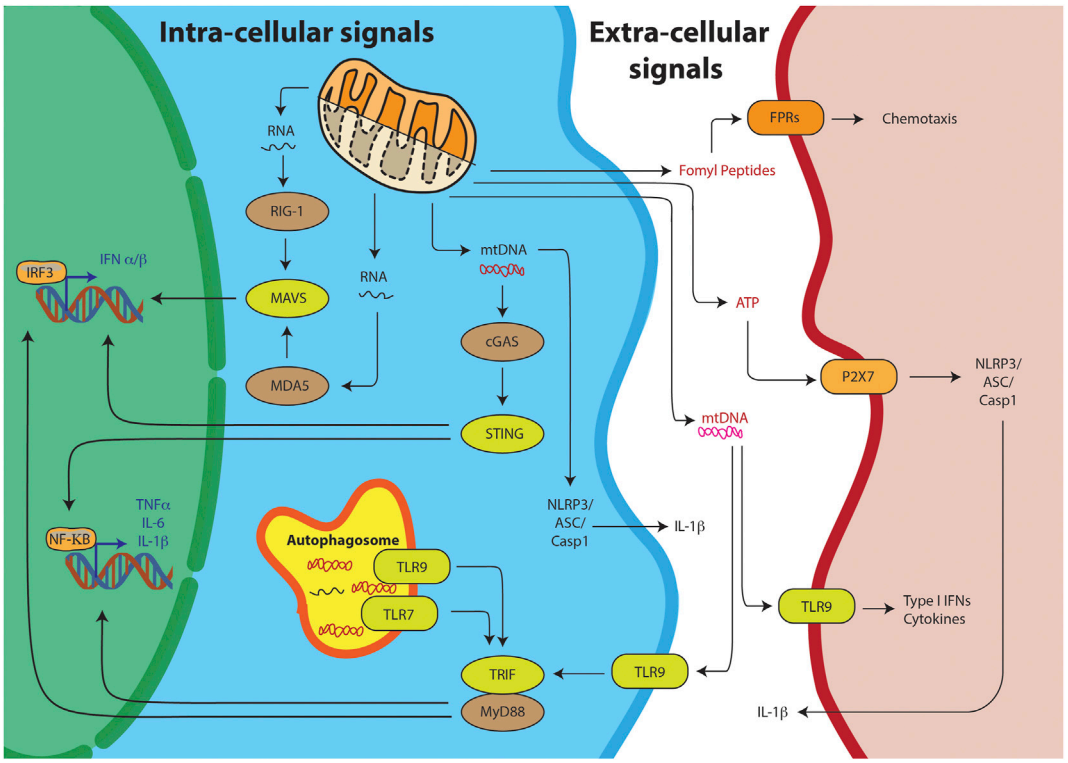

FIGURE 2 | Mitochondrial DAMPs can trigger the innate immunity through various pathways. Intra-cellular signals include the sensing of the mitochondrial nucleic acids, mtRNA or mtDNA, resulting into IRF3 or NFKB mediated T1-IFN response. Alternatively, TLR receptors on the autophagosome can sense mitochondrial nucleic acids and through TRIF/MyD88 stimulate the T1-IFN signaling. Free mtDNA can also stimulate the inflammasome for IL-1B production. DAMPs can also stimulate their respective receptors on other cells through extra-cellular signaling.

Extracellular TFAM inevitably elicits a pro-inflammatory response (Little et al., 2014). Injection of TFAM in rat brains have shown that different cells types elicit an upregulation of inflammatory mediators such as monocyte chemotactic protein (MCP)-1, IL-1β, IL-6, tumor necrosis factor (TNF)-α (Schindler et al., 2018). It serves in promoting plasmacytoid Dendritic Cell responses to mtDNA through engagement of Toll like receptor (TLR) nine receptors (Julian et al., 2012).

The last group of mtDs, which happen to be the focus of this review, are mitochondrial nucleic acids. mtDNA, a double stranded circular molecule, is often represented as a plasmid structure. But it is always packed as densely compacted nucleoprotein structures called nucleoids. Typically, a nucleoid contains one to two mtDNA molecules in mammals (Kukat et al., 2011). Since the volume of the purified mtDNA significantly exceeds that of the mitochondria itself, a considerable compaction and organization with the help of more than 50 different proteins are required for this structure to be packed in the matrix (Bogenhagen et al., 2003). Apart from this, specific bodies called "mitochondrial RNA granules" were found in mitochondrial matrix. These are complexes of RNase P with newly synthesized mtRNA (Jourdain et al., 2016; Xavier and Martinou, 2021). Thus, a radial organization of the genetic material is hypothesized, with the nucleoid at the core, surrounded by ring of RNA granules which are further surrounded by a cloud of mRNA being translated. Since, both mitochondrial nucleic acids are well sequestered in the matrix of the mitochondria, these escape the self-nonself discrimination of both the innate and adaptive immunity arms. The detailed mechanism of release and detection of both of these moieties is discussed in the next sections. Furthermore, they are associated with several "auto-immune" diseases affecting a multitude of organ systems, thus demanding a comprehensive look as well.

MITOCHONDRIA: THE HIDDEN PLAYER IN INNATE IMMUNE RESPONSE

Innate immunity is an evolutionarily conserved host defense mechanism. Mammals possess innate immune defenses in nearly every tissue, including the skin and mucosal surfaces of the respiratory and digestive tracts. In response to tissue damage, heat shock, infections, genotoxic or carcinogenic stress, the hematopoietic myeloid and lymphoid cells can trigger and further exert innate defense mechanisms. This is primarily mediated by the release of endogenous molecules such as uric acid, ATP, pathogenic molecules (DNA, RNA, proteins), *N*-formyl peptides (NFPs), heparan sulfate etc. during the above-mentioned events. These molecules further activate the pattern recognition receptors (PRRs) on innate immune cells

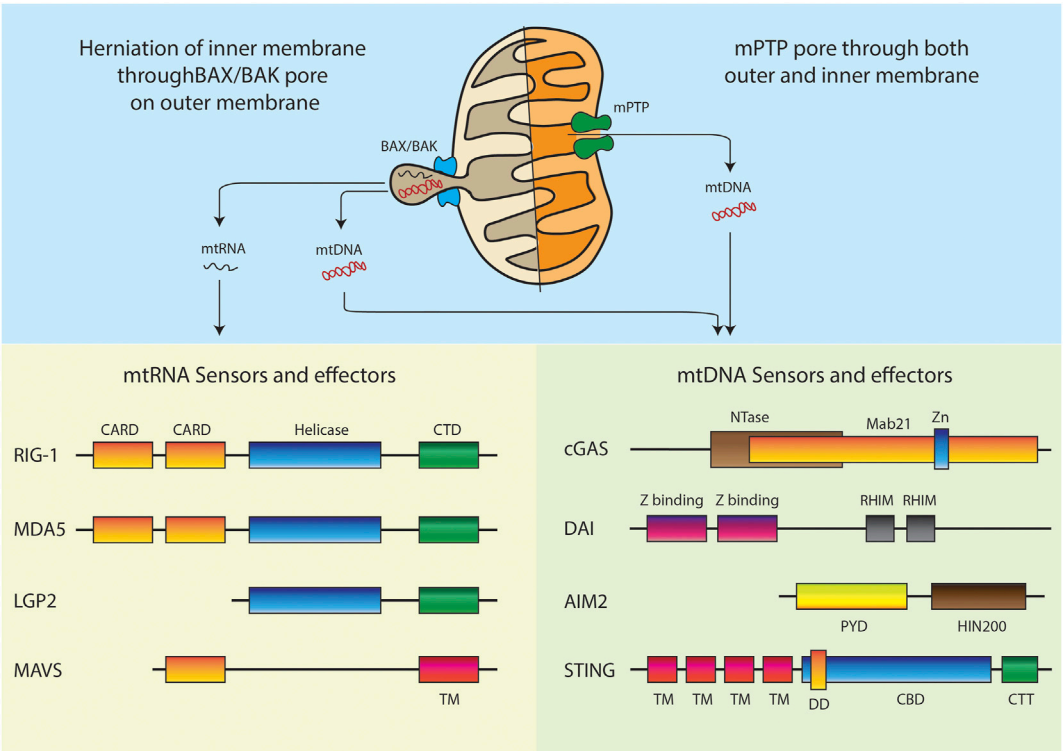

FIGURE 3 | Models of mitochondrial nucleic acids release and respective intracellular sensors and effectors. Domain abbreviations: Caspase activation and recruitment domains (CARD), C-terminal regulatory domain (CTD), Transmembrane (TM), Nucleotidyltransferase (NTase), Zinc ribbon insertion (Zn), Receptor-interacting protein (RIP) Homotypic interaction motifs (RHIM), Pyrin domain (PYD), Hematopoietic interferon-inducible nuclear protein with 200-amino-acid repeats (HIN200), Dimerization domain (DD), Cyclic dinucleotide (CDN) binding domain (CBD), C-terminal Tail (CTT).

(Brennan et al., 2015) (Takeuchi and Akira, 2009). In the event of viral infections, certain products of viral infections like viral proteins and nucleic acids, which are also known as pathogen associated molecular patterns (PAMPs) are sensed by PRRs as non-self to elicit antiviral innate immune response. This is primarily directed through type I and type III interferons (IFN) (Mesev et al., 2019). The identification of Mitochondrial antiviral-signaling protein (MAVS) not only changed the conception of innate immune responses by viral infections, but also implicated a new role of mitochondria in innate immunity (Seth et al., 2005). MAVS, which is a 540-amino acid long protein, primarily localizes on the outer mitochondrial membrane (Meylan et al., 2005). Moreover, it has also been detected on mitochondrial associated endoplasmic reticulum membranes and peroxisomes (Horner et al., 2011; Bender et al., 2015). The role of MAVS as a key adaptor protein in eliciting and promoting signal transduction against RNA viruses, paved the way towards a deeper understanding of viral RNA sensing and antiviral responses. In the next sections we will discuss more in detail about the mechanisms of viral RNA and DNA sensing is association with MAVS expression and signaling function.

RNA Sensors in the Cytosol

RIG-I-like receptors (RLRs) are a family of cytosolic pattern recognition receptors that play a pivotal role in detecting and distinguishing cytosolic viral RNA from cellular RNAs and activating downstream signaling events to initiate antiviral innate immune responses. This entire pathway is impelled by the interaction of RLRs with MAVS. MAVS consist of three domains: an N-terminal caspase recruitment domain (CARD), a middle proline-rich region, and a C-terminal transmembrane (TM) domain (**Figure 3**). While the RLR family primarily consists of three members: Retinoic acid-inducible gene I (RIG-I), Melanoma differentiation-associated gene 5 (MDA5), and Laboratory of genetics and physiology 2 (LGP2). All the three receptors of this family have a DExD/H box RNA helicase domain with ATPase activity and a carboxy-terminal domain (CTD). Binding of RNA requires both these domains. Additionally, the CTD of RIG-I and LGP2 has been shown to act as a repressor domain, which ensures that the receptors remain inactive, until they are bound by an activating RNA. An additional pair of caspase activation and recruitment domains (CARDs) are present at the N-terminus of both RIG-I and MDA5, which mediates downstream signal transduction by interacting with the CARD domain of the mitochondrial membrane-associated protein and MAVS. On the contrary, LGP2 lacks the N-terminal CARD domain and thus is not capable of interacting with MAVS. As a result, LGP2 is believed to regulate the RIG-I and MDA5 signaling pathways rather than acting independently as a signaling receptor. It is been

almost 16 years of the discovery that showed RIG-I and MDA5 induces type I interferons (T1-IFN) signaling through overexpression studies. (Yoneyama et al., 2004) Later on, RIG-I and MDA5 knockout studies in a mouse model of virus infection demonstrated that the receptors are essential for T1-IFN production and antiviral defense mechanism (Rehwinkel and Gack, 2020), (Kato et al., 2006)

RIG-1 Activation

In 2004, Takashi Fujita's group discovered that RIG-1, a cytoplasmic RNA helicase is responsible for promoting T1-IFN induction upon viral infections (Yoneyama et al., 2004). Later on many research findings showed that RIG-1 is a key PRR in sensing variety of RNA viruses including flaviviruses, alphaviruses, coronaviruses, reoviruses, paramyxoviruses, Orthohantavirus orthomyxoviruses, rhabdoviruses, arenaviruses, and bunyaviruses (Kell and Gale, 2015). RIG-1 has been shown to recognize multitude of PAMPs, including short double-stranded RNA (dsRNA) "containing either a 5′ triphosphate, 5" diphosphate or 5" monophosphate moiety (Hornung et al., 2006; Goubau et al., 2014; Spengler et al., 2015). It is now increasingly been shown that RIG-1 can also distinguish between the self-RNA from the viral RNA, based on post transcriptional modifications at 5′ triphosphate end of the RNA (Schuberth-Wagner et al., 2015; Devarkar et al., 2016).

In most cell types, RIG-I is expressed minimally. However, its abundance increases when exposed to IFN. RIG-1 contains a number of domains that regulates the sensing of PAMPs and consequently their activation (Kell and Gale, 2015). The Rig-1 protein consists of two N-terminal CARDs, followed by two tandem helicase domains (Hel1, Hel2) separated by an insertion domain (Hel2i). This is followed by a CTD, which is also referred as repressor domain (RD). In non-infected cells RIG-1 remains in its inactive form where the RD covers the RNA binding and helicase domains. RD also inhibits self-association of RIG-1, inhibiting its interaction with MAVS. In this close fit conformation, the CARDs are folded on top of each other in such a way that it keeps the protein in an auto-inhibited state (Saito et al., 2007; Kowalinski et al., 2011). The moment RIG-1 recognizes PAMP RNA, it hydrolyzes ATP and undergoes a conformational change which opens the RNA binding domain for closer interaction with PAMP RNA. The RD interacts with viral RNA and the helicase domains, resulting in the release of the CARDs for MAVS interaction and further signaling. Following the conformational change, both the RD and CARDs undergo posttranslational modifications. The RD is modified through E3 ubiquitin ligase RIPLET, which promotes ubiquitination at N-terminal sites by the TRIM25 protein (Gack et al., 2007; Oshiumi et al., 2010). This allows the CARD–CARD tetramer formation in the presence of ubiquitin. This tetramer of RIG-1 CARDs facilitates the interaction with MAVS and triggers MAVS mediated downstream signaling pathway.

MDA5 Activation

MDA5 was the first RLR gene that was fully cloned and characterized back in 2002, where the helicase core and CARD domains were found to be responsive to dsRNA (Kang et al., 2002). MDA5 also shows viral sensing for flaviviruses, alphaviruses, coronaviruses, reoviruses, and paramyxoviruses. But the detection of picornaviruses and caliciviruses is predominantly mediated through MDA5 (Kato et al., 2006) However, activation of MDA5 requires higher-order RNA web structures generated during viral infections rather than simply long molecules of dsRNA (Pichlmair et al., 2009). MDA5 thus is also a double-stranded RNA-dependent ATPase, consisting of both CARDs and an almost identical set of RNA helicase and RNA binding motifs. In addition, the CTD has a different function in MDA5 compared to RIG-1. Unlike RIG-1, the CTD of MDA5 has no RNA affinity and instead it is required for cooperative filament assembly (Peisley et al., 2011). However, similar to RIG-1, RNA binding with MDA5 results in the CARDs to interact with MAVS, leading to the transcription of the genes encoding IFNs (Wu et al., 2013). MDA5 senses longer dsRNA species and secondary structures which are usually viral replication intermediates and shows no requirement for terminal di-or triphosphates. For MDA5 activation and filament formation the ATP hydrolysis activity of the helicase domains is required (Motz et al., 2013). Further, these filaments expose the CARDs for interaction with the CARD motif of MAVS. Post translational modifications like protein phosphatase-1 (PP1) dephosphorylation of MDA5 CARDs have also been shown to regulate MDA5 activation (Wies et al., 2013). However, unlike RIG-I, not much is known about other post translational modifications such as ubiquitination that may regulate MDA5 activation. Overall, the underlaying mechanism and the biology about how the regulation and activation of MDA5 takes place has not been investigated at great depths.

LGP2 Activation

Similar to RIG-1 and MDA-5, LGP2 have also been identified as DExD/H box RNA helicases that function in the antiviral immune response (Rothenfusser et al., 2005). Although LGP2 is less well characterized than the other two. LGP2 lacks the CARD domain and acts as a negative regulator of RIG-1 and MDA5 mediated signaling while sometimes also acts as an enhancer of MDA5-directed signaling (Bruns et al., 2014) (Yoneyama et al., 2005) (Venkataraman et al., 2007). Structurally LGP2 consists of the similar helicase and RD domains like RIG-1 and MDA5 but lacks the N-terminal CARD domains, required for interaction with MAVS. Thus, its effect on downstream antiviral signaling is often due to interaction with dsRNA viral ligand or the other RLRs (RIG-I and MDA5). Uninfected cells express low levels of LGP2 but it accumulates as a result of viral infections (Komuro and Horvath, 2006). LGP2 can recognize various RNAs, irrespective of length or 5′ phosphate ends (Pippig et al., 2009). Although it seems that LGP2 serve multiple, diverse functions in response to different viruses, but there have been conflicting reports regarding LGP2's function in the immune response depending on the experimental approach taken (Zhu et al., 2014). Therefore, further research is needed to understand the role and function of LGP2 in the regulation of RNA virus sensing and downstream signaling events.

DNA Sensors in the Cytosol

In 2006, two parallel reports demonstrated that mammalian cells produce IFNs upon detection of cytosolic double-stranded DNA (dsDNA). This spurred the idea that cytosolic DNA sensing is a major mechanism by which the innate immune system detects pathogens (Ishii et al., 2006) (Stetson and Medzhitov, 2006). Afterwards several DNA sensors were identified, but only few have been proven to have a clear and definitive mechanism to induce IFN response to cytosolic DNA release. However, the presence of DNA in the cytosol is not only an indicator of pathogen infection, but it can also render to cellular damage and the cell's nuclear integrity. As far as pathogenic infections are concerned, with regards to DNA sensing, the cellular defense mechanism is triggered not only for DNA viruses, but also for bacterial and eukaryotic pathogens. While sensors and pathways related to detection of RNA viruses are well defined, most of the sensors of viral DNA have only been recently identified. Furthermore, the signaling pathways that lead to IFN production in response to viral DNA PAMPs are less well defined than pathways activated by viral RNA PAMPs. However, many discoveries in the past decade, have revealed key factors in the DNA-sensing through IFN-stimulatory DNA (ISD) pathway (Stetson and Medzhitov, 2006) (Yanai et al., 2018). The most well studied and relevant receptors in triggering the IFN pathways are the cGAS/STING, DAI and ALR pathway, which will be described in the next sections (Briard et al., 2020).

cGAS/Sting Pathway Activation

Amongst all the cytosolic DNA sensors, cGAS signaling is probably the most explored pathway. The pathway is triggered during infection with cytosolic bacterial pathogens and some DNA viruses resulting into transcriptional induction of T1-IFNs and the nuclear factor-κB (NF-κB) dependent expression of proinflammatory cytokines. The most common DNA viruses that cGAS senses are herpesviruses, human papillomavirus, adenovirus, and hepatitis B virus, as well as retroviruses such as human immunodeficiency virus-1 (HIV-1), simian immunodeficiency virus and murine leukemia virus (Ma and Damania, 2016). Although cGAS is known to play a role in the innate immune response to a number of positive-sense RNA viruses, the mechanism of RNA sensing and signaling remains largely unexplored (Schoggins et al., 2014).

Structurally cGAS is composed of N-terminal unstructured region and is also less conserved across species, followed by nucleotidyl transferase domain and a C terminal Mab21 domain (Sun et al., 2013). The DNA-sensing mechanism in this system mainly comprise of cGAS which is basically a DNA-sensing nucleotidyl transferase enzyme, its second-messenger product that is cyclic GMP–AMP (cGAMP) and the cGAMP sensor STING (also known as MITA13, ERIS14 or MPYS15,16). At resting state cGAS exists in a bilobal conformation, with a zinc thumb positioned between the lobes. The activation happens by direct DNA binding, which triggers conformational changes to induce the enzymatic activity (Civril et al., 2013) (Kranzusch et al., 2013; Li et al., 2013). Normally any DNA, foreign or self, can cause cGAS activation, but the length of the DNA is crucial for the trigger. Shorter DNA of approx. 20 bp can bind to cGAS, but longer dsDNAs of more than 45 bp can form more stable ladder-like networks of cGAS dimers, which consequently leads to stronger enzymatic activity (Li et al., 2013) (Zhang J.-Z et al., 2014) After the DNA binding, the catalytic pocket of cGAS is accessible for synthesis of cGAMP by converting GTP and ATP into cGAMP. This synthesis generates 2′3′-cGAMP, which is an endogenous cGAMP, containing two unique phosphodiester bonds (Sun et al., 2013; Schoggins et al., 2014) (Zhang X et al., 2013). 2′3′-cGAMP binds STING, which is an endoplasmic reticulum (ER)-localized adaptor. STING can also directly bind to cyclic dinucleotides produced by bacteria, including cyclic diGMP, cyclic diAMP and bacterial cGAMP, all of which have conventional (3′5′) phosphodiester linkages.

Although cGAS can directly bind to the DNA moieties, the production of cGAMP is essential for STING activation to induce T1-IFN. STING activation by cGAMP creates conformational change leading to STING dimerization and is then it is subjected to K63-linked ubiquitination by TRIM56, TRIM32 and MUL1 (Oshiumi et al., 2010; Tsuchida et al., 2010; Zhang et al., 2012; Ni et al., 2017) Further regulation of cGAS activity is governed by post translational modifications. Most post translational modification sites are found on the nucleotidyl transferase domain and on C-terminal domain of cGAS. The most predominant post-translational modifications of cGAS are phosphorylation, ubiquitination, acetylation, glutamylation, and sumoylation that are reported to profoundly affect its function (Wu and Li, 2020).

DAI Activation

DNA-dependent activator of IFN-regulatory factors (DAI) (also known as ZBP1 or DLM-1) is a cytosolic sensor molecule for dsDNA and is implicated in antiviral responses to some DNA viruses. It was the first cytosolic DNA sensor of antiviral innate immunity to be discovered by Taniguchi group in 2007 (Takaoka et al., 2007). Similar to cGAS pathway the dsDNA-stimulated DAI also activates IRF3 and NF-kB leading to the production of type-I interferons and inflammatory cytokines (Takaoka et al., 2007). Predominantly DAI can sense viruses including herpes simplex virus-1 (HSV-1), human cytomegalovirus (HCMV), mouse cytomegalovirus (MCMV) and Human immunodeficiency virus (HIV) (DeFilippis et al., 2010; Hayashi et al., 2010; Upton et al., 2019). Apart from recognizing DNA viruses, DAI is able to sense self-DNAs in the cytosol, which plays a crucial role in the development of autoimmune diseases like Systemic lupus erythematosus (SLE) (Zhang W et al., 2013). Increased DAI expression has been shown in SLE patients, where activation of DAI mediated by calcium signaling results in pathological macrophage activation in SLE disease (Zhang W et al., 2013). Another recent study shows that DAI also is involved in caspase independent cell death called necroptosis. This is induced by E3-Zα-domain-deleted vaccinia virus (VACVE3LΔ83N) (Koehler et al., 2017). Some reports also suggests that DAI plays a critical role in the activation of the NLRP3 inflammasome in Influenza A virus (IAV) infected bone marrow-derived macrophages (Kuriakose et al., 2016). In the same line of investigation a recent study shows that DAI is

capable of sensing Z-form RNAs produced during IAV infection, culminating into necroptosis (Zhang et al., 2020).

The overall mechanism by which DAI senses cytosolic DNA is scarcely known. Some studies have shown that DAI binds to DNA in a length-dependent manner, but is independent of sequence specificity. The DNA serves as a scaffold to mediate the formation of a tandem array of DAI molecules, which then recruit and activate downstream signaling molecules, such as TBK1 and IRF3 (Wang et al., 2008). Extensive research is needed to gain a better understanding of the underlaying mechanisms through which DAI senses DNA. There are no clear reports which demonstrates whether or not DAI signals through STING pathway (Radoshevich and Dussurget, 2016)-(Xu et al., 2015) Future studies to understand its role, mechanistic action and contribution in manifestation of innate immune response in variable infections needs to be thoroughly investigated.

AIM2-like Receptors (ALRs) Activation

The ALRs also participate in the detection of intracellular DNA and acts as sensors of the ISD pathway. They are known to activate inflammasomes in response to infections due to pathogens (Hornung et al., 2009). Since 2009 at least 10 or more proteins have been proposed as cytosolic DNA sensors. To name a few AIM2, IFI16, LRRFIP1, DHX9, DHX36, DDX41, Ku70, DNA-PK, MRE11, cGAS, STING and Rad50. However, it is only AIM2 and IFI16 that have been shown to detect viral dsDNA in the cytoplasm by direct binding via the AIM2 HIN200 domain. This further mediates inflammasome and transcription factor activation (Dempsey and Bowie, 2015) (Johnson et al., 2013) (Rathinam et al., 2010). During inflammasome activation, ASC (apoptosis-associated speck-like protein containing a CARD) brings caspase-1 to the inflammasome complex by CARD-CARD interactions. Activated caspase-1 then leads to the induction of a cell death pathway that is stimulated by a range of microbial infections called pyroptosis. This is mediated via the proteolytic cleavage of the N-terminal domain of gasdermin D that generates pores on the host cell membrane from which the proteolytically cleaved form of proinflammatory cytokines IL-1β and IL-18 are released (Sharma et al., 2019). Other than activating inflammasomes, IFI16 is also involved in activating the ISD pathway by sensing non-self DNA in both the nucleus and cytosol (Kerur et al., 2011). IFI16 has also been reported in regulating cellular transcription and act as a DNA virus restriction factor. IFI16 knockdown disrupts the latency of Kaposi's sarcoma associated herpesvirus (KSHV) and induced lytic transcripts (Roy et al., 2016). Mechanistically, IFI16's is reported to have an interaction with H3K9MTases leading to epigenetic silencing of foreign DNA (Roy et al., 2019). While these studies implicate IFI16 as an important sensor of both cytosolic and nuclear foreign DNA, several other reports suggest contradictorily. For example, in one study it was shown that ALRs are not required for the T1-IFN response to transfected DNA, DNA virus infection, or lentivirus infection. Moreover, IFI16 in primary human fibroblasts was shown to be dispensable for the ISD response to transfected DNA and HCMV infection (Gray et al., 2016). However, cGAS knockout cells did not generate an effective T1-IFN response. On the other hand, this study demonstrated the importance of cGAS as the primary DNA sensor in the ISD pathway. In conclusion, DNA sensing pathways like DAI ALRs like IFI16 may have a very specific cell type specific role or probably a redundant function in triggering ISD pathway. Therefore, the uncertainty that still thrives in this field of DNA sensors, needs to be studied at large to have deeper and clear understanding.

The Release of mtDNA

Although a lot is known about the role of mitochondrial nucleic acids in eliciting a pro-inflammatory response, the detailed mechanism of the actual release of the nucleic acids is highly elusive. A wide range of pathologies and infections are known to initiate the release of predominantly oxidized mtDNA into the cytoplasm triggering the recognition by sensors such as cGAS (West et al., 2015). TLR4 activation in experimental Autoimmune Myocarditis leads to significant amounts of circulating mtDNA in mice (Wu et al., 2017). They demonstrate a clear need for the circulating DNA to be oxidized. They also show that TLR4 activation induces ROS stress which may promote cardiomyocytes mtDNA damage and increase circulating mtDNA levels. Melatonin, which is synthesized by neuronal mitochondria and acts as an endogenous free radical scavenger, decreases with age and neurodegeneration. Studies with melatonin-deficient aralkylamine N-acetyltransferase (AANAT) knockout mice place ROS damage induced mitochondrial dysfunction as an initiating event for mtDNA release (Jauhari et al., 2020). Furthermore, infections with RNA viruses such as the dengue virus or bacterial pathogens such as *Mycobacterium tuberculosis* have been shown to increase mitochondrial stress and causes the release of mtDNA (Wiens and Ernst, 2016; Sun et al., 2017). It has been shown that various pathogens can induce limited mitochondrial membrane permeabilization called minority MOMP (Brokatzky et al., 2019). Under sub lethal stress conditions, minority MOMP triggers genomic DNA instability and engagement of mitochondrial apoptotic signaling.

Another interesting mechanism of mitochondrial nucleic acid release is found in breast cancer cells (Rabas et al., 2021). PINK1 association to mitochondria in metastatic cancer cells, promotes mitophagy and generation of extracellular vesicles in these "donor" cells. Thus, invasive characteristics are transferred to the "recipient" tumor cells. The key cargo in the vesicles is the mtDNA which activates TLR9 "recipient" tumor cells leading to increased endosomal trafficking which finally potentiates carcinoma progression. On the other hand, cancer cells also use similar mtDNA laden extracellular vesicles to target and induce the production of IFN and IL-6 from macrophages, which attenuates T-cell immunity in the tumor micro environment, thus promoting tumorigenesis (Cheng et al., 2020). They found oxidized mtDNA to be released into the cytosol when Lon is overexpressed. However, the mechanism of the DNA release and packaging into extracellular vehicles is still not clear.

A clear mechanism of mtDNA release is observed during programmed cell death. Studies have shown that under conditions of BAX and BAK mediated outer membrane permeabilization, the caspase inhibition can cause the pores to

increase considerably in size (McArthur et al., 2018; Riley et al., 2018). This allows inner membrane herniation and extrusion of mtDNA and dsRNA. It is still not clear if the herniated inner membrane forms a vesicle around the mitochondrial nucleic acids and continues to exist as vesicles in the cytoplasm. The other possibility is that such herniated structures are unstable and lead to release of the mitochondrial nucleic acids directly in the cytoplasm. Additionally, studies have also shown depletion of mitochondrial helicase SUV3 and polynucleotide phosphorylase (PNPase) leading to dsRNA release from mitochondria through BAX/BAK mediated outer membrane permeabilization (Dhir et al., 2018). One recent study further supported the mitochondrial herniation model. Here, mitochondrial TALENs were used to induce mtDNA breaks. This resulted in BAX/BAK mediated mtRNA release and activation of RIG-1/MAVS sensors (Tigano et al., 2021). Thus, it is very clear that apoptotic caspase activation must be shut down for hijacking the pore forming machinery to initiate mitochondrial nucleic acid mediated inflammation.

Another plausible mechanism is the engagement of the membrane permeability transition pore mPTP (Ricchelli et al., 2011). In many non-apoptotic models, the mPTP has been shown to be instrumental in release of mtDNA fragments (Kim et al., 2019). The study used cells lacking the mitochondrial endonuclease G to show release of 100–200 bp fragments. Another recent study has established the release through mPTP in YME1L deficient cells (Sprenger et al., 2021). All the studies which rely on this model show that VDAC oligomerization inhibitor, VBIT4 specifically blocks any mitochondrial nucleic acid release in these conditions (Yu et al., 2020; Torres-Odio et al., 2021). It is still not clear how a pore predicted to pass molecules smaller than 1.5 kDa is able to transport the entire mtDNA nucleoid. It could be possible that chronic opening of the pore causes swelling of the mitochondria and thus leads to a bigger pore size allowing efflux of nucleic acids.

Thus, in conclusion, more studies in different cell types and model organisms are necessary to establish the model and mechanics of mitochondrial nucleic acid release.

Signaling Pathways Triggered by Mitochondrial Nucleic Acid Sensing

mtDNA and mtRNA are dependent on different receptors and adaptors, but there is considerable overlap between the downstream signaling afterwards. This is evident from the fact that the final IFN response was attenuated only in double deletion of MAVS and STING both and not in situations where the individual gene were deleted (Brunette et al., 2012). Thus, sensing either of the nucleic acids leads to similar gene expression outcomes.

Following recognition of the mtRNAs, the PRRs activate the downstream signaling of the antiviral innate immunity pathway. The key player immediately downstream of PRRs is the mitochondrial antiviral signaling protein (MAVS). Upon activation, MAVS undergoes aggregation to form multimeric filaments (Hou et al., 2011). This filamentous form of MAVS is a platform on which other proteins can dock. At this point the signaling pathways splits into two molecular cascades. The first cascade relies on proteins Tank binding kinase-1 (TBK1) and IκB kinase epsilon (IKK ε). Both being serine/threonine kinases, phosphorylates the transcription factors IRF3 and IRF7 to trigger their dimerization and nuclear translocation (Hiscott, 2007). Once inside the nucleus, IRF3 and IRF7—which have great structural homology to each other—mediate the expression of type I and type III IFNs (Jefferies, 2019). The canonical interferon response element sequence (IRES) in the promoter of IFN-β and IFN-α is the binding site for IRF3 after its association with the co-activator CREB-binding protein (Jing et al., 2020). Similarly, route of homodimerization is adopted by IRF7 for its function as a transcription factor (Honda et al., 2005). Going back to the second cascade of MAVS signaling, the IKKα/β/γ complex is employed for NF-κB dependent upregulation of proinflammatory genes (Fang et al., 2017). Autocrine and paracrine responses, through the IFN-a/b receptor, is the ultimate result of T1-IFN production. This leads to the transcription of hundreds of IFN-stimulated genes (ISGs) through the activated JAK/STAT signaling pathway (Nan et al., 2017).

Recognition of the mtDNAs is signaled through cGAS-STING pathway. As discussed in the aforementioned section of cGAS activation, STING upon activation is then able to bind TBK1. Together they translocate to perinuclear endosomes via the Golgi (Zevini et al., 2017). Here in association with TBK1, STING interacts with and activates IRF3, thus leading to T1-IFN (Tanaka and Chen, 2012). STING is also able to cause NF-κB phosphorylation, nuclear translocation, and target gene expression (Abe and Barber, 2014). Thus, eliciting a similar response to that of mtRNA recognition.

PATHO-PHYSIOLOGY OF NUCLEIC ACID SENSING

mtDNA in (Auto) Immune-Diseases

The aforementioned signaling pathways represent a link between mtDAMPs and innate immune response leading to pathophysiology of autoimmune diseases. The common effect triggered by the PRRs is the release of a type 1 interferons (Hu et al., 2019), which has been reported over the years with increasing frequency in the context of various autoimmune diseases. Therefore, it is necessary to discuss the influence of mtDNA in the pathophysiology of Autoimmune diseases.

Most of the described phenotypes in such cases are related to one of the following events: 1. an excess release of mtDNA due to mitochondrial damages, 2. defective cytosolic nucleic acid degradation methods, 3. defective elimination of damaged mitochondria, 4. mutations in regulatory or stimulating molecules that contribute directly in the induction of interferons, especially by leukocytes. Thus, in the next sections we examine each disease individually and try to pin point which of the above mentioned events contribute to the pathology respectively.

Role of mtDNA Sensing in Systemic Lupus Erythematosus (SLE)

Kim et al. were first to show a direct connection between the recognition of cytosolic mtDNA, released by the engagement of the membrane permeability transition pore, and Lupus-like disease phenotype manifested by the production of Antinuclear Antibodies (Kim et al., 2019). The cGAS/STING pathway highlighted in this study appears to be associated with SLE and lupus-like interferon-associated diseases.

Another illustrative example of the pathogenesis of SLE by dysregulated DNA sensing mechanisms is that of Aicardi-Goutières syndrome (AGS). AGS is a hereditary systemic inflammatory disease which is characterized by overexpression of IFN1 (Crow and Manel, 2015). Here mutations, that are also often found in SLE, particularly affect various DNA sensing molecules. The excessive degradation of nucleic acids can lead to the expression of a lupus phenotype (Crow et al., 2006; Lee-Kirsch et al., 2007; Namjou et al., 2011). The phenotype seems to be closely related to the induction of interferons through the cGAS-STING pathway, as the deletion of involved factors led to a recovery of the phenotype (Stetson et al., 2008; Yan et al., 2010; Gall et al., 2012; Ablasser et al., 2014; Ahn et al., 2014). Similarly, an increase in STING activity also led to lupus-like symptoms and interferon induction (Jeremiah et al., 2014; Liu et al., 2014).

Proinflammatory Potential of Extracellular mtDNA in NETosis

Cell-free mtDNA released in the plasma plays a critical role in a recently addressed aspect of SLE—the formation of Neutrophil Extracellular Traps. This process is the ability of Neutrophils to release nucleic acids—also mtDNA—together with antimicrobial enzymes, as a first line defense mechanism against bacterial infection (Brinkmann et al., 2004; Wang et al., 2015). Physiologically, the factor TFAM gets activated by PKA and associates with pro-inflammatory oxidized mtDNA. This triggers its lysosomal degradation. However, dysfunction in the degradation of oxidized mtDNA, causes induction of type 1 interferons in leukocytes (Caielli et al., 2016). In SLE patients, PKA was found to be less active. This leads to NETs containing higher amounts of oxidized mtDNA (Lood et al., 2016). However, release and reaction to mtDNA is not only limited to Neutrophils. It was shown, that also Eosinophils and lymphocytes might trigger type 1 interferon response by releasing mtDNA in to the plasma (Yousefi et al., 2008; Ingelsson et al., 2018). The activation of leukocytes seems to be mediated mainly by TLRs. Interestingly, the NET formation seems to be also stimulated by cell-free mtDNA via TLR9 (Zhang et al., 2010), observed during primary graft dysfunction after lung transplantation. The authors hypothesized, that ischemic conditions might trigger the release of mtDNA which in turn led to the activation of neutrophils, causing increased NET formation resulting in lung injury (Mallavia et al., 2019).

All in all, the elevated concentrations of mtDNA in Plasma SLE patients, led to mtDNA being used as a possible new biomarker for SLE. This new biomarker not only correlates with the severity of the disease, but also with the development of a Lupus Nephritis (Truszewska et al., 2020).

MtDNA in Other Autoimmune Diseases

In addition to SLE, other autoimmune disorders are also highly related to an overactive IFN 1 response often in correlation with release and sensing of mtDNA. A group of diseases were termed type 1 interferonopathies, due to their origin of dysregulation of the type 1 interferon pathway. These include ISG15-and DNAse2 deficiency or AGS (described above), just to name a few. In conclusion this emphasizes the importance of mtDNA sensing as a possible trigger for an interferon induction in Autoimmune diseases.

Rheumatoid Arthritis

The pro-inflammatory potential of oxidized mtDNA in Rheumatologic diseases can be seen from the study where intra-articulary injection of oxidized mtDNA in mice caused progression of arthritis by stimulation of macrophages and induction of NF-KB (Collins et al., 2004) Moreover, circulating mtDNA was found in plasma and synovial fluid of RA patients ((Hajizadeh et al., 2003). Additionally, when there is dysfunction of DNAse I in apoptotic cells, there is insufficient degradation of extranuclear DNA. This leads to T1-IFN inflammation and arthritis in mice (Rodero et al., 2017). Thus, elimination of such apoptotic cells by macrophages might trigger a dysregulated systemic immune response through stimulation of cGAS, AIM2 and TLRs (Ahn et al., 2012; Baum et al., 2014; Jakobs et al., 2015).

Li N et al. (2019) demonstrated an important mechanism in the contribution of mtDNA in pro-inflammatory mediated $CD4^+$ T cells RA (Li Y. et al., 2019). It was shown, that defect of the mtDNA repair nuclease MRE11A, which seems to be associated in the progression of RA in humans (Li et al., 2016), caused not only leakage of mtDNA into the cytosol, but also its recognition by AIM3 and NLRP3. This leads to the stimulation of inflammasome, caspase1 and pyroptotic cell death. The phenotype was confirmed *in vivo*, showing aggressive tissue inflammation, caspase one activation and mtDNA accumulation in synovial tissue (Li Y. et al., 2019). Strikingly, not only does the interferon response appear to be conditioned by mitochondrial dysfunction, but T1-IFN itself also seems to worsen mitochondrial function. This self-reinforcing feedback occurs via suppression of NRF2 by interferon signaling, resulting in increased oxidative stress and enhanced proinflammatory cytokine responses (Lei et al., 2021).

Because increased levels of cell-free mtDNA are also associated with several other inflammatory diseases—e.g., granulomatosis with polyangiitis (Hashimoto et al., 2021), further intensive research on the pro-inflammatory role of mtDNA should be conducted.

mtDNA in Other Chronic Diseases

Apart from systemic inflammatory diseases, mitochondrial nucleic acid sensing seem to play a central role in the pathophysiology of the many organ specific inflammatory conditions. In the following sections we will focus on these

pathologies. We would also like to distinguish them from the effects of circulating mtDNA, which may result from acute tissue damages in these organs.

mtDNA in Neuroinflammatory Diseases

Parkinson's Disease

The influence of mitochondrial DNA on neuroinflammatory diseases has been most clearly demonstrated in Parkinson's disease (PD), a disease in which motor activity dysfunction results from the degeneration of dopaminergic neurons in the substantia nigra. Characteristically for pathology of PD, the so-called Lewy (protein) bodies are deposited in the affected brain areas and secretion of various cytokines indicate an inflammatory component of the disease (Mogi et al., 1994; Dobbs et al., 1999).

Early on, a link was recognized between defective mitophagy, the mechanism to eliminate malfunctioning mitochondria, and the pathogenesis of Parkinson's disease and neuroinflammation. Mutations in Parkin/PINK1, two key players in mitophagy, coordinating the lysosomal degradation by ubiquitination of the mitochondrial outer membrane proteins, were associated with a PD phenotype in several cell models (Abbas et al., 1999; Lücking et al., 2000; Valente et al., 2004; Lazarou et al., 2015; Wauer et al., 2015; Gladkova et al., 2018). However, the correlation between dysfunction of autophagy and development of PD was shown mainly *in vitro* and not *in vivo* experiments (Goldberg et al., 2003; Perez and Palmiter, 2005; Kitada et al., 2009). Thus, it looks like just the mutations are not sufficient to elicit the complete pathology of the disease. Recent studies shed new light on this aspect. In addition to the mutation in Parkin/PINK1, a second proinflammatory stimulus seems to be required to induce the onset of the disease *in vivo*. Sliter et al. showed that Parkin/PINK1 deficient mice at rest had no pathological differences in characteristic inflammatory cytokine levels (IL6, IFN b and circulating mtDNA). In contrast, by either exercise of the Parkin/PINK1 deficient mice or mice gathering further mtDNA mutations, the inflammatory stimulus was measured. Interestingly, this inflammatory response seemed to be strongly dependent on STING pathway and thus interferons (Sliter et al., 2018). This was based on the observations that, deletion of STING or receptor blockade of Interferon-alpha/beta receptor (IFNAR), respectively, completely prevented the release of cytokines. Recently, new evidence for the involvement of mitochondrial DNA in this pathophysiology has been revealed. The absence of PINK1, but also other autophagy molecules GBA and ATP13A2, led to accumulation of mtDNA in the cytosol and consequently to IFN1 induction in cultured neuroblastoma cells. This phenotype was completely prevented by overexpression of DNAse II, but also by depletion of IFI16, an mtDNA sensor molecule. Strikingly, DNAse II overexpression also improved symptoms in the zebrafish animal model of PD. A subsequent post-mortem analysis of PD patients showed an increase in cytosolic mtDNA and IFI16 levels in the medulla oblongata. It was striking that IFI16 was particularly associated with the Lewy bodies specific for the disease (Matsui et al., 2021).

Similar to other diseases, in PD circulating mtDNA was described, too. It seems to decrease due to affective treatment and thus can be discussed as a possible biomarker (Lowes et al., 2020).

Amyotrophic Lateral Sclerosis

Amyotrophic lateral sclerosis (ALS) is a neurodegenerative disease effecting the motor neurons. The disease pathology which is also connected to TLR signaling, interleukin release and activation of the inflammasome. A pathological marker for ALS is the accumulation of TDP-43 in the cytosol. This had been associated with interferon and NF-KB inflammatory signaling. Recently, it was shown, that mitochondrial DNA was released through mPTPs into the cytosol after TDP-43 treatment (Yu et al., 2020). This resulted in induction of interferons through NF-KB signaling. However, this could be prevented by deletion of cGAS/STING in cells and mice models. Furthermore, higher amounts of signaling intermediates of this pathway found in ALS patients spinal cord samples indicated, that mtDNA derived signaling might play a significant role in pathogenesis of ALS. Involvement of the cGAS-STING pathway and its activation by released mtDNA in neuroinflammation seems likely, which could be triggered by the absence of the antioxidant melatonin in a mouse line and was found in association with Huntington's disease (Jauhari et al., 2021).

Visual System

Mitochondrial dysfunction is often connected to pathologies associated with eye-related inherited disorders (Yu-Wai-Man and Newman, 2017). Recently, evidence for mtDNA induced inflammation in the visual system was shown in the experiments where cultivated retinal microvascular endothelial cells released mtDNA in response to oxidative stress (Guo et al., 2020). Also, in rat models, intravitreal injection of LPS and light injury in the retina triggered the release of mtDNA in retinal tissue (Guo et al., 2021). In both studies, the released mtDNA triggered the cGAS/STING pathway resulting in an T1-IFN upregulation. This, supports the need to investigate the significance of mitochondrial nucleic acid sensing in retinal neurodegeneration.

The central importance of mitochondrial DNA-triggered inflammation was also shown in studies of neuromyelitis optica - an autoimmune disease characterized by aquaporin four autoantibody-mediated damage to astrocytes. As a consequence, there are not only visual disturbances but also sensorimotor deficits. Shimizu et al. showed that astrocytes, upon treatment by the autoantibodies, released proinflammatory cytokines (CCL2) and mtDNA. The activation of TLR9, on the one hand increased the recruitment of monocytes, on the other hand mtDNA through *feedback loop* stimulated the further production of CCL2 (Shimizu et al., 2020). This indicates a central role of mtDNA in the pathophysiology in neuromyelitis optica.

Finally, mitochondrial autophagy regulators like Parkin/PINK1 seem to be crucial for retinal degeneration diseases, as they were reported to protect retinal photoreceptors from oxidative stress (Zhou B et al., 2021).

Role of mtDNA in Liver Disorders

The two important examples of a diseases strongly related to mitochondrial dysfunction are non-alcoholic fatty liver disease (NAFLD) and non-alcoholic steatohepatitis (NASH). Both these

conditions are precursor of hepatocellular carcinoma (HCC). HCC represents a central problem in industrialized countries with increasing numbers of cases. Although mitochondria also appear to be involved in dysregulated lipid metabolism in NAFLD (Longo et al., 2021), here we focus predominantly on pathologies triggered by mitochondrial nucleic acids.

The difference between NAFLD and NASH is mainly the inflammatory and fibrotic component of the later disease. Kupffer cells and macrophages are the main causative agent of fibrosis (Hirsova and Gores, 2015; Hirsova et al., 2017; Yuan et al., 2017). cGAS-STING signaling in Kupffer cells and macrophages might contribute in the development of NASH and fibrosis. It was found to be activated in hepatic tissue samples from NAFLD patients as well (Luo et al., 2018). Nonspecific induction of STING in macrophages and STING-IRF3 signaling, caused hepatic inflammation, steatosis and fibrosis. On the other hand, STING depletion ameliorated these consequences (Iracheta-Vellve et al., 2016; Luo et al., 2018; Qiao et al., 2018).

Strikingly, Yu et al. showed that mtDNA released by hepatocytes caused the secretion of TNF-a and IL-6 by Kupffer cells, which was attenuated by STING deletion. In addition, deletion of STING prevented the progression of hepatic steatosis (Yu et al., 2018). Furthermore, mtDNA can also directly activate hepatic stellate cells and push them to the progression of fibrosis (An et al., 2020). Also, in pathophysiology of NAFLD, the potential induction of TLR9 signaling by mtDNA seems to play a role, since Garcia-Martinez et al. were the first to show a direct link between the release of oxidized mitochondrial DNA from hepatocytes and its recognition by TLR9 in humans and in mouse model (Garcia-Martinez et al., 2016). This is supported by the observation that TLR9 deficient mice did not develop NASH on a provocative diet (Miura et al., 2010).

Thus, it becomes tempting to speculate, that the damaged hepatocytes are the drivers of mtDNA release, triggering the Kupffer cells and hepatic macrophages to induce pro-inflammatory and pro-fibrotic pathways.

Role of mtDNA in Pulmonary Diseases

The cell-free mtDNA concentrations changes with different pathologies associated with lungs. In case of acute lung injury the amounts go up, correlating to the extent of damage, whereas in lung carcinoma the amounts go down (Chen et al., 2018; Mao et al., 2021). This already indicates a possible involvement of mtDNA release and sensing in different pathologies of the pulmonary system.

Several independent studies indicate different paths leading to the same root cause. An analysis of samples from lung fibrosis patients showed higher levels of mtDNA mutations and dysfunction of the respiratory chain, indicating an involvement in fibrotic pathways (Jaeger et al., 2019). However, the authors did not address the contribution of mtDNA sensing pathways in these samples. This correlation was investigated in other studies, showing an induction of inflammatory pathways due to cell free mtDNA or cytosolic mtDNA. The triggering the of TLR9/NF-KB expression and the activation of the inflammasome pathway was observed in both, cultivated macrophages and lung tissue samples in mice (Zhang X et al., 2014; Wu et al., 2019). Injection of mtDNA caused the secretion of proinflammatory cytokines (IL-1b, IL18, TNFα) as well as the activation of Caspase -1. Both are associated with fibrotic and acute pulmonary injuries (Jäger et al., 2021).

While searching for possible triggers for mtDNA release, it was discovered that H_2O_2 released by *Streptococcus pneumoniae* caused severe mitochondrial- and histopathological damage. This, subsequently led to the release of mtDNA into the cytoplasm of human alveola cells. Further, an T1-IFN response was triggered, in which STING was found to be involved (Gao et al., 2019). Furthermore, ZBP1 is proposed to be involved as a mtDNA sensor and mediator of an interferon response (Szczesny et al., 2018). Sustained low level oxidative stress caused damage in the mtDNA of cultured pulmonary epithelia cells, but not the nuclear DNA. As a consequence, mtDNA was released into the cytosol and ZBP1 initiated T1-IFN response *via* TBK1. Interestingly, it was also shown that mtDNA was released extracellularly by exosomes, which also elicited an inflammatory response in healthy neighboring cells, suggesting an autocrine as well as a paracrine potential of mtDNA in lung pathologies.

Role of mtDNA in Kidney Diseases

Several kidney-related diseases including in diabetes, tubulo-nephritis show elevated mtDNA levels not only in the plasma, but also in the urine. Thus, it is important to discuss the role of the kidney in the involvement of elimination of potentially proinflammatory cell free mtDNA and look closely at the effect of mtDNA on the kidney itself (Whitaker et al., 2015; Wei et al., 2018; Chang et al., 2019).

As in other organ systems, TLR9, as well as cGas-STING signaling triggered by released mtDNA, seem to mediate inflammatory responses in acute kidney injury (Tsuji et al., 2016; Maekawa et al., 2019). STING mediated sensing of mtDNA might also be involved in kidney fibrosis, especially by triggering NF-KB, shown in renal cells of TFAM knockout mice. Since suppressing STING pathway ameliorated kidney fibrosis in mouse models of chronic kidney disease, it should be discussed as a possible target in fibrosis treatment strategies (Chung et al., 2019). Furthermore, activation of NLRP3 Inflammasome, which was reported in association with mitochondrial dysfunction was linked to renal tubular injury and tubulointerstitial fibrosis (Gong et al., 2016; Guo et al., 2017).

Role of mtDNA in Cardiovascular Diseases

The inflammatory potential of mtDNA is connected to different cardiac phenotypes, as extracellular mtDNA, which was found in higher concentrations in association with various cardiac pathologies. It was shown to activate NF-KB *via* TLR9 signalling in cardiomyocytes, even inducing its cell death (Bliksøen et al., 2016; Wu et al., 2017). One of the reasons for elevated circulating mtDNA levels can be cardiomyocyte necrosis. For example, in acute myocardial infarction (AMI) (Qin et al., 2017; Nakayama and Otsu, 2018), or ROS-dependent sepsis induced mitochondrial damages (Yao et al., 2015) cardiomyocyte necrosis led to mtDNA release. mtDNA sensing through both, TLR9 and the cGAS-STING pathway must

be highlighted as a potential driver of essential pathogenecity in pressure overload-induced heart failure (Hu et al., 2020). In response to pressure overload, the cGAS deficient mice showed not only lower inflammatory cardiac reactions, but more importantly also preserved LV contractile function. In these models, pathological remodeling—including cardiac hypertrophy, fibrosis, and apoptosis—was also very low (Hu et al., 2020).

STING signaling especially in infiltrating macrophages, triggered by mtDNA, might also be involved in inflammation after MI. This provokes IFN stimulation, cardiac expression of inflammatory cytokines and increase of cardiac inflammatory cell infiltration. After MI, the inhibition of IFNAR and IRF3 in mice attenuated ventricular dilation, improved left ventricular dysfunction and survival (King et al., 2017) Supporting its role in pathophysiological involvement in cardiac diseases, Li et al. reported that knockout of STING in mice treated with LPS (mimicking sepsis-induced cardiomyopathy) improved survival rate and cardiac function. Serum and myocardial cytokine levels were decreased and the knockout prevented the apoptosis, as well as NLRP3 mediated pyroptosis of cardiomyocytes (Li N. et al., 2019). Atherosclerosis is one of the major risk factors for MI. It was observed that, mtDNA damage in macrophages and smooth muscle cells (Yu et al., 2013), T1-IFN signaling (Goossens et al., 2010) and inflammasome activation seem to promote atherosclerosis (Duewell et al., 2010). Furthermore, STING-IRF3 pathway triggered endothelial inflammation *via* ICAM-1 in response to the release of mitochondrial DNA provoked by free fatty acids. This not only supported the importance of STING in several inflammatory pathways, but might also display an important connection between cardiovascular pathologies and metabolic syndromes (Mao et al., 2017).

Rising Knowledge of mtRNA in Pathophysiology

Although the role of mtDNA has been reported more extensively and further findings in this area appear to be of paramount importance, there is increasing evidence for a similar influence of mtRNA. mtRNA was identified as the main potential trigger of the innate T1-IFN immune response (Dhir et al., 2018). Physiologically, cytosolic dsRNA is contained in viruses as well as in mitochondria. But it is also formed to some extent in the cytosol in healthy individuals. It is degraded by a complex of SUV3 and PnPase, which is therefore called the degradosome (Szczesny et al., 2009, 2011; Borowski et al., 2012; Kim et al., 2018; Kotrys and Szczesny, 2019). This process is fundamental not only for defense against viral infections, but also to prevent excessive accumulation of mitochondrial dsRNA in the cytosol. Therefore, dysfunction of the complex also leads to an increased concentration of dsRNA in the cytosol of the affected cell (Pajak et al., 2019). Dhir et al. showed for the first time that, dysfunction of the degradosome and thus increased cytosolic mtRNA can trigger an interferon response via recognition by PRRs (Dhir et al., 2018). The most important receptors for recognition of foreign RNA, as described few sections before, are MDA5, RIG1, TLR3 and PKR (Chattopadhyay and Sen, 2014; Wu et al., 2014; Kim et al., 2018; Linder and Hornung, 2018). However, this mechanism seems to be far more complex, as Brachène et al. pointed out in their work on pancreatic beta cells, investigating the origin of an T1-IFN response observed in pancreatic islet cells in diabetes type 1 (Foulis et al., 1987; Brachène et al., 2021). Apparently, the accumulation of mtRNA in the cytosol is highly dependent on the proliferation state of the cell. Moreover, the induction of an T1-IFN response triggered by cytosolic mtRNA is by no means a general, ubiquitous mechanism of the innate immune system, but is conditioned by cell type (Brachène et al., 2021).

Since it appears that mitochondrial dsRNA (mtdsRNA), like mtDNA, can elicit an interferon response, it is not surprising that increasing evidence also points to a link between (autoimmune) diseases and mtdsRNA—although this is much less understood than for mtDNA. The effects of excessive cytosolic mtRNA can be seen in the study of Zhou et al., who discovered induction of NF-KB pathway by MDA5 upon detection of higher cytosolic concentrations of mtRNA (Zhou X et al., 2021). Excessive release of mtRNA was triggered by oxidative stress, provoked by common mtDNA deletions in collagen producing keratocytes. As a consequence, key signalling pathways such as the induction of IL8, key mediator of neutrophil immigration, and profibrotic molecules also appeared to be affected. Although this is a very specific example in keratocytes, it seems tempting to speculate that similar mechanisms could be at work in other organ systems, triggering local proinflammatory and fibrotic remodelling processes.

In addition, dsRNA as such might show proinflammatory effects in Myasthenia gravis (MG). MG is an autoimmune disease which is defined by the development of auto-antibodies against the AChReceptor, thus effecting the motoric nerve system (Cufi et al., 2012). An injection of dsRNA mimicking polyinosinic–polycytidylic acid [poly (I:C)] caused an activation of TLR3, PKR and induction of IFN beta in healthy mice. The analysis of human MG thymus cells further supported the hypothesis of dsRNA's role in the MG. Most interestingly, the injection of poly (I:C) also provoked a production of auto-antibodies also in wild type mice. This connection was likely strictly related to the interferon pathway, as the antibodies did not develop in T1-IFN Receptor deficient mice. However, this study did only show the pathophysiological potential of dsRNA in general, and not the mitochondrial dsRNA specifically. Apparently, the magnitude of the immune response as well as the organ manifestations depends on the circulating amount of dsRNA (McGarry et al., 2021).

MtdsRNA was found in higher concentration in circulating extracellular vesicles in Alzheimer's disease. These could be secreted by astrocytes, microglia and neurons under cellular stress (Kim et al., 2020). This might be an indication for considering circulating mtRNA as a potential biomarker for several diseases. However, the role of circulating mtdsRNA remains unclear and it is not investigated, whether it contributes to a systemic inflammatory response or if it is just a consequence of a damaged organ system. A look at the pathophysiology of autoimmune diseases suggests that mtdsRNA may also be involved in the progression of systemic immune responses.

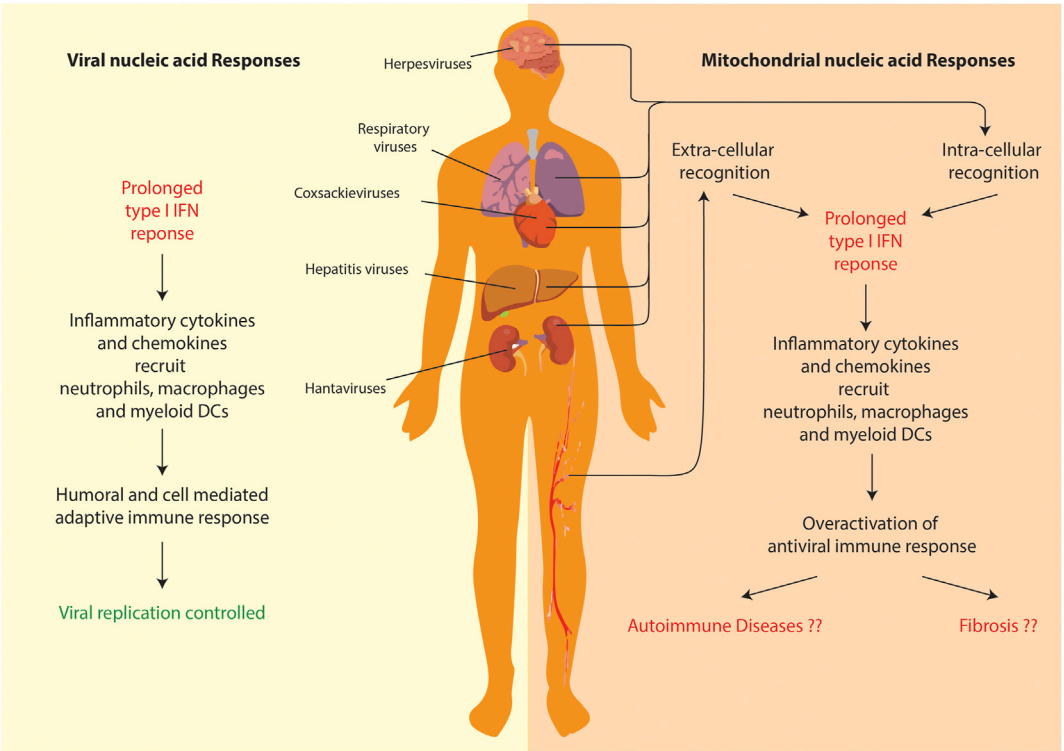

FIGURE 4 | Comparison of anti-viral and mitochondrial nucleic acid responses. Both lead to a prolonged T1-IFN inflammatory response. However, in case of mitochondrial nucleic acid sensing pathways, the overactivation of inflammation leads to systemic/organ-specific auto-immune diseases or even fibrosis in various organs.

Dermatomyositis is a disease that particularly attacks the striated muscle and skin. Besides intramuscular inflammation, hallmarks in diagnostics of this disease are the induction of interferon inducible genes—such as MHC1, ISG15, and RIG1—n muscle biopsies. There seems to be a strong link between hypoxic conditions and the expression of especially RIG1 in dermatomyositis. Thus, making it a potential inducer of the dysregulated immune response (Luna et al., 2017). Interestingly, mitochondrial transcription seems to be decreased under conditions of hypoxia and thus the amount of mtdsRNA is also reduced (Arnaiz et al., 2021). This represents a direct regulatory mechanism of the immune response triggered by RIG1 induction. Furthermore, dsRNA receptors were found in high expression in skin samples and keratinocytes from psoriasis patients (Rácz et al., 2011). Anti-MDA5 antibodies are found in association with idiopathic inflammatory myopathies, often indicating a lethal prognosis (Li et al., 2014). 40–50% of SLE patients are characterized by dsRNA antibodies (Schur et al., 1971; Davis et al., 1975). Although the development of auto-antibodies is a concept that is not understood in depth and require further investigation, specific auto-antibodies are crucial in diagnostics and prognosis of the diseases.

Finally, it was recently suggested, that mtRNA release might be linked to mtDNA integrity, as mtDNA double strand breaks triggered the release of mtRNA which caused activation of RIG1-MAVS dependent signaling (Tigano et al., 2021). Thus, in conclusion, the field of mtRNA sensing is a very promising for understanding the disease pathology, development of biomarkers and possible therapeutics.

DISCUSSION AND PERSPECTIVES

The field of mitochondrial nucleic acid-sensing has, in the recent years, made rapid progress owing to attention it drew from cell biologists, immunologists and clinicians alike. Since, the phenomenon directly connects all these branches of biology, the study requires a comprehensive understanding of all its aspects—including the nature of the molecular patterns, release and recognition in the cytoplasm, signaling and resulting patho-physiologies. Due to the bacterial ancestry of the mitochondrial genome, the molecular sensors of innate immunity can be easily repurposed to detect its extra-mitochondrial presence. Additionally, since an elaborate mechanism of anti-viral immunity exists to deal with viral pathogens, the molecular sensors involved can be also repurposed to detect mitochondrial nucleic acids outside their regular confines. However, it the response that mitochondrial nucleic acids garner from the over activation of antiviral immunity, which leads to a systemic patho-physiology (**Figure 4**). Additionally, a lot of critical shortcomings need to

be addressed particularly in the areas of mitochondrial nucleic acids release and the etiology of pathologies. Let us look at them one by one.

The major models of release from the mitochondrial matrix involve either 1. herniation of the inner membrane through BAX/BAK mediated outer membrane pore (McArthur et al., 2018) or 2. mPTP mediated channel pore formation (Kim et al., 2019). Both models require thorough mechanistic examination. Herniation would not lead to a vesicle like structure to protrude out form the outer membrane. The issue of how this vesicle gets permeabilized to release the mitochondrial nucleic acids into the cytoplasm has never been addressed. The molecular pathway of apoptotic caspase inactivation for BAX/BAK to generate the pore also needs to worked out. On the other hand, what causes the growth in pore size of the mPTP so as to allow the passage of the bulky nucleoid needs to be investigated. Furthermore, what is the effect of such a huge pore on the mitochondrial structural integrity needs to be explored.

With more and more reports of increased occurrence of mitochondrial DNA in connection with multiple different diseases, it seems increasingly important to shed light on this aspect. The central question is whether mitochondrial DNA is a concomitant of the disease itself or is just a side effect. Also, it is import to determine if mtDNA sensing may have an additional secondary influence on the course of the disease, or whether it is a primary patho-mechanistic determinant of the progression of the disease itself. mtDNA copy numbers do influence the mitochondrial health and any dysfunctions in the maintenance process are associated with neuroinflammatory diseases. A concept was proposed in the study by Dölle et al. that, dysregulation of mtDNA homeostasis might be a key process in the pathogenesis of neuronal loss in Parkinson's disease (Dölle et al., 2016). Physiologically, the amount of mtDNA in substantia nigra dopaminergic neurons increases with age, such that the wild-type mtDNA population is maintained in good numbers despite increasing deletions. This upregulation seems absent in PD patients, resulting in a depletion of the wild-type mtDNA population. In contrast, neuronal mtDNA point mutation load was not increased in PD, wich might be the trigger for its release and signaling. In a different context, the involvement of mtDNA signaling in pathogenesis of Alzheimer's disease (AD) is also currently under discussion, as several reports of mitochondrial dysfunction and also the dysfunction of Pink1/Parkin, excessive ROS production are reported in association with AD (Witte et al., 2009; Ye et al., 2015). However, a direct contribution of mtDNA in pathogenesis of AD was not proven yet, the inflammatory component, showing induction of the inflammasome, cytokines and NF-KB might hint a correlation of mtDNA accumulation in AD (Heneka et al., 2013; Ahmed et al., 2017; Hu et al., 2021).

Apart from the biogenesis and maintenance of mitochondrial nucleic acids, mitochondrial quality control might also play a role in various diseases. In pulmonary disorders, PINK1 was reported to attenuate mtDNA release in alveolar epithelial cells (Bueno et al., 2019). Both, ER stress and PINK1 deficiency in AECII led to oxidation and damage of mtDNA and subsequent extracellular release, which was recognized by TLR9 after endocytosis. Besides the inflammatory response, mtDNA triggered secretion of the profibrotic factor TGF-β. In addition, mtDNA oxidation and damage were found in IPF human lungs and circulating mtDNA plasma- and bronchoalveolar lavage levels were significantly elevated in patients with idiopathic pulmonary fibrosis (IPF). Strikingly, the induction of inflammation and autophagy seems to be cross-talking via STING, as activation of STING interfered with lysosomal acidification, hence disturbing autophagy in mtDNA mediated sepsis-induced acute lung injury. As a consequence, the induction of autophagy or STING deficiency alleviated lung injury (Liu et al., 2021). The proper functioning of the mitophagy also seems to be of great importance for the preservation of renal function. On the one hand, mitophagy seems to be essential in ischemic renal situations (Tang et al., 2018; Livingston et al., 2019), on the other hand, it also appears to be indispensable in the prevention of inflammatory and fibrotic processes (Szeto et al., 2016; Bhatia and Choi, 2019). Further, the role of mitophagy and its function to remove mitochondrial material has to be discussed, since inhibition of mitophagy molecules caused TLR9-mediated inflammatory responses in cardiomyocytes, myocarditis and dilated cardiomyopathy (Oka et al., 2012). Mitophagy-mediated mtDNA release aggravates stretching-induced inflammation and lung epithelial cell injury via the TLR9/MyD88/NF-κB pathway (Jing R et al., 2020). Thus, the molecular connections with autophagy/mitophagy and mitochondrial nucleic acid sensing pathways need to be examined in detail.

Lastly, the nature of the trigger and site of nucleic acid sensing also varies a lot for different diseases. Thus, we briefly touch upon the distinction of intracellular and extracellular DNA sensing. Usually there are two possible situations which lead to the occurrence of circulating mtDNA. The first situation may be a severe (acute) destruction of tissue. The other would be, mitochondria-related dysfunctions and resulting (chronic) pathologies of the organ system. However, the distinction between the two can be often murky as cell free mtDNA from acute damage in tissue might also contribute to additional inflammatory reactions in the tissue itself. Clinically, this might present as if the organ system failed and thus skew the interpretation towards the second hypothesis. Thus, while looking at the etiology of such pathologies one needs to carefully dissect the origin of the insult or signal. Similarly, although sensing of mitochondrial DNA/RNA is a widely established trigger for an enhanced (interferon) immune response, there appear to be fundamental differences in different cell/organ types that are studied. This is underscored by Brachene et al., who showed that triggering an interferon response by increased mtRNA is, by no means, a universal process (Brachène et al., 2021). Rather, it seems to depend not only on specific organ systems but also on the proliferative status of the cells. Also, the nucleic acid sensing pathways could aggravate the triggers for other unassociated disorders. Using the example of the influence of mitochondrial dysfunction in the pathogenesis of Parkinson's disease, it can be deduced that dysfunction in the mitochondrial system alone is not sufficient to trigger the disease. Much more, the chronic proinflammatory stress could be compensated in case of an intact regulatory system, which, however, could be omitted in case of another

mutation affecting this very compensatory mechanism. Thus, similar to tumorigenesis, a "second hit" hypothesis is being attempted: In addition to an underlying dysfunction in the mitochondrial system itself, it could be a second malfunction in the inflammatory pathway regulating mechanisms that ultimately triggers the onset of mitochondrial genome-driven disease.

However, there are a few studies which clearly contradict the role of mitochondrial nucleic acid sensing pathways in diseases. Studies in the autoimmune disease rheumatoid arthritis, show T cells in RA patients when treated with mtDNA actually have lower IFNB and IFIT1 transcripts (Li Y. et al., 2019). In other studies of chronic heart failure, although those patients show significantly higher levels of mtDNA than age- and sex-matched healthy controls, there is no association between the severity of heart failure and the levels of serum mtDNA (Dhondup et al., 2016). Additionally, one study even found TLR9 is not strongly involved in mtDNA-induced inflammation caused by cardiac ischemic injury (Omiya et al., 2016). Based on experiments using TLR9 null mice, they showed no differences in the number of infiltrating inflammatory cells and the levels of inflammatory cytokine mRNA in infarct hearts between TLR9-deficient and wild-type mice. Thus TLR9, in opposition to its role in invoking inflammation, actually promoted proliferation and differentiation of cardiac fibroblasts for cardiac remodeling. Thus, it is very clear that a thorough examination of mitochondrial nucleic acid sensing pathways is necessary. But overwhelming evidence do point in a direction of benefits of the pathway in diagnostics and treatments.

To conclude, the new insights into the key players of the patho-mechanisms of autoimmune diseases also bring forward new therapeutic options for discussion. Currently, the blocking of cGAS-STING pathways but also TLR are intensively discussed as potential therapeutic targets for the treatment of autoimmune diseases, for example SLE (Decout et al., 2021; Fillatreau et al., 2021). Apart from autoimmune diseases, circulating mtDNA can affect organ systems as well. Mechanically-induced cartilage injury also leads to leak of mtDNA into the synovial fluid through cell death/rupture (Seewald et al., 2020). Again, treatments with mitoprotective SS31 peptide, which interacts specifically with CL to affect membrane curvature and prevent peroxidative damage, significantly lower circulating mtDNA bringing it to similar levels to that of the controls. This clearly indicates a great potential for developing or re-tasking drugs for treating these systemic inflammatory diseases associated with mitochondrial energetics and metabolism. Additionally, new biomarkers of the mitochondrial nucleic acid sensing pathways could accelerate timely detection and life-saving therapeutic interventions (Borsche et al., 2020; Ward et al., 2021). Hence, it is necessary to have a comprehensive overview of the mitochondrial nucleic acid sensing pathways in order to study diseases of the OXPHOS dysfunction.

AUTHOR CONTRIBUTIONS

AC, SW, and AA wrote the manuscript. AC and AA prepared figures.

FUNDING

AA is funded by the Deutsche Forschungsgemeinschaft (DFG, German Research Foundation) under Germany's Excellence Strategy—EXC 2067/1- 390729940. AC is funded by the Deutsche Forschungsgemeinschaft (DFG, German Research Foundation) SFB1002.

REFERENCES

Abbas, N., Lucking, C. B., Ricard, S., Durr, A., Bonifati, V., De Michele, G., et al. (1999). A Wide Variety of Mutations in the Parkin Gene Are Responsible for Autosomal Recessive Parkinsonism in Europe. *Hum. Mol. Genet.* 8, 567–574. doi:10.1093/hmg/8.4.567

Abe, T., and Barber, G. N. (2014). Cytosolic-DNA-Mediated, STING-dependent Proinflammatory Gene Induction Necessitates Canonical NF-B Activation through TBK1. *J. Virol.* 88, 5328–5341. doi:10.1128/jvi.00037-14

Ablasser, A., Hemmerling, I., Schmid-Burgk, J. L., Behrendt, R., Roers, A., and Hornung, V. (2014). TREX1 Deficiency Triggers Cell-Autonomous Immunity in a cGAS-dependent Manner. *J.I.* 192, 5993–5997. doi:10.4049/jimmunol.1400737

Ahmed, M. E., Iyer, S., Thangavel, R., Kempuraj, D., Selvakumar, G. P., Raikwar, S. P., et al. (2017). Co-Localization of Glia Maturation Factor with NLRP3 Inflammasome and Autophagosome Markers in Human Alzheimer's Disease Brain. *Jad* 60, 1143–1160. doi:10.3233/jad-170634

Ahn, J., Gutman, D., Saijo, S., and Barber, G. N. (2012). STING Manifests Self DNA-dependent Inflammatory Disease. *Proc. Natl. Acad. Sci.* 109, 19386–19391. doi:10.1073/pnas.1215006109

Ahn, J., Xia, T., Konno, H., Konno, K., Ruiz, P., and Barber, G. N. (2014). Inflammation-driven Carcinogenesis Is Mediated through STING. *Nat. Commun.* 5, 5166. doi:10.1038/ncomms6166

An, P., Wei, L.-L., Zhao, S., Sverdlov, D. Y., Vaid, K. A., Miyamoto, M., et al. (2020). Hepatocyte Mitochondria-Derived Danger Signals Directly Activate Hepatic Stellate Cells and Drive Progression of Liver Fibrosis. *Nat. Commun.* 11, 2362. doi:10.1038/s41467-020-16092-0

Arnaiz, E., Miar, A., Dias, A. G., Prasad, N., Schulze, U., Waithe, D., et al. (2021). Hypoxia Regulates Endogenous Double-Stranded RNA Production via Reduced Mitochondrial DNA Transcription. *Front. Oncol.* 11, 779739. doi:10.3389/fonc.2021.779739

Ayyub, S. A., and Varshney, U. (2019). Translation Initiation in Mammalian Mitochondria- a Prokaryotic Perspective. *RNA Biol.* 17, 165–175–11. doi:10.1080/15476286.2019.1690099

Baum, R., Sharma, S., Carpenter, S., Li, Q.-Z., Busto, P., Fitzgerald, K. A., et al. (2014). Cutting Edge: AIM2 and Endosomal TLRs Differentially Regulate Arthritis and Autoantibody Production in DNase II-Deficient Mice. *J.I.* 194, 873–877. doi:10.4049/jimmunol.1402573

Bender, S., Reuter, A., Eberle, F., Einhorn, E., Binder, M., and Bartenschlager, R. (2015). Activation of Type I and III Interferon Response by Mitochondrial and Peroxisomal MAVS and Inhibition by Hepatitis C Virus. *Plos Pathog.* 11, e1005264. doi:10.1371/journal.ppat.1005264

Bhatia, D., and Choi, M. E. (2019). The Emerging Role of Mitophagy in Kidney Diseases. *JoLS* 1, 13–22. doi:10.36069/jols/20191203

Bliksøen, M., Mariero, L. H., Torp, M. K., Baysa, A., Ytrehus, K., Haugen, F., et al. (2016). Extracellular mtDNA Activates NF-Kb via Toll-like Receptor 9 and Induces Cell Death in Cardiomyocytes. *Basic Res. Cardiol.* 111, 42. doi:10.1007/s00395-016-0553-6

Bogenhagen, D. F., Wang, Y., Shen, E. L., and Kobayashi, R. (2003). Protein Components of Mitochondrial DNA Nucleoids in Higher Eukaryotes. *Mol. Cell Proteomics* 2, 1205–1216. doi:10.1074/mcp.m300035-mcp200

Borowski, L. S., Dziembowski, A., Hejnowicz, M. S., Stepien, P. P., and Szczesny, R. J. (2012). Human Mitochondrial RNA Decay Mediated by PNPase-hSuv3 Complex Takes Place in Distinct Foci. *Nucleic Acids Res.* 41, 1223–1240. doi:10.1093/nar/gks1130

Borsche, M., König, I. R., Delcambre, S., Petrucci, S., Balck, A., Brüggemann, N., et al. (2020). Mitochondrial Damage-Associated Inflammation Highlights Biomarkers in PRKN/PINK1 Parkinsonism. *Brain* 143, 3041–3051. doi:10.1093/brain/awaa246

Brennan, T. V., Rendell, V. R., and Yang, Y. (2015). Innate Immune Activation by Tissue Injury and Cell Death in the Setting of Hematopoietic Stem Cell Transplantation. *Front. Immunol.* 6, 101. doi:10.3389/fimmu.2015.00101

Briard, B., Place, D. E., and Kanneganti, T.-D. (2020). DNA Sensing in the Innate Immune Response. *Physiology* 35, 112–124. doi:10.1152/physiol.00022.2019

Brinkmann, V., Reichard, U., Goosmann, C., Fauler, B., Uhlemann, Y., Weiss, D. S., et al. (2004). Neutrophil Extracellular Traps Kill Bacteria. *Science* 303, 1532–1535. doi:10.1126/science.1092385

Brokatzky, D., Dörflinger, B., Haimovici, A., Weber, A., Kirschnek, S., Vier, J., et al. (2019). A Non-death Function of the Mitochondrial Apoptosis Apparatus in Immunity. *Embo J.* 38. doi:10.15252/embj.2018100907

Brunette, R. L., Young, J. M., Whitley, D. G., Brodsky, I. E., Malik, H. S., and Stetson, D. B. (2012). Extensive Evolutionary and Functional Diversity Among Mammalian AIM2-like Receptors. *J. Exp. Med.* 209, 1969–1983. doi:10.1084/jem.20121960

Bruns, A. M., Leser, G. P., Lamb, R. A., and Horvath, C. M. (2014). The Innate Immune Sensor LGP2 Activates Antiviral Signaling by Regulating MDA5-RNA Interaction and Filament Assembly. *Mol. Cel* 55, 771–781. doi:10.1016/j.molcel.2014.07.003

Buang, N., Tapeng, L., Gray, V., Sardini, A., Whilding, C., Lightstone, L., et al. (2021). Type I Interferons Affect the Metabolic Fitness of CD8+ T Cells from Patients with Systemic Lupus Erythematosus. *Nat. Commun.* 12, 1980. doi:10.1038/s41467-021-22312-y

Bueno, M., Zank, D., Buendia-Roldán, I., Fiedler, K., Mays, B. G., Alvarez, D., et al. (2019). PINK1 Attenuates mtDNA Release in Alveolar Epithelial Cells and TLR9 Mediated Profibrotic Responses. *Plos One* 14, e0218003. doi:10.1371/journal.pone.0218003

Caielli, S., Athale, S., Domic, B., Murat, E., Chandra, M., Banchereau, R., et al. (2016). Oxidized Mitochondrial Nucleoids Released by Neutrophils Drive Type I Interferon Production in Human Lupus. *J. Cel Biol* 213, 2132OIA85. doi:10.1083/jcb.2132oia85

Cekic, C., and Linden, J. (2016). Purinergic Regulation of the Immune System. *Nat. Rev. Immunol.* 16, 177–192. doi:10.1038/nri.2016.4

Chakraborty, K., Raundhal, M., Chen, B. B., Morse, C., Tyurina, Y. Y., Khare, A., et al. (2017). The Mito-DAMP Cardiolipin Blocks IL-10 Production Causing Persistent Inflammation during Bacterial Pneumonia. *Nat. Commun.* 8, 13944. doi:10.1038/ncomms13944

Chang, C.-C., Chiu, P.-F., Wu, C.-L., Kuo, C.-L., Huang, C.-S., Liu, C.-S., et al. (2019). Urinary Cell-free Mitochondrial and Nuclear Deoxyribonucleic Acid Correlates with the Prognosis of Chronic Kidney Diseases. *Bmc Nephrol.* 20, 391. doi:10.1186/s12882-019-1549-x

Chattopadhyay, S., and Sen, G. C. (2014). dsRNA-Activation of TLR3 and RLR Signaling: Gene Induction-dependent and Independent Effects. *J. Interferon Cytokine Res.* 34, 427–436. doi:10.1089/jir.2014.0034

Chen, J., Zhang, L., Yu, X., Zhou, H., Luo, Y., Wang, W., et al. (2018). Clinical Application of Plasma Mitochondrial DNA Content in Patients with Lung Cancer. *Oncol. Lett.* 16, 7074–7081. doi:10.3892/ol.2018.9515

Cheng, A. N., Cheng, L.-C., Kuo, C.-L., Lo, Y. K., Chou, H.-Y., Chen, C.-H., et al. (2020). Mitochondrial Lon-Induced mtDNA Leakage Contributes to PD-L1-Mediated Immunoescape via STING-IFN Signaling and Extracellular Vesicles. *J. Immunother. Cancer* 8, e001372. doi:10.1136/jitc-2020-001372

Chung, K. W., Dhillon, P., Huang, S., Sheng, X., Shrestha, R., Qiu, C., et al. (2019). Mitochondrial Damage and Activation of the STING Pathway Lead to Renal Inflammation and Fibrosis. *Cel Metab.* 30, 784–799. e5. doi:10.1016/j.cmet.2019.08.003

Civril, F., Deimling, T., de Oliveira Mann, C. C., Ablasser, A., Moldt, M., Witte, G., et al. (2013). Structural Mechanism of Cytosolic DNA Sensing by cGAS. *Nature* 498, 332–337. doi:10.1038/nature12305

Collins, L. V., Hajizadeh, S., Holme, E., Jonsson, I.-M., and Tarkowski, A. (2004). Endogenously Oxidized Mitochondrial DNA Induces *In Vivo* and *In Vitro* Inflammatory Responses. *J. Leukoc. Biol.* 75, 995–1000. doi:10.1189/jlb.0703328

Coomans de Brachène, A., Castela, A., Musuaya, A. E., Marselli, L., Marchetti, P., and Eizirik, D. L. (2021). Endogenous Mitochondrial Double-stranded RNA Is Not an Activator of the Type I Interferon Response in Human Pancreatic Beta Cells. *Autoimmun. Highlights* 12, 6. doi:10.1186/s13317-021-00148-2

Crow, Y. J., Leitch, A., Hayward, B. E., Garner, A., Parmar, R., Griffith, E., et al. (2006). Mutations in Genes Encoding Ribonuclease H2 Subunits Cause Aicardi-Goutières Syndrome and Mimic Congenital Viral Brain Infection. *Nat. Genet.* 38, 910–916. doi:10.1038/ng1842

Crow, Y. J., and Manel, N. (2015). Aicardi-Goutières Syndrome and the Type I Interferonopathies. *Nat. Rev. Immunol.* 15, 429–440. doi:10.1038/nri3850

Cufi, P., Dragin, N., Weiss, J. M., Martinez-Martinez, P., De Baets, M. H., Roussin, R., et al. (2012). Implication of Double-Stranded RNA Signaling in the Etiology of Autoimmune Myasthenia Gravis. *Ann. Neurol.* 73, 281–293. doi:10.1002/ana.23791

Davis, P., Cunnington, P., and Hughes, G. R. (1975). Double-stranded RNA Antibodies in Systemic Lupus Erythematosus. *Ann. Rheum. Dis.* 34, 239–243. doi:10.1136/ard.34.3.239

De Luna, N., Suárez-Calvet, X., Lleixà, C., Diaz-Manera, J., Olivé, M., Illa, I., et al. (2017). Hypoxia Triggers IFN-I Production in Muscle: Implications in Dermatomyositis. *Sci. Rep.* 7, 8595. doi:10.1038/s41598-017-09309-8

Decout, A., Katz, J. D., Venkatraman, S., and Ablasser, A. (2021). The cGAS-STING Pathway as a Therapeutic Target in Inflammatory Diseases. *Nat. Rev. Immunol.* 21, 548–569. doi:10.1038/s41577-021-00524-z

DeFilippis, V. R., Alvarado, D., Sali, T., Rothenburg, S., and Früh, K. (2010). Human Cytomegalovirus Induces the Interferon Response via the DNA Sensor ZBP1. *J. Virol.* 84, 585–598. doi:10.1128/jvi.01748-09

Dempsey, A., and Bowie, A. G. (2015). Innate Immune Recognition of DNA: A Recent History. *Virology* 479-480, 146–152. doi:10.1016/j.virol.2015.03.013

Devarkar, S. C., Wang, C., Miller, M. T., Ramanathan, A., Jiang, F., Khan, A. G., et al. (2016). Structural Basis for m7G Recognition and 2′-O-Methyl Discrimination in Capped RNAs by the Innate Immune Receptor RIG-I. *Proc. Natl. Acad. Sci. USA* 113, 596–601. doi:10.1073/pnas.1515152113

Dhir, A., Dhir, S., Borowski, L. S., Jimenez, L., Teitell, M., Rötig, A., et al. (2018). Mitochondrial Double-Stranded RNA Triggers Antiviral Signalling in Humans. *Nature* 560, 238–242. doi:10.1038/s41586-018-0363-0

Dhondup, Y., Ueland, T., Dahl, C. P., Askevold, E. T., Sandanger, Ø., Fiane, A., et al. (2016). Low Circulating Levels of Mitochondrial and High Levels of Nuclear DNA Predict Mortality in Chronic Heart Failure. *J. Card. Fail.* 22, 823–828. doi:10.1016/j.cardfail.2016.06.013

Dieudé, M., Striegl, H., Tyznik, A. J., Wang, J., Behar, S. M., Piccirillo, C. A., et al. (2011). Cardiolipin Binds to CD1d and Stimulates CD1d-Restricted γδ T Cells in the Normal Murine Repertoire. *J.I.* 186, 4771–4781. doi:10.4049/jimmunol.1000921

Dobbs, R. J., Charlett, A., Purkiss, A. G., Dobbs, S. M., Weller, C., and Peterson, D. W. (1999). Association of Circulating TNF-α and IL-6 with Ageing and Parkinsonism. *Acta Neurol. Scand.* 100, 34–41. doi:10.1111/j.1600-0404.1999.tb00721.x

Dölle, C., Flønes, I., Nido, G. S., Miletic, H., Osuagwu, N., Kristoffersen, S., et al. (2016). Defective Mitochondrial DNA Homeostasis in the Substantia Nigra in Parkinson Disease. *Nat. Commun.* 7, 13548. doi:10.1038/ncomms13548

Dudek, J., Rehling, P., and van der Laan, M. (2013). Mitochondrial Protein Import: Common Principles and Physiological Networks. *Biochim. Biophys. Acta (Bba) - Mol. Cel Res.* 1833, 274–285. doi:10.1016/j.bbamcr.2012.05.028

Duewell, P., Kono, H., Rayner, K. J., Sirois, C. M., Vladimer, G., Bauernfeind, F. G., et al. (2010). NLRP3 Inflammasomes Are Required for Atherogenesis and Activated by Cholesterol Crystals. *Nature* 464, 1357–1361. doi:10.1038/nature08938

Faas, M. M., Sáez, T., and de Vos, P. (2017). Extracellular ATP and Adenosine: The Yin and Yang in Immune Responses? *Mol. Aspects Med.* 55, 9–19. doi:10.1016/j.mam.2017.01.002

Fang, R., Jiang, Q., Zhou, X., Wang, C., Guan, Y., Tao, J., et al. (2017). MAVS Activates TBK1 and IKKε through TRAFs in NEMO Dependent and Independent Manner. *Plos Pathog.* 13, e1006720. doi:10.1371/journal.ppat.1006720

Fillatreau, S., Manfroi, B., and Dörner, T. (2021). Toll-like Receptor Signalling in B Cells during Systemic Lupus Erythematosus. *Nat. Rev. Rheumatol.* 17, 98–108. doi:10.1038/s41584-020-00544-4

Foulis, A., Farquharson, M., and Meager, A. (1987). IMMUNOREACTIVE α-INTERFERON IN INSULIN-SECRETING β CELLS IN TYPE 1 DIABETES MELLITUS. *The Lancet* 330, 1423–1427. doi:10.1016/s0140-6736(87)91128-7

Gack, M. U., Shin, Y. C., Joo, C.-H., Urano, T., Liang, C., Sun, L., et al. (2007). TRIM25 RING-finger E3 Ubiquitin Ligase Is Essential for RIG-I-Mediated Antiviral Activity. *Nature* 446, 916–920. doi:10.1038/nature05732

Gall, A., Treuting, P., Elkon, K. B., Loo, Y.-M., Gale, M., Barber, G. N., et al. (2012). Autoimmunity Initiates in Nonhematopoietic Cells and Progresses via Lymphocytes in an Interferon-dependent Autoimmune Disease. *Immunity* 36, 120–131. doi:10.1016/j.immuni.2011.11.018

Gao, Y., Xu, W., Dou, X., Wang, H., Zhang, X., Yang, S., et al. (2019). Mitochondrial DNA Leakage Caused by Streptococcus Pneumoniae Hydrogen Peroxide Promotes Type I IFN Expression in Lung Cells. *Front. Microbiol.* 10, 630. doi:10.3389/fmicb.2019.00630

Garcia-Martinez, I., Santoro, N., Chen, Y., Hoque, R., Ouyang, X., Caprio, S., et al. (2016). Hepatocyte Mitochondrial DNA Drives Nonalcoholic Steatohepatitis by Activation of TLR9. *J. Clin. Invest.* 126, 859–864. doi:10.1172/jci83885

Gilissen, J., Jouret, F., Pirotte, B., and Hanson, J. (2016). Insight into SUCNR1 (GPR91) Structure and Function. *Pharmacol. Ther.* 159, 56–65. doi:10.1016/j.pharmthera.2016.01.008

Gladkova, C., Maslen, S. L., Skehel, J. M., and Komander, D. (2018). Mechanism of Parkin Activation by PINK1. *Nature* 559, 410–414. doi:10.1038/s41586-018-0224-x

Goldberg, M. S., Fleming, S. M., Palacino, J. J., Cepeda, C., Lam, H. A., Bhatnagar, A., et al. (2003). Parkin-deficient Mice Exhibit Nigrostriatal Deficits but Not Loss of Dopaminergic Neurons. *J. Biol. Chem.* 278, 43628–43635. doi:10.1074/jbc.m308947200

Gong, W., Mao, S., Yu, J., Song, J., Jia, Z., Huang, S., et al. (2016). NLRP3 Deletion Protects against Renal Fibrosis and Attenuates Mitochondrial Abnormality in Mouse with 5/6 Nephrectomy. *Am. J. Physiology-Renal Physiol.* 310, F1081–F1088. doi:10.1152/ajprenal.00534.2015

Goossens, P., Gijbels, M. J. J., Zernecke, A., Eijgelaar, W., Vergouwe, M. N., van der Made, I., et al. (2010). Myeloid Type I Interferon Signaling Promotes Atherosclerosis by Stimulating Macrophage Recruitment to Lesions. *Cel Metab.* 12, 142–153. doi:10.1016/j.cmet.2010.06.008

Goubau, D., Schlee, M., Deddouche, S., Pruijssers, A. J., Zillinger, T., Goldeck, M., et al. (2014). Antiviral Immunity via RIG-I-Mediated Recognition of RNA Bearing 5′-diphosphates. *Nature* 514, 372–375. doi:10.1038/nature13590

Gray, E. E., Winship, D., Snyder, J. M., Child, S. J., Geballe, A. P., and Stetson, D. B. (2016). The AIM2-like Receptors Are Dispensable for the Interferon Response to Intracellular DNA. *Immunity* 45, 255–266. doi:10.1016/j.immuni.2016.06.015

Gray, M. W., Burger, G., and Lang, B. F. (1999). Mitochondrial Evolution. *Science* 283, 1476–1481. doi:10.1126/science.283.5407.1476

Grimolizzi, F., and Arranz, L. (20182018). Multiple Faces of Succinate beyond Metabolism in Blood. *Haematologica* 103, 1586–1592. haematol. doi:10.3324/haematol.2018.196097

Guo, H., Bi, X., Zhou, P., Zhu, S., and Ding, W. (20172017). NLRP3 Deficiency Attenuates Renal Fibrosis and Ameliorates Mitochondrial Dysfunction in a Mouse Unilateral Ureteral Obstruction Model of Chronic Kidney Disease. *Mediators Inflamm.* 2017, 1–10. doi:10.1155/2017/8316560

Guo, Y., Gan, D., Hu, F., Cheng, Y., Yu, J., Lei, B., et al. (2021). Intravitreal Injection of Mitochondrial DNA Induces Cell Damage and Retinal Dysfunction in Rats. doi:10.21203/rs.3.rs-538747/v1

Guo, Y., Gu, R., Gan, D., Hu, F., Li, G., and Xu, G. (2020). Mitochondrial DNA Drives Noncanonical Inflammation Activation via cGAS-STING Signaling Pathway in Retinal Microvascular Endothelial Cells. *Cell Commun Signal* 18, 172. doi:10.1186/s12964-020-00637-3

Hajizadeh, S., DeGroot, J., TeKoppele, J. M., Tarkowski, A., and Collins, L. V. (2003). Extracellular Mitochondrial DNA and Oxidatively Damaged DNA in Synovial Fluid of Patients with Rheumatoid Arthritis. *Arthritis Res. Ther.* 5, R234. doi:10.1186/ar787

Hashimoto, T., Ueki, S., Kamide, Y., Miyabe, Y., Fukuchi, M., Yokoyama, Y., et al. (2021). Increased Circulating Cell-free DNA in Eosinophilic Granulomatosis with Polyangiitis: Implications for Eosinophil Extracellular Traps and Immunothrombosis. *Front. Immunol.* doi:10.3389/fimmu.2021.801897

Hayashi, T., Nishitsuji, H., Takamori, A., Hasegawa, A., Masuda, T., and Kannagi, M. (2010). DNA-dependent Activator of IFN-Regulatory Factors Enhances the Transcription of HIV-1 through NF-Kb. *Microbes Infect.* 12, 937–947. doi:10.1016/j.micinf.2010.06.003

He, H.-Q., and Ye, R. (2017). The Formyl Peptide Receptors: Diversity of Ligands and Mechanism for Recognition. *Molecules* 22, 455. doi:10.3390/molecules22030455

Heneka, M. T., Kummer, M. P., Stutz, A., Delekate, A., Schwartz, S., Vieira-Saecker, A., et al. (2013). NLRP3 Is Activated in Alzheimer's Disease and Contributes to Pathology in APP/PS1 Mice. *Nature* 493, 674–678. doi:10.1038/nature11729

Hirsova, P., and Gores, G. J. (2015). Death Receptor-Mediated Cell Death and Proinflammatory Signaling in Nonalcoholic Steatohepatitis. *Cell Mol. Gastroenterol. Hepatol.* 1, 17–27. doi:10.1016/j.jcmgh.2014.11.005

Hirsova, P., Weng, P., Salim, W., Bronk, S. F., Griffith, T. S., Ibrahim, S. H., et al. (2017). TRAIL Deletion Prevents Liver Inflammation but Not Adipose Tissue Inflammation during Murine Diet-Induced Obesity. *Hepatol. Commun.* 1, 648–662. doi:10.1002/hep4.1069

Hiscott, J. (2007). Triggering the Innate Antiviral Response through IRF-3 Activation. *J. Biol. Chem.* 282, 15325–15329. doi:10.1074/jbc.r700002200

Honda, K., Yanai, H., Negishi, H., Asagiri, M., Sato, M., Mizutani, T., et al. (2005). IRF-7 Is the Master Regulator of Type-I Interferon-dependent Immune Responses. *Nature* 434, 772–777. doi:10.1038/nature03464

Horner, S. M., Liu, H. M., Park, H. S., Briley, J., and Gale, M. (2011). Mitochondrial-associated Endoplasmic Reticulum Membranes (MAM) Form Innate Immune Synapses and Are Targeted by Hepatitis C Virus. *Proc. Natl. Acad. Sci.* 108, 14590–14595. doi:10.1073/pnas.1110133108

Hornung, V., Ablasser, A., Charrel-Dennis, M., Bauernfeind, F., Horvath, G., Caffrey, D. R., et al. (2009). AIM2 Recognizes Cytosolic dsDNA and Forms a Caspase-1-Activating Inflammasome with ASC. *Nature* 458, 514–518. doi:10.1038/nature07725

Hornung, V., Ellegast, J., Kim, S., Brzo´zka, K., Jung, A., Kato, H., et al. (2006). 5'-Triphosphate RNA Is the Ligand for RIG-I. *Science* 314, 994–997. doi:10.1126/science.1132505

Hou, F., Sun, L., Zheng, H., Skaug, B., Jiang, Q.-X., and Chen, Z. J. (2011). MAVS Forms Functional Prion-like Aggregates to Activate and Propagate Antiviral Innate Immune Response. *Cell* 146, 841. doi:10.1016/j.cell.2011.08.013

Hu, D., Cui, Y.-X., Wu, M.-Y., Li, L., Su, L.-N., Lian, Z., et al. (2020). Cytosolic DNA Sensor cGAS Plays an Essential Pathogenetic Role in Pressure Overload-Induced Heart Failure. *Am. J. Physiology-Heart Circulatory Physiol.* 318, H1525–H1537. doi:10.1152/ajpheart.00097.2020

Hu, W. T., Ozturk, T., Kollhoff, A., Wharton, W., Christina Howell, J., Initiative, A. D. N., et al. (2021). Higher CSF sTNFR1-Related Proteins Associate with Better Prognosis in Very Early Alzheimer's Disease. *Nat. Commun.* 12, 4001. doi:10.1038/s41467-021-24220-7

Hu, X., Peng, X., Lu, C., Zhang, X., Gan, L., Gao, Y., et al. (2019). Type I IFN Expression Is Stimulated by Cytosolic Mt DNA Released from Pneumolysin-damaged Mitochondria via the STING Signaling Pathway in Macrophages. *Febs J.* 286, 4754–4768. doi:10.1111/febs.15001

Ingelsson, B., Söderberg, D., Strid, T., Söderberg, A., Bergh, A.-C., Loitto, V., et al. (2018). Lymphocytes Eject Interferogenic Mitochondrial DNA Webs in Response to CpG and Non-CpG Oligodeoxynucleotides of Class C. *Proc. Natl. Acad. Sci. USA* 115, E478–E487. doi:10.1073/pnas.1711950115

Iracheta-Vellve, A., Petrasek, J., Gyongyosi, B., Satishchandran, A., Lowe, P., Kodys, K., et al. (2016). Endoplasmic Reticulum Stress-Induced Hepatocellular Death Pathways Mediate Liver Injury and Fibrosis via Stimulator of Interferon Genes. *J. Biol. Chem.* 291, 26794–26805. doi:10.1074/jbc.m116.736991

Ishii, K. J., Coban, C., Kato, H., Takahashi, K., Torii, Y., Takeshita, F., et al. (2006). A Toll-like Receptor-independent Antiviral Response Induced by Double-Stranded B-form DNA. *Nat. Immunol.* 7, 40–48. doi:10.1038/ni1282

Iyer, S. S., He, Q., Janczy, J. R., Elliott, E. I., Zhong, Z., Olivier, A. K., et al. (2013). Mitochondrial Cardiolipin Is Required for Nlrp3 Inflammasome Activation. *Immunity* 39, 311–323. doi:10.1016/j.immuni.2013.08.001

Jaeger, V. K., Lebrecht, D., Nicholson, A. G., Wells, A., Bhayani, H., Gazdhar, A., et al. (2019). Mitochondrial DNA Mutations and Respiratory Chain

Dysfunction in Idiopathic and Connective Tissue Disease-Related Lung Fibrosis. *Sci. Rep.* 9, 5500. doi:10.1038/s41598-019-41933-4

Jäger, B., Seeliger, B., Terwolbeck, O., Warnecke, G., Welte, T., Müller, M., et al. (2021). The NLRP3-Inflammasome-Caspase-1 Pathway Is Upregulated in Idiopathic Pulmonary Fibrosis and Acute Exacerbations and Is Inducible by Apoptotic A549 Cells. *Front. Immunol.* 12, 642855. doi:10.3389/fimmu.2021.642855

Jakobs, C., Perner, S., and Hornung, V. (2015). AIM2 Drives Joint Inflammation in a Self-DNA Triggered Model of Chronic Polyarthritis. *Plos One* 10, e0131702. doi:10.1371/journal.pone.0131702

Jauhari, A., Baranov, S. V., Suofu, Y., Kim, J., Singh, T., Yablonska, S., et al. (2020). Melatonin Inhibits Cytosolic Mitochondrial DNA-Induced Neuroinflammatory Signaling in Accelerated Aging and Neurodegeneration. *J. Clin. Invest.* 130, 3124–3136. doi:10.1172/jci135026

Jauhari, A., Baranov, S. V., Suofu, Y., Kim, J., Singh, T., Yablonska, S., et al. (2021). Melatonin Inhibits Cytosolic Mitochondrial DNA-Induced Neuroinflammatory Signaling in Accelerated Aging and Neurodegeneration. *J. Clin. Invest.* 131, e150328. doi:10.1172/jci150328

Jefferies, C. A. (2019). Regulating IRFs in IFN Driven Disease. *Front. Immunol.* 10, 325. doi:10.3389/fimmu.2019.00325

Jeremiah, N., Neven, B., Gentili, M., Callebaut, I., Maschalidi, S., Stolzenberg, M.-C., et al. (2014). Inherited STING-Activating Mutation Underlies a Familial Inflammatory Syndrome with Lupus-like Manifestations. *J. Clin. Invest.* 124, 5516–5520. doi:10.1172/jci79100

Jing, T., Zhao, B., Xu, P., Gao, X., Chi, L., Han, H., et al. (2020). The Structural Basis of IRF-3 Activation upon Phosphorylation. *J.I.* 205, 1886–1896. doi:10.4049/jimmunol.2000026

Johnson, K. E., Chikoti, L., and Chandran, B. (2013). Herpes Simplex Virus 1 Infection Induces Activation and Subsequent Inhibition of the IFI16 and NLRP3 Inflammasomes. *J. Virol.* 87, 5005–5018. doi:10.1128/jvi.00082-13

Jourdain, A. A., Boehm, E., Maundrell, K., and Martinou, J.-C. (2016). Mitochondrial RNA Granules: Compartmentalizing Mitochondrial Gene Expression. *J. Cel Biol* 212, 611–614. doi:10.1083/jcb.201507125

Julian, M. W., Shao, G., Bao, S., Knoell, D. L., Papenfuss, T. L., VanGundy, Z. C., et al. (2012). Mitochondrial Transcription Factor A Serves as a Danger Signal by Augmenting Plasmacytoid Dendritic Cell Responses to DNA. *J.I.* 189, 433–443. doi:10.4049/jimmunol.1101375

Kang, D.-c., Gopalkrishnan, R. V., Wu, Q., Jankowsky, E., Pyle, A. M., and Fisher, P. B. (2002). mda-5: An Interferon-Inducible Putative RNA Helicase with Double-Stranded RNA-dependent ATPase Activity and Melanoma Growth-Suppressive Properties. *Proc. Natl. Acad. Sci.* 99, 637–642. doi:10.1073/pnas.022637199

Kato, H., Takeuchi, O., Sato, S., Yoneyama, M., Yamamoto, M., Matsui, K., et al. (2006). Differential Roles of MDA5 and RIG-I Helicases in the Recognition of RNA Viruses. *Nature* 441, 101–105. doi:10.1038/nature04734

Kell, A. M., and Gale, M. (2015). RIG-I in RNA Virus Recognition. *Virology* 479-480, 110–121. doi:10.1016/j.virol.2015.02.017

Kerur, N., Veettil, M. V., Sharma-Walia, N., Bottero, V., Sadagopan, S., Otageri, P., et al. (2011). IFI16 Acts as a Nuclear Pathogen Sensor to Induce the Inflammasome in Response to Kaposi Sarcoma-Associated Herpesvirus Infection. *Cell Host & Microbe* 9, 363–375. doi:10.1016/j.chom.2011.04.008

Kim, J., Gupta, R., Blanco, L. P., Yang, S., Shteinfer-Kuzmine, A., Wang, K., et al. (2019). VDAC Oligomers Form Mitochondrial Pores to Release mtDNA Fragments and Promote Lupus-like Disease. *Science* 366, 1531–1536. doi:10.1126/science.aav4011

Kim, K. M., Meng, Q., Perez de Acha, O., Mustapic, M., Cheng, A., Eren, E., et al. (2020). Mitochondrial RNA in Alzheimer's Disease Circulating Extracellular Vesicles. *Front. Cel Dev. Biol.* 8, 581882. doi:10.3389/fcell.2020.581882

Kim, Y., Park, J., Kim, S., Kim, M. A., Kang, M.-G., Kwak, C., et al. (2018). PKR Senses Nuclear and Mitochondrial Signals by Interacting with Endogenous Double-Stranded RNAs. *Mol Cell.* 71 (6), 1051–1063.e6. doi:10.1016/j.molcel.2018.07.029

King, K. R., Aguirre, A. D., Ye, Y.-X., Sun, Y., Roh, J. D., Ng, R. P., et al. (2017). IRF3 and Type I Interferons Fuel a Fatal Response to Myocardial Infarction. *Nat. Med.* 23, 1481–1487. doi:10.1038/nm.4428

Kiritsy, M. C., Mott, D., Behar, S. M., Sassetti, C. M., and Olive, A. J. (2020). Mitochondrial Respiration Contributes to the Interferon Gamma Response in Antigen Presenting Cells. *Biorxiv* 22, 393538. doi:10.1101/2020.11.22.393538

Kitada, T., Tong, Y., Gautier, C. A., and Shen, J. (2009). Absence of Nigral Degeneration in Aged parkin/DJ-1/PINK1 Triple Knockout Mice. *J. Neurochem.* 111, 696–702. doi:10.1111/j.1471-4159.2009.06350.x

Koehler, H., Cotsmire, S., Langland, J., Kibler, K. V., Kalman, D., Upton, J. W., et al. (2017). Inhibition of DAI-dependent Necroptosis by the Z-DNA Binding Domain of the Vaccinia Virus Innate Immune Evasion Protein, E3. *Proc. Natl. Acad. Sci. USA* 114, 11506–11511. doi:10.1073/pnas.1700999114

Komuro, A., and Horvath, C. M. (2006). RNA- and Virus-independent Inhibition of Antiviral Signaling by RNA Helicase LGP2. *J. Virol.* 80, 12332–12342. doi:10.1128/jvi.01325-06

Kotrys, A. V., and Szczesny, R. J. (2019). Mitochondrial Gene Expression and Beyond-Novel Aspects of Cellular Physiology. *Cells* 9, 17. doi:10.3390/cells9010017

Kowalinski, E., Lunardi, T., McCarthy, A. A., Louber, J., Brunel, J., Grigorov, B., et al. (2011). Structural Basis for the Activation of Innate Immune Pattern-Recognition Receptor RIG-I by Viral RNA. *Cell* 147, 423–435. doi:10.1016/j.cell.2011.09.039

Kranzusch, P. J., Lee, A. S.-Y., Berger, J. M., and Doudna, J. A. (2013). Structure of Human cGAS Reveals a Conserved Family of Second-Messenger Enzymes in Innate Immunity. *Cel Rep.* 3, 1362–1368. doi:10.1016/j.celrep.2013.05.008

Kraus, F., Roy, K., Pucadyil, T. J., and Ryan, M. T. (2021). Function and Regulation of the Divisome for Mitochondrial Fission. *Nature* 590, 57–66. doi:10.1038/s41586-021-03214-x

Kukat, C., Wurm, C. A., Spåhr, H., Falkenberg, M., Larsson, N.-G., and Jakobs, S. (2011). Super-resolution Microscopy Reveals that Mammalian Mitochondrial Nucleoids Have a Uniform Size and Frequently Contain a Single Copy of mtDNA. *Proc. Natl. Acad. Sci.* 108, 13534–13539. doi:10.1073/pnas.1109263108

Kuriakose, T., Man, S. M., Subbarao Malireddi, R. K., Karki, R., Kesavardhana, S., Place, D. E., et al. (2016). ZBP1/DAI Is an Innate Sensor of Influenza Virus Triggering the NLRP3 Inflammasome and Programmed Cell Death Pathways. *Sci. Immunol.* 1, aag2045. doi:10.1126/sciimmunol.aag2045

Lazarou, M., Sliter, D. A., Kane, L. A., Sarraf, S. A., Wang, C., Burman, J. L., et al. (2015). The Ubiquitin Kinase PINK1 Recruits Autophagy Receptors to Induce Mitophagy. *Nature* 524, 309–314. doi:10.1038/nature14893

Lechuga-Vieco, A. V., Justo-Méndez, R., and Enríquez, J. A. (2021). Not all Mitochondrial DNAs Are Made Equal and the Nucleus Knows it. *Iubmb Life* 73, 511–529. doi:10.1002/iub.2434

Lee-Kirsch, M. A., Chowdhury, D., Harvey, S., Gong, M., Senenko, L., Engel, K., et al. (2007). A Mutation in TREX1 that Impairs Susceptibility to Granzyme A-Mediated Cell Death Underlies Familial Chilblain Lupus. *J. Mol. Med.* 85, 531–537. doi:10.1007/s00109-007-0199-9

Lei, Y., Martinez, C. G., Torres-Odio, S., Bell, S. L., Birdwell, C. E., Bryant, J. D., et al. (2021). Elevated Type I Interferon Responses Potentiate Metabolic Dysfunction, Inflammation, and Accelerated Aging in mtDNA Mutator Mice. *Sci. Adv.* 7, eabe7548. doi:10.1126/sciadv.abe7548

Li, L., Wang, Q., Yang, F., Wu, C., Chen, S., Wen, X., et al. (2017). Anti-MDA5 Antibody as a Potential Diagnostic and Prognostic Biomarker in Patients with Dermatomyositis. *Oncotarget* 8, 26552–26564. doi:10.18632/oncotarget.15716

Li, N., Zhou, H., Wu, H., Wu, Q., Duan, M., Deng, W., et al. (2019). STING-IRF3 Contributes to Lipopolysaccharide-Induced Cardiac Dysfunction, Inflammation, Apoptosis and Pyroptosis by Activating NLRP3. *Redox Biol.* 24, 101215. doi:10.1016/j.redox.2019.101215

Li, X., Shu, C., Yi, G., Chaton, C. T., Shelton, C. L., Diao, J., et al. (2013). Cyclic GMP-AMP Synthase Is Activated by Double-Stranded DNA-Induced Oligomerization. *Immunity* 39, 1019–1031. doi:10.1016/j.immuni.2013.10.019

Li, Y., Shen, Y., Hohensinner, P., Ju, J., Wen, Z., Goodman, S. B., et al. (2016). Deficient Activity of the Nuclease MRE11A Induces T Cell Aging and Promotes Arthritogenic Effector Functions in Patients with Rheumatoid Arthritis. *Immunity* 45, 903–916. doi:10.1016/j.immuni.2016.09.013

Li, Y., Shen, Y., Jin, K., Wen, Z., Cao, W., Wu, B., et al. (2019). The DNA Repair Nuclease MRE11A Functions as a Mitochondrial Protector and Prevents T Cell Pyroptosis and Tissue Inflammation. *Cel Metab.* 30, 477–492. e6. doi:10.1016/j.cmet.2019.06.016

Linder, A., and Hornung, V. (2018). Mitochondrial dsRNA: A New DAMP for MDA5. *Develop. Cel* 46, 530–532. doi:10.1016/j.devcel.2018.08.019

Little, J. P., Simtchouk, S., Schindler, S. M., Villanueva, E. B., Gill, N. E., Walker, D. G., et al. (2014). Mitochondrial Transcription Factor A (Tfam) Is a Pro-inflammatory Extracellular Signaling Molecule Recognized by Brain Microglia. *Mol. Cell Neurosci.* 60, 88–96. doi:10.1016/j.mcn.2014.04.003

Liu, Q., Wu, J., Zhang, X., Li, X., Wu, X., Zhao, Y., et al. (2021). Circulating Mitochondrial DNA-Triggered Autophagy Dysfunction via STING Underlies Sepsis-Related Acute Lung Injury. *Cell Death Dis* 12, 673. doi:10.1038/s41419-021-03961-9

Liu, Y., Jesus, A. A., Marrero, B., Yang, D., Ramsey, S. E., Montealegre Sanchez, G. A., et al. (2014). Activated STING in a Vascular and Pulmonary Syndrome. *N. Engl. J. Med.* 371, 507–518. doi:10.1056/nejmoa1312625

Livingston, M. J., Wang, J., Zhou, J., Wu, G., Ganley, I. G., Hill, J. A., et al. (2019). Clearance of Damaged Mitochondria via Mitophagy Is Important to the Protective Effect of Ischemic Preconditioning in Kidneys. *Autophagy* 15, 2142–2162. doi:10.1080/15548627.2019.1615822

Longo, M., Meroni, M., Paolini, E., Macchi, C., and Dongiovanni, P. (2021). Mitochondrial Dynamics and Nonalcoholic Fatty Liver Disease (NAFLD): New Perspectives for a Fairy-Tale Ending? *Metabolism* 117, 154708. doi:10.1016/j.metabol.2021.154708

Lood, C., Blanco, L. P., Purmalek, M. M., Carmona-Rivera, C., De Ravin, S. S., Smith, C. K., et al. (2016). Neutrophil Extracellular Traps Enriched in Oxidized Mitochondrial DNA Are Interferogenic and Contribute to Lupus-like Disease. *Nat. Med.* 22, 146–153. doi:10.1038/nm.4027

Lowes, H., Pyle, A., Santibanez-Koref, M., and Hudson, G. (2020). Circulating Cell-free Mitochondrial DNA Levels in Parkinson's Disease Are Influenced by Treatment. *Mol. Neurodegeneration* 15, 10. doi:10.1186/s13024-020-00362-y

Lücking, C. B., Dürr, A., Bonifati, V., Vaughan, J., De Michele, G., Gasser, T., et al. (2000). Association between Early-Onset Parkinson's Disease and Mutations in theParkinGene. *N. Engl. J. Med.* 342, 1560–1567. doi:10.1056/nejm200005253422103

Luo, X., Li, H., Ma, L., Zhou, J., Guo, X., Woo, S.-L., et al. (2018). Expression of STING Is Increased in Liver Tissues from Patients with NAFLD and Promotes Macrophage-Mediated Hepatic Inflammation and Fibrosis in Mice. *Gastroenterology* 155, 1971–1984. e4. doi:10.1053/j.gastro.2018.09.010

Ma, Z., and Damania, B. (2016). The cGAS-STING Defense Pathway and its Counteraction by Viruses. *Cell Host & Microbe* 19, 150–158. doi:10.1016/j.chom.2016.01.010

Maekawa, H., Inoue, T., Jao, T.-M., Inoue, R., Nishi, H., Fujii, R., et al. (2019). Mitochondrial Damage Causes Inflammation via cGAS-STING Signaling in Acute Kidney Injury. *SSRN J.* doi:10.2139/ssrn.3366988

Mallavia, B., Liu, F., Lefrançais, E., Cleary, S. J., Kwaan, N., Tian, J. J., et al. (2020). Mitochondrial DNA Stimulates TLR9-dependent Neutrophil Extracellular Trap Formation in Primary Graft Dysfunction. *Am. J. Respir. Cel Mol Biol* 62, 364–372. doi:10.1165/rcmb.2019-0140oc

Mao, J.-y., Li, D.-k., Zhang, H.-m., Wang, X.-t., and Liu, D.-w. (2021). Plasma Mitochondrial DNA Levels Are Associated with Acute Lung Injury and Mortality in Septic Patients. *Bmc Pulm. Med.* 21, 66. doi:10.1186/s12890-021-01437-2

Mao, Y., Luo, W., Zhang, L., Wu, W., Yuan, L., Xu, H., et al. (2017). STING-IRF3 Triggers Endothelial Inflammation in Response to Free Fatty Acid-Induced Mitochondrial Damage in Diet-Induced Obesity. *Atvb* 37, 920–929. doi:10.1161/atvbaha.117.309017

Matsui, H., Ito, J., Matsui, N., Uechi, T., Onodera, O., and Kakita, A. (2021). Cytosolic dsDNA of Mitochondrial Origin Induces Cytotoxicity and Neurodegeneration in Cellular and Zebrafish Models of Parkinson's Disease. *Nat. Commun.* 12, 3101. doi:10.1038/s41467-021-23452-x

McArthur, K., Whitehead, L. W., Heddleston, J. M., Li, L., Padman, B. S., Oorschot, V., et al. (2018). BAK/BAX Macropores Facilitate Mitochondrial Herniation and mtDNA Efflux during Apoptosis. *Science* 359, eaao6047. doi:10.1126/science.aao6047

McGarry, N., Murray, C. L., Garvey, S., Wilkinson, A., Tortorelli, L., Ryan, L., et al. (2021). Double Stranded RNA Drives Innate Immune Responses, Sickness Behavior and Cognitive Impairment Dependent on dsRNA Length, IFNAR1 Expression and Age. *Biorxiv*. doi:10.1101/2021.01.09.426034

Mesev, E. V., LeDesma, R. A., and Ploss, A. (2019). Decoding Type I and III Interferon Signalling during Viral Infection. *Nat. Microbiol.* 4, 914–924. doi:10.1038/s41564-019-0421-x

Meylan, E., Curran, J., Hofmann, K., Moradpour, D., Binder, M., Bartenschlager, R., et al. (2005). Cardif Is an Adaptor Protein in the RIG-I Antiviral Pathway and Is Targeted by Hepatitis C Virus. *Nature* 437, 1167–1172. doi:10.1038/nature04193

Mills, E. L., Harmon, C., Jedrychowski, M. P., Xiao, H., Garrity, R., Tran, N. V., et al. (2021). UCP1 Governs Liver Extracellular Succinate and Inflammatory Pathogenesis. *Nat. Metab.* 3, 604–617. doi:10.1038/s42255-021-00389-5

Miura, K., Kodama, Y., Inokuchi, S., Schnabl, B., Aoyama, T., Ohnishi, H., et al. (2010). Toll-Like Receptor 9 Promotes Steatohepatitis by Induction of Interleukin-1β in Mice. *Gastroenterology* 139, 323–334. e7. doi:10.1053/j.gastro.2010.03.052

Mogi, M., Harada, M., Kondo, T., Riederer, P., Inagaki, H., Minami, M., et al. (1994). Interleukin-1β, Interleukin-6, Epidermal Growth Factor and Transforming Growth Factor-α Are Elevated in the Brain from Parkinsonian Patients. *Neurosci. Lett.* 180, 147–150. doi:10.1016/0304-3940(94)90508-8

Mottis, A., Herzig, S., and Auwerx, J. (2019). Mitocellular Communication: Shaping Health and Disease. *Science* 366, 827–832. doi:10.1126/science.aax3768

Motz, C., Schuhmann, K. M., Kirchhofer, A., Moldt, M., Witte, G., Conzelmann, K.-K., et al. (2013). Paramyxovirus V Proteins Disrupt the Fold of the RNA Sensor MDA5 to Inhibit Antiviral Signaling. *Science* 339, 690–693. doi:10.1126/science.1230949

Nakayama, H., and Otsu, K. (2018). Mitochondrial DNA as an Inflammatory Mediator in Cardiovascular Diseases. *Biochem. J.* 475, 839–852. doi:10.1042/bcj20170714

Namjou, B., Kothari, P. H., Kelly, J. A., Glenn, S. B., Ojwang, J. O., Adler, A., et al. (2011). Evaluation of the TREX1 Gene in a Large Multi-Ancestral Lupus Cohort. *Genes Immun.* 12, 270–279. doi:10.1038/gene.2010.73

Nan, Y., Wu, C., and Zhang, Y.-J. (2017). Interplay between Janus Kinase/Signal Transducer and Activator of Transcription Signaling Activated by Type I Interferons and Viral Antagonism. *Front. Immunol.* 8, 1758. doi:10.3389/fimmu.2017.01758

Ni, G., Konno, H., and Barber, G. N. (2017). Ubiquitination of STING at Lysine 224 Controls IRF3 Activation. *Sci. Immunol.* 2, eaah7119. doi:10.1126/sciimmunol.aah7119

Oka, T., Hikoso, S., Yamaguchi, O., Taneike, M., Takeda, T., Tamai, T., et al. (2012). Mitochondrial DNA that Escapes from Autophagy Causes Inflammation and Heart Failure. *Nature* 485, 251–255. doi:10.1038/nature10992

Omiya, S., Omori, Y., Taneike, M., Protti, A., Yamaguchi, O., Akira, S., et al. (2016). Toll-like Receptor 9 Prevents Cardiac Rupture after Myocardial Infarction in Mice Independently of Inflammation. *Am. J. Physiology-Heart Circulatory Physiol.* 311, H1497–H1485. doi:10.1152/ajpheart.00481.2016

Oshiumi, H., Miyashita, M., Inoue, N., Okabe, M., Matsumoto, M., and Seya, T. (2010). The Ubiquitin Ligase Riplet Is Essential for RIG-I-dependent Innate Immune Responses to RNA Virus Infection. *Cell Host & Microbe* 8, 496–509. doi:10.1016/j.chom.2010.11.008

Osteryoung, K. W., and Nunnari, J. (2003). The Division of Endosymbiotic Organelles. *Science* 302, 1698–1704. doi:10.1126/science.1082192

Pagliarini, D. J., Calvo, S. E., Chang, B., Sheth, S. A., Vafai, S. B., Ong, S.-E., et al. (2008). A Mitochondrial Protein Compendium Elucidates Complex I Disease Biology. *Cell* 134, 112–123. doi:10.1016/j.cell.2008.06.016

Pajak, A., Laine, I., Clemente, P., El-Fissi, N., Schober, F. A., Maffezzini, C., et al. (2019). Defects of Mitochondrial RNA Turnover lead to the Accumulation of Double-Stranded RNA *In Vivo*. *Plos Genet.* 15, e1008240. doi:10.1371/journal.pgen.1008240

Peisley, A., Lin, C., Wu, B., Orme-Johnson, M., Liu, M., Walz, T., et al. (2011). Cooperative Assembly and Dynamic Disassembly of MDA5 Filaments for Viral dsRNA Recognition. *Proc. Natl. Acad. Sci.* 108, 21010–21015. doi:10.1073/pnas.1113651108

Perez, F. A., and Palmiter, R. D. (2005). Parkin-deficient Mice Are Not a Robust Model of Parkinsonism. *Proc. Natl. Acad. Sci.* 102, 2174–2179. doi:10.1073/pnas.0409598102

Pichlmair, A., Schulz, O., Tan, C.-P., Rehwinkel, J., Kato, H., Takeuchi, O., et al. (2009). Activation of MDA5 Requires Higher-Order RNA Structures

Generated during Virus Infection. *J. Virol.* 83, 10761–10769. doi:10.1128/jvi.00770-09

Pippig, D. A., Hellmuth, J. C., Cui, S., Kirchhofer, A., Lammens, K., Lammens, A., et al. (2009). The Regulatory Domain of the RIG-I Family ATPase LGP2 Senses Double-Stranded RNA. *Nucleic Acids Res.* 37, 2014–2025. doi:10.1093/nar/gkp059

Pizzuto, M., and Pelegrin, P. (2020). Cardiolipin in Immune Signaling and Cell Death. *Trends Cel Biol.* 30, 892–903. doi:10.1016/j.tcb.2020.09.004

Qiao, J. T., Cui, C., Qing, L., Wang, L. S., He, T. Y., Yan, F., et al. (2018). Activation of the STING-IRF3 Pathway Promotes Hepatocyte Inflammation, Apoptosis and Induces Metabolic Disorders in Nonalcoholic Fatty Liver Disease. *Metabolism* 81, 13–24. doi:10.1016/j.metabol.2017.09.010

Qin, C., Gu, J., Liu, R., Xu, F., Qian, H., He, Q., et al. (2017). Release of Mitochondrial DNA Correlates with Peak Inflammatory Cytokines in Patients with Acute Myocardial Infarction. *Anatol. J. Cardiol.* 17 (3), 224–228. doi:10.14744/anatoljcardiol.2016.7209

Quirós, P. M., Mottis, A., and Auwerx, J. (2016). Mitonuclear Communication in Homeostasis and Stress. *Nat. Rev. Mol. Cel Biol* 17, 213–226. doi:10.1038/nrm.2016.23

Rabas, N., Palmer, S., Mitchell, L., Ismail, S., Gohlke, A., Riley, J. S., et al. (2021). PINK1 Drives Production of mtDNA-Containing Extracellular Vesicles to Promote Invasiveness. *J. Cel Biol* 220, e202006049. doi:10.1083/jcb.202006049

Rácz, E., Prens, E. P., Kurek, D., Kant, M., de Ridder, D., Mourits, S., et al. (2011). Effective Treatment of Psoriasis with Narrow-Band UVB Phototherapy Is Linked to Suppression of the IFN and Th17 Pathways. *J. Invest. Dermatol.* 131, 1547–1558. doi:10.1038/jid.2011.53

Radoshevich, L., and Dussurget, O. (2016). Cytosolic Innate Immune Sensing and Signaling upon Infection. *Front. Microbiol.* 7, 313. doi:10.3389/fmicb.2016.00313

Rath, S., Sharma, R., Gupta, R., Ast, T., Chan, C., Durham, T. J., et al. (2020). MitoCarta3.0: an Updated Mitochondrial Proteome Now with Sub-organelle Localization and Pathway Annotations. *Nucleic Acids Res.* 49, D1541–D1547. doi:10.1093/nar/gkaa1011

Rathinam, V. A. K., Jiang, Z., Waggoner, S. N., Sharma, S., Cole, L. E., Waggoner, L., et al. (2010). The AIM2 Inflammasome Is Essential for Host Defense against Cytosolic Bacteria and DNA Viruses. *Nat. Immunol.* 11, 395–402. doi:10.1038/ni.1864

Rehwinkel, J., and Gack, M. U. (2020). RIG-I-like Receptors: Their Regulation and Roles in RNA Sensing. *Nat. Rev. Immunol.* 20, 537–551. doi:10.1038/s41577-020-0288-3

Ricchelli, F., Šileikytė, J., and Bernardi, P. (20111807). Shedding Light on the Mitochondrial Permeability Transition. *Biochim. Biophys. Acta (Bba) - Bioenerg.* 1807, 482–490. doi:10.1016/j.bbabio.2011.02.012

Riley, J. S., Quarato, G., Cloix, C., Lopez, J., O'Prey, J., Pearson, M., et al. (2018). Mitochondrial Inner Membrane Permeabilisation Enables Mt DNA Release during Apoptosis. *Embo J.* 37. doi:10.15252/embj.201899238

Rodero, M. P., Tesser, A., Bartok, E., Rice, G. I., Della Mina, E., Depp, M., et al. (2017). Type I Interferon-Mediated Autoinflammation Due to DNase II Deficiency. *Nat. Commun.* 8, 2176. doi:10.1038/s41467-017-01932-3

Rothenfusser, S., Goutagny, N., DiPerna, G., Gong, M., Monks, B. G., Schoenemeyer, A., et al. (2005). The RNA Helicase Lgp2 Inhibits TLR-independent Sensing of Viral Replication by Retinoic Acid-Inducible Gene-I. *J. Immunol.* 175, 5260–5268. doi:10.4049/jimmunol.175.8.5260

Roy, A., Dutta, D., Iqbal, J., Pisano, G., Gjyshi, O., Ansari, M. A., et al. (2016). Nuclear Innate Immune DNA Sensor IFI16 Is Degraded during Lytic Reactivation of Kaposi's Sarcoma-Associated Herpesvirus (KSHV): Role of IFI16 in Maintenance of KSHV Latency. *J. Virol.* 90, 8822–8841. doi:10.1128/jvi.01003-16

Roy, A., Ghosh, A., Kumar, B., and Chandran, B. (2019). IFI16, a Nuclear Innate Immune DNA Sensor, Mediates Epigenetic Silencing of Herpesvirus Genomes by its Association with H3K9 Methyltransferases SUV39H1 and GLP. *Elife* 8, e49500. doi:10.7554/elife.49500

Ruprecht, J. J., King, M. S., Zögg, T., Aleksandrova, A. A., Pardon, E., Crichton, P. G., et al. (2019). The Molecular Mechanism of Transport by the Mitochondrial ADP/ATP Carrier. *Cell* 176, 435–447. e15. doi:10.1016/j.cell.2018.11.025

Ryan, M. T., and Hoogenraad, N. J. (2007). Mitochondrial-Nuclear Communications. *Annu. Rev. Biochem.* 76, 701–722. doi:10.1146/annurev.biochem.76.052305.091720

Saito, T., Hirai, R., Loo, Y.-M., Owen, D., Johnson, C. L., Sinha, S. C., et al. (2007). Regulation of Innate Antiviral Defenses through a Shared Repressor Domain in RIG-I and LGP2. *Proc. Natl. Acad. Sci.* 104, 582–587. doi:10.1073/pnas.0606699104

Schindler, S. M., Frank, M. G., Annis, J. L., Maier, S. F., and Klegeris, A. (2018). Pattern Recognition Receptors Mediate Pro-inflammatory Effects of Extracellular Mitochondrial Transcription Factor A (TFAM). *Mol. Cell Neurosci.* 89, 71–79. doi:10.1016/j.mcn.2018.04.005

Schoggins, J. W., MacDuff, D. A., Imanaka, N., Gainey, M. D., Shrestha, B., Eitson, J. L., et al. (2014). Pan-viral Specificity of IFN-Induced Genes Reveals New Roles for cGAS in Innate Immunity. *Nature* 505, 691–695. doi:10.1038/nature12862

Schuberth-Wagner, C., Ludwig, J., Bruder, A. K., Herzner, A.-M., Zillinger, T., Goldeck, M., et al. (2015). A Conserved Histidine in the RNA Sensor RIG-I Controls Immune Tolerance to N1-2′o-Methylated Self RNA. *Immunity* 43, 41–51. doi:10.1016/j.immuni.2015.06.015

Schur, P. H., Stollar, B. D., Steinberg, A. D., and Talal, N. (1971). Incidence of Antibodies to Double-Stranded RNA in Systemic Lupus Erythematosus and Related Diseases. *Arthritis Rheum.* 14, 342–347. doi:10.1002/art.1780140304

Seewald, L. A., Keller, L. E., Thomas, M., Casey, J. W., and Delco, M. L. (2020). Mitoprotection Prevents Increased Synovial Fluid Mitochondrial DNA Concentrations after Articular Injury. *Osteoarthritis and Cartilage* 28, S96. doi:10.1016/j.joca.2020.02.148

Seth, R. B., Sun, L., Ea, C.-K., and Chen, Z. J. (2005). Identification and Characterization of MAVS, a Mitochondrial Antiviral Signaling Protein that Activates NF-Kb and IRF3. *Cell* 122, 669–682. doi:10.1016/j.cell.2005.08.012

Shadel, G. S., and Clayton, D. A. (1997). MITOCHONDRIAL DNA MAINTENANCE IN VERTEBRATES. *Annu. Rev. Biochem.* 66, 409–435. doi:10.1146/annurev.biochem.66.1.409

Sharma, B. R., Karki, R., and Kanneganti, T. D. (2019). Role of AIM2 Inflammasome in Inflammatory Diseases, Cancer and Infection. *Eur. J. Immunol.* 49, 1998–2011. doi:10.1002/eji.201848070

Shimizu, M., Okuno, T., Kinoshita, M., Sumi, H., Fujimura, H., Yamashita, K., et al. (2020). Mitochondrial DNA Enhance Innate Immune Responses in Neuromyelitis Optica by Monocyte Recruitment and Activation. *Sci. Rep.* 10, 13274. doi:10.1038/s41598-020-70203-x

Sliter, D. A., Martinez, J., Hao, L., Chen, X., Sun, N., Fischer, T. D., et al. (2018). Parkin and PINK1 Mitigate STING-Induced Inflammation. *Nature* 561, 258–262. doi:10.1038/s41586-018-0448-9

Spengler, J. R., Patel, J. R., Chakrabarti, A. K., Zivcec, M., García-Sastre, A., Spiropoulou, C. F., et al. (2015). RIG-I Mediates an Antiviral Response to Crimean-Congo Hemorrhagic Fever Virus. *J. Virol.* 89, 10219–10229. doi:10.1128/jvi.01643-15

Sprenger, H.-G., MacVicar, T., Bahat, A., Fiedler, K. U., Hermans, S., Ehrentraut, D., et al. (2021). Cellular Pyrimidine Imbalance Triggers Mitochondrial DNA-dependent Innate Immunity. *Nat. Metab.* 3, 636–650. doi:10.1038/s42255-021-00385-9

Stetson, D. B., Ko, J. S., Heidmann, T., and Medzhitov, R. (2008). Trex1 Prevents Cell-Intrinsic Initiation of Autoimmunity. *Cell* 134, 587–598. doi:10.1016/j.cell.2008.06.032

Stetson, D. B., and Medzhitov, R. (2006). Recognition of Cytosolic DNA Activates an IRF3-dependent Innate Immune Response. *Immunity* 24, 93–103. doi:10.1016/j.immuni.2005.12.003

Sun, B., Sundström, K. B., Chew, J. J., Bist, P., Gan, E. S., Tan, H. C., et al. (2017). Dengue Virus Activates cGAS through the Release of Mitochondrial DNA. *Sci. Rep.* 7, 3594. doi:10.1038/s41598-017-03932-1

Sun, L., Wu, J., Du, F., Chen, X., and Chen, Z. J. (2013). Cyclic GMP-AMP Synthase Is a Cytosolic DNA Sensor that Activates the Type I Interferon Pathway. *Science* 339, 786–791. doi:10.1126/science.1232458

Szczesny, B., Marcatti, M., Ahmad, A., Montalbano, M., Brunyánszki, A., Bibli, S.-I., et al. (2018). Mitochondrial DNA Damage and Subsequent Activation of Z-DNA Binding Protein 1 Links Oxidative Stress to Inflammation in Epithelial Cells. *Sci. Rep.* 8, 914. doi:10.1038/s41598-018-19216-1

Szczesny, R. J., Borowski, L. S., Brzezniak, L. K., Dmochowska, A., Gewartowski, K., Bartnik, E., et al. (2009). Human Mitochondrial RNA Turnover Caught in Flagranti: Involvement of hSuv3p Helicase in RNA Surveillance. *Nucleic Acids Res.* 38, 279–298. doi:10.1093/nar/gkp903

Szczesny, R. J., Borowski, L. S., Malecki, M., Wojcik, M. A., Stepien, P. P., and Golik, P. (2012). RNA Degradation in Yeast and Human Mitochondria. *Biochim.*

Biophys. Acta (Bba) - Gene Regul. Mech. 1819, 1027–1034. doi:10.1016/j.bbagrm.2011.11.010

Szeto, H. H., Liu, S., Soong, Y., Seshan, S. V., Cohen-Gould, L., Manichev, V., et al. (2016). Mitochondria Protection after Acute Ischemia Prevents Prolonged Upregulation of IL-1β and IL-18 and Arrests CKD. *Jasn* 28, 1437–1449. doi:10.1681/asn.2016070761

Takaoka, A., Wang, Z., Choi, M. K., Yanai, H., Negishi, H., Ban, T., et al. (2007). DAI (DLM-1/ZBP1) Is a Cytosolic DNA Sensor and an Activator of Innate Immune Response. *Nature* 448, 501–505. doi:10.1038/nature06013

Takeuchi, O., and Akira, S. (2009). Innate Immunity to Virus Infection. *Immunol. Rev.* 227, 75–86. doi:10.1111/j.1600-065x.2008.00737.x

Tanaka, Y., and Chen, Z. J. (2012). STING Specifies IRF3 Phosphorylation by TBK1 in the Cytosolic DNA Signaling Pathway. *Sci. Signal.* 5, ra20. doi:10.1126/scisignal.2002521

Tang, C., Han, H., Yan, M., Zhu, S., Liu, J., Liu, Z., et al. (2018). PINK1-PRKN/PARK2 Pathway of Mitophagy Is Activated to Protect against Renal Ischemia-Reperfusion Injury. *Autophagy* 14, 880–897. doi:10.1080/15548627.2017.1405880

Taruno, A. (2018). ATP Release Channels. *Ijms* 19, 808. doi:10.3390/ijms19030808

Tigano, M., Vargas, D. C., Tremblay-Belzile, S., Fu, Y., and Sfeir, A. (2021). Nuclear Sensing of Breaks in Mitochondrial DNA Enhances Immune Surveillance. *Nature* 591, 477–481. doi:10.1038/s41586-021-03269-w

Torres-Odio, S., Lei, Y., Gispert, S., Maletzko, A., Key, J., Menissy, S. S., et al. (2021). Loss of Mitochondrial Protease CLPP Activates Type I IFN Responses through the Mitochondrial DNA-cGAS-STING Signaling Axis. *J.I.* 206, 1890–1900. doi:10.4049/jimmunol.2001016

Trauelsen, M., Hiron, T. K., Lin, D., Petersen, J. E., Breton, B., Husted, A. S., et al. (2021). Extracellular Succinate Hyperpolarizes M2 Macrophages through SUCNR1/GPR91-Mediated Gq Signaling. *Cel Rep.* 35, 109246. doi:10.1016/j.celrep.2021.109246

Truszewska, A., Wirkowska, A., Gala, K., Truszewski, P., Krzemień-Ojak, Ł., Perkowska-Ptasińska, A., et al. (2020). Cell-Free DNA Profiling in Patients with Lupus Nephritis. *Lupus* 29 (13), 1759–1772. doi:10.1177/0961203320957717

Tsuchida, T., Zou, J., Saitoh, T., Kumar, H., Abe, T., Matsuura, Y., et al. (2010). The Ubiquitin Ligase TRIM56 Regulates Innate Immune Responses to Intracellular Double-Stranded DNA. *Immunity* 33, 765–776. doi:10.1016/j.immuni.2010.10.013

Tsuji, N., Tsuji, T., Ohashi, N., Kato, A., Fujigaki, Y., and Yasuda, H. (2016). Role of Mitochondrial DNA in Septic AKI via Toll-like Receptor 9. *Jasn* 27, 2009–2020. doi:10.1681/asn.2015040376

Upton, J. W., Kaiser, W. J., and Mocarski, E. S. (2019). DAI/ZBP1/DLM-1 Complexes with RIP3 to Mediate Virus-Induced Programmed Necrosis that Is Targeted by Murine Cytomegalovirus vIRA. *Cell Host & Microbe* 26, 564. doi:10.1016/j.chom.2019.09.004

Vacchelli, E., Le Naour, J., and Kroemer, G. (2020). The Ambiguous Role of FPR1 in Immunity and Inflammation. *Oncoimmunology* 9, 1760061. doi:10.1080/2162402x.2020.1760061

Valente, E. M., Abou-Sleiman, P. M., Caputo, V., Muqit, M. M. K., Harvey, K., Gispert, S., et al. (2004). Hereditary Early-Onset Parkinson's Disease Caused by Mutations in PINK1. *Science* 304, 1158–1160. doi:10.1126/science.1096284

Venkataraman, T., Valdes, M., Elsby, R., Kakuta, S., Caceres, G., Saijo, S., et al. (2007). Loss of DExD/H Box RNA Helicase LGP2 Manifests Disparate Antiviral Responses. *J. Immunol.* 178, 6444–6455. doi:10.4049/jimmunol.178.10.6444

Wang, H., Li, T., Chen, S., Gu, Y., and Ye, S. (2015). Neutrophil Extracellular Trap Mitochondrial DNA and its Autoantibody in Systemic Lupus Erythematosus and a Proof-Of-Concept Trial of Metformin. *Arthritis Rheumatol.* 67, 3190–3200. doi:10.1002/art.39296

Wang, Z., Choi, M. K., Ban, T., Yanai, H., Negishi, H., Lu, Y., et al. (2008). Regulation of Innate Immune Responses by DAI (DLM-1/ZBP1) and Other DNA-Sensing Molecules. *Proc. Natl. Acad. Sci.* 105, 5477–5482. doi:10.1073/pnas.0801295105

Ward, G. A., McGraw, K. L., Abbas-Aghababazadeh, F., Meyer, B. S., McLemore, A. F., Vincelette, N. D., et al. (2021). Oxidized Mitochondrial DNA Released after Inflammasome Activation Is a Disease Biomarker for Myelodysplastic Syndromes. *Blood Adv.* 5, 2216–2228. doi:10.1182/bloodadvances.2020003475

Wauer, T., Simicek, M., Schubert, A., and Komander, D. (2015). Mechanism of Phospho-Ubiquitin-Induced PARKIN Activation. *Nature* 524, 370–374. doi:10.1038/nature14879

Wei, P. Z., Kwan, B. C., Chow, K. M., Cheng, P. M., Luk, C. C., Li, P. K., et al. (2018). Urinary Mitochondrial DNA Level Is an Indicator of Intra-renal Mitochondrial Depletion and Renal Scarring in Diabetic Nephropathy. *Nephrol. Dial. Transplant.* 33 (5), 784–788. doi:10.1093/ndt/gfx339

Wenceslau, C. F., McCarthy, C. G., Szasz, T., Spitler, K., Goulopoulou, S., Webb, R. C., et al. (2014). Mitochondrial Damage-Associated Molecular Patterns and Vascular Function. *Eur. Heart J.* 35, 1172–1177. doi:10.1093/eurheartj/ehu047

West, A. P., Khoury-Hanold, W., Staron, M., Tal, M. C., Pineda, C. M., Lang, S. M., et al. (2015). Mitochondrial DNA Stress Primes the Antiviral Innate Immune Response. *Nature* 520, 553–557. doi:10.1038/nature14156

Whitaker, R. M., Stallons, L. J., Kneff, J. E., Alge, J. L., Harmon, J. L., Rahn, J. J., et al. (2015). Urinary Mitochondrial DNA Is a Biomarker of Mitochondrial Disruption and Renal Dysfunction in Acute Kidney Injury. *Kidney Int.* 88, 1336–1344. doi:10.1038/ki.2015.240

Wiens, K. E., and Ernst, J. D. (2016). The Mechanism for Type I Interferon Induction by *Mycobacterium tuberculosis* Is Bacterial Strain-dependent. *Plos Pathog.* 12, e1005809. doi:10.1371/journal.ppat.1005809

Wies, E., Wang, M. K., Maharaj, N. P., Chen, K., Zhou, S., Finberg, R. W., et al. (2013). Dephosphorylation of the RNA Sensors RIG-I and MDA5 by the Phosphatase PP1 Is Essential for Innate Immune Signaling. *Immunity* 38, 437–449. doi:10.1016/j.immuni.2012.11.018

Willmes, D. M., and Birkenfeld, A. L. (2013). THE ROLE OF INDY IN METABOLIC REGULATION. *Comput. Struct. Biotechnol. J.* 6, e201303020–8. doi:10.5936/csbj.201303020

Witte, M. E., Bol, J. G. J. M., Gerritsen, W. H., Valk, P. v. d., Drukarch, B., Horssen, J. v., et al. (2009). Parkinson's Disease-Associated Parkin Colocalizes with Alzheimer's Disease and Multiple Sclerosis Brain Lesions. *Neurobiol. Dis.* 36, 445–452. doi:10.1016/j.nbd.2009.08.009

Wu, B., Ni, H., Li, J., Zhuang, X., Zhang, J., Qi, Z., et al. (2017). The Impact of Circulating Mitochondrial DNA on Cardiomyocyte Apoptosis and Myocardial Injury after TLR4 Activation in Experimental Autoimmune Myocarditis. *Cell Physiol Biochem* 42, 713–728. doi:10.1159/000477889

Wu, B., Peisley, A., Richards, C., Yao, H., Zeng, X., Lin, C., et al. (2013). Structural Basis for dsRNA Recognition, Filament Formation, and Antiviral Signal Activation by MDA5. *Cell* 152, 276–289. doi:10.1016/j.cell.2012.11.048

Wu, B., Peisley, A., Tetrault, D., Li, Z., Egelman, E. H., Magor, K. E., et al. (2014). Molecular Imprinting as a Signal-Activation Mechanism of the Viral RNA Sensor RIG-I. *Mol. Cel* 55, 511–523. doi:10.1016/j.molcel.2014.06.010

Wu, G., Zhu, Q., Zeng, J., Gu, X., Miao, Y., Xu, W., et al. (2019). Extracellular Mitochondrial DNA Promote NLRP3 Inflammasome Activation and Induce Acute Lung Injury through TLR9 and NF-Kb. *J. Thorac. Dis.* 11, 4816–4828. doi:10.21037/jtd.2019.10.26

Wu, Y., and Li, S. (2020). Role of Post-Translational Modifications of cGAS in Innate Immunity. *Ijms* 21, 7842. doi:10.3390/ijms21217842

Xavier, V. J., and Martinou, J.-C. (2021). RNA Granules in the Mitochondria and Their Organization under Mitochondrial Stresses. *Ijms* 22, 9502. doi:10.3390/ijms22179502

Xu, R.-H., Wong, E. B., Rubio, D., Roscoe, F., Ma, X., Nair, S., et al. (2015). Sequential Activation of Two Pathogen-Sensing Pathways Required for Type I Interferon Expression and Resistance to an Acute DNA Virus Infection. *Immunity* 43, 1148–1159. doi:10.1016/j.immuni.2015.11.015

Yan, N., Regalado-Magdos, A. D., Stiggelbout, B., Lee-Kirsch, M. A., and Lieberman, J. (2010). The Cytosolic Exonuclease TREX1 Inhibits the Innate Immune Response to Human Immunodeficiency Virus Type 1. *Nat. Immunol.* 11, 1005–1013. doi:10.1038/ni.1941

Yanai, H., Chiba, S., Hangai, S., Kometani, K., Inoue, A., Kimura, Y., et al. (2018). Revisiting the Role of IRF3 in Inflammation and Immunity by Conditional and Specifically Targeted Gene Ablation in Mice. *Proc. Natl. Acad. Sci. USA* 115, 5253–5258. doi:10.1073/pnas.1803936115

Yao, X., Carlson, D., Sun, Y., Ma, L., Wolf, S. E., Minei, J. P., et al. (2015). Mitochondrial ROS Induces Cardiac Inflammation via a Pathway through mtDNA Damage in a Pneumonia-Related Sepsis Model. *Plos One* 10, e0139416. doi:10.1371/journal.pone.0139416

Ye, X., Sun, X., Starovoytov, V., and Cai, Q. (2015). Parkin-mediated Mitophagy in Mutant hAPP Neurons and Alzheimer's Disease Patient Brains. *Hum. Mol. Genet.* 24, 2938–2951. doi:10.1093/hmg/ddv056

Yoneyama, M., Kikuchi, M., Matsumoto, K., Imaizumi, T., Miyagishi, M., Taira, K., et al. (2005). Shared and Unique Functions of the DExD/H-Box Helicases RIG-I, MDA5, and LGP2 in Antiviral Innate Immunity. *J. Immunol.* 175, 2851–2858. doi:10.4049/jimmunol.175.5.2851

Yoneyama, M., Kikuchi, M., Natsukawa, T., Shinobu, N., Imaizumi, T., Miyagishi, M., et al. (2004). The RNA Helicase RIG-I Has an Essential Function in Double-Stranded RNA-Induced Innate Antiviral Responses. *Nat. Immunol.* 5, 730–737. doi:10.1038/ni1087

Yousefi, S., Gold, J. A., Andina, N., Lee, J. J., Kelly, A. M., Kozlowski, E., et al. (2008). Catapult-like Release of Mitochondrial DNA by Eosinophils Contributes to Antibacterial Defense. *Nat. Med.* 14, 949–953. doi:10.1038/nm.1855

Yu, C.-H., Davidson, S., Harapas, C. R., Hilton, J. B., Mlodzianoski, M. J., Laohamonthonkul, P., et al. (2020). TDP-43 Triggers Mitochondrial DNA Release via mPTP to Activate cGAS/STING in ALS. *Cell* 183, 636–649. e18. doi:10.1016/j.cell.2020.09.020

Yu, E., Calvert, P. A., Mercer, J. R., Harrison, J., Baker, L., Figg, N. L., et al. (2013). Mitochondrial DNA Damage Can Promote Atherosclerosis Independently of Reactive Oxygen Species through Effects on Smooth Muscle Cells and Monocytes and Correlates with Higher-Risk Plaques in Humans. *Circulation* 128, 702–712. doi:10.1161/circulationaha.113.002271

Yu, Y., Liu, Y., An, W., Song, J., Zhang, Y., and Zhao, X. (2018). STING-mediated Inflammation in Kupffer Cells Contributes to Progression of Nonalcoholic Steatohepatitis. *J. Clin. Invest.* 129, 546–555. doi:10.1172/jci121842

Yu-Wai-Man, P., and Newman, N. J. (2017). Inherited Eye-Related Disorders Due to Mitochondrial Dysfunction. *Hum. Mol. Genet.* 26, R12–R20. doi:10.1093/hmg/ddx182

Yuan, D., Huang, S., Berger, E., Liu, L., Gross, N., Heinzmann, F., et al. (2017). Kupffer Cell-Derived Tnf Triggers Cholangiocellular Tumorigenesis through JNK Due to Chronic Mitochondrial Dysfunction and ROS. *Cancer Cell* 31, 771–789. e6. doi:10.1016/j.ccell.2017.05.006

Zevini, A., Olagnier, D., and Hiscott, J. (2017). Crosstalk between Cytoplasmic RIG-I and STING Sensing Pathways. *Trends Immunol.* 38, 194–205. doi:10.1016/j.it.2016.12.004

Zhang J.-Z, J.-Z., Liu, Z., Liu, J., Ren, J.-X., and Sun, T.-S. (2014). Mitochondrial DNA Induces Inflammation and Increases TLR9/NF-Kb Expression in Lung Tissue. *Int. J. Mol. Med.* 33, 817–824. doi:10.3892/ijmm.2014.1650

Zhang, J., Hu, M.-M., Wang, Y.-Y., and Shu, H.-B. (2012). TRIM32 Protein Modulates Type I Interferon Induction and Cellular Antiviral Response by Targeting MITA/STING Protein for K63-Linked Ubiquitination. *J. Biol. Chem.* 287, 28646–28655. doi:10.1074/jbc.m112.362608

Zhang, Q., Raoof, M., Chen, Y., Sumi, Y., Sursal, T., Junger, W., et al. (2010). Circulating Mitochondrial DAMPs Cause Inflammatory Responses to Injury. *Nature* 464, 104–107. doi:10.1038/nature08780

Zhang, T., Yin, C., Boyd, D. F., Quarato, G., Ingram, J. P., Shubina, M., et al. (2020). Influenza Virus Z-RNAs Induce ZBP1-Mediated Necroptosis. *Cell* 180, 1115–1129. e13. doi:10.1016/j.cell.2020.02.050

Zhang, W., Zhou, Q., Xu, W., Cai, Y., Yin, Z., Gao, X., et al. (2013). DNA-dependent Activator of Interferon-Regulatory Factors (DAI) Promotes Lupus Nephritis by Activating the Calcium Pathway. *J. Biol. Chem.* 288, 13534–13550. doi:10.1074/jbc.m113.457218

Zhang, X., Shi, H., Wu, J., Zhang, X., Sun, L., Chen, C., et al. (2013). Cyclic GMP-AMP Containing Mixed Phosphodiester Linkages Is an Endogenous High-Affinity Ligand for STING. *Mol. Cel* 51, 226–235. doi:10.1016/j.molcel.2013.05.022

Zhang, X., Wu, J., Du, F., Xu, H., Sun, L., Chen, Z., et al. (2014). The Cytosolic DNA Sensor cGAS Forms an Oligomeric Complex with DNA and Undergoes Switch-like Conformational Changes in the Activation Loop. *Cel Rep.* 6, 421–430. doi:10.1016/j.celrep.2014.01.003

Zhou, B., Fang, L., Dong, Y., Yang, J., Chen, X., Zhang, N., et al. (2021). Mitochondrial Quality Control Protects Photoreceptors against Oxidative Stress in the H2O2-Induced Models of Retinal Degeneration Diseases. *Cel Death Dis* 12, 413. doi:10.1038/s41419-021-03660-5

Zhou, X., Backman, L. J., and Danielson, P. (2021). Activation of NF-Kb Signaling via Cytosolic Mitochondrial RNA Sensing in Kerotocytes with Mitochondrial DNA Common Deletion. *Sci. Rep.* 11, 7360. doi:10.1038/s41598-021-86522-6

Zhu, Z., Zhang, X., Wang, G., and Zheng, H. (2014). The Laboratory of Genetics and Physiology 2: Emerging Insights into the Controversial Functions of This RIG-I-like Receptor. *Biomed. Res. Int.* 2014, 1–7. doi:10.1155/2014/960190

Zindel, J., and Kubes, P. (2020). DAMPs, PAMPs, and LAMPs in Immunity and Sterile Inflammation. *Annu. Rev. Pathol. Mech. Dis.* 15, 493–518. doi:10.1146/annurev-pathmechdis-012419-032847

Conflict of Interest: The authors declare that the research was conducted in the absence of any commercial or financial relationships that could be construed as a potential conflict of interest.

The handling editor declared a past collaboration with several of the authors AC, AA.

Publisher's Note: All claims expressed in this article are solely those of the authors and do not necessarily represent those of their affiliated organizations, or those of the publisher, the editors and the reviewers. Any product that may be evaluated in this article, or claim that may be made by its manufacturer, is not guaranteed or endorsed by the publisher.

frontiers in Cell and Developmental Biology

ORIGINAL RESEARCH
published: 17 February 2022
doi: 10.3389/fcell.2022.833127

Mitochondrial Inorganic Polyphosphate (polyP) Is a Potent Regulator of Mammalian Bioenergetics in SH-SY5Y Cells: A Proteomics and Metabolomics Study

*Mariona Guitart-Mampel[1], Pedro Urquiza[1], Fausto Carnevale Neto[2], James R. Anderson[3], Vedangi Hambardikar[4], Ernest R. Scoma[4], Gennifer E. Merrihew[5], Lu Wang[6], Michael J. MacCoss[5], Daniel Raftery[2,7], Mandy J. Peffers[3] and Maria E. Solesio[1,4]**

[1]Department of Biology, Rutgers University, Camden, NJ, United States, [2]Northwest Metabolomics Research Center, Department of Anesthesiology and Pain Medicine, University of Washington, Seattle, WA, United States, [3]Musculoskeletal and Ageing Science, Institute of Life Course and Medical Sciences, University of Liverpool, Liverpool, United Kingdom, [4]Center for Computational and Integrative Biology, Rutgers University, Camden, NJ, United States, [5]Department of Genome Sciences, University of Washington, Seattle, WA, United States, [6]Department of Environmental and Occupational Health Sciences, University of Washington, Seattle, WA, United States, [7]Public Health Sciences Division, Fred Hutchinson Cancer Research Center, Seattle, WA, United States

Inorganic polyphosphate (polyP) is an ancient, ubiquitous, and well-conserved polymer which is present in all the studied organisms. It is formed by individual subunits of orthophosphate which are linked by structurally similar bonds and isoenergetic to those found in ATP. While the metabolism and the physiological roles of polyP have already been described in some organisms, including bacteria and yeast, the exact role of this polymer in mammalian physiology still remains poorly understood. In these organisms, polyP shows a co-localization with mitochondria, and its role as a key regulator of the stress responses, including the maintenance of appropriate bioenergetics, has already been demonstrated by our group and others. Here, using Wild-type (Wt) and MitoPPX (cells enzymatically depleted of mitochondrial polyP) SH-SY5Y cells, we have conducted a comprehensive study of the status of cellular physiology, using proteomics and metabolomics approaches. Our results suggest a clear dysregulation of mitochondrial physiology, especially of bioenergetics, in MitoPPX cells when compared with Wt cells. Moreover, the effects induced by the enzymatic depletion of polyP are similar to those present in the mitochondrial dysfunction that is observed in neurodegenerative disorders and in neuronal aging. Based on our findings, the metabolism of mitochondrial polyP could be a valid and innovative pharmacological target in these conditions.

Keywords: mitochondria, bioenergetics, mitochondrial metabolism, OXPHOS, inorganic polyphosphate, metabolomics, proteomics, SH-SY5Y cells

OPEN ACCESS

Edited by:
Gloria Garrabou, Institut d'Investigacions Biomèdiques August Pi i Sunyer (IDIBAPS), Spain

Reviewed by:
Jaume Amengual, University of Illinois at Urbana-Champaign, United States
Heather M. Wilkins, University of Kansas Medical Center Research Institute, United States
Pasquale D'Acunzo, Vita-Salute San Raffaele University, Italy

****Correspondence:***
Maria E. Solesio
m.solesio@rutgers.edu

Specialty section:
This article was submitted to Cellular Biochemistry, a section of the journal Frontiers in Cell and Developmental Biology

Received: *10 December 2021*
Accepted: *21 January 2022*
Published: *17 February 2022*

Citation:
Guitart-Mampel M, Urquiza P, Carnevale Neto F, Anderson JR, Hambardikar V, Scoma ER, Merrihew GE, Wang L, MacCoss MJ, Raftery D, Peffers MJ and Solesio ME (2022) Mitochondrial Inorganic Polyphosphate (polyP) Is a Potent Regulator of Mammalian Bioenergetics in SH-SY5Y Cells: A Proteomics and Metabolomics Study. Front. Cell Dev. Biol. 10:833127. doi: 10.3389/fcell.2022.833127

1 INTRODUCTION

Inorganic polyphosphate (polyP) is an evolutionary conserved polymer, which is wide spread across all studied organisms, from bacteria to mammals (Kornberg et al., 1999; Kulakovskaya et al., 2010). It is composed of multiple monomers of orthophosphate linked by high-energy phosphoanhydride bonds, similar to those present in ATP (Kornberg et al., 1999). The concentration and length of polyP has shown to be variable in different subcellular locations and organisms (Kumble and Kornberg, 1995). In mammalian cells, polyP is usually formed by a couple of hundred monomers of orthophosphate, and it is found within the micromolar range (Kumble and Kornberg, 1995). The metabolism of polyP in these cells still remains poorly understood, even though a study showing the effects of the mitochondrial F_0F_1-ATP synthase in the synthesis and degradation of the polymer in the presence of mitochondrial respiration substrates and phosphates has been recently published (Bayev et al., 2020). However, additional pathways independent of the ATP synthase are probably also involved in the metabolism of polyP in mammalian cells (Borden et al., 2021; McIntyre and Solesio, 2021; Patro et al., 2021). In bacteria and yeast, the metabolism of the polymer is well-described. For example, it is known that polyP is converted into inorganic phosphate by the exopolyphosphatase (PPX) enzyme (Kornberg et al., 1999; Kulakovskaya et al., 2010).

PolyP has been proposed as a key molecule in the cellular stress response in a wide range of organisms, including mammals (Judge and Leeuwenburgh, 2007; Paradies et al., 2010; Armstrong et al., 2018). Accordingly, polyP has an important regulatory role in many cellular processes that are commonly dysregulated in neurodegenerative disorders, such as generation of reactive oxygen species (ROS), inflammation, apoptosis, energy metabolism, calcium signaling, and protein homeostasis (Muller et al., 2009; Kim et al., 2011; Morrissey et al., 2012; Solesio et al., 2016a; Amodeo et al., 2017; Angelova et al., 2018; Yoo et al., 2018; Maiolino et al., 2019; Solesio et al., 2020). In mammalian cells, polyP has been found in the cytoplasm, the nucleus, associated with membrane proteins (Kumble and Kornberg, 1995), in the extracellular space (Suess et al., 2017), and in different organelles such as acidocalcisomes and mitochondria, where the levels of the polymer correlate with those of ATP (Abramov et al., 2007; Solesio et al., 2016a). In fact, polyP synthesis is dependent on the metabolic status of the cell (Pavlov et al., 2005; Pavlov et al., 2010). Moreover, we have already demonstrated the role of polyP in the regulation of the intra-mitochondrial levels of free calcium, which are closely related to mitochondrial metabolism and ATP generation (Solesio et al., 2016b; Solesio et al., 2020). Indeed, intra-mitochondrial calcium signaling activates mitochondrial dehydrogenases, which leads to the increased levels of NADH and ATP (McCormack et al., 1990), present in stress response and in aging (Baltanas et al., 2013; Picard et al., 2018).

Mitochondrial function, including oxidative phosphorylation (OXPHOS) regulation, is especially relevant to high-energy cells, such as neurons (Zheng et al., 2016). Changes in energy metabolism can compromise brain function and be components in the etiopathology of multiple diseases, including neurodegenerative disorders, such as Parkinson's (PD) and Alzheimer's disease (AD) (Lin and Beal, 2006; Schon and Przedborski, 2011; Koopman et al., 2013). Moreover, increased ROS production, a well-known consequence of dysfunctional mitochondrial bioenergetics, is also a common aspect of neurodegeneration (Kudryavtseva et al., 2016; Singh et al., 2019). Furthermore, our research group has recently investigated the impact of mitochondrial polyP in the regulation of mammalian OXPHOS. By using HEK293 cells that are enzymatically depleted of mitochondrial polyP (MitoPPX), we demonstrated a significant shift from OXPHOS to glycolysis, globally affecting mitochondrial physiology (Solesio et al., 2021). MitoPPX cells are created by the stable transfection of Wt cells with a plasmid containing the sequence for the mitochondrial expression of the exopolyphosphatase enzyme (PPX), which is the enzyme in charge of the degradation of polyP in yeast. The homolog of the PPX enzyme in mammalian cells still remains unknown. Previous studies have shown that the effects induced by transfection with MitoPPX are due to the elimination of polyP and not to the transfection procedure or other effects of PPX on mammalian cellular physiology (Abramov et al., 2007; Seidlmayer et al., 2012; Seidlmayer et al., 2015).

Here, we conducted a comprehensive proteomics and metabolomics study of the role of mitochondrial polyP in SH-SY5Y cells, a cellular model widely used for experimental research in the field of neurodegeneration (Xicoy et al., 2017). Our goal is to better understand the contribution of mitochondrial polyP to the molecular mechanisms that regulate cellular bioenergetics. To achieve this, we used Wild-type (Wt) and MitoPPX SH-SY5Y cells. Proteomics and metabolomics approaches were conducted to identify phenotypic differences between the cell lines, particularly focused on mitochondrial metabolism and bioenergetics. Our data suggested that the enzymatic depletion of mitochondrial polyP has a deleterious impact on various metabolic pathways, including mitochondrial bioenergetics, where several subunits of the Electron Transfer Chain (ETC) as well as metabolites, are altered. These integrated proteomics and metabolomics profiles could bring new insights into the specific role(s) of mitochondrial polyP in mammalian cells, as well as contribute to finding new therapeutic approaches using mitochondrial polyP as a valid target against dysfunctional organelle in human pathologies.

2 MATERIALS AND METHODS

2.1 Reagents

Dulbecco's Modified Eagle medium (DMEM):F12; 4′,6-diamino-2-phenylindole (DAPI); penicillin-streptomycin; G418; lipofectamine; trypsin; alkaline phosphatase; Pierce BCA protein assay kit; Pierce ECL western blotting substrate; phosphoric acid; heat-inactivated fetal bovine serum (FBS); acetonitrile (ACN); methanol; ammonium acetate; Pierce Halt protease and phosphatase Inhibitor Cocktails; and acetic acid Optima LC-MS grade were purchased from Thermo Fisher

Scientific (Waltham, MA, US). Phosphate-Buffered Saline (PBS); β-mercaptoethanol; tris(hydroxymethyl)-1,3-propanediol hydrochloride (TRIS-HCl); glycerol; Bovine Serum Albumin (BSA); phenylmethylsulfonyl fluoride (PMSF); Tween-20; triethylammonium bicarbonate buffer (TEAB); dimethyl sulfoxide (DMSO); iodoacetamide (IAA); yeast enolase protein; and potassium chloride were obtained from Sigma-Aldrich (San Louis, Missouri, US). All the materials and reagents used in the Western Blotting experiments, including secondary antibodies, polyvinylidene (PVDF) membranes, fat-free milk, protein ladders, and polyacrylamide-precast gels were obtained from BioRad (Hercules, California, US). Primary antibodies anti-OXPHOS, anti-PPX and anti-β-actin were obtained from Abcam (Cambridge, United Kingdom), and anti-eGFP from Cell Signaling (Danvers, MA, US). Deionized water was obtained using an 18 MΩ Milli-Q from EMD Millipore Corporation (Billerica, Massachusetts, US).

2.2 Cell Growing and Maintenance

Wt SH-SY5Y cells were obtained from the American Type Culture Collection (Manassas, Virginia, US), and grown following the instructions of the provider, as previously done (Solesio et al., 2012; Solesio et al., 2013; Fossati et al., 2016; Angiulli et al., 2018; Solesio et al., 2018). Specifically, we used DMEM:F12 media, supplemented with 20 units/mL penicillin-streptomycin and 10% (v/v) heat-inactivated fetal bovine serum (FBS). Cells were grown in a humidified cell culture incubator, under a 5% CO_2 atmosphere at 37°C until around 80% optimal confluence was reached, as previously reported (Solesio et al., 2012; Solesio et al., 2013). MitoPPX cells were generated adapting the protocol from (Solesio et al., 2020) to SH-SY5Y neuroblastoma cells. 50,0000 cells were plated in 6-well plate. 24 h later, the cells were transiently transfected using lipofectamine and a DNA construct containing the sequence for the mammalian expression of a mitochondrial targeting sequence (MTS), green fluorescent (eGFP) protein, and PPX (Solesio et al., 2020). After 24 h, 0.5 mg/mL of geneticin (the selection antibody) were added to the cells for 2 weeks. Subsequently, individual clones were selected, transferred into a 96-well plate and amplified. MitoPPX cells were grown and maintained in the presence of geneticin to assure the expression of the construct.

2.3 PPX Enzymatic Assay

The binding between polyP-DAPI shifts the wavelength of emission of DAPI up to 550 nm (Aschar-Sobbi et al., 2008). Therefore, this is a widely used method to assay the presence of polyP in various organisms, including mammalian cells (Abramov et al., 2007; Aschar-Sobbi et al., 2008). Using this principle, the enzymatic activity of MitoPPX cells was assayed following the protocol previously published in (Solesio et al., 2021).

2.4 Protein Extraction and Quantification

Cells were plated and grown to 90% confluency. Afterwards, cells were scrapped on ice-cold PBS 1x, and centrifuged at 1,000 rpm for 5 min at 4°C. Pellets were re-suspended in lysis buffer (300 mM NaCl, 50 mM Tris-HCl pH 7.5, 1% TritonX-100) and shaken for 15 min at 4°C. Cell suspensions were centrifuged at 13,000 rpm for 5 min at 4°C, and supernatants were directly frozen at–80°C. Protein content was measured through the bicinchoninic acid colorimetric (BCA) assay following manufacturer's instructions. Aliquots of the samples were prepared and stored at -80°C for further Western Blotting validation.

2.5 Western Blotting

Western Blotting analyses were conducted as previously published (Baltanas et al., 2013; Liu et al., 2019; Castro et al., 2020; Khong et al., 2020). 20 μg of protein per sample was separated using 12% Mini-Protean TGX Precast Gel, and transferred into PVDF membranes. Non-specific protein binding was blocked using 5% fat-free milk and 0.1% Tween-20 in PBS 1x for 1 h. Membranes were then hybridized with the specific primary antibodies overnight at 4°C (PPX 45 kDa; eGFP 25 kDa; CV-ATP5A 54 kDa; CIII-UQCRC2 48 kDa; CII-SDHB 29 kDa; CIV-COXII 22 kDa; CI-NDUFB8 18 kDa; all of them at 1:1,000 dilution). The levels of protein expression were normalized using β-actin content (47 kDa; 1:1000). The signal was detected using Piece ECL Substrate kit following manufacturer's instructions and the Gel Doc XR Image System from BioRad (Hercules, California, US). Finally, the intensity of the signal was quantified by densitometry analysis using ImageJ software from NIH (Bethesda, Maryland, US).

2.6 Proteomics Assay

Wt and MitoPPX cells were scraped, washed with cold PBS, and immediately preserved at–80°C (five replicates, collected on two independent days). Cells were shipped overnight on dry ice for further protein profiling at the Department of Genome Science of University of Washington (Seattle, Washington, United States).

2.6.1 Protein Lysis and Digestion

Cell pellets were resuspended in 100 μL of 5% SDS, 50 mM Triethylammonium bicarbonate (TEAB), 2 mM $MgCl_2$, and 1x Pierce Halt protease and phosphatase inhibitor cocktail, vortexed and briefly probe sonicated. Protein concentration was measured with a BCA assay. Homogenate of 50 ug was added to a process control of 800 ng of yeast enolase protein, which was then reduced with 20 mM DTT, and alklyated with 40 mM of IAA. Lysates were then prepared for S-trap column (Protifi, Long Island, New York, US), binding by the addition of 1.2% phosphoric acid and 350 μL of binding buffer (90% methanol, 100 mM TEAB). The acidified lysate was bound to the column incrementally, followed by three wash steps with binding buffer to remove SDS, three wash steps with 50:50 methanol:chloroform to remove lipids, and a final wash step with binding buffer. Trypsin (1:10) in 50 mM TEAB was then added to the S-trap column for digestion at 47°C for 1 h. Hydrophilic peptides were then eluted with 50 mM TEAB and hydrophobic peptides were eluted with a solution of 50% acetonitrile in 0.2% formic acid. The elute was pooled, speed vacuumed and resuspended in 0.1% formic acid. A heavy labeled Peptide Retention Time Calibrant (PRTC) mixture

(Pierce, Waltham, Massachusetts, US) was added to each sample.

2.6.2 Proteomic Profiling by LC-MS

One μg of each sample with 150 femtomole of PRTC were loaded onto a 30 cm fused silica picofrit (New Objective, Littleton, Massachusetts, US) 75 μm column and 3.5 cm 150 μm fused silica Kasil1 (PQ Corporation, Malvern, Pennsylvania, US) frit trap loaded with 3 μm Reprosil-Pur C18 (Dr. Maisch, Ammerbuch, Entringen, Germany) reverse-phase resin analyzed with a Thermo Easy nano-LC 1200. The PRTC mixture was used to assess quality of the columns before and during analysis. Four of these quality control runs were analyzed prior to any sample analysis and then after every six to eight sample runs, another quality control run was analyzed.

Buffer A was 0.1% formic acid in water and Buffer B was 0.1% formic acid in 80% acetonitrile. The 40-min QC gradient consists of a 0–16% B in 5 min, 16–35% B in 20 min, 35–75% B in 1 min, 75–100% B in 5 min, followed by a wash of 9 min and a 30 min column equilibration. The 110 min sample LC gradient consists of a 2–7% for 1 min, 7–14% B in 35 min, 14–40% B in 55 min, 40–60% B in 5 min, 60–98% B in 5 min, followed by a 9-min wash and a 30-min column equilibration. Peptides were eluted from the column with a 50°C heated source (CorSolutions, Ithaca, New York, US) and electrosprayed into a Thermo Orbitrap Fusion Lumos Mass Spectrometer with the application of a distal 3 kV spray voltage. For the quality control analysis, a cycle of one 120,000 resolution full-scan mass spectrum (350–2000 *m/z*) followed by data-independent MS/MS spectra on the loop count of 76 data-independent MS/MS spectra using an inclusion list at 15,000 resolution, AGC target of 4e5, 20 s maximum injection time, 33% normalized collision energy with a 8 *m/z* isolation window. For the sample digestion, first a chromatogram library of six independent injections is analyzed from a pool of all samples within a batch. For each injection, a cycle of one 120,000 resolution full-scan mass spectrum with a mass range of 100 *m/z* (400–500 *m/z*, 500–600 *m/z* … 900–1,000 *m/z*) followed by data-independent MS/MS spectra on the loop count of 26 at 30,000 resolution, AGC target of 4e5, 60 s maximum injection time, 33% normalized collision energy with a 4 *m/z* overlapping isolation window. The chromatogram library data generated from a pooled samples was used to detect proteins from individual quantitative sample runs. These individual runs consist of a cycle of one 120,000 resolution full-scan mass spectrum with a mass range of 350–2000 *m/z*, AGC target of 4e5, 100 m maximum injection time followed by data-independent MS/MS spectra on the loop count of 76 at 15,000 resolution, AGC target of 4e5, 20 s maximum injection time, 33% normalized collision energy with an overlapping 8 *m/z* isolation window. Application of the mass spectrometer and LC solvent gradients are controlled by the ThermoFisher XCalibur data system (Waltham, Massachusetts, US).

2.6.3 Proteomics Data Analysis

Thermo RAW files were converted into mzML format using Proteowizard (version 3.0.20064; Palo Alto, CA, US) using vendor peak picking and demultiplexing (Amodei et al., 2019). Chromatogram libraries were created by analyzing the six narrow window gas phase fractionated runs on the pool sample using default settings (10 ppm tolerances, trypsin digestion, HCD b- and y-ions) of EncyclopeDIA (version 0.9.5) using a Prosit predicted spectra library (Gessulat et al., 2019) based on Uniprot human canonical FASTA background (april 2019) as described previously (Pino et al., 2020). Prosit library was created using the settings one missed cleavage, 33% Normalized Collison Energy (NCE), charge states of 2 and 3, m/z range of 396.4–1,002.7, and a default charge state of 3. The resulting chromatogram library empirically corrected the on-column chromatographic retention times and the product ion intensities and only included peptides detected in the pooled sample (Pino et al., 2020).

The individual quantitative analyses were analyzed using EncyclopeDIA with the Chromatogram library generated from the narrow window gas phase fractionated data. EncyclopeDIA was set to require a minimum of three quantitative ions and filtering peptides at a 1% False Discovery Rate (FDR) using Percolator 3.01 (Kall et al., 2008). The output of the EncyclopeDIA Quant Report was imported into Skyline (version 20.1.9.234; Fairfield, Ohio, US) with the human uniprot FASTA as the background proteome to map peptides to proteins. We used a library of predicted spectra and retention times. In Skyline, data was normalized to the total ion current (TIC) and unique peptides were summed to protein TAF (total area fragment) quantities. If a peptide mapped to more than one protein, Skyline selected the first protein on the list. A csv file of unique protein TAFs for each replicate was exported. The Skyline documents and raw files for DIA library generation and DIA sample analyses are available at Panorama Public (ProteomeXchange ID: PXD028185; access URL: https://panoramaweb.org/MitoPPX.url)

2.7 Metabolomics Assay

2.7.1 Sample Preparation

Cells were prepared as for the proteomics assay (five replicates, collected on two independent days), and shipped over night on dry ice for metabolite profiling at the University of Washington's Northwest Metabolomics Research Center (Seattle, Washington, US).

Aqueous metabolites were extracted using a protein precipitation method (Mathon et al., 2019). Cell samples were first homogenized in 200 μL purified deionized water at 4°C, and then 800 μL of methanol containing $^{13}C_6$-glucose and $^{13}C_2$-glutamate (reference internal standards used to monitor sample preparation) were added. Afterwards samples were vortexed, stored for 30 min at–20°C, sonicated in an ice bath for 10 min, centrifuged for 15 min at 14,000 rpm and 4°C, and then 600 μL of supernatant was collected from each sample. Lastly, recovered supernatants were dried on an Eppendorf Vacufuge (Brinkmann Instruments, Westbury, NY, US) and reconstituted in 1 ml of LC-matching solvent containing $^{13}C_2$-tyrosine and $^{13}C_3$-lactate (reference internal standards used to monitor instrument performance). Protein pellets that were left

over from the sample preparation were used for BCA protein assay.

2.7.2 Metabolite Profiling by LC-MS

Targeted LC-MS metabolite analysis was performed on a duplex-LC-MS system composed of two Shimadzu Nexera XR LC-20AD pumps, CTC Analytics PAL HTC-xt temperature-controlled auto-sampler (Shimadzu, Kyoto, Japan) and AB Sciex 6,500 + Triple Quadrupole MS equipped with ESI ionization source (AB Sciex, Framingham, MA, US) (Meador et al., 2020). UPLC pumps were connected to the auto-sampler in parallel to allow two independent chromatography separations: while one column performed separation and MS data acquisition in ESI + ionization mode, the other column was equilibrated for sample injection, chromatographic separation and MS data acquisition in ESI- mode. Samples were injected on two identical Waters XBridge BEH Amide XP analytical columns (-2.5 μm, 130 Å, 2.1 × 150 mm) (Waters Corporation, Milford, MA, US). Each chromatography separation was 18 min (total analysis time per sample was 36 min). MS data acquisition was performed in multiple-reaction-monitoring (MRM) mode. LC-MS system was controlled using AB Sciex Analyst 1.6.3 software (AB Sciex, Framingham, MA, US).

2.7.3 Metabolomics Data Analysis

Measured MS peaks were integrated using AB Sciex MultiQuant 3.0.3 software. The LC-MS assay targeted 363 metabolites (plus four spiked reference internal standards). In addition to the study samples, two sets of quality control (QC) samples were used to monitor the assay performance as well as data reproducibility. One QC [QC(I)] was a pooled human serum sample used to monitor system performance over extended time and the other QC [QC(S)] was a pooled study sample, which was used to monitor data reproducibility. Each QC sample was injected per every 10-study samples. The data were well reproducible with a median CV of 5.86%.

2.8 Statistical Analysis

For the proteomics data, we used TIC-normalized protein TAF quantities for the downstream analysis. Data were run in two batches. There were 5,847 proteins detected in run batch1 and 5,600 proteins detected in run batch2. We included 4,232 proteins with <20% missingness in both batches for the imputation. We used a quantile regression approach for the imputation of left-censored missing data (QRILC), which has been suggested as the favored imputation method for left-censored Missing Not At Random (MNAR) data (Wei et al., 2018). This was implemented in the R imputeLCMD package. We fitted a linear model to the protein level data to detect the genotype group differences while adjusting for run batch and sample collection day in the model using the Bioconductor limma package (Ritchie et al., 2015). The limma package uses empirical Bayes moderated statistics, which improves power by 'borrowing strength' between proteins in order to moderate the residual variance (Smyth, 2004).

For the targeted metabolomics assay, we performed a median normalization where we adjusted the data, so all samples have the same median value of the metabolite abundance post $\log_2$ transformation. Only metabolites with <20% missingness and a coefficient of variation (CV) < 20% in the pooled sample QC data were included in further analyses. Out of the possible 363 metabolites that the assay could detect, 151 metabolites passed these filtering criteria, which were included in the imputation step. We used the same imputation method as described above for the proteomics data. We fit a linear model to the imputed data to detect the genotype group differences while adjusting for collection day and protein amount in the model using the Bioconductor limma package.

For the unsupervised learning, the batch effects (run batch and sample collection day) and covariates (protein amount) were removed using the limma removeBatchEffect function prior to the PCA (principal component analysis) and clustering analysis. We used MetaboAnalyst (v 5.0) to perform univariate methods (*t*-test), multivariate analysis (PCA) and hierarchical clustering (Euclidean distance and Ward's linkage) (Pang et al., 2021). Statistical analysis and graphical representation of the data were conducted using GraphPad (San Diego, California, US), and Origins Lab (Northampton, Massachusetts, US) software.

2.9 Pathway Analysis

Ingenuity Pathway Analysis (IPA, Ingenuity Systems, Redwood City, California, US), was used to analyze the proteomics and metabolomics data for canonical pathways, upstream regulators, and disease and function analysis using the list of differentially expressed proteins ($\log_2$FC cutoff of 1.5 and FDR<0.001) and metabolites (FDR<0.05). Protein and metabolite symbols were used as identifiers. All molecules were overlaid onto a global molecular network contained in the Ingenuity Knowledge base. Networks of network-eligible molecules were algorithmically generated based on their connectivity. The functional analyses identified the canonical pathways, upstream regulators and biological functions and diseases that were most significant to the data set. A right-tailed Fisher's exact test was used to calculate the raw *p*-values. The z-score was used to predict the activation or inhibition state of the molecules in our datasets. Canonical pathways, upstream regulators and biological functions and diseases which were likely activated (based on the pattern of differentially abundant proteins or metabolites) were presented in orange (positive z-score), those that were likely inhibited were presented in blue (negative z-score), and those with a z-score which is zero (or close to zero) or ineligible for prediction were presented in white or grey, respectively (NaN z-score).

3 RESULTS

3.1 SH-SY5Y Cells Overexpressing the PPX Enzyme in Mitochondria Showed Decreased Levels of polyP and Affected ETC

SH-SY5Y MitoPPX cells successfully expressed eGFP and the PPX enzyme, while these proteins were not observed in the Wt samples (**Figure 1A**). In addition, the activity of the PPX

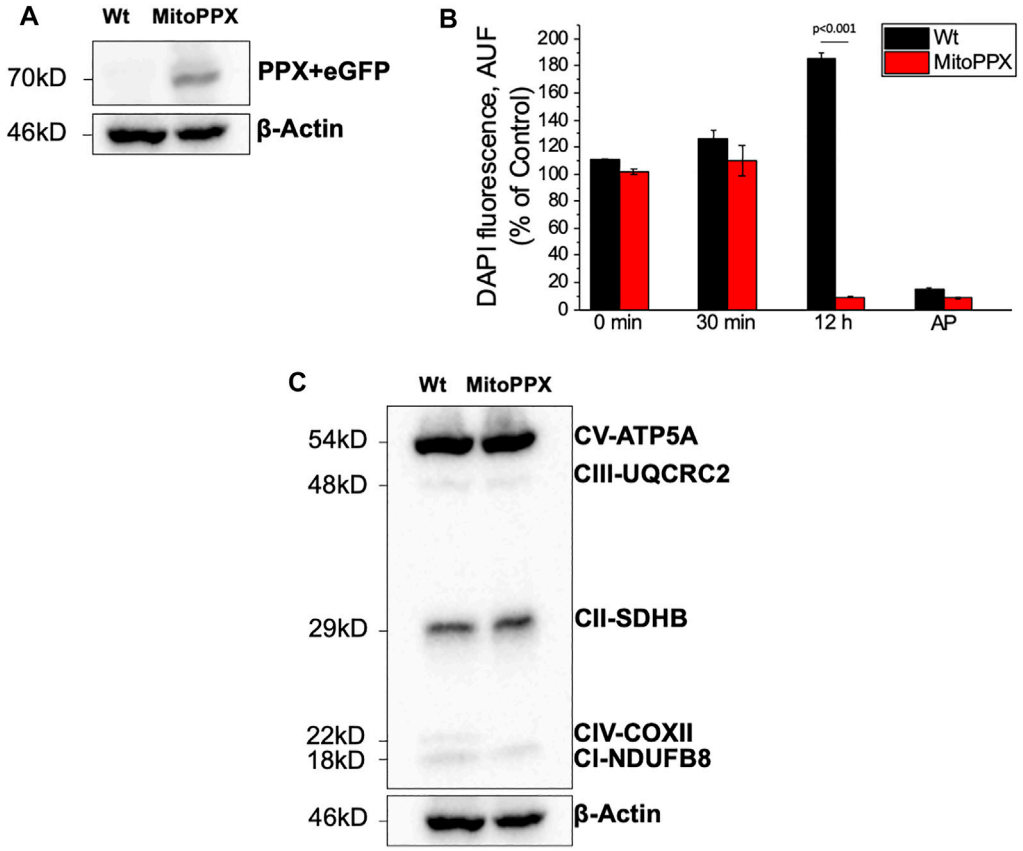

FIGURE 1 | SH-SY5Y neuroblastoma cells overexpressing exopolyphosphatase (PPX) enzyme. **(A)** Western Blotting confirming the expression of PPX (70 kDa together with eGFP protein) in the MitoPPX cells. PPX antibody was used to conduct this experiment. However, the molecular weight shown is the combined molecular weight of PPX and GFP, as the GFP protein is expressed jointly with PPX. **(B)** Enzymatic assay demonstrating the activity of the PPX enzyme in our MitoPPX SH-SY5Y samples. After 12 h of treatment with exogenous polyP, the levels of the polymer were decreased in MitoPPX cells, compared to Wt ($p < .001$). These decreased levels were comparable to the levels seen in the positive control, which was conducted with alkaline phosphatase (AP), an enzyme known to degrade polyP (Lorenz and Schroder, 2001). Results are expressed as mean ± SEM of three experiments. *t*-test was used to seek for statistical analysis between groups. **(C)** Western Blotting that shows the expression of different subunits of the ETC complexes in SH-SY5Y Wt and MitoPPX samples that were shipped for metabolomics and proteomics assays ($n = 1$).

enzyme was assayed through the measurement of the cellular levels of exogenous polyP, using DAPI fluorescence as previously described (Aschar-Sobbi et al., 2008; Solesio and Pavlov, 2016). A significant decrease of cellular polyP was observed in MitoPPX cells after 12 h of incubation with exogenous polyP, when compared with Wt (**Figure 1B**). This indicated the functional activity of the overexpressed PPX enzyme in MitoPPX cells.

The expression of some subunits of the ETC complexes was assayed using Western Blotting in our Wt and MitoPPX SH-SY5Y cells. Decreased protein expression of NDUFB8-complex I and COXII- complex IV subunits were observed in MitoPPX cells, compared to Wt. These results will be confirmed by our data obtained from the proteomics and metabolomics assays, and they show the important role of polyP in the regulation of the function of the ETC (**Figure 1C**. Different exposure times of the membrane are included in **Supplementary Figure S1**).

3.2 Pathway Analysis of Proteomics and Metabolomics Data Show Significant Changes in MitoPPX SH-SY5Y Cells, Compared With Wt Cells, Including Differences in Bioenergetics

The global effects of the enzymatic depletion of mitochondrial polyP were investigated through the IPA software. We focused our studies especially on the pathways that relate to mitochondrial metabolism. Each dataset was analyzed separately and later integrated via meta-analysis. A complete summary of each IPA analysis (Proteomics, Metabolomics and Meta-analysis) can be accessed in the **Supplementary Material S1**.

3.2 1 Differential Protein Expression

Proteomics analysis led to the annotation of 4,232 proteins with less than 20% missingness in all samples. Out of 4,214 mapped

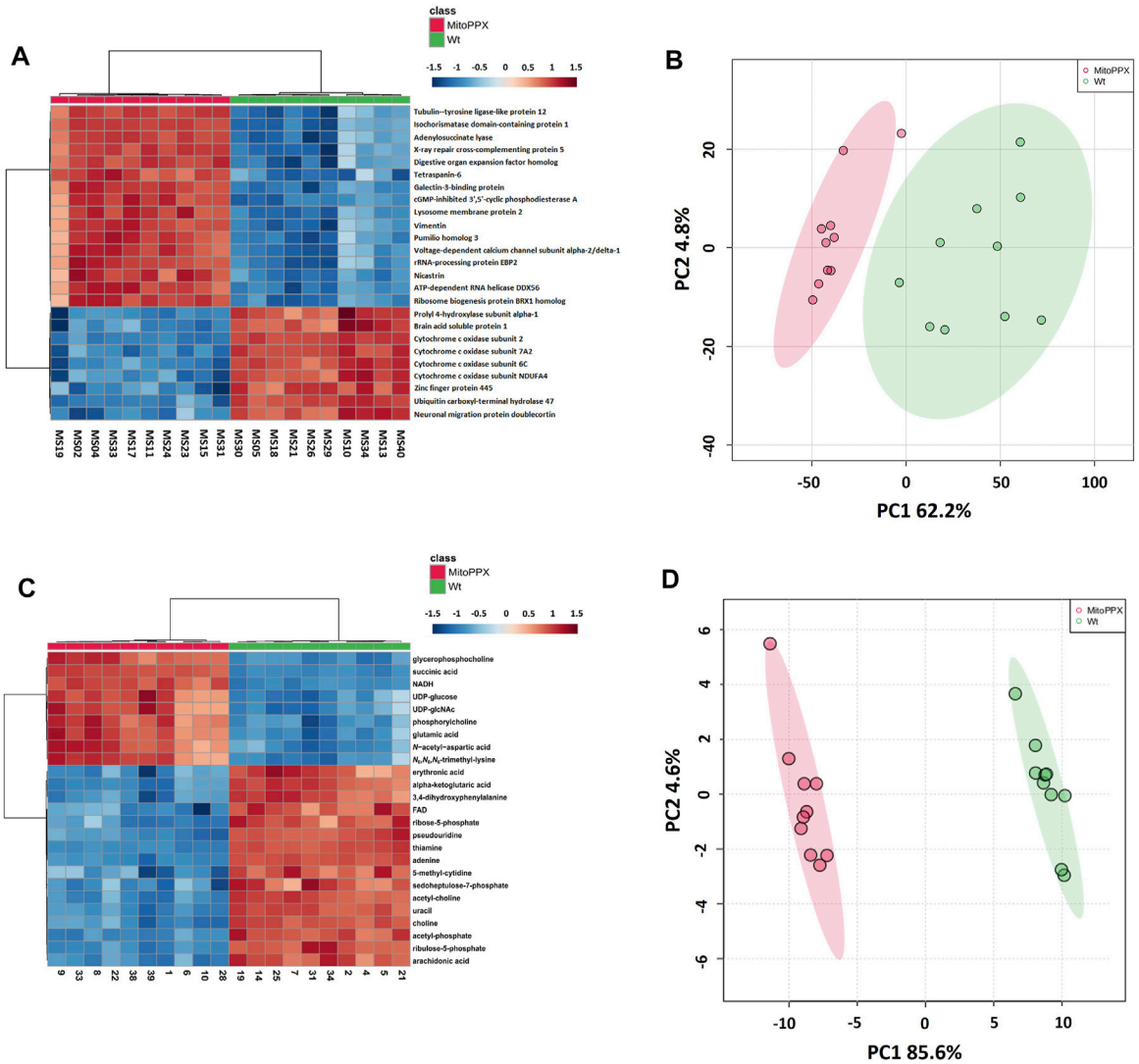

FIGURE 2 | Heat maps and principal component analysis (PCA) showed that SH-SY5Y Wt and MitoPPX have different proteomics and metabolomics profiles. Heat maps identified the top 25 most significantly expressed proteins (*t*-test *p*-value<.05) **(A)** and metabolites (*t*-test *p*-value<.05) **(C)** detected in MitoPPX cells with respect to Wt cells, some of them related to the status of mitochondrial physiology. Red colors depict proteins or metabolites that were upregulated in the MitoPPX cells and blue colors depict those downregulated in the same samples. PCA identified clear separation between groups for both proteomics **(B)** and metabolomics **(D)** datasets. Shaded areas depict regions with at least 95% confidence.

proteins in IPA, we identified 405 differentially expressed proteins in MitoPPX cells compared to Wt (log2FC < 1.5 and FDR<0.001), of which 386 were upregulated, whereas 19 were downregulated. The top 25 most significantly expressed proteins with a *t*-test *p*-value<0.05 were depicted in a heat map (**Figure 2A**). PCA demonstrated a clear discrimination between the two groups (in red MitoPPX cells and in green Wt cells; **Figure 2B**).

3.2.2 Differential Metabolite Abundance

Out of 363 metabolites, the metabolomics profiling in IPA resulted in the detection of 151 metabolites with less than 20% missingness in all samples, and 80 abundant metabolites were significantly different in MitoPPX compared to Wt (FDR<0.05), of which 52 were upregulated and 36 were downregulated. The top 25 most significant metabolites (*t*-test *p*-value<0.05) were shown in a heat map (**Figure 2C**). PCA showed two clear populations (in red MitoPPX cells and in green Wt cells; **Figure 2D**).

3.2.3 Identification of Canonical Pathways

The most significant dysregulated pathways in the proteomics analysis included assembly of RNA polymerase II complex (raw *p*-value<.001), androgen signaling (raw *p*-value<.001),

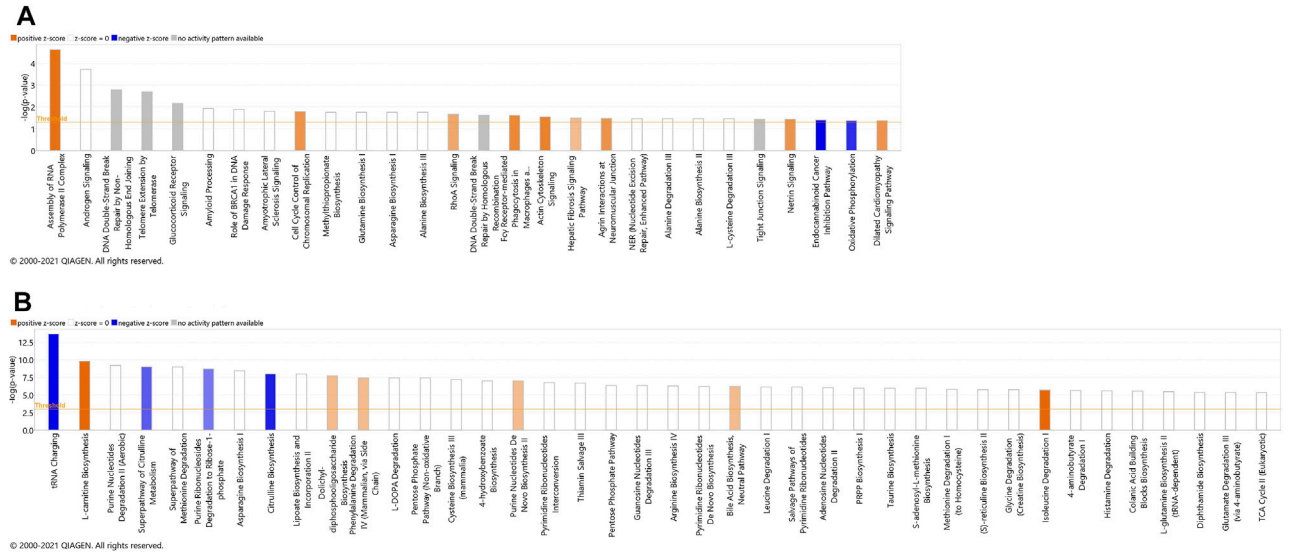

FIGURE 3 | Canonical pathways identified using IPA analysis, based on proteins **(A)** and metabolites **(B)** that were identified using label-free quantification proteomics ($log_2FC \geq 1.5$ and FDR<0.05) and metabolomics (FDR<0.05). The bars represent the significance of the canonical pathway as calculated by a right-sided Fisher's exact test (threshold is showing raw *p*-value<.05 for proteomics and raw *p*-value<.001 for metabolomics). Therefore, the tallest bars represent the canonical pathways that are the least likely to have been identified due to molecules being in the canonical pathway by random chance. Canonical pathways which are likely activated (based on the pattern of differentially abundant proteins or metabolites) are presented in orange (positive z-score) and pathways that are likely inhibited are presented in blue (negative z-score).

TABLE 1 | List of the five altered proteins of the OXPHOS pathway in MitoPPX cells compared to Wt, identified by IPA software. ETC components showed significant differences in their expression levels ($log_2FC < 0$ means decreased expression and $log_2FC > 0$ means increased expression) in MitoPPX cells, compared to Wt. Alterations in these proteins allowed the IPA software to predict a decrease in the OXPHOS system. The 'Expected' column indicates the state that protein is predicted to have if the pathway were activated. FDR: False Discovery Rate.

Symbol	Gene Name	UniProt	Log_2FC	FDR	Expected
COX6C	Cytochrome c oxidase subunit 6C	P09669	−2.67	2.40E-21	Up
COX7A2	Cytochrome c oxidase subunit 7A2	P14406	−2.31	1.89E-21	Up
COX7C	Cytochrome c oxidase subunit 7C	P15954	−1.54	2.78E-07	Up
NDUFA4	NDUFA4 mitochondrial complex associated	O00483	−2.00	3.82E-17	Up
SDHC	Succinate dehydrogenase complex subunit C	Q99643	2.61	3.38E-06	Up

DNA double-strand break repair by non-homologous end joining (raw *p*-value<.01), telomere extension by telomerase (raw *p*-value < .01), glucocorticoid receptor signaling (raw *p*-value<.01), and amyloid processing (raw *p*-value<.05) (**Figure 3A**). In the metabolomics analysis, the most significant dysregulated pathways comprised tRNA changing, L-carnitine biosynthesis, purine nucleotides degradation II–aerobic, super pathway of citrulline metabolism, and super pathway of methionine degradation (all of them raw *p*-value<0.001) (**Figure 3B**).

Both proteomics and metabolomics analyses showed the differential expression of the OXPHOS pathway in MitoPPX cells, compared to Wt samples (raw *p*-value<.05 and <.001, respectively). Proteomics data indicated that the variation in OXPHOS occurred at different subunits of the ETC complexes (**Table 1** and **Figure 4A**) which was accompanied by alterations in the abundance of ATP, ADP, NADH and NAD + metabolites, all of them directly involved in OXPHOS (**Table 2**; **Figure 4B**). These results were supported by IPA prediction of decreased OXPHOS activity in the MitoPPX cells, when compared to Wt, proposed in both proteomics (negative z-score = -1.34; **Figure 3A**) and metabolomics datasets (negative z-score = -1). The dysregulation of the tricarboxylic acid (TCA) cycle observed in the metabolomics data (**Figure 3B**), with increased succinate and decreased oxoglutarate, also suggested a global effect of polyP depletion on mitochondrial function and energetic metabolism (**Figure 4C**).

3.2.4 Analysis of Upstream Regulators

We performed upstream regulator analysis (URA) in IPA software to explore the potential upstream regulators of the protein and metabolite regulatory networks affected by changes in gene expression.

From 308 predicted upstream regulators of different molecule types identified in the proteomics analysis, only 11 were further considered based on FDR<0.05 (**Table 3** and **Supplementary**

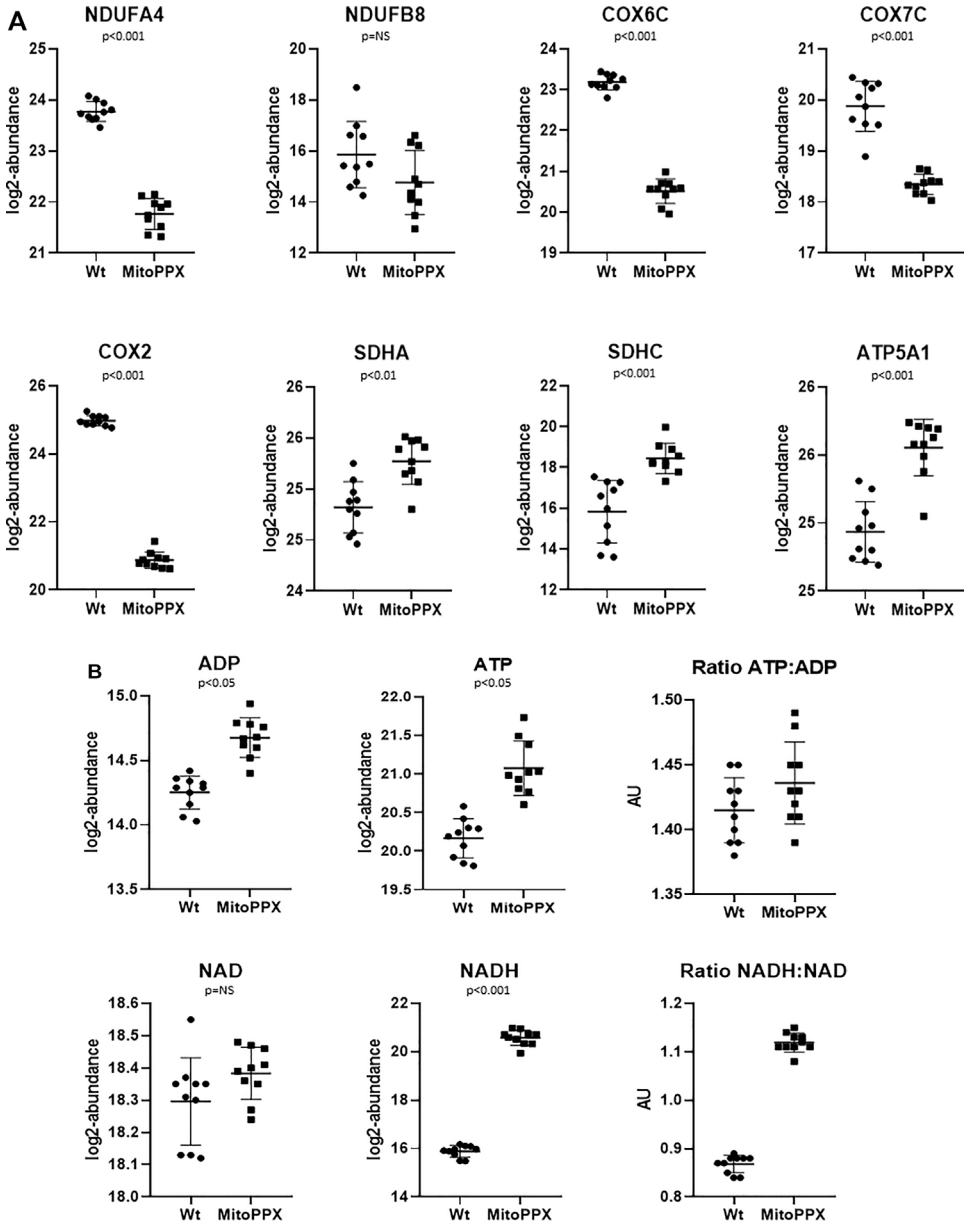

FIGURE 4 | SH-SY5Y MitoPPX cells showed alterations in OXPHOS and in TCA. **(A)** Proteomics data showed decreased and increased protein expression of distinct subunits of the ETC complexes in MitoPPX cells compared to Wt. **(B)** Metabolomics data showed increased presence of different metabolites involved in mitochondrial metabolism in MitoPPX cells compared to Wt. **(C)** Metabolomics data showed alterations in the levels of succinate and 2-oxoglutarate metabolites in MitoPPX cells as well as in the levels of ATP and NADH metabolites lead to a dysfunction of TCA. Ten biological samples (five replicates, collected on two independent days) were used for each experiment. All results were expressed as mean ± SD and a right-tailed Fisher's exact test was used to calculate the raw *p*-values.

Material S1). The transcriptional regulator KDM5A (lysine-specific demethylase 5A), a histone demethylase, was increased in MitoPPX cells within our data set, compared to Wt (log_2FC = 0.203) and appears as one of the predicted upstream regulators (negative z-score = -0.632, FDR<0.05) of ten proteins, three of them being dysregulated subunits of the ETC complexes in MitoPPX cells: COX7A2-complex IV, NDUFA4-complex I, and SDHC-complex I (**Figure 5A**). In addition, KDM5A was a predicted upstream regulator of two other mitochondrial proteins: Txn2, a mitochondrial-specific thioredoxin, and Misato 1 (Msto 1), which is a cytosolic protein, involved in the regulation of mitochondrial distribution, morphology, fusion, and network formation (Kimura and Okano, 2007; Gal et al., 2017; Nasca et al., 2017) (**Figure 5A**).

The metabolomics analysis resulted in 1,013 upstream regulators, with 69 FDR<0.001 (**Supplementary Material**

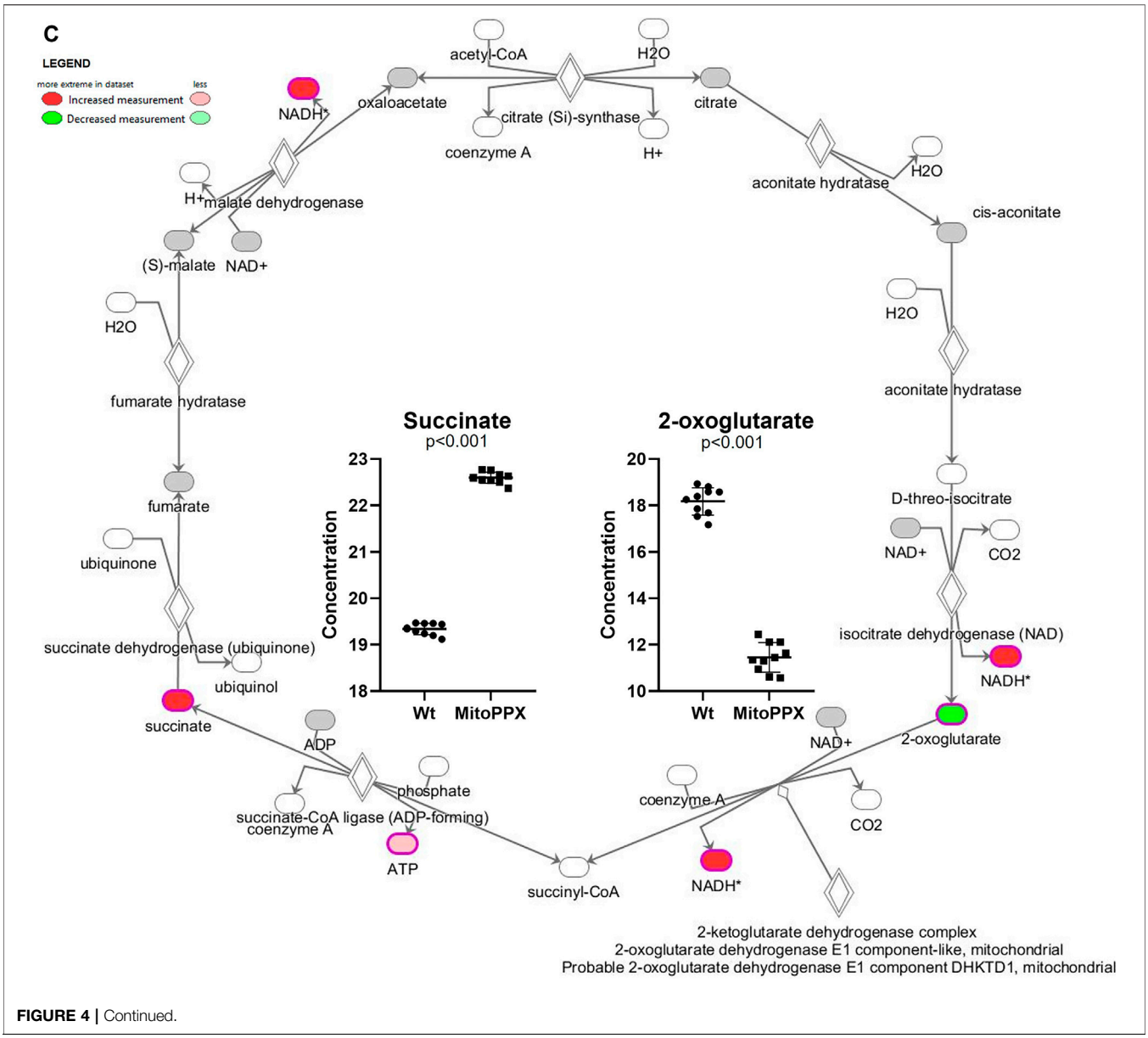

FIGURE 4 | Continued.

TABLE 2 | List of the four altered metabolites involved in the OXPHOS pathway in MitoPPX cells compared to Wt, identified by IPA software. Metabolites which were significantly different ($log_2FC < 0$ means decreased expression and $log_2FC > 0$ means increased expression) in MitoPPX cells compared to Wt. Alterations in these metabolites allowed the IPA software to predict a decrease in the OXPHOS system. The 'Expected' column indicates the state that protein is predicted to be in if the pathway were activated. FDR: False Discovery Rate.

Symbol	Human Metabolome Database (HMDB)	Log_2FC	FDR	Expected
Adenine-riboflavin dinucleotide	HMDB01248	−1.13	7.78E-05	Up
ATP	HMDB00538	0.91	2.69E-02	Up
NADH	HMDB01487	4.70	8.55E-06	Down
Succinic acid	HMDB00254	3.26	5.61E-13	Down

S1). Creatine, an endogenous compound in neuronal cells which is also involved in bioenergetics, was decreased in MitoPPX cells within our data set, compared to Wt (log_2FC = -0.019). This metabolite was predicted to be an upstream regulator of seven metabolites (positive z-score = 2.383), including phosphocreatine, AMP and ATP

TABLE 3 | Analysis of upstream regulators generated from protein changes between MitoPPX and Wt cells identified using IPA software. The 11 predicted upstream regulators with an FDR set at 0.05 are listed below. The activation z-score can be used to infer likely activation states of the upstream regulators based on the direction of protein abundance change in the dataset, i.e. a negative activation z score indicates that the upstream regulator is downregulated in MitoPPX cells compared to Wt. NP indicates no prediction of activation status was generated by the IPA software.

Upstream Regulator	Activation z-score	FDR	Target molecules in dataset
APBB1	0.762	5.97E-03	ACTA2, EGFR, TAGLN, TYMS, VLDLR
CST5	−2.828	5.97E-03	ADSL, AHNAK, BRIX1, EXOC3, MALSU1, MSN, PDCL3, PITRM1, PPAN, PRKACB, ACTA2, EGFR, VIM
GLIPR2	NP	1.66E-02	ACTA2, EGFR, VIM
HNF4A	0.751	1.66E-02	AAMDC, ABCF3, ACTA2, AHNAK, ARFGAP1, ARFIP2, AS3MT, ASNS, C11orf58, CCDC25
miR-382-5p (miRNAs w/seed AAGUUGU)	NP	2.37E-02	SEPTIN3, TAGLN, VIM
MIR143-145a	NP	2.37E-02	ACTA2, DES, TAGLN
KDM5A	−0.632	4.31E-02	COQ7, COX7A2, GPT2, MCAT, MSTO1, NDUFA4, PDE3A, SDHC, TOMM22, TXN2
XAV939	NP	4.31E-02	AHNAK, CSRP1, DES, DHX36, IGFBP2
TP53	1.751	4.31E-02	A2M, ACOT11, ACTA2, ALDH1B1, ASNS, ATG7, BICD2, BID, CHEK1, CNN2
MED28	NP	4.85E-02	ACTA2, CNN2, TAGLN
miR-145-5p (and other miRNAs w/seed UCCAGUU)	−1.851	4.96E-02	ACTA2, AHNAK, C11orf58, CCDC25, NDUFA4, TAGLN, UNG

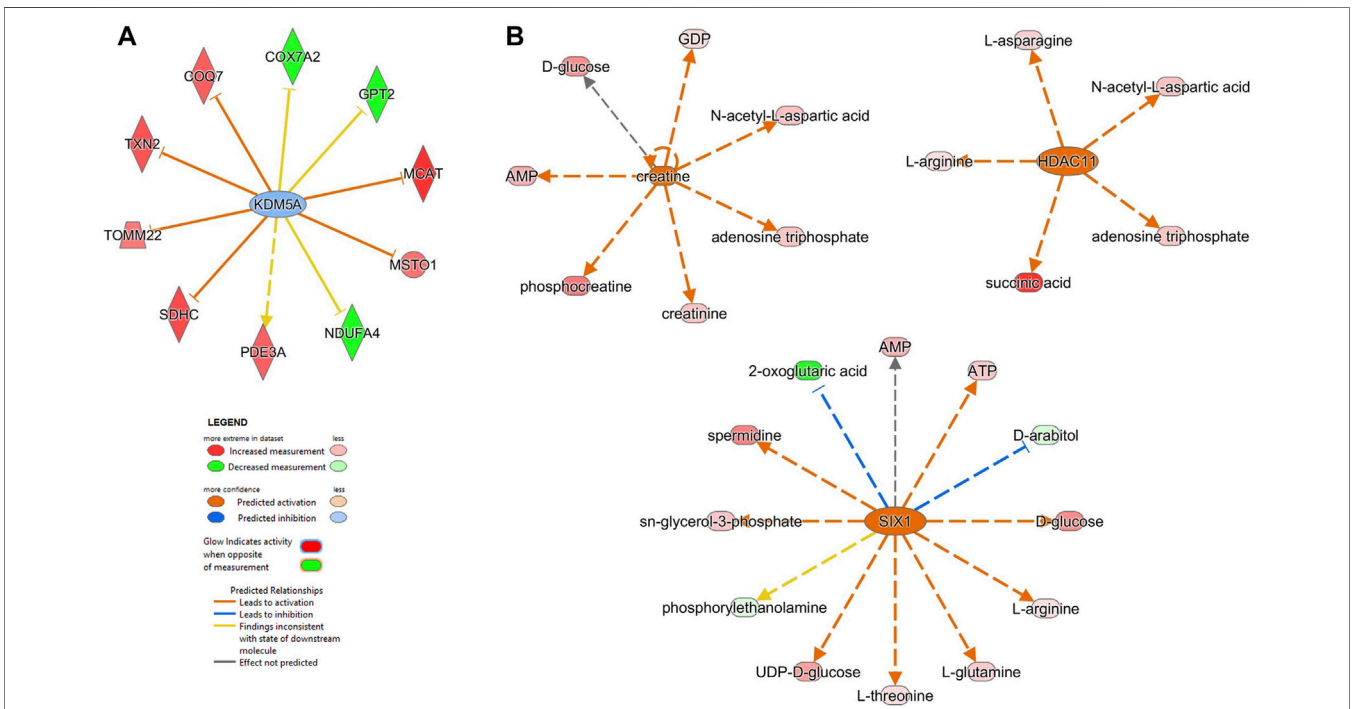

FIGURE 5 | Upstream analysis using proteomics and metabolomics datasets showed potential up-regulators mediating the effects of the enzymatic depletion of mitochondrial polyP in SH-SY5Y MitoPPX cells. **(A)** The proteomics analysis showed that KDM5A (lysine-specific demethylase 5A) is one of the first 10 upstream regulators, which is predicted to regulate different mitochondrial proteins such as COX7A2 subunit of complex IV and NDUFA4 subunit of complex I. **(B)** The metabolomics analysis identified creatine, SIX1 (homeobox protein SIX1) and HDAC 11 (histone deacetylate 11) as upstream molecules predicted to regulate different mitochondrial metabolites such as ATP, AMP, phosphocreatine, succinic acid and 2-oxoglutaric acid. This figure was prepared using IPA predictions from the same samples used for the metabolomics and proteomics assays (five replicates, collected on two independent days).

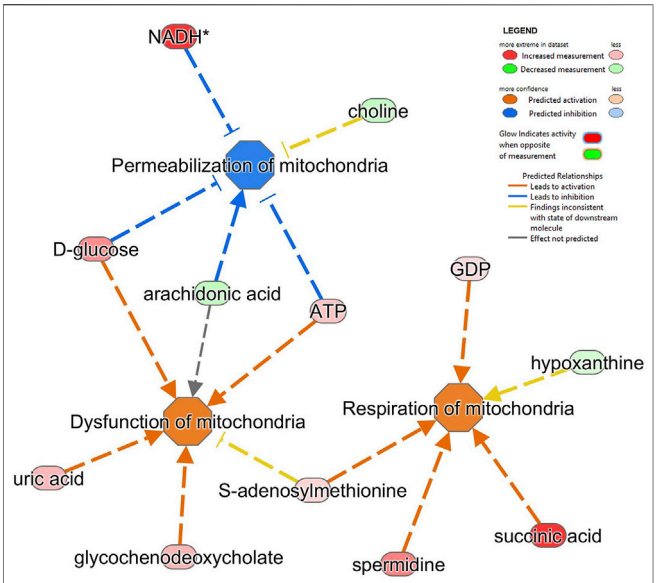

FIGURE 6 | Alterations in several metabolites identified impacts on different mitochondrial pathways in SH-SY5Y MitoPPX cells. Respiration of mitochondria, dysfunction of mitochondria and permeabilization of mitochondria (all of them FDR<0.001) were the top three significantly affected mitochondrial-related pathways shown by 'disease and function' analysis in IPA software from the metabolomics data.

(**Figure 5B**). In addition, SIX1 (Homeobox protein SIX1) and HDAC 11 (histone deacetylate 11) were predicted as upstream regulators (positive z-score = 2.714 and 2.200, respectively). SIX1 is a transcription factor predicted to lead to decreased levels of 2-oxoglutaric acid and the increase of AMP and ATP (**Figure 5B**). Also, HDAC11 is predicted to lead to increased succinate levels (**Figure 5B**).

3.2.5 Analysis of Diseases and Functions

We also applied the 'disease and function analysis' from IPA to examine the biological context of proteomics and metabolomics alterations in MitoPPX and Wt cells (**Supplementary Material S1**). In our proteomics analysis, the top five significant diseases or functions were cancer (raw *p* value range: 4.8E-29 - 5.46E-03), organismal injury and abnormalities (raw *p* value range: 4.8E-29 - 5.46E-03), endocrine system disorders (raw *p* value range: 2.98E-20 - 4.12E-03) gastrointestinal disease (raw *p* value range: 2.17E-13 - 4.78E-03); and DNA replication, recombination, and repair (raw *p* value range: 1.1E-07 - 2.56E-03). Cancer was one of the top results. In fact, the role of polyP in carcinogenesis has already been demonstrated (Wang et al., 2003; Tsutsumi et al., 2017; Arelaki et al., 2018; Kulakovskaya et al., 2018). Neurological disease is within the top ten affected 'disease and functions', showing 283 proteins involved. In our metabolomics analysis, the top five significant 'disease or functions' are cellular growth and proliferation (raw *p*-value range: 5.27E-23 - 2.74E-03), organismal development (raw *p*-value range: 5.27E-23 - 2.74E-03), inflammatory disease (raw *p*-value range: 1.02E-15 - 2.74E-03), inflammatory response (raw *p*-value range: 1.02E-15 - 2.74E-03), organismal injury and abnormalities (raw *p*-value range: 1.02E-15 - 2.74E-03). Within all the detected 'disease and function', ten of them were related to mitochondria and affected in neurodegeneration. The most significant included dysfunction of mitochondria, permeabilization of mitochondria, and respiration of mitochondria (all of them FDR<0.001; **Figure 6**).

3.3 Meta-Analysis Corroborates Proteomics and Metabolomics Findings

Next, we combined the proteins and metabolites differentially expressed together into an IPA analysis. The meta-analysis of both proteomics and metabolomics assays suggested altered canonical pathways associated with abundant metabolites and proteins in MitoPPX cells (**Supplementary Material S1**). The most significant pathways found included asparagine biosynthesis I, L-carnitine biosynthesis, tRNA charging, lipoate biosynthesis and incorporation II, and purine ribonucleosides degradation to ribose-1-phosphate (all of them raw *p*-value<.001). The meta-analysis further supported the decreased OXPHOS pathway in MitoPPX cells

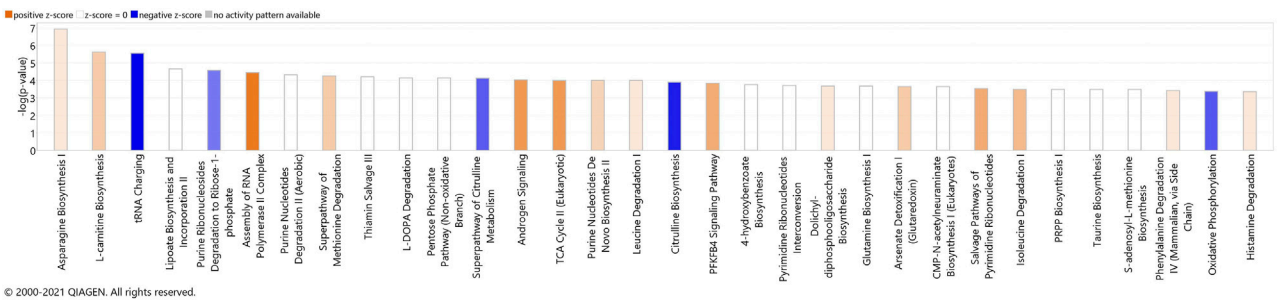

FIGURE 7 | Canonical pathways identified using IPA analysis, based on the meta-analysis. The bars represent the significance of the canonical pathway as calculated by a right-sided Fisher's exact test. Therefore, the tallest bars represent the canonical pathways that are the least likely to have been identified due to molecules being in the canonical pathway by random chance. Canonical pathways which are likely activated (based on the pattern of differentially abundant proteins or metabolites) are presented in orange (positive z-score) and pathways that are likely inhibited are presented in blue (negative z-score).

TABLE 4 | List of the proteins and metabolites found altered in the mitochondrial dysfunction pathway in MitoPPX cells compared to Wt (meta-analysis conducted by IPA software). Table shows increase ($log_2FC > 0$) or decrease ($log_2FC < 0$) of different proteins and metabolites involved in the canonical pathway of mitochondrial dysfunction in the meta-analysis. FDR: False Discovery Rate.

Symbol	Uniprot/Human Metabolome Database (HMDB)	Log2FC	FDR
Adenine-riboflavine dinucleotide	HMDB01248	−1.13	7.78E-05
ATP	HMDB00538	0.91	2.69E-02
COX6C	P09669	−2.67	2.40E-21
COX7A2	P14406	−2.31	1.89E-21
COX7C	P15954	−1.54	2.78E-07
Glutathione disulfide	HMDB03337	0.99	2.54E-03
NADH	HMDB01487	4.70	8.55E-06
NDUFA4	O00483	−2.00	3.82E-17
SDHC	Q99643	2.61	3.38E-06
TXN2	Q99757	2.45	1.76E-09

(negative z-score = -1.76, **Figure 7**), observed in both the proteomics and metabolomics study, as well as the change in TCA (positive z-score = 2.00, **Figure 7**) observed in the metabolomics analysis. In addition, the meta-analysis revealed the presence of mitochondrial dysfunction in MitoPPX cells, when compared with Wt samples (grey z-score = NaN, **Table 4**). Using the 'Molecule Activity Predictor' (MAP) option in IPA software, we predicted up- and downstream properties/activities of molecules participating in mitochondrial function (**Figure 8**). These included an increase in the glutathione levels (GSH), probably to counteract the potential increased oxidative stress in MitoPPX cells, as well as an increase of TRX2, which is a mitochondrial protein important for the control of mitochondrial ROS homeostasis, leading to an increase of NADP + levels (**Figure 8**).

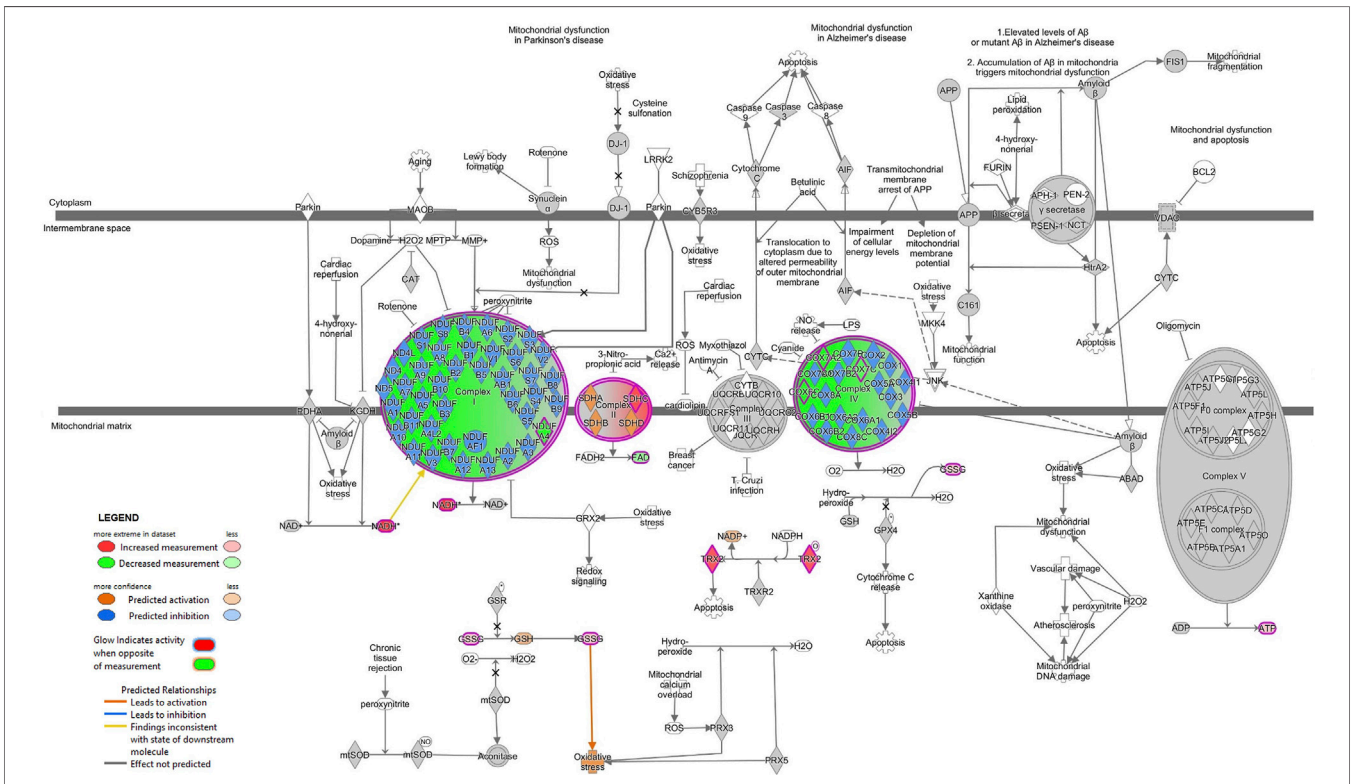

FIGURE 8 | Mitochondrial dysfunction is predicted in SH-SY5Y MitoPPX cells (meta-analysis). Predicted up- and downstream pathways of molecules participating in mitochondrial function were performed using the 'MAP' option in IPA software. The decrease of some of the subunits of ETC complex I and IV together with an increase of some of the subunits of ETC complex II lead to an unbalanced functioning of OXPHOS. The prediction states an increase in the glutathione (GSH) and NADP + levels (due to increase in GSSG and TRX2, respectively), probably as an attempt to counteract the potential oxidative stress consequence of a potential mitochondrial dysfunction.

Moreover, we identified 57 different upstream regulators with FDR set at 0.05 (**Supplementary Material S1**). The analysis distinguished 40 regulators as genes, RNAs or proteins, such as the previously mentioned SIX1 (activation z-score = 2.714, FDR<0.001) and HDAC11 (positive z-score = 2.200, FDR<0.01). Additionally, IPA predicted another upstream regulated protein, UCP1 (uncoupling protein one; positive z-score = 2.027, FDR<0.01).

Finally, the meta-analysis showed top five most significant dysregulated pathways as cancer (raw *p* value range: 1.66E-18–2.95E-03), organismal injury and abnormalities (raw *p* value range: 1.66E-18–2.95E-03), cellular growth and proliferation (raw *p* value range: 8.04E-13–2.44E-03), organismal development (raw *p* value range: 8.04E-13–2.68E-03), and endocrine system disorders (raw *p* value range: 2.77E-11–2.68E-03). In line with metabolomics data, we identified several significantly affected mitochondrial-related pathways, such as dysfunction of mitochondria, release of mitochondrial DNA, respiration of mitochondria, and activation of mitochondria (all of them FDR<0.05; **Supplementary Material S1**).

4 DISCUSSION

A wide range of mitochondrial alterations have been described in the etiopathology of various human diseases. These alterations include but are not limited to dysregulation of the ETC complexes, which will ultimately affect OXPHOS functionality, increasing ROS levels and unbalancing the cellular antioxidant system (Guzun et al., 2011; Gonzalez-Casacuberta et al., 2018; Gonzalez-Casacuberta et al., 2019). However, the exact molecular basis of the mechanism(s) underlying mitochondrial dysfunction still remain mostly unknown.

PolyP has been described as a key molecule in the cellular stress response, including the regulation of several mitochondrial functions, such as energy metabolism (including calcium homeostasis), and protein homeostasis (Gray et al., 2014; Dahl et al., 2015; Gray and Jakob, 2015; Solesio et al., 2016a; Cremers et al., 2016; Lempart and Jakob, 2019; Xie and Jakob, 2019; Solesio et al., 2020; Solesio et al., 2021). However, the exact molecular mechanism explaining the effects of polyP in the regulation of mitochondrial function are still unclear, especially under stress conditions, such as in human disease.

To our knowledge, this is the first time that a comprehensive study of the effects of polyP on the proteome and the metabolome of mammalian cells has been conducted. Specifically, in the present study, a large number of protein expression and metabolite abundance alterations were described in SH-SY5Y cells that were enzymatically depleted of mitochondrial polyP (MitoPPX). These findings highlighted the importance of polyP in maintaining the proper cellular function, either through direct or indirect regulation of all proteins and metabolites that are differentially expressed in MitoPPX cells.

The number of differentially expressed mitochondrial proteins and the different abundance of mitochondrial metabolites observed in MitoPPX cells showed the clear impact that enzymatical depletion of mitochondrial polyP has in the metabolism of the organelle. Two of the main dysregulated mitochondrial metabolic pathways identified by IPA software were OXPHOS and TCA. In our case, when we used IPA, the background was set for all proteins identified in the samples and not for the entire protein coding transcriptome (default in IPA). Specifically, ETC complex I, complex II, and complex IV showed differential protein expression of some of their subunits, leading to a potential alteration of their activity. Moreover, altered levels of succinate and oxoglutarate evidenced the dysregulation of the TCA. Indeed, the observed increased succinate ETC complex II subunits could indicate a blockage of this complex. In addition, further evidence that demonstrated that mitochondrial metabolism was affected, were increased levels of ATP, ADP, NAD, and NADH in MitoPPX cells. These findings reinforced the importance of polyP in the maintenance of mitochondrial and cellular function. One plausible mechanism explaining this differential pattern of protein and metabolites presence in MitoPPX cells could be the reduced chaperoning effects due to the lack of polyP in our model (Gray et al., 2014; Gray and Jakob, 2015; Lempart and Jakob, 2019). It is well known that the chaperoning ability of the cells is critical in the activation of the stress response. Indeed, the lack of mitochondrial polyP could promote the activation of the cellular stress response in MitoPPX cells. This explanation is supported by our proteomic analysis data, showing increased expression of some antioxidant enzymes (including several peroxiredoxins, thioredoxins, SOD1 and catalase), as well as of proteins involved in the regulation of the cellular stress response (including KEAP, Kelch-like ECH-associated protein 1). This entire cellular stress environment could further deleteriously affect mitochondrial metabolism.

The observed effects of polyP could also be at least partially mediated by the direct interaction between the polymer and the altered proteins within the OXPHOS and TCA which were identified in our analysis. In contrast to the mentioned increased expression of several antioxidant enzymes, mitochondrial SOD2 expression was decreased in MitoPPX cells, which hints at this enzyme as a potential target of polyP. Mitochondrial SOD2 is a superoxide dismutase enzyme dependent on manganese, which is known to form complexes with polyP (Gray and Jakob, 2015). This property suggests a role for polyP in the detoxification process mediated by SOD2. Although we did not show direct evidence of increased ROS levels in these MitoPPX cells, the regulatory effects of the polymer on ROS have already been demonstrated in other organisms (Gray and Jakob, 2015). As previously mentioned, our data showed that ETC complexes I and IV were affected in MitoPPX cells. Some authors have evidenced an overall alteration of oxygen consumption as a consequence of these deficiencies in the ETC, which was also demonstrated by previous work, which was conducted in HEK293 cells (Solesio et al., 2021).

Thanks to our analysis, we were able to identify several upstream regulators of these changes in IPA analysis. For example, KDM5A was identified to regulate mitochondrial proteins, confirming that the lack of polyP could be involved

in the decrease of KDM5A leading to the decrease of ETC subunits (COX7A2-complex IV and NDUFA4-complex I), and the increase of catalase and TXN2 (both participating in the antioxidant defense). KDM5A is a well-known regulator of the expression of mitochondrial proteins, especially of those involved in mitochondrial respiration (Varaljai et al., 2015). Furthermore, SIX1, a transcriptional factor described to regulate mitochondrial apoptosis (Du et al., 2017), was predicted to lead to decreased levels of 2-oxoglutaric acid and increased ATP levels. These alterations could be the potential cause underlying the TCA abnormalities observed in MitoPPX cells. Finally, creatine was identified to upregulate ATP and phosphocreatine among others. Creatine is an endogenous chemical converted into phosphocreatine, which is used to produce new ATP under certain circumstances (i.e. during high-intensity exercise) (Guzun et al., 2011). Moreover, the protective role of creatine in maintaining mitochondrial physiology is also known (Barbieri et al., 2016), and it has been demonstrated that the dietary supplementation with this molecule could improve cellular bioenergetics and mitochondrial function, therefore decreasing neuronal cell death in neurodegeneration (Adhihetty and Beal, 2008; Smith et al., 2014). In addition, IPA predicted three upregulated proteins, SIX1, UCP1, and HDAC 11, all of them involved in the upstream regulation of mitochondrial proteins and metabolites, as well as mitochondrial bioenergetics (Fedorenko et al., 2012; Kazak et al., 2015; Chowdhury et al., 2017; Yang et al., 2017; Bhaskara, 2018; Hurtado et al., 2021). In general, the 'upstream regulators' analysis hinted at a cellular compensatory response in MitoPPX cells, in which increased presence of proteins involved in cell stress response, including ATP generation, was present, when compared with the Wt samples.

This study has some limitations. We recognize that the use of geneticin exclusively in the MitoPPX cells could exert some effects on the physiology of the SH-SY5Y cells. Additionally, transfection with the MitoPPX contrast could change the amount and/or type of proteins in mitochondria. Moreover, our data was not sufficient to clarify the exact molecular mechanisms by which mitochondrial polyP was involved in the regulation of bioenergetics within the organelle and therefore, in the regulation of mitochondrial physiology. Indeed, the present proteomics ad metabolomics approaches were not focused on the investigation of these mechanisms but to obtain a snapshot of mitochondrial metabolism. Further research is needed to better understand the role of polyP within mitochondria, especially in the context of neurodegeneration. However, this proteomics and metabolomics analysis bring new insights towards elucidating the role of polyP in the regulation of mitochondrial physiology in mammalian cells. Moreover, targeting the metabolism of polyP could provide us with novel therapeutic approaches for diseases where mitochondrial dysfunction has been broadly described as an early and triggering event, such as in neurodegenerative disorders.

DATA AVAILABILITY STATEMENT

Further information and requests for resources and reagents should be directed to and will be fulfilled by the corresponding author, MS (m.solesio@rutgers.edu). Proteomics data (skyline documents and raw files for DIA library generation and DIA sample analysis) has been deposited in Panorama Public (ProteomeXchange ID: PXD028185. Access URL: https://panoramaweb.org/MitoPPX.url). The full data set from the metabolomics assay can be found at **Supplementary Information**.

AUTHOR CONTRIBUTIONS

Conceived and designed the study: MG-M, MM, DR, and MS. Collected the data: MG-M. Contributed data or analysis tools: MG-M, PU, FCN, JA, VH, ES, GM, and MP. Performed the analysis and wrote the paper: MG-M, FCN, JA, LW, MP, and MS.

FUNDING

This study was supported by the National Institutes of Health (1K99AG055701-01A1 and 4R00AG055701-03 to MS; 1S10OD021562-01 to the Northwest Metabolomics Research Center; and P30 AG013280 and P01 AG001751 to MJM), by the Start Up funds from Rutgers University to MS, by the Horserace Betting Levy Board (T15) to JA, and by the Welcome Trust Clinical Intermediate Fellowship 107471/Z/15/Z to MP.

ACKNOWLEDGMENTS

We kindly thank Dr. Toshikazu Shiba, from Kitasato University, Tokyo, Japan, for providing us with synthetic polyP, as well as Dr. Evgeny V. Pavlov, from New York University, New York City, United States for providing us with the MitoPPX construct. We also would like to thank Dr. John A. Collins, from Jefferson University, Philadelphia, United States , for connecting some of the members of this team, as well as Mitch Maleki, Esq., for editing the manuscript.

SUPPLEMENTARY MATERIAL

The Supplementary Material for this article can be found online at: https://www.frontiersin.org/articles/10.3389/fcell.2022.833127/full#supplementary-material

REFERENCES

Abramov, A. Y., Fraley, C., Diao, C. T., Winkfein, R., Colicos, M. A., Duchen, M. R., et al. (2007). Targeted Polyphosphatase Expression Alters Mitochondrial Metabolism and Inhibits Calcium-Dependent Cell Death. *Proc. Natl. Acad. Sci.* 104, 18091–18096. doi:10.1073/pnas.0708959104

Adhihetty, P. J., and Beal, M. F. (2008). Creatine and its Potential Therapeutic Value for Targeting Cellular Energy Impairment in Neurodegenerative Diseases. *Neuromol Med.* 10, 275–290. doi:10.1007/s12017-008-8053-y

Amodei, D., Egertson, J., MacLean, B. X., Johnson, R., Merrihew, G. E., Keller, A., et al. (2019). Improving Precursor Selectivity in Data-Independent Acquisition Using Overlapping Windows. *J. Am. Soc. Mass. Spectrom.* 30, 669–684. doi:10.1007/s13361-018-2122-8

Amodeo, G. F., Solesio, M. E., and Pavlov, E. V. (2017). From ATP Synthase Dimers to C-Ring Conformational Changes: Unified Model of the Mitochondrial Permeability Transition Pore. *Cel. Death Dis.* 8, 1. doi:10.1038/s41419-017-0042-3

Angelova, P. R., Iversen, K. Z., Teschemacher, A. G., Kasparov, S., Gourine, A. V., and Abramov, A. Y. (2018). Signal Transduction in Astrocytes: Localization and Release of Inorganic Polyphosphate. *Glia* 66, 2126–2136. doi:10.1002/glia.23466

Angiulli, F., Solesio, M. E., Debure, L., Cejudo, J. R., Wisniewski, T., and Fossati, S. (2018). P3-464: Carbonic Anhydrase Inhibitors Ameliorate Neurovascular Dysfunction in a Mouse Model of Cerebral Amyloid Angiopathy. *Alzheimer's Demen.* 14, P1296. doi:10.1016/j.jalz.2018.06.1828

Arelaki, S., Arampatzioglou, A., Kambas, K., Sivridis, E., Giatromanolaki, A., and Ritis, K. (2018). Mast Cells Co-Expressing CD68 and Inorganic Polyphosphate Are Linked with Colorectal Cancer. *PLoS One* 13, e0193089. doi:10.1371/journal.pone.0193089

Armstrong, J. A., Cash, N. J., Ouyang, Y., Morton, J. C., Chvanov, M., Latawiec, D., et al. (2018). Oxidative Stress Alters Mitochondrial Bioenergetics and Modifies Pancreatic Cell Death Independently of Cyclophilin D, Resulting in an Apoptosis-To-Necrosis Shift. *J. Biol. Chem.* 293, 8032–8047. doi:10.1074/jbc.RA118.003200

Aschar-Sobbi, R., Abramov, A. Y., Diao, C., Kargacin, M. E., Kargacin, G. J., French, R. J., et al. (2008). High Sensitivity, Quantitative Measurements of Polyphosphate Using a New DAPI-Based Approach. *J. Fluoresc* 18, 859–866. doi:10.1007/s10895-008-0315-4

Baltanás, A., Solesio, M. E., Zalba, G., Galindo, M. F., Fortuño, A., and Jordán, J. (2013). The Senescence-Accelerated Mouse Prone-8 (SAM-P8) Oxidative Stress Is Associated with Upregulation of Renal NADPH Oxidase System. *J. Physiol. Biochem.* 69, 927–935. doi:10.1007/s13105-013-0271-6

Barbieri, E., Guescini, M., Calcabrini, C., Vallorani, L., Diaz, A. R., Fimognari, C., et al. (2016). Creatine Prevents the Structural and Functional Damage to Mitochondria in Myogenic, Oxidatively Stressed C2C12 Cells and Restores Their Differentiation Capacity. *Oxid. Med. Cel. Longev.* 2016, 1–12. doi:10.1155/2016/5152029

Bayev, A. Y., Angelova, P. R., and Abramov, A. Y. (2020). Inorganic Polyphosphate Is Produced and Hydrolysed in F0F1-ATP Synthase of Mammalian Mitochondria. *Biochem. J.* 477 (8), 1515–1524. doi:10.1042/BCJ20200042

Bhaskara, S. (2018). Histone Deacetylase 11 as a Key Regulator of Metabolism and Obesity. *EBioMedicine* 35, 27–28. doi:10.1016/j.ebiom.2018.08.008

Borden, E. A., Furey, M., Gattone, N. J., Hambardikar, V. D., Liang, X. H., Scoma, E. R., et al. (2021). Is There a Link between Inorganic Polyphosphate (polyP), Mitochondria, and Neurodegeneration. *Pharmacol. Res.* 163, 105211. doi:10.1016/j.phrs.2020.105211

Castro, C. M., Corciulo, C., Solesio, M. E., Liang, F., Pavlov, E. V., and Cronstein, B. N. (2020). Adenosine A2A Receptor (A2AR) Stimulation Enhances Mitochondrial Metabolism and Mitigates Reactive Oxygen Species-mediated Mitochondrial Injury. *FASEB j.* 34, 5027–5045. doi:10.1096/fj.201902459R

Chowdhury, S. R., Ray, U., Chatterjee, B. P., and Roy, S. S. (2017). Targeted Apoptosis in Ovarian Cancer Cells through Mitochondrial Dysfunction in Response to Sambucus Nigra Agglutinin. *Cel. Death Dis.* 8, e2762. doi:10.1038/cddis.2017.77

Cremers, C. M., Knoefler, D., Gates, S., Martin, N., Dahl, J.-U., Lempart, J., et al. (2016). Polyphosphate: A Conserved Modifier of Amyloidogenic Processes. *Mol. Cel.* 63, 768–780. doi:10.1016/j.molcel.2016.07.016

Dahl, J.-U., Gray, M. J., and Jakob, U. (2015). Protein Quality Control under Oxidative Stress Conditions. *J. Mol. Biol.* 427, 1549–1563. doi:10.1016/j.jmb.2015.02.014

Du, P., Zhao, J., Wang, J., Liu, Y., Ren, H., Patel, R., et al. (2017). Sine Oculis Homeobox Homolog 1 Regulates Mitochondrial Apoptosis Pathway via Caspase-7 in Gastric Cancer Cells. *J. Cancer* 8, 636–645. doi:10.7150/jca.16018

Fedorenko, A., Lishko, P. V., and Kirichok, Y. (2012). Mechanism of Fatty-acid-dependent UCP1 Uncoupling in Brown Fat Mitochondria. *Cell* 151, 400–413. doi:10.1016/j.cell.2012.09.010

Fossati, S., Giannoni, P., Solesio, M. E., Cocklin, S. L., Cabrera, E., Ghiso, J., et al. (2016). The Carbonic Anhydrase Inhibitor Methazolamide Prevents Amyloid Beta-Induced Mitochondrial Dysfunction and Caspase Activation Protecting Neuronal and Glial Cells *In Vitro* and in the Mouse Brain. *Neurobiol. Dis.* 86, 29–40. doi:10.1016/j.nbd.2015.11.006

Gal, A., Balicza, P., Weaver, D., Naghdi, S., Joseph, S. K., Várnai, P., et al. (2017). MSTO 1 Is a Cytoplasmic Pro-mitochondrial Fusion Protein, Whose Mutation Induces Myopathy and Ataxia in Humans. *EMBO Mol. Med.* 9, 967–984. doi:10.15252/emmm.201607058

Gessulat, S., Schmidt, T., Zolg, D. P., Samaras, P., Schnatbaum, K., Zerweck, J., et al. (2019). Prosit: Proteome-wide Prediction of Peptide Tandem Mass Spectra by Deep Learning. *Nat. Methods* 16, 509–518. doi:10.1038/s41592-019-0426-7

González-Casacuberta, I., Morén, C., Juárez-Flores, D.-L., Esteve-Codina, A., Sierra, C., Catalán-García, M., et al. (2018). Transcriptional Alterations in Skin Fibroblasts from Parkinson's Disease Patients with Parkin Mutations. *Neurobiol. Aging* 65, 206–216. doi:10.1016/j.neurobiolaging.2018.01.021

González-Casacuberta, I., Juárez-Flores, D.-L., Ezquerra, M., Fucho, R., Catalán-García, M., Guitart-Mampel, M., et al. (2019). Mitochondrial and Autophagic Alterations in Skin Fibroblasts from Parkinson Disease Patients with Parkin Mutations. *Aging* 11, 3750–3767. doi:10.18632/aging.102014

Gray, M. J., and Jakob, U. (2015). Oxidative Stress protection by Polyphosphate-New Roles for an Old Player. *Curr. Opin. Microbiol.* 24, 1–6. doi:10.1016/j.mib.2014.12.004

Gray, M. J., Wholey, W.-Y., Wagner, N. O., Cremers, C. M., Mueller-Schickert, A., Hock, N. T., et al. (2014). Polyphosphate Is a Primordial Chaperone. *Mol. Cel.* 53, 689–699. doi:10.1016/j.molcel.2014.01.012

Guzun, R., Timohhina, N., Tepp, K., Gonzalez-Granillo, M., Shevchuk, I., Chekulayev, V., et al. (2011). Systems Bioenergetics of Creatine Kinase Networks: Physiological Roles of Creatine and Phosphocreatine in Regulation of Cardiac Cell Function. *Amino Acids* 40, 1333–1348. doi:10.1007/s00726-011-0854-x

Hurtado, E., Núñez-Álvarez, Y., Muñoz, M., Gutiérrez-Caballero, C., Casas, J., Pendás, A. M., et al. (2021). HDAC11 Is a Novel Regulator of Fatty Acid Oxidative Metabolism in Skeletal Muscle. *Febs J.* 288, 902–919. doi:10.1111/febs.15456

Judge, S., and Leeuwenburgh, C. (2007). Cardiac Mitochondrial Bioenergetics, Oxidative Stress, and Aging. *Am. J. Physiol.-Cel. Physiol.* 292, C1983–C1992. doi:10.1152/ajpcell.00285.2006

Käll, L., Storey, J. D., MacCoss, M. J., and Noble, W. S. (2008). Assigning Significance to Peptides Identified by Tandem Mass Spectrometry Using Decoy Databases. *J. Proteome Res.* 7, 29–34. doi:10.1021/pr700600n

Kazak, L., Chouchani, E. T., Jedrychowski, M. P., Erickson, B. K., Shinoda, K., Cohen, P., et al. (2015). A Creatine-Driven Substrate Cycle Enhances Energy Expenditure and Thermogenesis in Beige Fat. *Cell* 163, 643–655. doi:10.1016/j.cell.2015.09.035

Khong, M. L., Li, L., Solesio, M. E., Pavlov, E. V., and Tanner, J. A. (2020). Inorganic Polyphosphate Controls Cyclophilin B-mediated Collagen Folding in Osteoblast-like Cells. *Febs J.* 287, 4500–4524. doi:10.1111/febs.15249

Kim, S., Kim, S. F., Maag, D., Maxwell, M. J., Resnick, A. C., Juluri, K. R., et al. (2011). Amino Acid Signaling to mTOR Mediated by Inositol Polyphosphate Multikinase. *Cel. Metab.* 13, 215–221. doi:10.1016/j.cmet.2011.01.007

Kimura, M., and Okano, Y. (2007). Human Misato Regulates Mitochondrial Distribution and Morphology. *Exp. Cel. Res.* 313, 1393–1404. doi:10.1016/j.yexcr.2007.02.004

Koopman, W. J. H., Distelmaier, F., Smeitink, J. A., and Willems, P. H. (2013). OXPHOS Mutations and Neurodegeneration. *EMBO J.* 32, 9–29. doi:10.1038/emboj.2012.300

Kornberg, A., Rao, N. N., and Ault-Riché, D. (1999). Inorganic Polyphosphate: a Molecule of many Functions. *Annu. Rev. Biochem.* 68, 89–125. doi:10.1146/annurev.biochem.68.1.89

Kudryavtseva, A. V., Krasnov, G. S., Dmitriev, A. A., Alekseev, B. Y., Kardymon, O. L., Sadritdinova, A. F., et al. (2016). Mitochondrial Dysfunction and Oxidative Stress in Aging and Cancer. *Oncotarget* 7, 44879–44905. doi:10.18632/oncotarget.9821

Kulakovskaya, T. V., Lichko, L. P., Vagabov, V. M., and Kulaev, I. S. (2010). Inorganic Polyphosphates in Mitochondria. *Biochem. Mosc.* 75, 825–831. doi:10.1134/s0006297910070035

Kulakovskaya, E. V., Zemskova, M. Y., and Kulakovskaya, T. V. (2018). Inorganic Polyphosphate and Cancer. *Biochem. Mosc.* 83, 961–968. doi:10.1134/S0006297918080072

Kumble, K. D., and Kornberg, A. (1995). Inorganic Polyphosphate in Mammalian Cells and Tissues. *J. Biol. Chem.* 270, 5818–5822. doi:10.1074/jbc.270.11.5818

Lempart, J., and Jakob, U. (2019). Role of Polyphosphate in Amyloidogenic Processes. *Cold Spring Harb Perspect. Biol.* 11, a034041. doi:10.1101/cshperspect.a034041

Lin, M. T., and Beal, M. F. (2006). Mitochondrial Dysfunction and Oxidative Stress in Neurodegenerative Diseases. *Nature* 443, 787–795. doi:10.1038/nature05292

Liu, Z., Solesio, M. E., Schaffler, M. B., Frikha-Benayed, D., Rosen, C. J., Werner, H., et al. (2019). Mitochondrial Function Is Compromised in Cortical Bone Osteocytes of Long-Lived Growth Hormone Receptor Null Mice. *J. Bone Miner Res.* 34, 106–122. doi:10.1002/jbmr.3573

Lorenz, B., and Schröder, H. C. (2001). Mammalian Intestinal Alkaline Phosphatase Acts as Highly Active Exopolyphosphatase. *Biochim. Biophys. Acta (Bba) - Protein Struct. Mol. Enzymol.* 1547, 254–261. doi:10.1016/s0167-4838(01)00193-5

Maiolino, M., O'Neill, N., Lariccia, V., Amoroso, S., Sylantyev, S., Angelova, P. R., et al. (2019). Inorganic Polyphosphate Regulates AMPA and NMDA Receptors and Protects against Glutamate Excitotoxicity via Activation of P2Y Receptors. *J. Neurosci.* 39, 6038–6048. doi:10.1523/JNEUROSCI.0314-19.2019

Mathon, C., Bovard, D., Dutertre, Q., Sendyk, S., Bentley, M., Hoeng, J., et al. (2019). Impact of Sample Preparation upon Intracellular Metabolite Measurements in 3D Cell Culture Systems. *Metabolomics* 15, 92. doi:10.1007/s11306-019-1551-0

McCormack, J. G., Halestrap, A. P., and Denton, R. M. (1990). Role of Calcium Ions in Regulation of Mammalian Intramitochondrial Metabolism. *Physiol. Rev.* 70, 391–425. doi:10.1152/physrev.1990.70.2.391

McIntyre, B., and Solesio, M. (2021). Mitochondrial Inorganic Polyphosphate (polyP): the Missing Link of Mammalian Bioenergetics. *Neural Regen. Res.* 16, 2227–2228. doi:10.4103/1673-5374.310687

Meador, J. P., Bettcher, L. F., Ellenberger, M. C., and Senn, T. D. (2020). Metabolomic Profiling for Juvenile Chinook salmon Exposed to Contaminants of Emerging Concern. *Sci. Total Environ.* 747, 141097. doi:10.1016/j.scitotenv.2020.141097

Morrissey, J. H., Choi, S. H., and Smith, S. A. (2012). Polyphosphate: an Ancient Molecule that Links Platelets, Coagulation, and Inflammation. *Blood* 119, 5972–5979. doi:10.1182/blood-2012-03-306605

Müller, F., Mutch, N. J., Schenk, W. A., Smith, S. A., Esterl, L., Spronk, H. M., et al. (2009). Platelet Polyphosphates Are Proinflammatory and Procoagulant Mediators *In Vivo*. *Cell* 139, 1143–1156. doi:10.1016/j.cell.2009.11.001

Nasca, A., Scotton, C., Zaharieva, I., Neri, M., Selvatici, R., Magnusson, O. T., et al. (2017). Recessive Mutations in MSTO1 Cause Mitochondrial Dynamics Impairment, Leading to Myopathy and Ataxia. *Hum. Mutat.* 38, 970–977. doi:10.1002/humu.23262

Pang, Z., Chong, J., Zhou, G., de Lima Morais, D. A., Chang, L., Barrette, M., et al. (2021). MetaboAnalyst 5.0: Narrowing the gap between Raw Spectra and Functional Insights. *Nucleic Acids Res.* 49, W388–W396. doi:10.1093/nar/gkab382

Paradies, G., Petrosillo, G., Paradies, V., and Ruggiero, F. M. (2010). Oxidative Stress, Mitochondrial Bioenergetics, and Cardiolipin in Aging. *Free Radic. Biol. Med.* 48, 1286–1295. doi:10.1016/j.freeradbiomed.2010.02.020

Patro, S., Ratna, S., Yamamoto, H. A., Ebenezer, A. T., Ferguson, D. S., Kaur, A., et al. (2021). ATP Synthase and Mitochondrial Bioenergetics Dysfunction in Alzheimer's Disease. *Int. J. Mol. Sci.* 22, 11185. doi:10.3390/ijms222011185

Pavlov, E., Zakharian, E., Bladen, C., Diao, C. T. M., Grimbly, C., Reusch, R. N., et al. (2005). A Large, Voltage-dependent Channel, Isolated from Mitochondria by Water-Free Chloroform Extraction. *Biophys. J.* 88, 2614–2625. doi:10.1529/biophysj.104.057281

Pavlov, E., Aschar-Sobbi, R., Campanella, M., Turner, R. J., Gómez-García, M. R., and Abramov, A. Y. (2010). Inorganic Polyphosphate and Energy Metabolism in Mammalian Cells. *J. Biol. Chem.* 285, 9420–9428. doi:10.1074/jbc.M109.013011

Picard, M., McEwen, B. S., Epel, E. S., and Sandi, C. (2018). An Energetic View of Stress: Focus on Mitochondria. *Front. Neuroendocrinol.* 49, 72–85. doi:10.1016/j.yfrne.2018.01.001

Pino, L. K., Just, S. C., MacCoss, M. J., and Searle, B. C. (2020). Acquiring and Analyzing Data Independent Acquisition Proteomics Experiments without Spectrum Libraries. *Mol. Cel. Proteomics* 19, 1088–1103. doi:10.1074/mcp.P119.001913

Ritchie, M. E., Phipson, B., Wu, D., Hu, Y., Law, C. W., Shi, W., et al. (2015). Limma powers Differential Expression Analyses for RNA-Sequencing and Microarray Studies. *Nucleic Acids Res.* 43, e47. doi:10.1093/nar/gkv007

Schon, E. A., and Przedborski, S. (2011). Mitochondria: the Next (Neurode) Generation. *Neuron* 70, 1033–1053. doi:10.1016/j.neuron.2011.06.003

Seidlmayer, L. K., Gomez-Garcia, M. R., Blatter, L. A., Pavlov, E., and Dedkova, E. N. (2012). Inorganic Polyphosphate Is a Potent Activator of the Mitochondrial Permeability Transition Pore in Cardiac Myocytes. *J. Gen. Physiol.* 139, 321–331. doi:10.1085/jgp.201210788

Seidlmayer, L. K., Juettner, V. V., Kettlewell, S., Pavlov, E. V., Blatter, L. A., and Dedkova, E. N. (2015). Distinct mPTP Activation Mechanisms in Ischaemia-Reperfusion: Contributions of Ca2+, ROS, pH, and Inorganic Polyphosphate. *Cardiovasc. Res.* 106, 237–248. doi:10.1093/cvr/cvv097

Singh, A., Kukreti, R., Saso, L., and Kukreti, S. (2019). Oxidative Stress: A Key Modulator in Neurodegenerative Diseases. *Molecules* 24, 1583. doi:10.3390/molecules24081583

Smith, R. N., Agharkar, A. S., and Gonzales, E. B. (2014). A Review of Creatine Supplementation in Age-Related Diseases: More Than a Supplement for Athletes. *F1000Res* 3, 222. doi:10.12688/f1000research.5218.1

Smyth, G. K. (2004). Linear Models and Empirical Bayes Methods for Assessing Differential Expression in Microarray Experiments. *Stat. Appl. Genet. Mol. Biol.* 3, 1–25. Article3. doi:10.2202/1544-6115.1027

Solesio, M. E., and Pavlov, E. V. (2016). "Methods of Inorganic Polyphosphate (PolyP) Assay in Higher Eukaryotic Cells," in *Inorganic Polyphosphates in Eukaryotic Cells* (New York, NY: Springer), 81–89. doi:10.1007/978-3-319-41073-9_6

Solesio, M. E., Saez-Atienzar, S., Jordán, J., and Galindo, M. F. (2012). Characterization of Mitophagy in the 6-hydoxydopamine Parkinson's Disease Model. *Toxicol. Sci.* 129, 411–420. doi:10.1093/toxsci/kfs218

Solesio, M. E., Saez-Atienzar, S., Jordan, J., and Galindo, M. F. (2013). 3-Nitropropionic Acid Induces Autophagy by Forming Mitochondrial Permeability Transition Pores rather Than Activatiing the Mitochondrial Fission Pathway. *Br. J. Pharmacol.* 168, 63–75. doi:10.1111/j.1476-5381.2012.01994.x

Solesio, M. E., Demirkhanyan, L., Zakharian, E., and Pavlov, E. V. (2016a). Contribution of Inorganic Polyphosphate towards Regulation of Mitochondrial Free Calcium. *Biochim. Biophys. Acta (Bba) - Gen. Subj.* 1860, 1317–1325. doi:10.1016/j.bbagen.2016.03.020

Solesio, M. E., Elustondo, P. A., Zakharian, E., and Pavlov, E. V. (2016b). Inorganic Polyphosphate (polyP) as an Activator and Structural Component of the Mitochondrial Permeability Transition Pore. *Biochem. Soc. Trans.* 44, 7–12. doi:10.1042/BST20150206

Solesio, M. E., Peixoto, P. M., Debure, L., Madamba, S. M., de Leon, M. J., Wisniewski, T., et al. (2018). Carbonic Anhydrase Inhibition Selectively Prevents Amyloid β Neurovascular Mitochondrial Toxicity. *Aging Cell* 17, e12787. doi:10.1111/acel.12787

Solesio, M. E., Garcia Del Molino, L. C., Elustondo, P. A., Diao, C., Chang, J. C., and Pavlov, E. V. (2020). Inorganic Polyphosphate Is Required for Sustained Free Mitochondrial Calcium Elevation, Following Calcium Uptake. *Cell Calcium* 86, 102127. doi:10.1016/j.ceca.2019.102127

Solesio, M. E., Xie, L., McIntyre, B., Ellenberger, M., Mitaishvili, E., Bhadra-Lobo, S., et al. (2021). Depletion of Mitochondrial Inorganic Polyphosphate (polyP) in Mammalian Cells Causes Metabolic Shift from Oxidative Phosphorylation to Glycolysis. *Biochem. J.* 478, 1631–1646. doi:10.1042/BCJ20200975

Suess, P. M., Watson, J., Chen, W., and Gomer, R. H. (2017). Extracellular Polyphosphate Signals through Ras and Akt to Prime Dictyostelium Discoideum Cells for Development. *J. Cel Sci.* 130, 2394–2404. doi:10.1242/jcs.203372

Tsutsumi, K., Matsuya, Y., Sugahara, T., Tamura, M., Sawada, S., Fukura, S., et al. (2017). Inorganic Polyphosphate Enhances Radio-Sensitivity in a Human Non-small Cell Lung Cancer Cell Line, H1299. *Tumour Biol.* 39, 101042831770503. doi:10.1177/1010428317705033

Váraljai, R., Islam, A. B. M. M. K., Beshiri, M. L., Rehman, J., Lopez-Bigas, N., and Benevolenskaya, E. V. (2015). Increased Mitochondrial Function Downstream from KDM5A Histone Demethylase Rescues Differentiation in pRB-Deficient Cells. *Genes Dev.* 29, 1817–1834. doi:10.1101/gad.264036.115

Wang, L., Fraley, C. D., Faridi, J., Kornberg, A., and Roth, R. A. (2003). Inorganic Polyphosphate Stimulates Mammalian TOR, a Kinase Involved in the Proliferation of Mammary Cancer Cells. *Proc. Natl. Acad. Sci.* 100, 11249–11254. doi:10.1073/pnas.1534805100

Wei, R., Wang, J., Su, M., Jia, E., Chen, S., Chen, T., et al. (2018). Missing Value Imputation Approach for Mass Spectrometry-Based Metabolomics Data. *Sci. Rep.* 8, 663. doi:10.1038/s41598-017-19120-0

Xicoy, H., Wieringa, B., and Martens, G. J. M. (2017). The SH-Sy5y Cell Line in Parkinson's Disease Research: a Systematic Review. *Mol. Neurodegener.* 12, 10. doi:10.1186/s13024-017-0149-0

Xie, L., and Jakob, U. (2019). Inorganic Polyphosphate, a Multifunctional Polyanionic Protein Scaffold. *J. Biol. Chem.* 294, 2180–2190. doi:10.1074/jbc.REV118.002808

Yang, Z., Feng, Z., Gu, J., Li, X., Dong, Q., Liu, K., et al. (2017). microRNA-488 Inhibits Chemoresistance of Ovarian Cancer Cells by Targeting Six1 and Mitochondrial Function. *Oncotarget* 8, 80981–80993. doi:10.18632/oncotarget.20941

Yoo, N. G., Dogra, S., Meinen, B. A., Tse, E., Haefliger, J., Southworth, D. R., et al. (2018). Polyphosphate Stabilizes Protein Unfolding Intermediates as Soluble Amyloid-like Oligomers. *J. Mol. Biol.* 430, 4195–4208. doi:10.1016/j.jmb.2018.08.016

Zheng, X., Boyer, L., Jin, M., Mertens, J., Kim, Y., Ma, L., et al. (2016). Metabolic Reprogramming during Neuronal Differentiation from Aerobic Glycolysis to Neuronal Oxidative Phosphorylation. *Elife* 5, e13374. doi:10.7554/eLife.13374

Conflict of Interest: The authors declare that the research was conducted in the absence of any commercial or financial relationships that could be construed as a potential conflict of interest.

The handling editor declared a past collaboration with one of the authors (MGM).

Publisher's Note: All claims expressed in this article are solely those of the authors and do not necessarily represent those of their affiliated organizations, or those of the publisher, the editors and the reviewers. Any product that may be evaluated in this article, or claim that may be made by its manufacturer, is not guaranteed or endorsed by the publisher.

frontiers in Cell and Developmental Biology

ORIGINAL RESEARCH
published: 01 March 2022
doi: 10.3389/fcell.2022.786268

Applying Sodium Carbonate Extraction Mass Spectrometry to Investigate Defects in the Mitochondrial Respiratory Chain

David R. L. Robinson[1], *Daniella H. Hock*[1], *Linden Muellner-Wong*[1,2], *Roopasingam Kugapreethan*[1], *Boris Reljic*[1,3], *Elliot E. Surgenor*[3,4], *Carlos H. M. Rodrigues*[1,5], *Nikeisha J. Caruana*[1,6] *and David A. Stroud*[1,2]*

[1]Department of Biochemistry and Pharmacology, Bio21 Molecular Science and Biotechnology Institute, University of Melbourne, Parkville, VIC, Australia, [2]The Royal Children's Hospital, Murdoch Children's Research Institute, Parkville, VIC, Australia, [3]Department of Biochemistry and Molecular Biology, Monash Biomedicine Discovery Institute, Monash University, Clayton, VIC, Australia, [4]The Walter and Eliza Hall Institute of Medical Research, Parkville, VIC, Australia, [5]Baker Heart and Diabetes Institute, Melbourne, VIC, Australia, [6]Institute for Health and Sport (IHES), Victoria University, Melbourne, VIC, Australia

OPEN ACCESS

Edited by:
Sylvie Callegari, Walter and Eliza Hall Institute of Medical Research, Australia

Reviewed by:
Martin Ott, Stockholm University, Sweden
Karthik Mohanraj, University of Bern, Switzerland

***Correspondence:**
David A. Stroud
david.stroud@unimelb.edu.au

Specialty section:
This article was submitted to Cellular Biochemistry, a section of the journal Frontiers in Cell and Developmental Biology

Received: *30 September 2021*
Accepted: *03 February 2022*
Published: *01 March 2022*

Citation:
Robinson DRL, Hock DH, Muellner-Wong L, Kugapreethan R, Reljic B, Surgenor EE, Rodrigues CHM, Caruana NJ and Stroud DA (2022) Applying Sodium Carbonate Extraction Mass Spectrometry to Investigate Defects in the Mitochondrial Respiratory Chain. Front. Cell Dev. Biol. 10:786268. doi: 10.3389/fcell.2022.786268

Mitochondria are complex organelles containing 13 proteins encoded by mitochondrial DNA and over 1,000 proteins encoded on nuclear DNA. Many mitochondrial proteins are associated with the inner or outer mitochondrial membranes, either peripherally or as integral membrane proteins, while others reside in either of the two soluble mitochondrial compartments, the mitochondrial matrix and the intermembrane space. The biogenesis of the five complexes of the oxidative phosphorylation system are exemplars of this complexity. These large multi-subunit complexes are comprised of more than 80 proteins with both membrane integral and peripheral associations and require soluble, membrane integral and peripherally associated assembly factor proteins for their biogenesis. Mutations causing human mitochondrial disease can lead to defective complex assembly due to the loss or altered function of the affected protein and subsequent destabilization of its interactors. Here we couple sodium carbonate extraction with quantitative mass spectrometry (SCE-MS) to track changes in the membrane association of the mitochondrial proteome across multiple human knockout cell lines. In addition to identifying the membrane association status of over 840 human mitochondrial proteins, we show how SCE-MS can be used to understand the impacts of defective complex assembly on protein solubility, giving insights into how specific subunits and sub-complexes become destabilized.

Keywords: mitochondria, proteomic analyses, membrane protein, OXPHOS (oxidative phosphorylation), respiratory chain assembly, carbonate extraction

1 INTRODUCTION

Mitochondria are double membrane-bound eukaryotic organelles that perform critical cellular functions including producing the bulk of cellular energy, acting as hubs for synthesis of various biomolecules, and driving the apoptotic response. Mitochondria produce the majority of the cell's ATP through oxidative phosphorylation (OXPHOS), which involves five multi-protein complexes (complexes I-IV and the F_1-F_0 ATP Synthase, or complex V) found within the inner mitochondrial

membrane (IMM) (Hatefi, 1985; Rich and Maréchal, 2010; Hock et al., 2020). Mitochondria evolved from endosymbiotic prokaryotes, and therefore have their own genome, known as mitochondrial DNA (mtDNA), and their own ribosomes, known as mitoribosomes. Most protein coding genes in mtDNA were lost or transferred to the nucleus early in eukaryotic evolution, and numerous machineries have evolved to import and process these >1,000 proteins (Adams and Palmer, 2003; Roger et al., 2017; Rath et al., 2021). Following synthesis in the cytosol, nuclear encoded proteins are imported into the mitochondria through translocases of the inner and outer membranes, TIM and TOM respectively (Jackson et al., 2018; Pfanner et al., 2019). In humans, 13 proteins are encoded by mtDNA, all hydrophobic transmembrane subunits of the OXPHOS complexes that are translated on mitoribosomes and co-translationally inserted into the IMM (Ott and Herrmann, 2010; Thompson et al., 2018).

Complexes I-IV act as an electron transport chain with electrons from metabolic sources such as the tricarboxylic acid (TCA) cycle passing from complex to complex in a series of redox reactions. The energy from this process is used to pump protons from the mitochondrial matrix to the intermembrane space (IMS), creating a proton gradient used by complex V to synthesize ATP (Jonckheere et al., 2012). Mitochondrial respiratory complexes I, III and IV are found together in higher-order complexes, so called supercomplexes (SCs), that have well defined stoichiometry (Schagger and Pfeiffer, 2000; Letts et al., 2016; Wu et al., 2016; Guo et al., 2017). These include complex I and III (I/III_2), complex III and IV (III_2/IV), and complex I, III and IV ($I/III_2/IV$), the latter referred to as the respirasome and considered the dominant form.

Complex III (CIII) or the cytochrome bc_1 complex is at the center of the OXPHOS system, using electrons received from complexes I, II and other sources via ubiquinone to reduce cytochrome *c*, while also pumping protons into the IMS (Crofts et al., 2008; Fernandez-Vizarra and Zeviani, 2015). Mammalian CIII forms an obligate homodimer, with each subunit composed of 9 nuclear encoded proteins and one mtDNA-encoded protein, cytochrome *b* (MT-CYB) (Schagger et al., 1986). Complex III biogenesis begins with the synthesis of mtDNA-encoded MT-CYB on mitoribosomes and its co-translational insertion into the IMM. Two small membrane bound subunits UQCRB and UQCRQ then associate with MT-CYB (Hildenbeutel et al., 2014), while in parallel to this, peripherally associated subunits UQCRC1 and UQCRC2 form a tetramer of two UQCRC1-UQCRC2 dimers which is thought to coalesce on the nascent MT-CYB assembly along with additional membrane bound subunits CYC1, UQCR10 and UQCRH to yield a dimeric intermediate of CIII called pre-$CIII_2$ (Stephan and Ott, 2020). Finally, UQCR11 and catalytic subunit UQCRFS1 and incorporated to form the mature, active complex (Smith et al., 2012; Fernandez-Vizarra and Zeviani, 2018; Ndi et al., 2018). Although complexes I and IV are structurally independent from CIII, complete complex III assembly is critical for their biogenesis (Acin-Perez et al., 2004; Protasoni et al., 2020). Although the molecular details of this necessity are not yet fully understood, loss of CIII leads to inhibition of the final step of Complex I assembly; addition of the catalytic NADH dehydrogenase module (N-module) (Protasoni et al., 2020). Mutations in MT-CYB and 5 of the 9 nuclear encoded subunits in Complex III, along with mutations in many Complex I and IV subunits and assembly factors required for the biogenesis of OXPHOS complexes, impact complex and result in mitochondrial disease, a debilitating metabolic disorder affecting at least 1 in 5,000 live births (Fernandez-Vizarra and Zeviani, 2015; Gorman et al., 2016; Hock et al., 2020). For the majority of mitochondrial diseases there are no effective treatments, thus a nuanced understanding the molecular impact of dysfunctional assembly will be critical to the future development of therapeutics (Gorman et al., 2016).

Sodium carbonate extraction is a ~30 year old experimental technique used to determine whether a specific protein is an integral membrane protein, peripherally associated with the membrane, or a soluble protein. In the original method, cellular isolates containing membranes are solubilized in 0.1 M sodium carbonate, pH 11.5 (Fujiki et al., 1982a; Fujiki et al., 1982b). The alkaline carbonate solution disrupts protein-protein interactions without disrupting the membrane. Ultracentrifugation is then used to generate a pellet fraction, containing integral membrane proteins, and a supernatant fraction containing soluble and membrane-associated proteins. These fractions can then be analyzed by immunoblotting with specific antibodies.

The mitochondrial inner membrane is one of the most densely packed eukaryotic membranes with a high protein: lipid ratio. As a result of this, the transmembrane domains (TMDs) of mitochondrial membrane proteins are less hydrophobic compared to ER membrane proteins (von Heijne, 1986). This, along with the unique lipid content of mitochondrial membranes may explain the observation that mitochondrial proteins with single, moderately hydrophobic TMDs are susceptible to carbonate extraction at pH 11.0 (Kim et al., 2015). Thus, sodium carbonate extraction alone may yield false negatives as to the presence of TMDs in mitochondrial proteins, and that proteins may be present in both the pellet and supernatant fractions in different proportions, depending on their level of membrane integration (Fujiki et al., 1982a). One approach to overcome this is the use of multiple carbonate solutions with increasingly lower pH, as at lower pH peripheral membrane proteins are partially retained in the pellet fraction (Lytovchenko et al., 2014).

Here we describe a technique combining sodium carbonate extraction with quantitative mass spectrometry (SCE-MS) applicable to routine use in molecular investigations. We used SCE-MS to generate membrane association profiles for over 840 mitochondrial proteins in human embryonic kidney (HEK293T) cells, grouping them into 6 distinct clusters based on their resistance to sodium carbonate extraction across multiple pH conditions. By coupling SCE-MS with stable isotope labelling of amino acids in cell culture (SILAC), we were able to track changes in the membrane integration of mitochondrial proteins in gene-edited knockout cell-lines lacking different CIII subunits. We find that loss of single pass membrane-spanning subunit UQCR10 leads to defective complex assembly. SCE-MS revealed that while the majority of CIII subunits remained membrane associated, peripherally associated core-module subunits UQCRC1 and UQCRC2 became more soluble, consistent with the

destabilization and detachment of the core-module from the membrane bound CIII intermediate. Additionally, we found that arrest of CIII assembly, either through loss of UQCR10 or UQCRC1, leads to partial loss of the Complex I N-module as has been previously shown in CIII deficient cells (Protasoni et al., 2020). Using SCE-MS we found that while a population of N-module remained associated with Complex I, N-module subunits had increased solubility relative to other CI subunits, suggesting the modules attachment to the complex becomes unstable in the presence of a structural CIII defect. Thus, we see SCE-MS as a novel and unbiased means to assess the destabilization of protein complexes; a concept often cited to describe the impact of an assembly defect, but generally without a clear molecular definition.

2 MATERIALS AND METHODS

2.1 Tissue Culture and Generation of Knockout Cell Lines

HEK293T cells were cultured in Dulbecco's Modified Eagle's medium (DMEM High Glucose), supplemented with 10% (v/v) fetal calf serum (FCS; CellSera, Rutherford, NSW, Australia), penicillin/streptomycin (Thermo Fisher Scientific, Scoresby, VIC, Australia) and 50 μg ml^{-1} uridine (Sigma-Aldrich, North Ryde, NSW, Australia) at 37°C under an atmosphere of 5% CO_2. Guide (g) RNA sequences for CRISPR-Cas9 gene editing were designed using the CHOPCHOP software (Labun et al., 2019) and corresponding oligonucleotides were cloned into pSPCas9(BB)-2A-GFP (PX458) plasmid (a gift from F. Zhang;RRID:Addgene_48138) as previously described. The gRNA sequences used were 5′-CGA CTGCAGCTGGAAGATGG for UQCRC1^{KO} and 5′-TGGACT GTGAAGAAACATGG for UQCR10^{KO}. HEK293T cells were transfected with constructs using Lipofectamine LTX (Thermo Fisher Scientific) according to manufacturer's instructions. Single GFP-positive cells were sorted into 96 well plates and expanded for screening. To verify mutations caused by CRISPR/Cas9, genomic DNA of positive clones was extracted using Quick-DNA kit (Zymo Research, Irvine, CA) according to manufacturer's specifications. Screening primers designed by the CHOPCHOP software were used to amplify target regions that were cloned into the pGEM4Z plasmid (Yanisch-Perron et al., 1985) for M13 primed Sanger sequencing as described previously (Stroud et al., 2016). (Stroud et al., 2016). UQCRC1^{KO} clone 1 contained the following mutations c.[1-6T_11del]; [1-3A_4del] while clone 2 contained c.[1-126T_69+66delins]; [3G_4del] c.[1-126T_69+65delins]. UQCR10^{KO} clone 1 contained the following mutations c.[1-217G_30del] while UQCR10^{KO} clone 2 contained c.[1-27G_8del]; [1-11T_14del]; [1-28G_128delins]. All mutations disrupted the start codon and as such no protein product is predicted.

2.2 SDS-PAGE, BN-PAGE and Western Blotting

SDS-PAGE was performed using samples solubilized in LDS sample buffer (Thermo Fisher Scientific) with the 100 mM DTT and separated on Invitrogen Bolt Bis-Tris 4–12% protein gels according to manufacturer's conditions. BN-PAGE was performed using mitochondrial proteins solubilized in 1% (w/v) digitonin buffer as previously described (Wittig et al., 2006; Lazarou et al., 2007). Mitochondria were isolated as previously described (Johnston et al., 2002) with protein concentration determined using the Pierce Protein Assay Kit (Thermo Fisher Scientific). Detergent solubilized complexes were separated on Invitrogen NativePAGE Bis-Tris gels (3–12%) according to manufacturer's instructions. Western blotting of SDS-PAGE gels was undertaken using the Invitrogen iBlot2 Dry Blotting System using PVDF based stacks as per manufacturer's instructions. Western transfer of BN-PAGE gels onto PVDF (Merck, Bayswater, VIC, Australia) was performed using the Invitrogen Mini Blot Module transfer system as per manufactures recommendations. Immunoblots were developed using horseradish peroxidase-conjugated mouse and rabbit secondary antibodies (Cell Signaling Technology, Danvers, MA) and ECL chemiluminescent substrates (Bio-Rad, Gladesville, NSW, Australia) and visualized using a ChemiDoc XRS+ gel documentation system (Bio-Rad). Commercial antibodies were acquired for COXI (Abcam Cat# ab14705, RRID:AB_2084810), COXII (Thermo Fisher Scientific Cat# A-6404, RRID:AB_221584), COX4 (Abcam Cat# ab110261, RRID:AB_10862101), CYC1 (Sigma-Aldrich Cat# HPA001247, RRID:AB_1078602), CYCS (BD Biosciences Cat# 556433, RRID:AB_396417), NDUFV1 (Proteintech Cat# 11238-1-AP, RRID:AB_2149040), SDHA (Abcam Cat# ab14715, RRID:AB_301433), TIMM50 (Proteintech Cat# 22229-1-AP, RRID:AB_2879039), UQCRC1 (Abcam Cat# ab110252, RRID:AB_10863633), UQCRFS1 (Abcam Cat# ab14746, RRID:AB_301445), UQCRH (Abcam Cat# ab134949, RRID:AB_2800504), and UQCRQ (Abcam Cat# ab110255, RRID:AB_10865309). The generation of polyclonal antibodies for MT-HSP70 (Stroud et al., 2013), VDAC2 (Ma et al., 2014), NDUFAF1 (Dunning et al., 2007) and NDUFA9 (Lazarou et al., 2007) has been previously described. In-gel activity assay was performed as previously described (Zerbetto et al., 1997).

2.3 Sodium Carbonate Extraction for SDS-PAGE and BN-PAGE

Mitochondria were isolated from HEK293T cells were pelleted at 12,000 x g for 5 min at 4°C before being resuspended in 100 mM Na_2CO_3, pH 9.5 or 11.5 and incubated on ice for 30 min. Half the volume of each sample was reserved for a "Total" fraction. The remainder was centrifuged at 125,000 x g for 30 min at 4°C to generate "Pellet" and "Supernatant" fractions. The pellet fraction was solubilized for SDS-PAGE as described above. Total and supernatant fractions were made up to a final concentration of 15% trichloroacetic acid (TCA) and incubated on ice for 30 min before centrifugation at 20,000 x g for 10 min at 4°C. The supernatant was discarded, and the protein precipitates were washed with ice cold acetone before further centrifugation at 20,000 x g for 10 min at 4°C. The supernatant was discarded, and the protein pellets allowed to air dry before being solubilized for SDS-PAGE as above. For BN-PAGE analysis of pellet fractions, pellets were resuspended in 1% (w/v) digitonin buffer as

previously described (Wittig et al., 2006; Lazarou et al., 2007) and subjected to shaking at 1500 rpm for 90 min at 4°C. Samples were centrifuged at 20,000 x g for 10 min at 4°C and BN-PAGE analysis and Western blotting were carried out as described above.

2.4 Sodium Carbonate Extraction for Mass Spectrometry

HEK293T, UQCRC1^{KO}, and UQCR10^{KO} cells were cultured in DMEM for SILAC (Thermo Scientific, 88364), supplemented with 10% (v/v) dialyzed FCS (Thermo Scientific, 30067334), penicillin/streptomycin (Thermo Fisher Scientific, Scoresby, VIC, Australia), 50 μg ml^{-1} uridine (Sigma-Aldrich, North Ryde, NSW, Australia), 600 mg L^{-1} L-proline and, either regular "light" or "heavy" ($^{13}C_6{}^{15}N_2$ lysine and $^{13}C_6{}^{15}N_4$-arginine) arginine and lysine (Silantes, 201604102 and 211604102) at the concentrations of 42 mg L^{-1} L-arginine and 146 mg L^{-1} L-lysine at 37°C and 5% CO_2 for at least 5 passages. Cells were collected, washed in PBS and counted. Samples were prepared in triplicate with a label switch. Equal numbers of HEK293T cells (2 independent samples grown in heavy DMEM and one grown in light DMEM) and knockout cells (1 sample grown in heavy DMEM and 2 independent samples grown in light DMEM) were mixed in heavy/light HEK293T/knockout pairs and used for isolation of mitochondria as previously described (Stroud et al., 2016). SILAC-labelled mitochondria were pelleted at 12,000 x g for 5 min at 4°C before being resuspended in 100 mM Na_2CO_3, pH 9.5 or 11.5 and incubated on ice for 30 min. One fifth of the volume of each sample was aliquoted as the "Total" fraction. The remainder was centrifuged at 125,000 x g for 30 min at 4°C to generate "Pellet" and "Supernatant" fractions. Peptides were prepared using the S-Trap system (Hailemariam et al., 2018) as per manufacturer's instructions. The total fraction was solubilized using 1X S-Trap solubilization buffer while pellet and supernatant fractions were prepared using 3X S-Trap solubilization buffer. The total fraction samples were processed using Micro S-Trap columns, while the pellet and supernatant fractions were processed using Mini S-Trap columns. Proteins were digested with trypsin (Thermo Fisher Scientific) at a 1:25 trypsin:protein ratio overnight at 37°C. Peptides were eluted from S-Trap columns according to manufacturer's instructions, prior to drying in a CentriVap Benchtop Vacuum Concentrator (Labconco, Kansas City, MO) and reconstitution in 0.1% TFA and 2% ACN for analysis by Liquid chromatography (LC) - MS/MS on an Orbitrap Exploris 480 (Thermo Fisher Scientific) coupled with an Ultimate 3000 HPLC (Thermo Fisher Scientific) and NanoESI interface. The LC system was equipped with an Acclaim Pepmap nano-trap column (Dinoex-C18, 100 Å, 75 μm × 2 cm) and an Acclaim Pepmap RSLC analytical column (Dinoex-C18, 100 Å, 75 μm × 50 cm). The tryptic peptides were injected to the enrichment column at an isocratic flow of 5 μl/min of 2% v/v CH_3CN containing 0.1% v/v formic acid for 5 min applied before the enrichment column was switched in-line with the analytical column. The eluents were 5% DMSO in 0.1% v/v formic acid (solvent A) and 5% DMSO in 100% v/v CH_3CN and 0.1% v/v formic acid (solvent B). The flow gradient was 1) 0–6 min at 3% B, 2) 6–95 min, 3-22% B 3) 95–105 min 22–40% B 4) 105–110 min, 40–80% B 5) 110–115 min, 80–80% B 6) 115–117 min, 80–3% and equilibrated at 3% B for 10 min before the next sample injection. The mass spectrometer was operated in the data-dependent acquisition mode, whereby full MS1 spectra were acquired in a positive mode at 1,20,000 resolution. The "top speed" acquisition mode with 3 s cycle time on the most intense precursor ion was used, whereby ions with charge states of 2–7 were selected. MS/MS analyses were performed by 1.6 m/z isolation with the quadrupole, fragmented by HCD with collision energy of 30%. MS2 resolution was at 15,000. Dynamic exclusion was activated for 30 s. AGC target was set to standard with auto maximum injection mode. Dynamic exclusion was activated for 30 s. Raw files were processed using the MaxQuant software package (Version 1.6.17.0, RRID:SCR_014485) (Tyanova et al., 2016a), and searched against the UniProt human database, including unreviewed proteins, (193557 entries, March 2021). For this search, Arg10 and Lys8 were set as the heavy labels and Trypsin/P cleavage specificity (cleaves after lysine or arginine, even when proline is present) was used with a maximum of 2 missed cleavages. Oxidation of methionine and N-terminal acetylation were specified as variable modifications. Carbamidomethylation of cysteine was set as a fixed modification. The settings "LFQ," "re-quant" and "Match between runs" were enabled with otherwise default settings.

2.5 Steady State Proteomics

SILAC labeled isolated mitochondria were prepared as described above, and peptides were prepared using Mini S-Trap columns (Hailemariam et al., 2018) as described above for analysis by LC-MS/MS on an Orbitrap Eclipse. The LC was carried out as described above. The mass spectrometer was operated in the data-dependent acquisition mode, whereby full MS1 spectra were acquired in a positive mode at 120,000 resolution. The "top speed" acquisition mode with 3 s cycle time on the most intense precursor ion was used, whereby ions with charge states of 2–7 were selected. MS/MS analyses were performed by 1.6 m/z isolation with the quadrupole, fragmented by HCD with normalized collision energy of 30%. MS2 resolution was at 15,000. Dynamic exclusion was activated for 30 s. AGC target was set to standard with auto maximum injection mode. Raw files were processed as described above, however without the "LFQ" option enabled.

2.6 Complexome Mass Spectrometry

SILAC labelled heavy UQCRC1^{KO}/light HEK293T isolated mitochondria were prepared as described above and analyzed via BN-PAGE as described above. Detergent solubilized complexes were separated on a 4–16% acrylamide gel, run overnight. The blue native gel containing separated SILAC-labelled mitochondria was transferred into fixing solution (50% v/v methanol, 10% v/v acetic acid, 10 mM ammonium acetate) and incubated for 30 min, followed by a 30-minute incubation in Coomassie solution (0.025% (w/v) Coomassie, 10% v/v acetic acid). The gel was destained in 10% acetic acid for several hours until background was clear, then washed in

water at least three times. The lane containing the SILAC-labelled mitochondria was excised and cut into 60 even slices. Each slice was further diced into smaller pieces and placed into individual wells of an Acroprep™ 30-40 µm PP/PE filtered microtiter plate containing 50 mM ammonium bicarbonate (ABC) for in-gel tryptic digest as previously described (Giese et al., 2021). Briefly, the ABC was removed by centrifugation before destaining. All centrifugation steps were performed at 1,500 x g. The destain and wash process was repeated 2–3 times as required. Gel peices were incubated for 60 min with gentle shaking in destain solution (60% methanol v/v, 50 mM ABC). Gel pieces were washed in 50% v/v acetonitrile (ACN), 50 mM ABC and incubated in 10 mM dithiothreitol, 50 mM ABC for 60 min at 56°C without shaking. Gel pieces were then incubated in 40 mM chloroacetamide, 50 mM ABC for 45 min before being washed twice with 50% v/v ACN, 50 mM ABC. Gel pieces were then allowed to air dry for 40–45 min without agitation, before digestion solution (10 ng/µl trypsin (Thermo Fisher Scientific), 10% v/v ACN, 0.01% (w/v) ProteaseMAX surfactant (Promega), 1 mM $CaCl_2$, 50 mM ABC) was added, and topped up with 50 mM ABC, for overnight incubation at 37°C in a pre-humidified incubator. Digested peptides were eluted the next day into a fresh microtiter plate by centrifugation before adding additional elution buffer (30% [v/v] ACN, 3% [v/v] formic acid (FA)) to gel pieces before gentle shaking for a further 20 min. The second elution was collected by centrifugation and both elutions were pooled. Peptide solutions were dried using a CentriVap concentrator (Labconco) then reconstituted in 2% [v/v] ACN, 0.1% [v/v] TFA. Samples were desalted on stagetips containing 2x 14G plugs of 3M™ Empore™ SDB-XC extraction Disks (Sigma-Aldrich), which were pre-activated with 100% ACN and equilibrated with 2% [v/v] ACN, 0.1% [v/v] TFA before loading. Stagetips were washed with 2% [v/v] ACN, 0.1% [v/v] TFA and samples were eluted with 80% [v/v] ACN, 0.1% [v/v] TFA. All centrifugation steps were performed at 3,000 x g. Elutions were dried and reconstituted in 2% [v/v], 0.1% TFA [v/v] for LC-MS/MS analysis. The LC system was equipped with an Acclaim Pepmap nano-trap column (Dinoex-C18, 100 Å, 75 µm × 2 cm) and an Acclaim Pepmap RSLC analytical column (Dinoex-C18, 100 Å, 75 µm × 50 cm). The tryptic peptides were injected to the enrichment column at an isocratic flow of 5 µl/min of 2% v/v CH_3CN containing 0.05% [v/v] TFA for 6 min applied before the enrichment column was switched in-line with the analytical column. The eluents were 5% DMSO in 0.1% [v/v] formic acid (solvent A) and 5% DMSO in 100% [v/v] CH_3CN and 0.1% [v/v] formic acid (solvent B). The flow gradient was 1) 0-6min at 2% B, 2) 6–25 min, 2–23% B 3) 25–35 min 23–40% B 4) 35–40 min, 40–80% B 5) 40–42 min, 80–80% B 6) 42–42.1 min, 80–2% and equilibrated at 2% B for 10 min before the next sample injection. The QExactive plus mass spectrometer was operated in the data-dependent mode, whereby full MS1 spectra were acquired in positive mode, 70 000 resolution, AGC target of $3e^6$ and maximum IT time of 50 ms. Fifteen of the most intense peptide ions with charge states ≥2 and intensity threshold of $4e^4$ were isolated for MSMS. The isolation window was set at 1.2m/z and precursors fragmented using normalized collision energy of 30, 17 500 resolution, AGC target of $5e^4$ and maximum IT time of 50 ms. Dynamic exclusion was set to be 30sec. Raw files were processed using the MaxQuant platform (version 1.6.17.0) against the UniProt human canonical and isoforms database (42,360 entries, August 2020) using settings for the standard identification of light and heavy (Arg-10 and Lys-8) SILAC-labelled peptides. Oxidation of methionine and N-terminal acetylation were specified as variable modifications, and carbamidomethylation of cysteine was set as a fixed modification. Trypsin/P cleavage specificity was used with a maximum of 2 missed cleavages, and a search tolerance of 4.5 ppm was used for MS1 and 20 ppm for MS2 matching. False discovery rates (FDR) were determined through the target-decoy approach set to 1% for both peptides and proteins. The calculation of intensity-based absolute quantification (iBAQ) intensities was enabled with the Log fit function disabled.

2.7 Proteomics Data Analysis

The ProteinGroups.txt files generated by the SCE-MS search was imported into Perseus (version 1.6.15.0, RRID:SCR_015753) (Tyanova et al., 2016b). Normalized H/L Ratios and individual LFQ Heavy (H) and Light (L) intensities were Log_2-transformed and grouped by cell line and fraction. Proteins were filtered for mitochondrial localization based on the MitoCarta3.0 dataset (Rath et al., 2021) added through matching by Uniprot ID. For comparing "Total" fractions and "Pellet" and "Supernatant" fractions prior to normalization, for each fraction, proteins were filtered for H/L ratio quantitation in at least two samples and a one-sample two-sided t-test was conducted with results expressed as a volcano plot. For normalized comparisons, Log_2-transfrormed ratios of each replicate of the "Total" fraction was subtracted from the corresponding "Pellet" or "Supernatant" fraction. Proteins without quantified ratios in both "Total" and either "Pellet" or "Supernatant" fractions were excluded from comparisons. A one-sample two-sided t-test was conducted, and results expressed as a volcano plot. For comparisons between "Supernatant" and "Pellet" fractions in the same cell line, proteins were filtered for those quantified in at least two third of samples for at least two of pH 9.5 "Pellet", pH 9.5 "Supernatant", pH 11.5 "Pellet" or pH 11.5 "Supernatant". The number of transmembrane domains for each protein were added using the Uniprot database (The Uniprot Consortium, 2021). Missing values were imputed based on the normal distribution with a width of 0.3 and a down-shift of 1.8, and a two-sample t-test was performed between "Pellet" and "Supernatant" groups with the results displayed as a volcano plot. For cluster analysis, each fraction was averaged and Z-scored. Hierarchical clustering was then performed with default settings. Clusters were defined in HEK293T samples using the define row cluster tool. Samples were then un-Z-scored and principal component analysis plots generated. For transmembrane domain prediction, the FASTA sequences of proteins in cluster 1 were analyzed using HMMTOP (Bioinformatics Toolkit, RRID:SCR_010277) (Tusnády and Simon, 2001), TMHMM (RRID:SCR_014935) (Krogh et al., 2001), TMPred (Hofmann, 1993) and Phobius (RRID:SCR_015643) (Käll et al., 2004).

For the steady-state experiment, the ProteinGroups.txt file was imported into Perseus. Normalized H/L ratios were Log_2-

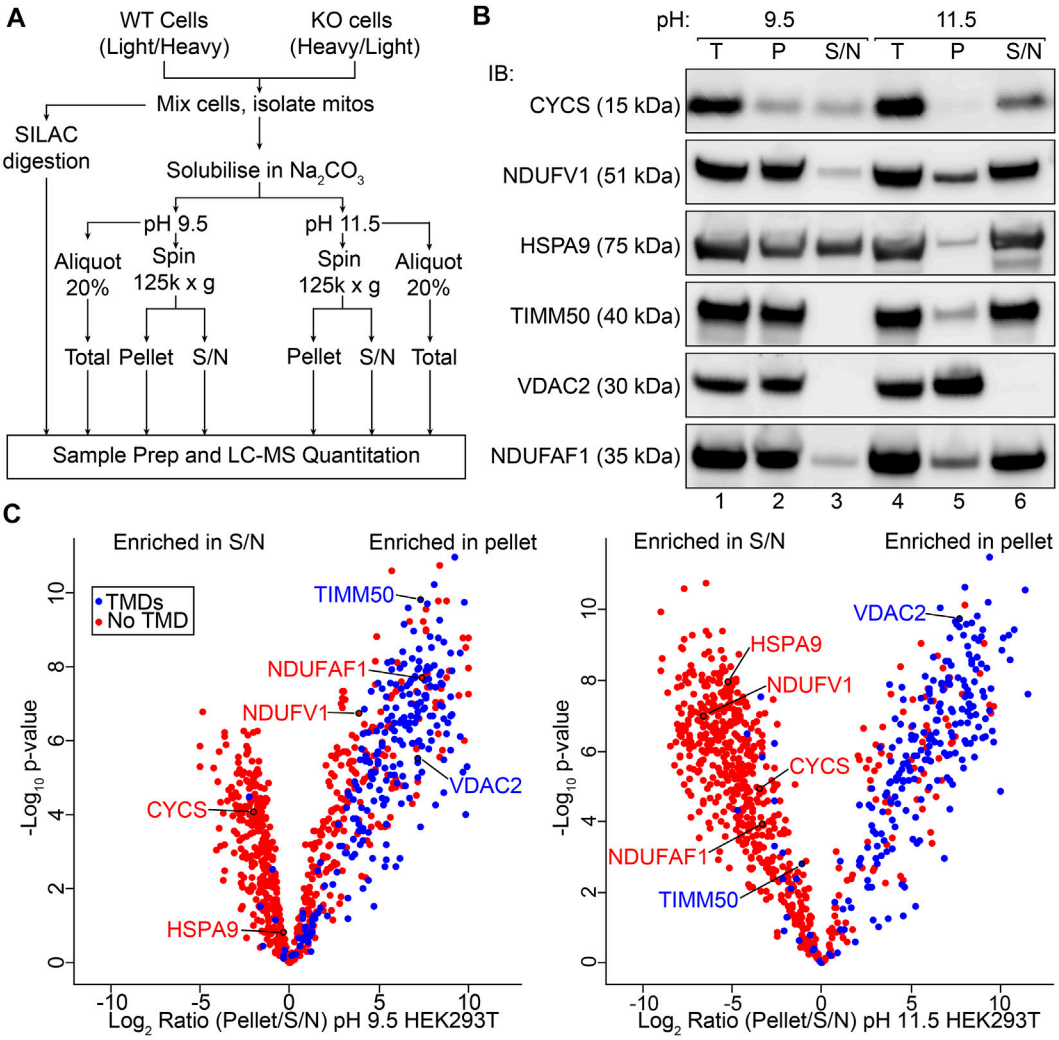

FIGURE 1 | Sodium carbonate extraction MS to assess membrane association on a mitochondrial proteome wide scale. **(A)** Protocol for SILAC coupled sodium carbonate extraction experiment. SILAC heavy and light labeled WT and KO cells are mixed and mitochondria isolated from the resultant pool of cells. Pooled mitochondria are then used directly for quantitative mass spectrometry or for sodium carbonate extraction (Na_2CO_3) MS. Total, Pellet and Supernatant (S/N) fractions generated by carbonate extraction and analyzed by LC-MS. **(B)** Mitochondria isolated from the HEK293T cell line were subjected to sodium carbonate extraction and total (T), pellet (P) and supernatant (S/N) fractions were analyzed by SDS-PAGE and immunoblotting (IB) with indicated antibodies. **(C)** Volcano plots depicting relative abundance of mitochondrial proteins in the pellet and supernatant fractions after sodium carbonate extraction at pH 9.5 and 11.5.

transformed and grouped by cell line. Proteins were filtered for mitochondrial localization based on Mitocarta3.0 and ratios were normalized by subtracting the median of each column. A one-sample two-sided t-test was conducted, and result expressed as a volcano plot and topographical heatmap as previously described (Stroud et al., 2016) with -2 and 2 as minimum and maximum values respectively.

For complexome analysis, heavy and light iBAQ intensities were imported into Perseus (version 1.6.15.0), filtered and annotated for mitochondrial proteins listed in MitoCarta 3.0 (Rath et al., 2021), then imported into NOVA (version 0.8.0.0) for complexome analysis and visualisation. Mass scale calibration was performed by exponential interpolation in NOVA by inputting apparent protein masses selected from **Supplementary Table S5** from (Maclean et al., 2021). Selected proteins of interest underwent hierarchical clustering using default settings, with optimised leaf ordering, average linkage, and a Person Correlation Distance function, without normalisation. Exported heatmaps with iBAQ values were normalised in Excel, by row average for heatmap generation, and by maximum intensity for profile plot generation. Figures were generated in GraphPad Prism 9 (RRID:SCR_002798).

2.8 Oxygen Consumption Measurements

Mitochondrial oxygen consumption rates were measured in live cells using a Seahorse Bioscience XFe-96 Analyzer (Agilent Mulgrave, VIC, Australia). Briefly, 25,000 cells were plated per well in culture plates treated with 50 µg/ml poly-d-lysine (Sigma-

Aldrich). For each assay cycle, there were 3 measurements of 2 min followed by mixing, 2 min wait, and 3 min measure. The following inhibitor concentrations were used: 1 µm oligomycin, 1 µm carbonyl cyanide 4-(trifluoromethoxy)phenylhydrazone (FCCP), 0.5 µm rotenone and 0.5 µm antimycin A. Data were normalized using the Pierce Protein Assay Kit (Thermo Fisher Scientific) and analyzed using Wave (version 2.6.0, Agilent, RRID:SCR_014526) and Prism (version 8.0.2, GraphPad, RRID:SCR_005375) software packages.

3 RESULTS

To assess the membrane association of the mitochondrial proteome in an unbiased manner, we adapted a sodium carbonate extraction protocol for use with quantitative proteomics workflows (**Figure 1A**). This included the use of stable isotope labelling using amino acids in cell culture (SILAC) to allow the impact of perturbations (such as CRISPR/Cas9 knockout of a protein of interest) to be quantitatively assessed, as discussed in subsequent results sections. In order to validate our protocol, we first analyzed sodium carbonate extraction data for only control HEK293T mitochondria, separated from the dataset *in silico* and treated in a similar way as would be done in a label free quantification (LFQ; see *Materials and Methods* for more detail). SDS-PAGE and immunoblotting using antibodies against mitochondrial proteins with varied localizations and membrane integration was also performed to establish baseline profiles for proteins with known behavior (**Figure 1B**). At pH 11.5, outer membrane channel VDAC2 and peripheral IMM electron carrier cytochrome *c* (CYCS) are found exclusively in the pellet and supernatant fractions respectively as expected (Ma et al., 2014;Letts et al., 2016). Complex I N-module/matrix arm subunit NDUFV1 and assembly factor NDUFAF1, both peripherally associated with the membrane (Stroud et al., 2016), along with import translocase components TIMM50 and mt-HSP70 are found in both fractions at pH 11.5. At pH 9.5, a reduction in carbonate extraction is observed for each protein, with only cytochrome *c* and mt-HSP70 found in equal proportions in both the pellet and supernatant fractions, possibly due to their localization in both soluble and peripherally membrane associated pools (Kang et al., 2018;Timón-Gómez et al., 2018). Using SCE-MS we were able to quantify the relative abundance of 844 mitochondrial proteins (Rath et al., 2021) from control HEK293T cells at both pH 9.5 and 11.5 (**Figure 1C**; **Supplementary Table S1**). This represents 74% of the known mitochondrial proteome. Under both extraction conditions the majority of proteins with transmembrane domains annotated in UniProt (The Uniprot Consortium, 2021) were detected at greater abundance in the pellet fraction. Proteins without annotated TMDs were found most enriched in the supernatant extracted at pH 11.5, but were more evenly distributed between supernatant and pellet fractions following extraction at the lower pH, as expected.

In order to classify the mitochondrial proteome based on extraction properties, we performed hierarchical clustering on our SCE-MS data (**Figure 2A**; **Supplementary Table S2**) and used this to define six distinct clusters that could be readily visualized using principal component analysis (PCA; **Figure 2B**; **Supplementary Table S2**). Cluster 1 contains 276 proteins that are resistant to membrane extraction at both pH 9.5 and 11.5. This includes hydrophobic proteins such as mitochondrial transporter family SLC25A members and all detected mtDNA encoded proteins. Cluster 2 contains 44 proteins that are resistant to extraction at pH 9.5 but are partially susceptible to extraction at pH 11.5. Cluster 3 contains 20 proteins that are resistant to extraction at pH 9.5 but very susceptible at pH 11.5. Cluster 4 contains 128 proteins that are moderately resistant to extraction at pH 9.5 but highly susceptible at pH 11.5, including 21 subunits of the small subunits of the mitoribosome, 16 of the large subunit and 6 out of the 9 detected subunits of the N-module of complex I. Cluster 5 contains 278 proteins that are partially resistant to extraction at pH 9.5 but very susceptible at pH 11.5. Cluster 6 contains 88 proteins that are susceptible to extraction at both pH 9.5 and 11.5. A total of 10 proteins quantified in this analysis did not segregate into a cluster.

To further validate our dataset, we cross-referenced the number of predicted TMDs present in proteins found within each cluster. Predictions were drawn from UniProt (The Uniprot Consortium, 2021), which annotates TMDs automatically based on the TMD being identified by both TMHMM (Krogh et al., 2001) and Phobius (Käll et al., 2004) algorithms with substantial overlap. Nearly every protein with two or more annotated TMDs was found in cluster 1 (**Figure 2C**), along with the majority of single TMD proteins. The remaining proteins with single TMDs are distributed across the other clusters, with a bias toward clusters 2 and 4. Of the 276 proteins in cluster 1, 73 had no TMD annotated in Uniprot (**Figure 2D**). Using a number of additional bioinformatics tools for predicting TMDs, including TMPred (Hofmann, 1993) and HMMTOP (Bioinformatics Toolkit, RRID:SCR_010277) (Tusnády and Simon, 2001), as well as TMHMM (RRID:SCR_014935) (Krogh et al., 2001) and Phobius (RRID:SCR_015643) (Käll et al., 2004) without the overlap constraint used by UniProt, we identified an additional 30 proteins that had TMDs identified by at least two algorithms. A number of these proteins have been experimentally determined to be genuine membrane proteins, including complex I subunit NDUFB2 through high resolution structural studies (Zhu et al., 2016) recently identified complex III assembly factor OCIAD1 through classical carbonate extraction studies (Le Vasseur et al., 2021) and pro-survival protein FUNDC2 through mutation and localization analysis (Ma et al., 2019).

Next, we wanted to demonstrate the usefulness of SCE-MS in identifying changes in membrane integration following a perturbation. We used the CRISPR/Cas9 system to generate knockout cell lines where the expression of complex III subunits UQCRC1 and UQCR10 was disrupted. Two individual clones for each knockout were validated by sequencing of targeted alleles (see *Materials and Methods*). To determine changes in OXPHOS complex assembly, we analyzed mitochondria from two clones of each knockout using Blue Native (BN) PAGE and immunoblotting (**Figure 3A**). Mitochondria from both knockouts retained a ~150 kDa

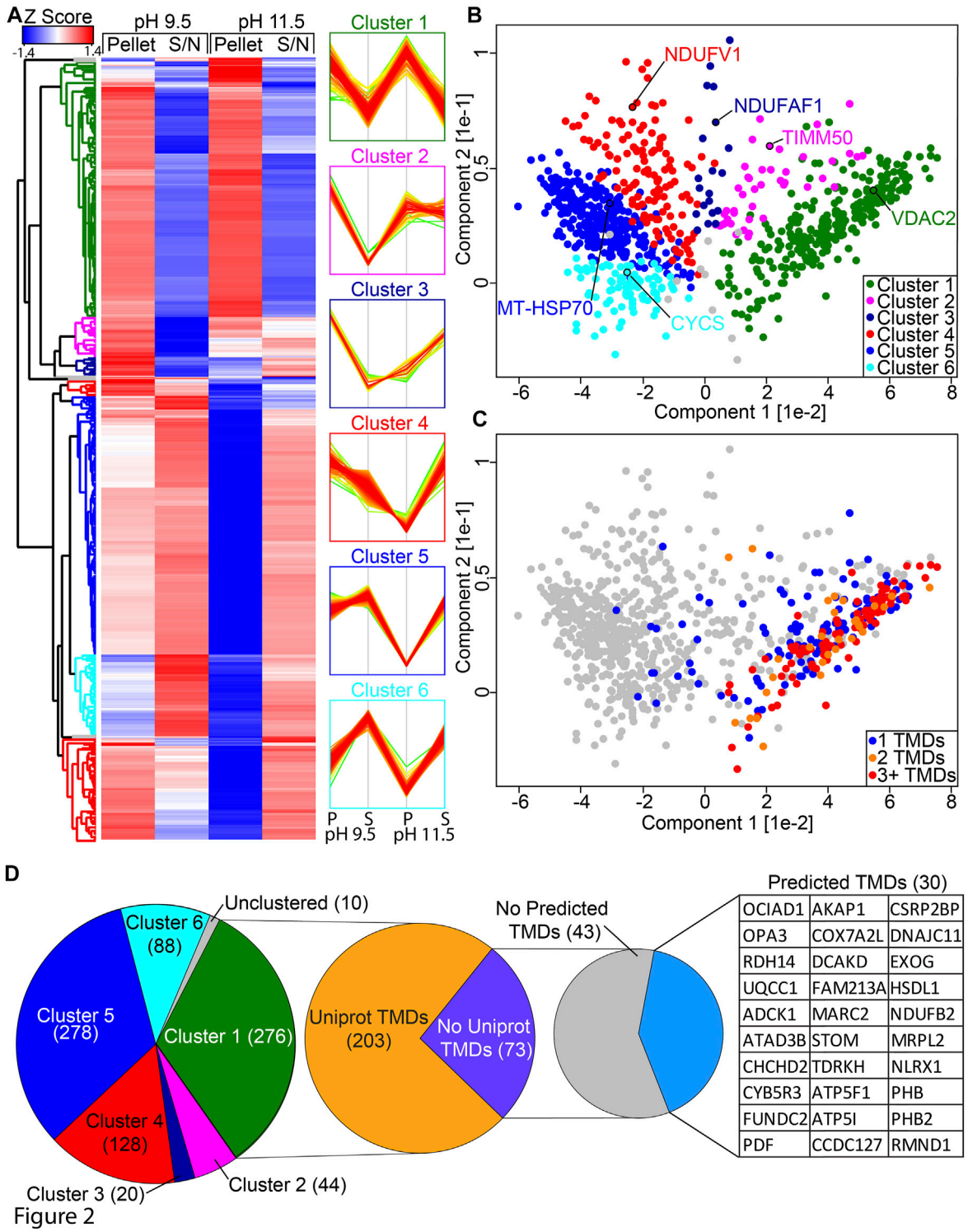

FIGURE 2 | Classification of protein clusters. **(A)** HEK293T mitochondrial proteome SCE-MS data was Z-scored and hierarchical clustering was performed. Results are expressed in a heatmap and the profiles of each cluster are shown. The *x*-axis on the profiles indicates relative abundance, where higher is equal to more abundant. Coloring reflects distance to the mean of the profile, where red is closest, green is most distant. **(B)** Principal component analysis of HEK293T supernatant and pellet fractions at pH 9.5 and 11.5, colored according to the clusters identified in **(A)**. **(C)** as for B but with coloring according to the number of transmembrane domains. **(D)** Breakdown of Cluster 1 showing number of proteins with TMDs annotated in Uniprot and predicted by at least two single TM prediction algorithms (TMPred, HMMTOP, TMHMM or Phobius).

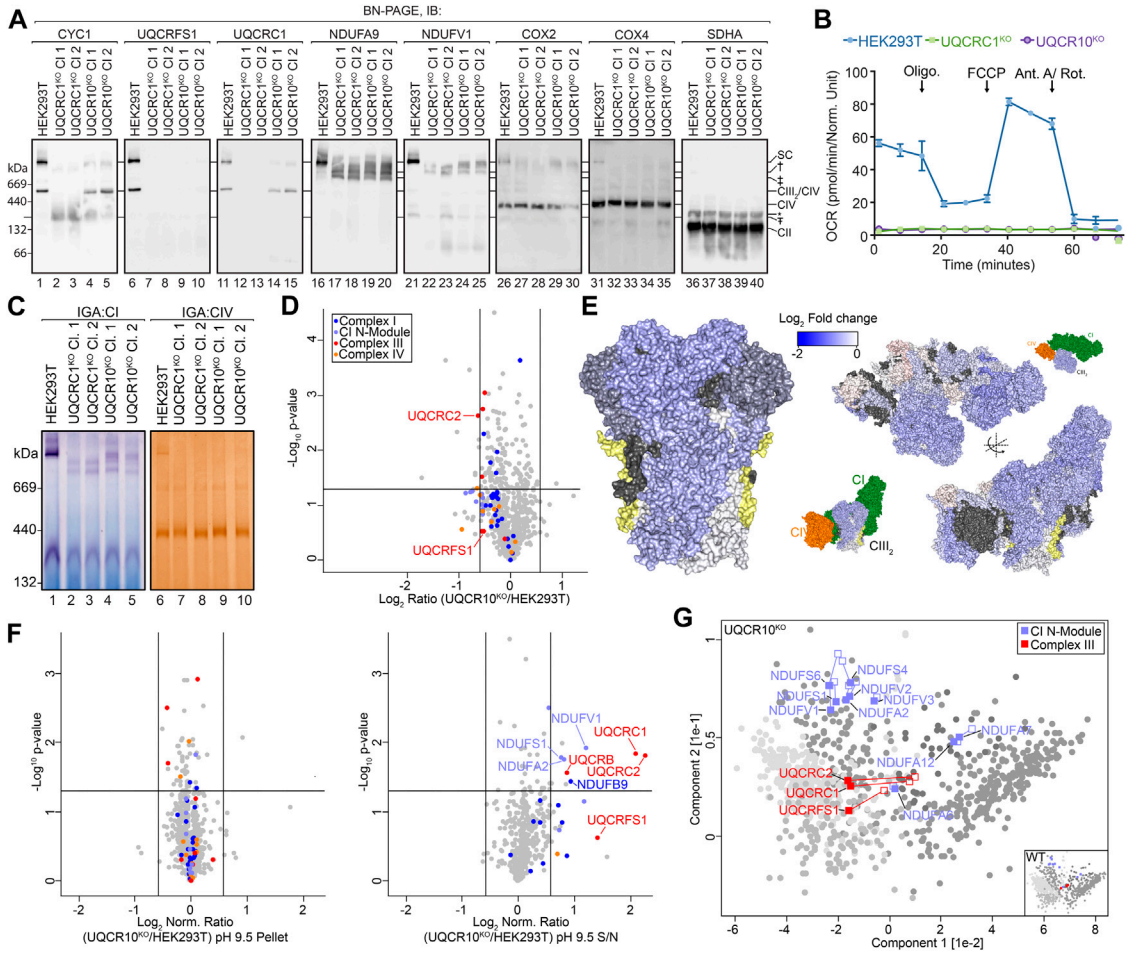

FIGURE 3 | Loss of UQCR10 leads to destabilization and accumulation of a soluble core-module. **(A)** Mitochondria isolated from indicated cell lines were solubilized in 1% digitonin and analyzed by BN-PAGE and immunoblotting with the indicated antibodies. ∓, † and ‡ represent sub-assemblies discussed in text. *non-specific complex. **(B)** Oxygen consumption rates of HEK293T, UQCRC1^{KO} and UQCR10^{KO} cell lines. Oligo, oligomycin; FCCP, carbonyl cyanide 4-(trifluoromethoxy) phenylhydrazone; Ant A, antimycin A; Rot, rotenone. **(C)** Mitochondria isolated from indicated cell lines were analyzed using BN-PAGE and the activity of complex I and IV determined through in-gel assays. **(D)** Volcano plot depicting relative abundances of mitochondrial proteins in UQCR10^{KO} compared to HEK293T. **(E)** Topographical heatmap showing changes in abundance of CIII and respirasome subunits in UQCR10^{KO} using the CIII (PDB 5XTE) and respirasome (PDB 5XTH) structures. UQCR10 shown in yellow. **(F)** Volcano plots depicting relative abundance of proteins in pH 9.5 carbonate extraction pellet and supernatant fractions in UQCR10^{KO} compared to HEK293T mitochondria following normalization against the total fraction. Data prior to normalization and pH 11.5 data can be found in **Supplementary Figures S1, S2**. **(G)** Principal component analysis showing overall membrane association profiles in UQCR10^{KO} relative to HEK293T mitochondria. Complex I N-module and CIII subunits are labeled, with their position in control data shown as empty squares and position in knockout data as filled squares. Clusters defined in **Figure 2A** are colored in grey.

subassembly containing CYC1 that was more abundant in the UQCRC1^{KO} than UQCR10^{KO} (**Figure 3A**, compare lanes 2–5 with 1; subassembly indicated by ∓). Cells lacking UQCR10 retained a $CIII_2$-like assembly containing CYC1 and UQCRC1 (compare lanes 4–5 with 1). No signal for complex III subunit UQCRFS1 was observed in either UQCRC1^{KO} or UQCR10^{KO} clones (compare lanes 7–10 with 6), indicating that UQCRFS1 is not assembled into CIII in either knockout cell line in agreement with existing assembly models that describe incorporation of that subunit to be a late stage assembly event (Fernandez-Vizarra and Zeviani, 2018), and despite UQCRFS1 levels being only slightly reduced in UQCR10^{KO} (see **Figure 3D** and **Figure 4A**; UQCRFS1 is decreased by a fold-change of ~2 in UQCRC1^{KO}). Interestingly, the $CIII_2$-like complex in UQCR10^{KO} appeared to migrate slightly faster than wildtype $CIII_2$ (**Figure 3A**), leading us to speculate that it could represent the pre-$CIII_2$ intermediate (Fernandez-Vizarra and Zeviani, 2018). In the absence of peripheral core-module subunit UQCRC1, no supercomplex assemblies were observed, with CI migrating in two major sub-assemblies (compare lanes 22–23 with 21; assemblies indicated by † and ‡). In the absence of single-spanning membrane subunit UQCR10, similar CI sub-assemblies were observed, in addition to a supercomplex-like structure, albeit at a lower abundance than in control cells (compare lanes 24–25 with 21). In both UQCRC1^{KO} and UQCR10^{KO}, assembly of holo CIV appears to be unperturbed,

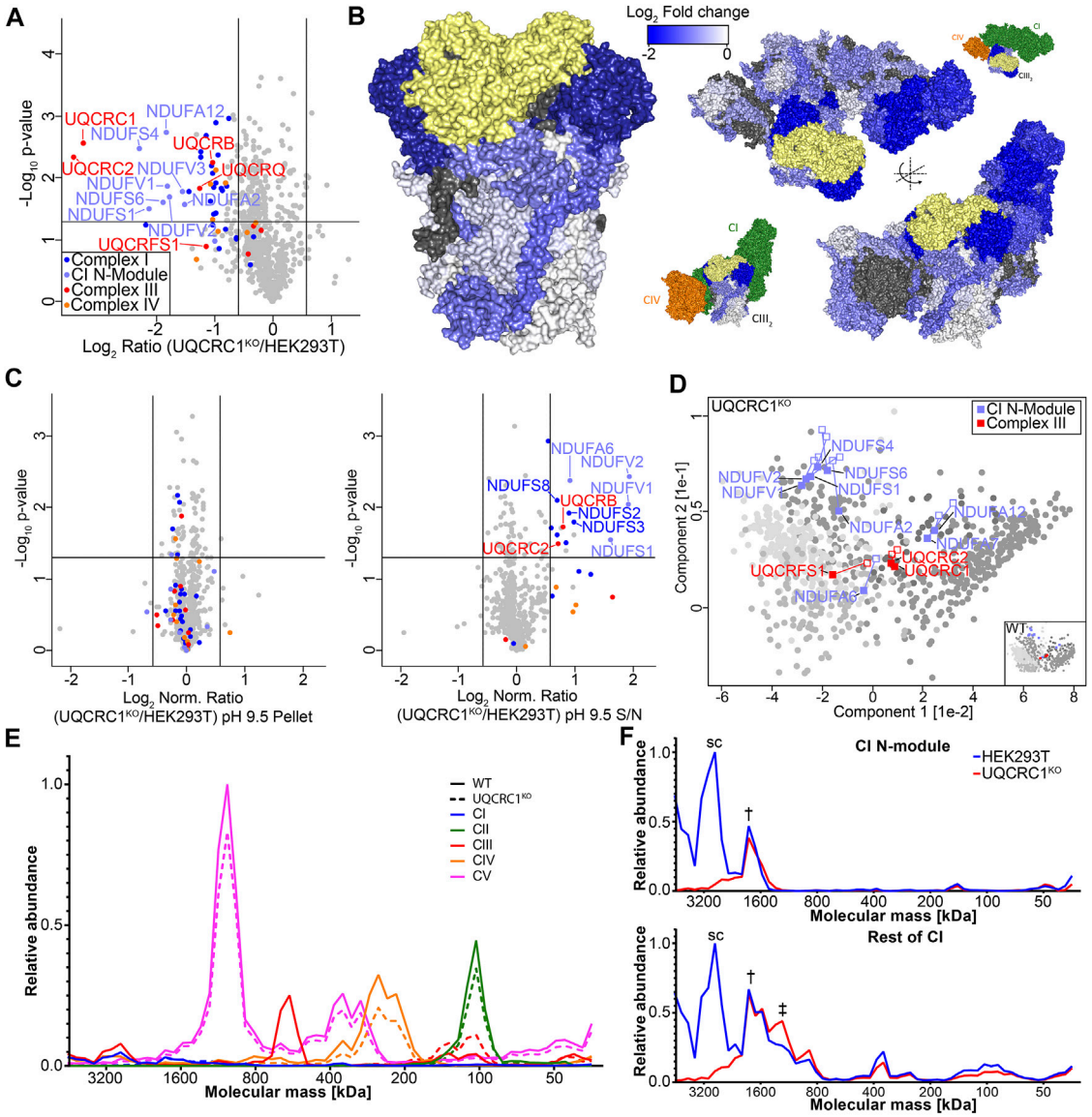

FIGURE 4 | Loss of UQCRC1 destabilizes the N-module of complex I. **(A)** Volcano plot depicting relative abundances of mitochondrial proteins in UQCRC1^{KO} compared to HEK293T. **(B)** Topographical heatmap showing changes in abundance of CIII and respirasome subunits in UQCRC1^{KO} using the CIII (PDB 5XTE) and respirasome (PDB 5XTH) structures. UQCRC1 shown in yellow **(C)** Volcano plots depicting relative abundance of proteins in pH 9.5 carbonate extraction pellet and supernatant fractions in UQCR10^{KO} compared to HEK293T mitochondria following normalization against the total fraction. **(D)** Principal component analysis showing overall membrane association profiles in UQCRC1^{KO} relative to control mitochondria. Complex I N-module and CIII subunits are labeled, with their position in control data shown as empty squares and position in knockout data as filled squares. Clusters defined in **Figure 2A** are colored in grey. **(E)** Complexome profile of mitochondrial respiratory complexes in UQCRC1^{KO} and HEK293T mitochondria. Graphs plot relative intensities of peptides averaged across all subunits of each complex with the maximum set as 1.0. Molecular mass calculated as described in *Materials and Methods*. **(F)** Complexome profile of CI subunits, separated into N-module and the rest of the complex, as in **(E)**. The symbols used to indicate peaks represent the equivalent complex in **Figure 3A**.

however higher order CIV assemblies are mostly absent, with the exception of a low abundance complex migrating at a similar molecular weight to the supercomplex in UQCR10^{KO}. Given the reported role of CIII in CI and CIV assembly and function (Protasoni et al., 2020) and the unexpected impact of the loss of UQCRC1 and UQCR10 on CI seen in **Figure 3A**, we wanted to determine if CI and CIV activity was retained in our knockouts. Surprisingly, despite the loss of catalytic complex III subunit UQCRFS1 from all CIII-containing complexes and sub-assemblies (**Figure 3A**) and thus the loss of overall respiration via OXPHOS (**Figure 3B**), partial complex I in-gel activity was observed in the remnant supercomplex-like structure in UQCR10^{KO} (**Figure 3C**, compare lanes 4–5 with 1) and in the lower molecular weight assemblies seen in both knockouts (**Figure 3C**). Despite the low abundance band seen in immunoblotting, no Complex IV activity was observed in the

supercomplex-like structure found in UQCR10^{KO}, with the only activity found holo CIV (**Figure 3C**). Given the reproducible phenotype between multiple independent sequence-verified clones complementation experiments were not performed. Clones 1 of UQCRC1^{KO} and UQCR10^{KO} were used for all subsequent experiments.

We first focused our SCE-MS analysis on UQCR10 knockout mitochondria. Assembly of the dimeric pre-CIII$_2$ occurs with the addition of membrane subunits UQCR10, CYC1 and UQCRH and peripherally associated core-module subunits UQCRC1 and UQCRC2 (Stephan and Ott, 2020). We reasoned that loss of UQCR10 may result in accumulation of a soluble core-module observable through SCE-MS, demonstrating how the technique can provide additional insights into CIII assembly. First we assessed the baseline steady-state levels of proteins in UQCR10^{KO} and controls using quantitative mass spectrometry of isolated mitochondria, as baseline data would be critical to interpretating SCE-MS data since some proteins may have an overall reduced cellular abundance due to perturbed assembly. Knockout and control HEK293T cells were subjected to SILAC labeling using light or heavy ($^{13}C_6{}^{15}N_2$ lysine and $^{13}C_6{}^{15}N_4$-arginine) amino acids, and the relative abundance of mitochondrial proteins in the knockouts compared to HEK293T was determined. In total, we quantified relative changes in abundance of 749 mitochondrial proteins (**Supplementary Table S3**). While UQCR10 itself was not detected in UQCR10^{KO} mitochondria (**Supplementary Table S3**), OXPHOS subunits including most CIII subunits were only minimally reduced in abundance, with only UQCRC2 reaching our significance threshold of 1.5 fold change (**Figure 3D**). The non-specific trend in reduced abundance of CIII and supercomplex subunits is also evident using topographical heatmaps (Stroud et al., 2016) (**Figure 3E**) where the fold change for individual proteins observed in steady state proteomics is mapped to the cryo-electron microscopy structure of the human CI/CIII$_2$/CIV supercomplex (Gu et al., 2016).

We next turned to SCE-MS, which was performed as outlined in **Figure 1A** using SILAC labelled UQCR10^{KO} and control cell lines (**Supplementary Figure S1**, **Supplementary Table S4**). To account for the overall decreased steady-state abundance of some proteins seen in **Figure 3D** we also measured proteome changes in a "Total" fraction containing sodium carbonate solubilized material prior to ultracentrifugation (**Supplementary Figure S1**, left panels), using this data to normalize pellet and supernatant SCE-MS results (**Figure 3F** shows normalized data at pH 9.5. Normalized data for pH 11.5 can be found in **Supplementary Figure S2**, and raw ratios in **Supplementary Figure S1**). Following carbonate extraction at pH 9.5, the normalized pellet fraction had no significant changes in the levels of OXPHOS subunits. However in contrast, CIII subunits UQCRC1 and UQCRC2 were found to be relatively more abundant in supernatant in UQCRC10^{KO}. Similar results were observed following extraction at pH 11.5, however under these conditions the effect was reversed, with UQCRC1 and UQCRC2 being less abundant in the pellet fraction of UQCRC10^{KO} (**Supplementary Figure S2B**). To more easily visualize changes in membrane association of CIII subunits we compared the proteome wide changes to membrane association across both extraction conditions, assigning protein solubility in the knockout to the previously identified clusters (**Figure 2B**). While in the knockouts most proteins fell into the same clusters as in control cells, the clustering of core-module subunits UQCRC1 and UQCRC2 changed from clusters 2 to 5 in the knockout (**Figure 3G**, compare filled to empty squares) indicating altered membrane association. Also notable is UQCRFS1, the last assembled subunit (Fernandez-Vizarra and Zeviani, 2018), which moved from cluster 2 to 5. Cluster 5 contains proteins that are partially resistant to extraction at pH 9.5 but very susceptible at pH 11.5 and predominantly includes soluble matrix proteins such as those found in the mitoribosome and various tRNA ligases, along with proteins having mixed peripheral and soluble localization such as mt-HSP70 (Kang et al., 2018; Timón-Gómez et al., 2018) (**Supplementary Table S2**). These data, taken together with our BN-PAGE analysis that shows UQCRC1 remains associated with CIII$_2$ in the UQCR10^{KO} under native-electrophoresis conditions (**Figure 3A**, compare lanes 14–15 with 11), suggest that the interaction between core module subunits UQCRC1 and UQCRC2 and the nascent CIII membrane assembly is destabilized in the absence of UQCR10, evidenced by the increased resistance of UQCRC1 and UQCRC2 to extraction at pH 9.5.

A concern we had over the validity of our SCE-MS data is the impact of the carbonate extraction procedure on protein complex stability. Our knockouts harbor sub-assemblies with different protein composition to that found in control cells. Should the presence of carbonate lead to selective partial breakdown of these complexes but not the comparable control complex, this would potentially lead to artefactual results caused by altered extractability of these breakdown sub-complexes. An example sub-assembly would be the CIII$_2$-like complex lacking UQCRFS1 and UQCR10 that we suspect may represent pre-CIII$_2$ (**Figure 3A**, compare lanes 4–5 with 1), as in the above experiments we are directly comparing the extractability of UQCRC1 and UQCRC2 from this and wildtype holo-CIII$_2$ (along with other assemblies). To address this, we analyzed membrane fractions from our control and knockout cells extracted at both pH 9.5 and 11.5 using BN-PAGE and immunoblotting (**Supplementary Figure S3**). While the relative abundance of some sub-assemblies changed under different conditions as expected based on our SCE-MS data, their migration on BN-PAGE did not. We also did not observe any sub-complexes unique to either carbonate extraction condition. Taken together, we conclude that the presence of sodium carbonate does not alter the composition of the complexes and sub-assemblies being discussed in this study.

We next turned our attention to the UQCRC1 knockout. To obtain a baseline of proteome changes in the knockout, we performed steady state quantitative mass-spectrometry on isolated mitochondria, as described above (**Supplementary Table S3**). Loss of UQCRC1 led to a significant decrease in the levels of subunits present in CI, CIII and CIV, particularly the

subunits of the core module of CIII, UQCRC1 and UQCRC2, and of the N-module of Complex I (**Figure 4A**). We again used topographical heatmaps to interpret the data in the context of the CI/$CIII_2$/IV supercomplex (**Figure 4B**) (Gu et al., 2016), which clearly visualized the greatest impact of UQCRC1 loss to be on the core module of CIII and the N-module of Complex I. While this is consistent with recent reports that dysfunctional CIII assembly prevents addition of the N-module to Complex I (Protasoni et al., 2020), the molecular underpinnings of this phenomenon are not fully understood. To investigate this further, we performed SCE-MS on $UQCRC1^{KO}$ as described above. In mitochondria from this knockout we observed a significant increase in the solubility of several CI subunits, with the greatest increase seen in N-module subunits (**Figure 4C**, right panel). Also moderately increased in solubility were the CIII subunits UQCRC2 and UQCRB. As done for $UQCR10^{KO}$, we used a PCA-based approach incorporating both extraction conditions to better understand the implication of proteome solubility changes seen in the $UQCRC1^{KO}$. While most proteins quantified in $UQCRC1^{KO}$ could be assigned to the same clusters as in control cells (**Figure 2B**), the clustering of Complex I N-module subunits changed (**Figure 4D**, compare filled to empty squares) indicating altered membrane association. In the control HEK293T dataset, whereas most N-module subunits appeared at the intersect of cluster 3 and 4, these proteins migrated toward cluster 5 in $UQCRC1^{KO}$ (**Figure 4D**). Complex III subunits were largely unchanged, with the exception of UQCRFS1, which like in $UQCR10^{KO}$ moved from cluster 2 to 5. Similar trends in respect to N-module solubility were observed, though with less severity, for $UQCR10^{KO}$ (**Figure 3G**). Despite N-module subunits being increasingly soluble in $UQCRC1^{KO}$ and given the results of Protasoni and colleagues (2020) we were surprised by the relatively large amount of catalytic N-module subunit NDUFV1 still migrating with other Complex I subunits in $UQCRC1^{KO}$ (**Figure 3A**), and moreover, CI-linked NADH dehydrogenase activity, an enzymatic reaction performed by the N-module, retained in $UQCRC1^{KO}$ (**Figure 3C**). Interestingly, Protasoni and colleagues (2020) also observed low amounts of Complex I activity in their model of CIII dysfunction, however complexome profiling, a technique where lanes from BN-PAGE gels are excised into ~60 slices and the protein distribution obtained by MS analysis, showed that the majority of holo-Complex I lacked associated N-module subunits. To better understand our results, we performed complexome profiling on the $UQCRC1^{KO}$ (**Figure 4E**; **Supplementary Figure S4**; **Supplementary Table S5**) which accurately recapitulated observations we made using traditional BN-PAGE and immunoblotting (**Figure 3A**). A closer inspection of the dataset revealed multiple high molecular weight Complex I sub-assemblies in $UQCRC1^{KO}$, including a dominant assembly containing all Complex I subunits, and at least two assemblies lacking the N-module (**Figure 4F**, † indicates assembly containing N-module, ‡ the assembly lacking N-module observed in **Figure 3A**). Taken together with our SCE-MS and in-gel activity data, we conclude that while the severe structural defect in CIII assembly found in $UQCRC1^{KO}$ leads to the association between the N-module and the Complex I membrane assembly being destabilized, the N-module still retains an ability to associate with the complex. We suspect the differences in N-module association between our study and Protasoni et al. (2020) can be attributed to cell type and other confounders (see *Discussion*), and while our data broadly supports their conclusions it raises additional questions as to the molecular nature of Complex I N-module assembly.

4 DISCUSSION

Sodium carbonate extraction is technique commonly used to identify integral membrane proteins. The technique has been adapted for use in both immunoblotting and radiolabeled *in vitro* import based assays (Stojanovski et al., 2007) and in addition to being useful in the characterization of newly identified proteins, is commonly used to gain mechanistic insights into membrane protein complex biogenesis through the use of mutant and gene-edited cell lines where the assembly process is blocked at specific steps. The use of multiple pH extraction conditions and control proteins with known localization additionally allows proteins with peripheral membrane association to be assessed (Lytovchenko et al., 2014). Here we describe a technique that combines sodium carbonate extraction with quantitative proteomics applicable for routine use in the study of mitochondrial complex assembly. Sodium carbonate extraction has previously been coupled with mass-spectrometry (Vögtle et al., 2017) however in that study the technique was combined with several other biochemical fractionation protocols to develop a steady state map of the *Saccharomyces cerevisiae* mitochondrial proteome. Vögtle and colleagues utilized SILAC multiplexing to compare crude and highly pure yeast mitochondria, allowing novel mitochondrial proteins to be confidently identified (Vögtle et al., 2017), but making their protocol not applicable to routine comparative analysis. Using SCE-MS we profiled the membrane association of 844 mitochondrial proteins in the commonly used human HEK293T cell line, roughly 75% of the human mitochondrial proteome (Rath et al., 2021). We applied bioinformatic tools to this dataset in order to cluster proteins based on their membrane association profiles, identifying 6 well defined clusters with decreasing membrane association. Clusters were validated against proteins with known membrane association and readily separate proteins with genuine membrane integration via TMDs (Cluster 1) such the polytopic SLC25A family of solute carriers found in the IMM (Palmieri, 2013) from truly soluble proteins (Cluster 6). One interesting outcome of this analysis is the large proportion of proteins that behave as peripherally associated membrane proteins. We identified four different clusters, accounting for almost 60% of proteins quantified, with varying levels of extraction at both pH 11.5 but partial resistance to extraction at pH 9.5, suggesting at least some peripheral association with the membrane. Our dataset, available in **Supplementary Table S2**, can be used as a general

reference for the membrane association of a protein of interest in HEK293T cells.

One caveat of our dataset that could explain the profiles seen for some proteins is the tendencies for large soluble complexes such as the mitoribosome (subunits of which are predominantly found in Cluster 4) to sediment at the high centrifugation speeds used in our assay (Aibara et al., 2020). This highlights the need for biology and the nature of co-clustering proteins to be considered when interpreting SCE-MS data. For example, the mitoribosome is known to associate with the IMM translocase OXA1 to facilitate co-translational membrane insertion (Itoh et al., 2021) while Cluster 4 also contains subunits found in the membrane associated matrix arm of complex I. Together these lines of evidence suggest the presence of mitoribosome proteins in this cluster may reflect at least some degree of membrane association. To further test our clusters for biological significance we assessed the number of TMDs predicted for each protein. As expected, the majority of proteins with predicted TMDs were resistant to extraction and as such clustered together in Cluster 1. Through bioinformatic analysis of Cluster 1 proteins, we identified 30 proteins with likely TMDs that are not annotated on the Uniprot database. The presence of the other 43 proteins lacking annotated TMDs within Cluster 1 suggests that these proteins may contain transmembrane beta barrels or may be associated with the membrane through post-translational modifications, such as glycosylphosphatidylinositol (GPI) anchors or covalent lipid modifications. While proteins with two or more TMDs are almost exclusively found within Cluster 1, a number of single TMD proteins were found in all other clusters, including two proteins with single TMDs in Cluster 6, which is made up of mostly soluble proteins susceptible to carbonate extraction. One of these, the serine protease HTRA2, contains an N-terminal transmembrane domain that is inserted into the IMM during import, the protein is subsequently cleaved, releasing the soluble domain into the IMS (Challa et al., 2007).

As a test case for SCE-MS as a tool to complement techniques such as BN-PAGE in understanding the assembly pathways of OXPHOS complexes, we decided to investigate the impact of different complex III structural defects on the assembly of complex III and the wider OXPHOS system. While both UQCRC1 and UQCR10 are thought to be incorporated into CIII at the same step (Smith et al., 2012;Ndi et al., 2018), as UQCRC1 is required for the dimerization of CIII (Stephan and Ott, 2020) we hypothesized that UQCRC1^{KO} would exhibit a more severe CIII defect, more closely mimicking the loss of MT-CYB (Protasoni et al., 2020) that is known to lead to assembly of the Complex I N-module being blocked. We anticipated that the loss of the small membrane subunit UQCR10 would have minimal impact on CIII assembly, but may lead to the presence of a pool of soluble UQCRC1-UQCRC2 core-module. Both situations where chosen as they were predicted to highlight the utility of SCE-MS to observe aspects of OXPHOS assembly defects not accessible through other techniques. In UQCR10^{KO}, while the abundance of complex III subunits were only moderately altered when observed through steady state quantitative proteomics (**Figure 3D**), SCE-MS showed UQCRC1 and UQCRC2 to increase in solubility (**Figure 3F**), migrating from a cluster defined by the presence of membrane proteins to one containing predominantly soluble matrix proteins (**Figure 3G**). Interestingly, we also found that UQCRFS1 is not present in the CIII intermediate found in UQCR10^{KO} that we suspect to be pre-$CIII_2$, and like the core module is found predominantly in soluble clusters (**Figure 4D**). In the high resolution structure of the mature CIII dimer (Gu et al., 2016), the transmembrane domains of UQCRFS1 and UQCR10 sit next to each other. Taken together with our data, this may suggest that UQCR10 plays a direct role in stabilizing UQCRFS1 incorporation into the complex through a coordinated interaction with the translocase BCS1L (Wagener and Neupert, 2012). As expected, UQCRC1^{KO} lacks the later stage CIII intermediates (**Figure 3A**) and has a greater impact on the steady state abundance of CIII subunits (**Figure 4A**) than UQCR10^{KO}. Loss of UQCRC1 also strongly impacts the abundance of Complex I and blocks its assembly into the supercomplex (**Figure 3A**). This is unsurprising as assembly of Complex III is known to be critical to the assembly of Complex I (Acin-Perez et al., 2004; Schägger et al., 2004; Protasoni et al., 2020). This was most recently demonstrated using human cybrids lacking MT-CYB, where it was shown through complexome profiling and other techniques that complex I is blocked at the step where the N-module is incorporated (Protasoni et al., 2020). While our steady state proteomic data for the UQCRC1^{KO} showed a decrease in the abundance of N-module subunits (**Figures 4A,B**) SCE-MS suggested the remaining population trended to being more soluble (**Figures 4C,D**). We performed complexome profiling on UQCRC1^{KO} to investigate this further, finding multiple holo-Complex I assemblies with and without N-module. Importantly, these results were supported by our in-gel NADH dehydrogenase activity assay (**Figure 3C**) which confirmed the presence of the N-module on at least one remnant Complex I assembly. Taken together, our data suggests that while Complex I biogenesis strongly relies on the presence of the CIII dimer for efficient assembly, it appears to be able to retain a partial ability to assemble without the structural involvement of CIII. This is not without precedent, as Protasoni and colleagues (2020) also find that 6% of Complex I in their model system remains fully assembled, however unlike in their study we find that the relative amounts of N-module and non-N-module complex I subunits are approximately the same in control and UQCRC1^{KO} cells. Moreover, Protasoni and colleagues show that restoration of the Coenzyme Q pool through expression of an alternative oxidase in their CIII deficient cell line was able to partly restore complex I activity and re-association of the N-module to holo-Complex I. Such an experiment followed by SCE-MS could provide further insights into the nature of N-module association. Possible reasons for the discrepancy between our results and Protasoni et al. (2020) could be cell line specific differences (HEK293 derived from embryonic kidney in our study, and 143B cybrids derived from an osteosarcoma in Protasoni et al., 2020) and resulting differences in the Q-pool, as potential differences in detergent solubilization and BN-PAGE protocols, as well as the nature of the CIII assembly defect. While it is tempting to speculate that the largest confounder is the latter,

our UQCRC1^{KO} contains an uncharacterized ~150 kDa CIII sub-assembly containing MT-CYB, CYC1, UQCRB, UQCRQ and UQCR10 (**Figure 3A**, **Supplementary Figure S4**) while their cybrid system harbors no comparable sub-assembly, the ~150 kDa sub-assembly present in our cell line does not appear to be associated with any Complex I sub-assemblies (**Supplementary Figure S4**). Thus we conclude that while structural association between Complex III assemblies and the nascent Complex I membrane arm is not required for N-module association, its absence may lead to the interaction being more labile, reflected in an increased susceptibility of N-module subunits to carbonate extraction.

Finally, two additional caveats to SCE-MS introduced by the use of knockout cell lines harboring severe defects in OXPHOS complex assembly should be considered. The first is the potential impact of the carbonate solution on protein complex stability. Since we are directly comparing extractability of proteins from two different complexes, differences in complex stability during the carbonate extraction has the potential to confound results. For example, a sub-assembly unique to a knockout may collapse in the presence of sodium carbonate leading to some subunits being artificially susceptible to extraction from the membrane, whereas the comparable assembly in control cell lines is unaffected. We analyzed membrane fractions from our control and knockout cells extracted at both pH 9.5 and 11.5 using BN-PAGE and immunoblotting (**Supplementary Figure S3**). This experiment showed that while the susceptibility to extraction changed for some complexes as we expected it would, complexes resistant to carbonate extraction migrated similarly to those solubilized from intact mitochondria. An additional caveat that could be considered is effect of the loss of a protein of interest on mitochondrial lipid composition, which may indirectly alter extractability of proteins. For example, dysfunctional respiratory chain assembly is also known to alter the abundance of cardiolipin (Xu et al., 2019), a mitochondrial specific phospholipid that is critical in the stability of mitochondrial complexes, including OXPHOS complexes (Zhang et al., 2002; Pfeiffer et al., 2003; Mckenzie et al., 2006; Kutik et al., 2008; Gebert et al., 2009). Such alterations could reasonably impact the extractability of complexes between control and knockout cells in a similar way as described above. While measurement of lipid content in our cell lines was out of the scope of our study, we note that while defects in cardiolipin biosynthesis alter the migration and conceivably composition of the pre-sequence translocase of the inner membrane (TIM23 complex) (Kutik et al., 2008), the extractability of Tim23 is not altered (Claypool et al., 2008). Given that the migration of carbonate resistant complexes is not altered in our knockouts (**Supplementary Figure S3**) we suspect that potential changes in mitochondrial lipid composition would not alter our conclusions.

In summary, SCE-MS is technique that can be used to identify dynamic changes in membrane association on a proteome wide scale. "Destabilization" is an oft-cited concept to describe the impact of an assembly defect on a specific subunit or part of a complex. In most cases it is used speculatively upon observing a reduction in protein abundance, but without other molecular precedent. SCE-MS provides additional insight into "destabilization" by revealing a change in solubility of a protein or population of proteins between two conditions. The quantitative accuracy and high dynamic range of mass-spectrometry relative to techniques such as immunoblotting allow overall reduction in protein abundance to be accounted for, and the global nature of the technique affords the use of 100's of proteins with known solubility profiles as internal controls. In conclusion, SCE-MS is an easy to implement tool that can add an extra dimension to our understanding of respiratory chain complex assembly.

DATA AVAILABILITY STATEMENT

The original contributions presented in the study are publicly available. This data can be found here: ProteomeXChange/PXD028935.

AUTHOR CONTRIBUTIONS

DR and DS designed the research, DR, LM-W, RK, BR, and ES performed experiments, DH developed methodology, DR, DH, LM-W, CR, and NC performed bioinformatic analysis, DR and DS wrote the manuscript, all authors analyzed data and participated in revising the manuscript.

FUNDING

This research was supported by an Australian National Health and Medical Research Council (NHMRC) project grant (1140906 to DS) and fellowship (1140851 to DS). DH is supported by the Melbourne Research Scholarship and the Mito Foundation top-up Scholarship.

ACKNOWLEDGMENTS

We thank all members of the Stroud lab, Diana Stojanovski and members of the Stojanovski lab for input into experimental design and interpretation of data. We thank Diana Stojanovski, Mike Ryan, and David Ascher for provision of reagents and computational resources respectively. We thank the Bio21 Mass Spectrometry and Proteomics Facility (MMSPF) for the provision of instrumentation, training, and technical support, and the Mito Foundation for the provision of instrumentation through the large equipment grant support scheme.

SUPPLEMENTARY MATERIAL

The Supplementary Material for this article can be found online at: https://www.frontiersin.org/articles/10.3389/fcell.2022.786268/full#supplementary-material

REFERENCES

Acin-Perez, R., Bayona-Bafaluy, M. A. P., Fernández-Silva, P., Moreno-Loshuertos, R., Pérez-Martos, A., Bruno, C., et al. (2004). Respiratory Complex III Is Required to Maintain Complex I in Mammalian Mitochondria. *Mol. Cel* 13, 805–815.

Adams, K., and Palmer, J. D. (2003). Evolution of Mitochondrial Gene Content: Gene Loss and Transfer to the Nucleus. *Mol. Phylogenet. Evol.* 29, 380–395. doi:10.1016/s1055-7903(03)00194-5

Aibara, S., Singh, V., Modelska, A., and Amunts, A. (2020). Structural Basis of Mitochondrial Translation. *eLife* 9, e58362. doi:10.7554/eLife.58362

Challa, M., Malladi, S., Pellock, B. J., Dresnek, D., Varadarajan, S., Yin, Y. W., et al. (2007). Drosophila Omi, a Mitochondrial-Localized IAP Antagonist and Proapoptotic Serine Protease. *Embo j* 26, 3144–3156. doi:10.1038/sj.emboj.7601745

Claypool, S. M., Boontheung, P., Mccaffery, J. M., Loo, J. A., and Koehler, C. M. (2008). The Cardiolipin Transacylase, Tafazzin, Associates with Two Distinct Respiratory Components Providing Insight into Barth Syndrome. *MBoC* 19, 5143–5155. doi:10.1091/mbc.e08-09-0896

Crofts, A. R., Holland, J. T., Victoria, D., Kolling, D. R. J., Dikanov, S. A., Gilbreth, R., et al. (2008). The Q-Cycle Reviewed: How Well Does a Monomeric Mechanism of the Bc1 Complex Account for the Function of a Dimeric Complex? *Biochim. Biophys. Acta (Bba) - Bioenerg.* 1777, 1001–1019. doi:10.1016/j.bbabio.2008.04.037

Dunning, C. J. R., Mckenzie, M., Sugiana, C., Lazarou, M., Silke, J., Connelly, A., et al. (2007). Human CIA30 Is Involved in the Early Assembly of Mitochondrial Complex I and Mutations in its Gene Cause Disease. *Embo j* 26, 3227–3237. doi:10.1038/sj.emboj.7601748

Fernandez-Vizarra, E., and Zeviani, M. (2018). Mitochondrial Complex III Rieske Fe-S Protein Processing and Assembly. *Cell Cycle* 17, 681–687. doi:10.1080/15384101.2017.1417707

Fernández-Vizarra, E., and Zeviani, M. (2015). Nuclear Gene Mutations as the Cause of Mitochondrial Complex III Deficiency. *Front. Genet.* 6, 134. doi:10.3389/fgene.2015.00134

Fujiki, Y., Fowler, S., Shio, H., Hubbard, A. L., and Lazarow, P. B. (1982a). Polypeptide and Phospholipid Composition of the Membrane of Rat Liver Peroxisomes: Comparison with Endoplasmic Reticulum and Mitochondrial Membranes. *J. Cel Biol* 93, 103–110. doi:10.1083/jcb.93.1.103

Fujiki, Y., Hubbard, A. L., Fowler, S., and Lazarow, P. B. (1982b). Isolation of Intracellular Membranes by Means of Sodium Carbonate Treatment: Application to Endoplasmic Reticulum. *J. Cel Biol* 93, 97–102. doi:10.1083/jcb.93.1.97

Gebert, N., Joshi, A. S., Kutik, S., Becker, T., Mckenzie, M., Guan, X. L., et al. (2009). Mitochondrial Cardiolipin Involved in Outer-Membrane Protein Biogenesis: Implications for Barth Syndrome. *Curr. Biol.* 19, 2133–2139. doi:10.1016/j.cub.2009.10.074

Giese, H., Meisterknecht, J., Heidler, J., and Wittig, I. (2021). "Mitochondrial Complexome Profiling," in *Mitochondrial Gene Expression: Methods and Protocols*. Editors M. Minczuk, and J. Rorbach (New York, NY: Springer US), 269–285. doi:10.1007/978-1-0716-0834-0_19

Gorman, G. S., Chinnery, P. F., Dimauro, S., Hirano, M., Koga, Y., Mcfarland, R., et al. (2016). Mitochondrial Diseases. *Nat. Rev. Dis. Primers* 2, 16080. doi:10.1038/nrdp.2016.80

Gu, J., Wu, M., Guo, R., Yan, K., Lei, J., Gao, N., et al. (2016). The Architecture of the Mammalian Respirasome. *Nature* 537, 639–643. doi:10.1038/nature19359

Guo, R., Zong, S., Wu, M., Gu, J., and Yang, M. (2017). Architecture of Human Mitochondrial Respiratory Megacomplex I2III2IV2. *Cell* 170, 1247–1257. doi:10.1016/j.cell.2017.07.050

Hailemariam, M., Eguez, R. V., Singh, H., Bekele, S., Ameni, G., Pieper, R., et al. (2018). S-trap, an Ultrafast Sample-Preparation Approach for Shotgun Proteomics. *J. Proteome Res.* 17, 2917–2924. doi:10.1021/acs.jproteome.8b00505

Hatefi, Y. (1985). The Mitochondrial Electron Transport and Oxidative Phosphorylation System. *Annu. Rev. Biochem.* 54, 1015–1069. doi:10.1146/annurev.bi.54.070185.005055

Hildenbeutel, M., Hegg, E. L., Stephan, K., Gruschke, S., Meunier, B., and Ott, M. (2014). Assembly Factors Monitor Sequential Hemylation of Cytochrome B to Regulate Mitochondrial Translation. *J. Cel Biol.* 205, 511–524. doi:10.1083/jcb.201401009

Hock, D. H., Robinson, D. R. L., and Stroud, D. A. (2020). Blackout in the Powerhouse: Clinical Phenotypes Associated with Defects in the Assembly of OXPHOS Complexes and the Mitoribosome. *Biochem. J.* 477, 4085–4132. doi:10.1042/bcj20190767

Hofmann, K. (1993). TMbase-A Database of Membrane Spanning Proteins Segments. *Biol. Chem. Hoppe-seyler* 374, 166.

Itoh, Y., Andréll, J., Choi, A., Richter, U., Maiti, P., Best, R. B., et al. (2021). Mechanism of Membrane-Tethered Mitochondrial Protein Synthesis. *Science* 371, 846–849. doi:10.1126/science.abe0763

Jackson, T. D., Palmer, C. S., and Stojanovski, D. (2018). Mitochondrial Diseases Caused by Dysfunctional Mitochondrial Protein Import. *Biochem. Soc. Trans.* 46, 1225–1238. doi:10.1042/bst20180239

Johnston, A. J., Hoogenraad, J., Dougan, D. A., Truscott, K. N., Yano, M., Mori, M., et al. (2002). Insertion and Assembly of Human Tom7 into the Preprotein Translocase Complex of the Outer Mitochondrial Membrane. *J. Biol. Chem.* 277, 42197–42204. doi:10.1074/jbc.m205613200

Jonckheere, A. I., Smeitink, J. A. M., and Rodenburg, R. J. T. (2012). Mitochondrial ATP Synthase: Architecture, Function and Pathology. *J. Inherit. Metab. Dis.* 35, 211–225. doi:10.1007/s10545-011-9382-9

Käll, L., Krogh, A., and Sonnhammer, E. L. (2004). A Combined Transmembrane Topology and Signal Peptide Prediction Method. *J. Mol. Biol.* 338, 1027–1036. doi:10.1016/j.jmb.2004.03.016

Kang, Y., Fielden, L. F., and Stojanovski, D. (2018). Mitochondrial Protein Transport in Health and Disease. *Semin. Cel Dev. Biol.* 76, 142–153. doi:10.1016/j.semcdb.2017.07.028

Kim, H., Botelho, S. C., Park, K., and Kim, H. (2015). Use of Carbonate Extraction in Analyzing Moderately Hydrophobic Transmembrane Proteins in the Mitochondrial Inner Membrane. *Protein Sci.* 24, 2063–2069. doi:10.1002/pro.2817

Krogh, A., Larsson, B., Von Heijne, G., and Sonnhammer, E. L. L. (2001). Predicting Transmembrane Protein Topology with a Hidden Markov Model: Application to Complete genomes11Edited by F. Cohen. *J. Mol. Biol.* 305, 567–580. doi:10.1006/jmbi.2000.4315

Kutik, S., Rissler, M., Guan, X. L., Guiard, B., Shui, G., Gebert, N., et al. (2008). The Translocator Maintenance Protein Tam41 Is Required for Mitochondrial Cardiolipin Biosynthesis. *J. Cel Biol* 183, 1213–1221. doi:10.1083/jcb.200806048

Labun, K., Montague, T. G., Krause, M., Torres Cleuren, Y. N., Tjeldnes, H., and Valen, E. (2019). CHOPCHOP V3: Expanding the CRISPR Web Toolbox beyond Genome Editing. *Nucleic Acids Res.* 47, W171–W174. doi:10.1093/nar/gkz365

Lazarou, M., Mckenzie, M., Ohtake, A., Thorburn, D. R., and Ryan, M. T. (2007). Analysis of the Assembly Profiles for Mitochondrial- and Nuclear-DNA-Encoded Subunits into Complex I. *Mol. Cel Biol* 27, 4228–4237. doi:10.1128/mcb.00074-07

Le Vasseur, M., Friedman, J., Jost, M., Xu, J., Yamada, J., Kampmann, M., et al. (2021). Genome-wide CRISPRi Screening Identifies OCIAD1 as a Prohibitin Client and Regulatory Determinant of Mitochondrial Complex III Assembly in Human Cells. *Elife* 10, e67624. doi:10.7554/eLife.67624

Letts, J. A., Fiedorczuk, K., and Sazanov, L. A. (2016). The Architecture of Respiratory Supercomplexes. *Nature* 537, 644–648. doi:10.1038/nature19774

Lytovchenko, O., Naumenko, N., Oeljeklaus, S., Schmidt, B., Malsburg, K., Deckers, M., et al. (2014). The INA Complex Facilitates Assembly of the Peripheral Stalk of the Mitochondrial F 1 F O - ATP Synthase. *Embo J.* 33, 1624–1638. doi:10.15252/embj.201488076

Ma, Q., Zhu, C., Zhang, W., Ta, N., Zhang, R., Liu, L., et al. (2019). Mitochondrial PIP3-Binding Protein FUNDC2 Supports Platelet Survival via AKT Signaling Pathway. *Cell Death Differ* 26, 321–331. doi:10.1038/s41418-018-0121-8

Ma, S. B., Nguyen, T. N., Tan, I., Ninnis, R., Iyer, S., Stroud, D. A., et al. (2014). Bax Targets Mitochondria by Distinct Mechanisms before or during Apoptotic Cell Death: a Requirement for VDAC2 or Bak for Efficient Bax Apoptotic Function. *Cel Death Differ* 21, 1925–1935. doi:10.1038/cdd.2014.119

Maclean, A. E., Bridges, H. R., Silva, M. F., Ding, S., Ovciarikova, J., Hirst, J., et al. (2021). Complexome Profile of Toxoplasma Gondii Mitochondria Identifies Divergent Subunits of Respiratory Chain Complexes Including New Subunits of Cytochrome Bc1 Complex. *Plos Pathog.* 17, e1009301. doi:10.1371/journal.ppat.1009301

Mckenzie, M., Lazarou, M., Thorburn, D. R., and Ryan, M. T. (2006). Mitochondrial Respiratory Chain Supercomplexes Are Destabilized in Barth Syndrome Patients. *J. Mol. Biol.* 361, 462–469. doi:10.1016/j.jmb.2006.06.057

Ndi, M., Marin-Buera, L., Salvatori, R., Singh, A. P., and Ott, M. (2018). Biogenesis of the Bc1 Complex of the Mitochondrial Respiratory Chain. *J. Mol. Biol.* 430, 3892–3905. doi:10.1016/j.jmb.2018.04.036

Ott, M., and Herrmann, J. M. (2010). Co-translational Membrane Insertion of Mitochondrially Encoded Proteins. *Biochim. Biophys. Acta (Bba) - Mol. Cel Res.* 1803, 767–775. doi:10.1016/j.bbamcr.2009.11.010

Palmieri, F. (2013). The Mitochondrial Transporter Family SLC25: Identification, Properties and Physiopathology. *Mol. Aspects Med.* 34, 465–484. doi:10.1016/j.mam.2012.05.005

Pfanner, N., Warscheid, B., and Wiedemann, N. (2019). Mitochondrial Proteins: from Biogenesis to Functional Networks. *Nat. Rev. Mol. Cel Biol* 20, 267–284. doi:10.1038/s41580-018-0092-0

Pfeiffer, K., Gohil, V., Stuart, R. A., Hunte, C., Brandt, U., Greenberg, M. L., et al. (2003). Cardiolipin Stabilizes Respiratory Chain Supercomplexes. *J. Biol. Chem.* 278, 52873–52880. doi:10.1074/jbc.m308366200

Protasoni, M., Pérez-Pérez, R., Lobo-Jarne, T., Harbour, M. E., Ding, S., Peñas, A., et al. (2020). Respiratory Supercomplexes Act as a Platform for Complex III-Mediated Maturation of Human Mitochondrial Complexes I and IV. *EMBO J.* 39, e102817. doi:10.15252/embj.2019102817

Rath, S., Sharma, R., Gupta, R., Ast, T., Chan, C., Durham, T. J., et al. (2021). MitoCarta3.0: an Updated Mitochondrial Proteome Now with Sub-organelle Localization and Pathway Annotations. *Nucleic Acids Res.* 49, D1541–d1547. doi:10.1093/nar/gkaa1011

Rich, P. R., and Maréchal, A. (2010). The Mitochondrial Respiratory Chain. *Essays Biochem.* 47, 1–23. doi:10.1042/bse0470001

Roger, A. J., Muñoz-Gómez, S. A., and Kamikawa, R. (2017). The Origin and Diversification of Mitochondria. *Curr. Biol.* 27, R1177–r1192. doi:10.1016/j.cub.2017.09.015

Schägger, H., De Coo, R., Bauer, M. F., Hofmann, S., Godinot, C., and Brandt, U. (2004). Significance of Respirasomes for the Assembly/Stability of Human Respiratory Chain Complex I. *J. Biol. Chem.* 279, 36349–36353. doi:10.1074/jbc.M404033200

Schägger, H., Link, T. A., Engel, W. D., and Von Jagow, G. (1986). [22] Isolation of the Eleven Protein Subunits of the Bc1 Complex from Beef Heart. *Methods Enzymol.* 126, 224–237. doi:10.1016/s0076-6879(86)26024-3

Schagger, H., and Pfeiffer, K. (2000). Supercomplexes in the Respiratory Chains of Yeast and Mammalian Mitochondria. *Embo j* 19, 1777–1783. doi:10.1093/emboj/19.8.1777

Smith, P. M., Fox, J. L., and Winge, D. R. (2012). Biogenesis of the Cytochrome Bc1 Complex and Role of Assembly Factors. *Biochim. Biophys. Acta (Bba) - Bioenerg.* 1817, 276–286. doi:10.1016/j.bbabio.2011.11.009

Stephan, K., and Ott, M. (2020). Timing of Dimerization of the Bc Complex during Mitochondrial Respiratory Chain Assembly. *Biochim. Biophys. Acta (Bba) - Bioenerg.* 1861, 148177. doi:10.1016/j.bbabio.2020.148177

Stojanovski, D., Pfanner, N., and Wiedemann, N. (2007). "Import of Proteins into Mitochondria," in *Methods in Cell Biology* (Academic Press), 783–806. doi:10.1016/s0091-679x(06)80036-1

Stroud, D. A., Formosa, L. E., Wijeyeratne, X. W., Nguyen, T. N., and Ryan, M. T. (2013). Gene Knockout Using Transcription Activator-like Effector Nucleases (TALENs) Reveals that Human NDUFA9 Protein Is Essential for Stabilizing the junction between Membrane and Matrix Arms of Complex I. *J. Biol. Chem.* 288, 1685–1690. doi:10.1074/jbc.c112.436766

Stroud, D. A., Surgenor, E. E., Formosa, L. E., Reljic, B., Frazier, A. E., Dibley, M. G., et al. (2016). Accessory Subunits Are Integral for Assembly and Function of Human Mitochondrial Complex I. *Nature* 538, 123–126. doi:10.1038/nature19754

The Uniprot Consortium (2021). UniProt: the Universal Protein Knowledgebase in 2021. *Nucleic Acids Res.* 49, D480–D489. doi:10.1093/nar/gkaa1100

Thompson, K., Mai, N., Oláhová, M., Scialó, F., Formosa, L. E., Stroud, D. A., et al. (2018). OXA1L Mutations Cause Mitochondrial Encephalopathy and a Combined Oxidative Phosphorylation Defect. *EMBO Mol. Med.* 10, e9060. doi:10.15252/emmm.201809060

Timón-Gómez, A., Nývltová, E., Abriata, L. A., Vila, A. J., Hosler, J., and Barrientos, A. (2018). Mitochondrial Cytochrome C Oxidase Biogenesis: Recent Developments. *Semin. Cel Dev. Biol.* 76, 163–178. doi:10.1016/j.semcdb.2017.08.055

Tusnády, G. E., and Simon, I. (2001). The HMMTOP Transmembrane Topology Prediction Server. *Bioinformatics* 17, 849–850. doi:10.1093/bioinformatics/17.9.849

Tyanova, S., Temu, T., and Cox, J. (2016a). The MaxQuant Computational Platform for Mass Spectrometry-Based Shotgun Proteomics. *Nat. Protoc.* 11, 2301–2319. doi:10.1038/nprot.2016.136

Tyanova, S., Temu, T., Sinitcyn, P., Carlson, A., Hein, M. Y., Geiger, T., et al. (2016b). The Perseus Computational Platform for Comprehensive Analysis of (Prote)omics Data. *Nat. Methods* 13, 731–740. doi:10.1038/nmeth.3901

Vögtle, F. N., Burkhart, J. M., Gonczarowska-Jorge, H., Kücükköse, C., Taskin, A. A., Kopczynski, D., et al. (2017). Landscape of Submitochondrial Protein Distribution. *Nat. Commun.* 8, 290. doi:10.1038/s41467-017-00359-0

Von Heijne, G. (1986). Why Mitochondria Need a Genome. *FEBS Lett.* 198, 1–4. doi:10.1016/0014-5793(86)81172-3

Wagener, N., and Neupert, W. (2012). Bcs1, a AAA Protein of the Mitochondria with a Role in the Biogenesis of the Respiratory Chain. *J. Struct. Biol.* 179, 121–125. doi:10.1016/j.jsb.2012.04.019

Wittig, I., Braun, H.-P., and Schägger, H. (2006). Blue Native PAGE. *Nat. Protoc.* 1, 418–428. doi:10.1038/nprot.2006.62

Wu, M., Gu, J., Guo, R., Huang, Y., and Yang, M. (2016). Structure of Mammalian Respiratory Supercomplex I 1 III 2 IV 1. *Cell* 167, 1598–1609. doi:10.1016/j.cell.2016.11.012

Xu, Y., Anjaneyulu, M., Donelian, A., Yu, W., Greenberg, M. L., Ren, M., et al. (2019). Assembly of the Complexes of Oxidative Phosphorylation Triggers the Remodeling of Cardiolipin. *Proc. Natl. Acad. Sci. USA* 116, 11235–11240. doi:10.1073/pnas.1900890116

Yanisch-Perron, C., Vieira, J., and Messing, J. (1985). Improved M13 Phage Cloning Vectors and Host Strains: Nucleotide Sequences of the M13mpl8 and pUC19 Vectors. *Gene* 33, 103–119. doi:10.1016/0378-1119(85)90120-9

Zerbetto, E., Vergani, L., and Dabbeni-Sala, F. (1997). Quantification of Muscle Mitochondrial Oxidative Phosphorylation Enzymesvia Histochemical Staining of Blue Native Polyacrylamide Gels. *Electrophoresis* 18, 2059–2064. doi:10.1002/elps.1150181131

Zhang, M., Mileykovskaya, E., and Dowhan, W. (2002). Gluing the Respiratory Chain Together. *J. Biol. Chem.* 277, 43553–43556. doi:10.1074/jbc.c200551200

Zhu, J., Vinothkumar, K. R., and Hirst, J. (2016). Structure of Mammalian Respiratory Complex I. *Nature* 536, 354–358. doi:10.1038/nature19095

Conflict of Interest: The authors declare that the research was conducted in the absence of any commercial or financial relationships that could be construed as a potential conflict of interest.

Publisher's Note: All claims expressed in this article are solely those of the authors and do not necessarily represent those of their affiliated organizations, or those of the publisher, the editors and the reviewers. Any product that may be evaluated in this article, or claim that may be made by its manufacturer, is not guaranteed or endorsed by the publisher.

frontiers | Frontiers in Cell and Developmental Biology

PERSPECTIVE
published: 01 April 2022
doi: 10.3389/fcell.2022.874596

Mitochondrial Respiratory Chain Dysfunction—A Hallmark Pathology of Idiopathic Parkinson's Disease?

Irene H. Flønes[1,2,3] *and Charalampos Tzoulis*[1,2,3]*

[1]Neuro-SysMed, Department of Neurology, Haukeland University Hospital, Bergen, Norway, [2]K.G Jebsen Center for Translational Research in Parkinson's Disease, University of Bergen, Bergen, Norway, [3]Department of Clinical Medicine, University of Bergen, Bergen, Norway

Parkinson's disease (PD) is the most common age-dependent neurodegenerative synucleinopathy. Loss of dopaminergic neurons of the substantia nigra pars compacta, together with region- and cell-specific aggregations of α-synuclein are considered main pathological hallmarks of PD, but its etiopathogenesis remains largely unknown. Mitochondrial dysfunction, in particular quantitative and/or functional deficiencies of the mitochondrial respiratory chain (MRC), has been associated with the disease. However, after decades of research in this field, the pervasiveness and anatomical extent of MRC dysfunction in PD remain largely unknown. Moreover, it is not known whether the observed MRC defects are pathogenic, compensatory responses, or secondary epiphenomena. In this perspective, we give an overview of current evidence for MRC dysfunction in PD, highlight pertinent knowledge gaps, and propose potential strategies for future research.

Keywords: neurodegeneration, mitochondrial complex I, mitochondria, oxidative phosphorylation, Parkinson's disease

OPEN ACCESS

Edited by:
Sylvie Callegari,
The University of Melbourne, Australia

Reviewed by:
Cristofol Vives-Bauza,
University of the Balearic Islands, Spain
Christos Proukakis,
University College London, United Kingdom

***Correspondence:**
Charalampos Tzoulis
chtzoulis@gmail.com

Specialty section:
This article was submitted to Cellular Biochemistry, a section of the journal Frontiers in Cell and Developmental Biology

Received: *12 February 2022*
Accepted: *10 March 2022*
Published: *01 April 2022*

Citation:
Flønes IH and Tzoulis C (2022) Mitochondrial Respiratory Chain Dysfunction—A Hallmark Pathology of Idiopathic Parkinson's Disease? Front. Cell Dev. Biol. 10:874596. doi: 10.3389/fcell.2022.874596

INTRODUCTION

Parkinson's disease (PD) is the most common neurodegenerative synucleinopathy, and affects approximately 1.8% of the population above the age of 65 years (de Rijk et al., 2000). Idiopathic PD is the predominant form of the disease, whereas monogenic forms of PD are rare, generally accounting for <5% of the cases in most populations (Bloem et al., 2021). This work will focus on idiopathic PD, which will be henceforth referred to simply as PD, unless otherwise stated. Region-specific formation of Lewy pathology (LP), of which misfolded and aggregated α-synuclein is a main constituent, and loss of the dopaminergic neurons of the substantia nigra pars compacta (SNc), are the pathological hallmarks of PD (Dickson, 2012; Surmeier et al., 2017). Neuronal loss is not limited to the SNc, but occurs across multiple brain regions, and is commonly accompanied by astro- and microgliosis. In addition to LP, accumulation of tau and beta-amyloid is also commonly observed in PD (Dickson, 2012).

Mitochondria have been the subject of intensive research in PD, following the discovery that chemical inhibition of complex I (CI) of the mitochondrial respiratory chain (MRC) can cause a

Abbreviations: CI, complex I; CIV, complex IV; IHC, immunohistochemistry; LP, Lewy pathology; MRC, mitochondrial respiratory chain; MRS, magnetic resonance spectroscopy; mtDNA, mitochondrial DNA; PD, Parkinson's disease; PET, positron-emission tomography; ROS, reactive oxygen species; SNc, substantia nigra pars compacta; TFAM, mitochondrial transcription factor A.

parkinsonian phenotype in humans and other primates, with dopaminergic neuron loss and inclusions resembling LP in the SNc (Langston et al., 1983; Ramsay et al., 1986; Betarbet et al., 2000). Shortly after, it was demonstrated that CI deficiency occurs in the SNc of individuals with PD. While CI deficiency in the dopaminergic neurons of the SNc has been a consistent finding in subsequent studies of PD, reports from other brain regions are variable and conflicting. A comprehensive review of studies on this topic was recently published by Subrahmanian et al. (Subrahmanian and LaVoie, 2021). Thus, the pervasiveness and anatomical extent of CI deficiency in PD remains a subject of debate, four decades since its first description. Moreover, the etiopathogenesis and downstream impact of CI deficiency in PD are unknown. Here, we provide a brief overview of current evidence, regarding the role of MRC deficiency in PD.

STATE OF THE ART ON MITOCHONDRIAL RESPIRATORY CHAIN DYSFUNCTION IN PARKINSON'S DISEASE

Evidence of Mitochondrial Respiratory Chain Dysfunction in Parkinson's Disease

The brain constitutes approximately 2% of the total body weight, yet it accounts for 20% of the resting metabolic rate (Mary et al., 2012). The majority of ATP synthesis occurs at the MRC, via the process of oxidative phosphorylation (Berg et al., 2007) (**Figure 1A**). Studies of the MRC in PD have generally relied on two types of methodological approaches, quantitative and functional. Quantitative assays are based primarily on immunodetection, either in bulk, homogenized tissue (e.g., by immunoblot), or *in situ* by immunohistochemistry (IHC) (Subrahmanian and LaVoie, 2021). Functional assays measure the specific activity of each respiratory complex by quantifying substrate conversion, usually in mitochondria isolated from homogenized bulk tissue (Birch-Machin and Turnbull, 2001).

Evidence for both quantitative and functional MRC deficiency has been reported in PD, but findings vary depending on the study and brain region being examined (Subrahmanian and LaVoie, 2021). In the SNc, most studies report evidence of MRC deficiency in PD, affecting mostly CI and, to a lesser degree, complexes II-IV (Subrahmanian and LaVoie, 2021) (**Figures 1B,C**). That said, the dopaminergic neurons of the SNc exhibit pronounced MRC deficiencies of similar type also with neurologically healthy aging (Bender et al., 2006; Kraytsberg et al., 2006). While subjects with PD generally show more severe deficiency than age-matched controls at the group level, there is substantial overlap at the individual level (Chen et al., 2021), so that disease-specific effects cannot be fully disentangled from the impact of aging.

MRC deficiencies have been reported in regions outside the SNc. However, findings are inconsistent and, in part, contradictory, with several studies showing no significant difference between cases and controls at the group level (Subrahmanian and LaVoie, 2021). Furthermore, the question of whether non-neuronal cells in the central nervous system exhibit MRC dysfunction in PD is only starting to be explored, with one recent study reporting quantitative reduction in all MRC complexes, normalized for total mitochondrial mass, in SNc astrocytes (Chen et al., 2022). Studies in peripheral tissues of individuals with PD, including platelets, skeletal muscle and lymphocytes, have produced similarly conflicting results, with some, but not all, detecting functional and/or quantitative reduction of CI and other MRC complexes, compared to controls (Subrahmanian and LaVoie, 2021).

Thus, while MRC dysfunction, mainly in the form of CI deficiency, is undoubtfully a phenomenon associated with PD, its presence shows high anatomical/regional and individual variation. Methodological differences may partly account for this variability. For instance, studies in homogenized bulk tissue may be less sensitive in detecting cell-specific changes, and prone to bias from altered tissue cell composition. That said, results vary also between studies using cell-specific approaches (Subrahmanian and LaVoie, 2021). This variability raises the pertinent question of whether MRC dysfunction is a universal feature of PD, or rather one characterizing a particular subset of individuals.

The Origin of Mitochondrial Respiratory Chain Deficiency in Parkinson's Disease Remains Largely Unknown

A unique feature of the MRC is that it is encoded by two genomes: 13 of its subunits are encoded by the mitochondrial DNA (mtDNA) and the remaining by the nuclear DNA (Mukherjee and Ghosh, 2020). Thus, the question arises of whether variation in any, or both, of these genomes is responsible for MRC dysfunction in PD. Genetic association studies suggest that polygenic variation enrichment in nuclear genes regulating the processes of mtDNA maintenance (Billingsley et al., 2019), mitophagy and mitochondrial translation (van der Walt et al., 2003; Pyle et al., 2005), all of which are critical for MRC integrity and function, is associated with PD. Moreover, inherited variation in the mtDNA itself appears to be important, as certain mtDNA haplogroups have been associated with lower risk of PD (van der Walt et al., 2003; Pyle et al., 2005). The reported associations are, however, relatively weak, and unlikely to be, alone, driving the observed MRC deficit in PD.

Somatic mtDNA changes are an established cause of MRC deficiency and have been associated with PD (Bender et al., 2006). Dopaminergic neurons of the SNc accumulate high levels of somatic mtDNA deletions with age (Bender et al., 2006), and this can reach even higher levels in PD (Dölle et al., 2016). Moreover, while neurologically healthy individuals appear to compensate for the accumulation of age-dependent mtDNA deletions by increasing their total mtDNA copy number, this response is blunted in PD, resulting in loss of wild-type mtDNA (Dölle et al., 2016). In line with this observation, single SNc neurons with MRC deficiencies show both a decrease in mitochondrial transcription factor A (TFAM) expression and total mtDNA copy number in PD (Chen et al., 2020). The role of mtDNA point mutations (i.e., single nucleotide variants, SNV), is more controversial. While some studies report no increase in

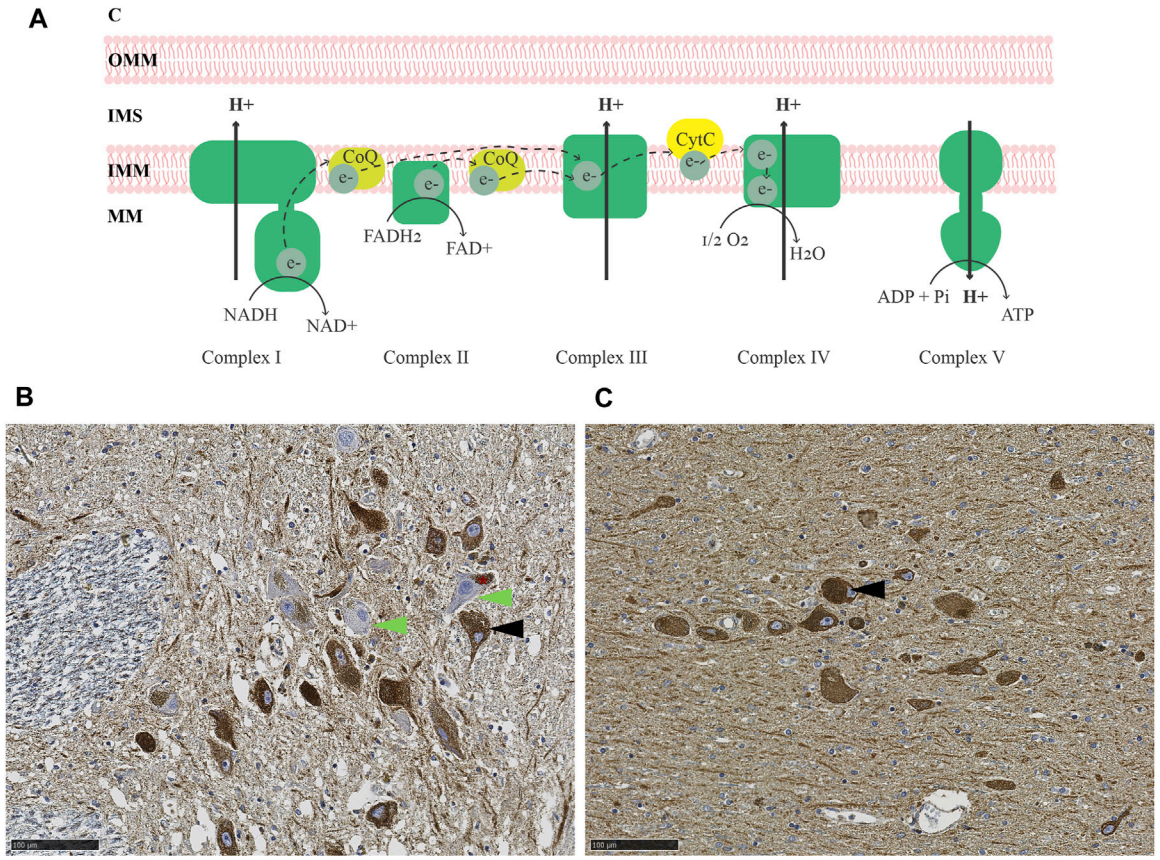

FIGURE 1 | MRC deficiency in PD. **(A)** Schematic representation of the MRC. Electrons are transferred from NADH and $FADH_2$ to complex I and II, respectively, and carried by ubiquinol (coenzyme Q; CoQ) to complex III. From there, electrons are further transferred to cytochrome c and transported to complex IV, which finally transfers the electrons onto molecular oxygen, generating water. The energy released during the series of electron transfers and redox reactions is used to pump protons out of the mitochondrial matrix (MM) via complexes I, III, and IV, creating an electrochemical and pH gradient. Protons flow back into the mitochondrial matrix via complex V and this flux is coupled with the phosphorylation of ADP to generate ATP. **(B–C)** Immunohistochemistry for the CI subunit NDUFS4 **(B)** and mitochondrial mass marker VDAC1 **(C)** in the SNc of an individual with idiopathic PD. The asterisk in **(B)** indicates neuromelanin in dopaminergic neurons of the SNc. Arrowheads show examples of CI deficient (green) and intact (black) neurons. Magnification 20X. Scalebar: 100 µm. C: cytosol, OMM: outer mitochondrial membrane, IMS: intermembrane space, IMM: inner mitochondrial membrane, MM: mitochondrial matrix, CoQ: coenzyme Q, CytC: cytochrome C, NADH: reduced nicotinamide adenine dinucleotide, NAD^+: oxidized nicotinamide adenine dinucleotide, $FADH_2$: reduced flavin adenine dinucleotide, FAD^+: oxidized flavin adenine dinucleotide, O_2: molecular oxygen, H_2O: water, ADP: adenosine diphosphate, Pi: phosphate, ATP: adenosine triphosphate.

point mutational load in PD (Simon et al., 2000; Vives-Bauza et al., 2002), others indicate that heteroplasmic point mutations occur in genes encoding subunits of CI (Parker and Parks, 2005) and CIV (Coxhead et al., 2016). Moreover, increased levels of mtDNA point mutations have been reported in single SNc neurons in early PD and incidental Lewy-body disease, indicating that point mutations may be present in early stages of PD (Lin et al., 2012).

An alternative hypothesis is that neuronal mtDNA changes in PD may be the result, rather than the cause, of MRC dysfunction. Under this model, mtDNA deletions and, potentially, point mutations arise during the repair of double-strand breaks, caused by increased reactive oxygen species (ROS) generation in CI deficient neurons (Verkaart et al., 2007; Zsurka et al., 2018). Yet another hypothesis, based on cell culture experiments, proposes that CI loss in PD may be mediated by an intra-mitochondrial LON-ClpP proteolytic quality control axis, which cleaves the peripheral arm of the complex, in response to ROS generation in depolarized mitochondria (Pryde et al., 2016). In this scenario, CI deficiency would be a compensatory response to mitigate ROS-related damage. While an intriguing hypothesis, the role of ROS in the pathogenesis of PD remains highly uncertain (Nissanka and Moraes, 2018).

Since heritability only accounts for part of the PD risk (Nalls et al., 2019). It is reasonable to assume that the environment also contributes to the observed MRC dysfunction. The fact that chemical CI inhibition causes SNc degeneration and parkinsonism has led to the hypothesis that chronic exposure to mitochondrial toxins, such as the ones contained in various pesticides, may contribute to MRC dysfunction in individuals with PD (Brown et al., 2006). Indeed, several epidemiological studies have found associations between exposure to pesticides known to inhibit CI and the incidence/prevalence of PD. However, to date, no direct causality has been established

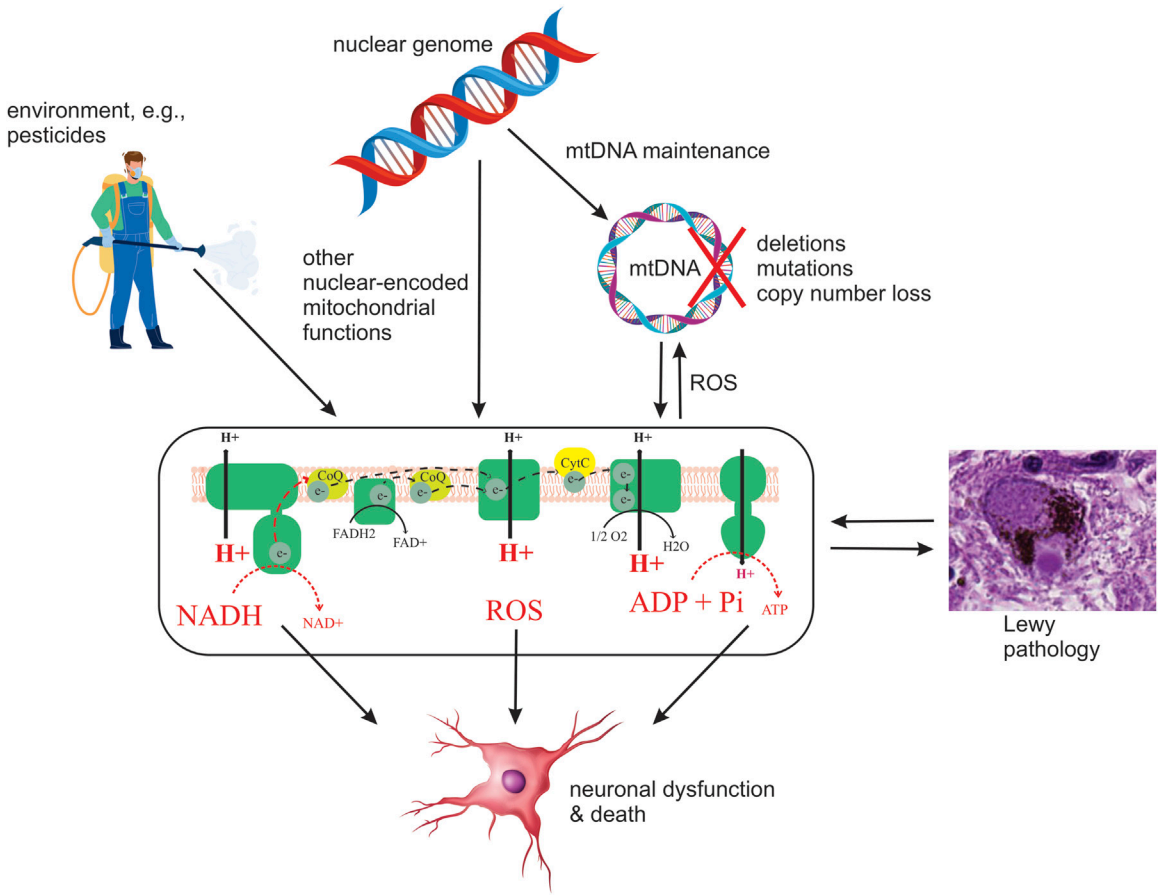

FIGURE 2 | Schematic depiction of current hypotheses on the origin and role of MRC deficiency in PD. Potential upstream etiologies are summarized, including genetic and environmental factors. Four potential downstream consequences of deficient MRC function are shown: decreased oxidation of NADH to NAD^+ by CI, decreased electron transfer, resulting in decreased proton pumping and, in turn, loss of membrane potential and lower ATP production, and increased generation of ROS. It should be emphasized that this is by no means an exhaustive list of possible causes or consequences of MRC deficiency in PD.

(**Figure 2**). Epidemiologic and toxicologic evidence of association between pesticide exposure and the risk of PD and/or parkinsonism has been reviewed by Brown et al. (Brown et al., 2006).

Is Mitochondrial Respiratory Chain Dysfunction Linked to α-Synuclein Pathology in Parkinson's Disease?

The question of whether and how mitochondria and α-synuclein interact in health and disease has been a topic of investigation ever since α-synuclein was recognized as a main constituent of LP, along with mitochondria (Spillantini et al., 1997; Shahmoradian et al., 2019). In its native state, α-synuclein is a monomer of multiple conformational states, which is believed to be involved in the regulation of synaptic vesicle trafficking and neurotransmission (Bobela et al., 2015; Alam et al., 2019). The conformational plasticity of α-synuclein monomers has been suggested to facilitate the formation of fibrils and/or oligomers, which have been suggested to be cytotoxic, although their pathogenic contribution in PD remains uncertain (Alam et al., 2019; Kumar et al., 2020; Mahul-Mellier et al., 2020; Bisi et al., 2021; Outeiro, 2021).

Studies in cell and animal models generally support a link between mitochondria and α-synuclein, but the dynamics of this relationship remains poorly understood. In yeast it was shown that functional mitochondria are required for α-synuclein-induced toxicity and cell death (Büttner et al., 2008). However, several studies in mammalian cells and animals revealed a different picture, suggesting that α-synuclein and MRC dysfunction may act synergistically in PD. Namely, α-synuclein knockout mice were resistant to CI inhibition by parkinsonism-inducing neurotoxins (Klivenyi et al., 2006), whereas mice overexpressing α-synuclein were more vulnerable to the same toxins (Song et al., 2004). Studies in cybrid-derived neurons from mouse fibroblasts carrying pathogenic mtDNA mutations revealed that α-synuclein aggregates inhibit CI function in wild-type and complex IV(CIV)-deficient cells, resulting in increased levels of apoptosis, although they did not exacerbate established CI

deficiency (Reeve et al., 2015). Furthermore, it has been shown that aggregated α-synuclein induces mitochondrial dysfunction, including CI deficiency and opening of the permeability transition pore, in co-cultures of rat neurons and astrocytes, as well as in human induced pluripotent stem cells (iPSC)-derived neurons (Ludtmann et al., 2018).

To our knowledge, few studies have explored the link between MRC dysfunction and α-synuclein pathology in the human brain. Two studies revealed an inverse association between neuronal CI deficiency and the presence of LP, in the form of Lewy bodies or pale bodies, in PD and Parkinson's disease dementia—i.e., neurons deficient for CI were significantly less likely to contain formed LP aggregates (Reeve et al., 2012; Flones et al., 2017). The mechanisms underlying this inverse association are unknown. One possibility is that functional MRC is required for LP formation, similar to what has been shown in yeast (Büttner et al., 2008). Alternatively, the coexistence of MRC deficiency and LP may be additively, or even synergistically, deleterious, so that neurons that suffer a "double hit" are lost early in the disease (Reeve et al., 2012).

Whether and How Mitochondrial Respiratory Chain Dysfunction Contributes to Neuronal Dysfunction and Death in Parkinson's Disease Remains Unknown

Irrespective of the etiopathogenesis of MRC deficiency in PD, given the neuronal dependency on mitochondrial respiration (Mary et al., 2012), it is likely to compromise the metabolic and bioenergetic status of neurons, and possibly other cell types, thereby contributing to cellular dysfunction and death in PD (**Figure 2**). The deleterious effect of MRC dysfunction was recently illustrated in a mouse model of CI deficiency specific to dopaminergic neurons, in which it was shown that isolated CI deficiency is sufficient to cause degeneration, beginning with axonal loss of function, with progressive levodopa-responsive parkinsonism (González-Rodríguez et al., 2021). While it is unknown whether similar effects take place in PD, CI deficiency is an established cause of neuronal dysfunction and death across multiple brain regions, including the dopaminergic SNc, in patients with mitochondrial disease (Tzoulis et al., 2016; Carelli et al., 2015; Fløne and Tzoulis, 2018). Therefore, it stands to reason that the MRC deficiency observed in PD is deleterious to neuronal function and survival and contributes to the neurodegenerative process (**Figure 2**). However, as with LP, there is not a high correlation between neuronal loss and reported MRC deficiency in PD (Dickson, 2012; Subrahmanian and LaVoie, 2021).

FUTURE PERSPECTIVES

Regardless of the variable and partly conflicting evidence, little doubt remains that MRC dysfunction, as a phenomenon, is associated with idiopathic PD. Specifically, CI deficiency in the SNc appears to be the most pronounced and consistently reported defect, whereas other complexes may also be affected, albeit to a lesser degree. In spite of having had this knowledge since 1989 (Schapira et al., 1989), the role of MRC dysfunction in PD, and whether it is deleterious, compensatory, or an innocent bystander, remain unknown. Several obstacles have prevented major breakthroughs in this field, including the inability to assess and track MRC function in the human brain during life, and the lack of reliable disease models. Below, we summarize three key knowledge gaps in this field, and propose potential strategies to explore and address them in future research.

Is Mitochondrial Respiratory Chain Dysfunction a Pervasive Phenomenon in Parkinson's Disease?

While referred to as a single entity, PD is a heterogeneous clinical syndrome, defined based on a constellation of phenotypical features (Bloem et al., 2021). Individuals with PD exhibit high phenotypic variability, on the basis of which several classification systems have been proposed, clustering subjects e.g., according to age of onset, combinations of motor and non-motor feature, rate of disease progression and variable treatment response (Espay et al., 2017; Greenland et al., 2019; Bloem et al., 2021). This phenotypical diversity has led to the hypothesis that biological subtypes of PD may exist, driven by different molecular mechanisms (Espay et al., 2017). Considering the clinicopathological heterogeneity of PD and striking variability in the reported MRC findings, it is not unreasonable to hypothesize that MRC dysfunction may characterize only a subgroup of individuals with PD. If true, this would imply that mitochondrial dysfunction underpins a distinct subtype of PD, and, at the same time, provide the opportunity to interrogate and decipher the role of mitochondrial dysfunction in the disease. With the appropriate markers, PD samples and cohorts could be stratified according to MRC deficiency, thereby increasing the signal-to-noise ratio in both basic and clinical research and increasing the chances for success, while moderating the need for large sample sizes. Exploring the pervasiveness of MRC dysfunction in PD should be feasible with today's technology, but will require systematic characterization of large samples, preferably with accompanying clinical and environmental information.

What Is the Etiopathogenesis of Mitochondrial Respiratory Chain Dysfunction in Parkinson's Disease?

In terms of the etiology of MRC dysfunction, current evidence suggests that genetics may play a role, but this has not been adequately explored. While associations at the pathway level have been highlighted (Gaare et al., 2018; Billingsley et al., 2019), these studies were underpowered for detecting signal at the level of individual variants or genes. Moreover, they did not consider complex interactions between nuclear and mtDNA variation. Addressing these questions would require single-base resolution genetic data from larger populations, probably in the order of 5–10,000 samples (Gaare et al., 2018). Since such datasets are now available via international consortia, this should be feasible to assess. That said, genetics are unlikely to be the sole

driver of MRC dysfunction in PD, and the potential role of environmental factor, including exposure to MRC-inhibitors, ought to be better resolved as multiple clinical cohorts of increasing sizes are being studied across most populations.

In terms of the mechanisms underlying the observed decrease in MRC complexes, evidence supports that this is, at least partly, mediated by somatic mtDNA changes. While we know that this type of mtDNA alterations can cause MRC deficiencies in models and other diseases, proving that this is the case in PD is no trivial challenge. Having no cell or animal models that recapitulate the pathogenesis of PD, answers ultimately rely on the study of postmortem brain tissue. Since MRC deficiencies occur in a mosaic distribution (Flones et al., 2017), this question must be addressed at a cell-specific level, e.g., by combining immunostaining with laser-microdissection. A handful of such studies have been reported in the SNc with results corroborating the link between mtDNA changes and MRC defects (Bender et al., 2006; Grünewald et al., 2016). Similar studies are warranted in other areas and cell-types showing MRC deficiencies in PD and assessing the full spectrum of mtDNA changes (deletions, copy number, point mutations) in each cell. A similar approach can be used to assess the transcriptomic profile of MRC-deficient and competent cells. If these deficiencies are mediated by mtDNA changes, it stands to reason that the expression of MRC subunits will be decreased in these cells.

What Is the Downstream Impact of Mitochondrial Respiratory Chain Dysfunction in Parkinson's Disease?

To understand the impact of MRC deficiencies in PD there is a need to combine experiments in appropriate models of MRC deficiency with cell-specific molecular signatures of the PD-brain. In this integrated approach, models can interrogate causality, while brain studies will establish relevance for the disease. Good models would reflect the type and magnitude of the MRC deficiencies observed without perturbing other biological systems. A paradigm of such a model was recently reported (González-Rodríguez et al., 2021). Cell-specific molecular studies of the PD-brain should differentiate between subtypes of neurons and/or glia, and distinguish between states of cell-specific pathology (i.e., presence, type and severity of MRC deficiency and α-synuclein pathology), so that specific molecular-pathological associations may be derived. Conducting such studies to full extent with current technology would be challenging. Immunostaining combined with laser-capture microdissection is a highly versatile, but also cumbersome approach. Moreover, the quality of derived omics, such as transcriptomics or proteomics, is often poor. Medium and high-throughput technologies (Nagy et al., 2020) are under rapid development and will hopefully provide us with the means to perform such studies at higher volume, efficiency, and precision.

To determine whether MRC dysfunction contributes to the initiation and progression of PD, there is a need to understand how it evolves over time, as well as if/how it is connected to disease progression. Doing so requires extra-neural and/or non-invasive brain markers of mitochondrial pathology. Currently, no imaging biomarkers have been shown to directly detect mitochondrial dysfunction, in the PD brain. A recently developed positron-emission tomography (PET) tracer for quantitative imaging of CI has shown promise in neurotoxic models of PD, but detected no changes in a human trial (Wilson et al., 2020). Even if the MRC itself cannot be directly assessed in the living brain, it may be possible to detect associated metabolic changes, measurable by e.g., phosphorus (31P) magnetic resonance spectroscopy (MRS), which assesses phosphorylated metabolites including NAD and ATP (Lu et al., 2014), and/or metabolomic analyses in cerebrospinal fluid. However, the potential of these powerful technologies has not been fully harnessed in PD. Furthermore, it is important to settle the question of whether signs of MRC deficiency can be detected in peripheral tissues of individuals with PD. The contradictory results of previous studies, in this regard, are consistent with a heterogeneous effect, where MRC dysfunction only occurs in a subpopulation of PD subjects. Addressing this heterogeneity will require studies in larger patient groups, employing multidisciplinary methodologies (e.g., immunodetection, functional assays, mtDNA assessment, and targeted metabolomics), and assessing interindividual variability and the potential for stratification of the examined cohorts.

In conclusion, two centuries since PD was first described, our pathophysiological insight still relies largely on phenomenology. Along with LP, MRC dysfunction is a phenomenon associated with PD, albeit less consistently, but whose potential role in disease initiation and progression remains poorly understood. We hope that future studies will provide the much-sought answers to these pertinent questions and begin to unwind the mystery of mitochondrial dysfunction in PD.

DATA AVAILABILITY STATEMENT

The original contributions presented in the study are included in the article/Supplementary Material, further inquiries can be directed to the corresponding author.

AUTHOR CONTRIBUTIONS

IF and CT: conception, design, wrote the manuscript.

FUNDING

This work is supported by grants from The Research Council of Norway (288164), Bergen Research Foundation (BFS2017REK05) and the Western Norway Regional Health Authority (F-10229-D11661).

REFERENCES

Alam, P., Bousset, L., Melki, R., and Otzen, D. E. (2019). α-synuclein Oligomers and Fibrils: a Spectrum of Species, a Spectrum of Toxicities. *J. Neurochem.* 150 (5), 522–534. doi:10.1111/jnc.14808

Bender, A., Krishnan, K. J., Morris, C. M., Taylor, G. A., Reeve, A. K., Perry, R. H., et al. (2006). High Levels of Mitochondrial DNA Deletions in Substantia Nigra Neurons in Aging and Parkinson Disease. *Nat. Genet.* 38 (5), 515–517. doi:10.1038/ng1769

Berg, J. M. T., and Stryer, L. J. (2007). "Oxidative Phosphorylation," in *Biochemistry*. Editors J. M. T. Berg and J. L. Stryer (W. H. Freeman and CompanyUnited States of America), 502–540.

Betarbet, R., Sherer, T. B., MacKenzie, G., Garcia-Osuna, M., Panov, A. V., and Greenamyre, J. T. (2000). Chronic Systemic Pesticide Exposure Reproduces Features of Parkinson's Disease. *Nat. Neurosci.* 3 (12), 1301–1306. doi:10.1038/81834

Billingsley, K. J., au, fnm., Barbosa, I. A., Bandrés-Ciga, S., Quinn, J. P., Bubb, V. J., et al. (2019). Mitochondria Function Associated Genes Contribute to Parkinson's Disease Risk and Later Age at Onset. *Npj Parkinsons Dis.* 5, 8. doi:10.1038/s41531-019-0080-x

Birch-Machin, M. A., and Turnbull, D. M. (2001). Chapter 5 Assaying Mitochondrial Respiratory Complex Activity in Mitochondria Isolated from Human Cells and Tissues. *Methods Cel Biol* 65, 97–117. doi:10.1016/s0091-679x(01)65006-4

Bisi, N., Feni, L., Peqini, K., Pérez-Peña, H., Ongeri, S., Pieraccini, S., et al. (2021). α-Synuclein: An All-Inclusive Trip Around its Structure, Influencing Factors and Applied Techniques. *Front. Chem.* 9, 666585. doi:10.3389/fchem.2021.666585

Bloem, B. R., Okun, M. S., and Klein, C. (2021). Parkinson's Disease. *The Lancet* 397 (10291), 2284–2303. doi:10.1016/s0140-6736(21)00218-x

Bobela, W., Aebischer, P., and Schneider, B. (2015). Alpha-Synuclein as a Mediator in the Interplay between Aging and Parkinson's Disease. *Biomolecules* 5 (4), 2675–2700. doi:10.3390/biom5042675

Brown, T. P., Rumsby, P. C., Capleton, A. C., Rushton, L., and Levy, L. S. (2006). Pesticides and Parkinson's Disease-Is There a Link? *Environ. Health Perspect.* 114 (2), 156–164. doi:10.1289/ehp.8095

Büttner, S., Bitto, A., Ring, J., Augsten, M., Zabrocki, P., Eisenberg, T., et al. (2008). Functional Mitochondria Are Required for Alpha-Synuclein Toxicity in Aging Yeast. *J. Biol. Chem.* 283 (12), 7554–7560.

Carelli, V., Musumeci, O., Caporali, L., Zanna, C., La Morgia, C., Del Dotto, V., et al. (2015). Syndromic Parkinsonism and Dementia Associated with OPA 1 Missense Mutations. *Ann. Neurol.* 78 (1), 21–38. doi:10.1002/ana.24410

Chen, C., Mossman, E., Malko, P., McDonald, D., Blain, A. P., Bone, L., et al. (2022). Astrocytic Changes in Mitochondrial Oxidative Phosphorylation Protein Levels in Parkinson's Disease. *Mov. Disord.* 37, 302–314. doi:10.1002/mds.28849

Chen, C., McDonald, D., Blain, A., Sachdeva, A., Bone, L., Smith, A. L. M., et al. (2021). Imaging Mass Cytometry Reveals Generalised Deficiency in OXPHOS Complexes in Parkinson's Disease. *Npj Parkinsons Dis.* 7 (1), 39. doi:10.1038/s41531-021-00182-x

Chen, C., Vincent, A. E., Blain, A. P., Smith, A. L., Turnbull, D. M., and Reeve, A. K. (2020). Investigation of Mitochondrial Biogenesis Defects in Single Substantia Nigra Neurons Using post-mortem Human Tissues. *Neurobiol. Dis.* 134, 104631. doi:10.1016/j.nbd.2019.104631

Coxhead, J., Kurzawa-Akanbi, M., Hussain, R., Pyle, A., Chinnery, P., and Hudson, G. (2016). Somatic mtDNA Variation Is an Important Component of Parkinson's Disease. *Neurobiol. Aging* 38, 217–e6. doi:10.1016/j.neurobiolaging.2015.10.036

de Rijk, M. C., Launer, L. J., Berger, K., Breteler, M. M., Dartigues, J. F., Baldereschi, M., et al. (2000). Prevalence of Parkinson's Disease in Europe: A Collaborative Study of Population-Based Cohorts. Neurologic Diseases in the Elderly Research Group. *Neurology* 54 (11 Suppl. 5), S21–S23.

Dickson, D. W. (2012). Parkinson's Disease and Parkinsonism: Neuropathology. *Cold Spring Harb Perspect. Med.* 2 (8). doi:10.1101/cshperspect.a009258

Dölle, C., Fløne, I., Nido, G. S., Miletic, H., Osuagwu, N., Kristoffersen, S., et al. (2016). Defective Mitochondrial DNA Homeostasis in the Substantia Nigra in Parkinson Disease. *Nat. Commun.* 7, 13548. doi:10.1038/ncomms13548

Espay, A. J., Schwarzschild, M. A., Tanner, C. M., Fernandez, H. H., Simon, D. K., Leverenz, J. B., et al. (2017). Biomarker-driven Phenotyping in Parkinson's Disease: A Translational Missing Link in Disease-modifying Clinical Trials. *Mov Disord.* 32 (3), 319–324. doi:10.1002/mds.26913

Fløne, I. H., and Tzoulis, C. (2018). Movement Disorders in Mitochondrial Disease: a Clinicopathological Correlation. *Curr. Opin. Neurol.* 31 (4), 472–483. doi:10.1097/WCO.0000000000000583

Flones, I. H., Fernandez-Vizarra, E., Lykouri, M., Brakedal, B., Skeie, G. O., Miletic, H., et al. (2017). Neuronal Complex I Deficiency Occurs throughout the Parkinson's Disease Brain, but Is Not Associated with Neurodegeneration or Mitochondrial DNA Damage. *Acta Neuropathol.*.

Gaare, J. J., Nido, G. S., Sztromwasser, P., Knappskog, P. M., Dahl, O., Lund-Johansen, M., et al. (2018). Rare Genetic Variation in Mitochondrial Pathways Influences the Risk for Parkinson's Disease. *Mov Disord.* 33 (10), 1591–1600. doi:10.1002/mds.64

González-Rodríguez, P., Zampese, E., Stout, K. A., Guzman, J. N., Ilijic, E., Yang, B., et al. (2021). Disruption of Mitochondrial Complex I Induces Progressive Parkinsonism. *Nature* 599 (7886), 650–656.

Greenland, J. C., Williams-Gray, C. H., and Barker, R. A. (2019). The Clinical Heterogeneity of Parkinson's Disease and its Therapeutic Implications. *Eur. J. Neurosci.* 49 (3), 328–338. doi:10.1111/ejn.14094

Grünewald, A., Rygiel, K. A., Hepplewhite, P. D., Morris, C. M., Picard, M., and Turnbull, D. M. (2016). Mitochondrial DNA Depletion in Respiratory Chain-Deficient P Arkinson Disease Neurons. *Ann. Neurol.* 79 (3), 366–378. doi:10.1002/ana.24571

Klivenyi, P., Siwek, D., Gardian, G., Yang, L., Starkov, A., Cleren, C., et al. (2006). Mice Lacking Alpha-Synuclein Are Resistant to Mitochondrial Toxins. *Neurobiol. Dis.* 21 (3), 541–548. doi:10.1016/j.nbd.2005.08.018

Kraytsberg, Y., Kudryavtseva, E., McKee, A. C., Geula, C., Kowall, N. W., and Khrapko, K. (2006). Mitochondrial DNA Deletions Are Abundant and Cause Functional Impairment in Aged Human Substantia Nigra Neurons. *Nat. Genet.* 38 (5), 518–520. doi:10.1038/ng1778

Kumar, S. T., Jagannath, S., Francois, C., Vanderstichele, H., Stoops, E., and Lashuel, H. A. (2020). How Specific Are the Conformation-specific α-synuclein Antibodies? Characterization and Validation of 16 α-synuclein Conformation-specific Antibodies Using Well-Characterized Preparations of α-synuclein Monomers, Fibrils and Oligomers with Distinct Structures and Morphology. *Neurobiol. Dis.* 146, 105086. doi:10.1016/j.nbd.2020.105086

Langston, J. W., Ballard, P., Tetrud, J. W., and Irwin, I. (1983). Chronic Parkinsonism in Humans Due to a Product of Meperidine-Analog Synthesis. *Science* 219 (4587), 979–980. doi:10.1126/science.6823561

Lin, M. T., Cantuti-Castelvetri, I., Zheng, K., Jackson, K. E., Tan, Y. B., Arzberger, T., et al. (2012). Somatic Mitochondrial DNA Mutations in Early Parkinson and Incidental Lewy Body Disease. *Ann. Neurol.* 71 (6), 850–854. doi:10.1002/ana.23568

Lu, M., Zhu, X.-H., Zhang, Y., and Chen, W. (2014). Intracellular Redox State Revealed by *In Vivo*31P MRS Measurement of NAD+and NADH Contents in Brains. *Magn. Reson. Med.* 71 (6), 1959–1972. doi:10.1002/mrm.24859

Ludtmann, M. H. R., Angelova, P. R., Horrocks, M. H., Choi, M. L., Rodrigues, M., Baev, A. Y., et al. (2018). α-Synuclein Oligomers Interact with ATP Synthase and Open the Permeability Transition Pore in Parkinson's Disease. *Nat. Commun.* 9 (1), 2293. doi:10.1038/s41467-018-04422-2

Mahul-Mellier, A.-L., Burtscher, J., Maharjan, N., Weerens, L., Croisier, M., Kuttler, F., et al. (2020). The Process of Lewy Body Formation, rather Than Simply α-synuclein Fibrillization, Is One of the Major Drivers of Neurodegeneration. *Proc. Natl. Acad. Sci. U.S.A.* 117 (9), 4971–4982. doi:10.1073/pnas.1913904117

Mary, C. Mc. Kenna., Ursula Sonnewald, G. A. D., Waagepetersen, Helle. S., and Schousboe, Arne., *Energy Metabolism of the Brain*. Eighth ed. *Basic Neurochemistry*, 2012, Springer

Mukherjee, S., and Ghosh, A. (2020). Molecular Mechanism of Mitochondrial Respiratory Chain Assembly and its Relation to Mitochondrial Diseases. *Mitochondrion* 53, 1–20. doi:10.1016/j.mito.2020.04.002

Nagy, C., Maitra, M., Tanti, A., Suderman, M., Théroux, J.-F., Davoli, M. A., et al. (2020). Single-nucleus Transcriptomics of the Prefrontal Cortex in Major Depressive Disorder Implicates Oligodendrocyte Precursor Cells and Excitatory Neurons. *Nat. Neurosci.* 23 (6), 771–781. doi:10.1038/s41593-020-0621-y

Nalls, M. A., Blauwendraat, C., Vallerga, C. L., Heilbron, K., Bandres-Ciga, S., Chang, D., et al. (2019). Identification of Novel Risk Loci, Causal Insights, and Heritable Risk for Parkinson's Disease: a Meta-Analysis of Genome-wide Association Studies. *Lancet Neurol.* 18 (12), 1091–1102. doi:10.1016/S1474-4422(19)30320-5

Nissanka, N., and Moraes, C. T. (2018). Mitochondrial DNA Damage and Reactive Oxygen Species in Neurodegenerative Disease. *FEBS Lett.* 592 (5), 728–742. doi:10.1002/1873-3468.12956

Outeiro, T. F. (2021). Alpha-Synuclein Antibody Characterization: Why Semantics Matters. *Mol. Neurobiol.* 58 (5), 2202–2203. doi:10.1007/s12035-020-02269-7

Parker, W. D., Jr., and Parks, J. K. (2005). Mitochondrial ND5 Mutations in Idiopathic Parkinson's Disease. *Biochem. Biophysical Res. Commun.* 326 (3), 667–669. doi:10.1016/j.bbrc.2004.11.093

Pryde, K. R., Taanman, J. W., and Schapira, A. H. (2016). A LON-ClpP Proteolytic Axis Degrades Complex I to Extinguish ROS Production in Depolarized Mitochondria. *Cel Rep.* 17 (10), 2522–2531. doi:10.1016/j.celrep.2016.11.027

Pyle, A., Foltynie, T., Tiangyou, W., Lambert, C., Keers, S. M., Allcock, L. M., et al. (2005). Mitochondrial DNA Haplogroup Cluster UKJT Reduces the Risk of PD. *Ann. Neurol.* 57 (4), 564–567. doi:10.1002/ana.20417

Ramsay, R. R., Salach, J. I., and Singer, T. P. (1986). Uptake of the Neurotoxin 1-Methyl-4-Phenylpyridine (MPP+) by Mitochondria and its Relation to the Inhibition of the Mitochondrial Oxidation of NAD+-linked Substrates by MPP+. *Biochem. Biophysical Res. Commun.* 134 (2), 743–748. doi:10.1016/s0006-291x(86)80483-1

Reeve, A. K., Park, T. K., Jaros, E., Campbell, G. R., Lax, N. Z., Hepplewhite, P. D., et al. (2012). Relationship between Mitochondria and α-Synuclein. *Arch. Neurol.* 69 (3), 385–393. doi:10.1001/archneurol.2011.2675

Reeve, A. K., Ludtmann, M. H., Angelova, P. R., Simcox, E. M., Horrocks, M. H., Klenerman, D., et al. (2015). Aggregated α-synuclein and Complex I Deficiency: Exploration of Their Relationship in Differentiated Neurons. *Cell Death Dis* 6, e1820. doi:10.1038/cddis.2015.166

Schapira, A. H. V., Cooper, J. M., Dexter, D., Jenner, P., Clark, J. B., and Marsden, C. D. (1989). Mitochondrial Complex I Deficiency in Parkinson's Disease. *The Lancet* 333 (8649), 1269. doi:10.1016/s0140-6736(89)92366-0

Shahmoradian, S. H., Lewis, A. J., Genoud, C., Hench, J., Moors, T. E., Navarro, P. P., et al. (2019). Lewy Pathology in Parkinson's Disease Consists of Crowded Organelles and Lipid Membranes. *Nat. Neurosci.* 22 (7), 1099–1109. doi:10.1038/s41593-019-0423-2

Simon, D. K., Mayeux, R., Marder, K., Kowall, N. W., Beal, M. F., and Johns, D. R. (2000). Mitochondrial DNA Mutations in Complex I and tRNA Genes in Parkinson's Disease. *Neurology* 54 (3), 703. doi:10.1212/wnl.54.3.703

Song, D. D., Shults, C. W., Sisk, A., Rockenstein, E., and Masliah, E. (2004). Enhanced Substantia Nigra Mitochondrial Pathology in Human α-synuclein Transgenic Mice after Treatment with MPTP111-Methyl-4-Phenyl-1,2,3,6-Tetrahydropyridine. *Exp. Neurol.* 186 (2), 158–172. doi:10.1016/s0014-4886(03)00342-x

Spillantini, M. G., Schmidt, M. L., Lee, V. M.-Y., Trojanowski, J. Q., Jakes, R., and Goedert, M. (1997). α-Synuclein in Lewy Bodies. *Nature* 388 (6645), 839–840. doi:10.1038/42166

Subrahmanian, N., and LaVoie, M. J. (2021). Is There a Special Relationship between Complex I Activity and Nigral Neuronal Loss in Parkinson's Disease? A Critical Reappraisal. *Brain Res.* 1767, 147434. doi:10.1016/j.brainres.2021.147434

Surmeier, D. J., Obeso, J. A., and Halliday, G. M. (2017). Selective Neuronal Vulnerability in Parkinson Disease. *Nat. Rev. Neurosci.* 18 (2), 101–113. doi:10.1038/nrn.2016.178

Tzoulis, C., Schwarzlmüller, T., Biermann, M., Haugarvoll, K., and Bindoff, L. A. (2016). Mitochondrial DNA Homeostasis Is Essential for Nigrostriatal Integrity. *Mitochondrion* 28, 33–37. doi:10.1016/j.mito.2016.03.003

van der Walt, J. M., Nicodemus, K. K., Martin, E. R., Scott, W. K., Nance, M. A., Watts, R. L., et al. (2003). Mitochondrial Polymorphisms Significantly Reduce the Risk of Parkinson Disease. *Am. J. Hum. Genet.* 72 (4), 804–811. doi:10.1086/373937

Verkaart, S., Koopman, W. J. H., van Emst-de Vries, S. E., Nijtmans, L. G. J., van den Heuvel, L. W. P. J., Smeitink, J. A. M., et al. (2007). Superoxide Production Is Inversely Related to Complex I Activity in Inherited Complex I Deficiency. *Biochim. Biophys. Acta (Bba) - Mol. Basis Dis.* 1772 (3), 373–381. doi:10.1016/j.bbadis.2006.12.009

Vives-Bauza, C., Andreu, A. L., Manfredi, G., Beal, M. F., Janetzky, B., Gruenewald, T. H., et al. (2002). Sequence Analysis of the Entire Mitochondrial Genome in Parkinson's Disease. *Biochem. Biophysical Res. Commun.* 290 (5), 1593–1601. doi:10.1006/bbrc.2002.6388

Wilson, H., Pagano, G., Natale, E. R., Mansur, A., Caminiti, S. P., Polychronis, S., et al. (2020). Mitochondrial Complex 1, Sigma 1, and Synaptic Vesicle 2A in Early Drug-Naive Parkinson's Disease. *Mov Disord.* 35 (8), 1416–1427. doi:10.1002/mds.28064

Zsurka, G., Peeva, V., Kotlyar, A., and Kunz, W. S. (2018). Is There Still Any Role for Oxidative Stress in Mitochondrial DNA-dependent Aging? *Genes (Basel)* 9 (4). doi:10.3390/genes9040175

Conflict of Interest: The authors declare that the research was conducted in the absence of any commercial or financial relationships that could be construed as a potential conflict of interest.

Publisher's Note: All claims expressed in this article are solely those of the authors and do not necessarily represent those of their affiliated organizations, or those of the publisher, the editors and the reviewers. Any product that may be evaluated in this article, or claim that may be made by its manufacturer, is not guaranteed or endorsed by the publisher.

Advantages of publishing in Frontiers

OPEN ACCESS
Articles are free to read for greatest visibility and readership

FAST PUBLICATION
Around 90 days from submission to decision

HIGH QUALITY PEER-REVIEW
Rigorous, collaborative, and constructive peer-review

TRANSPARENT PEER-REVIEW
Editors and reviewers acknowledged by name on published articles

Frontiers
Avenue du Tribunal-Fédéral 34
1005 Lausanne | Switzerland

Visit us: www.frontiersin.org
Contact us: frontiersin.org/about/contact

REPRODUCIBILITY OF RESEARCH
Support open data and methods to enhance research reproducibility

DIGITAL PUBLISHING
Articles designed for optimal readership across devices

FOLLOW US
@frontiersin

IMPACT METRICS
Advanced article metrics track visibility across digital media

EXTENSIVE PROMOTION
Marketing and promotion of impactful research

LOOP RESEARCH NETWORK
Our network increases your article's readership